

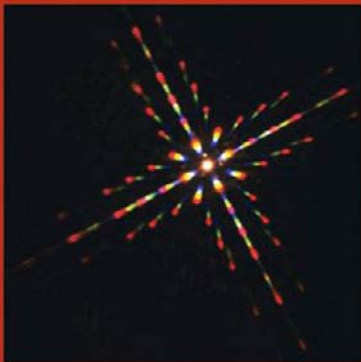
IUCr TEXTS ON CRYSTALLOGRAPHY · 14

Crystal Structure Analysis

A Primer

Third Edition

JENNY PICKWORTH GLUSKER
AND KENNETH N. TRUEBLOOD



INTERNATIONAL UNION OF CRYSTALLOGRAPHY
OXFORD SCIENCE PUBLICATIONS



INTERNATIONAL UNION OF CRYSTALLOGRAPHY
BOOK SERIES

IUCr BOOK SERIES COMMITTEE

J. Bernstein, *Israel*
G. R. Desiraju, *India*
J. R. Helliwell, *UK*
T. Mak, *China*
P. Müller, *USA*
P. Paufler, *Germany*
H. Schenk, *The Netherlands*
P. Spadon, *Italy*
D. Viterbo (*Chairman*), *Italy*

IUCr Monographs on Crystallography

- 1 *Accurate molecular structures*
A. Domenicano, I. Hargittai, editors
- 2 *P.P. Ewald and his dynamical theory of X-ray diffraction*
D.W.J. Cruickshank, H.J. Juretschke, N. Kato, editors
- 3 *Electron diffraction techniques, Vol. 1*
J.M. Cowley, editor
- 4 *Electron diffraction techniques, Vol. 2*
J.M. Cowley, editor
- 5 *The Rietveld method*
R.A. Young, editor
- 6 *Introduction to crystallographic statistics*
U. Shmueli, G.H. Weiss
- 7 *Crystallographic instrumentation*
L.A. Aslanov, G.V. Fetisov, J.A.K. Howard
- 8 *Direct phasing in crystallography*
C. Giacovazzo
- 9 *The weak hydrogen bond*
G.R. Desiraju, T. Steiner
- 10 *Defect and microstructure analysis by diffraction*
R.L. Snyder, J. Fiala and H.J. Bunge
- 11 *Dynamical theory of X-ray diffraction*
A. Authier
- 12 *The chemical bond in inorganic chemistry*
I.D. Brown
- 13 *Structure determination from powder diffraction data*
W.I.F. David, K. Shankland, L.B. McCusker, Ch. Baerlocher, editors

- 14 *Polymorphism in molecular crystals*
J. Bernstein
- 15 *Crystallography of modular materials*
G. Ferraris, E. Makovicky, S. Merlino
- 16 *Diffuse x-ray scattering and models of disorder*
T.R. Welberry
- 17 *Crystallography of the polymethylene chain: an inquiry into the structure of waxes*
D.L. Dorset
- 18 *Crystalline molecular complexes and compounds: structure and principles*
F. H. Herbst
- 19 *Molecular aggregation: structure analysis and molecular simulation of crystals and liquids*
A. Gavezzotti
- 20 *Aperiodic crystals: from modulated phases to quasicrystals*
T. Janssen, G. Chapuis, M. de Boissieu
- 21 *Incommensurate crystallography*
S. van Smaalen
- 22 *Structural crystallography of inorganic oxysalts*
S.V. Krivovichev
- 23 *The nature of the hydrogen bond: outline of a comprehensive hydrogen bond theory*
G. Gilli, P. Gilli
- 24 *Macromolecular crystallization and crystal perfection*
N.E. Chayen, J.R. Helliwell, E.H. Snell

IUCr Texts on Crystallography

- 1 *The solid state*
A. Guinier, R. Julien
- 4 *X-ray charge densities and chemical bonding*
P. Coppens
- 7 *Fundamentals of crystallography, second edition*
C. Giacovazzo, editor
- 8 *Crystal structure refinement: a crystallographer's guide to SHELXL*
P. Müller, editor
- 9 *Theories and techniques of crystal structure determination*
U. Shmueli
- 10 *Advanced structural inorganic chemistry*
Wai-Kee Li, Gong-Du Zhou, Thomas Mak
- 11 *Diffuse scattering and defect structure simulations: a cook book using the program DISCUS*
R. B. Neder, T. Proffen
- 12 *The basics of crystallography and diffraction, third edition*
C. Hammond
- 13 *Crystal structure analysis: principles and practice, second edition*
W. Clegg, editor
- 14 *Crystal structure analysis: a primer, third edition*
J.P. Glusker, K.N. Trueblood

Crystal Structure Analysis

A Primer

Third Edition

Jenny Pickworth Glusker

The Institute for Cancer Research, Fox Chase Cancer Center, Philadelphia

Kenneth N. Trueblood

University of California, Los Angeles

OXFORD
UNIVERSITY PRESS

OXFORD

UNIVERSITY PRESS

Great Clarendon Street, Oxford OX2 6DP

Oxford University Press is a department of the University of Oxford.
It furthers the University's objective of excellence in research, scholarship,
and education by publishing worldwide in

Oxford New York

Auckland Cape Town Dar es Salaam Hong Kong Karachi

Kuala Lumpur Madrid Melbourne Mexico City Nairobi

New Delhi Shanghai Taipei Toronto

With offices in

Argentina Austria Brazil Chile Czech Republic France Greece

Guatemala Hungary Italy Japan Poland Portugal Singapore

South Korea Switzerland Thailand Turkey Ukraine Vietnam

Oxford is a registered trade mark of Oxford University Press
in the UK and in certain other countries

Published in the United States

by Oxford University Press Inc., New York

© Jenny Pickworth Glusker and Kenneth N. Trueblood 2010

The moral rights of the authors have been asserted

Database right Oxford University Press (maker)

Third edition published 2010

All rights reserved. No part of this publication may be reproduced,
stored in a retrieval system, or transmitted, in any form or by any means,
without the prior permission in writing of Oxford University Press,
or as expressly permitted by law, or under terms agreed with the appropriate
reprographics rights organization. Enquiries concerning reproduction
outside the scope of the above should be sent to the Rights Department,
Oxford University Press, at the address above

You must not circulate this book in any other binding or cover
and you must impose the same condition on any acquirer

British Library Cataloguing in Publication Data

Data available

Library of Congress Cataloging in Publication Data

Glusker, Jenny Pickworth.

Crystal structure analysis : a primer / Jenny Pickworth Glusker, Kenneth N.
Trueblood. — 3rd ed.

p. cm.

ISBN 978-0-19-957635-7 1. X-ray crystallography. I. Trueblood, Kenneth N. II. Title.
QD945.G58 2010

548'.81—dc22

2010010910

Typeset by SPI Publisher Services, Pondicherry, India

Printed in Great Britain

on acid-free paper by

CPI Antony Rowe, Chippenham, Wiltshire

ISBN 978-0-19-957635-7 (Pbk)

ISBN 978-0-19-957634-0 (Hbk)

1 3 5 7 9 10 8 6 4 2

*To those who taught us crystallography,
most especially Dorothy Crowfoot Hodgkin,
A. Lindo Patterson, J. H. Sturdivant,
Robert B. Corey, and Verner Schomaker.*

Preface to the third edition

Our aim in this book is to explain how and why the detailed three-dimensional architecture of molecules can be determined from the diffraction patterns produced when X rays or neutrons are scattered by the atoms in single crystals. The diffraction pattern can be analyzed (by the methods described here in this book) to provide molecular structures of the components of the crystal and information on their interactions with each other. In the last 25 years, since the second edition was published, the experimental procedures for achieving molecular structure in this manner have greatly improved and computing facilities (expensive and mostly confined to scientific laboratories in the 1970s and 1980s) are now available to all. Larger and larger molecules can now be investigated at higher and higher resolutions and methods for solving the phase problem (which allow us to convert experimental diffraction data into a map of the material that did the scattering) are now much more efficient. Therefore we thought that it is time for an updated version of this book. We have not changed the overall scheme of the book, merely tried to bring it into the twenty-first century.

Sadly my coauthor, Ken Trueblood, died in May 1998—a big loss to X-ray crystallography. This book was the last scientific item he worked on. He strongly urged me to try hard not to increase the length of the book, and I have tried to comply with this request. It has, however, not been possible with this new edition to make full use of Ken's wisdom and insight. We have had a long history of collaboration since the early days when I was a graduate student in Dorothy Hodgkin's laboratory in Oxford working on the crystal structure of a vitamin B₁₂ derivative, and Ken was at UCLA programming the massive computer, SWAC, for crystallographic programs that tackled large structures. Several teaching examples in this book came from this collaboration across the miles between Los Angeles and Oxford.

This new edition has been improved by generous assistance from Dr. Peter Müller at MIT and Dr. Virginia Pett at the College of Wooster, Ohio. They both read the entire manuscript and made invaluable suggestions for improving it. I also wish to extend sincere thanks to Pat Bateman and Eileen Pytko for typing assistance and to Karen Albert, Carol Brock, Sue Byram, Bud Carrell, Bryan Craven, Dick Dickerson, Dave Duchamp, David Eisenberg, Debra Foster, Bob Hesse, Amy Katz, Bill Stallings, and Karen Trush. The staff at Oxford University Press have been most helpful, and my thanks go to Emma Lonie, April Warman, and Sonke Adlung. The copy-editor Douglas Meekison and the

illustrators at SPi Publishing also deserve thanks. Finally the National Institutes of Health (CA-10925 to JPG and CA-06927 to FCCC) provided the support through the years which made this book possible.

There are numerous additional sources of information now available for students of the subject (see the References and further reading section). These include the IUCr texts and monographs on crystallography listed at the beginning of the book, *International Tables for Crystallography* and the World Wide Web. The latter contains many examples of crystallography courses given at various universities and research organizations throughout the world. They often contain useful illustrations and some are interactive; unfortunately the identifying URLs of the sites of these teaching items do not seem to last with time so it is better for a student to use a search engine and define the specific subject of interest.

Finally my thanks to all of you who have provided me through the years with encouragement, counsel, and advice on the teaching of this subject.

Jenny P. Glusker
Philadelphia, Pennsylvania
March 2010

Preface to the second edition

In the thirteen years since the first edition of this book appeared there have been numerous advances in the practice of structural crystallography. Furthermore, many users of the first edition have suggested ways in which the book might have been improved. In this revision, we have endeavored to incorporate those suggestions and to describe the most significant advances in practice. The major changes include a considerable elaboration of the treatment of direct methods, a new chapter on anomalous dispersion and absolute configuration, a more detailed treatment of biological macromolecules, a reorganization and expansion into a separate chapter of the discussion of microcrystalline and non-crystalline materials, enlargement of the section on experimental methods to include discussion of area detectors and synchrotron radiation, and a new appendix on molecular geometry. The bibliography has been expanded by more than 50 percent, and the glossary doubled in length.

Our aim is to explain how and why the detailed three-dimensional architecture of molecules can be determined by an analysis of the diffraction patterns produced when X rays (or neutrons) are scattered by the atoms in single crystals. As with the first edition, the book is intended primarily for those who want to understand the fundamental concepts on which crystal structure determination is based without necessarily themselves becoming specialists in crystallography—an audience that includes advanced undergraduates who have studied some physics and chemistry, as well as graduate students and other research workers.

This book is divided, as before, into three parts; each has been expanded, the last two significantly. Part I, comprising the first four chapters, deals with the nature of the crystalline state, certain relevant facts about diffraction generally and diffraction by crystals in particular, and the experimental procedures used. Part II, consisting of Chapters 5 through 10, examines the problem of converting the experimentally obtained data (directions and intensities of diffracted beams) into a model of the atomic arrangement that scattered these beams—in other words, the problem of determining the approximate structure of this scattering matter, a “trial structure” suitable for refinement. Part III (Chapters 11 through 14) is concerned with techniques for refining this approximate structure to the degree warranted by the experimental

data and with discussions of the structural parameters and other information that can be derived from a careful structure determination. It also includes a discussion of microcrystalline materials and glasses, and an overall summary of the various stages in structure analysis.

We wish to thank those who have helped us in this endeavor, particularly Bill Stallings and John Stezowski, who read through our manuscript and made most helpful comments, and Jack Dunitz who helped us with the glossary. We are also grateful to Margaret J. Adams, Bob Bryan, Bud Carrell, Philip Coppens, Dick Dickerson, Jose Donnay, David Eisenberg, Doris Evans, Setsuo Kashino, Henry Katz, Lisa Keefe, Bill Parrish, Eileen Pytko, Miriam Rossi, Christopher Smart, Verner Schomaker and David Zacharias for their help. One of us (J.P.G.) acknowledges financial support from the National Institutes of Health, U.S.P.H.S. (grant CA-10925).

Finally, we appreciate the help of all of you who have encouraged us through the years with your comments and constructive criticisms.

Philadelphia
Los Angeles
April 1985

J.P.G.
K.N.T.

Preface to the first edition

This book, which developed from a talk to the California Association of Chemistry Teachers at Asilomar in 1966, is designed to serve as an introduction to the principles underlying structure analysis by X-ray diffraction from single crystals. It is intended both for undergraduates who have had some previous chemistry and physics and for graduate students and other research workers who do not intend to become specialists in crystallography but who want to understand the fundamental concepts on which this widely used method of structure determination is based. We have included many illustrations, with legends that form an important part of the text, a rather detailed glossary of common terms, an extensive annotated bibliography, and a list of the symbols used.

Our aim is to explain how and why the detailed three-dimensional architecture of molecules can be determined by an analysis of the diffraction patterns produced when X rays (or neutrons) are scattered by the atoms in single crystals. Part I, consisting of the first four chapters, deals with the nature of the crystalline state, certain relevant facts about diffraction generally and diffraction by crystals in particular, and, briefly the experimental procedures that are used. Part II comprises an examination of the problem of converting the experimentally obtained data (directions and intensities of diffracted beams) into a model of the atomic arrangement that scattered these beams, that is, the problem of determining the approximate structure of this scattering matter. Part III is concerned with techniques for refining this approximate structure to the degree warranted by the experimental data, and also includes a brief discussion of some of the auxiliary information, beyond the geometric details of the structure, that can be learned from modern structure analysis. Most mathematical details have been relegated to several Appendices.

We are indebted to D. Adzei Bekoe, Helen Berman, Herbert Bernstein, Carol Ann Casciato, Anne Chomyn, Joyce Dargay, David Eisenberg, Emily Maverick, Walter Orehowsky, Jr., Joel Sussman, and David E. Zacharias for their help in suggesting revisions of earlier drafts, and to all those writers on crystallography whose ideas and illustrations we have included here.

One of us (J.P.G.) acknowledges financial support from the National Institutes of Health, U.S.P.H.S. (grants CA-10925, CA-06927 and RR-05539), and an appropriation from the Commonwealth of

Pennsylvania. This book is Contribution No. 2609 from the Department of Chemistry, University of California, Los Angeles.

Finally, we want to express our gratitude to Miss Doris E. Emmott for her patient, painstaking, and precise typing of the manuscript and to Miss Leona Capeless of Oxford University Press for her help through the stages of publication.

Philadelphia
Los Angeles
April 1971

J.P.G.
K.N.T.

This page intentionally left blank

Contents

| | |
|---------------------------|-----|
| List of figures | xv |
| Symbols used in this book | xix |

PART I CRYSTALS AND DIFFRACTION

| | |
|-----------------------------|----|
| 1 Introduction | 3 |
| 2 Crystals | 9 |
| 3 Diffraction | 25 |
| 4 Experimental measurements | 46 |

PART II DIFFRACTION PATTERNS AND TRIAL STRUCTURES

| | |
|---|-----|
| 5 The diffraction pattern obtained | 71 |
| 6 The phase problem and electron-density maps | 86 |
| 7 Symmetry and space groups | 101 |
| 8 The derivation of trial structures. I. Analytical methods for direct phase determination | 115 |
| 9 The derivation of trial structures. II. Patterson, heavy-atom, and isomorphous replacement methods | 130 |
| 10 Anomalous scattering and absolute configuration | 151 |

PART III STRUCTURE REFINEMENT AND STRUCTURAL INFORMATION

| | |
|---|-----|
| 11 Refinement of the trial structure | 167 |
| 12 Structural parameters: Analysis of results | 181 |
| 13 Micro- and noncrystalline materials | 196 |
| 14 Outline of a crystal structure determination | 206 |

Appendices

| | | |
|-----------|---|------------|
| 1 | The determination of unit-cell constants and their use in ascertaining the contents of the unit cell | 216 |
| 2 | Some information about crystal systems and crystal lattices | 217 |
| 3 | The reciprocal lattice | 220 |
| 4 | The equivalence of diffraction by a crystal lattice and the Bragg equation | 222 |
| 5 | Some scattering data for X rays and neutrons | 225 |
| 6 | Proof that the phase difference on diffraction is $2\pi(hx + ky + lz)$ | 225 |
| 7 | The 230 space groups | 227 |
| 8 | The Patterson function | 228 |
| 9 | Vectors in a Patterson map | 231 |
| 10 | Isomorphous replacement (centrosymmetric structure) | 232 |
| 11 | Diffraction data showing anomalous scattering | 233 |
| 12 | Molecular geometry | 234 |
| | Glossary | 236 |
| | References and further reading | 259 |
| | Index of scientists referred to in the text | 271 |
| | Index | 273 |

List of figures

| | |
|---|----|
| 1.1. Analogies between light microscopy and X-ray diffraction | 5 |
| 1.2. A sinusoidal wave | 6 |
| 2.1. Crystals being grown by the vapor diffusion method | 12 |
| 2.2. Unit-cell axes | 14 |
| 2.3. An electron micrograph of a crystalline protein | 14 |
| 2.4. Indexing faces of a crystal | 15 |
| 2.5. The determination of the probable shape of the unit cell from interfacial angles in the crystal | 16 |
| 2.6. The crystal lattice and choices of unit cells | 18 |
| 2.7. The birefringence of calcite (Iceland spar) | 22 |
| 3.1. Diffraction patterns of single narrow slits | 27 |
| 3.2. Interference of two waves. Summation of waves | 28 |
| 3.3. Diffraction by a single slit | 30 |
| 3.4. Orders of diffraction | 31 |
| 3.5. Diffraction by two slits | 32 |
| 3.6. Diffraction patterns from equidistant parallel slits | 34 |
| 3.7. Diagrams of diffraction patterns from one- and two-dimensional arrays. Relation between the crystal lattice and reciprocal lattice | 36 |
| 3.8. X-ray diffraction photographs taken by the precession method | 37 |
| 3.9. The effect of different lattice samplings on the diffraction pattern | 39 |
| 3.10. The optical diffraction pattern of an array of templates resembling the skeleton of a phthalocyanine molecule | 40 |
| 3.11. Diagram of "reflection" of X rays by imaginary planes through points in the crystal lattice | 42 |
| 4.1. The diffraction experiment | 48 |
| 4.2. Mounting a crystal | 49 |
| 4.3. Centering a crystal | 50 |
| 4.4. The Ewald sphere (sphere of reflection) | 53 |
| 4.5. An X-ray tube | 54 |
| 4.6. Energy levels and X rays | 55 |

| | |
|---|-----|
| 4.7. Source, crystal, and detector | 58 |
| 4.8. The relation between the crystal orientation and the diffraction pattern | 58 |
| 4.9. The reciprocal lattice | 59 |
| 4.10. Layer lines | 59 |
| 4.11. Indexing a precession photograph | 60 |
| 4.12. An automatic diffractometer | 61 |
| 4.13. Wilson plot | 66 |
| 5.1. The representation of sinusoidal waves | 73 |
| 5.2. Vector representation of structure factors | 75 |
| 5.3. Atomic scattering factors | 77 |
| 5.4. Atomic-scattering-factor curves | 78 |
| 5.5. The meaning of “relative phase.” | 81 |
| 5.6. The relative phase angle on diffraction | 81 |
| 6.1. Scattered waves and their relative phases | 89 |
| 6.2. Fourier synthesis of the Bragg reflections from Figure 6.1 | 90 |
| 6.3. Summing Fourier transforms | 92 |
| 6.4. Overview of X-ray diffraction | 94 |
| 6.5. Comparison of electron-density maps when the phases are correct and when they are incorrect and random | 95 |
| 6.6. Different stages of resolution for a given crystal structure | 98 |
| 7.1. A four-fold rotation axis | 104 |
| 7.2. A mirror plane | 105 |
| 7.3. A two-fold screw axis | 107 |
| 7.4. A four-fold screw axis | 108 |
| 7.5. A glide plane | 108 |
| 7.6. Part of a page from <i>International Tables for X-Ray Crystallography</i> | 109 |
| 7.7. A structure that crystallizes in the space group $P2_12_12_1$ | 110 |
| 8.1. Summing density waves | 118 |
| 8.2. Aiming for nonnegative electron density | 119 |
| 8.3. X-ray scattering by point atoms and normal atoms | 120 |
| 8.4. Numerical use of Eqn. (8.2) to derive phases of a crystal structure | 122 |
| 8.5. An excerpt from an <i>E</i> -map | 124 |
| 8.6. A triple product in diffraction by hexamethylbenzene | 124 |
| 9.1. Peaks in a Patterson (vector) map | 131 |

| | |
|--|-----|
| 9.2. The calculation of a Patterson map for a one-dimensional structure | 133 |
| 9.3. The analysis of a Patterson map | 135 |
| 9.4. The vector superposition method | 136 |
| 9.5. A Patterson search by rotation | 139 |
| 9.6. Patterson projections for a cobalt compound in the space group $P2_12_12_1$ | 141 |
| 9.7. The heavy-atom method. A difference Patterson map | 142 |
| 9.8. The heavy-atom method | 143 |
| 9.9. Isomorphous replacement for a noncentrosymmetric structure | 146 |
| 9.10. Protein backbone fitting by computer-based interactive graphics | 147 |
| 9.11. Multiple Bragg reflections | 148 |
| 10.1. Absolute configurations | 152 |
| 10.2. Absorption of X rays of various wavelengths by a cobalt atom | 153 |
| 10.3. Phase change on anomalous scattering | 154 |
| 10.4. Path differences on anomalous scattering in a noncentrosymmetric structure | 156 |
| 10.5. Polarity sense of zinc blende | 158 |
| 10.6. Absolute configurations of biological molecules | 159 |
| 10.7. Effects of anomalous scattering on F values | 161 |
| 10.8. Isomorphous replacement plus anomalous scattering | 162 |
| 11.1. Fourier maps phased with partially incorrect trial structures | 168 |
| 11.2. Hydrogen atoms found from a difference map | 171 |
| 11.3. Refinement by difference maps | 172 |
| 12.1. Crystal structure of sodium chloride | 183 |
| 12.2. Crystal structure of iron pyrite | 183 |
| 12.3. Crystal structure of diamond | 184 |
| 12.4. Torsion angles | 184 |
| 12.5. Torsion angles in the isocitrate ion | 185 |
| 12.6. Crystal structure of benzene | 186 |
| 12.7. Anisotropic molecular motion | 188 |
| 12.8. Root-mean-square displacements at two different temperatures | 189 |
| 12.9. Libration | 190 |

| | |
|--|-----|
| 12.10. Projection of the neutron scattering density for crystalline benzene | 192 |
| 13.1. Radial distribution functions | 198 |
| 13.2. Some diffraction patterns of DNA and polynucleotides | 200 |
| 13.3. Powder diffraction | 204 |
| 14.1. The course of a structure determination by single-crystal X-ray diffraction | 208 |
| 14.2. The course of a structure determination by single-crystal X-ray diffraction | 209 |

Symbols used in this book

| | |
|--|--|
| A | Amplitude of a wave. |
| $A, B, A(hkl),$ $B(hkl), A_j B_j$ | Values of $ F \cos \alpha$ and $ F \sin \alpha$, respectively; that is, the components of a structure factor $F = A + iB$. The subscript j denotes the atom j . |
| $A', B', A'', B'', A_d,$ B_d | Values of A and B taking into account f' (to give A' and B'), f'' and f''' (to give A'' and B''), and the anomalously scattering atom (A_d and B_d). |
| Abs | Absorption factor. |
| a | The width of each of a series of (or single) diffracting slits. |
| a, b, c | Unit-cell axial lengths. |
| $\mathbf{a}, \mathbf{b}, \mathbf{c}$ | Unit-cell vectors of the direct lattice. |
| a^*, b^*, c^* | Lengths of the unit-cell edges of the reciprocal lattice. |
| $\mathbf{a}^*, \mathbf{b}^*, \mathbf{c}^*$ | Unit-cell vectors in reciprocal space. |
| a, b, c, n, d, g | Glide planes. The row parallel to the translation is designated; it is the side of the net (a , b , or c) or its diagonal (n in a primitive net, d in a centered net). In two dimensions, a glide-reflection line is represented by g . |
| B_{iso}, B | Isotropic atomic displacement (or temperature or vibration) parameter. |
| $b^{11}, b^{22}, b^{33}, b^{12},$ $b^{23}, b^{31}, b_{ij}, b_{11j}$ | Six anisotropic vibration parameters representing anisotropic temperature motion; a third subscript j denotes the atom j . |
| c_i, c_1, c_2, c_r | Wave amplitudes (see Chapter 5). |
| d | The distance between two diffracting slits. |
| d_{hkl}, d | The spacing between the lattice planes (hkl) in the crystal. |
| $d_{\text{A-B}}$ | Bond distance between atoms A and B. |
| E, E_{hkl}, E_H | Values of F corrected to remove thermal-motion and scattering-factor effects. These are called "normalized structure factors." |
| F | Face-centered lattice. |
| $F(hkl), F, F(000)$ | The structure factor for the unit cell, for the reflection hkl . It is the ratio of the amplitude of the wave scattered by the entire contents of the unit cell to that scattered by a single electron. A phase angle for the scattered wave is also involved. $F(000)$ is thus equal to the total number of electrons in the unit cell. |
| $ F(hkl) , F $ | The amplitude of the structure factor for hkl with no phase implied. |
| $ F_o , F_c $ | Amplitudes of structure factors observed ($ F_o $), that is, derived from measurements of the intensity of the diffracted beam, and calculated ($ F_c $) from a postulated trial structure. |

| | |
|--|--|
| $F_P, F_{PH1}, F_{PH2}, F_{H1}, F_{H2}, F_M, F_{M'}, F_R, F_T, F_{T'}$ | Structure factors for a given value of hkl for a protein (P), two heavy-atom derivatives ($PH1$ and $PH2$), the parts of F due to certain atoms ($M, M', H1$ and $H2$) and the rest of the molecule (R), and for the total structure (T and T'). |
| F | Structure factor when represented as a vector. |
| F_{novib} | Value of F for a structure containing only nonvibrating atoms. |
| F_+, F_- | Values of $F(hkl)$ and $F(\bar{h}\bar{k}\bar{l})$ when anomalous-dispersion effects are measurable. |
| $f(hkl), f, f_j$ | Atomic scattering factor, also called atomic form factor, for the hkl reflection relative to the scattering by a single electron. The subscript j denotes atom j . |
| f', f'' | When an anomalous scatterer is present the value of f is replaced by $(f + f') + if''$. |
| $G(r)$ | Radial distribution function. |
| G, H | Values of A and B with the scattering factor contribution $(f + f' + f'')$ removed (see Chapter 10). |
| H | Reciprocal lattice vector. |
| H, K | Indices of two Bragg reflections. $H = h, k, l$; $K = h', k', l'$. |
| $hkl, -h, -k, -l, \bar{h}\bar{k}\bar{l}, hkil$ | Indices of the Bragg reflection from a set of parallel planes; also the coordinates of a reciprocal lattice point. If h, k , or l are negative they are represented as $-h, -k, -l$ or $\bar{h}\bar{k}\bar{l}$. In hexagonal systems a fourth index, $i = -(h + k)$, may be used (see Appendix 2). |
| (hkl) | Indices of a crystal face, or of a single plane, or of a set of parallel planes. |
| I | Body-centered lattice. |
| $I(hkl), I$ | Intensity (on an arbitrary scale) for each reflection. |
| I_{corr} | Value of I corrected for Lp and Abs. |
| i | An "imaginary number," $i = \sqrt{-1}$ |
| i, j | Any integers. |
| Lp | Lorentz and polarization factors. These are factors that are used to correct values of I for the geometric conditions of their measurement |
| l | The distance between two points in the unit cell (e.g., bond length). |
| l | A direction cosine. |
| M | Molecular weight of a compound. |
| M_1, M_2, M, M' | Atoms or groups of atoms that are interchanged during the preparation of an isomorphous pair of crystals. Heavy atoms substituted in a protein, P . |
| m | Mirror planes. |
| N | The number of X-ray reflections observed for a structure. |
| N_{Avog} | Avogadro's number. The number of molecules in the molecular weight in grams, 6.02×10^{23} . |
| n | Any integer. Used for n -fold rotation axes. Also used as a general constant. |
| n_r | Screw axis designations, where n and r are integers (2, 3, 4, 6 and 1, ..., $(n - 1)$, respectively). |
| $P, PH1, PH2$ | Protein (P), also heavy-atom derivatives $PH1$ and $PH2$. |
| $P(uvw), P, P_s(uvw)$ | The Patterson function, evaluated at points of u, v, w in the unit cell. The $P_s(uvw)$ function is used with anomalous-dispersion data (see Chapter 10). |

| | |
|--|--|
| P, A, B, C, F, I | Lattice symbols. Primitive (P), centered on one set of faces (A, B, C), or all faces (F) of the unit cell, or body-centered (I). |
| P_+ | Probability that a triple product is positive (see Eqns. 8.6 and 8.7). |
| p, q | Path differences. |
| Q | The quantity minimized in a least-squares calculation. |
| R | Discrepancy index $R = \frac{\sum (F_o - F_c)}{ F_o }$. Also called R factor, R value, or residual. |
| R/S | System of Cahn and Ingold for describing the absolute configuration of a chiral molecule. |
| r | The distance on a radial distribution function. |
| $s(hkl)$ | The sign of the reflection hkl for a centrosymmetric structure. |
| t | Crystal thickness. |
| U^{11}, U^{ii}, U^{ij} | Anisotropic vibration parameters. |
| $\langle u^2 \rangle$ | Mean square amplitude of atomic vibration. |
| u, v, w | The coordinates of any one of a series of systematically spaced points, expressed as fractions of a, b , and c , in the unit cell for a Patterson (or similar) function. |
| V_c, V, V^* | The unit-cell volume in direct and reciprocal space. |
| V_M | Matthews coefficient, volume on \AA^3 per dalton of protein. |
| $w(hkl)$ | The weight of an observation in a least-squares refinement. |
| X, Y, Z | Cartesian coordinates for atomic positions. |
| $x, y, z; x_j, y_j, z_j;$ x, y, z, u | Atomic coordinates as fractions of a, b , and c . The subscript j denotes the atom under consideration. If the system is hexagonal a fourth coordinate, u , may be added (see Appendix 2). |
| x_1, x_2, x_j, x_r | Displacements of a wave at a given point. The waves are each designated 1, 2, j ; r is the resultant wave from the summation of several waves. |
| x, y, z | Coordinates of any one of a series of systematically spaced points, expressed as fractions of a, b, c filling the unit cell at regular intervals. |
| Z | Number of molecules in a unit cell. |
| Z_i, Z_j | The atomic number (total number of diffracting electrons) of atoms i and j . |
| α, β, γ | Interaxial angles between \mathbf{b} and \mathbf{c} , \mathbf{a} and \mathbf{c} , and \mathbf{a} and \mathbf{b} , respectively (alpha, beta, gamma). |
| $\alpha^*, \beta^*, \gamma^*$ | Interaxial angles in reciprocal space. |
| $\alpha(hkl), \alpha, \alpha_M, \alpha_P,$ α_H | Phase angle of the structure factor for the reflection hkl . $\alpha = \tan^{-1}(B/A)$. |
| $\alpha_1, \alpha_2, \alpha_j, \alpha_r$ | Phases of waves 1, 2, j , and r , the resultant of the summation of waves, relative to an arbitrary origin. |
| $\Delta F $ | The difference in the amplitudes of the observed and calculated structure factors, $ F_o - F_c $ (delta $ F $). |
| $\Delta\rho$ | Difference electron density. |
| δ | Interbond angle. |
| δ_{ij} | An index that is 1 when $i = j$ and 0 elsewhere; i and j are integers (delta). |

| | |
|--|--|
| ε | Epsilon factor used in calculating normalized structure factors (see Glossary). |
| θ, θ_{hkl} | The glancing angle (complement of the angle of incidence) of the X-ray beam to the "reflecting plane." 2θ is the deviation of the diffracted beam from the direct X-ray beam (two theta). |
| κ | A device for aligning the crystal and detector in a diffractometer that utilizes κ geometry (Figure 4.12) (kappa). |
| λ | Wavelength, usually that of the radiation used in the diffraction experiment (lambda). |
| μ/ρ | Mass absorption coefficient. μ , linear absorption coefficient; ρ , density. |
| $\rho(xyz), \rho_{\text{obs}}, \rho_{\text{calc}}$ | Electron density, expressed as number of electrons per unit volume, at the point x, y, z in the unit cell (rho). |
| Σ | Summation sign (sigma). |
| Σ_1, Σ_2 | Listing of triple products of normalized structure factors (see Chapter 8). |
| τ | Torsion angle. |
| ϕ | An angular variable, proportional to the time, for a traveling wave. It is of the form $2\pi\nu t$, where ν is a frequency and t is the time (phi). |
| ϕ | Angle on spindle axis of goniometer head. See diffractometer (Figure 4.12). |
| ϕ_H | The phase angle of the structure factor of the Bragg reflection H . |
| χ | Angle between ϕ axis and diffractometer axis (see Figure 4.12) (chi). |
| ψ | Angle incident beam makes with lattice rows (see Appendix 4) (psi). |
| ω | Angle between diffraction vector and plane of χ circle on diffractometer (Figure 4.12) (omega). |
| $\langle \rangle$ | The mean value of a quantity. |
| 1, 2, 3, 4, 6 | Rotation axes. |
| $\bar{1}, \bar{2}, \bar{3}, \bar{4}, \bar{6}$ | Rotatory-inversion axes. |
| $2_1, 4_1, 4_2, 4_3$ | Screw axes n_r . |

CRYSTALS AND DIFFRACTION

**Part
I**

This page intentionally left blank

Introduction

1

Much of our present knowledge of the architecture of molecules has been obtained from studies of the diffraction of X rays or neutrons by crystals. X rays* are scattered by the electrons of atoms and ions, and the interference between the X rays scattered by the different atoms or ions in a crystal can result in a diffraction pattern. Similarly, neutrons are scattered by the nuclei of atoms. Measurements on a crystal diffraction pattern can lead to information on the arrangement of atoms or ions within the crystal. This is the experimental technique to be described in this book.

X-ray diffraction was first used to establish the three-dimensional arrangement of atoms in a crystal by William Lawrence Bragg in 1913 (Bragg, 1913), shortly after Wilhelm Conrad Röntgen had discovered X rays and Max von Laue had shown in 1912 that these X rays could be diffracted by crystals (Röntgen, 1895; Friedrich et al., 1912). Later, in 1927 and 1936 respectively, it was also shown that electrons and neutrons could be diffracted by crystals (Davisson and Germer, 1927; von Halban and Preiswerk, 1936; Mitchell and Powers, 1936). Bragg found from X-ray diffraction studies that, in crystals of sodium chloride, each sodium is surrounded by six equidistant chlorines and each chlorine by six equidistant sodiums. No discrete molecules of NaCl were found and therefore Bragg surmised that the crystal consisted of sodium ions and chloride ions rather than individual (noncharged) atoms (Bragg, 1913); this had been predicted earlier by William Barlow and William Jackson Pope (Barlow and Pope, 1907), but had not, prior to the research of the Braggs, been demonstrated experimentally. A decade and a half later, in 1928, Kathleen Lonsdale used X-ray diffraction methods to show that the benzene ring is a flat regular hexagon in which all carbon-carbon bonds are equal in length, rather than a ring structure that contains alternating single and double bonds (Lonsdale, 1928). Her experimental result, later confirmed by spectroscopic studies (Stoicheff, 1954), was of great significance in chemistry. Since then X-ray and neutron diffraction have served to establish detailed features of the molecular structure of every kind of crystalline chemical species, from the simplest to those containing many thousands of atoms.

We address ourselves here to those concerned with or interested in structural aspects of chemistry and biology who wish to know how

* "X ray" for a noun, "X-ray" for an adjective.

crystal diffraction methods can be made to reveal the underlying three-dimensional structure within a crystal and how the results of such structure determinations may be critically assessed. In order to explain why molecular structure can be determined by single-crystal diffraction of X rays or neutrons, we shall try to answer several questions: Why use crystals and not liquids or gases? Why use X rays or neutrons and not other types of radiation? What experimental measurements are needed? What are the stages of a typical structure determination? How are the structures of macromolecules such as proteins and viruses determined? Why is the process of structure analysis sometimes lengthy and complex? Why is it necessary to “refine” the approximate structure that is first obtained? How can one assess the reliability of a crystal structure analysis?

This book should be regarded not as an account of “how to do it” or of practical procedural details, but rather as an effort to explain “why it is possible to do it.” We aim to give an account of the underlying physical principles and of the kinds of experiments and methods of handling the experimental data that make this approach to molecular structure determination such a powerful and fruitful one. Practitioners are urged to look elsewhere for details.

The primary aim of a crystal structure analysis by X-ray or neutron diffraction is to obtain a detailed three-dimensional picture of the contents of the crystal at the atomic level, as if one had viewed it through an extremely powerful microscope. Once this information is available, and the positions of the individual atoms are therefore known precisely, one can calculate interatomic distances, bond angles, and other features of the molecular geometry that are of interest, such as the planarity of a particular group of atoms, the angles between planes, and conformation angles around bonds. Frequently the resulting three-dimensional representation of the atomic contents of the crystal establishes a structural formula and geometrical details hitherto completely unknown. Such information is of great interest to chemists, biochemists, and molecular biologists who are interested in the relation of structural features to chemical and biological effects. Furthermore, precise molecular dimensions (and information about molecular packing, molecular motion in the crystal, and molecular charge distribution) may be obtained by this method. These results expand our understanding of electronic structure, molecular strain, and the interactions between molecules.

Atoms and molecules are very small and therefore an extensive magnification is required to visualize them. The usual way to view a very small object is to use a lens, or, if even higher magnification is required, an optical or electron microscope. Light scattered by the object that we are viewing is recombined by the lens system of the microscope to give an image of the scattering matter, appropriately magnified, as shown in Figure 1.1a. This will be discussed and illustrated later, in Chapter 3. What is important is how the various scattered light waves interact with each other, that is, the overall relationship between the relative phases** of the various scattered waves (defined

** Relative phases (discussed in Chapter 3) describe the relationships between the various locations of peaks and troughs of a series of sinusoidal wave motions. They are described as “relative” phases because they are measured with respect to a fixed point in space, such as but not necessarily the selected origin of the unit cell.

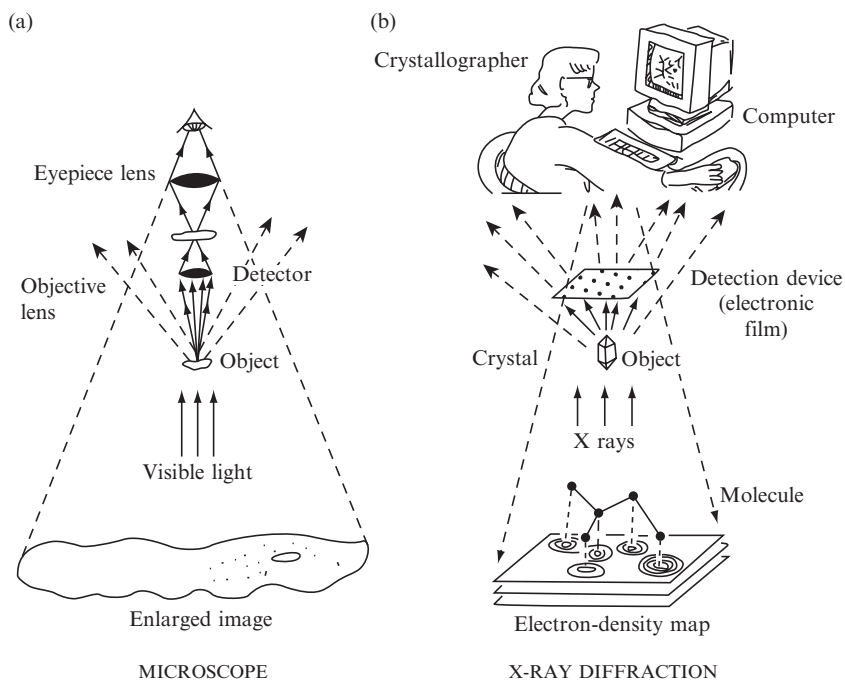


Fig. 1.1 Analogies between light microscopy and X-ray diffraction. Analogies between the two methods of using scattered radiation for determining structure are shown here—optical microscopy on the left, X-ray diffraction on the right. The sample that is under study in both instruments scatters some of the incident radiation and this gives a diffraction pattern.

- (a) In the ordinary optical microscope there are two lenses. The lower objective lens gathers light that has been scattered by the object under study and focuses and magnifies it. The eyepiece or ocular lens, which is the one we look through, increases this magnification. There is no need to record a diffraction pattern because the light that is scattered by the object under examination is focused by these lenses and gives a magnified image of that object. The closer the objective lens is to the object, the wider the angle through which scattered radiation is caught by this lens and focused to form a high-resolution image. The rest of the radiation is lost to the surroundings.
- (b) With X rays the diffraction pattern has to be recorded electronically or photographically, because X rays cannot (at this time) be focused by any known lens system. Therefore the recombination of the diffracted beams (which is done by an objective lens in the optical microscope) must, when X rays are used, be done mathematically by a crystallographer with the aid of a computer. As stressed later (Chapter 5), this recombination cannot be done directly, because the phase relations among the different diffracted beams cannot usually be measured directly. However, once these phases have been derived, deduced, guessed, or measured indirectly, an image can be constructed of the scattering matter that caused diffraction—the electron density in the crystal.

in Figure 1.2); this is because, when two scattered waves proceed in the same direction, the intensity of the combined wave will depend on the difference in the phases of the two scattered beams. If they are “in phase” they will enhance each other and give an intense beam, but if they are “out of phase” they will destroy each other and there will be no apparent diffracted beam. Generally it is found that such enhancement or destruction is only partial, so that the diffracted beams have some intensity and the diffraction pattern that is obtained contains diffracted beams that have differing intensities—some are weak and some are intense.

In an optical microscope, that is, a microscope that uses light that is visible to the human eye, the radiation scattered by the object is

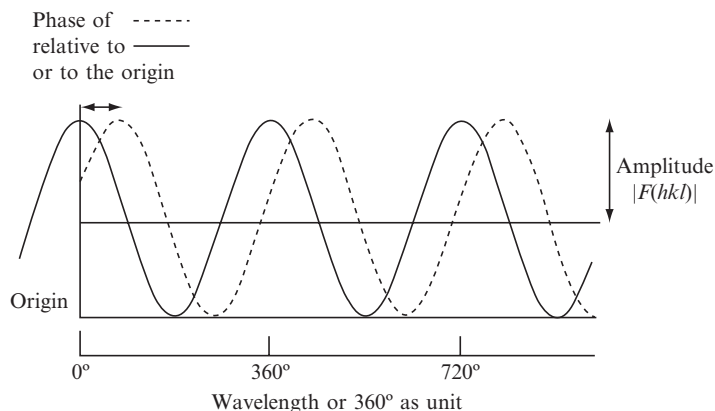


Fig. 1.2 A sinusoidal wave.

A sinusoidal wave, showing its amplitude, phase relative to the origin, and wavelength. Sine and cosine functions are sinusoidal waves with different phases [$\cos x = \sin(x + \pi/2)$ when the distance traveled is measured in radians]. Shown is a cosine wave (black line), which has a peak at the wave origin. This wave origin coincides with the origin in space that has been selected by the crystallographer. A second wave (dashed line) has its peak in a different location. The distance between these two peaks defines their “relative phase.”

recombined by the lens system (the objective lens) so that a magnified image of the object under study is obtained (Figure 1.1a). Light flows through and beyond the lens system of the microscope in such a way that the relationships between the phases of the scattered waves are maintained, even after these waves have been recombined by the second lens (the eyepiece lens). In a similar way, X rays are scattered by the electrons in atoms and ions (Figure 1.1b), but, in contrast to the situation with visible light, these scattered X rays cannot be focused by any presently known experimental techniques. This is because no electric or magnetic field or material has yet been found that can refract X rays sufficiently to give a practicable X-ray lens. Therefore an X-ray microscope cannot yet be used to view atoms (which have dimensions too small to permit them to be visible with an ordinary light microscope). Much research on a possible X-ray lens is currently in progress (see Shapiro et al., 2005; Sayre, 2008). The information obtained from an X-ray diffraction experiment, however, is three-dimensional, and therefore the great usefulness of this method will doubtless continue after an X-ray lens can be made.

Since a lens system cannot be used to recombine scattered X rays to obtain images at atomic resolution, some other technique must be used if one wishes to view molecules. In practice, the diffracted (scattered) X rays or neutrons are intercepted and measured by a detecting system, but this means that the relationships between the phases of the scattered waves are lost; only the intensities (not the relative phases) of the diffracted waves can be measured. If the values of the phases of the diffracted beams were known, it would be possible to combine them with the experimental measurements of the diffraction pattern

and *simulate the recombination of the scattered radiation*—just as if a lens had done it—by an appropriate, though complicated, calculation (done by a crystallographer and a computer in Figure 1.1b). Then we would have an electron-density map, that is, an image of the material that had scattered the X rays. This mathematical calculation, the *Fourier synthesis* of the pattern of scattered or “diffracted” radiation (Fourier, 1822; Porter, 1906; Bragg, 1915), is a method for summing sinusoidal waves in order to obtain a representation of the material that scattered the radiation. Such a Fourier synthesis is a fundamental step in crystal structure determination by diffraction methods and is a central subject of our discussion (described in detail in Chapters 5, 6, 8, and 9). The difficult part of correctly summing these sinusoidal waves is termed the “phase problem,” that is, finding where the peaks of each sinusoidal wave should lie with respect to the others in the summation. Any of several methods (to be described) can be used to overcome this difficulty and determine the phases of the various diffracted beams with respect to each other. When the correct phases are known (that is, derived, deduced, guessed, or measured indirectly), the three-dimensional structure of the atomic contents of the crystal (and hence of the molecules or ions that it contains) will be revealed as a result of a Fourier synthesis.

Why make the effort to carry out a crystal structure analysis? The reason is that when the method is successful, it is unique in providing an unambiguous and complete *three-dimensional representation of the atoms in the crystal*. This three-dimensionality is incredibly useful because chemical and biological reactions occur in three dimensions, not two; surface and internal structures of molecules, plus information on their interactions with other molecules, are revealed by this powerful technology. Other experimental methods can also provide structural information. For example, large molecules, such as those of viruses, can also be visualized by use of an electron microscope, but individual atoms deep inside each virus molecule cannot currently be distinguished. Newer technologies such as field ion microscopy and scanning tunneling microscopy (or atomic force microscopy) are now providing views of molecules on the surfaces of materials, but they also do not provide the detailed and precise information about the internal structure of larger molecules that X-ray and neutron diffraction studies do. Infrared and microwave spectroscopic techniques give quantitative structural information for simple molecules. High-field nuclear magnetic resonance (NMR), the main alternative method currently used for structure determination, can also provide distances between identified atoms and can be used to study fairly large molecules. No other method can, however, give the entire detailed three-dimensional picture that X-ray and neutron diffraction techniques can produce.

Crystal diffraction methods do, however, have their limitations, chiefly connected with obtaining samples with the highly regular long-range three-dimensional order characteristic of the ideal crystalline

state. The success of high-resolution diffraction analysis requires that the sample be prepared as an ordered array (e.g., a crystal). Molecular motion or static disorder within the regular array of molecules in a crystal may result in a time-averaged or space-averaged representation of the molecular structure. Freedom of molecular motion is, in general, much more restricted in solids than it is in liquids or gases. Even in solids, however, both overall and intramolecular motion can be appreciable, and precise diffraction data may reveal enlightening information about atomic and molecular motion.

When a crystal structure analysis by diffraction methods is completed, a wealth of information results. It reveals the shapes of molecules and the way they interact, and gives geometrical data for each. The method can be adapted to a wide range of temperatures, pressures, and environments and has been successfully used to establish the molecular architecture and packing of an enormous diversity of substances, from elementary hydrogen and simple salts to molecules such as buckminsterfullerene and to proteins and nucleic acids and their assemblages in viruses and other cellular structures. X-ray diffraction methods have also contributed significantly to our understanding of natural and synthetic partially crystalline materials such as polyethylene and fibers of DNA. Although structure determinations of organic and biochemically significant molecules have received the most attention in recent years, the contributions of the technique to inorganic chemistry have been equally profound, initially through the clarification of the chemistry of the silicates and of other chemical mysteries of minerals and inorganic solids, and then with applications to such diverse materials as the boron hydrides, alloys, hydrates, compounds of the rare gases, and metal-cluster compounds.

Throughout the book you may encounter symbols or terms that are unfamiliar, such as d_{010} or d_{110} in Figure 2.5. We have included a list of symbols at the start, and a glossary (to provide definitions of such symbols and words) and a list of references at the end of the book. We urge you to use all of these sections frequently as you work your way through the book.

Crystals

2

The elegance and beauty of crystals have always been a source of delight. What is a crystal? *A crystal is defined as a solid that contains a very high degree of long-range three-dimensional internal order of the component atoms, molecules, or ions.* This implies a repetitious internal organization, at least ideally.* By contrast, the internal organization of atoms and ions within a noncrystalline material is totally random, and the material is described as “amorphous.” Studies of crystal morphology, that is, of the external features of crystals, have been made since early times, particularly by those interested in minerals (for practical as well as esthetic reasons) (Groth, 1906–1919; Burke, 1966; Schneer, 1977).

It was Max von Laue who realized in 1912 that this internal regularity of crystals gave them a grating-like quality so that they should be able to diffract electromagnetic radiation of an appropriate wavelength. From Avogadro’s number (6.02×10^{23} , the number of molecules in the molecular weight in grams of a compound) and the volume that this one “gram molecule” of material fills, von Laue was able to reason that distances between atoms or ions in a crystal were of the order of 10^{-9} to 10^{-10} m (now described as 10 to 1 Å).** A big debate at that time was whether X rays were particles or waves. If X rays were found to be wavelike (rather than particle-like), von Laue estimated they would have wavelengths of this same order of magnitude, 10^{-9} to 10^{-10} m. Therefore, since diffraction was viewed as a property of waves rather than particles, von Laue urged Walther Friedrich and Paul Knipping to test if X rays could be diffracted by crystals. Their resulting diffraction experiment was dramatically successful. The crystal, because of its internal regularity, had indeed acted as a diffraction grating. This experiment was therefore considered to have demonstrated that X rays have wavelike properties (Friedrich et al., 1912). We now know that particles, such as neutrons or electrons, can also be diffracted. The X-ray diffraction experiment in 1912 was, in spite of this later finding, highly significant because it led to an extremely useful technique for the study of molecular structure. An analysis of the X-ray diffraction pattern of a crystal, by the methods to be described in this book, will give precise geometrical information on the molecules and ions that comprise the crystal.

The most obvious external characteristic of a crystal is that it has flat faces bounded by straight edges, but this property is not necessary

* Real crystals often exhibit a variety of imperfections—for example, short-range or long-range disorder, dislocations, irregular surfaces, twinning, and other kinds of defects—but, for our present purposes, it is a good approximation to consider that in a specimen of a single crystal the order is perfect and three-dimensional. We discuss very briefly in Chapter 13 the way in which our discussion must be modified when some disorder is present—for example, when the order is only one-dimensional, as in many fibers.

** Crystallographic interatomic distances are usually listed in Å. $1 \text{ Å} = 10^{-8} \text{ cm} = 10^{-10} \text{ m}$.

or sufficient to define a crystal. Glass and plastic, neither of which is crystalline, can be cut and polished so that they have faces that are flat with straight edges. However, they have not been made crystalline by the polishing, because their disordered internal structures have not been made regular (even though the word “crystal” is often used for some quality glassware). Therefore the presence of flat faces or straight edges in a material does not necessarily indicate that it is crystalline. It is the internal order, rather than external appearance, that defines a crystal. One way to check whether or not this internal order is present is to examine the diffraction pattern obtained when the material is targeted by a beam of X rays; the extent of the crystallinity (that is, the quality of its regular internal repetition) will be evident in any diffraction pattern obtained.

The fact that crystals have an internal structure that is periodic (regularly repeating) in three dimensions has long been known. It was surmised by Johannes Kepler, who wrote about the six-cornered snowflake, and by Robert Hooke, who published some of the earliest pictures of crystals viewed under a microscope (Kepler, 1611; Hooke, 1665; Bentley, 1931). They both speculated that crystals are built up from an ordered packing of roughly spheroidal particles. The Danish physician Nicolaus Steno (Niels Stensen) noted that although the faces of a crystalline substance often varied greatly in shape and size (depending on the conditions under which the crystals were formed), the angles between certain pairs of faces were always the same (Steno, 1669). From this observation Steno and Jean Baptiste Louis Romé de Lisle postulated the “Law of Constancy of Interfacial Angles” (Romé de Lisle, 1772). Such angles between specific faces of a crystal can be measured approximately with a protractor or more precisely with an optical goniometer (Greek: *gonia* = angle), and a great many highly precise measurements of the interfacial angles in crystals have been recorded over the past three centuries. This constancy of the interfacial angles for a given crystalline form of a substance is a result of its internal regularity (its molecular or ionic packing) and has been used with success as an aid in characterizing and identifying compounds in the old science of “pharmacognosy.” Investigations of crystal form were carried out further by Torbern Olof Bergman in 1773 and René Just Haüy in 1782; they concluded independently, as a result of studies of crystals that had cleaved into small pieces when accidentally dropped, that crystals could be considered to be built up of building bricks of specific sizes and shapes for the particular crystal. These ideas led to the concept of the “unit cell,” the basic building block of crystals (Bergman, 1773; Haüy, 1784; Burke, 1966; Lima-de-Faria, 1990).

Obtaining and growing crystals

The growth of crystals is a fascinating experimental exercise that the reader is urged to try (Holden and Singer, 1960; McPherson, 1982;

Ducruix and Giegé, 1999; Bergfors, 2009). Considerable perseverance and patience are necessary, but the better the quality of the crystal the more precise the resulting crystal structure. Generally crystals are grown from solution, but other methods that can be used involve cooling molten material or sublimation of material onto a surface.

In order to obtain crystals from solution it is necessary to dissolve the required substance (the solute) in a suitable solvent until it is near its saturation point, and then increase the concentration of the solute in the solution by slowly evaporating or otherwise removing solvent. This provides a saturated or supersaturated solution from which material will separate, and the aim is to make this separation occur in the form of crystals. During the growth process, solute molecules meet in solution and form small aggregates, a process referred to as “nucleation.” Extraneous foreign particles (such as those from a person’s beard or hair, or “seeds,” or dust) may serve as initiators of such nucleation. More molecules are then laid down on the surface of this nucleus, and eventually a crystal may separate from the solution. Crystal growth will continue until the concentration of the material being crystallized falls below the saturation point:

Saturated solution → Supersaturation → Nucleation → Crystal growth

The crystallization process is essentially a controlled precipitation onto an appropriate nucleation site. If growth conditions are achieved too quickly, many nucleation sites may form and crystals may be smaller than those obtained under slower crystallization conditions. If too few nucleation sites form, crystals may not grow. Crystal habit (overall shape) may be modified by the addition of soluble foreign materials to the crystallization solution. These added molecules may bind to growing crystal faces and inhibit their growth. As a result, different sets of crystal faces may become more prominent.

When a molecule or ion approaches a growing crystal, it will form more interactions than otherwise if it can bind at a step in the formation of layers of molecules in the crystal. Various irregularities or defects (dislocations) in the internal order of stacking can facilitate the formation of steps and therefore aid in the crystallization process. Most real crystals are not perfect; that is, the regularity of packing of molecules may not be exact. In general, they tend to be composed of small blocks of precisely aligned unit cells (domains) that may each be slightly misaligned with respect to each other. The extent to which this occurs is referred to as the “mosaicity” of the crystal, and its measurement indicates the degree of long-range crystalline order (regularity) in the crystal under study. Most real crystals are described as “ideally imperfect” if they have a mosaic structure composed of slightly misoriented very small crystal domains.

Several of the methods that are now used to facilitate the growth of crystals involve changing the experimental conditions so that

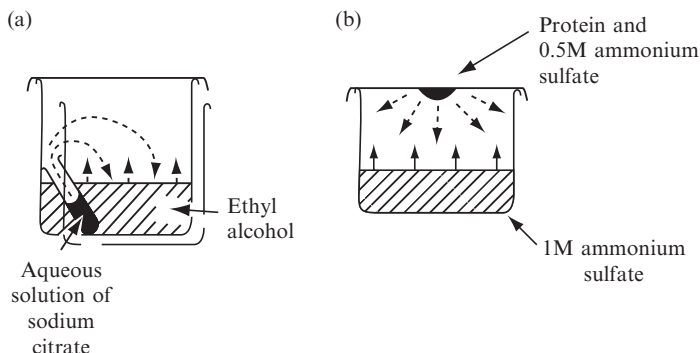


Fig. 2.1 Crystals being grown by the vapor diffusion method.

- (a) The sample (sodium citrate) to be crystallized is soluble in water but is not very soluble in ethyl alcohol. A test tube containing sodium citrate dissolved in water is sealed in a beaker containing ethyl alcohol. An equilibrium between the two liquids is then approached. Vapor phase diffusion of the water molecules from the test tube into the larger volume in the reservoir and of alcohol into the smaller volume in the test tube takes place. The result is that crystals separate out in the test tube as the solution in it becomes more concentrated and the alcohol helps the citrate to separate out.
- (b) Pure protein is usually available only in limited quantities and therefore the following scheme has been adopted to circumvent this problem. A drop of protein solution is placed on a cover slip, which is sealed with grease over a container (a beaker or one of the many small wells in a biological culture tray). In this sealed system, the protein drop contains precipitant at a concentration below the point at which protein precipitation would be expected; the sealed container (the well) contains a much larger volume of precipitant at or slightly above the concentration of the precipitation point of the protein. Water evaporates slowly from the protein-containing drop into the container until the concentration of precipitant in the hanging drop is the same as that in the well, and crystallization may occur. This method works best for a protein if it is highly purified.

saturation of the solution will be exceeded, generally by a slow precipitation method (see Figure 2.1). In one method, a precipitant (that is, a liquid or solution of a compound in which the substance is insoluble) is layered on a solution of the material to be crystallized. For example, alcohol, acting as a precipitant, when carefully layered on top of a saturated aqueous solution of sodium citrate and left for a day or so, will generally give good diffraction-quality crystals. Alternatively, some of the solvent may be slowly removed from the solution by equilibration through the vapor phase in a closed system, thereby increasing the concentration of the material being crystallized. This can be done, as shown in Figure 2.1a, with an aqueous solution of sodium citrate in a test tube, placed in a covered beaker containing ethyl alcohol alone; equilibration of the solvents in this sealed container will (hopefully) then cause the formation of crystals. This vapor diffusion method is also used for macromolecules. An aqueous solution of the protein, together with a precipitant (a salt such as ammonium sulfate, or an alcohol such as methylpentanediol) in the same solution but at a concentration below

that which will cause precipitation, is put in a dish, or suspended as a droplet on a microscope slide, in a sealed container. Then another, more concentrated, precipitant solution is placed at the bottom of the same sealed container (Figure 2.1b). Water will be transferred through the vapor phase from the solution that is less concentrated in the precipitant (but containing protein) to that which is more concentrated (but lacking protein). The result is a loss of water from the suspended droplet containing protein. As the precipitation point of the protein is reached in the course of this dehydration, factors such as pH, temperature, ionic strength, and choice of buffer will control whether the protein will separate from the solution as a crystal or as an amorphous precipitate.

In summary, the main factors affecting the growth of good crystals are an appropriate choice of solvent, suitable generation of nucleation sites, control of the rate of crystal growth, and a lack of any disturbance of the crystallization system (see Chayen, 2005). In practice the equipment for doing this is now increasingly sophisticated, and often, for macromolecules, a robot setup is used that provides a wide variety of conditions for crystallization (Snook et al., 2000). For example, it has been found that protein crystallization may be more successful on space shuttles, where gravity is reduced (DeLucas et al., 1999). The components do not then separate as quickly and fluid flow at the site of crystallization is reduced.

Crystals suitable for modern single-crystal diffraction need not be large. For X-ray work, specimens with dimensions of 0.2 to 0.4 mm or less on an edge are usually appropriate. Such a crystal normally weighs only a small fraction of a milligram and, unless there is radiation damage or crystal deterioration during X-ray exposure, can be reclaimed intact at the end of the experiment. Larger crystals are needed for neutron diffraction studies, although this requirement is becoming less strict as better sources of neutrons become available.

Sometimes a crystal is difficult to prepare or is unstable under ordinary conditions. It may react with oxygen or water vapor, or may effloresce (that is, lose solvent of crystallization and form a noncrystalline powder) or deliquesce (that is, take up water from the atmosphere and eventually form a solution). Many crystals of biologically interesting materials are unstable unless the relative humidity is extremely high; since such crystals contain a high proportion of water, they are fragile and crush easily. Special techniques, such as sealing the crystal in a capillary tube in a suitable atmosphere, cooling the crystal, or growing it at very low temperatures, can be used to surmount such experimental difficulties. Sometimes a twinned crystal may be formed as the result of an intergrowth of two separate crystals in a variety of specific configurations. This may complicate optical and diffraction studies, but methods have been devised for working with them because sometimes only twinned crystals, and no single crystals, can be obtained.

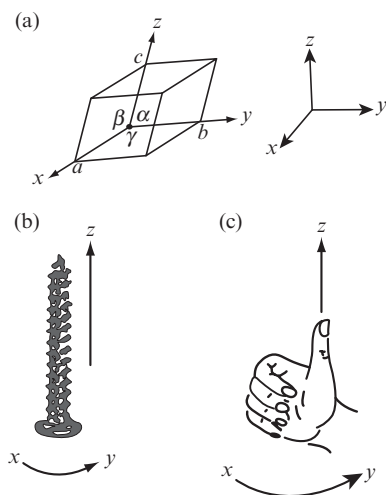


Fig. 2.2 Unit-cell axes.

(a) A unit cell showing the axial lengths a , b , and c and the interaxial angles (α between b and c , β between c and a , and γ between a and b). The directions of axes are given in a right-handed system, as shown by the screw in (b) and the human fist in (c). As x is moved to y , the screw in (b) or the thumb in (c) moves in the z -direction in a right-handed manner.

[†] A parallelepiped is a *three-dimensional* polyhedron with six faces, each a parallelogram that is parallel to a similarly shaped opposite face. It does not have any requirement that all or any angles at the corners of the six faces be 90° . Each face, a parallelogram, is a four-sided *two-dimensional* polygon with two pairs of parallel sides.

The unit cell of a crystal

Any crystal may be regarded as being built up by the continuing *three-dimensional translational repetition* of some basic structural pattern, which may consist of one or more atoms, a molecule or ion, or even a complex assembly of molecules and ions; the simplest component of this three-dimensional pattern is called the “unit cell.” It is analogous to a building brick. The word “translational” in the above definition of a crystal implies that there is within it a repetition of an arrangement of atoms in a specific direction at regular intervals; this repeat distance defines a measure of the unit-cell dimension in that direction.

The basic building block of a crystal is an imaginary three-dimensional parallelepiped,[†] the “unit cell,” that contains one unit of the translationally repeating pattern. It is defined by three noncoplanar vectors (the crystal axes) \mathbf{a} , \mathbf{b} , and \mathbf{c} , with magnitudes a , b , and c (Figure 2.2a). These vectors are arranged, for convenience, in the sequence \mathbf{a} , \mathbf{b} , \mathbf{c} , in a right-handed axial system (see Figures 2.2b and c). The angles between these axial vectors are α between \mathbf{b} and \mathbf{c} , β between \mathbf{a} and \mathbf{c} , and γ between \mathbf{a} and \mathbf{b} (see Figure 2.2). Thus, the size and shape of the unit cell are defined by the dimensions a , b , c , α , β , γ . As will be described later, atomic positions along each of the unit-cell directions are generally measured as fractions x , y , and z of the repeat lengths a , b , and c .

The unit cell is a complete representation of the contents of the repeating unit of the crystal. As a building block, it must pack in three-dimensional space without any gaps. The unit cells of most crystals are, of course, extremely small, because they contain comparatively few molecules or ions, and because normal interatomic distances are of the order of a few Å. For example, a diamond is built up of a three-dimensional network of tetrahedrally linked carbon atoms, 1.54 Å apart. This atomic arrangement lies in a cubic unit cell, 3.6 Å on an edge. A one-carat diamond, which has approximately the volume of

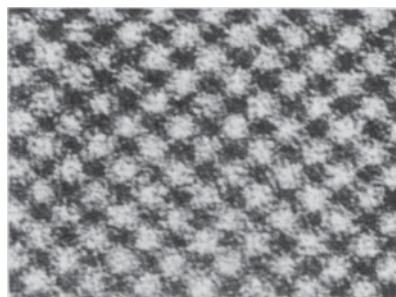


Fig. 2.3 An electron micrograph of a crystalline protein.

An electron micrograph of a crystalline protein, fumarase, molecular weight about 200,000. The individual molecules, in white, are visible as approximately spherical structures at low resolution. Note that several choices of unit cell are possible. (Photograph courtesy of Dr. L. D. Simon)

a cube a little less than 4 mm on a side, thus contains 10^{21} unit cells of the diamond structure.[‡] A typical crystal suitable for X-ray structure analysis, a few tenths of a millimeter in average dimension, contains 10^{12} to 10^{18} unit cells, each with identical contents that can diffract X rays in unison. Figure 2.3 shows an electron micrograph of a protein crystal and the regularity of its molecular packing. The existence of unit cells in this micrograph is evident.

[‡]The unit cell of diamond is cubic. The unit cell edges are 3.6 Å. Given that the density is 3.5 g cm^{-3} we can calculate that there are 8 atoms of C in the unit cell. 1 carat weighs 0.2 g.

The faces of a crystal

There is a need to be able to describe a specific face of a crystal, and this is done with respect to the chosen unit cell. Finding three integers that characterize a given crystal face or plane is known as “indexing.” As shown in Figure 2.4, a crystal face or crystal plane is indexed with three numbers, h , k , and l , with these indices relatively prime (not each divisible by the same factor), when the crystal face or plane makes intercepts a/h , b/k , c/l with the edges of the unit cell (lengths a , b , and c). This is derived from the “Law of Rational Indices,” which states that each face of a crystal may be described by three whole (rational) numbers; these three numbers describing a crystal face are enclosed in parentheses as (hkl) . This nomenclature was introduced by William Whewell and William Hallowes Miller (see Haüy, 1784, 1801; Miller, 1839). If a crystal face is parallel to one crystal axis, its intercept on that axis is at infinity, so that the corresponding “Miller index” is zero, as shown in Figure 2.4a. If a crystal face intersects the unit-cell edge at one-third its length, the value of the index is 3, as shown in Figure 2.4b. When the crystal faces have been indexed and the angles between them measured, it is possible to derive the ratio of the lengths of the unit

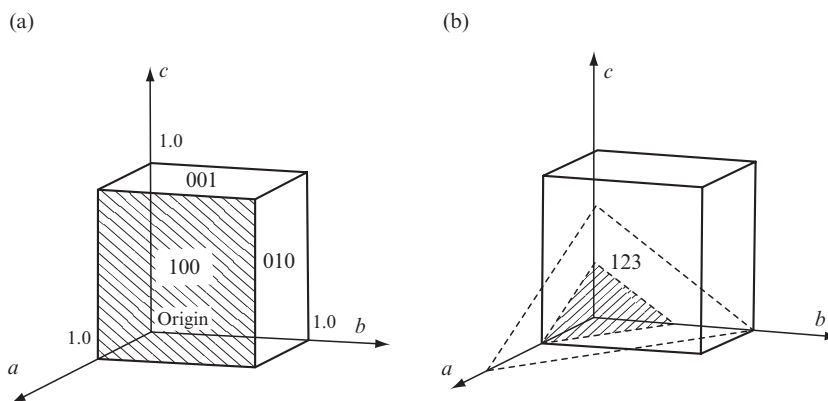


Fig. 2.4 Indexing faces of a crystal.

A crystal face or plane (hkl) makes intercepts a/h , b/k , c/l with the edges of the unit cell of lengths a , b , and c . (a) The (100) , (010) , and (001) faces are shown. (b) The (123) face makes intercepts $a/1$, $b/2$, and $c/3$ with the unit-cell axes. A parallel crystal plane (unshaded) is also indicated; it makes the same intercepts with the next unit cell nearer to the observer.

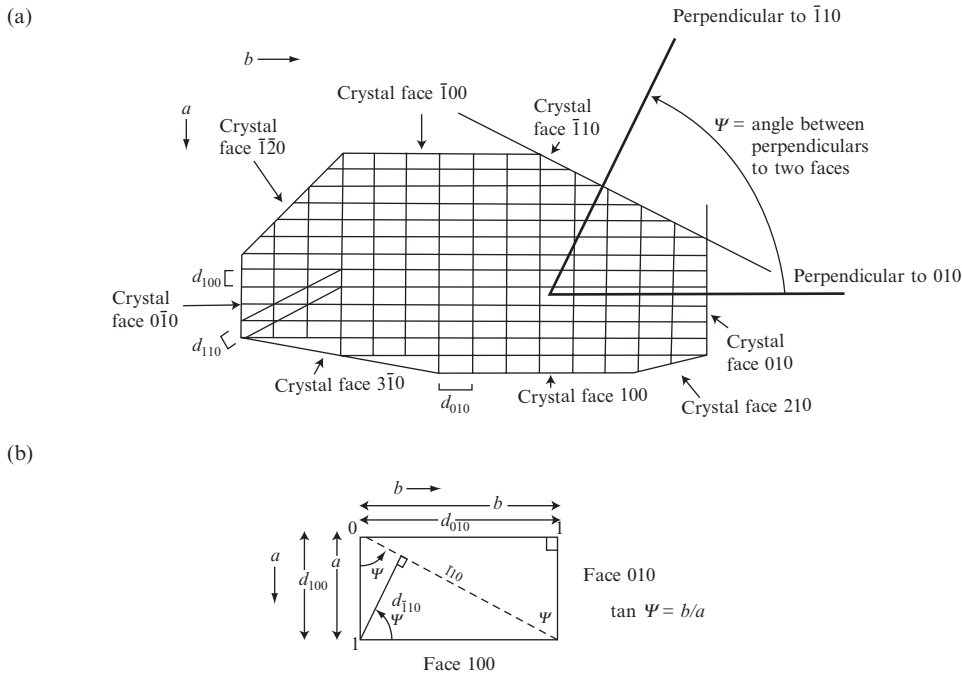


Fig. 2.5 The determination of the probable shape of the unit cell from interfacial angles in the crystal.

(a) A cross section of a crystal viewed down the c -axis. For each face in this figure, $l = 0$. If the faces can be indexed and the angles between these faces measured, it is possible to derive the ratio of the lengths of the unit cell edges (in this example b/a). This will then give the shape (but not the absolute dimensions) of the unit cell. (b) One unit cell, showing the indices of some faces and the interplanar spacings d_{hkl} (the spacing between crystal lattice planes (hkl) in the crystal).

cell edges and hence the shape (but not the absolute dimensions) of the unit cell.

The relative lengths of some interplanar spacings, d_{hkl} (the spacing between the crystal lattice planes (hkl) in the crystal), are indicated in both Figures 2.5a and b. An index (hkl) with a line above any of these entries means that the value is negative. For example, $(3\bar{1}0)$ means $h = 3$, $k = -1$, $l = 0$; the intercepts with the axes are $a/3$ and $-b$, and the faces or planes lie parallel to c , since $l = 0$ (intercept infinity). Sets of planes that are equivalent by symmetry (such as (100) , (010) , (001) , $(\bar{1}00)$, $(0\bar{1}0)$, and $(00\bar{1})$) constitute a crystal form, represented (with “squiggly” brackets) as $\{100\}$. Square brackets enclosing three integers indicate a crystal lattice row; for example, $[010]$ denotes the direction of the \mathbf{b} axis, that is, a line connecting the unit-cell origin to a point with coordinates $x = 0$, $y = 1$, $z = 0$. Before the discovery of X-ray diffraction in 1912, it was possible to deduce only the relative lengths of the unit-cell axes and the values of the interaxial angles from measurements of interfacial angles in crystalline specimens by means of a special instrument (an optical goniometer), as shown in Figure 2.5a. As we shall see shortly, however, X rays provide a tool for measuring the actual lengths of these axes, and therefore the size, as well as the shape, of the unit

cell of any crystal can be found. In addition, if the density of a crystal is measured, one can calculate the weight (and hence, in most cases, the atomic contents) of atoms in the unit cell. The method for doing this is described in Appendix 1.

The crystal lattice

The *crystal lattice* highlights the repetition of the unit-cell contents within the crystal. If, in a diagram of a crystal, *each complete repeating unit (unit cell) is replaced by a point*, the result is the crystal lattice. It is an infinite three-dimensional network of points that may be generated from a single starting point (at a chosen position in the unit cell) by an extended repetition of a set of translations that are, in most cases, the conventional unit-cell vectors just described. This highlights the regularly repeating internal structure of the crystal, as shown in Figure 2.6.

The term “crystal lattice” is sometimes, misleadingly, used to refer to the crystal structure itself. It is important to remember that a *crystal structure is an ordered array of objects (atoms, molecules, ions) that make up a crystal, while a crystal lattice is merely an ordered array of imaginary points*. Although crystal lattice points are conventionally placed at the corners of the unit cell, there is no reason why this need be done. The crystal lattice may be imagined to be free to move in a straight line (although not to rotate) in any direction relative to the structure. A crystal lattice point may be positioned anywhere in the unit cell, but exactly the same position in the next unit cell is chosen for the next crystal lattice point. As a result every crystal lattice point in the unit cell will have the same environment as every other crystal lattice point in the crystal. The most general kind of crystal lattice, composed of unit cells with three unequal edges and three unequal angles, is called a triclinic crystal lattice. Once the crystal lattice is known, the entire crystal structure may be described as a combination (convolution[§]) of the crystal lattice with the contents of one unit cell, as shown in Figure 2.6.

The two-dimensional example of the regular translational repetition of apples, illustrated in Figure 2.6, might serve as a pattern for wallpaper (which generally has two-dimensional translational repetitions). Several possible choices of unit cell, however, can be made from the two-dimensional arrangement of apples in it. How, then, can we speak of *the unit cell* for a given crystal? In general, we can't. The conventional choice of unit cell is made by examining the crystal lattice of the crystal and choosing a unit cell whose shape displays the full symmetry of the crystal lattice—rotational as well as translational—and that is convenient. For example, the axial lengths may be the shortest possible ones that can be chosen and the interaxial angles may be as near as possible to 90°. There may be several possibilities that fit these conditions. It is usual to derive the Niggli reduced cell (Niggli, 1928; de

[§] A convolution (with axes u, v, w) is a way of combining two functions $A(x, y, z)$ and $B(x, y, z)$ (with axes x, y, z). It is an integral that expresses the extent to which one function overlaps another function as it is shifted over it. The convolution of these two functions A and B at a point (u_0, v_0, w_0) is found by multiplying together the values $A(x, y, z)$ and $B(x + u_0, y + v_0, z + w_0)$ for all possible values of $x, y,$ and z and summing all these products. This process must then be repeated for each value of $u, v,$ and w of the convolution. A crystal structure, for example, can be viewed as the convolution of a crystal lattice (function A) with the contents of a single unit cell (function B) (see Figure 2.6). This is a simple example because the crystal lattice exists only at discrete points and the rest of this function A has zero values. This convolution converts a specific unit of pattern into a series of identical copies arranged on the crystal lattice. All that is needed is information on the geometry of the crystal lattice and on the unit of pattern; the convolution of these two functions gives the crystal structure.

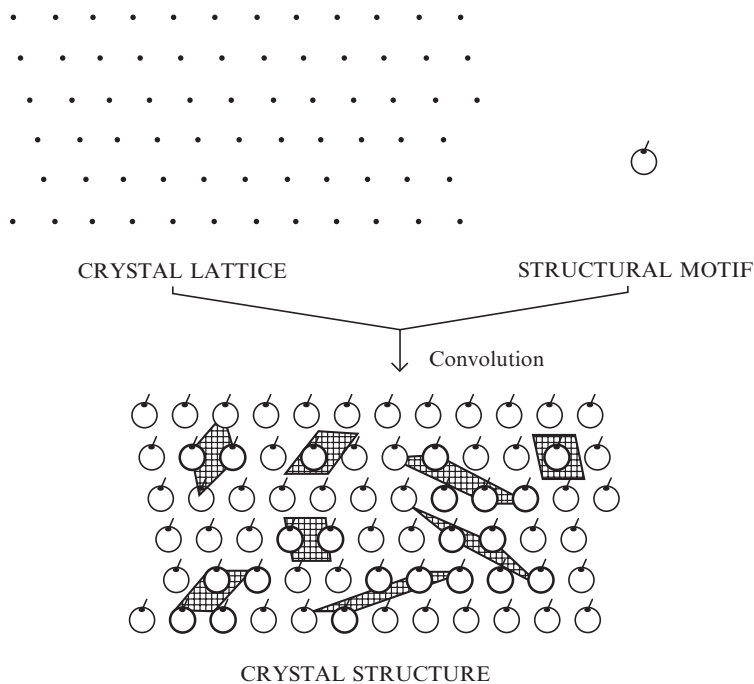


Fig. 2.6 The crystal lattice and choices of unit cells.

The generation of a two-dimensional “crystal structure” from a crystal lattice and a structural motif (an apple in this example). The crystal lattice is obtained from the crystal structure by replacing each complete repeating unit by a point. The replacement of each point in the crystal lattice by an apple would lead to a two-dimensional crystal structure. This *crystal structure* may be described alternatively as the *convolution of an apple and the crystal lattice*. There are many ways in which unit cells may be chosen in the repeating pattern of apples. Some possible alternative choices are shaded, each having the same area despite varying shape. This can be verified by noting that the total content of any chosen unit cell in this figure is one apple. Infinite repetition in two dimensions of any one of these choices for unit cell will reproduce the entire pattern.

Wolff and Gruber, 1991), that is, to select the three shortest noncoplanar vectors in the crystal lattice. This may help in establishing whether two crystals with different unit-cell dimensions are really the same or not.

It is a common misconception, perhaps arising from the abundance of illustrations of the simplest elementary and ionic structures in textbooks, that an atom must lie at the corner (origin) of each unit cell. It is possible to choose the origin arbitrarily and place it at the site of an atom, but in most structures the choice of origin is dictated by convenience, because of its relation to symmetry elements that may be present (i.e., the appropriate space group), and in the great majority of known structures no atom is present at the origin. Another misconception is that what a chemist finds convenient to regard as a single molecule or formula unit must lie entirely within one unit cell. Portions of a single bonded aggregate may lie in two or more adjacent unit

cells. If this does happen, however, any single unit cell will necessarily still contain all of the independent atoms in the molecule—the atoms simply comprise portions of different molecules. This is illustrated in Figure 2.6, which shows that a given unit cell may contain only one apple or portions of two or more apples.

Crystal symmetry

Unit cells and crystal lattices are *classified according to their rotational symmetry*. If an object is rotated 180° and then appears identical to the starting structure, the object is said to have a two-fold rotation axis (the axis about which the 180° rotation occurred). The presence of an n -fold rotation axis, where n is any integer, means that when the unit cell is rotated $(360/n)^\circ$ about this axis, the crystal lattice so obtained is indistinguishable from original before rotation. If you closed your eyes, rotated the crystal lattice, and opened your eyes again, nothing would appear to have changed. The symmetry of an isolated crystal can be found by examination, and it can give us some very useful information about the internal atomic arrangement. If the crystal is set down on a flat surface, it is possible to note if there is another face on top of the crystal that is parallel to the lower face lying on the flat surface. Then one can determine if there is a center of symmetry between these upper and lower faces of the crystal. Similarly, one can examine the crystal for two-, three-, four- and six-fold rotation axes. The result of such examinations is the determination of the point group of the crystal, that is, a group of symmetry operations, such as an n -fold rotation axis, that leaves at least one point unchanged within the crystal.

It is shown in Appendix 2 that there are seven ways in which different types of applicable rotational symmetry (such as two-, three-, four-, and six-fold rotation axes) lead to infinitely repeatable unit cells. These seven are called the *seven crystal systems*—triclinic, monoclinic, orthorhombic, tetragonal, trigonal/rhombohedral, hexagonal, and cubic. They are distinguished by their different rotational symmetries. For example, in a triclinic crystal lattice there is no rotational (only one-fold) symmetry; this defines the term “triclinic.” As a result, usually (but not always) in a triclinic crystal lattice, all unit-cell lengths (a , b , and c) are unequal, as are all interaxial angles (α , β , and γ). A monoclinic crystal lattice ($\alpha = \gamma = 90^\circ$) has a two-fold rotation axis parallel to the b axis (where b is chosen, by convention for this crystal system, to be unique). This means that a rotation of the crystal lattice by 180° about the b axis gives a crystal lattice indistinguishable from the original. In an orthorhombic crystal lattice, with three mutually perpendicular rotation axes, all interaxial angles (α , β , and γ) are 90° . A cubic crystal is defined by three-fold axes along the cube diagonals, not by its four-fold axes. It must be stressed that it is the symmetry of the crystal lattice that is important in defining the crystal system, not the magnitude of the interaxial angles. Some monoclinic crystals have been found with

$\beta = 90^\circ$, and some triclinic crystals with all interaxial angles very close to 90° ; this is why symmetry rather than unit cell dimensions are used to define which is the correct crystal system for the material under study. In the diagrams of these seven crystal systems in Appendix 2 all crystal lattice points (designated by small circles) are equivalent by translational symmetry. All crystal lattices except the triclinic crystal lattice display more than one-fold rotational symmetry (see Chapter 7 for details).

It is customary when choosing a unit cell to take advantage of the highest symmetry of the crystal lattice. If a unit cell includes only one crystal lattice point (obtained from the fractions at each corner), it is said to be primitive and the crystal lattice is designated *P*. Sometimes it is more convenient to choose a unit cell that contains more than one crystal lattice point (a “nonprimitive” unit cell). Nonprimitive unit cells are chosen because they display the full symmetry of the crystal lattice, or are more convenient for calculation; any given crystal lattice may always be described in terms of either primitive or nonprimitive unit cells. The latter type of crystal lattices have lattice points not only at the corners of the conventional unit cell, but also at the center of this unit cell (*I* for the German *innenzentrierte*), at the center of one pair of opposite faces (*A*, *B*, or *C*), or at the center of all three pairs of opposite faces (*F*) (see Appendix 2). More than one crystal lattice point is then associated with a unit cell so chosen, but the requirement that every crystal lattice point must have identical surroundings is still fulfilled. That there are 14, and only 14, distinct types of crystal lattices was deduced by Moritz Ludwig Frankenheim and Auguste Bravais in the nineteenth century, and these crystal lattices are named after Bravais (Bravais, 1850). The Bravais crystal lattices are obtained from a combination of the seven crystal systems (triclinic, monoclinic, orthorhombic, tetragonal, trigonal/rhombohedral, hexagonal, and cubic) with the four crystal lattice types (*P*, *A* or *B* or *C*, *F*, and *I*) after the elimination of any equivalencies. The unit cells of these 14 Bravais crystal lattices are shown in Appendix 2.

Space groups

Since the atomic contents in each unit cell are identical (or nearly so), the symmetry of the arrangement of atoms in each unit cell must be related by certain symmetry operations (in addition to translation) that ensure identity from unit cell to unit cell. This means that the atomic arrangement in one unit cell is related by defined symmetry operations to the arrangement in all other unit cells. The smallest part of a crystal structure from which the complete structure can be obtained by space-group symmetry operations (including translations) is called the asymmetric unit. The operation of the correct space-group symmetry elements (other than crystal lattice translations) on the asymmetric unit

will generate the entire contents of a primitive unit cell. When one considers the possible combinations of symmetry elements (centers of symmetry, mirror planes, glide planes, rotation axes, and screw axes) that are consistent with the 14 Bravais crystal lattices, and thus the possible symmetry elements of the structures that can be arranged on the crystal lattices, it is found that 230, and only 230, distinct combinations of the possible symmetry elements exist for three-dimensional crystals (and only 17 plane groups for two-dimensional wallpaper). Thus the many different ways of arranging atoms or ions in structures to give a regularly repeating three-dimensional arrangement in a crystal fall into 230, and only 230, different three-dimensional crystallographic space groups. They are listed in *International Tables for (X-ray) Crystallography* (referred to here as *International Tables*), and these Tables, listed at the end of this book in the "References and further reading" section, are constantly used by crystallographers. The important result is that if the location of one atom in a crystal of known space group has been found, then application of the space-group symmetry operations (listed for convenience in *International Tables*) will give the locations of all other such specific atoms in the unit cell. This can be repeated for each atom in the ions or molecules that make up the crystal. Symmetry and space groups are discussed further in Chapter 7.

Physical properties of crystals

Optical properties

The interaction of light with crystals is one of the reasons they are used for ornamentation (as jewelry). It may also reveal information about crystalline symmetry and, in certain cases, the internal structure of the crystal (Hartshorne and Stuart, 1950; Wood, 1977; Wahlstrom, 1979). Particularly useful information may be obtained from the refractive index of the crystal. This gives a measure of the change in the velocity of light when it enters the crystal. Refraction is evident when a straight stick or rod is partially inserted in water; the rod appears to be bent at the point of entry. The change in the velocity of light as it passes from air to water is revealed by the angle to which the rod appears to be bent; when this angle is measured it gives information on the ratio of the two velocities (that is, the refractive index of water). The refractive index of a crystal is generally measured by immersing it in liquids of known refractive index, and determining when the crystal becomes "invisible." The crystal and the liquid surrounding it now have the same refractive index.

Some crystals, such as cubic crystals, are optically isotropic: the refractive index is independent of the direction from which the crystal is viewed. Other crystals may be birefringent, with different refractive indices in different directions. When a test tube containing birefringent



Fig. 2.7 The birefringence of calcite (Iceland spar).

View through an Iceland spar crystal (calcite) with the word "BIREFRINGENCE" written on a strip of paper behind it. Light is broken into two polarized beams as it passes through the crystal. The word is split into two images, hence the term "birefringence." As the crystal is rotated, the image made by the extraordinary ray moves around the image made by the ordinary ray. Iceland spar crystals are believed to have been used in the Arctic regions for ages in navigation to determine the direction of the sun on a cloudy day, and hence which direction to sail in.

crystals in their mother liquor is shaken, the crystals glisten (unlike the situation for isotropic cubic crystals). Birefringence, or double refraction, is the decomposition of light into two rays, each polarized. One ray, the "ordinary ray," travels through the crystal with the same velocity in every direction. The other ray, the "extraordinary ray," travels with a velocity that depends on the direction of passage through the crystal. The result of this can readily be seen for a calcite crystal (Iceland spar) in Figure 2.7, in which two images are formed when light passes through the crystal. If a birefringent crystal is colored, it may show different colors when viewed in different directions. If the crystal structure contains an approximately planar group, measurements of refractive indices may permit deduction of the orientation of this planar group within the chosen unit cell. This method, combined with unit-cell measurements, was used to study steroid dimensions and packing long before any complete structure determination was or could be initiated. It led to a correct chemical formula for atoms in the steroid ring structure (Bernal, 1932).

There are many other interesting optical properties of crystals. Second-harmonic generation (SHG, also called frequency doubling) was first demonstrated when a ruby laser with a wavelength of 694 nm was focused into a quartz crystal (Dougherty and Kurz, 1976). Analysis with a spectrometer indicated that light was produced with a wavelength of 347 nm (half the wavelength and twice the frequency of the incident light). Only noncentrosymmetric crystal structures can double the frequency, and therefore SHG provides a useful method for testing the symmetry of a crystal. Green laser pointers combine a noncentrosymmetric (nonlinear) crystal with a red neodymium laser to produce green light.

Electrical properties

Certain crystals display piezoelectricity. This word is derived from a Greek word meaning "to squeeze" or "press." Piezoelectricity is the creation of an electrical potential by a crystal in response to an applied mechanical stress. This effect is reversible in that materials exhibiting the direct piezoelectric effect also exhibit the converse piezoelectric effect (the production of stress when an electric field is applied). The piezoelectric effect was first reported by Pierre and Jacques Curie in 1880, who detected a voltage across the faces of a compressed Rochelle salt crystal (Curie and Curie, 1880). The phenomenon has many industrial uses. For example, when the button of a cigarette lighter or gas burner is pressed, the high voltage produced by the compression of a crystal causes an electric current to flow across a small spark gap, so that the gas is ignited. Another example is in the airbag sensor of a car. The intensity of the shock of a car crash to a crystal causes an electrical signal that triggers expansion of the airbag. In the analogous phenomenon of pyroelectricity, a crystal can generate an electrical potential in response to a change in temperature.

The significance of the unit cell

In this chapter we have described crystals and their representation by a repeating component, the unit cell. Since a crystal is built up of an extremely large number of regularly stacked cells, each of which has identical contents, the problem of determining the structure of a crystal is reduced to that of determining the spatial arrangement of the atoms *within a single unit cell*, or *within the smaller asymmetric unit* if (as is usual) the unit cell has some internal symmetry. If there is some static disorder in the structure, the arrangements of atoms in different unit cells may not be precisely identical, varying in an apparently random fashion. There may also be dynamic disorder in a structure as various part of the molecules move. Since the frequencies of atomic vibrations are of the order of 10^{13} per second, and since sets of X-ray diffraction data are measured over periods ranging from seconds to hours, time-averaging of the atomic distribution is always involved. What one finds for the arrangement of atoms in a crystal is the space-averaged structure of all of its component unit cells.

Summary

A crystal is, by definition, a solid that has a regularly repeating internal structure (arrangement of atoms). This internal periodicity was surmised in the seventeenth century from the regularities of the shapes of crystals, and was proved in 1912 when it was shown that a crystal could act as a three-dimensional diffraction grating for X rays, since X rays have wavelengths comparable to the distances between atoms in crystals.

Crystals are generally grown by concentrating a solution of the material of interest until material separates (hopefully in a crystalline state). Experimental conditions should ensure a good choice of solvent, the generation of a suitable number of nucleation sites, control of the rate of growth, and a lack of disturbance of the setup.

The *unit cell* of a crystal is its basic building block and is described by three axial lengths a , b , c and three interaxial angles α , β , γ . When describing a crystal face or plane it is necessary to consider intercepts on the three axes of the unit cell. The hkl face or plane makes intercepts a/h , b/k , c/l with the three axes. The internal regularity of a crystal is expressed in the *crystal lattice*; this is a regular three-dimensional array of points (each with identical environments) upon which the contents of the unit cell (*the motif*) are arranged by infinite repetition to build up the crystal structure. There are seven ways in which rotational symmetry can lead to infinitely repeatable unit cells. These are the seven crystal systems—triclinic, monoclinic, orthorhombic, tetragonal, trigonal/rhombohedral, hexagonal, and cubic (see Appendix 2). These seven crystal lattices are combined with the four crystal lattice types (primitive P , single-face-centered A or B or C , face-centered F , and

body-centered I) to give 14 Bravais lattices. Symmetry elements (center of symmetry, mirror planes, glide planes, rotation axes, and screw axes) combined with these 14 Bravais lattices give the 230 different combinations of symmetry elements (the 230 space groups) that are possible for arranging objects in a regularly repeating manner in three dimensions, as in the crystalline state.

Diffraction

3

A common approach to crystal structure analysis by X-ray diffraction presented in texts that have been written for nonspecialists involves the Bragg equation, and a discussion in terms of “reflection” of X rays from crystal lattice planes (Bragg, 1913). While the Bragg equation, which implies this “reflection,” has proved extremely useful, it does not really help in understanding the process of X-ray diffraction. Therefore we will proceed instead by way of an elementary consideration of *diffraction phenomena* generally, and then diffraction from periodic structures (such as crystals), making use of optical analogies (Jenkins and White, 1957; Taylor and Lipson, 1964; Harburn et al., 1975).

Visualizing small objects

The eyes of most animals, including humans, comprise efficient optical systems for forming images of objects by the recombination of visible radiation scattered by these objects. Many things are, of course, too small to be detected by the unaided human eye, but an enlarged image of some of them can be formed with a microscope—using visible light for objects with dimensions comparable to or larger than the wavelength of this light (about 6×10^{-7} m), or using electrons of high energy (and thus short wavelength) in an electron microscope. In order to “see” the fine details of molecular structure (with dimensions 10^{-8} to 10^{-10} m), it is necessary to use radiation of a wavelength comparable to, or smaller than, the dimensions of the distances between atoms. Such radiation is readily available

- (1) in the X rays produced by bombarding a target composed of an element of intermediate atomic number (for example, between Cr and Mo in the Periodic Table) with fast electrons, or from a synchrotron source,*
- (2) in neutrons from a nuclear reactor or spallation source, or
- (3) in electrons with energies of 10–50 keV.

Each of these kinds of radiation is scattered by the atoms of the sample, just as is ordinary light, and if we could recombine this scattered radiation, as a microscope can, we could form an image of the scattering matter. This recombination of radiation scattered by atoms

* Synchrotron radiation is an intense and versatile source of X rays that is emitted by high-energy electrons, such as those in an electron storage ring, when their path is bent by a magnetic field. The radiation is characterized by a continuous spectral distribution (which can, however, be “tuned” by appropriate selection), a very high intensity (many times that of conventional X-ray generators), a pulsed time structure, and a high degree of polarization.

** When X rays hit an atom, its electrons are set into oscillation about their nuclei as a result of perturbation by the rapidly oscillating electric field of the X rays. The frequency of this oscillation is equal to that of the incident X rays. The oscillating dipole so formed acts, in accord with electromagnetic theory, as a source of radiation with the same frequency as that of the incident beam. This is referred to as “elastic scattering” and is the type of scattering discussed in this book. When there is energy loss, resulting in a wavelength change on scattering, the phenomenon is described as “inelastic scattering.” This effect is generally ignored by crystallographers interested in structure and will not be discussed in this book.

is, however, found to be more complicated than that necessary for viewing through a microscope, and it is the major subject of this book.

X rays are scattered by the electrons in an atom,** neutrons are scattered by the nuclei and also, by virtue of their spin, by any unpaired electrons in the atom, and electrons are scattered by the electric field of the atom, which is of course a consequence of the combined effects of both its nuclear charge and its extranuclear electrons. However, neither X rays nor neutrons of the required wavelengths can be focused by any known lens system, and high-energy electrons cannot (at least at present) be focused sufficiently well to show individually resolved atoms. Thus, the formation of an atomic-resolution image of the object under scrutiny, which is the self-evident aim of any method of crystal structure determination—and is a process that we take for granted when we use our eyes or any kind of microscope—is not directly possible when X rays, neutrons, or high-energy electrons are used as a probe. Unfortunately, the atoms that we wish to see are too small to be seen without these short-wavelength radiation sources.

When, however, X rays or neutrons are diffracted by crystalline materials, a measurable pattern of diffracted beams is obtained and these results can be analyzed to give a three-dimensional map of the atomic arrangement within the crystal and hence the molecular structures involved. In order for the reader to understand the process involved it is necessary to consider diffraction in general, and easier to start with the effects of visible light on masks that are readily visible. Scattering of light by slits will serve as a preliminary model for the scattering of X rays by atoms. When the dimensions of both the slits and the wavelength of visible light are reduced by several orders of magnitude, analogous results can be obtained for atoms and X rays.

Diffraction of visible light by single slits

The pattern of radiation scattered by any object is called the *diffraction pattern* of that object. Diffraction occurs whenever the wavefront of a light beam is obstructed in some way. We are accustomed to think of light as traveling in straight lines and thus casting sharply defined shadows, but that is only because the dimensions of the objects normally illuminated in our experience are much larger than the wavelength of visible light. When light from a point source passes through a narrow slit or a very fine pinhole, the light is found to spread into the region that normally would be expected to be in shadow. In explanation of this effect, each point on the wavefront within the slit or pinhole is considered to act as a secondary source, radiating in all directions. The secondary wavelets so generated interfere with each other, either reinforcing or partially destroying each other, as originally described by Francesco Maria Grimaldi, Christiaan Huygens, Thomas Young, and Augustin Jean Fresnel (Grimaldi, 1665; Huygens, 1690; Young, 1807;

de Sénarmont et al., 1866). As these waves combine, the extent of interference will depend on their relative phases and amplitudes. It is assumed that any phase change on scattering is the same for each atom and therefore this change is generally ignored.[†] There are, however, exceptions to this assumption, for example when the wavelength of the radiation can cause changes in the atom (see Chapter 10).

The phenomenon of diffraction by a regular two-dimensional pattern may be illustrated by holding a woven fabric handkerchief taut between your eyes and a distant point source of light, such as a street light. Instead of just one spot of light, as expected, a cluster of lights will be seen. The same phenomenon can also be demonstrated with a fine sieve (see the cover of this book). The narrowly and regularly spaced threads of the fabric or wires of the sieve are considered to produce this diffraction effect. The larger the spacing between the wires of the sieve, the closer diffraction spots are found around the central spot.

Keeping in mind that we are interested in scattering (diffraction) by atoms, we begin with a discussion of diffraction by slits because these involve visible light and therefore help with the description of the various principles of diffraction. Two examples of the diffraction of light when it passes through a single slit are given in Figure 3.1; in one,

[†] The reader will remember that an electromagnetic wave has a constant velocity *in vacuo* (the speed of light) and consists of successive crests and troughs. Two crests are a wavelength apart, and this distance, which is inversely proportional to the frequency of the radiation, defines the properties of the electromagnetic wave (such as color red or blue, X ray or infrared, etc.). The wave has an amplitude (the maximum value measured from its mean value), which is related to the square root of the intensity of the beam. It also has a “relative phase,” which is the distance of the crest of the wave measured from a chosen origin of the wave or with respect to the crest of another wave (see Figure 1.2). It was shown by John Joseph Thomson that when radiation is scattered by an electron, there is a phase change of 180° in the sense that the electric field in the scattered wave at a given point is opposed to that of the direct (incident) wave at that same point (Thomson, 1906). This is discussed in detail by Reginald William James (1965).

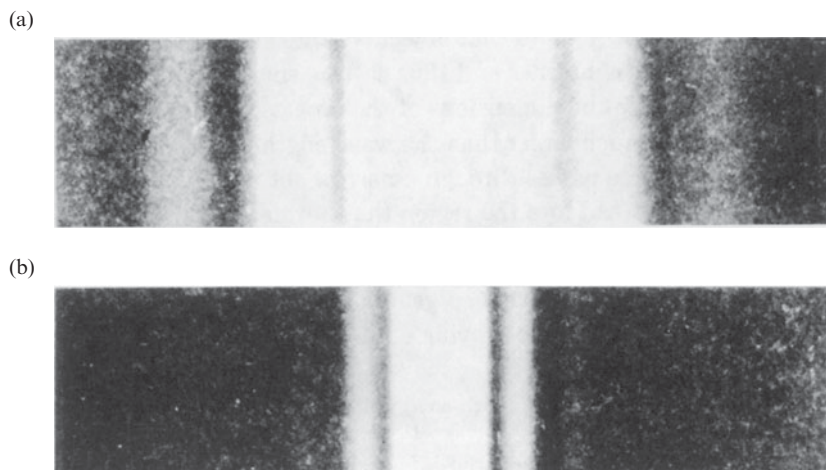


Fig. 3.1 Diffraction patterns of single narrow slits.

The diffraction patterns of two single slits of different width, both illuminated with light of the same single wavelength.

- (a) The diffraction pattern of a narrow slit.
- (b) The diffraction pattern of a slit 2.2 times wider than that used in (a). The diffraction pattern is now narrower by a factor of 2.2.

Note that the wider slit gives the narrower diffraction pattern.

From *Fundamentals of Optics* by Francis A. Jenkins and Harvey E. White, 3rd edition (1957) (Figure 16A). Copyright © 1957, McGraw-Hill Book Company. Used with permission of McGraw-Hill Book Company.

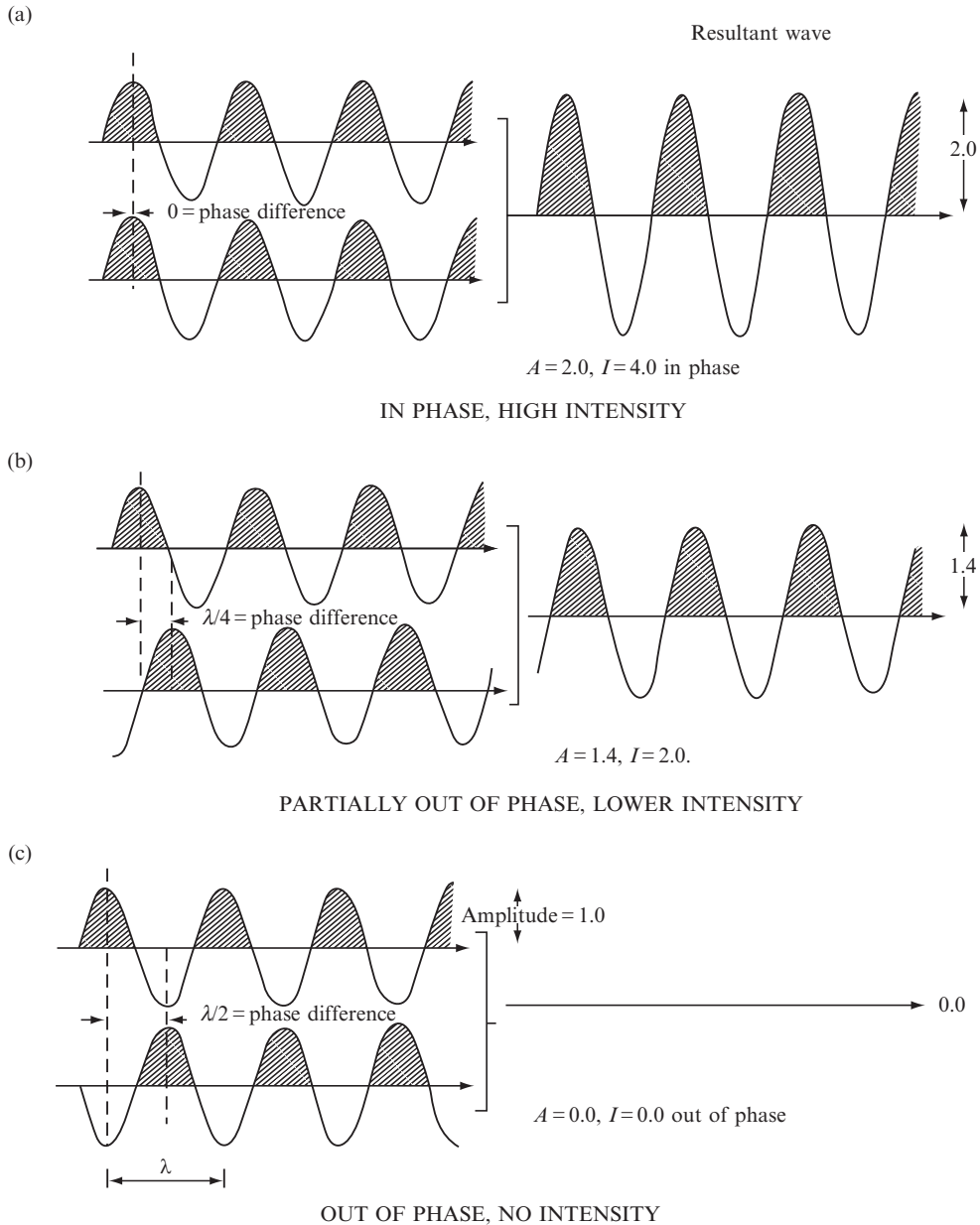


Fig. 3.2 Interference of two waves. Summation of waves.

Three examples are shown of what happens when two parallel waves of the same wavelength and equal amplitude add. In each example, the two separate waves are shown on the left and their sum or resultant wave on the right. The different examples are characterized by varying phase differences. The *relative phase* of a wave is the position of a crest relative to some arbitrary point (see Figure 1.2). This position (relative phase) is usually expressed as a fraction of the wavelength, and often this fraction is multiplied by 360° or 2π radians, so that the phase will be given as an angle. Thus a phase difference of $\lambda/4$ may be given as $1/4$, 90° , or $2/\pi$ radians. The resultant wave has the same wavelength, λ , as the original two waves. The intensity, I , of the resultant wave is proportional to the square of its amplitude, A , obtained on wave summation.

Figure 3.1a, the slit is narrow and the diffraction pattern is wide, while in the other, Figure 3.1b, the slit has a greater width but the diffraction pattern is narrower. This implies that there is a reciprocal relation between the angular spread of the scattering or diffraction pattern in a particular direction and the corresponding dimension of the object causing the scattering. The smaller the object, the larger the angular spread of the diffraction pattern. What is actually involved is the ratio of λ (the wavelength of the radiation used) to the minimum dimension, a , of the scattering object (for example, the width of the slit); the larger the value of λ/a (wavelength divided by slit width), the greater the spread of the pattern. Therefore Figure 3.1b might equally well be a view of the same slit as in Figure 3.1a, illuminated with radiation of wavelength about 2.2 times shorter than that used in Figure 3.1a. It is, in fact, possible to produce this change of scale by any change in a and λ whose combined effect is to decrease the value of λ/a by a factor of 2.2.

The phenomenon of interference between two waves traveling in the same direction and the importance of phase differences between these two parallel waves are illustrated in Figure 3.2. The amplitude of the wave resulting from the interaction of two separate waves traveling in the same direction with the same wavelength, and a constant phase difference, depends markedly on the size of this phase difference. Figure 3.2 shows how such waves may be summed[‡] for three examples of different phase differences (zero, a quarter, and half a wavelength). The intensity of the resulting beam is proportional to the square of the amplitude of the summed waves in each case.

The variations in intensity seen in Figure 3.1 arise from the interference of the secondary wavelets generated within the slit, as shown in Figure 3.3. In the direction of the direct beam, the waves scattered by the slit are totally in phase and reinforce one another to give maximum intensity. However, at other scattering angles, as illustrated in Figure 3.3, the relative phases of the waves cause interference between waves traveling in the same direction so that the intensity falls off as a function of scattering angle; this leads to an overall intensity contour of the diffraction peak, and we term this “the envelope.” At most scattering angles the different scattered waves are neither completely in phase nor completely out of phase, so that there is partial reinforcement and thus an intermediate intensity of the diffracted beam. The result is illustrated in the single-slit diffraction pattern (the envelope) shown on the right of Figure 3.3.

[‡] The displacements from the mean (zero), parallel to the vertical axis (the ordinates), are directly summed at many points along the horizontal axis (the abscissae) to give the resultant wave.

-
- (a) Phase difference zero. In this case there is total reinforcement, and the waves are said to be “in phase” or to show “constructive interference”. If the original waves are of unit amplitude, the resultant wave has amplitude 2, intensity 4.
 - (b) Phase difference $\lambda/4$. Partial reinforcement occurs in this case to give a resultant wave of amplitude 1.4, intensity 2.
 - (c) Phase difference $\lambda/2$. The waves are now completely “out of phase” and there is destructive interference, which gives no resultant wave (that is, a wave with amplitude 0, intensity 0).

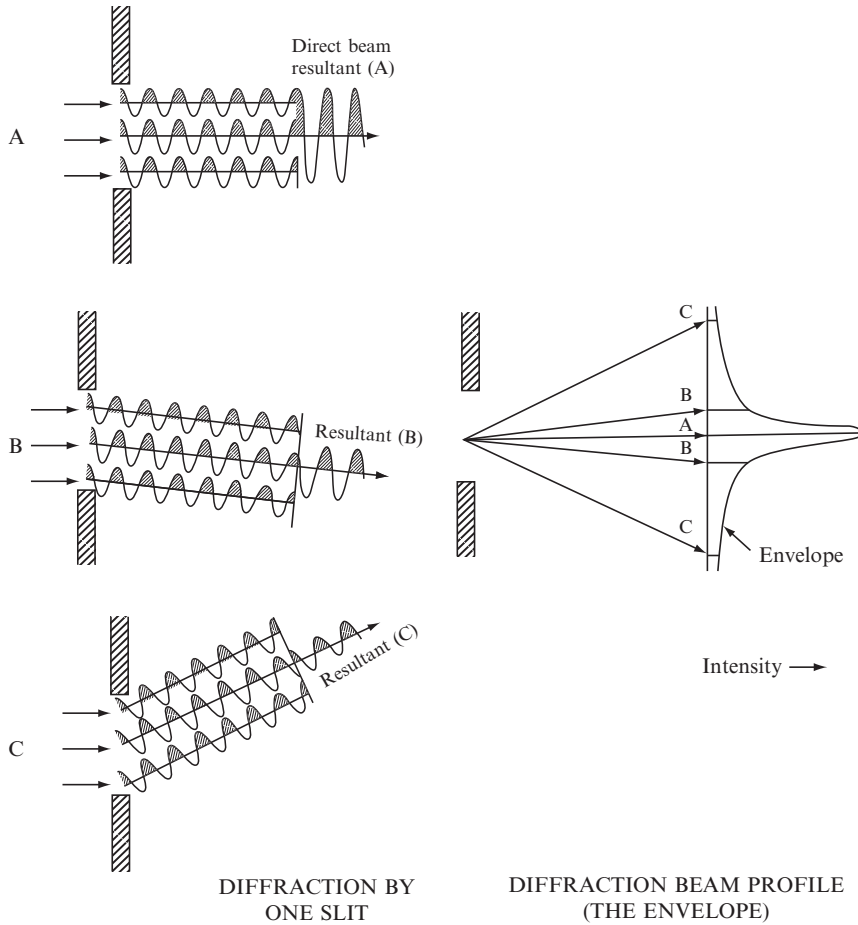


Fig. 3.3 Diffraction by a single slit.

Diffraction from a single slit is diagrammed by the superposition of waves generated within the area of the slit. The variation in intensity with increasing angle is shown by the different amplitudes of the resultant waves (A, B, and C) at different angles. Left-hand side: diffraction by a single slit; right-hand side: diffracted beam profile (the envelope), showing the location of A, B, and C on this envelope.

Diffraction of light by regular arrays of slits

In order to consider what happens when a crystal that has a periodic internal structure diffracts radiation, we now describe diffraction by a series of equidistantly aligned slits. Reinforcement of the diffracted beam occurs at angles at which the path difference between two parallel waves is an integral number of wavelengths; for example, when the two waves are out of phase by three wavelengths ($n = 3$), there will be reinforcement at a specific scattering angle and the wave will be described as the "third order of diffraction" (see Figure 3.4). As shown in Figure 3.5, the diffraction pattern of a single slit is modified by interference effects when increasing numbers of slits are placed

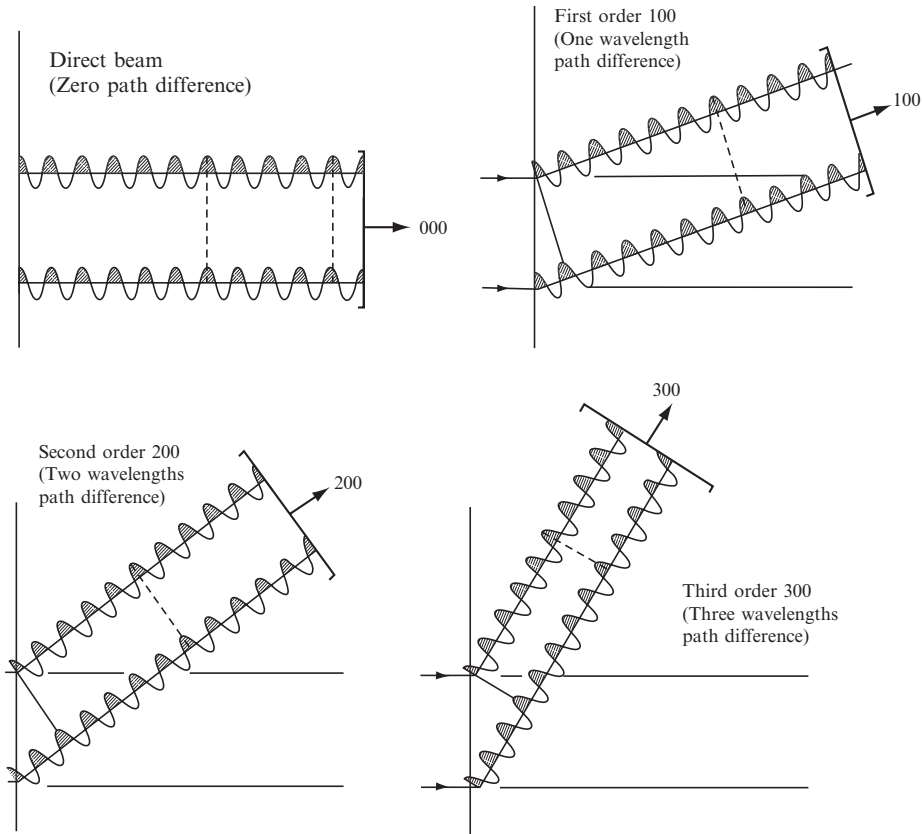


Fig. 3.4 Orders of diffraction.

First, second, third, and higher orders of diffraction are obtained as scattered waves differ by one, two, three, and more wavelengths. Readers should satisfy themselves that with a smaller spacing a between scattering objects, the angle at which a given order of diffraction occurs is proportionally increased.

side by side in a regular manner to form a one-dimensional grating. Sometimes rays proceeding in a specific direction after scattering are in phase and sometimes they are not. The important point to note is that the *diffraction pattern from a grating of slits is a sampling of the single-slit pattern in narrow regions that are representative of the spacings between the slits* (see Figure 3.5). With even as few as 20 slits in the “grating” (see Figure 3.6), the small subsidiary maxima vanish almost completely and the lines in the diffraction pattern are sharp. The overall diffraction pattern of a series of slits is thus composed of an “envelope” and a series of “sampling regions” within the envelope. This envelope represents the diffraction pattern of a single slit (see Figure 3.3). The “sampling regions” result from interference of waves scattered from equivalent points in different slits; the spacing of these sampling regions in the diffraction pattern (see Figure 3.6) is inversely related to the spacing of the slits.

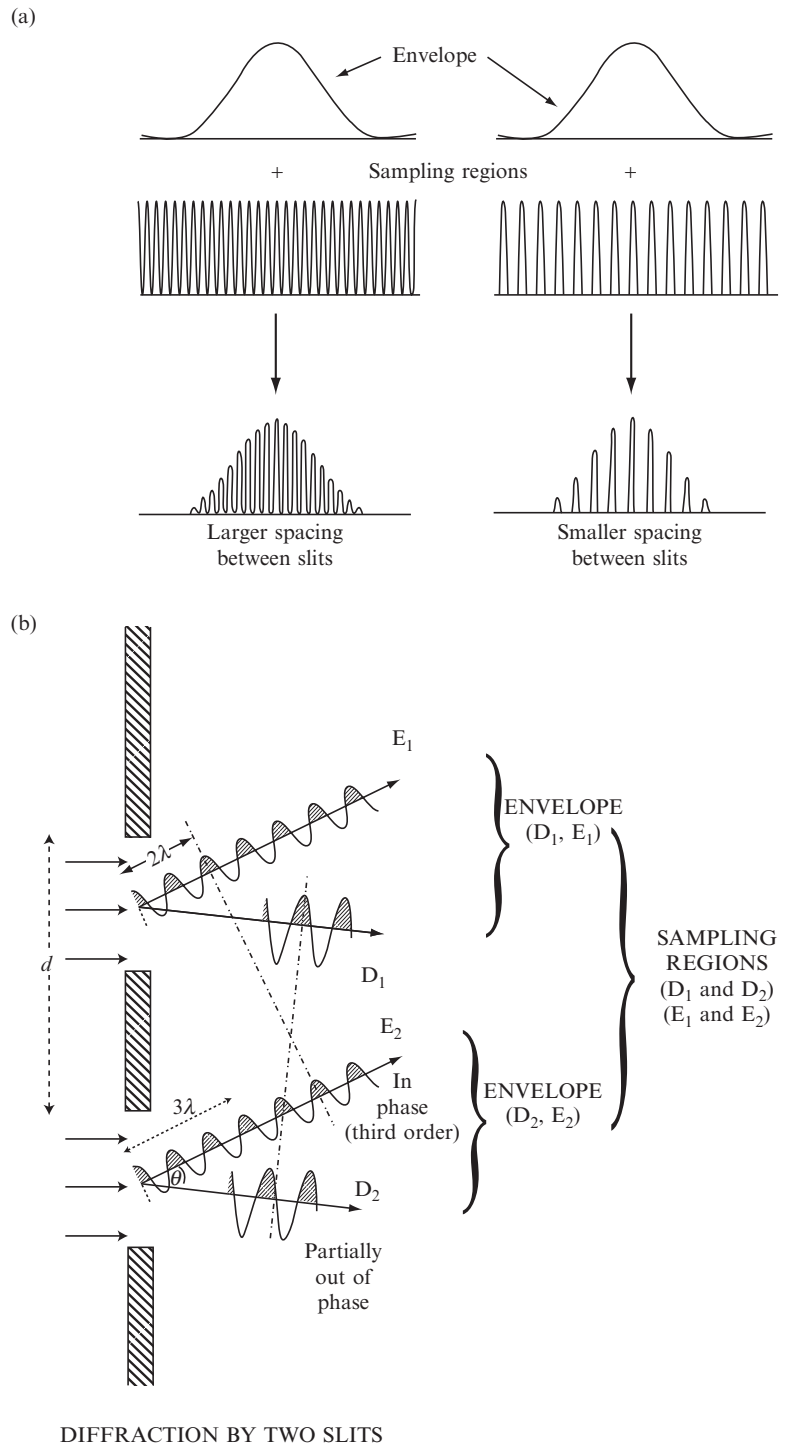


Fig. 3.5 Diffraction by two slits.

Figure 3.7 shows schematically how a two-dimensional regular arrangement of simple scattering objects, in this case holes in an opaque sheet (drawn as black spots on the left), produces a two-dimensional diffraction pattern (drawn as lines or spots on the right). Each of the one-dimensional gratings in Figures 3.7a and b produces (in two dimensions) a pattern of scattered light (the diffraction pattern) consisting of lines (representing the maxima of light, as seen on the right). These lines are perpendicular to the direction of the original grating because interference effects between light scattered from adjacent holes reduce the scattered light intensity effectively to zero in all directions except that perpendicular to the repeat direction of the original grating. Hence lines of diffracted light are formed. In Figure 3.7c, a combination of both kinds of one-dimensional gratings that were shown in (a) and (b) are present at once. This gives a regular two-dimensional grating. The lattice of the diffraction pattern in Figure 3.7c is necessarily, then, the “reciprocal” of the lattice of the original scattering objects (the crystal lattice) shown on its left; see Figure 3.7d. This will now be described.

The reciprocal lattice

In addition to the lattice of the crystal structure in real or crystal space (discussed earlier), there is a second lattice, related to the first, that is of importance in diffraction experiments and in many other aspects of solid state physics. This is the *reciprocal lattice*, introduced by Josiah Willard Gibbs in 1884, long before X-ray diffraction was known (Gibbs, 1901; Ewald, 1921). Its definition in terms of the crystal lattice vectors is shown in Appendix 3. In the reciprocal lattice a point, (hkl) , is drawn at a distance $1/d_{hkl}$ from the origin (the direct beam, (000)), and in the direction of the perpendicular distance between the (hkl) crystal lattice planes (Figure 3.7d). The relationship between these two important lattices (the crystal and reciprocal lattices) is a particularly simple one if the fundamental translations of the crystal lattice are all perpendicular to one another; then the

-
- (a) An overview of the envelope profile (equivalent to diffraction by a single slit or an atomic arrangement) and the sampling regions (equivalent to the diffraction of a series of equidistant slits or a crystal lattice). The envelope is accessed at the sampling regions only.
- (b) When diffraction occurs from two slits, there are two effects to consider:
- (1) The variation in intensity with angle as a result of interference of the waves generated within each slit separately. Interference between D_1 and E_1 and between D_2 and E_2 gives the “envelope,” as obtained for a single slit (see also Figure 3.3). This is the equivalent of diffraction by a single slit.
 - (2) The interference of scattered waves at a given angle with those at the same angle from the adjacent slit (D_1 with D_2 from the next slit, E_1 with E_2 from the next slit, etc.). At angles of constructive interference, when the two resultant waves are in phase, “sampling” of the “envelope” occurs, as shown in part (a). At certain other angles, no diffraction is observed. This sampling is the result of the distance between the two slits.

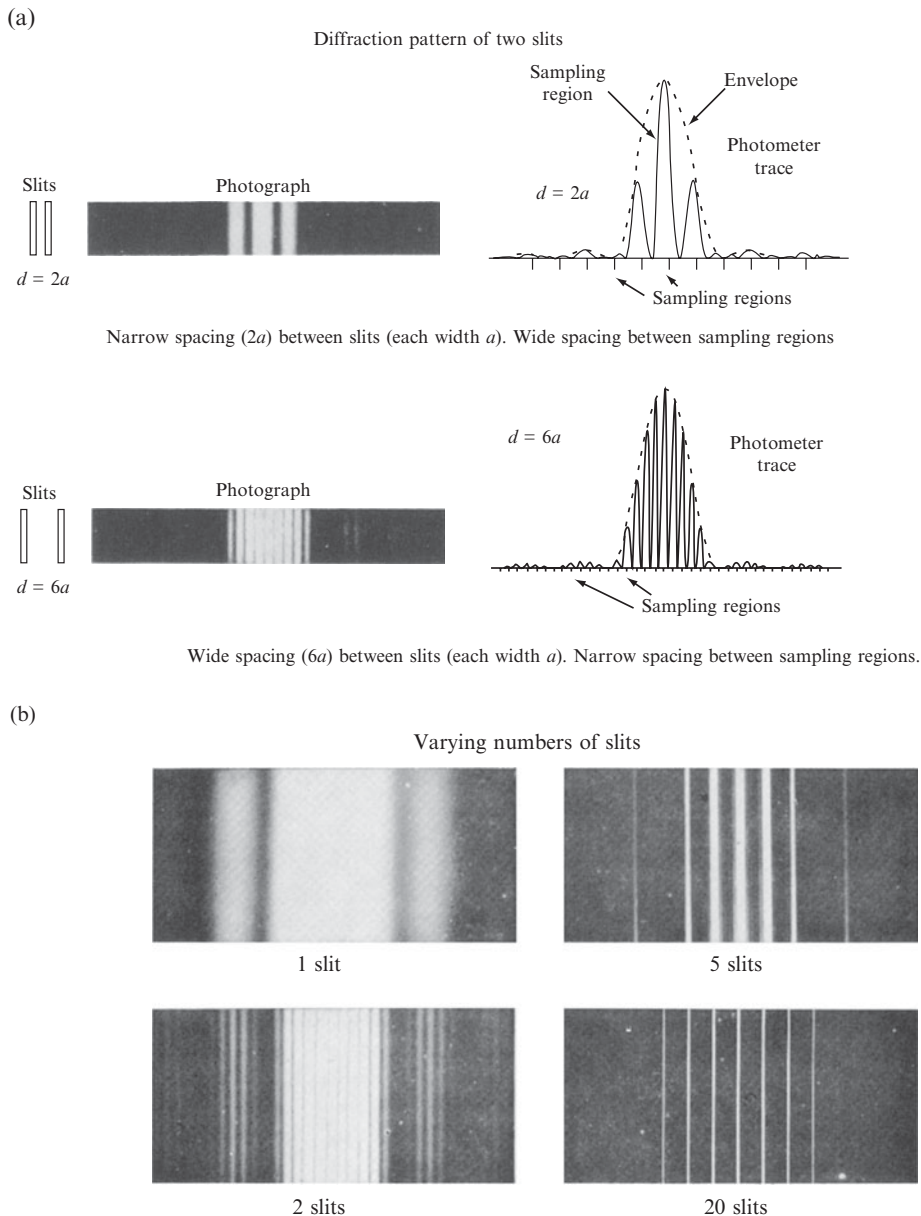


Fig. 3.6 Diffraction patterns from equidistant parallel slits.

- (a) The effect of varying the distance, d , between two slits of constant width, a , is shown. On the left is a diagram of the slits with spacings of $2a$ and $6a$, respectively, between them. In the center is shown a photograph of the diffraction pattern. On the right, a photometer tracing of the diffraction pattern for the combination of the two slits is drawn as a solid line, and the diffraction pattern for a single slit, referred to in the text as the "envelope," is drawn as a dashed line. The envelope in both cases has the same shape because it represents the diffraction pattern of a single slit of the same width. The regions of the "envelope" that are sampled are indicated by short vertical lines at the lower edge of the drawings on the right. When there is a relatively narrow spacing between the slits ($d = 2a$), the distance between sampling regions is relatively large, as shown in the upper diagram. When there is a relatively wide spacing between the slits ($d = 6a$), the distance between sampling regions has decreased; that is, there is an inverse relationship of the spacing of the sampling regions to the spacing of the slits.

fundamental translations of the reciprocal lattice are parallel to those of the crystal lattice, and the lengths of these translations are inversely proportional to the lengths of the corresponding translations of the crystal lattice. With nonorthogonal axes, the relationships between the crystal lattice and the reciprocal lattice are not hard to visualize geometrically; a two-dimensional example is given in Figure 3.7d. As we shall see shortly, the fundamental importance of the reciprocal lattice in crystal diffraction arises from the fact that *if a structure is arranged on a given lattice, then its diffraction pattern is necessarily arranged on the lattice that is reciprocal to the first.*[§]

Diffraction of X rays by atoms in crystals

It is a principle of optics that the diffraction pattern of a mask with very small holes in it is approximately equivalent to the diffraction pattern of the “negative” of the mask—that is, an array of small dots at the positions of the holes, each dot surrounded by empty space. This equivalence is discussed lucidly by Richard Feynman (Feynman et al., 1963). In a crystal, the *electrons in the atoms act, by scattering, as sources of X rays, just as the wavefront in the slits in a grating may be regarded as sources of visible light.* There is thus an analogy between atoms in a crystal, arranged in a regular array, and slits in a grating, arranged in a regular array. In diffraction of X rays by crystals, as of visible light by slits in a grating, the intensities of the diffraction maxima show a variation in different directions and also vary significantly with angle of scattering.

Most unit cells contain a complex assembly of atoms, and each atom is comparable in linear dimensions to the wavelength of the X rays or neutrons used. Figure 3.8a shows a typical X-ray diffraction photograph, taken by the “precession method,” which records the reciprocal lattice without distortion. Considerable variation in intensity of the individual diffracted beams is evident; this is a result of the arrangement of atoms (and their accompanying electron density) in the structure. The analogy with Figures 3.3, 3.5, and 3.6 holds; that is, *the X-ray photograph is merely a scaled-up sampling of the diffraction pattern of the contents of a single unit cell.* The “envelope,” which is shown by the

[§]This may be stated alternatively as follows. The diffraction pattern of a molecular crystal is the product of the diffraction pattern of the molecule (also called the molecular transform) with the diffraction pattern of the crystal lattice (which is also a lattice, the reciprocal lattice, described above). The result is a sampling of the molecular transform at each of the reciprocal lattice points. The diffraction pattern of a single molecule is too weak to be observable. However, when it is reinforced in a crystal (containing many billions of molecules in a regular array) it can be readily observed, but only at the reciprocal lattice points.

- (b) Diffraction patterns are shown for gratings containing 1, 2, 5, and 20 equidistant slits, illuminated by parallel radiation of the same wavelength. The diffraction pattern for a grating composed of 20 (or more) slits consists only of sharp lines, the intervening minor maxima having disappeared; similarly, the diffraction pattern for a crystal composed of many unit cells contains sharp diffraction maxima.

Summary of key points:

- (1) The size and shape of the envelope are determined by the diffraction pattern of a single slit.
- (2) The positions of the regions in which the envelope is sampled are determined by the spacing between the slits.

From *Fundamentals of Optics* by Francis A. Jenkins and Harvey E. White, 3rd edition (1957) (Figures 16E and 17A). Copyright © 1957, McGraw-Hill Book Company. Used with permission of McGraw-Hill Book Company.

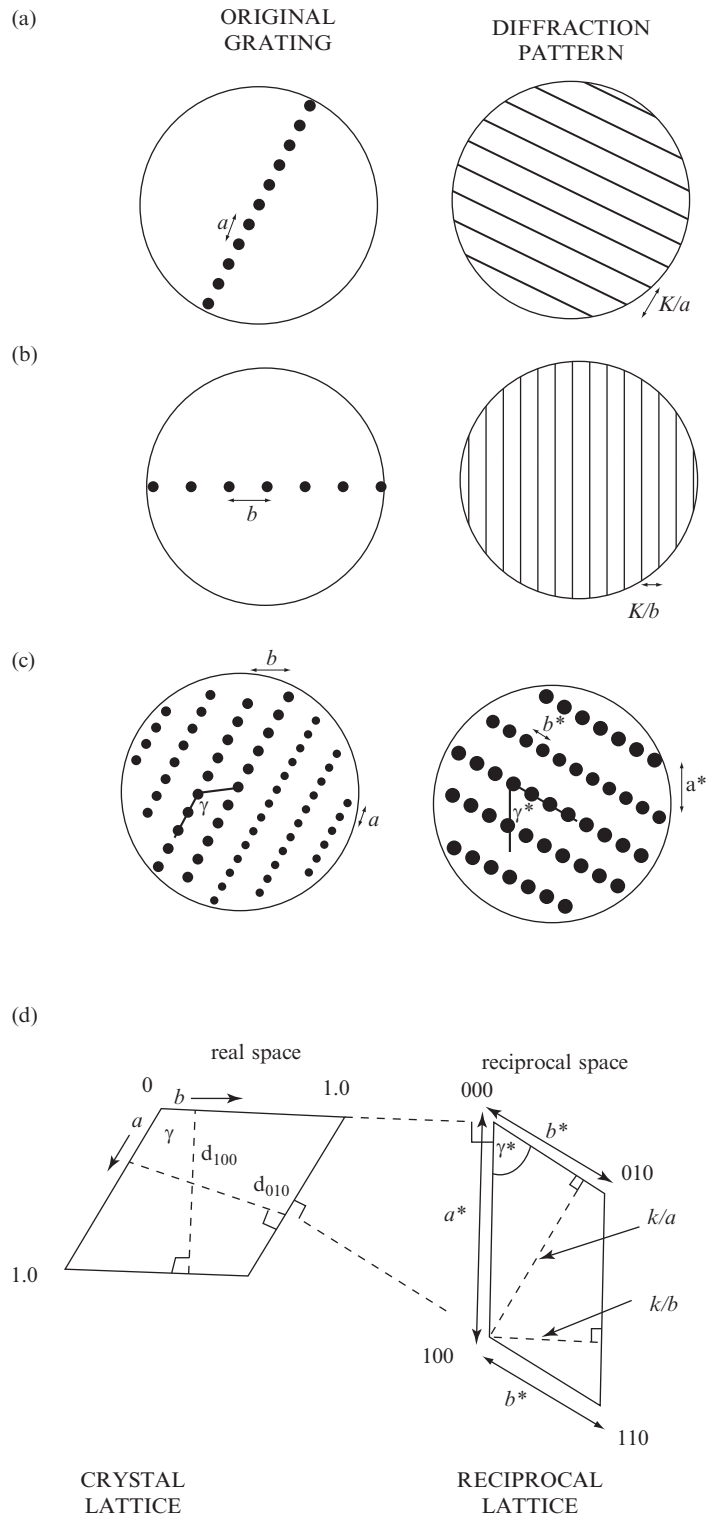


Fig. 3.7 Diagrams of diffraction patterns from one- and two-dimensional arrays. Relation between the crystal lattice and reciprocal lattice.

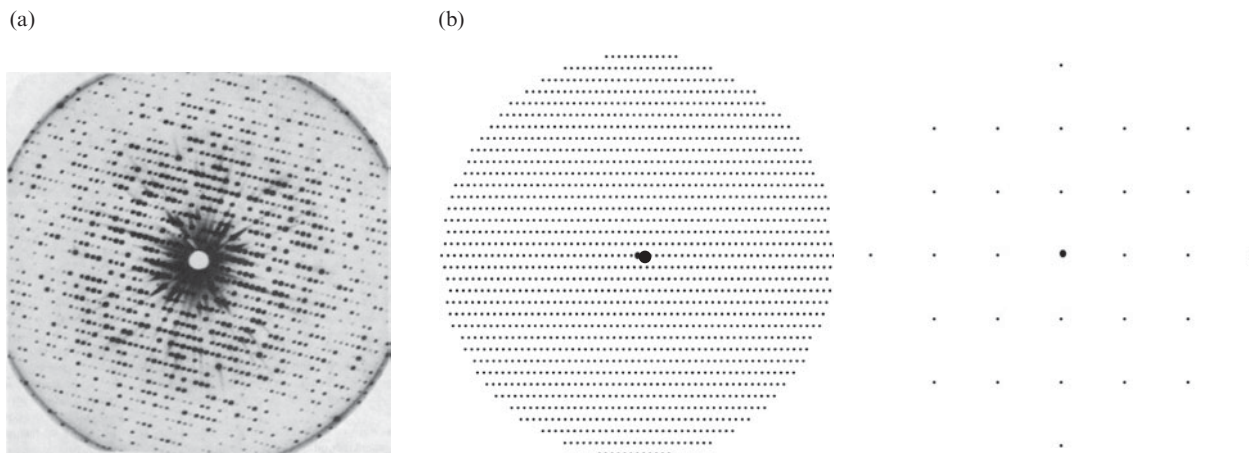


Fig. 3.8 X-ray diffraction photographs taken by the precession method.

- (a) The precession method gives an undistorted representation of one layer of the reciprocal lattice. An X-ray precession photograph of a crystal of myoglobin is shown here. The direct X-ray beam, which might otherwise “fog” the film, has been intercepted, hence the white hole in the middle of the photograph. The radial streaks, found for very intense Bragg reflections, occur because the X rays are not truly monochromatic (one wavelength) but contain background radiation of varying wavelength but lower intensity. As a result the spot appears somewhat smeared out (that is, for each Bragg reflection, $\sin \theta/\lambda$ is constant but since λ varies for the background “white radiation,” $\sin \theta$ must also vary, giving rise to a streak rather than a spot on the film). Note the regularity of the positions of spots in this photograph but the wide variation in intensity (from a very black spot to one that is almost or apparently absent). The positions of the spots (diffracted beams) give information on unit cell dimensions; the intensities of the spots give information on the arrangement of atoms in that unit cell.

Photograph courtesy Dr. J. C. Kendrew.

- (b) A comparison of diagrams of the diffraction patterns of myoglobin (large unit cell, monoclinic, $a = 64.5 \text{ \AA}$, $b = 30.9 \text{ \AA}$ not shown, $c = 34.7 \text{ \AA}$, $\beta = 106.0^\circ$) on the left and potassium chloride (small unit cell, cubic, $a = 6.29 \text{ \AA}$) on the right. The larger the unit cell, the nearer together the diffraction spots if the wavelength of the radiation is the same for both. Variations in Bragg reflection intensities are not shown in these diagrams. Note that many Bragg reflections are measured when the unit cell is large.

variation in intensities of the individual diffracted-beam spots, is the diffraction pattern of the scattering matter (the electrons of the atoms) in a single unit cell. The “sampling regions,” which are the positions of the diffracted-beam spots, are arranged on a lattice that is “reciprocal” to the crystal lattice. Measurements of the distances between these will lead to the dimensions of the unit cell, and they sample the diffraction

(a, b, c) On the left is shown the grating used and, on the right, the corresponding diffraction pattern (such as might be obtained by holding the original grating in front of a point source of light). **a** and **b** are direct lattice vectors in the crystal or grating, and **a*** and **b*** are vectors in the diffraction pattern (*a* and *b* are the spacings of the original gratings, and *a** and *b** are spacings in the diffraction pattern). The reciprocal relationships of *a* and *b* to the spacings of certain rows in the diffraction pattern are shown. These are diagrams, and no intensity variation is indicated. The black dots on the left-hand side represent holes that cause diffraction, giving the pattern on the right-hand side, in which black lines or spots represent appreciable intensity for diffracted light.

Adapted from H. Lipson and W. Cochran. *The Crystalline State. Volume III. The Determination of Crystal Structures*. Cornell University Press: Ithaca, New York; G. Bell and Sons: London (1966) (Lipson and Cochran, 1966).

(d) The relationships of **a** and **b** in the crystal lattice to **a*** and **b*** in the corresponding reciprocal lattice are shown.

pattern of a single unit cell. A comparison of the reciprocal lattices of the protein myoglobin (Figure 3.8a) with that of potassium chloride (with a much smaller unit cell) is shown in Figure 3.8b.

Some diffraction patterns of individual and assembled molecules are illustrated in Figures 3.9 and 3.10, which have been prepared using a special optical device that permits photographs to be made of the diffraction patterns of arrays of holes cut in an opaque sheet. By an appropriate choice of the optical components, the effective ratio of the wavelength of the light used to the sizes of these holes can be made similar to the ratio of X-ray wavelengths to the sizes of atoms. One can, then, simulate X-ray diffraction photographs of crystals by making patterns of holes in opaque sheets that are similar, except for scale, to the patterns of arrangement of the atoms in the crystals.

The relationship between the diffraction pattern of a single “molecule” and various “samplings” that can be produced by regular arrangements of such molecules are shown in Figure 3.9. The left-hand side of each part of the figure shows different arrangements of molecules and the right-hand side shows the corresponding diffraction patterns. This figure also shows, from the dimensions of the unit cell, that the lattice of the diffraction pattern is reciprocal to that of the “crystal”. Figure 3.9b shows the diffraction pattern of two “molecules” side by side (horizontally in the orientation shown here) and illustrates the interference arising from the interaction of the scattering by the two molecules, exactly analogous to the interference caused by the presence of two adjacent slits that gives rise to Figure 3.6a. Figure 3.9c shows the pattern arising from four “molecules” arranged in a parallelogram; now there is interference parallel to each of the two axes of the incipient crystal lattice. Figure 3.9d shows the diffraction pattern of an extended regularly spaced row of the molecules—that is, from a one-dimensional crystal; there is sharpening of the diffraction effects parallel to the direction of ordering, but no interference at all in other directions. Figure 3.9e shows the pattern obtained by placing two lengthy rows

-
- (c) Four molecules arranged in a parallelogram.
 - (d) Many molecules horizontally side by side (a one-dimensional crystal). Only part of the row is shown.
 - (e) Two rows of molecules arranged on an oblique lattice. Only parts of the rows are shown.

In comparing (e) with (d), note again the analogy with the relation of the one-slit and two-slit patterns of Figures 3.1 and 3.6.

- (f) Two-dimensional crystal of molecules. Only part of the crystal and part of the diffraction pattern are shown. Compare this with Figure 3.8a.

From C. A. Taylor and H. Lipson. *Optical Transforms. Their Preparation and Application to X-ray Diffraction Problems*. Plate 26. G. Bell and Sons, London (1964). Published with permission.

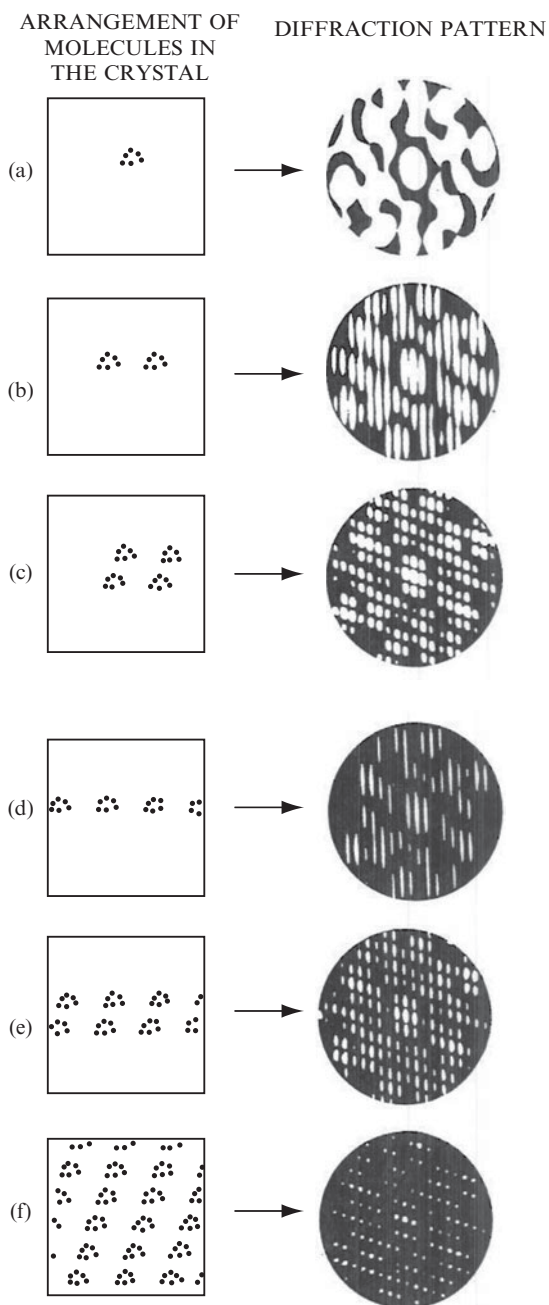


Fig. 3.9 The effect of different lattice samplings on the diffraction pattern.

This shows the relationship between the diffraction pattern of a "molecule" and various regular arrangements of such molecules. The optical mask is on the left (black points as holes) and its diffraction pattern is on the right.

(a) A single molecule.

(b) Two molecules horizontally side by side.

In comparing (b) with (a), note the analogy with the one-slit and two-slit patterns of Figures 3.1 and 3.6.

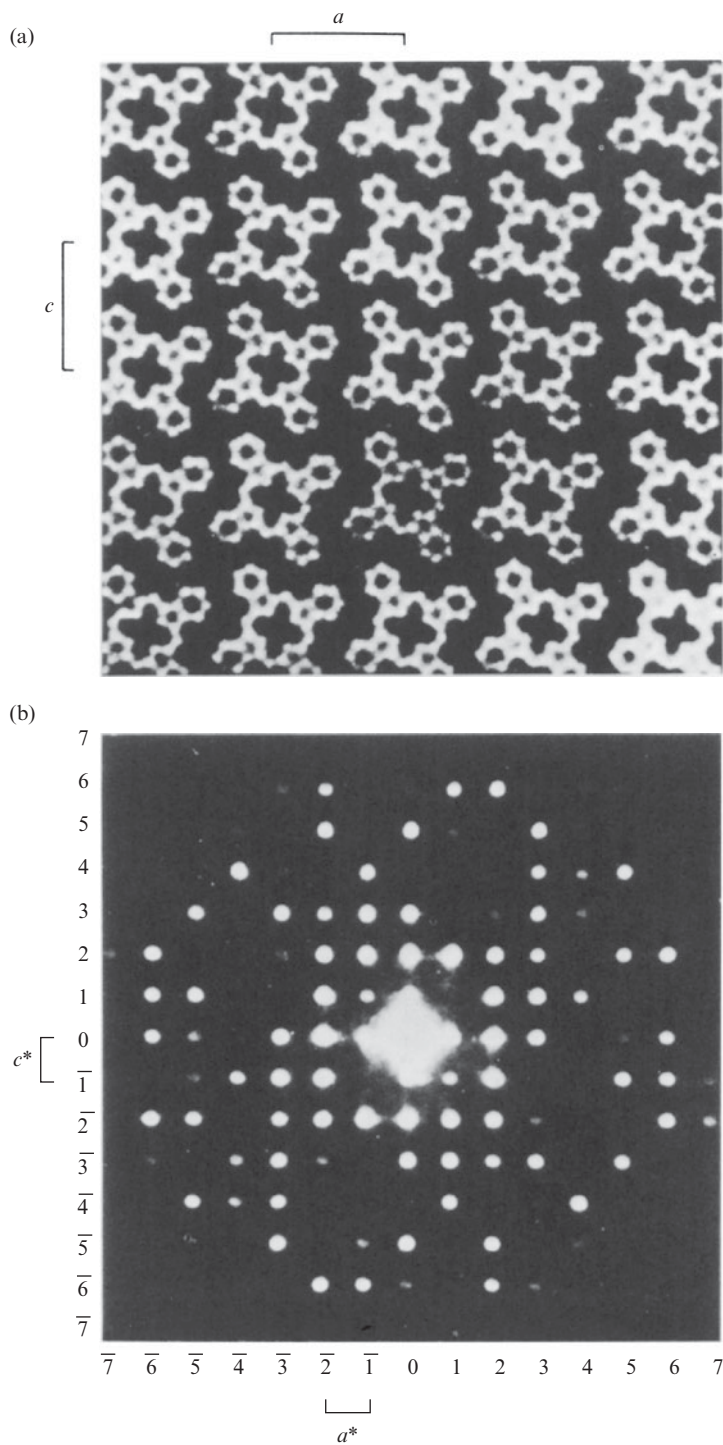


Fig. 3.10 The optical diffraction pattern of an array of templates resembling the skeleton of a phthalocyanine molecule.

side by side and, finally, Figure 3.9f shows the pattern obtained from a two-dimensional crystal of these “molecules.” The resemblance to the precession photograph in Figure 3.8a is good. Figure 3.9a is being sampled at reciprocal lattice points to give Figure 3.9f.

In Figure 3.10a arrays of holes, each of which has the shape of the skeleton of a phthalocyanine molecule, are shown, together with the optical diffraction pattern obtained (with visible light) from these arrays (Figure 3.10b). Note that the intensity variation in the optical diffraction pattern (shown as intensities in Figure 3.10b) parallels that found in the corresponding pattern obtained by the diffraction of X rays (listed in Figure 3.10c).

Diffraction and the Bragg equation: Two ways of analyzing the same phenomenon

Von Laue, who, with Friedrich and Knipping, discovered the diffraction of X rays by crystals in 1912, interpreted the observed X-ray diffraction

(c) Relative intensities for the phthalocyanine crystal

| $h \rightarrow$ | 0 | 1 | 2 | 3 | 4 | 5 | 6 | 7 |
|-----------------|----|----|----|----|----|----|----|----|
| 7 | 6 | 0 | 2 | 7 | 0 | 6 | 0 | 0 |
| 6 | 25 | 52 | 45 | 11 | 4 | 0 | 3 | 0 |
| 5 | 36 | 1 | 0 | 58 | 0 | 1 | 2 | 0 |
| 4 | 3 | 17 | 0 | 14 | 0 | 38 | 0 | 9 |
| 3 | 15 | 1 | 2 | 14 | 4 | 4 | 2 | 1 |
| 2 | 72 | 85 | 21 | 16 | 0 | 8 | 27 | 1 |
| 1 | 61 | 0 | 64 | 30 | 2 | 2 | 1 | 3 |
| 0 | | 94 | 72 | 10 | 0 | 2 | 17 | 1 |
| -1 | 61 | 29 | 55 | 0 | 2 | 7 | 10 | 5 |
| -2 | 72 | 46 | 23 | 3 | 0 | 0 | 18 | 14 |
| -3 | 15 | 37 | 14 | 10 | 2 | 21 | 2 | 0 |
| -4 | 3 | 13 | 0 | 10 | 18 | 2 | 1 | 0 |
| -5 | 36 | 0 | 18 | 3 | 19 | 0 | 0 | 0 |
| -6 | 25 | 5 | 35 | 5 | 2 | 0 | 1 | 0 |
| -7 | 6 | 0 | 2 | 0 | 14 | 2 | 0 | 0 |
| $l \uparrow$ | | | | | | | | |

From C. W. Bunn. *Chemical Crystallography: An Introduction to Optical and X-ray Methods*. 2nd edition. Plate XIV. Oxford at the Clarendon Press: Oxford (1961).

- The array used to obtain the optical diffraction pattern. This models a crystal structure of phthalocyanine.
- The optical diffraction pattern obtained from (a).
- Relative $h0l$ intensities measured from the X-ray diffraction pattern of a phthalocyanine crystal. Qualitative comparison of these values with the intensities of the corresponding spots in the optical diffraction pattern shown in (b) indicates that the model used is a surprisingly good one. *Note:* Intensities for $h0l$ and $-h0-l$ (not listed below) are equal.

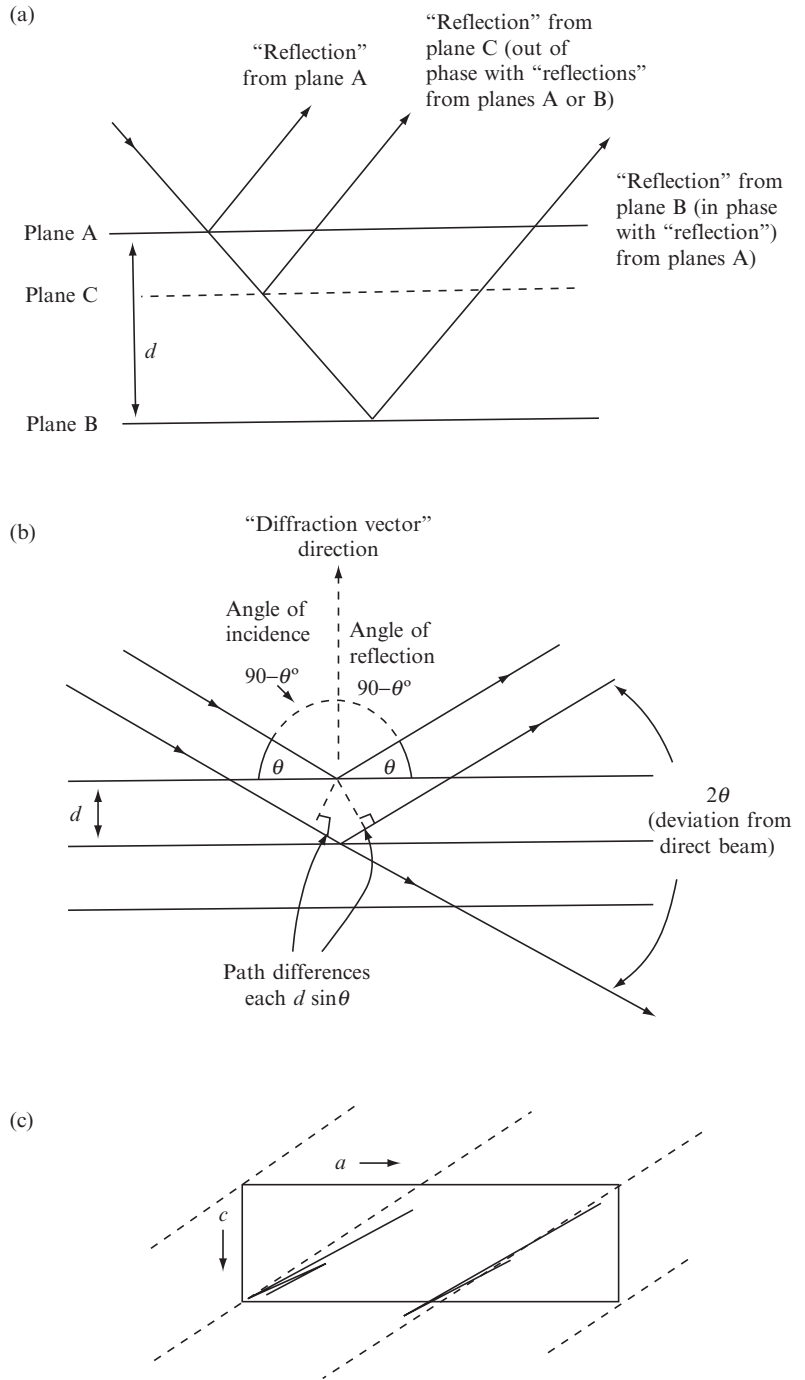


Fig. 3.11 Diagram of "reflection" of X rays by imaginary planes through points in the crystal lattice.

patterns of crystals in terms of a theory analogous to that used to treat optical diffraction by gratings, extended to three dimensions. On the other hand, William Lawrence Bragg, who worked out the first crystal structures with his father, William Henry Bragg, during the summer of 1913, showed that the angular distribution of scattered radiation could be understood by considering that the diffracted X-ray beams behaved *as if they were reflected* from planes passing through points of the crystal lattice (Bragg, 1913). This “reflection” is analogous to that from a mirror, for which the angle of incidence of radiation is equal to the angle of reflection, as shown in Figure 3.11a. Waves scattered from adjacent crystal lattice planes will be just in phase (i.e., the difference in the paths traveled by these waves will be an integral multiple of the wavelength, $n\lambda$) only for certain angles of scattering, as shown in Figure 3.11. From such considerations Bragg derived the famous equation that now bears his name:

$$n\lambda = 2d \sin \theta \quad \text{The Bragg equation} \quad (3.1)$$

In this equation λ is the wavelength of the radiation used, n is an integer (analogous to the order of diffraction from a grating, so that $n\lambda$ is the total path difference between waves scattered from adjacent crystal lattice planes with equivalent indices), d is the perpendicular spacing between the lattice planes in the crystal, and θ is the complement ($90^\circ - \theta$) of the angle of incidence of the X-ray beam (and thus also the complement of the angle of scattering or “reflection”). Since it appears as if reflection has occurred from these crystal lattice planes, so that the direct beam is deviated by the angle 2θ from its original direction, diffracted beams are commonly referred to as “reflections.” Because the Bragg equation is easily visualized, it is commonly presented in elementary discussions in diagrams such as those in Figures 3.11a and b; in Appendix 4 we show how it can be related to diffraction by a crystal lattice (as described above).

The Bragg equation can be derived by considering the path difference between waves scattered from adjacent parallel crystal lattice planes; the path difference must be an integral number of wavelengths

-
- (a) Constructive and destructive interference as waves are “reflected” from imaginary planes, spacing d , in a crystal. Constructive interference of planes A and B (the unit-cell repeat distance d apart), and partial destructive interference of plane C with A and B.
 - (b) Diffraction geometry. Since the path difference of waves scattered by two adjacent planes is $2d \sin \theta$, this must equal $n\lambda$ for total reinforcement to occur to give a diffracted beam (as illustrated in Figures 3.3, 3.4, and 3.5).
 - (c) Planes (2 0 1) in a crystal that has many atoms in its structure (see Figure 9.3d); the planes lie perpendicular to the plane of the paper. Note that the planes intersect the unit-cell edges once in the c direction and twice in the a direction. The 201 Bragg reflection is intense in this structure.

if constructive interference (reinforcement) is to occur. The equation is satisfied, and thus diffraction maxima occur, when and only when the relation of wavelength, interplanar spacing, and angle of incidence is appropriate. If a nearly monochromatic beam of X rays is used with a single-crystal specimen, diffraction maxima will be observed only for special values of the angle of incidence of the beam of X rays, and not necessarily for other arbitrary angles. If the crystal is rotated in the beam, it may be in a position (at certain rotation angles) to form additional diffracted beams. Therefore rotation of the crystal increases the number of observed Bragg reflections available for measurement. We use the term "Bragg reflections" for the diffracted beams to remind the reader that they will only occur when the angle of incidence of the X-ray beam is such as to satisfy Eqn. (3.1) for some set of crystal lattice spacings present in the crystal. This means that λ , d , and θ must all be such that the Bragg equation holds. The chance of this happening for a perfect crystal is low. However, real crystals have a mosaic spread (as if composed of minute blocks of unit cells, each block being misaligned by a few tenths of a degree with respect to its neighbors), and the X rays used are never truly monochromatic, so that, in practice, a Bragg reflection can be observed over a small range of θ and therefore some Bragg reflections are observed in almost any orientation of a single crystal. With a powdered crystalline specimen many different orientations of tiny crystallites are present simultaneously, and for any set of crystal planes, Eqn. (3.1) will be satisfied in some of the crystallites so that the complete diffraction pattern will be observed for any orientation of the specimen with respect to the X-ray beam. It is also possible to get a diffraction pattern from a stationary single crystal by the use of a wide range of wavelengths simultaneously. This was, in fact, the way in which von Laue, Friedrich, and Knipping did their original experiment; the technique is known as the *Laue method*, and is now currently used for studies of biological macromolecules with high-energy X rays (see Moffat et al., 1984).

The Bragg equation says nothing about the intensities of the diffraction maxima that will be observed when it is satisfied. If, however, a particular set of crystal lattice planes happens to coincide, in orientation and position, with some densely populated planar or nearly planar arrays of atoms in a crystal, and if there are no intervening densely populated planes, the corresponding diffraction maximum will be an intense one because the scattering from all atoms is approximately in phase. In an example cited in Chapter 9 (Figure 9.3d) involving a planar organic molecule, the "reflection" with indices $h = 2$, $k = 0$, $l = 1$ (written $2\ 0\ 1$, i.e., second order in h , direct for k , and first order for l) is very intense because the molecules lie nearly parallel to the crystal lattice plane with indices $(2\ 0\ 1)$ and are separated by a spacing very nearly the same as the interplanar spacing of this crystal lattice plane. This is shown in Figure 3.11c.

Summary

To explain what happens when a crystal diffracts X rays, we first examined optical analogies with slits and then with templates resembling two-dimensional crystals. The pattern of radiation scattered by any object is called the diffraction pattern of the object. For diffraction from a slit, the wider the slit the narrower the diffraction pattern for a given wavelength of radiation. The diffraction pattern of many parallel and equidistant slits consists of a sampling of the single-slit pattern in regions that are representative of the spacings between the slits.

For a series of several slits, the diffraction of light of a given wavelength leads to the information that:

- (1) The size and shape of the “envelope” of the intensity variation is determined by the characteristic diffraction pattern of a *single slit*. This intensity variation tells us the shape and size of the diffracting object.
- (2) The spacings between the “sampling regions” in this “envelope” are inversely related to the *spacings between the slits*. Thus the differences between diffracting objects are revealed by the distances between diffraction maxima.

These principles may be extended to three dimensions and to crystals, in which the electrons in the atoms act as scatterers for X rays, just as the areas within the slits behave as if they were scatterers for visible light. The diffraction pattern of a crystal is arranged on a lattice that is reciprocal to the lattice of the crystal. The analogy with the optical example holds; the X-ray photograph is merely a scaled-up “sampling region” of the diffraction pattern of a single unit cell, with the “envelope” being the diffraction pattern produced by scattering from the electrons in the atoms of the unit cell, and the “sampling regions” arranged on the lattice reciprocal to the crystal lattice. In an analogous manner, diffraction of X rays of a given wavelength by a series of unit cells in a crystal gives an envelope, related to the arrangement of atoms in the unit cell, and sampling regions, related to the unit-cell dimensions.

This phenomenon of X-ray diffraction by crystals can be considered in terms of a theory analogous to that of diffraction by gratings and extended to three dimensions (von Laue) or be considered in terms of reflection from planes through points in the crystal lattice (Bragg). While these two treatments are equivalent, we have chosen to emphasize the first approach because it provides more insight into the process of structure analysis by diffraction methods.

4

Experimental measurements

The analysis of a crystal structure by X-ray or neutron diffraction consists of three stages:

- (1) *Data collection.* This involves experimental measurement of the directions of scatter of the diffracted beams so that a unit cell can be selected and its dimensions measured. The intensities of as many as possible of the diffracted beams (Bragg reflections) from that same crystal are then recorded. These intensities depend on the nature of the atoms present in the crystal and their relative positions within the unit cell.
- (2) *Finding a “trial structure.”* This is the deduction by some method (such as one of those described in Chapters 8 and 9) of a suggested atomic arrangement (a “trial structure”). This is listed as atomic coordinates that have been measured with respect to the unit-cell axes. The intensity of each Bragg reflection corresponding to this trial structure can then be calculated (see Chapter 5) and its value then compared with the corresponding experimentally measured intensity in order to determine whether the trial structure is “good,” meaning that it is essentially correct.
- (3) *Refinement of the trial structure.* This involves modification (refinement) of a good trial structure until the calculated and measured intensities agree with each other within the limits of any errors in the observations (see Chapter 11). This is usually done by a least-squares refinement, although difference electron-density maps may also prove useful. The result of the refinement is information on the three-dimensional atomic coordinates in this particular crystal, together with atomic displacement parameters.

This chapter is concerned with the first of these stages, the experimental measurements. This is a rapidly changing area of science as more powerful and precise equipment and detection devices become available. The *experimental data* that may be derived from measurements of an X-ray or neutron diffraction pattern include:

- (1) The *overall appearance* of the Bragg reflections at the detection system. Ideally these diffraction maxima should be sharp,

well-resolved peaks. Blurred, double spots or arcs may indicate disorder or poor *crystal quality*.

- (2) The *angles or directions of scattering* (including 2θ , the angular deviation from the direct beam).^{*} These can be used to determine the order, hkl , of each Bragg reflection and lead to a selection of a *unit cell* and a measurement of its *size and shape*.
- (3) The *intensities, $I(hkl)$* , of the diffracted beams, which may be analyzed to give *the positions of the atoms* within the unit cell.

^{*} See Figure 3.11 for a diagrammatic definition of θ .

The result is a set of values— $2\theta, h, k, l, I(hkl)$ —and some measure of the precision, $\sigma(I)$, for each Bragg reflection. The diffraction pattern is uniquely characteristic of the atomic identities and arrangement in the particular crystal under study, and will only be the same for other crystals of the same material grown under the same conditions and having the same unit-cell dimensions and atomic composition. This means that a diffraction pattern can serve as a “fingerprint,” and can be used for identifying material.

The experimental setup

The apparatus that is used to measure an X-ray diffraction pattern has the same configuration as that used in the very first diffraction experiment in 1912. The overall setup, illustrated in Figure 4.1, consists of:

- (1) *The crystal that has been selected for study*. It is checked to ensure that it is a single crystal and is mounted in the measurement apparatus so that the incident radiation can pass through it and be diffracted by it.
- (2) *An incident beam of radiation*. This is a fine pencil-like beam of X rays or a larger beam of neutrons directed at the crystal. The source of such radiation may be an X-ray tube, a synchrotron source, or neutrons from a nuclear reactor or spallation source. The beam may be monochromatic (one wavelength) or polychromatic (many wavelengths, known as “white radiation”).
- (3) *A system to detect the diffraction pattern*. This is usually an image plate or a charge-coupled device that can detect, measure, and electronically record the directions and intensities of Bragg reflections. Measurements may be serial (one Bragg reflection at a time) or may involve as much as possible of the entire diffraction pattern. The apparatus that aligns the incident beam, crystal, and detector, ready for measurement, is a diffractometer.

There have been many improvements to these components of the setup through the years and they are now significantly more efficient and “user-friendly.” Advances in their design have now made it possible to study the crystal structures of extremely large biological

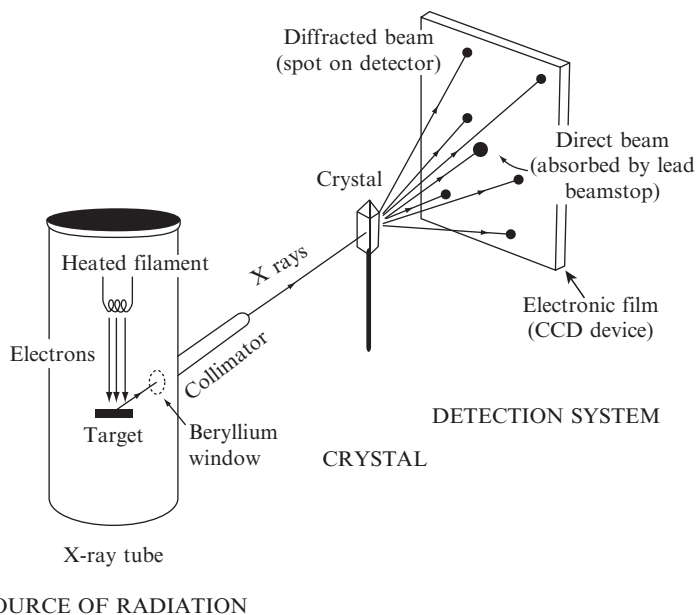


Fig. 4.1 The diffraction experiment.

The experimental setup used by von Laue, Friedrich, and Knipping to measure X-ray diffraction intensities in 1912. The important components of the experimental equipment consist of an X-ray source that provides a finely collimated beam of radiation, a crystal that can scatter this radiation, and a detection device that can detect the diffraction pattern and measure the directions and intensities of the diffracted beams. Currently this same arrangement of equipment is used by X-ray crystallographers, but each component is now much more sophisticated.

macromolecules (Blundell and Johnson, 1976; Helliwell, 1992; McRee, 1993; Drenth, 1999).

Selection of a suitable crystal

A crystal whose structure is to be determined should be a single crystal, not cracked or a conglomerate. This may be checked by examining it under a microscope, with polarized light, since most crystals are birefringent** (Blundell and Johnson, 1976; Wahlstrom, 1979; Hartshorne and Stuart, 1950). In the polarizing microscope two Nicol prisms each transmit only plane-polarized light, that is, light vibrating in a specific direction. One prism, the polarizer, produces plane-polarized light and the other prism, the analyzer, is only able to transmit light if the two prisms are in the same orientation. They are set perpendicular to each other so that no light can pass through. An optically isotropic crystal placed between the prisms will not change this, but if the crystal is birefringent and is rotated on the stage, it will show sharp extinction of light at four rotation positions 90° apart. These extinctions occur when the vibration directions of the Nicol prisms are the same as those of the

** One crystal form of the enzyme citrate synthase is cubic (Rubin et al., 1983) and shows no birefringence when a test tube containing crystals is shaken.

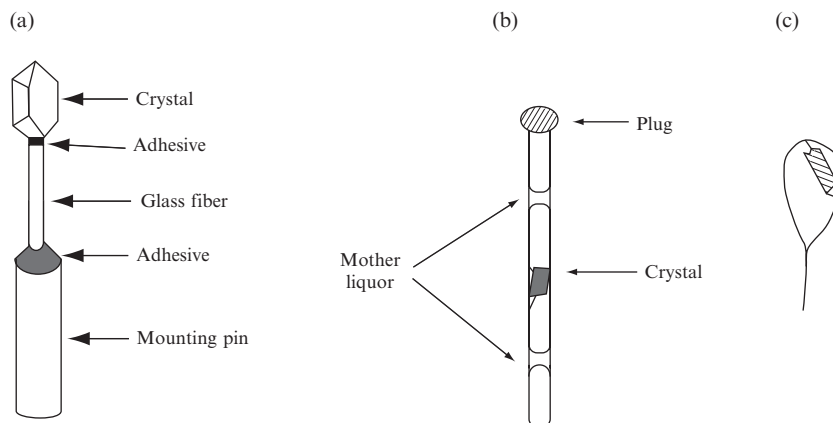


Fig. 4.2 Mounting a crystal.

Methods for mounting crystals. (a) A crystal mounted on a glass fiber, as used for a small-molecule crystal that does not decompose on exposure to air. (b) A crystal that does not diffract if it dries out is mounted in a sealed capillary tube with its mother liquor. (c) A protein crystal frozen on a thin film of solvent in a loop.

crystal under examination. Generally, if multiple crystals are present, only one part of the crystal will extinguish, and others will extinguish on further rotation of the crystal (Bunn, 1961). In this way one can check that a crystal is single.

If the crystal is too large, and therefore will not be fully bathed by the incident X-ray beam, it may be possible to cut it safely with a razor blade or with a solvent-coated fiber. Ideally one can try to find a crystal that can be shaped, often by grinding, until it is approximately spherical so that corrections for absorption of X rays are simplified. Some crystals, however, are too soft, fragile, or sensitive even for a delicate cutting and must be used as they have grown. For example, crystals of macromolecules contain 30–70% water, sometimes more, and they break very readily because the forces between such large molecules are weak in view of the macromolecular size; therefore attempts to cut the crystals may destroy them (Bernal and Crowfoot, 1934; McPherson, 1982; Bergfors, 2009).

The ultimate test of how good a crystal is comes from an inspection of the diffraction pattern obtained. Crystals are mounted on an aligning device (such as a goniometer head, see Figures 4.2 and 4.3), so that they can be positioned in the direct X-ray or neutron beam, ready for diffraction. The centering of the crystal in the beam is checked by rotating and viewing it through a microscope to make sure the center of the crystal is fixed in space during the rotation, and therefore does not move out of the incident beam during data collection.

A crystal to be studied is generally attached to a glass fiber with glue or some similar material. If the crystal is unstable, it is put into a thin-walled glass capillary tube (generally by gentle suction or simple capillary action) and the capillary is then sealed. An appropriate atmosphere is then maintained in the capillary to ensure stability of the crystal;

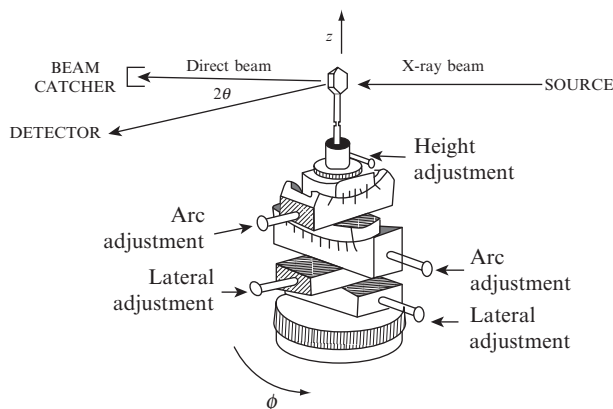


Fig. 4.3 Centering a crystal.

A goniometer head is used for orienting and centering a crystal in the incident X-ray beam. The goniometer arcs and lateral adjustments provide the means for the crystallographer to orient the crystal so that, in spite of reorientations of the centering device during data collection, the crystal is always centered in the incident X-ray beam. The angle ϕ and the position z define the orientation and height of the crystal.

for example, protein crystals require a small amount of mother liquor to prevent drying out and disordering or collapse of the crystalline structure. The fiber or capillary is fixed onto a brass pin by shellac or glue and this pin is then attached to the diffraction equipment, as shown in Figure 4.2. For biological macromolecules, such as enzymes, it is currently more usual to capture the crystal in a tiny loop (made of rayon, nylon, or plastic and attached to a tiny rod). The crystal is mounted or positioned for cryocrystallography in the thin film that forms when the small loop is immersed in real or synthetic mother liquor, as shown in Figure 4.2c; the crystal in the loop is then flash-cooled in liquid nitrogen. The aim of this cooling is to reduce radiation damage caused by the X rays, but it can sometimes cause the crystal to crack or form ice on its surface; therefore it may be necessary to soak the crystal in a cryoprotectant solution, such as glycerol, prior to cooling. Cooling will also increase the maximum resolution of the diffraction data and the value of $I(hkl)/\sigma(I)$. The crystals are then kept at a low temperature (just above the boiling point of nitrogen) for data measurement. If its quality is still poor the crystal can be annealed by warming the crystal, and then flash-cooling it for a second time (Harp et al., 1998). Newer methods of crystal mounting continue to be designed and reported on in the literature.

Radiation damage usually occurs as a result of free-radical formation and heating effects; it will continue after X-ray exposure has stopped. It is generally believed that such radiation damage can be reduced by the use of incident monochromatic X rays, or by lowering the temperature with appropriate attention to the solvent. If a small group of Bragg reflections is measured at regular intervals throughout a sequential measurement process, it will be possible to determine the amount of

crystal decay as a function of time. In practice, each Bragg reflection is affected in a unique manner, depending on the nature of the atomic movement during damage, but an average fall-off in intensity will give some (but not precise) information that is suitable for use in correcting intensities for radiation damage. A neutron beam generally does not cause any radiation damage to the crystal.

Unit-cell dimensions and density

The dimensions of the unit cell ($a, b, c, \alpha, \beta, \gamma$) can be found from the angles, 2θ , of the deviation of given diffracted beams from the direction of the incident beam, because each value of 2θ at which a diffraction maximum is observed is a function only of the cell dimensions and of the known wavelength of the radiation used, see Appendix 1. The spatial orientation of these diffracted beams allows indexing so that the determination of cell dimensions is simplified; however, it is also possible to determine unit-cell dimensions from powder photographs.

The density of the crystal can be measured by flotation, but generally the value is now assumed to be the same as that of crystals with a similar composition. Most crystals of organic compounds have a density near 1.3 g cm^{-3} , otherwise described as 18 \AA^3 per atom, excluding hydrogen atoms. For macromolecular crystals, which may have a high water content, the Matthews coefficient (V_M , volume per dalton of protein), calculated as the unit-cell volume, V , divided by the molecular weight, MW, times the number of asymmetric units in the unit cell, Z , should lie in the range 1.7 to 3.5 \AA^3 per dalton (average near 2.3) (Matthews, 1968; Kantardjieff and Rupp, 2003):

$$\text{Matthews coefficient } V_M = V / \{Z \text{ times MW}\} \text{ cubic \AA per dalton} \quad (4.1)$$

If the nature of the atomic contents of the crystal is uncertain, it still may be necessary to measure its density. Experimentally, this is done by mixing two miscible liquids in which the crystal is insoluble (one more dense, one less dense than the crystal) in such proportion that the crystal remains suspended in the mixture (it neither sinks nor rises to the surface of the resulting mixture). The density of the liquid mixture (with the same density as that of the crystal) is then found by weighing a known volume in a "specific gravity bottle" or "pycnometer." For macromolecules, a "density gradient column" is prepared by layering an organic liquid (in which the protein is insoluble) on another that is miscible with the first. This column can be calibrated by measuring the equilibrium positions along the column of drops of aqueous solutions of known density. Some protein crystals are then added to the column and their equilibrium positions read; these positions can be directly converted to densities using the previously prepared chart. As seen in Appendix 1, the density of the crystal, combined with its unit-cell dimensions, will give the weight of the contents of the unit cell. If the elemental analysis of the crystal is known, then the number of each type

of atom in each unit cell can be determined. Then a decision can be made whether or not to proceed with a structure analysis.

The Bragg reflections to be measured

The Bragg equation (Eqn. 3.1) is only satisfied for a few diffracted beams if the crystal is stationary. Therefore it is usual to oscillate the crystal in order to obtain more diffraction data. The maximum number of Bragg reflections that can be accessed, N , will depend on appropriate oscillation of the crystal, the wavelength λ of the radiation, the volume V of the unit cell, and the number n of crystal lattice points in the unit cell, according to the formula

$$N = (4\pi/3)(8V/n\lambda^3) \quad (4.2)$$

How do we tell which Bragg reflections can be measured with a selected arrangement of the diffraction-measuring apparatus? There is a geometric construction that does exactly this. It is the Ewald sphere, named after Paul Ewald, who was involved in discussions with von Laue that led to the first crystal diffraction experiments in 1912 (Ewald, 1913). For the crystal under consideration, the Ewald sphere is a sphere of radius $1/\lambda$ (for a reciprocal lattice with dimensions $d^* = 1/d$), drawn with its diameter along the incident beam direction. This is shown in the diagrams of its construction in Figure 4.4. The origin of the reciprocal lattice is positioned at the point at which the incident beam emerges from the Ewald sphere. The reciprocal lattice is then rotated about its origin (in the same manner as that planned for data measurement). Whenever a reciprocal lattice point P touches the surface of the Ewald sphere, the conditions for a diffracted beam are satisfied. A Bragg reflection, with the hkl indices of that reciprocal lattice point P , will result. Thus, for a particular orientation of the crystal relative to the incident beam, it is possible to predict which reciprocal lattice points and thus which Bragg reflections will be observed. If radiation of a different wavelength is used, the radius $1/\lambda$, drawn in the Ewald sphere, can be adjusted accordingly, and the angles through which the crystal is rotated can be accounted for.

The incident radiation: X rays or neutrons

X rays are produced, as mentioned in Chapter 3, when a high voltage is applied between a cathode and an anode in an evacuated glass bulb; this voltage causes the cathode to emit fast-moving electrons,[†] and they are directed at the anode (a metal target), and are suddenly decelerated when they hit it. As a result of this impact, X rays are emitted. The intensity of this initial source of X rays is controlled by the applied voltage and amperage. A diagram of an X-ray tube is provided in Figure 4.5. X ray-tubes have a relatively low flux and the background

[†] The type of diffraction discussed in this book is referred to as “kinematical diffraction” and assumes that the incident beam is diffracted and leaves the crystal. In “dynamical diffraction,” which is particularly evident in electron diffraction, the diffracted beams interact with the crystal and each other (Ewald, 1969). This repeated scattering makes analysis of the diffraction pattern much more complicated.

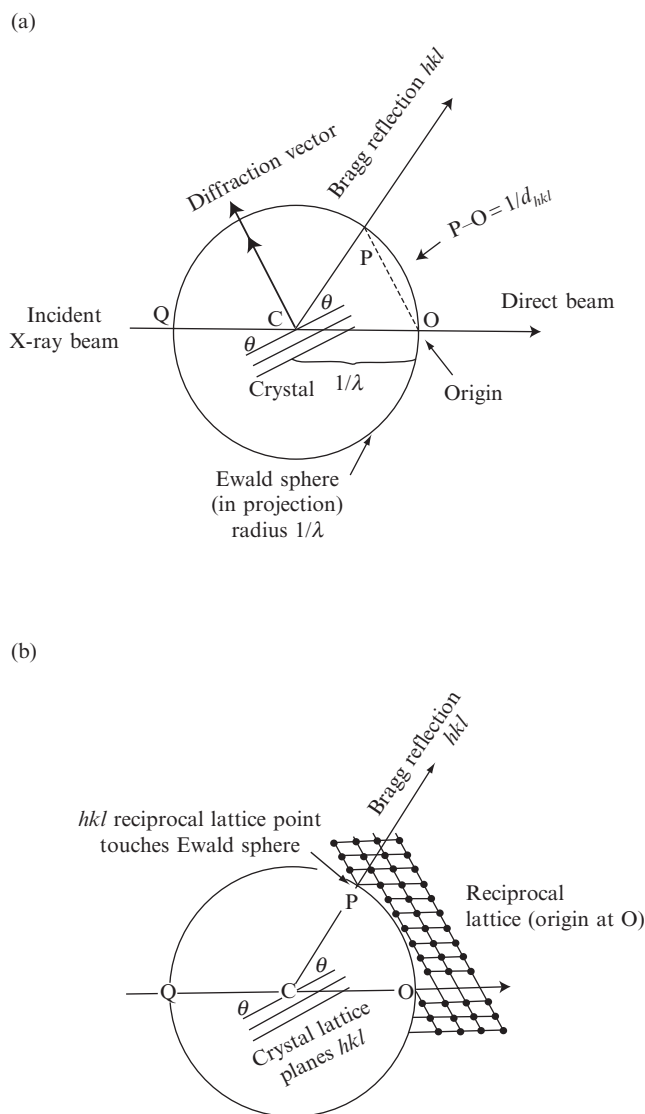


Fig. 4.4 The Ewald sphere (sphere of reflection).

(a) A sphere of radius $1/\lambda$ is drawn. (b) The origin of the reciprocal lattice, drawn on the same scale, is placed with its origin on the surface of the sphere, at O. When a reciprocal lattice point hits the surface of the Ewald sphere, a Bragg reflection will occur. To increase the likelihood of this happening the crystal is rotated in the diffractometer, an event that is represented in the Ewald construction by a similar rotation of the reciprocal lattice. If white radiation is used, it will be necessary to draw spheres at the two limits of radiation.

radiation is appreciable, unless filters or a monochromator are used. The greater the intensity of radiation from an X-ray tube, the more extensive the diffraction pattern (since weak Bragg reflections are made visible) and the better the signal-to-noise ratio. Since diffracted beams are much weaker in intensity than the direct (undiffracted) beam, it is

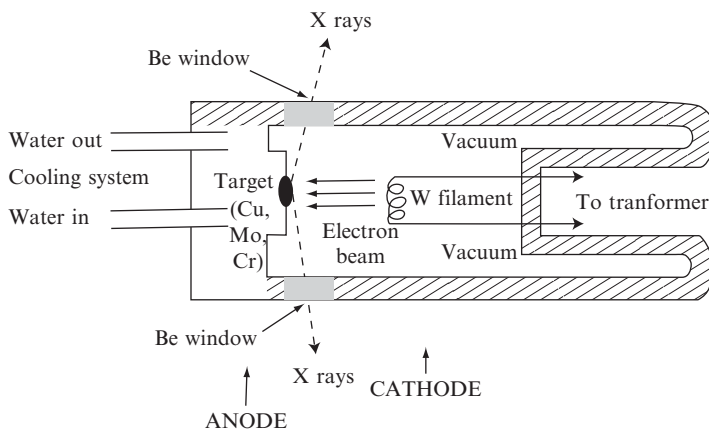


Fig. 4.5 An X-ray tube.

Diagram of the structure of an X-ray tube. Electrons are emitted from the tungsten filament (cathode) and are attracted to the target in the anode. On hitting the target (Cu, Mo, Cr, for example), X rays are emitted and exit the tube through beryllium windows.

necessary to intercept the direct beam by means of a small metal cup (a “beam stop”) so that the detection system is not overloaded by the high intensity of the direct incident beam of X rays.

Two types of X rays are produced in the X-ray tube (see Figure 4.6a). The first has the label “Bremsstrahlung,” which means “braking radiation” (in German), and is produced when accelerated electrons are suddenly decelerated by a collision with the electrical field of an atom in the metal target of an X-ray tube. This radiation, which generally serves as background, has a continuous spectrum. The kinetic energy of the fast electrons has been converted into radiation, including X rays. The second type of radiation, called “characteristic radiation,” is produced when the fast electrons cause a change in the atom that they hit; this change is the ejection of an electron from an inner shell of an atom in the metal target anode. When another electron from an outer shell of the same atom moves to fill the void left by the ejected electron, an X ray photon will be emitted with a wavelength representative of the difference between the energy levels of the ejected electron and of the electron that takes its place. The X-ray spectrum obtained is therefore characteristic of the metal in the target anode. It is approximately monochromatic, and all but one narrow wavelength band can be selected and used for diffraction studies. Characteristic X rays from copper and molybdenum target anodes (wavelengths 1.54 \AA and 0.71 \AA , respectively) are most commonly used in X-ray diffraction experiments, but many other targets are available for use when necessary. The X rays are labeled by the shell of the ejected electron (K, L, M, etc.) and the number of shells that the replacement electron has passed through (α for one shell, β for two, etc.) (see Figure 4.6b). For example, $K\alpha$ radiation corresponds to a transition from $n = 2$ to $n = 1$ (the innermost, highest-energy atomic level, where n is the principal quantum number

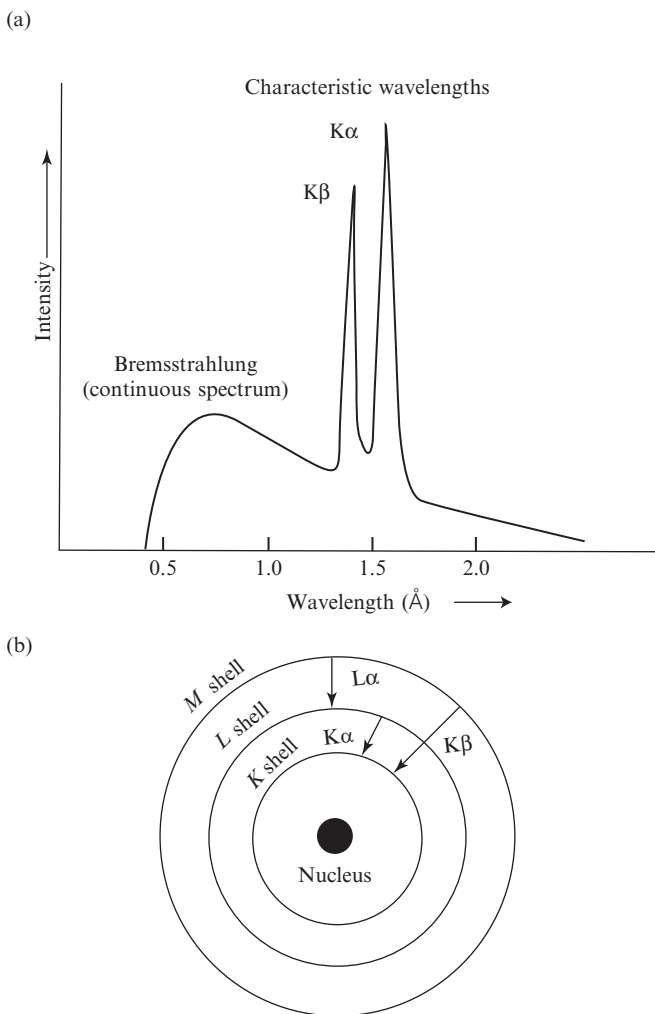


Fig. 4.6 Energy levels and X rays.

(a) The characteristic X-ray spectrum of copper radiation, produced with a copper target in the X-ray tube. (b) X rays are labeled by the shell of the ejected electron (K, L, M, etc.) and the number of shells the replacement electron has passed through (α for one shell, β for two, etc.).

of a shell). This means that when a K-shell vacancy is formed, it is filled by an electron from the adjacent L shell, and $K\alpha$ radiation is emitted. $K\beta$ radiation corresponds to a transition from $n = 3$ to $n = 1$; that is, a K-shell vacancy is filled by an M-shell electron, and so forth.

A monochromator, which transmits only a mechanically selectable small range of wavelengths (its bandpass) from a larger range, is used to tune X rays to a required wavelength. One type of monochromator selects (by slits) a single Bragg reflection from an appropriate crystal, such as one of graphite, silicon, germanium or copper, and this selected Bragg reflection becomes the new incident beam for diffraction studies.

Another type employs optical methods, that is, a combination of a collimating mirror, a diffraction grating, and a focusing mirror, to give the required spectral range; X rays can be focused by mirrors if the angle of incidence is extremely small (less than 0.1°). Sometimes two monochromators are used, acting in tandem.

A major problem when X rays are produced in a sealed tube (as just described) is that considerable heat is generated and must be eliminated, for example by cooling the tube with flowing water. It has been found that if the anode is rotated at high speed and the fast-electron beam is directed at its outer edge, this heat can be dissipated, and, as a result, it becomes possible to generate more intense X rays. This is the principle of the *rotating-anode generator*, and, because of the high flux of the X rays produced, it is possible to measure extensive diffraction data for crystalline biological macromolecules.

Synchrotron radiation, however, currently provides the most intense X rays suitable for diffraction studies. The emission of radiation is a property of accelerated charged particles. Electromagnetic radiation (which includes X rays) is emitted when accelerating electrons, traveling at near the speed of light, are forced, by a magnetic field, to travel in a circular orbit, as in an electron storage ring. The wavelength of this radiation will depend on the strength of the magnetic field, the speed of the electrons, and the size of the storage ring. These factors can be appropriately chosen and combined to give a good source of X rays. Synchrotron radiation has very high intensity (and therefore is good for single-crystal diffraction studies), and low divergence (so that there is good intrinsic collimation, a large signal-to-noise ratio, and a high resolution). It is also highly polarized (which is useful for distinguishing electronic from magnetic scattering) and is emitted in short pulses (which facilitates fast time-resolved studies). It is multiwavelength (white) radiation and, if a single wavelength is required, selection (tuning) with a monochromator is essential. Its range of wavelengths is wide, so that selection can be made of radiation near the absorption edge of an atom contained in the crystal; therefore anomalous-dispersion experiments, as described in Chapter 10, can be done.

Another type of radiation used in crystal diffraction studies consists of neutrons (Bacon, 1975; Dianoux and Lander, 2003; Willis and Carlile, 2009). Neutron diffraction can provide information that complements that from X-ray diffraction. Neutrons are uncharged particles, highly penetrating, but their beams are relatively weak, and, when not in nuclei, they decay with a mean lifetime of about 15 minutes. They were discovered by James Chadwick in 1932, and were subsequently shown to be diffracted by crystals (even though they are particles) (Chadwick, 1932; von Halban and Preiswerk, 1936; Mitchell and Powers, 1936).[‡] This dual identity of neutrons is in line with the postulate of Louis Victor de Broglie in 1923 that particles and waves should have both particle-like and wavelike properties (de Broglie, 1923). Their wavelength can be calculated from his equation $\lambda = h/mv$, where λ is the wavelength, m is the mass of a neutron (1.67×10^{-24} g), v is its

[‡] This was long after von Laue studied diffraction of X rays by crystals in 1912 and therefore decided that X rays are waves (Friedrich et al., 1912).

velocity, and h is Planck's constant ($6.626 \times 10^{-34} \text{ kg m}^2 \text{ s}^{-1}$) (Planck, 1901). The faster the neutron, the shorter its apparent wavelength.

X-ray diffraction probes the electron-density arrangement in the crystal, while neutron diffraction probes the positions of atomic nuclei in the crystal. Therefore, when the results of X-ray and neutron diffraction by a crystal are compared, a large amount of structural and chemical information, for example, on the asymmetry of the electron distribution around a particular atomic nucleus, is obtained. This will be described later in Chapter 12. Neutrons also have a spin of $1/2$ and therefore can also be used to probe the magnetic structure of a material.

Neutrons are generally produced at nuclear reactors, so that it is necessary to visit a national atomic energy center for neutron diffraction studies. A large number of neutrons are produced in a reactor by nuclear fission. They may also be produced at spallation sources. The word "spallation" describes the ejection of material on impact. Neutrons are obtained at a spallation source when short bursts of high-energy protons bombard a target of heavy atomic nuclei (such as mercury, lead, or uranium); each proton produces several high-energy neutrons in a pulsed manner. Slow neutrons with wavelengths of 1 to 2 Å are required for diffraction studies. Therefore fast neutrons produced by either of these two processes must be slowed down by moderators (such as heavy water) that reduce their kinetic energy and provide neutrons with wavelengths that are approximately the same as those used for X-ray diffraction studies. For further information on the practical aspects of neutron diffraction, there are several excellent texts (Bacon, 1975; Wilson, 2000; Willis and Carlile, 2009).

Equipment for diffraction studies

When X rays are used for crystal diffraction studies, it is found to be necessary, in order to get a large number of Bragg reflections, to oscillate or rotate the crystal, or to use polychromatic radiation (the Laue method). The general geometry of the detection system is shown in Figure 4.7. The relationship between the diffraction pattern and the crystal orientation is diagrammed in Figure 4.8. While the crystal lattice defines the crystal, the reciprocal lattice (Figure 4.9) represents the diffraction pattern, and this information is useful when interpreting the diffraction pattern in terms of Bragg reflections.

We first briefly describe the old film methods, as they are part of the literature on the subject and they illustrate some of the principles that the reader needs to know. Then we proceed to the more modern methods. The old methods mostly involve photographic film; this is a good X-ray detector, but has now been superseded by more efficient electronic devices. To take an oscillation or rotation diffraction photograph, a crystal, mounted on a goniometer head, is either rotated continuously in one direction (to give a rotation photograph) or oscillated back and forth through a small angle (to give an oscillation photograph). The

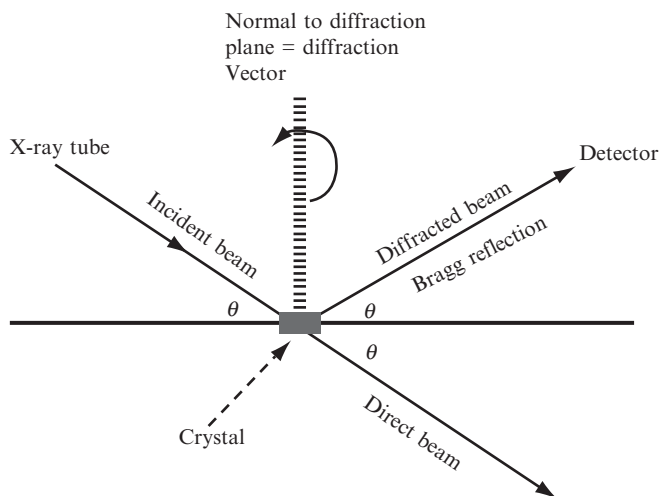


Fig. 4.7 Source, crystal, and detector.

Diagram of the relative arrangement of the X-ray source, the detector, and the crystal and their relationship to the diffraction vector. All are in the same plane.

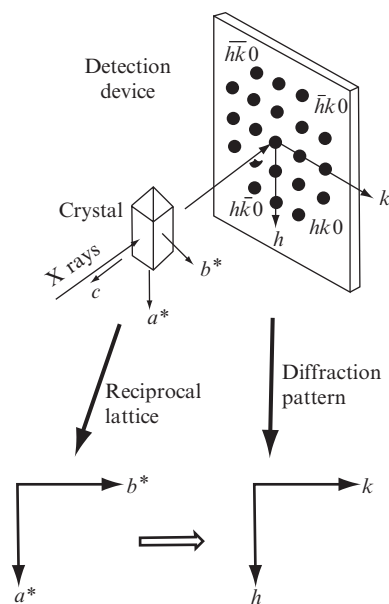


Fig. 4.8 The relation between the crystal orientation and the diffraction pattern.

The relative orientation of the reciprocal lattice of a crystal (expressed here as a^* and b^*), and its indexed X-ray diffraction pattern (expressed here as h and k). Note the relationship of a^* to h and b^* to k . From the positions of diffracted beams on the detection device it is possible to deduce the dimensions of the reciprocal lattice and hence of the crystal lattice; hence the indices h , k , and l of each Bragg reflection.

resulting diffraction pattern is recorded on photographic film placed around the crystal. If the axis of rotation or oscillation is perpendicular to the X-ray beam, the resulting photograph contains lines (layers) of Bragg reflections (see Figure 4.10). As can be seen in this figure, many of the Bragg reflections overlap each other, so that indexing them may be difficult. Therefore the Weissenberg camera was invented, in which the camera is moved as the crystal is rotated or oscillated. Only one layer from an oscillation photograph is selected, by the positioning of a metal screen with a slit in it, between the film and the X-ray source (Weissenberg, 1924). The crystal is oscillated back and forth, while the slit ensures that only one layer of Bragg reflections (for example, a specific value for the h index) is recorded on the film. At the same time the camera moves in a direction parallel to the axis of crystal oscillation. The most important feature is that the motion of the camera is coupled to the oscillation of the crystal, which helps in interpreting the photograph. Bragg reflections on a Weissenberg photograph can therefore be more readily indexed than on an oscillation photograph.

An even more useful type of X-ray diffraction photograph is produced by a precession camera (Figures 3.8a and 4.11) (Buerger, 1964). It gives an undistorted view of one selected plane of the reciprocal lattice. This makes it particularly useful for measuring unit-cell dimensions and assigning a space group to the crystal. Here the camera motion is more complicated in order that the recorded image of the diffraction pattern may be simple. In fact, direct measurement of all reciprocal lattice parameters is possible from a series of precession photographs, with an appropriate scale factor taken into

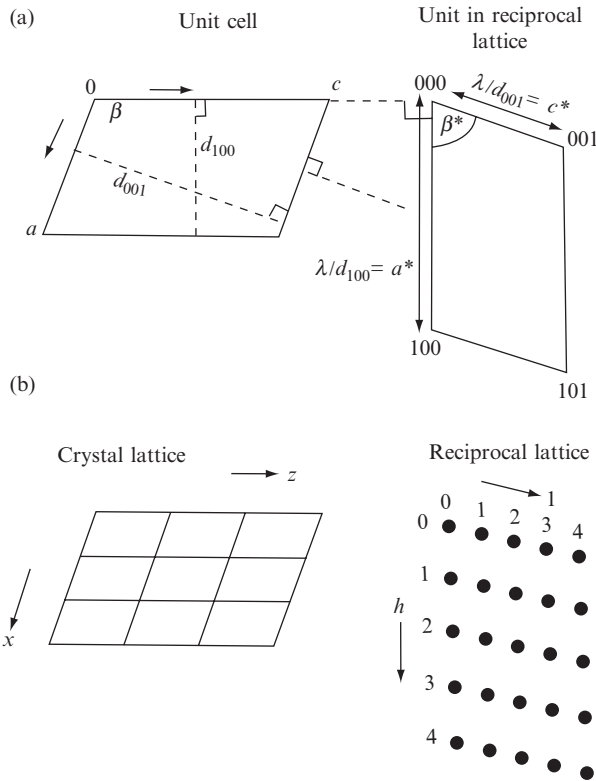


Fig. 4.9 The reciprocal lattice.

(a) The relationship between the unit cell of a crystal and its reciprocal lattice. (b) Indexing of a reciprocal lattice.

consideration. An axis of the crystal perpendicular to the required reciprocal lattice plane is inclined by an angle μ (typically 30°) to the direct incident X-ray beam, and this then precesses (like the motion of a toy spinning top) about the incident X-ray beam. The flat film holder, which has an annular screen that isolates a single plane of the reciprocal lattice, follows the precession motion, ensuring that the film is always parallel to the selected reciprocal lattice plane of the crystal being photographed. It does this in such a way that the direct beam always hits the center of the film. The photograph that results from this complicated set of motions is simple to interpret. This method is very useful for triclinic crystals and for macromolecular crystals.

Generally, crystal symmetry, crystal lattice constants, and diffraction data are currently measured with a diffractometer (Figure 4.12). The incident radiation may be X rays from a sealed tube, a rotating anode, or a synchrotron source, or it may be a neutron beam. A diffractometer requires a collimated incident beam and a beamstop to collect that part of the direct beam that has passed undeflected through the crystal. The

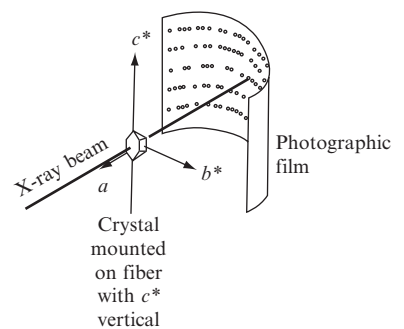
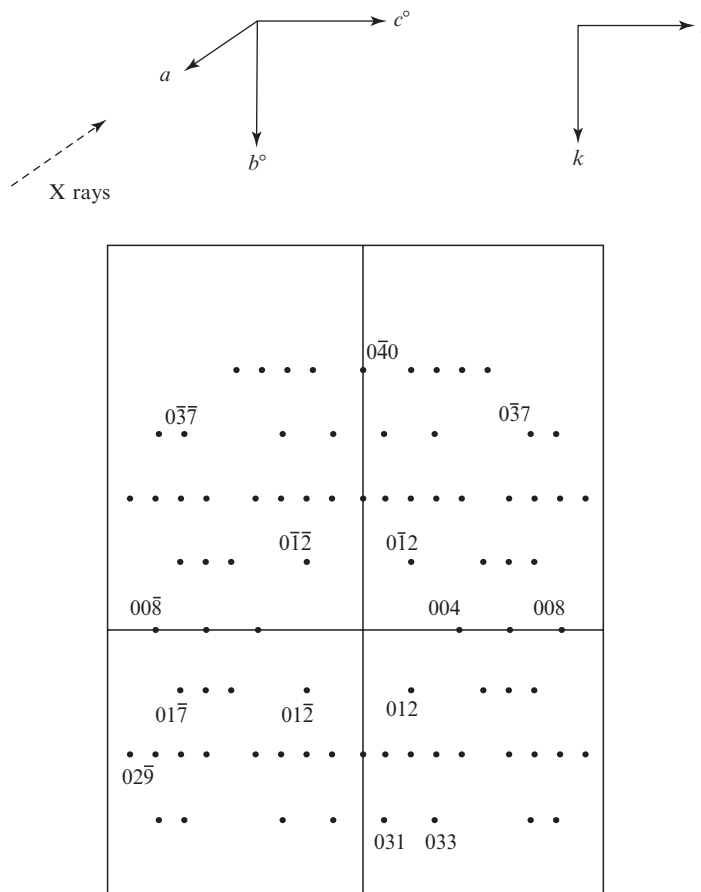


Fig. 4.10 Layer lines.

An X-ray diffraction photograph is obtained from a crystal mounted with the reciprocal lattice axis, c^* , vertical. On oscillation about this vertical axis the diffraction pattern shows layer lines, each with a constant value for the index l along them.



PARTIALLY INDEXED PRECESSION PHOTOGRAPH

Fig. 4.11 Indexing a precession photograph.

The indexing of Bragg reflections on a precession photograph. Note the systematic absences— $0k0$ with k odd and $00l$ with l odd. By convention the positive direction of a is toward the X-ray source.

detection system is an image plate or a charge-coupled device, rarely photographic film. Many modern diffractometers do not require any orientation of the crystal, only centering of the crystal, so that no matter how the instrument is oriented the crystal is always centered in the incident beam. A goniometer head can, however, be used to align the crystal, if required. Protein crystals, mounted with mother liquor in a capillary, are also put in a centering device. While both imaging with film and digital signaling are employed for the detection of diffracted radiation, they operate in different ways. A film records light as the result of a series of chemical reactions, while charge-coupled devices convert light (caused when X-ray photons hit a phosphor) directly into a digital signal.

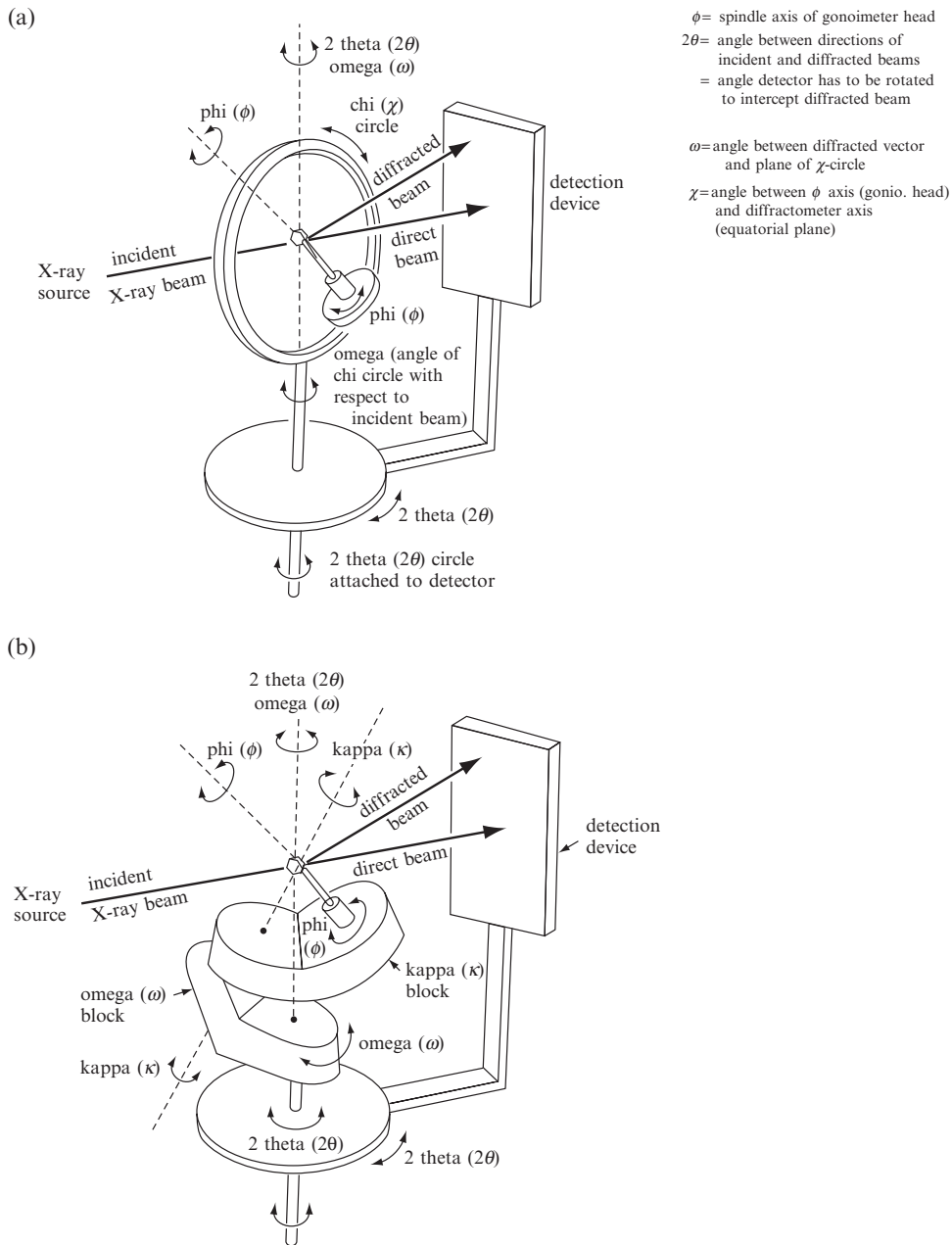


Fig. 4.12 An automatic diffractometer.

(a) A four-circle diffractometer. The crystal is mounted on a goniometer head, for which the spindle axis is ϕ . The goniometer head is attached to the χ circle. The angle χ is the angle between the ϕ axis of the goniometer head and the base of the diffractometer. The χ circle can be rotated about the ω axis, where ω is the angle between the diffraction vector and the plane of the χ circle. The detector is moved on the 2θ circle, where 2θ is the angle between the incident and diffracted X-ray beams. The detection device can be an image plate or a charge-coupled device. The setup for serial measurement is shown here. (b) A diffractometer with kappa (κ) geometry. The omega block rotates about the base plate while the kappa block rotates about the omega block as shown. This simulates the chi circle motions in the instrument in (a) but avoids clashes.

There are several types of diffractometers. Some move a detector to measure each Bragg reflection sequentially, and some employ a flat detection device, an “area detector,” that measures a large number of Bragg reflections at one time. The source of radiation is usually fixed in space and, in a sequentially measuring diffractometer, the required angular settings for the crystal and detector with respect to the incident beam are calculated in advance once a few Bragg reflections have been located and identified. This type of diffractometer is composed of several mechanical circles that rotate the crystal or the detection system with respect to the X-ray beam, as shown in Figure 4.12a. In this “four-circle diffractometer” the crystal can be rotated around three axes (χ , ϕ , and ω) independently, and the detector can be rotated about a fourth angle (2θ , concentric with, but independent of, ω), in the equatorial plane parallel to the base of the instrument. The crystal is mounted on a goniometer head and can be rotated about the vertical ϕ axis (phi) of this mounting (see Figure 4.12a). The goniometer head is mounted on the χ circle, which tilts the crystal about the horizontal χ axis (chi). The 2θ circle is attached to the detector device. This is concentric with the ω circle that rotates the sample. The χ circle is mounted on top of the ω circle, and the ϕ circle is mounted on top of the χ circle. Usually the entire instrument is controlled by a computer and the data collection is then done automatically. There are also diffractometers that utilize the kappa (κ) geometry (Figure 4.12b). This type of diffractometer was designed specifically to reduce mechanical clashes during data collection. The ω , ϕ , and 2θ circles remain, but the χ circle is replaced by a κ block that sits on the ω block (which replaces the ω circle) and this controls the orientation of the crystal and its goniometer head.

If the measurement is to be sequential, the intensity of a Bragg reflection is measured with the detector and recorded, together with measurements of the background intensity near the Bragg reflection, and then a new set of angles is calculated and another intensity measurement made. One normally advances incrementally through the Miller indices, hkl . In this way a systematic scan of all desired Bragg reflections is done completely automatically. Alternatively, if the crystal is stationary and white radiation is used, an image plate or charge-coupled device will be positioned to receive and record as many as possible of the diffracted beams. For this Laue diffraction, the incident radiation is white radiation with a range of wavelengths. It has proved useful for studies of enzyme reactions (Hajdu et al., 1987). For example, a crystal of the enzyme glycogen phosphorylase *b* was mounted in a flow cell and substrate solution was passed over it. Laue photographs (stationary crystal, white radiation) were taken with synchrotron white radiation (over 10,000 Bragg reflections per second) at a series of times after initiation of the biochemical reaction. A comparison of electron-density maps from the various data sets showed the course of the reaction as a substrate was converted to product (by phosphorylation).

Detection systems

The intensities of the diffracted beams are measured by intercepting the beams with a detecting material or device that is sensitive to X rays. The intensity at the peak of the diffraction spot is measured, or, better, the peak profile is scanned. Measurements of background counts are also made, or calculated from the profile of the peak, and used to correct the recorded intensities. Measurements may be done electronically or photographically and may concentrate on one diffracted beam at a time (as is often done with a diffractometer) or on many diffracted beams at the same instant (as with electronic analogues of photographic film).

The simplest detection device for X rays is photographic film. This contains silver halide in an emulsion on its surface. When the film is developed, black metallic silver is deposited at the positions at which the diffracted beams hit the photographic film. The darkness of each spot so formed is a measure of the intensity of the diffracted beam. These intensities can be measured with a film scanner. Film is not used much nowadays, because of the development of electronic detection devices (with superior detection capabilities) and current problems in obtaining photographic film suitable for X-ray studies.

Electronic detectors of X rays that have an appreciable area for detection of the diffraction pattern, and offer the possibility of resolving and individually measuring the intensities of diffraction maxima at different points across this area, are now preferred. They consist of scintillation counters, television-enhanced scanning devices, image plates, and charge-coupled devices, and are the equivalent of electronic film. Position-sensitive detectors can measure the position at which a Bragg reflection hits the detection device. These various devices represent the development of improved ways of recording a diffraction pattern electronically in a computer-readable manner, and image plates and charge-coupled devices are the current instruments of choice for this. Whereas photographic film records photons through a series of chemical reactions, charge-coupled devices convert light directly into a digital signal. Scintillation counters make use of the ability of certain substances to emit visible light by fluorescence when X rays hit them. The intensity of the emitted light is measured by a photomultiplier tube. Similarly, television area detectors contain a phosphor that produces visible light when hit by X rays. The photon signal is intensified and then detected by a television photocathode. These methods of detection are now less used than image plates and charge-coupled devices. Neutrons, which lack any charge, and readily penetrate materials, are detected by gas or scintillator detectors; these are similar to the X ray detectors described above (Wilson, 2000).

An image plate is a storage phosphor on which a latent image is formed when X rays hit it. It contains plastic sheets with powdered

phosphor crystals, doped with divalent europium ions, on their surfaces. When X rays hit these sheets, the divalent europium ions are converted to metastable trivalent ions and the electrons that are liberated are stored ready for release when scanned by a laser beam of visible light. When trivalent europium ions are encountered, blue light (wavelength 3900 Å) is emitted that can be scanned and converted to a digital image. This latent image has to be read; it is exposed to laser light, which causes the emission of light of a different wavelength, which is then detected. The image plate can then be erased, ready for the next use, while the data from the scanning of the latent image, which are in a computer-readable form, are then ready for use in structure determination. The location of the direct beam is evident on the image, and from the positions of diffracted beams it is possible to determine the direction, as well as the intensity, of each Bragg reflection. Neutrons can only be detected if they have undergone some reaction that results in the emission of energetic charged particles; this means that a converter must be used. Neutron image plates contain elements such as gadolinium (which has a very high neutron, but not proton, capture cross-section, or stopping power) that absorb neutrons and act as a converter to enable the neutrons to emit electromagnetic radiation (such as gamma rays), which can be detected like the X rays in the description above.

Charge-coupled devices are used widely in X-ray diffraction equipment. They are two-dimensional grids of radiation-sensitive semiconductor capacitors that have the capability of transferring charge between their neighbors. They acquire a charge when hit by a photon, and electron-hole pairs are generated by the photoelectric effect. The total charge that is built up is a measure of the number of photons that have been detected (the radiation intensity), and it is collected in an array of electrodes. The charge and position of each pixel are transferred as a result of a differential voltage across the electrodes, and the data are read and digitized by a computer (see Ladd and Palmer, 2003). This gives an immediate computer listing of the intensity and position on the detection device, and therefore this device is closer to a direct detector than is an image plate.

When white radiation is incident on a crystal, as in the Laue method, it is necessary to know the wavelength of the radiation that causes a particular Bragg reflection. The time-of-flight neutron diffraction technique depends on the fact that neutrons with different energies (wavelengths) travel at different speeds. Therefore a measurement of the time of flight will reveal the wavelength of the diffracted beam (generally selected from a multiwavelength incident beam). The instant at which the diffracted beam hits the crystal and then impacts on the detection system is measured and recorded. This, with the known distance traveled, gives the velocity of the neutron and hence its wavelength. Therefore the wavelength of each diffracted neutron can be measured.

Preparing measured $I(hkl)$ for subsequent analysis

Since the intensity $I(hkl)$ of any radiation propagated as a wave is proportional to the square of its amplitude, $|F(hkl)|$ the intensity of the diffracted beam corresponding to the diffraction maximum for each set of planes hkl is proportional to $|F(hkl)|^2$. Modifications to $I(hkl)$ are necessary in order to correct for the geometry of measurement. Weak Bragg reflections are measured carefully, rather than being ignored. Of the various correction factors that are used, the Lorentz factor takes into account the time that it takes for a Bragg reflection, represented as a reciprocal lattice point with a finite size, to cross the surface of the sphere of reflection; the longer the time, the higher the intensity. The Lorentz factor equalizes the time taken to measure each Bragg reflection. The polarization factor depends on the state of polarization of the incident X-ray beam; X rays are polarized on scattering, with reduction of the intensity of the Bragg reflection. Corrections for absorption of X rays by the crystal are also made; ideally, the path lengths through the crystal of many component waves of each diffracted beam are computed, and the diminution in intensity resulting from absorption can then be determined. Semiempirical absorption corrections, based on the intensity variation as certain intense Bragg reflections are scanned while the crystal is rotated, are more generally used. If a crystal is strongly absorbing for the radiation used, it may be shaped (with a scalpel or razor blade) until it is approximately spherical so that absorption corrections may be more uniform. Generally it is better to avoid using a crystal larger than the primary beam, although this may be necessary for protein crystals that are damaged by the X-ray beam, so that one can move the crystal to an undamaged area during data collection. The aim is to keep the amount of matter exposed to radiation independent of the crystal orientation.

It is then possible to determine the absolute value (without phase) of the structure factor $F(hkl)$ from these measurements, as follows:

$$\begin{aligned} I(hkl) &= k_1 \{\lambda^3 V_c \text{Lp Abs} / \omega V^2\} |F(hkl)|^2 = K \{\text{Lp Abs}\} |F(hkl)|^2 \\ &= k_2 |F(hkl)|^2 \end{aligned} \quad (4.3)$$

where k_1 , k_2 , and K are constants, V_c is the volume of the crystal that is bathed in the incident beam, V is the volume of the unit cell, Lp consists of the Lorentz and polarization factors, Abs is an absorption correction, and ω is the angular velocity of the crystal. Thus, values of $k_2 |F(hkl)|^2$ and hence of $k_2^{1/2} |F(hkl)|$ are immediately available once intensity measurements have been made. The values of Lp and Abs contain only known quantities and therefore can readily be computed for each Bragg reflection.

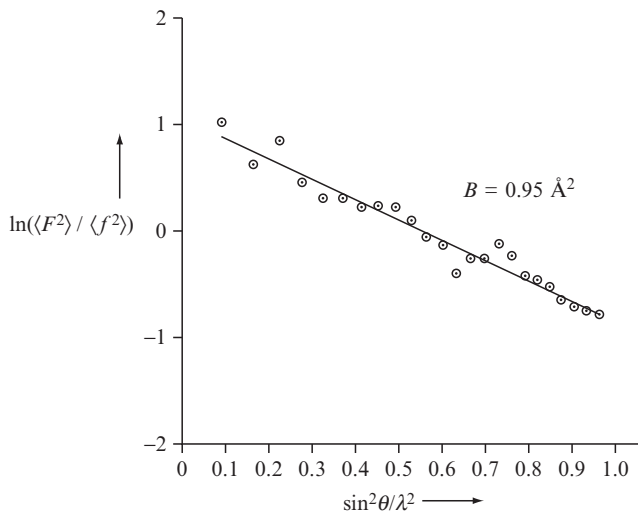


Fig. 4.13 Wilson plot.

A Wilson plot of $\sin^2 \theta / \lambda^2$ versus the logarithm of a function of the measured structure factors, $F(hkl) = F$. The slope gives an overall measure of the displacement factors. The intercept gives the scale factor necessary to obtain intensities on an absolute scale.

If the value of $I(hkl)$, corrected for Lp and Abs, is called I_{corr} , we can say

$$I_{\text{corr}} = I(hkl) / \{Lp \text{ Abs}\} = K |F(hkl)|^2 = K |F_{\text{novib}}|^2 \exp(-2B_{\text{iso}} \sin^2 \theta / \lambda^2) \quad (4.4)$$

where $|F_{\text{novib}}|$ is the value of $|F(hkl)|$ for a structure composed of non-vibrating point atoms. The application of the Lp correction involves no knowledge of the structure. An estimation of Abs can be made from a knowledge of the shape, orientation, and composition of the crystal. The value of $|F(hkl)|$ so derived contains information on the atomic displacement factors, B . Thus $F = |F_{\text{novib}}| \exp(-B_{\text{iso}} \sin^2 \theta / \lambda^2)$ (see Trueblood et al., 1996). It is possible to derive B_{iso} and K in Eqn. (4.4) from the experimental data by a "Wilson plot" (Wilson, 1942). It is assumed that, to a first approximation, the average intensity of Bragg reflections at a certain value of 2θ depends only on the atoms present in the cell, not on their positions—that is, that the arrangement of atoms in the crystal structure is random. By comparison of the averages of the observed intensities in ranges (shells) of $\sin^2 \theta / \lambda^2$ with the theoretical values for a unit cell with the same atomic contents, approximate values for K and B_{iso} can be found from the Wilson plot (Figure 4.13). Values of the resulting scale factor K can then be used for preparation of a full list of values of $|F(hkl)|$ on an approximately absolute scale (relative to the scattering by one electron) for all Bragg reflections measured. The value of B_{iso} obtained from this graph will indicate the extent of disorder from unit cell to unit cell in the crystal structure.

The reader should note that the intensity, $I(hkl)$, is a simple function of the structure amplitude $|F|$. However, an inspection of Eqn. (4.4) shows that *each value of $|F(hkl)|$, and hence of the intensity, $I(hkl)$, of the diffracted beams contains, with few exceptions, a contribution from every atom in the unit cell.* The unraveling of these contributions makes the structure solution complicated.

Summary

The diffraction of a crystal by X rays results from the constructive and destructive interference of the X rays that have been scattered by each individual atom in the structure. Three types of experimental diffraction data may be obtained:

- (1) The angle of scattering (2θ , the angular deviation from the direct undeviated beam), which is used to measure the spacings of the reciprocal lattice and hence the spacings of the crystal lattice. These spacings can be used to derive the size and shape of the unit cell.
- (2) The orders of diffraction (hkl) of each diffracted beam.
- (3) The intensities of the diffracted beams, $I(hkl)$, which may be analyzed to give the positions of the atoms within the unit cell. These atomic positions are usually expressed as fractions of the unit-cell edges.

This page intentionally left blank

DIFFRACTION PATTERNS AND TRIAL STRUCTURES

**Part
II**

This page intentionally left blank

The diffraction pattern obtained

5

In this chapter we will describe those factors that control the intensities of Bragg reflections and how to express them mathematically so that we can calculate an electron-density map. The Bragg reflections have intensities that depend on the arrangement of atoms in the unit cell and how X rays scattered by these atoms interfere with each other. Therefore the diffraction pattern has a wide variety of intensities in it (see Figure 3.8a). Measured X-ray diffraction data consist of a list of the relative intensity $I(hkl)$, its indices (h , k , and l), and the scattering angle 2θ (see Chapter 4), for each Bragg reflection. All the values of the intensity $I(hkl)$ are on the same relative scale, and this entire data set describes the “diffraction pattern.” It is used as part of the input necessary to determine the crystal structure.

As already indicated from a study of the diffraction patterns from slits and from various arrangements of molecules (Figures 3.1 and 3.9 especially), the angular positions (2θ) at which scattered radiation is observed depend only on the dimensions of the crystal lattice and the wavelength of the radiation used, while the intensities $I(hkl)$ of the different diffracted beams depend mainly on the nature and arrangement of the atoms within each unit cell. It is these two items, the unit-cell dimensions of the crystal and its atomic arrangement, that comprise what we mean by “the crystal structure.” Their determination is the primary object of the analysis described here.

Representation of the superposition of waves

As illustrated in Figure 1.1b and the accompanying discussion, and mentioned again at the start of Chapter 3, X rays scattered by the electrons in the atoms of a crystal cannot be recombined by any known lens. Consequently, to obtain an image of the scattering matter in a crystal, the “structure” of that crystal, we need to simulate this recombination, which means that *we must find a way to superimpose the scattered waves, with the proper phase relations between them, to give an image of the material that did the scattering, that is, the electrons in the atoms.* We call this image

an “electron-density map.” It shows approximately zero values at sites in the unit cell where there are no atoms, and positive values at sites of atoms. The electron-density values are higher for heavier atoms than for lighter atoms (an effect expressing the number of electrons in each atomic nucleus) so that this electron-density map may permit discrimination between atoms that have different atomic numbers.

How then can the superposition of waves be represented? There are several ways. Electromagnetic waves, such as X rays, may be regarded as composed of many individual waves. When this radiation is scattered with preservation of the phase relationships among the scattered waves, the amplitude of the resultant beam in any direction may be determined by summing the individual waves scattered in that direction, taking into account their relative phases (see Figure 3.2). We use a cosine wave (or a sine wave, which differs from it by a phase change of $\pi/2$ radians or 90°). The phase for this cosine wave may be calculated by noting the position of some point on it, such as a maximum. This is measured relative to an arbitrarily chosen origin (see Figures 1.2 and 5.1a).

There are several ways of representing electromagnetic waves so that they can be summed to give information on the nature of the combined wave.

Graphical representation

The usual way to represent electromagnetic waves graphically is by means of a sinusoidal function. Unfortunately, graphical superposition of waves of the type illustrated in Figure 3.2 is not convenient with a digital computer. Therefore, for speed and convenience in computing, other representations are preferred.

Algebraic representation

When we represent a wave by a trigonometric (cosine) function, we use the following algebraic expressions for the vertical displacements (x_1 or x_2) of two waves at a particular moment in time:

$$x_1 = c_1 \cos(\phi + \alpha_1) \quad (5.1)$$

$$x_2 = c_2 \cos(\phi + \alpha_2) \quad (5.2)$$

Here c_1 and c_2 are the amplitudes of the two waves (their maximum vertical displacements). The value of ϕ is, at a given instant, proportional to the time (or distance) for the traveling wave and is the same for all waves under consideration; α_1 and α_2 are the phases, expressed relative to an arbitrary origin. We will assume here that the wavelengths of the scattered waves are identical, inasmuch as the X rays used in structure analyses are generally monochromatic (only one wavelength). Because the wavelengths are the same, the phase difference between the two scattered waves ($\alpha_1 - \alpha_2$), remains constant (assuming that no change in the phase of either wave has taken place during scattering).

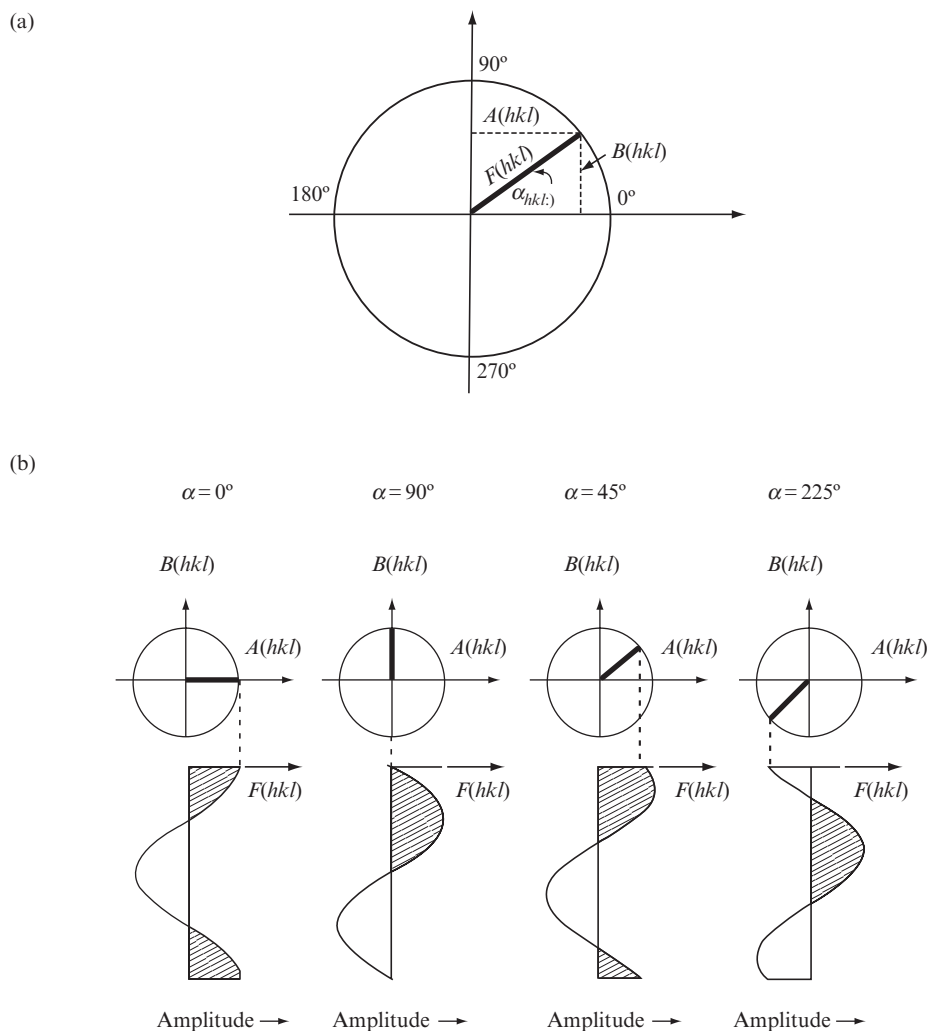


Fig. 5.1 The representation of sinusoidal waves.

(a) Graphical representation of a sinusoidal cosine wave, amplitude $F(hkl)$ represented by the radius of the circle, and phase α_{hkl} represented by the counterclockwise angle measured at the center of the circle. (b) Four examples of a phase angle, represented as shown in (a), and the cosine wave it represents. Note the relationship of the phase angle in the circular representation to the location of the peak of the cosine wave.

When the waves are superimposed, the resulting displacement, x_r , is, at any time, simply the sum of the individual displacements, as shown earlier in a graphical manner in Figure 3.2:

$$x_r = x_1 + x_2 = c_1 \cos(\phi + \alpha_1) + c_2 \cos(\phi + \alpha_2) \quad (5.3)$$

which, since $\cos(A + B) = \cos A \cos B - \sin A \sin B$, may be rewritten as

$$x_r = c_1 \cos \phi \cos \alpha_1 - c_1 \sin \phi \sin \alpha_1 + c_2 \cos \phi \cos \alpha_2 - c_2 \sin \phi \sin \alpha_2 \quad (5.4)$$

or

$$x_r = (c_1 \cos \alpha_1 + c_2 \cos \alpha_2) \cos \phi - (c_1 \sin \alpha_1 + c_2 \sin \alpha_2) \sin \phi \quad (5.5)$$

If we define the amplitude, c_r , and phase, α_r , of the resulting wave such that

$$c_r \cos \alpha_r = c_1 \cos \alpha_1 + c_2 \cos \alpha_2 = \sum_j c_j \cos \alpha_j \quad (5.6)$$

and

$$c_r \sin \alpha_r = c_1 \sin \alpha_1 + c_2 \sin \alpha_2 = \sum_j c_j \sin \alpha_j \quad (5.7)$$

then we can rewrite Eqn. (5.5) as

$$x_r = c_r \cos \alpha_r \cos \phi - c_r \sin \alpha_r \sin \phi = c_r \cos(\phi + \alpha_r) \quad (5.8)$$

Thus the resultant of adding two waves of equal wavelength is a wave of the same frequency, with a phase α_r (relative to the same origin) given by Eqns. (5.6) and (5.7) or, more compactly, by the following equation:

$$\tan \alpha_r = \frac{c_r \sin \alpha_r}{c_r \cos \alpha_r} = \frac{\sum_j c_j \sin \alpha_j}{\sum_j c_j \cos \alpha_j} \quad (5.9)$$

The amplitude of the resultant wave, c_r , is given by

$$\begin{aligned} c_r &= [(c_r \cos \alpha_r)^2 + (c_r \sin \alpha_r)^2]^{1/2} \\ &= \left[\left(\sum_j c_j \cos \alpha_j \right)^2 + \left(\sum_j c_j \sin \alpha_j \right)^2 \right]^{1/2} \end{aligned} \quad (5.10)$$

Vectorial representation

These relationships can all be expressed alternatively in terms of two-dimensional vectors, as illustrated in Figures 5.1a and b. You will remember that a vector has a magnitude (measure), direction (angle from the horizontal), and sense (where it starts and ends) (see Glossary). The length of the j th vector is its amplitude, c_j , and the angle that it makes with the arbitrary zero of angle (usually taken as the direction of the horizontal axis pointing to the right, with positive angles measured counterclockwise) is the phase angle α_j . This is shown in Figures 5.1a and 5.2a, where c_j is represented as $F(hkl)$, the structure factor. The components of the vectors along orthogonal axes are just $A = c_j \cos \alpha_j$ and $B = c_j \sin \alpha_j$ and the components of the vector resulting from addition of two (or more) vectors are just the sums of the components of the individual vectors making up the sum, a result expressed in Eqns. (5.6) and (5.7). The relationship of the vector representation of a

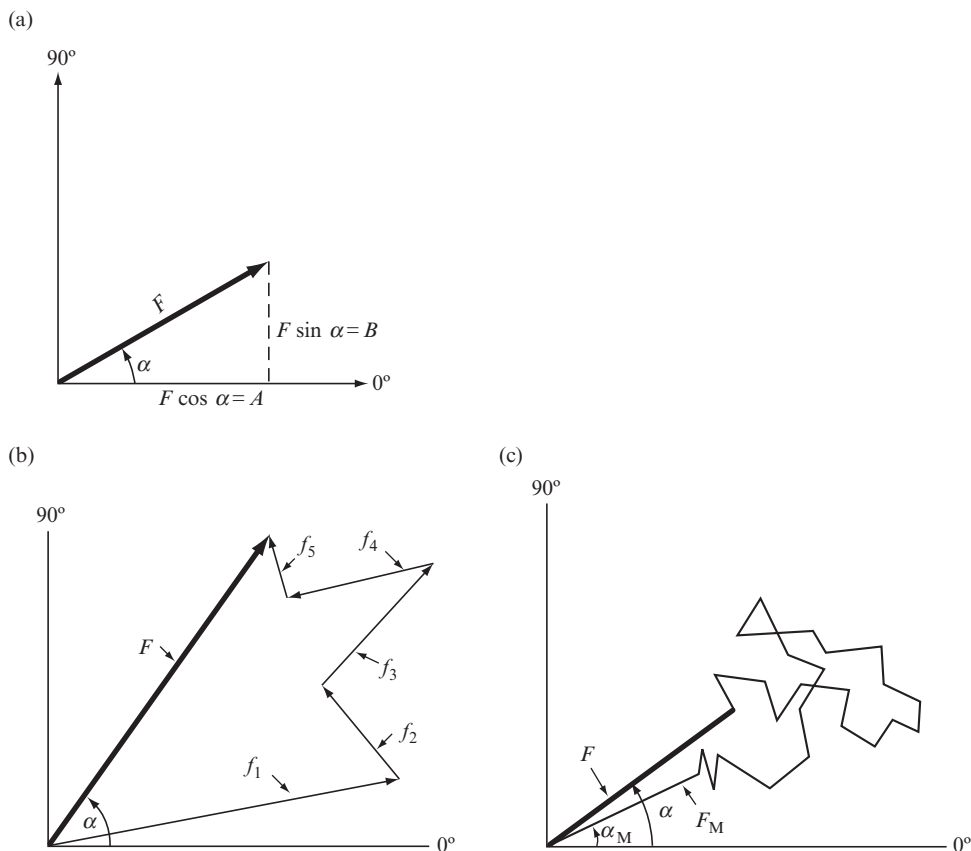


Fig. 5.2 Vector representation of structure factors.

- The relation of the vector F to A and B .
- The vector addition of the contribution of each atom to give a resultant F .
- If a "heavy" atom (M) has a much higher atomic number, and hence a much longer vector in a diagram (like that in Figure 5.2b) than any of the other atoms present, then the effect on the vector diagram for F is normally as if a short-stepped random walk had been made from the end of F_M . Since the steps or f -values for the lighter atoms are relatively small, there is a reasonable probability that the angle between F and F_M will be small and an even higher probability that α (for the entire structure) will lie in the same quadrant as α_M (for the heavy atom alone). Thus the heavy-atom phase, α_M , may be used as a first approximation to the true phase, α .

wave to its sinusoidal appearance and phase angle is shown in Figure 5.1b. When there are several atoms in the unit cell, the various component scattering vectors can be added, as shown in Figures 5.2b and c.

Exponential representation (complex numbers)

For computational convenience, vector algebra is an improvement over graphical representation, but an even simpler notation is that involving so-called "complex" numbers, often represented as exponentials. The *exponential representation* is particularly simple because multiplication of

exponentials involves merely addition of the exponents. Equations (5.6) and (5.7) express the components of the resulting wave; Eqn. (5.10) expresses the amplitude of the resulting wave as the square root of the sum of the squares of its components, which we will now abbreviate as A and B . Equations (5.6), (5.7), and (5.10) may be rewritten as

$$A = c_r \cos \alpha_r = \sum_j c_j \cos \alpha_j \quad (5.11)$$

$$B = c_r \sin \alpha_r = \sum_j c_j \sin \alpha_j \quad (5.12)$$

and

$$c_r = (A^2 + B^2)^{1/2} \quad (5.13)$$

We will, as is conventional, let i represent $\sqrt{-1}$, an “imaginary” number. A complex number, C , is defined as the sum of a “real” number, x , and an “imaginary” number, iy (where y is real),

$$C = x + iy \quad (5.14)$$

The magnitude of C , written as $|C|$, is defined as the square root of the product of C with its complex conjugate C^* (which is defined as $x - iy$) so that

$$|C| \equiv [CC^*]^{1/2} = [(x + iy)(x - iy)]^{1/2} = [x^2 - i^2y^2]^{1/2} = [x^2 + y^2]^{1/2} \quad (5.15)$$

Comparison of Eqns. (5.14) and (5.15) with Eqns. (5.10)–(5.13) shows that the *vector representations of a wave and the complex number representations are parallel*, provided that we identify the vector itself as $A + iB$. The result is that c_r of Eqn. (5.13) is identified with $|C|$ of Eqn. (5.15), and hence the vector components A and B are identified with x and y , respectively. A and B [as given by Eqns. (5.11) and (5.12)] represent components along two mutually orthogonal axes (called, with enormous semantic confusion, the “real” and “imaginary” axes, although both are perfectly real). The magnitude of the vector is given, as is usual, by the square root of the sum of the squares of its components along orthogonal axes, $(A^2 + B^2)^{1/2}$, as in Eqns. (5.13) and (5.15).

One advantage of the complex representation follows from the identity

$$e^{i\alpha} \equiv \cos \alpha + i \sin \alpha \quad (5.16)$$

(which can easily be proved using the power-series expansions for these functions). We then have our expression for the total scattering as

$$A + iB = c_r \cos \alpha_r + ic_r \sin \alpha_r \equiv c_r e^{i\alpha_r} \quad (5.17)$$

Note that the amplitude of this scattered wave is c_r and its phase angle is α_r , as before, with $\alpha_r = \tan^{-1}(B/A)$, as in Eqn. (5.9).

Thus Eqn. (5.17) provides a mathematical means that is computer-usable for summing values of A and iB . It is often said, when this representation of the result of the superposition of scattered waves is used,

that A is the “real” component and B the “imaginary” component, a terminology that causes considerable uneasiness among those who prefer their science firmly founded and not flirting with the unreal or imaginary. It cannot be stressed too firmly that *the complex representation is merely a convenient way of representing two orthogonal vector components in one equation*, with a notation designed to keep algebraic manipulations of the components in different directions separate from one another. Each component is entirely real, as is evident from Figures 5.1 and 5.2.

Scattering by an individual atom

Electrons are the only components of the atom that scatter X rays significantly, and they are distributed over atomic volumes with dimensions comparable to the wavelengths of X rays used in structure analysis. The amplitude of scattering for an atom is known as the “atomic scattering factor” or “atomic form factor”, and is symbolized as f . It is the scattering power of an atom measured relative to the scattering by a single electron under similar conditions. If the electron density is known for computed atomic orbitals (see Hartree, 1928; James, (1965); Stewart et al., 1965; Pople, 1999), then atomic scattering factors can be calculated from this electron density as shown in Figure 5.3. The electron densities of the atomic orbitals form the basis of the scattering

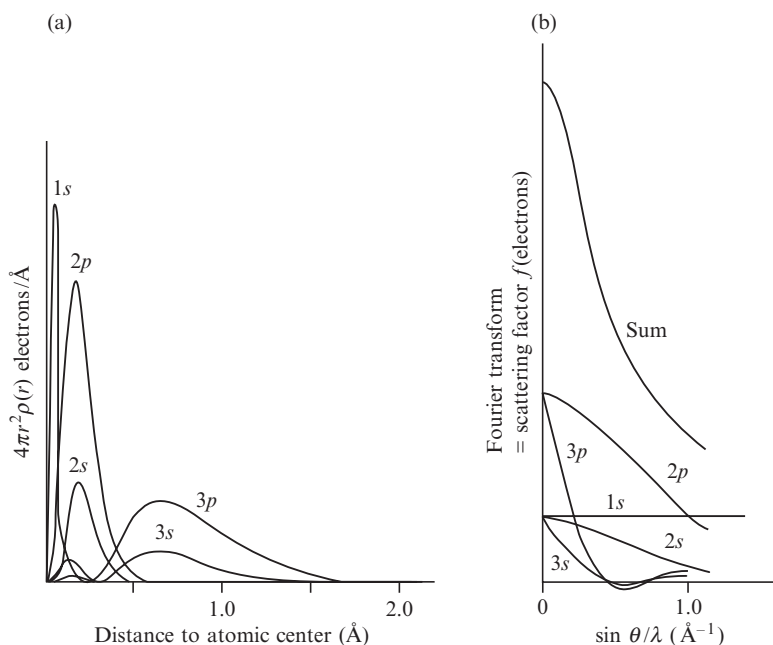


Fig. 5.3 Atomic scattering factors.

(a) Radial electron density distribution in atomic orbitals from theoretical calculations and (b) the scattering factors derived from them. The scattering curves in Figure 5.4 are similar to the uppermost curve (marked “Sum”) in (b) here.

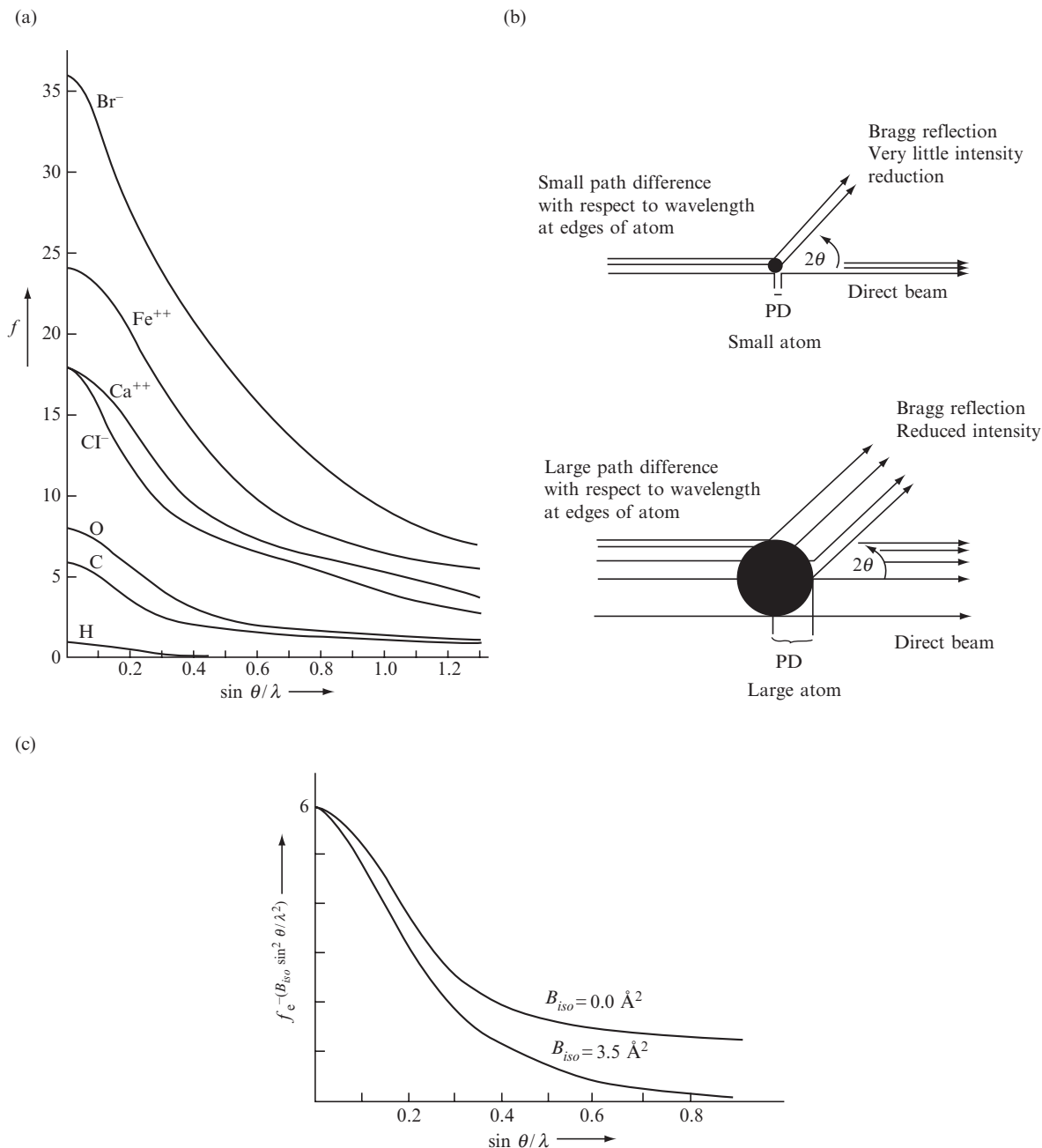


Fig. 5.4 Atomic-scattering-factor curves.

- (a) Some atomic-scattering-factor curves for atoms, given as a function of $\sin \theta/\lambda$ so that they will be independent of wavelength. (Remember that 2θ is the deviation of the diffracted beam from the direct X-ray beam, wavelength λ .) The scattering factor for an atom is the ratio of the amplitude of the wave scattered by the atom to that of the wave scattered by a single electron. At $\sin \theta/\lambda = 0$ the value of the scattering factor of a neutral atom is equal to its atomic number, since all electrons then scatter in phase. Note that calcium (Ca^{++}) and chloride (Cl^-) are isoelectronic; that is, they have the same number of extranuclear electrons.

factors as a function of $\sin \theta/\lambda$; they are published and available in *International Tables*. Some values are given in Appendix 5.

For most purposes in structure analysis it is adequate to assume that atoms themselves are spherically symmetrical, but, with some of the best data now available, small departures from spherical symmetry (attributable to covalent bonding, lone pairs of electrons, and nonspherical orbitals, for example) are detectable. However, in our discussions, unless stated otherwise, we will assume spherical symmetry of atoms. This means that the scattering by an assemblage of atoms—that is, by the structure—can be very closely approximated by summing the contributions to each scattered wave from each atom independently, taking appropriate account of differences in the phase angles of each wave. Some atomic scattering factors, plotted as a function of $\sin \theta/\lambda$, are shown in Figure 5.4a. Since the diffraction pattern is the sum of the scattering from all unit cells, and this can be represented by the average contents of a single one of these unit cells, vibrations or disorder may be considered the equivalent of the smearing out of the electron density, so that there is a greater fall-off in the intensity of the diffraction pattern at a higher $\sin \theta/\lambda$ values (cf. the optical analogy in Figure 3.1: the wider the slit, the narrower the diffraction pattern). This modification of the fall-off by atomic vibration, motion or disorder, which results in a larger apparent atomic size as shown in Figure 5.4b, increases the falloff in scattering power as a function of scattering angle (Figure 5.4c). This fall-off may be isotropic (equal in all directions) or anisotropic (greater in certain directions in the unit cell than in others). Information obtained from an analysis of such atomic motion or disorder is discussed in Chapter 12. It leads, in nearly all crystal structures, to a model with anisotropic displacement parameters representing an inexact register of atomic positions from unit cell to unit cell. By contrast to X-ray scattering, neutrons are scattered by atomic nuclei, rather than by electrons around a nucleus, and hence, since the nucleus is so small (equivalent to a “point atom”), the neutron scattering for a nonvibrating nucleus is almost independent of scattering angle.

The positively charged calcium ion pulls electrons closer to the nucleus than does the chloride ion, which is negatively charged and has a lower atomic number. The resulting “narrower atom” for Ca^{++} will, for reasons shown in Figure 3.1, give a broader diffraction pattern. This is shown at high values of $\sin \theta/\lambda$ by higher values of f for Ca^{++} than for Cl^- .

- (b) When radiation is scattered by particles that are very small relative to the wavelength of the radiation, such as neutrons, the scattered radiation has approximately the same intensity in all directions. When it is scattered by larger particles, the radiation scattered from different regions of the particle will still be in phase in the forward direction, but at higher scattering angles there is interference between radiation scattered from various parts of the particle. The intensity of radiation scattered at higher angles is thus less than for that scattered in the forward direction. This effect is greater the larger the size of the particle relative to the wavelength of the radiation used.
- (c) The effects of isotropic vibration on the scattering by a carbon atom. Values are shown for a stationary carbon atom (B_{iso} of 0.0 \AA^2) and for one with a room temperature isotropic displacement factor (B_{iso} of 3.5 \AA^2) that corresponds to a root-mean-square amplitude of vibration of 0.21 \AA . Vibration and disorder result in an apparently relatively greater size for the atoms (since we are considering an average of millions of unit cells), and consequently a decrease in scattering intensity with increasing scattering angle. If B_{iso} is large, no Bragg reflections may be detectable at high values of 2θ ; that is, a narrower diffraction pattern is obtained from the “smeared-out” electron cloud of a vibrating atom (cf. Figure 3.1).

Scattering by a group of atoms (a structure)

The X radiation scattered by one unit cell of a structure in any direction in which there is a diffraction maximum has a particular combination of amplitude and relative phase, known as the *structure factor* and symbolized by F or $F(hkl)$ (Sommerfeld, 1921). It is the ratio of the amplitude of the radiation scattered in a particular direction by the contents of one unit cell to that scattered by a single electron at the origin of the unit cell under the same conditions. The intensity of the scattered radiation is proportional to the square of the amplitude, $|F(hkl)|^2$. In the manner just discussed [see Eqn. (5.17)], the structure factor can be represented either exponentially or as an ordinary complex number:

$$F(hkl) = |F(hkl)|e^{ia(hkl)} = A(hkl) + iB(hkl) \quad (5.18)$$

with $|F|$ or $|F(hkl)|$ representing the amplitude of the scattered wave, and $a(hkl)$ its phase relative to the chosen origin of the unit cell.* As before (Figure 5.1), $a = \tan^{-1}(B/A)$ and $c_r = |F(hkl)| = (A^2 + B^2)^{1/2}$. The quantities A and B , representing the components of the wave in its vector representation (see Figure 5.2), can be calculated, if one knows the structure, merely by summing the corresponding components of the scattering from each atom separately. These components are [by Eqns. (5.6) and (5.7)] the products of the individual atomic-scattering-factor amplitudes, f_j , and the cosines and sines of the phase angles, α_j , of the waves scattered from the individual atoms:

$$A(hkl) = \sum_j f_j \cos \alpha_j \quad (5.19)$$

and

$$B(hkl) = \sum_j f_j \sin \alpha_j \quad (5.20)$$

But how do we calculate α_j for each atom?

If an atom lies at the origin of the unit cell and if other atoms lie one or several unit-cell translations (a) from it, then this grating of atoms will give a series of Bragg reflections $h00$ on diffraction. If there is another atom between two of them, at a distance xa from the origin (where x is less than 1), radiation scattered by this atom will interfere with the other resultant Bragg reflection by an amount that depends on the value of x . This can be generalized so that, for each $h00$ Bragg reflection, the phase difference (interference) will depend on the value of hx as illustrated in Figures 5.5 and 5.6. We show in Appendix 6 that the phase of the wave scattered in the direction of a reciprocal lattice point (hkl) by an atom situated at a position x, y, z in the unit cell (where x, y , and z are expressed as fractions of the unit-cell lengths a, b , and c , respectively) is just $2\pi(hx + ky + lz)$ radians, relative to the phase of the wave scattered in the same direction by an atom at the origin. This is important because it defines the effect of the location of an atom in the unit cell. The “relative phase angle” for an atom at x, y, z , where these numbers are defined

*The structure factor F may be represented as a vector, but it is not conventionally written in bold face, so we, as is common, will use F for the vector and $|F|$ for its amplitude.

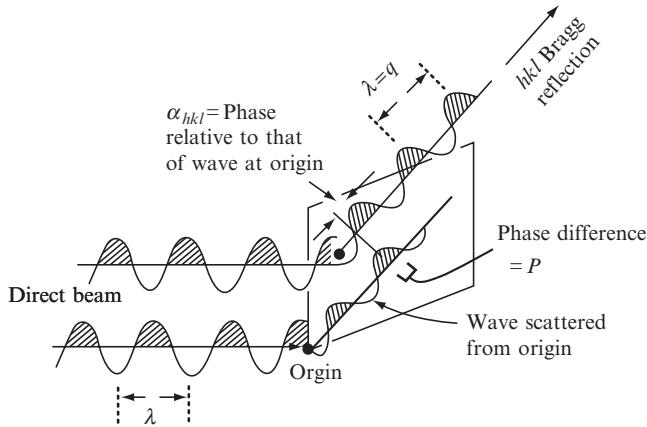


Fig. 5.5 The meaning of "relative phase."

The relative phase angle α_{hkl} of a Bragg reflection hkl is the difference between the phase of a wave scattered by an atom (shown as a black circle within the unit cell) and the phase of a wave scattered in the same direction by an imaginary atom at the chosen origin of the unit cell.

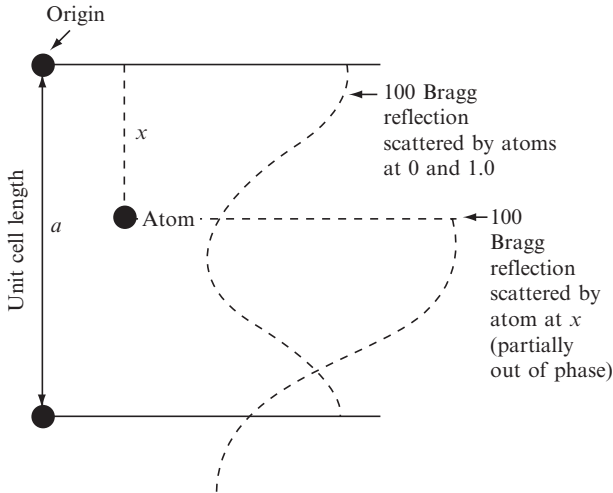


Fig. 5.6 The relative phase angle on diffraction.

If a one-dimensional structure with a repeat distance a has an atom at 0.0 (and this is repeated from unit cell to unit cell by other atoms at 1.0, 2.0, etc.) and an atom at x/a , the phase difference between the atom at 0.0 and the atom at x/a is $2\pi hx$ radians. Suppose that the atom at 0.0 is at the chosen origin of the system. Its phase angle for a cosine function is 0° . The phase angle of the atom at x is $2\pi hx$ radians. This is the difference of its phase with that of the atom at the origin, and hence the radiation scattered by the atom at x is considered to have a relative phase of $2\pi hx$ radians.

with respect to a chosen origin at 0, 0, 0, is $2\pi(hx + ky + lz)$ radians. If the location of the chosen origin is changed, the relative phase will also be changed. Each structure factor is the sum of the scattering from all atoms j in the unit cell. Thus Eqns. (5.19) and (5.20) (for all atoms j) can be rewritten as

$$A(hkl) = \sum_j f_j \cos 2\pi(hx_j + ky_j + lz_j) \quad (5.21)$$

$$B(hkl) = \sum_j f_j \sin 2\pi(hx_j + ky_j + lz_j) \quad (5.22)$$

where the value of f_j chosen is that corresponding to the value of $\sin \theta/\lambda$ for the Bragg reflection in question, modified to take into account any thermal vibration of the atom. A comparison with Eqns. (5.19) and (5.20) shows that we now know the phase α_j . The magnitude of $|F(hkl)|$ depends only on the relative positions of the atoms in the unit cell, except to the extent that f_j is a function of the scattering angle. The size and shape of the unit cell do not appear as such in the expressions for A and B . In Figure 5.2, F is represented as a vector. Note that a shift in the chosen origin of the unit cell will add a constant to the phase angle of each atom [see Eqns. (5.21) and (5.22)]; that is, it will rotate the phase diagrams in Figure 5.2 relative to the coordinate axes, but will leave the length of $|F(hkl)|$, and hence the values of $|F(hkl)|^2$ and the intensity, unchanged.

Effects of atomic vibration and displacements on atomic scattering

Atomic vibrations in a crystal, that is, displacements from equilibrium positions, have a frequency of the order of 10^{13} per second. This is much slower than the frequencies of X rays used to study crystals; these are of the order of 10^{18} per second. Therefore a vibrating atom will appear stationary to X rays but displaced in a random manner within the vibration amplitude. Atoms in other unit cells will also exhibit this random deviation from their equilibrium positions, different for each such atom in the various unit cells throughout the crystal. Because minor static displacements of atoms appear similar to displacements caused by atomic vibrations, it is usual to use the term "atomic displacement parameter" rather than "atomic temperature factor" for the correction factor. When $2\theta = 0$, all electrons in the atom scatter in phase, and the scattering power of an atom at this angle, expressed relative to the scattering power of a free electron, is just equal to the number of electrons present (the atomic number for neutral atoms).

However, an atom has size (relative to the wavelength of the X rays used), with the result that X rays scattered from one part of an atom interfere with those scattered from another part of the same atom at all angles of scattering greater than 0° . This causes the scattering to

fall off with increasing scattering angle or, more precisely, increasing values of $\sin \theta/\lambda$, as indicated in Figure 5.4b. The fall-off in intensity with higher scattering angle (Figure 5.4c) increases as the vibrations of atoms become greater, and these vibrations in turn increase in extent with rising temperature. Atoms are in motion in the crystalline state, however, even when the temperature is reduced to near absolute zero. This vibration, coupled with displacements of some atoms, leads to a significant reduction in intensity that can be approximated by an exponential function that has a large effect at high 2θ values (illustrated in Figure 5.4c); this indicates, as noted by Peter J. W. Debye and Ivar Waller, that atomic motion endows a larger “apparent size” to atoms (Debye, 1914; Waller, 1923). Effectively, since atoms are displaced different amounts from unit cell to unit cell at the given instant in time that measurement occurs, atoms appear to have become smeared in the average of all the unit cells in the crystal. If the displacement amplitude is sufficiently high, essentially no diffracted intensity will be observed beyond some limiting value of the scattering angle; that is, the “slit” is effectively widened by the vibration and so the “envelope” is narrow (Figure 3.5a). If the displacements are nearly isotropic—that is, do not differ greatly in different directions—the exponential factor can be written as $\exp(-2B_{\text{iso}} \sin^2 \theta/\lambda^2)$, with B_{iso} called the *atomic displacement factor*.^{**} B_{iso} is equal to $8\pi^2 \langle u^2 \rangle$, where $\langle u^2 \rangle$ is the mean square amplitude of displacement of the atom from its equilibrium position. The type of disorder found in a crystal may be static, with the atom in one site in one unit cell and a different site in another unit cell. Alternatively, it may be dynamic, which implies that the atom moves from one site to another. The overall effect in both cases is a reduction in the scattering factors of the atoms involved as $\sin \theta/\lambda$ increases (see Willis and Pryor, 1975).

If the motion or disorder is anisotropic, it is necessary to replace B_{iso} by six terms. This is usually necessary for all atoms except hydrogen atoms; these have only weak scattering power. Atoms in crystals rarely have isotropic environments. The six parameters define the orientations of the principal axes of the ellipsoid that represents the anisotropic displacements and the magnitudes of the displacements along these axes. The results are often displayed in an ORTEP[†] diagram, in which the atomic displacement factors are drawn as ellipsoids (Johnson, 1965). If the anisotropy is severe, the ellipsoid representing the displacement probability and its direction may be abnormally extended in shape and may be better represented as disorder in two positions.

Macromolecules, such as proteins, show interesting thermal and displacement effects. While their structures are generally, but not always, measured at a lower resolution than for small molecules, anisotropic displacement parameters are rarely determined, but isotropic displacements give information on the motion and flexibility of various portions in the molecule. One domain of the molecule may appear to move in a hingelike manner with respect to another part of the same molecule. Also, side chains at the surface of the macromolecule may have

^{**} Many crystallographers omit the subscript “iso,” relying on the context to avoid confusion with the quantity B defined in $F = A + iB$.

[†] ORTEP = Oak Ridge Thermal Ellipsoid Plot (Johnson, 1965).

alternate atomic positions from unit cell to unit cell as they interact with the various water molecules that fill nearly half of the crystal volume.

Calculating a structure factor

With a method for expressing a structure factor by means of an equation (Eqn. 5.18), and information on the components of this equation, it is possible to obtain a calculated value for the structure factor. This can be compared with the experimental value derived from $I(hkl)$. The data needed in order to calculate a structure factor include the values of x , y , and z for each atom; h , k , l , and $\sin \theta/\lambda$ for the Bragg reflection under consideration; and the scattering factor f_j for each atom at that value of $\sin \theta/\lambda$, modified by atomic displacement factors. Then it is necessary to calculate $2\pi(hx_j + ky_j + lz_j)$ and its sine and cosine for each atom and the Bragg reflection for which $F(hkl)$ is being calculated. This gives all the information necessary to sum the results for each atom and obtain $A(hkl)$ and $B(hkl)$ according to Eqns. (5.21) and (5.22). These lead to $F(hkl)$, that is, $(A^2 + B^2)^{1/2}$, and the relative phase angle $\alpha(hkl)$, that is, $\tan^{-1}(B/A)$, for the Bragg reflection with indices h , k , and l when all the atomic coordinates are known. This process has to be repeated for all of the other Bragg reflections. It demonstrates how important computers are to the X-ray crystallographer.

Information on the electron-density map will have to wait until we know the phase of the structure factor (so that we can determine the atomic positions x , y , and z). All we have so far are the experimentally measured structure amplitudes, $|F(hkl)|$, but we can calculate $F(hkl) = A(hkl) + iB(hkl)$ (including its relative phase angle $\alpha = \tan^{-1}(B(hkl)/A(hkl))$, see Eqns. 5.21 and 5.22) if we have x , y , and z for a model in a unit cell of known dimensions and space group.

Summary

When X rays are diffracted by a crystal, the intensity of X-ray scattering at any angle is the result of the combination of the waves scattered from different atoms and the manner in which they modify this intensity by various degrees of constructive and destructive interference. A structure determination involves a matching of the observed intensity pattern to that calculated from a postulated model, and it is thus imperative to understand how this intensity pattern can be calculated for any desired model. The combination of the scattered waves can be represented in various ways:

- (1) The waves may be drawn *graphically* and the displacements (ordinates, vertical axis) at a given position (abscissae, horizontal axis) summed.

- (2) A wave may be represented *algebraically* as

$$x_j = c_j \cos(\phi + a_j) \quad (\text{for the } j\text{th wave})$$

and the displacements, x_j , of several such waves summed to give a resultant wave.

- (3) The waves may be expressed as *two-dimensional vectors* in an orthogonal coordinate system, amplitude c_j , with the relative phase angle a_j measured in a counterclockwise direction from the horizontal axis. This is the equivalent of representing one complete wavelength as 360° , so that the periodicity of the wave is expressed. The phase relative to some origin is given as a fraction of a revolution. The vectors may then be summed by vectorial addition of their components.
- (4) The waves may be represented in *complex notation*

$$A_j + iB_j = c_j e^{ia_j}$$

which is merely a convenient way of representing two orthogonal vector components (at 0° and 90°) in one equation. By convention A is the component at 0° and B the component at 90° .

X rays are scattered by electrons. The extent of scattering depends on the atomic number of the atom and the angle of scattering, 2θ , and is represented by an atomic scattering factor f . For a group of atoms, the amplitude (relative to the scattering by a single electron) and the relative phase of the X rays scattered by one unit cell are represented by the structure factor $F(hkl) = A(hkl) + iB(hkl)$ for each Bragg reflection. For a known structure with atoms j at positions x_j, y_j, z_j , this may be calculated from

$$A(hkl) = \sum_j f_j \cos 2\pi(hx_j + ky_j + lz_j)$$

and

$$B(hkl) = \sum_j f_j \sin 2\pi(hx_j + ky_j + lz_j)$$

where the summation is over all atoms in the unit cell. The relative phase angle $a(hkl)$ is $\tan^{-1}(B/A)$ and the structure factor amplitude $|F(hkl)|$ is $\{(A(hkl)^2 + B(hkl)^2)\}^{1/2}$. The value of $F(hkl)$ may be reduced as a result of thermal vibration and atomic displacement so that if F_{novib} is the value for a structure containing stationary atoms, the experimental values will correspond to $F(hkl) = F_{\text{novib}} \exp(-B_{\text{iso}} \sin^2 \theta / \lambda^2)$, where B_{iso} , the atomic displacement parameter, is a measure of the amount of vibration and/or displacement ($B_{\text{iso}} = 8\pi^2 \langle u^2 \rangle$, where $\langle u^2 \rangle$ is the mean square amplitude of displacement). With precise experimental data, it is possible to measure the anisotropy of vibration and displacement.

6

The phase problem and electron-density maps

In order to obtain an image of the material that has scattered X rays and given a diffraction pattern, which is the aim of these studies, one must perform a three-dimensional Fourier summation. The theorem of Jean Baptiste Joseph Fourier, a French mathematician and physicist, states that a continuous, periodic function can be represented by the summation of cosine and sine terms (Fourier, 1822). Such a set of terms, described as a Fourier series, can be used in diffraction analysis because the electron density in a crystal is a periodic distribution of scattering matter formed by the regular packing of approximately identical unit cells. The Fourier series that is used provides an equation that describes the electron density in the crystal under study. Each atom contains electrons; the higher its atomic number the greater the number of electrons in its nucleus, and therefore the higher its peak in an electron-density map. We showed in Chapter 5 how a structure factor amplitude, $|F(hkl)|$, the measurable quantity in the X-ray diffraction pattern, can be determined if the arrangement of atoms in the crystal structure is known (Sommerfeld, 1921). Now we will show how we can calculate the electron density in a crystal structure if data on the structure factors, including their relative phase angles, are available.

Calculating an electron-density map

The Fourier series is described as a “synthesis” when it involves structure amplitudes and relative phases and builds up a picture of the electron density in the crystal. By contrast, a “Fourier analysis” leads to the components that make up this series. The term “relative” is used here because the phase of a Bragg reflection is described relative to that of an imaginary wave diffracted in the same direction at a chosen origin of the unit cell (see Figure 6.1). The number of electrons per unit volume, that is, the electron density at any point x, y, z , represented by $\rho(xyz)$, is given by the following expression (for an electron-density map,

a Fourier synthesis):

$$\rho(xyz) = \frac{1}{V_c} \sum_{\text{all } hkl} \sum \sum F(hkl) \exp[-2\pi i(hx + ky + lz)] \quad (6.1)$$

Here V_c is the volume of the unit cell, and $F(hkl)$ is the structure factor for the Bragg reflection with indices h , k , and l . The triple summation is over all values of the indices h , k , and l . This summation, first calculated in 1925, represents a mathematical analogy to the process effected physically in the microscope (Duane, 1925; Havighurst, 1925; Waser, 1968). As described in Chapter 4, the amplitude of $F(hkl)$, that is, $|F(hkl)|$, is easily derived [Eqn. (4.3)] from the intensity of the Bragg reflection. The phase of that same Bragg reflection $\alpha(hkl)$, however, is not.

We will simplify the following equations by putting

$$\phi = 2\pi(hx + ky + lz) \quad (6.2)$$

We then abbreviate $A(hkl)$ and $B(hkl)$ to A and B , respectively,* and $F(hkl) = |F(hkl)|e^{i\phi}$ to $F = A + iB$. This leads to Eqn. (6.3) (from Eqns. (5.16) to (5.18) for $|F(hkl)| = F(hkl)e^{-i\phi}$). In this equation, $e^{-i\phi} = \cos \phi - i \sin \phi$ and $i^2 = -1$:

$$F e^{-i\phi} = (A + iB)(\cos \phi - i \sin \phi) = A \cos \phi + B \sin \phi - i(A \sin \phi - B \cos \phi) \quad (6.3)$$

Because the summation in Eqn. (6.1) is over all values of the indices h , k , and l , it includes, in addition to every Bragg reflection hkl , the corresponding one with all indices having the opposite signs, $-h$, $-k$, $-l$ (also denoted \bar{h} , \bar{k} , \bar{l}). The *magnitude* of each term ($A(hkl)$, $B(hkl)$, $\cos \phi$, and $\sin \phi$) is normally the same** for a Bragg reflection with indices hkl as for that with indices $-h$, $-k$, $-l$. The *sign* of the term will change for these pairs of Bragg reflections if the term involves sine functions [since $\sin(-x) = -\sin x$], but will remain unchanged if it involves cosine functions [since $\cos(-x) = \cos x$]. Both $A(hkl)$ [the sum of cosines, by Eqn. (5.19)] and $\cos \phi$ have the same sign for hkl as for $-h$, $-k$, $-l$, whereas $B(hkl)$ [the sum of sines, by Eqn. (5.20)] and $\sin \phi$ have opposite signs for this pair of Bragg reflections. Therefore, when Eqn. (6.3) is substituted in Eqn. (6.1) and the summation is made, the $i(A \sin \phi - B \cos \phi)$ terms cancel for each pair of Bragg reflections hkl and $\bar{h}\bar{k}\bar{l}$ and vanish completely. The remaining terms, $A \cos \phi$ and $B \sin \phi$, need be summed over only half of the Bragg reflections. All those with any one index (for example, h) negative are omitted and a factor of 2 is introduced to account for this. Therefore we may write, by Eqns. (6.1) and (6.3),

$$\rho(xyz) = \frac{1}{V_c} \left\{ |F(000)| + 2 \sum_{\substack{h \geq 0, \text{ all } k, l \\ \text{excluding } F(000)}}^{\infty} (A \cos \phi + B \sin \phi) \right\} \quad (6.4)$$

* Note that the exponential terms in the expressions for F (the structure factor) and ρ (the electron density) are opposite in sign; $F = \sum f e^{i\phi}$ and $\rho = (1/V) \sum F e^{-i\phi}$. This is because these are Fourier transforms of each other (Glasser, 1987a,b; Carslaw, 1930).

** This implies that "Friedel's Law" $|F(hkl)|^2 = |F(\bar{h}\bar{k}\bar{l})|^2$ is obeyed (Friedel, 1913); deviations from this law are considered in Chapter 10.

Since $A = |F| \cos \alpha$ and $B = |F| \sin \alpha$ [by Eqn. (5.17), where α is the relative phase angle of $F(hkl)$, and $\cos X \cos Y + \sin X \sin Y = \cos(X - Y)$], the above expression for the electron density (Eqn. (6.4)) may be rewritten[†]

$$\rho(xyz) = \frac{|F(000)|}{V_c} + \frac{2}{V_c} \sum_{\substack{h \geq 0, \text{ all } k, l \\ \text{excluding } F(000)}}^{\infty} (|F| \cos(\phi - \alpha)) \quad (6.5)$$

This may be alternatively expressed as

$$\rho(xyz) = \frac{|F(000)|}{V_c} + \frac{2}{V_c} \sum_{\substack{h \geq 0, \text{ all } k, l \\ \text{excluding } F(000)}}^{\infty} |F(hkl)| \cos[2\pi(hx + ky + lz) - \alpha(hkl)]$$

Remembering that $\phi = 2\pi(hx + ky + lz)$, an inspection of Eqn. (6.5) shows that we need both the magnitudes $|F(hkl)|$ and the relative phases $\alpha(hkl)$ of the radiation that has been diffracted in different directions. These are necessary for us to be able to form an image of the scattering matter, $\rho(xyz)$. *If we knew $|F(hkl)|$ and $\alpha(hkl)$, we could then calculate the Fourier summation in Eqn. (6.5) and plot the values of $\rho(xyz)$, thereby obtaining a three-dimensional electron-density map.* By assuming that atoms lie at the centers of peaks in this map, we would then know the atomic structure of the crystal.

However, as we have already stressed many times, we can normally obtain only the structure factor amplitudes $|F(hkl)|$ and not the relative phase angles $\alpha(hkl)$ [‡] directly from the experimental measurements. We must *derive* $\alpha(hkl)$, either from values of $A(hkl)$ and $B(hkl)$ that are computed from structures we have deduced in various ways (“trial structures”), or by purely analytical methods. The problem of getting estimates of the phase angles so that an image of the scattering matter can be calculated is called the *phase problem* and is the central one in X-ray crystallography. Chapters 8 and 9 are devoted to methods used to solve the phase problem, either by deriving a trial structure and then calculating approximate values of $\alpha(hkl)$ for each Bragg reflection, or by trying to find values of $\alpha(hkl)$ directly. Recall that, for the third-order Bragg reflection, the path difference between waves scattered one repeat unit (a) apart (that is, by equivalent atoms in adjacent unit cells) is three wavelengths. The important fact for the reader to understand is that each resultant wave should be traced back and its phase compared with that of an imaginary wave being scattered at the origin of the repeat unit (with a relative phase angle of 0°); that is why we call it a “relative phase,” the origin being in a position chosen by the investigator (see Nyburg, 1961).

How do we derive the relative phases of the density waves, that is, their phases relative to a chosen origin? We attempt to show, in Figure 6.1, how the X rays scattered from different atoms are summed to give the resultant X ray beams of various amplitudes (and hence inten-

[†] A schematic example of the calculation of the function described in Eqn. (6.5) is shown in Figure 6.2.

[‡] Under certain conditions, when two-beam diffraction occurs, some phase information may be derived from experimental measurements (see Chapter 10).

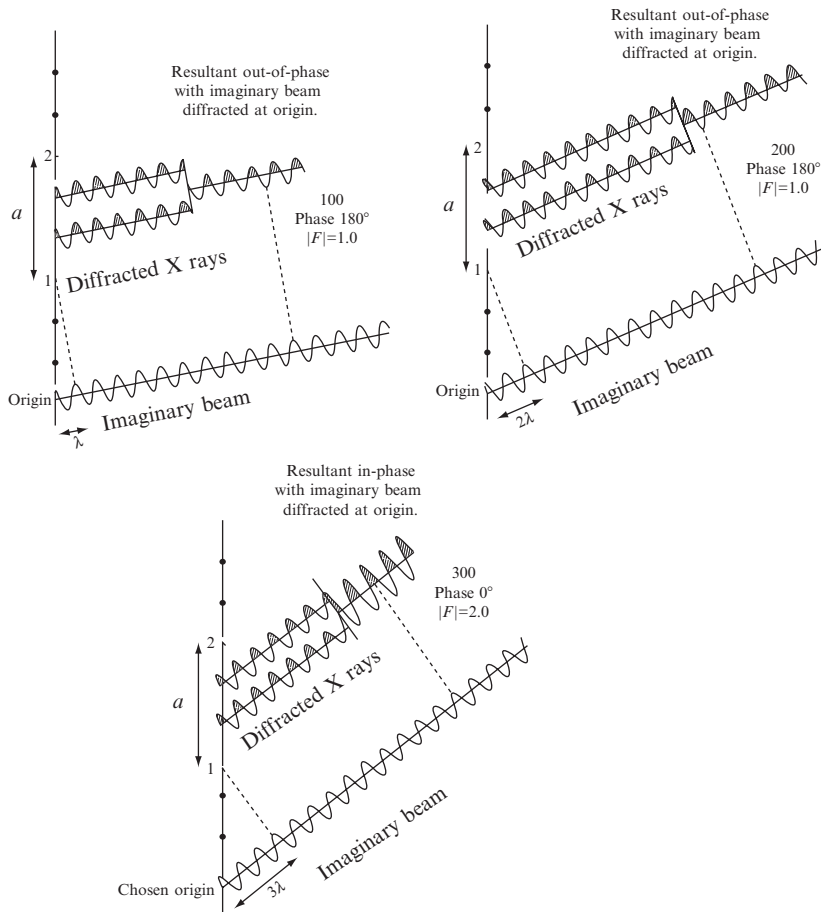


Fig. 6.1 Scattered waves and their relative phases.

A one-dimensional crystal with two atoms in the unit cell, one at $x = 1/3$ and the other at $x = 2/3$. Shown are the Bragg reflections (a) 100, (b) 200, and (c) 300 and their relationships to an imaginary wave scattered at the chosen origin of the unit cell (which leads to the "relative phase angle"). Note that the most intense of these three is the 300 Bragg reflection.

sities). A unit cell containing two atoms, one at $x = 1/3$ and the other at $x = 2/3$, is used to illustrate how relative phases are derived. Compared with an imaginary atom at the origin, the atom at $x = 1/3$ scatters for a third order reflection with a path difference of one wavelength and the atom at $x = 2/3$ scatters with a path difference of two wavelengths. Thus both scatter in phase with the wave scattered at $x = 0$. However, for the second order, the atom at $x = 1/3$ scatters X rays with a path difference of 0.67 wavelengths from that scattered by the imaginary atom at the origin, and the atom at $x = 2/3$ scatters with a path difference of 1.33 wavelengths from the wave scattered at the origin. The resultant wave is then $(0.33 + 0.67)/2 = 0.50$ wavelengths out of phase with the wave scattered by the imaginary atom at the origin. Thus, in summing

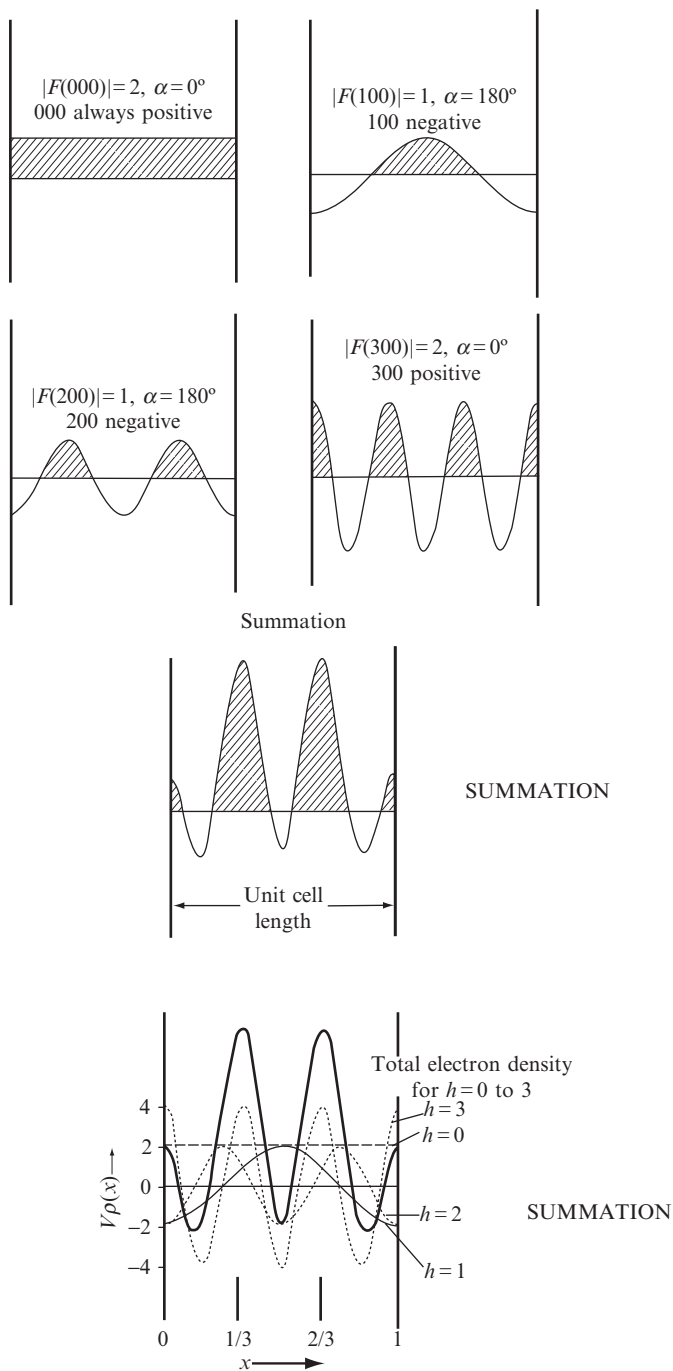


Fig. 6.2 Fourier synthesis of the Bragg reflections from Figure 6.1.

The Fourier summation of density waves to give an electron-density map with peaks at $x = \pm 1/3$. At any point x, y, z in the unit cell, volume V_c , the electron density $\rho(xyz)$ may be calculated by use of Eqn. (6.5). The following data have been used for this one-dimensional example:

density waves, as shown in Figure 6.2, the 300 wave has a relative phase angle of 0° and the 200 density wave has a relative phase angle of 180° .

Fourier transforms

We have shown that the electron density $\rho(xyz)$ (Eqn. 6.1) can be expressed in an equation that involves the structure factors $F(hkl)$ as coefficients,

$$\rho = (1/V)\Sigma F e^{-i\phi} \quad (6.6)$$

It is also possible to express the structure factors in terms of the electron density:

$$F = \Sigma f e^{i\phi} \quad (6.7)$$

The relationship between these two is referred to as a Fourier transform or Fourier inversion. These equations show that the structure factor is the Fourier transform of the scattering density (electrons in the molecule) sampled at the reciprocal lattice point hkl , while the electron density is the Fourier transform of the structure factors (which contain their relative phases). The intensity at a particular point of the diffraction pattern of an object (a set of relative $|F(hkl)|^2$ values) is proportional to the square of the Fourier transform of the object (with the distribution of matter in the object described by $\rho(x, y, z)$). Examples of Fourier transforms are shown in Figure 6.3, with electron density and density waves on the left and structure factors, with their relative phases, shown on the right as positive or negative ($\alpha = 0^\circ$ or 180°). Equation (6.6) or (6.7) (whichever

| h | -3 | -2 | -1 | 0 | 1 | 2 | 3 |
|---------------------------|----------------|----------------|----------------|----|----------------|----------------|----------------|
| $ F(hkl) $ | 2 | 1 | 1 | 2 | 1 | 1 | 2 |
| $\alpha(hkl)^\circ$ | 0 | 180 | 180 | 0 | 180 | 180 | 0 |
| $\cos[2\pi(hx - \alpha)]$ | $+\cos 6\pi x$ | $-\cos 4\pi x$ | $-\cos 2\pi x$ | +1 | $-\cos 2\pi x$ | $-\cos 4\pi x$ | $+\cos 6\pi x$ |

Therefore $\rho(x) = |F(000)|/V_c + (4 \cos 6\pi x - 2 \cos 4\pi x - 2 \cos 2\pi x + 2)/V_c$.

When $h = 0$, the function does not depend on x and so is a straight line (but drawn with half its amplitude to conform to the electron-density map equation with positive and negative values of h). The phase angle of this is necessarily 0° . The function for $h = 1$ is $-\cos 2\pi x$, the negative sign resulting from the relative phase angle of 180° , and so forth. These functions are summed for each value of x to give the result shown by the heavy solid line. It has peaks at $x = \pm 1/3$. Clearly, unless the phases were known, it would not be possible to sum the waves correctly. This kind of calculation must be made, with thousands of Bragg reflections, at each of many thousands of points to give a complete electron-density map in three dimensions. Therefore high-speed computers are essential. For a three-dimensional electron-density map it is not possible to plot heights of peaks (because we have no fourth spatial dimension), and therefore contours of equal electron density (or height) are drawn on sections through the three-dimensional map. Atomic centers appear at the centers of areas of high electron density, which look like circular mountains on a topographical map. The larger values of F dominate the Fourier summation.

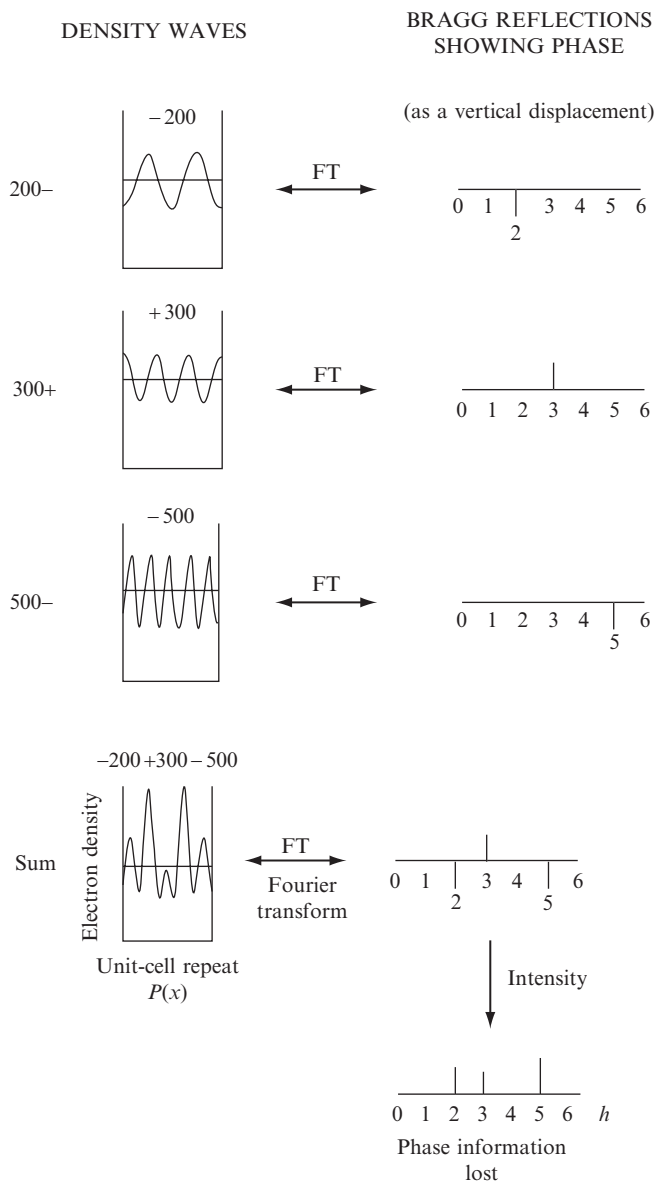


Fig. 6.3 Summing Fourier transforms.

Density waves for the 200, 300, and 500 Bragg reflections and their Fourier transforms. When the columns are summed, the density waves (on the left) give the electron density map, while their Fourier transforms (on the right) give the phases of the individual density waves. When intensities are measured, the phase information is lost. Note: This is a different structure from that in Figures 6.1 and 6.2.

is most appropriate) is used for the transformations. As will be seen later, it is convenient to be able to move readily between real (electron density) and reciprocal (structure factor) space, and this is how it is done. For example, one may want to modify an electron-density map

and calculate a new data set of structure factors for comparison with experimental values or may calculate the theoretical electron density for an atom or ion and then examine the atomic scattering factors relevant to this density (as mentioned in Chapter 5). Alternatively, one may want to change some (or all) of the structure factors and investigate the effect of this on the electron-density map. The Fourier transform equations make this possible.

Summing density waves to obtain an electron-density map

We have emphasized the analogy between the action of a lens in collecting and refocusing radiation to give an image of the scattering matter, and the process of Fourier summation, a mathematical technique for forming an image by use of information about the amplitudes and relative phases of the scattered waves. Fourier summation techniques can be applied even when the waves cannot be refocused, as in the X-ray experiment. With a lens the light waves are (ideally) brought together with the same phases that they had when they left the object; in the X-ray diffraction experiment these phases are usually not measurable, although if they can be found in some way, then it is possible to calculate an electron-density map as shown in Figures 6.3 and 6.4.

The individual waves in Eqn. (6.5) that are summed to give the electron-density map are referred to, for convenience in this book, as “density waves” (see Bijvoet et al., 1948). In other words, each term $|F(hkl)| \cos[2\pi(hx + ky + lz) - \alpha(hkl)]$, calculated as a function of x , y , and z , is a density wave, as illustrated in Figure 6.4. In effect, Eqn. (6.5) could be rewritten to say that *the electron density $\rho(x, y, z)$ at a point in space x, y, z is equal to the sum of these density waves*. Thus each Bragg reflection with its relative phase can be considered to produce a density wave in the crystal, with an amplitude that can be derived from the intensity of the Bragg reflection; the superposition of these density waves, once their phases are known, produces the electron-density map for the crystal:

$$\rho(xyz) = \frac{1}{V_c} \left\{ |F(000)| + 2 \sum_{\text{all density waves}} \sum_{\infty} |F(hkl)| \cos[2\pi(hx + ky + lz) - \alpha(hkl)] \right\} \quad (6.8)$$

The determination of the phases of these density waves is the subject of much of the rest of this book. But what is the wavelength of a density wave and how is it related to the order (h, k, l) of the diffracted beam? Their wavelengths depend on h , k , and l , not the wavelength of the X rays that caused each Bragg reflection. A close examination of Eqn. (6.5) shows that $|F(hkl)|$ is modified by a cosine function

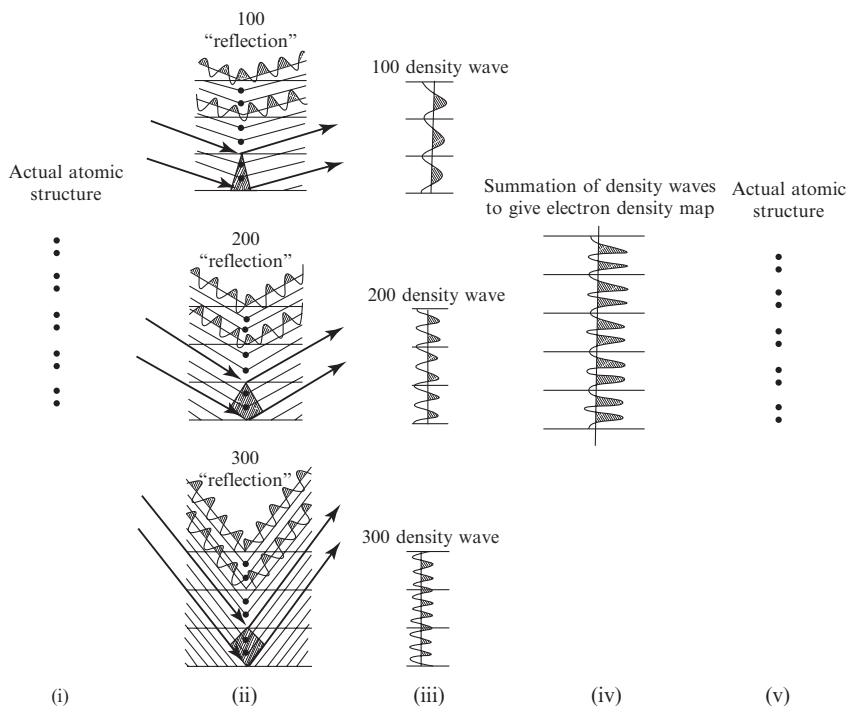


Fig. 6.4 Overview of X-ray diffraction.

Summary of the diffraction experiment, showing (i) the atomic structure (one-dimensional in this case); (ii) diffraction of X rays by the crystal structure; (iii) density waves; (iv) summation of the density waves to give the electron-density map; and the result is an image of the actual structure (v), which is the same as (i).

of $(2\pi(hx + ky + lz) - \alpha(hkl))$; thus it becomes a periodic function of h , k , and l . In the simple case (Figure 6.2) where k and l are both zero, $\cos 2\pi(hx)$ is at a maximum value when $x = 1/h$; that is, this cosine term has an apparent wavelength of a/h (where a is the unit-cell length in the x direction and x is expressed as a fraction of this dimension a).

In summary, the wavelengths of the density waves are $d_{hkl} = \lambda/2 \sin \theta$, their amplitudes are $|F(hkl)|$, and their phases are $\alpha(hkl)$. For example, the wavelength of the 1 0 0 density wave is the repeat distance $a (= d_{100})$ (see Figure 6.2), the wavelength of the 2 0 0 density wave is $a/2$ because the second order of diffraction occurs at a $\sin \theta$ value twice that of the first order, and so forth. For the 1 0 0 reflection, phase π , Eqn. 6.8 gives the function $\cos [2\pi x + \pi]$ which is maximal at $x = 1/2$ (see Figure 6.4). These are the density waves that are summed to give the electron-density map shown in Figure 6.2. "High resolution" implies a high value of $\sin \theta$ and thus a small value for the effective wavelength of the density wave; as we shall see later, high-resolution Bragg reflections (short wavelength density waves) are needed to provide high-resolution images of molecules.

The density waves, derived by arguments such as these, are summed as shown in Figures 6.2 and 6.4 to give the electron density of the

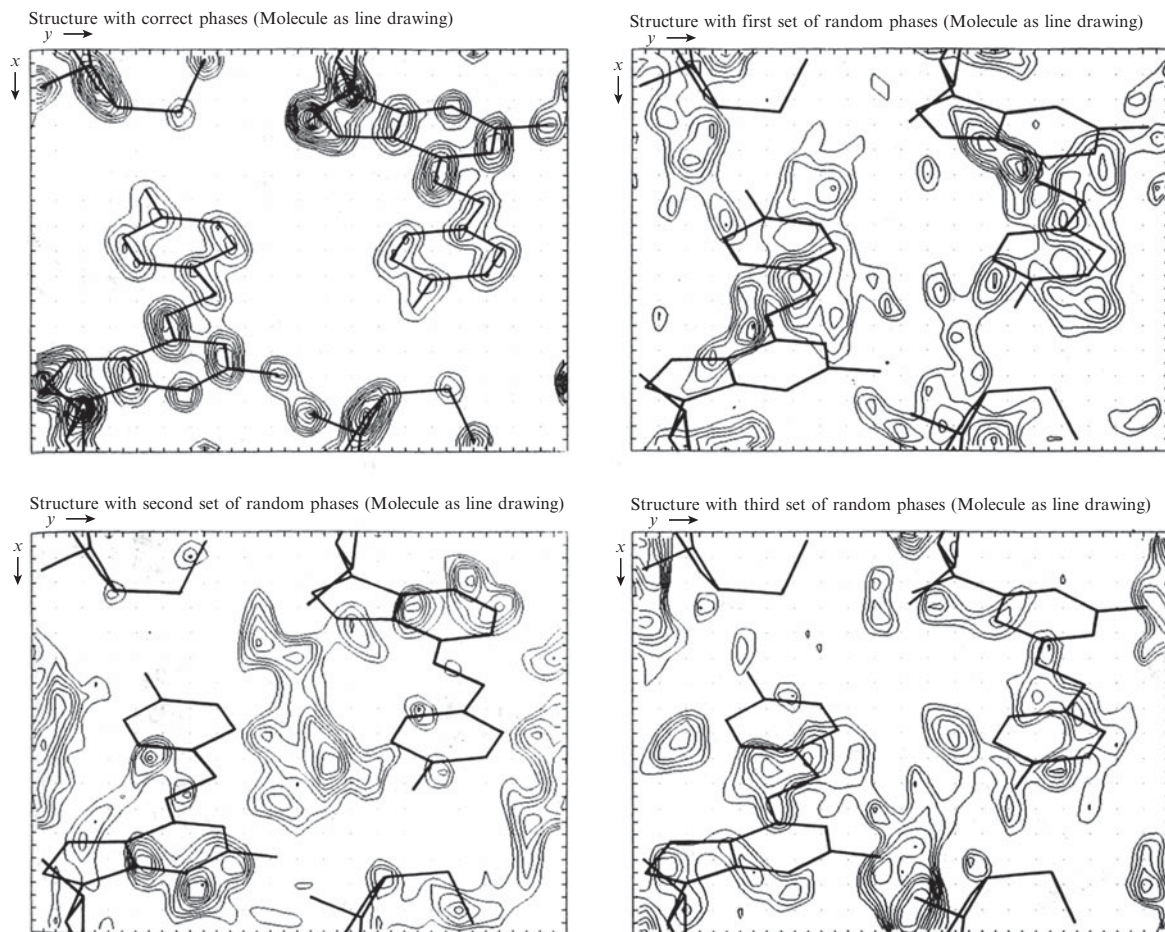


Fig. 6.5 Comparison of electron-density maps when the phases are correct and when they are incorrect and random.

In the computation of all maps shown here, the same $|F(hkl)|$ values but different phases were used. The upper left electron-density map (a) is the correct result; the other three maps (b) to (d) have incorrect relative phases, and provide an incorrect electron-density map. The phases of these three “random phase” maps were found by a computer program for random number generation. Since the structure is noncentrosymmetric, the phase for each Bragg reflection could have any value between 0° and 360° . In each case, the molecular skeleton is shown by solid lines in the correct position, but it is clear that only the first map (top left) correctly represents the true structure.

Courtesy H. L. Carrell.

structure, and the peaks in such a map correspond to the centers of atoms. The importance of the phases in determining a structure is illustrated in Figure 6.5. Each of the four electron-density maps in this figure has the same values of $|F|$, but differs in the phases used in the calculation. For clarity, the true crystal structure is indicated by a line diagram. As can be seen, only the first map correctly gives peaks at atomic positions. An electron-density map with correct phases much more nearly approximates the correct structure than does an electron-density map with incorrect phases, even if each has the correct magnitudes for the $|F(hkl)|$ values. The analysis of electron-density and Patterson maps has

benefited greatly from the improvements in computer graphics so that now it is possible to view the three-dimensional map on a computer screen and rotate and move it at will in order to obtain structural information. However, automatic fitting of a three-dimensional model structure to the electron-density map is now possible by computer without any need for display (Lamzin et al. 2001; Oldfield, 2003).

An initial trial structure

At the start of a structure determination one does not know the positions of all the atoms in the structure (for if one did, the structure would probably not need to be investigated), but one can often deduce an approximation to the correct structure. The calculated phases for this initial (approximate) trial structure will provide a starting point for structure determination. This trial structure may be one that completely fills the unit cell or else it may be only a partial structure (even, for example, one heavy atom). It is possible to calculate an approximation to the true electron density by a three-dimensional Fourier summation of the observed structure factor amplitudes, $|F_o|$, with phases calculated from an initial trial structure which may be only partially complete. It has been found that the general features of an electron-density map depend much more on the phase angles than on the structure factor amplitudes. Therefore a map calculated with only approximately correct phases will be an imperfect representation of the structure. However, it is biased toward the correct structure because the observed structure amplitudes $|F_o|$ were used in the calculation. By comparison with a similar synthesis using the calculated amplitudes $|F_c|$, or even more simply by computing the difference ($|F_o| - |F_c|$) to obtain a “difference synthesis”, one can deduce the changes in the model needed to give better agreement with observation. The positions of some hitherto unrecognized atoms may be indicated, and shifts in the positions of some atoms already included will normally be suggested as well.

Correctness of the trial structure

Once the approximate positions and identities of all the atoms in the asymmetric unit are known (that is, when the true crystal structure is known), the amplitudes and phases of the structure factors can readily be calculated (see Chapter 5). These calculated amplitudes, $|F(hkl)_c|$, may be compared with the observed amplitudes, $|F(hkl)_o|$. If the structural model is a correct one and the experimentally observed data are reasonably precise, the agreement should be good. The situation is different for phases. The phases calculated for a trial structure cannot be compared with observed phases, because normally *phases are not*

observed; they depend on where the origin of the unit cell was chosen to be.

One measure of the correctness of a structure is the so-called discrepancy index (or reliability index or conventional residual), R , defined as

$$R = \frac{\sum (|F_o| - |F_c|)}{\sum (|F_o|)} \quad (6.9)$$

It is a measure of how closely the experimentally observed structure factor amplitudes are matched by the values calculated for a proposed trial structure. At present, R values in the range of 0.02 to 0.06 (alternatively described as 2 percent to 6 percent) are being quoted for the most reliably determined structures of small molecules. An R value of 0.83 corresponds to a random centrosymmetric structure; that is, with proper scaling a randomly incorrect structure with a center of symmetry would give an R value of about 0.83 (0.59 for a noncentrosymmetric crystal structure) (Wilson, 1950). A refinable trial structure may have an R value between 0.25 and 0.35, or even somewhat higher. This value will (hopefully) be decreased by methods described in Chapter 11 to a much lower value. If one atom of high atomic number is present, the initial trial value of R may be much lower because the position of this atom can usually be determined reasonably well even at an early stage, and a heavy atom normally dominates the scattering, as illustrated in the atomic scattering factors in Figure 5.4a. If the trial structure is a reasonable approximation to the correct structure, the R value goes down appreciably as refinement proceeds.

The discrepancy index R is, however, only one measure of the precision (but not necessarily the accuracy) of the derived structure. It denotes how well the calculated model fits the observed data. Many complications can cause errors in the observed or calculated structure factors or both—for example, absorption of the X-radiation by the crystal, or atomic scattering factors and temperature factors that do not adequately describe the experimental situation. The fit of the calculated structure factors to the observed ones may then be good, but if the observations are systematically in error, the *accuracy* of the derived structure may be low, despite an apparently high *precision*. Hence care must be taken in interpreting R values. In general, the lower the R value the better the structure determination, but if one or more very heavy atoms are present, they may dominate the structure factor calculation to such an extent that the contributions from light atoms may not have noticeable effects on R , especially if the structure has not been refined extensively. The positions of the light atoms may then be significantly in error. Also the resolution of the data (i.e., the maximum value of $\sin \theta/\lambda$) must be taken into account in assessing the meaning of an R value. A few grossly incorrect trial structures have been refined to R values as low as 0.10. Fortunately this situation is not common.

Resolution of a crystal structure

The variation of resolving power with scattering angle in structural diffraction studies has a direct analogy with the resolution of an ordinary microscope image (Abbé, 1873; Porter, 1906). If some of the radiation scattered by an object under examination with a microscope escapes

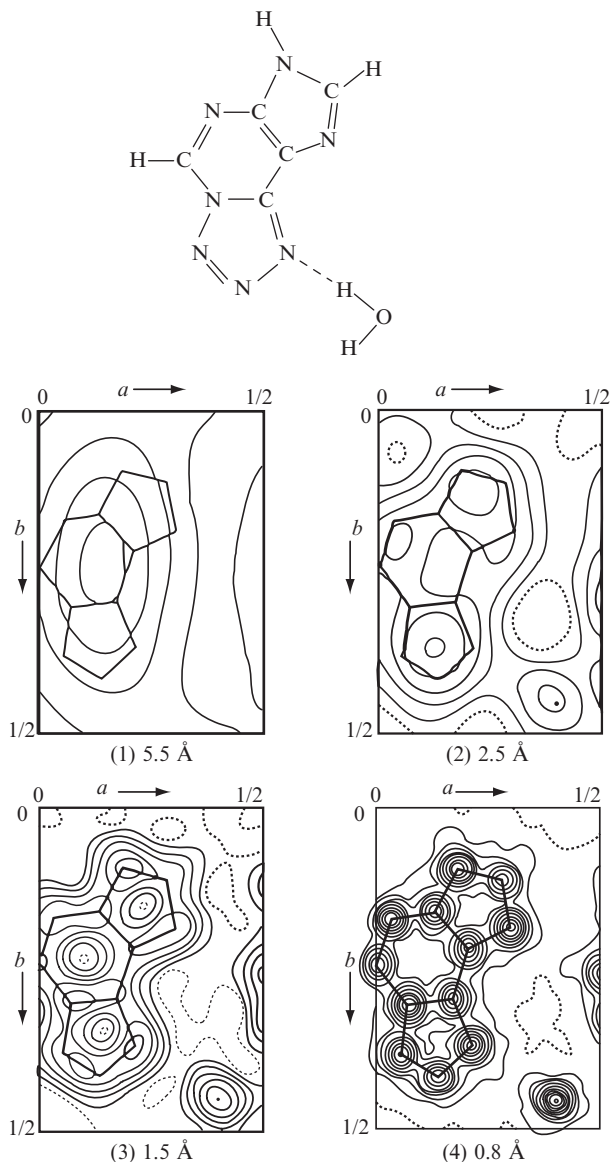


Fig. 6.6 Different stages of resolution for a given crystal structure.

The electron-density maps shown were calculated after eliminating all observed $|F(hkl)|$ measured beyond a given 2θ value. The “resolution” obtained is usually expressed in terms of the interplanar spacings $d = \lambda/(2 \sin \theta)$ corresponding to the maximum observed 2θ values ($\lambda = 1.54 \text{ \AA}$ for copper radiation in this example).

rather than being recombined to form an image (as shown in Figure 1.1), the image that is formed will be, to some degree, an imperfect representation of the scattering object. More particularly, fine detail will remain unresolved. Similarly, with X rays, if the diffraction pattern for the customary wavelengths is observed only out to a relatively small scattering angle, the resolution of the corresponding image reconstructed from it will be low. Furthermore, the resolution will be limited by the wavelength chosen even if the entire pattern is observed. Some examples of electron-density maps calculated with data out to a listed resolution are shown in Figure 6.6. As can be seen, lower numbers, indicating higher resolution, give more detailed pictures of the molecule. As in any process of image formation by recombination of scattered radiation, detail significantly smaller than the wavelength used cannot be distinguished by *any* scheme. On the other hand, the positions of well-resolved objects of known shape can be measured with high precision, and fortunately *all* interatomic distances are well resolved in three dimensions with the X rays we generally use. Hence, the positions of the resolved atoms can be measured and the details of molecular geometry calculated quite precisely.

The basic data in X-ray crystal studies

It is important to stress here which are the experimental data in an X-ray or neutron diffraction experiment. *The experimental results are the intensities of the diffracted beams* (combined with their indices hkl) and their conversion to $|F(hkl)|$ values. The relative phases are generally not measured, but are derived by the methods described in Chapters 8 and 9; isomorphous replacement and Renninger reflection measurements may, however, give some initial phase information. *The electron-density maps that follow are generally not primary experimental data but are the*

| | $d(\text{\AA})$ | Maximum $2\theta(^{\circ})$ | Relative number of Bragg reflections included in each calculation |
|-----|-----------------|-----------------------------|---|
| (1) | 5.5 | 16 | 7 |
| (2) | 2.5 | 36 | 27 |
| (3) | 1.5 | 62 | 71 |
| (4) | 0.8 | 162 | 264 |

In each of the maps, the skeleton of the actual structure from which the data were taken has been superimposed. The first stage (1) (upper left) is typical of those encountered early in the determination of a protein structure. For protein structures, a degree of resolution between (2) and (3) is generally as much as is possible. The detail shown in (4) is characteristic of a structure determination with good crystals of low-molecular-weight compounds with radiation from an X-ray tube with a copper target. These electron-density maps may be compared to views of an object through a microscope, each corresponding to a different aperture (from Glusker et al., 1968). Note the lower peak heights of the carbon atoms compared with the nitrogen atoms. Also note that in the high-resolution structure, hydrogen atom locations are indicated.

results of estimated phase angles and, as shown in Figure 6.5, may or may not be correct. Therefore, if the final structure is not as expected, rereview the methods used to obtain the phases and to refine the proposed trial structure.

Summary

The electron density at a point x, y, z in a unit cell of volume V_c is

$$\rho(xyz) = \frac{1}{V_c} \sum_{\text{all } hkl} \sum |F(hkl)| \cos[2\pi(hx + ky + lz) - \alpha(hkl)]$$

[see Eqn. (6.5)]. Therefore, if we knew $|F(hkl)|$ and $\alpha(hkl)$ (for each h, k, l) we could compute $\rho(x, y, z)$ for all values of x, y , and z and plot the values obtained to give a three-dimensional electron-density map. Then, assuming atomic nuclei to be at the centers of peaks, we would know the entire structure. However, we can usually obtain only the structure factor amplitudes $|F(hkl)|$ and not the relative phase angles $\alpha(hkl)$ directly from experimental measurements. *This is the phase problem.* We must usually derive values of $\alpha(hkl)$ either from values of $A(hkl)$ and $B(hkl)$ computed from suitable “trial” structures or by the use of purely analytical methods. In practice, approximations to electron-density maps can be calculated with experimentally observed values of $|F(hkl)|$ and calculated values of $\alpha(hkl)$. If the trial structure is not too grossly in error, the map will be a reasonable representation of the correct electron-density map, and the structure can be refined to give a better fit of observed and calculated $|F(hkl)|$ values. The discrepancy index R is one measure of the correctness of a structure determination. However, it is at best a measure of the precision of the fit of the model used to the experimental data obtained, not a measure of the accuracy. Some structures with low R values have been shown to be incorrect.

Symmetry and space groups

7

A certain degree of symmetry is apparent in much of the natural world, as well as in many of our creations in art, architecture, and technology. Objects with high symmetry are generally regarded with pleasure. Symmetry is perhaps the most fundamental property of the crystalline state and is a reason that gemstones have been so appreciated throughout the ages. This chapter introduces some of the fundamental concepts of symmetry—symmetry operations, symmetry elements, and the combinations of these characteristics of finite objects (point symmetry) and infinite objects (space symmetry)—as well as the way these concepts are applied in the study of crystals.

An object is said to be symmetrical if after some movement, real or imagined, it is or would be indistinguishable (in appearance and other discernible properties) from the way it was initially. The movement, which might be, for example, a rotation about some fixed axis or a mirror-like reflection through some plane or a translation of the entire object in a given direction, is called a symmetry operation. The geometrical entity with respect to which the symmetry operation is performed, an axis or a plane in the examples cited, is called a symmetry element. *Symmetry operations are actions* that can be carried out, while *symmetry elements are descriptions* of possible symmetry operations. The difference between these two symmetry terms is important.

It is possible not only to determine the crystal system of a given crystalline specimen by analysis of the intensities of the Bragg reflections in the diffraction pattern of the crystal, but also to learn much more about its symmetry, including its Bravais lattice and the probable space group. As indicated in Chapter 2, the 230 space groups represent the distinct ways of arranging identical objects on one of the 14 Bravais lattices by the use of certain symmetry operations to be described below. The determination of the space group of a crystal is important because it may reveal some symmetry within the contents of the unit cell. Space group determination also vastly simplifies the analysis of the diffraction pattern because different regions of this pattern (and hence of the atomic arrangement in the crystal) may then be known to be identical. Furthermore, symmetry greatly reduces the number of required calcu-

lations because only the contents of the asymmetric portion of the unit cell (the asymmetric unit) need to be considered in detail. In summary, the concept of the unit cell reduces the amount of structural information that needs to be determined for a crystal. It is not necessary to determine the locations of millions of molecules in a crystal experimentally, only the locations of those in one unit cell. The concept of the space group further reduces the information required to the “asymmetric unit,” which is a portion of the unit cell that is defined by the space group of the crystal structure. Once the locations of atoms in the asymmetric unit are known, it is possible to calculate the positions of all other atoms in the unit cell and also of all those in the entire crystal by application of the space-group symmetry operations. These have been meticulously tabulated and are readily available in *International Tables* (Hahn, 2005).

Scrutiny of diffraction patterns of crystals reveals that there are often systematically related positions where diffraction maxima might occur but where, in fact, the observed intensity is zero. For example, if molecules pack in a crystal so that there is a two-fold screw axis parallel to the a axis, this means that each atom is moved a distance $a/2$ and then rotated 180° about the screw axis (from x, y, z to $1/2 + x, -y, 1/2 - z$). A result is that for every atom at position x there is another at $1/2 + x$. As far as $h\ 0\ 0$ Bragg reflections are concerned, the unit-cell size has been halved (to $a/2$) and the reciprocal lattice spacing has doubled (to $2a^*$). Bragg reflections will then only be observed for *even* values of h . This situation is made evident by summing in Eqns. (5.21) and (5.22) for atoms at x and $1/2 + x$ when k and l are zero.*

$$\begin{aligned} & * \cos x + \cos y \\ & = 2 \cos [(x + y)/2] \cos [(x - y)/2] \end{aligned}$$

$$\begin{aligned} & \sin x + \sin y \\ & = 2 \sin [(x + y)/2] \cos [(x - y)/2] \end{aligned}$$

$$\cos 0 \text{ and } \cos 2\pi = 1, \cos \pi = -1$$

$$\cos \frac{\pi}{2} \text{ and } \cos \frac{3\pi}{2} = 0$$

$$\begin{aligned} A(h00) &= f \cos 2\pi(hx) + f \cos 2\pi(hx + h/4) \\ &= 2f \cos 2\pi(hx + h/4) \cos 2\pi(h/4) \end{aligned} \quad (7.1)$$

$$\begin{aligned} B(h00) &= f \sin 2\pi(hx) + f \sin 2\pi(hx + h/4) \\ &= 2f \sin 2\pi(hx + h/4) \cos 2\pi(h/4) \end{aligned} \quad (7.2)$$

$A(h00)$ and $B(h00)$ are both zero if h is odd, and therefore no Bragg reflection is observed. By contrast, if h is even, values may be found for $A(h00)$ and $B(h00)$.

Most, but not all, combinations of symmetry elements give rise to systematic relationships among the indices of some of the systematically “absent reflections.” The word “systematically” implies some numerical relationship between the indices hkl of the Bragg reflections. For example, the only $h\ k\ 0$ Bragg reflections with a measurable intensity may be those for which $(h + k)$ is even. Such systematic relationships imply certain symmetry relations in the packing in the structure. Before continuing with an account of methods of deriving trial structures, we present a short account of symmetry and, particularly, its relation to the possible ways of packing molecules or ions in a crystal.

Symmetry groups

Any isolated object, such as a crystal, can possess “point symmetry”. This term means that *any symmetry operation*, such as a rotation of, say, 180° , when applied to the object, *must leave at least one point within the object fixed* (unmoved). “Space symmetry” is different, because it includes *translational symmetry* (which is not permitted in a point group because this requires one point to be fixed in space). A translation operation is a space-symmetry operation; it leaves no point unchanged, since it moves all points equal distances in parallel directions. For example, an infinite array of points, such as a crystal lattice (or an ideal unbounded crystal structure), has translational symmetry, since unit translation (motion in a straight line, without rotation) along any unit crystal lattice vector moves the crystal lattice into self-coincidence. Because most macroscopic crystals consist of 10^{12} or more unit cells, it is a fair approximation to regard the arrangement of atoms throughout most (if not all) of a real crystal as possessing translational symmetry.

Symmetry elements (defined above as descriptions of possible symmetry operations) can be classified into groups (Cotton, 1971). A group, in the mathematical sense, is a set of elements, one of which must be the identity element, and the product of any two elements must also be an element in that same group. In addition, the order in which symmetry elements are combined must not affect the resulting element, and, for every element in the group, there must be another that is its inverse so that when the two are multiplied together the identity element is obtained. Studies of crystal symmetry involve point groups (one point unmoved when symmetry operations are applied) that are used in descriptions of crystals, and space groups (which also allow translational symmetry) that are used in descriptions of atomic arrangements within crystals.

Point symmetry and point groups

The operations of rotation, mirror reflection, and inversion through a point are point-symmetry operations, since each will leave at least one point of the object in a fixed position. The geometrical requirements of crystal lattices restrict the number of possible types of point-symmetry elements that a crystal can have to these three:

- (1) *n-fold rotation axes*. A rotation of $(360/n)^\circ$ leaves the object or structure apparently unchanged (self-coincident). The order of the axis is said to be n , where n is an integer. When $n = 1$ (that is, a rotation of 360°), the operation is equivalent to no rotation at all (0°), and is said to be the “identity operation.” A four-fold rotation axis, 90° rotation at each step, is shown in Figure 7.1, and is denoted by the number 4. It may be proved that only axes of

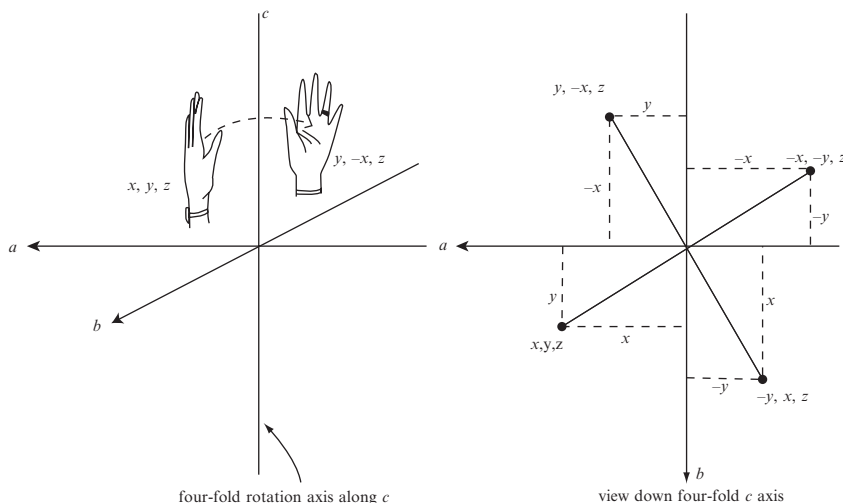


Fig. 7.1 A four-fold rotation axis.

In the figures in this chapter, in order to make the distinction of left and right hands clearer, a ring and watch have been indicated on the left hand but not on the right (even after reflection from the left hand). A four-fold rotation axis, parallel to c and through the origin of a tetragonal unit cell ($a = b$), moves a point at x, y, z to a point at $(y, -x, z)$ by a rotation of 90° about the axis. The sketch on the right shows all four equivalent points resulting from successive rotations; only two of these are illustrated in the left-hand sketch.

order 1, 2, 3, 4, and 6 are compatible with structures built on three-dimensional (or even two-dimensional) crystal lattices. Isolated molecules can have symmetry axes of other orders (5, 7, 8, or 17, for example), but when crystals are formed from a molecule with, for example, a five-fold axis of symmetry, *this five-fold axis cannot be a symmetry axis of the crystal*, although it can be a symmetry axis of the molecule. The molecule may still retain its five-fold symmetry in the crystal, but it can never occur at a position such that this symmetry is a necessary consequence of five-fold symmetry in the crystalline environment. In other words, five-fold symmetry is local and not crystallographic—that is, not required by any space group. This results from the requirement that there be no empty spaces in the packing in a crystal. Pentagonal tiles will not cover a floor without leaving untiled spaces.

- (2) *n-fold rotatory-inversion axes*. The inversion operation, with the origin of coordinates as the “center of inversion,” implies that every point x, y, z is moved to $-x, -y, -z$. From a point at x, y, z one could consider an imaginary straight line to proceed through the center of symmetry (at 0, 0, 0) and, further, an equal distance to $-x, -y, -z$. This inversion can also be augmented by a rotation to give an n -fold rotatory-inversion axis. This involves a rotation of $(360/n)^\circ$ (where n is 1, 2, 3, 4, or 6) followed by inversion through some point on the axis so that no apparent change in the object or structure occurs. The one-fold case, $\bar{1}$, is the inversion operation itself and is often merely called a center of symmetry. A two-fold rotatory-inversion axis, denoted $\bar{2}$, is

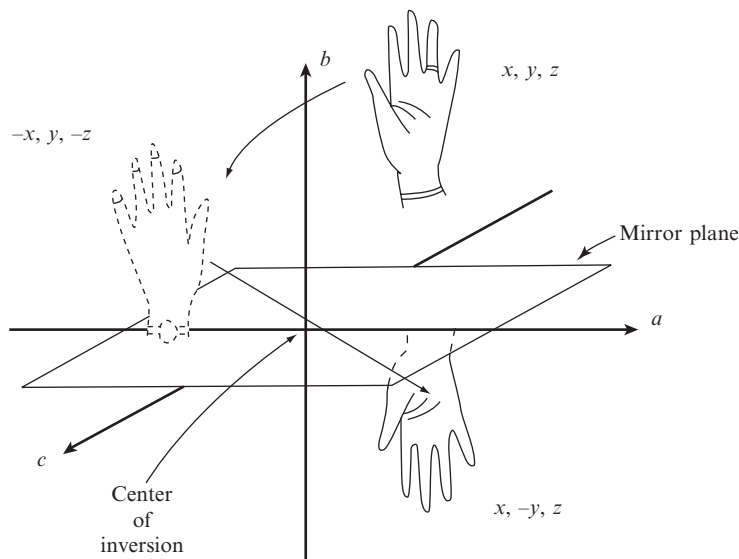
Two-fold rotatory-inversion axis *or* mirror plane

Fig. 7.2 A mirror plane.

The operation $\bar{2}$, a two-fold rotatory-inversion axis parallel to b and through the origin, converts a point at x, y, z to a point at $x, -y, z$. One way of analyzing this change is to consider it as the overall result of first a two-fold rotation about an axis through the origin and parallel to b (x, y, z to $-x, y, -z$) and then an inversion about the origin ($-x, y, -z$ to $x, -y, z$). This is the same as the effect of a mirror plane perpendicular to the b axis. Note that a left hand has been converted to a right hand. The hand illustrated by broken lines is an imaginary intermediate for the symmetry operation $\bar{2}$.

shown in Figure 7.2. In general, these axes are symbolized as \bar{n} .

The rotatory-inversion operations differ from the pure rotations in an important respect; they convert an object into its mirror image. Thus a pure rotation can convert a left hand only into a left hand. By contrast, a rotatory-inversion axis will, on successive operations, convert a left hand into a right hand, then that right hand back into a left hand, and so on. Chiral objects that cannot be superimposed on their mirror images cannot possess any element of rotatory-inversion symmetry.

- (3) *Mirror planes.* We are all familiar with mirrors. They convert a left-handed molecule into a right-handed molecule. As shown in Figure 7.2, a mirror plane is equivalent to a two-fold rotatory-inversion axis, $\bar{2}$, with the axis oriented perpendicular to the plane. The symbol m is more common for this symmetry element.

The point symmetry operations listed above (1, 2, 3, 4, 6, $\bar{1}$, $\bar{2}$ or m , $\bar{3}$, $\bar{4}$, and $\bar{6}$) can be combined together in just 32 ways in three dimensions to form the 32 three-dimensional *crystallographic point groups* (Phillips, 1963). There are, of course, other point groups, appropriate to isolated molecules and other figures, containing, for example, five-fold axes, but objects with such symmetry will have problems packing without gaps in three-dimensional space. The 32 crystallographic point groups or

symmetry classes may be applied to the shapes of crystals or other finite objects (Groth, 1906–1919); the point group of a crystal may sometimes be deduced by an examination of any symmetry in the development of faces. For example, a study of crystals of beryl shows that each has a six-fold axis perpendicular to a plane of symmetry ($6/m$), with two more symmetry planes parallel to the six-fold axis and at 30° to each other (mm). The corresponding point group is designated $6/mmm$. This external symmetry is a manifestation of the symmetry in the internal structure of the crystal. Frequently, however, the environment of a crystal during growth is sufficiently perturbed that the external form or morphology of the crystal does not reflect, to the extent that it might, the internal symmetry. Diffraction studies then help to establish the point group as well as the space group.

Space symmetry

A combination of the point-symmetry operations with translations gives rise to various kinds of space-symmetry operations, in addition to the pure translations.

- (1) *n-fold screw axes*. A two-fold screw axis, 2_1 , is shown in Figure 7.3. Screw axes result from the combination of translation (by distances such as $1/r$ of the repeat axis) and pure rotation (by an n -fold axis) and are symbolized by n_r . They involve a rotation of $(360/n^\circ)$ (where $n = 1, 2, 3, 4$ or 6) and a translation parallel to the axis by the fraction r/n of the identity period along that axis (where r is less than n and both are integers). If we consider a quantity $p = n - r$, then the axes n_r and n_p (such as 4_1 and 4_3 screw axes) are enantiomorphous; that is, they are mirror images of one another, like left and right hands. It is important, however, to note that it is only the *screw axes* that are enantiomorphous; structures built on them will not be enantiomorphous unless the objects in the structure are themselves enantiomorphous. Thus a left hand operated on by a 4_1 will give an arrangement that is the mirror image of that produced by the operation of a 4_3 on a right hand, but not, of course, the mirror image of that produced by the operation of a 4_3 on another left hand, as shown in Figure 7.4 (far left and far right).
- (2) *Glide planes*. These symmetry elements result from the combination of translation with a mirror operation (or its equivalent, 2 , normal to the plane), as illustrated in Figure 7.5. The glide must be parallel to some crystal lattice vector, and, because the mirror operation is two-fold, a point equivalent by a simple translational symmetry operation (a crystal lattice vector) must be reached after two glide translations. Thus these translations may be half of the repeat distance along a unit-cell edge, in which case the glide plane is referred to as an *a*-glide, *b*-glide, or *c*-glide, depending

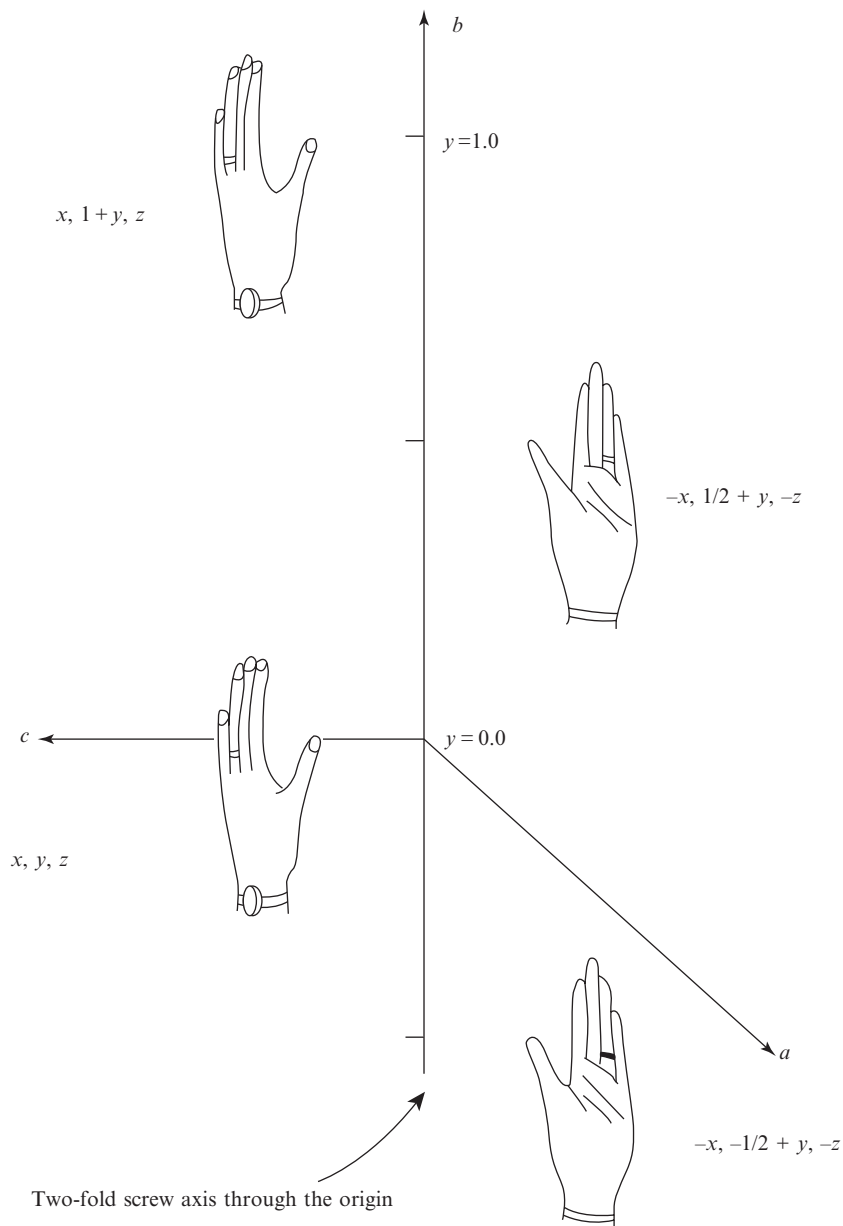


Fig. 7.3 A two-fold screw axis.

A two-fold screw axis, 2_1 , parallel to b and through the origin, which combines both a two-fold rotation (x, y, z to $-x, y, -z$) and a translation of $b/2$ ($-x, y, -z$ to $-x, 1/2 + y, -z$). A second screw operation will convert the point $-x, 1/2 + y, -z$ to $x, 1 + y, z$, which is the equivalent of x, y, z in the next unit cell along b . Note that the left hand is never converted to a right hand by this screw axis.

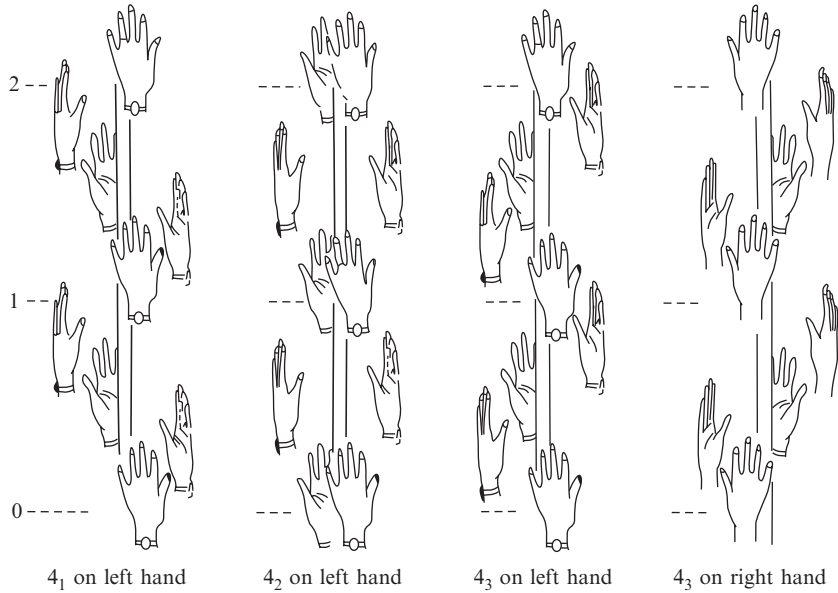


Fig. 7.4 A four-fold screw axis.

Some crystallographic four-fold screw axes showing two identity periods for each. Note that the effect of 4_1 on a left hand is the mirror image of the effect of 4_3 on a right hand.

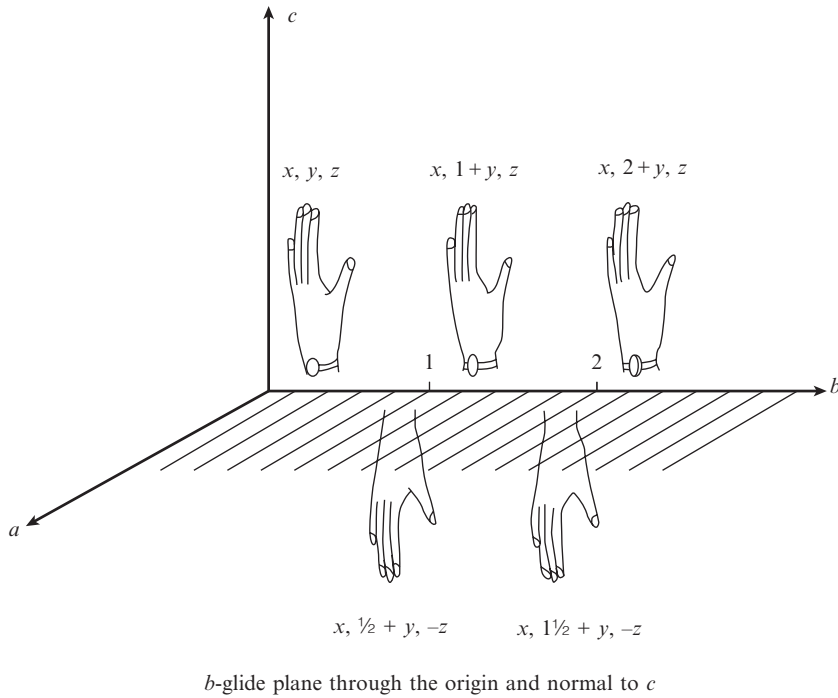


Fig. 7.5 A glide plane.

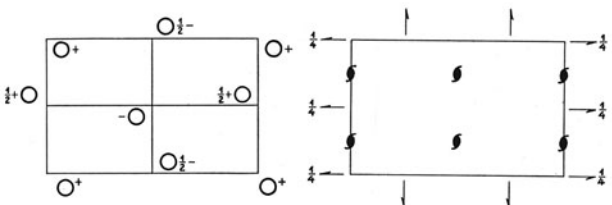
A b -glide plane normal to c and through the origin involves a translation of $b/2$ and a reflection in a plane normal to c . It converts a point at x, y, z to one at $x, 1/2 + y, -z$. Note that left hands are converted to right hands, and vice versa.

on the edge parallel to the translation. Alternatively, the glide may be parallel to a face diagonal. No glide operation involves fractional translational components other than $\frac{1}{2}$ or $\frac{1}{4}$, and the latter occurs only for glide directions parallel to a face diagonal or a body diagonal in certain nonprimitive space groups.

Space groups

We showed in Chapter 2 how an investigation of the symmetries of crystal lattices led to the seven crystal systems (triclinic, monoclinic, orthorhombic, tetragonal, hexagonal, rhombohedral, and cubic). These, when combined with unit-cell centering (face- or body-centering), gave the 14 Bravais lattices (see Appendix 2). If the 14 Bravais lattices are

| | | | | |
|--------------|-----|-----------------|--------|----------------------------|
| Orthorhombic | 222 | $P 2_1 2_1 2_1$ | No. 19 | $P 2_1 2_1 2_1$ D_2^7 |
|--------------|-----|-----------------|--------|----------------------------|



Origin halfway between three pairs of non-intersecting screw axes

| Number of positions, Wyckoff notation, and point symmetry | Co-ordinates of equivalent positions | Conditions limiting possible reflections |
|---|---|---|
| 4 <i>a</i> 1 | $x, y, z; \frac{1}{2} - x, \bar{y}, \frac{1}{2} + z; \frac{1}{2} + x, \frac{1}{2} - y, \bar{z}; \bar{x}, \frac{1}{2} + y, \frac{1}{2} - z.$ | $hkl:$ $0kl:$ $h0l:$ $hk0:$ $h00: h=2n$ $0k0: k=2n$ $00l: l=2n$ |
| Symmetry of special projections | | |
| (001) <i>pgg</i> ; $a' = a, b' = b$ | (100) <i>pgg</i> ; $b' = b, c' = c$ | (010) <i>pgg</i> ; $c' = c, a' = a$ |

Fig. 7.6 Part of a page from *International Tables for X-Ray Crystallography*.

Information on the space group $P 2_1 2_1 2_1$. The crystal is orthorhombic and there are three sets of mutually perpendicular nonintersecting screw axes. P denotes a primitive crystal lattice (that is, one lattice point per cell with no face- or body-centering) and 2_1 denotes a two-fold screw axis. The origin of the cell, chosen so that it lies halfway between these three pairs of nonintersecting screw axes, lies in the upper left-hand corner with the x direction down and the y direction across to the right; x is parallel to a and y is parallel to b . The symbol (\bullet) refers to a two-fold screw axis perpendicular to the plane of the paper. The symbol ($-$) refers to a two-fold screw axis in a plane parallel to the plane of the paper; the fractional height of this plane above the plane $z = 0$ is shown (unless the screw axis is in the plane $z = 0$). The operations of the space group on the point (x, y, z) give three additional equivalent positions, whose coordinates are listed. Thus the screw axis parallel to c at $x = \frac{1}{4}, y = 0$ converts an atom at x, y, z to one at $\frac{1}{2} - x, -y, \frac{1}{2} + z$. Similar transformations are effected by the other two sets of screw axes (parallel to a and b , respectively). The diffraction patterns of crystals with this space group show systematic absences only for $h 0 0$ when h is odd, $0 k 0$ when k is odd, and $0 0 l$ when l is odd. Such crystals contain only molecules of one handedness (chirality). This diagram is from Volume 1 of *International Tables*. The current Volume A of *International Tables* contains the same information and more. Reproduced with permission of the International Union of Crystallography.

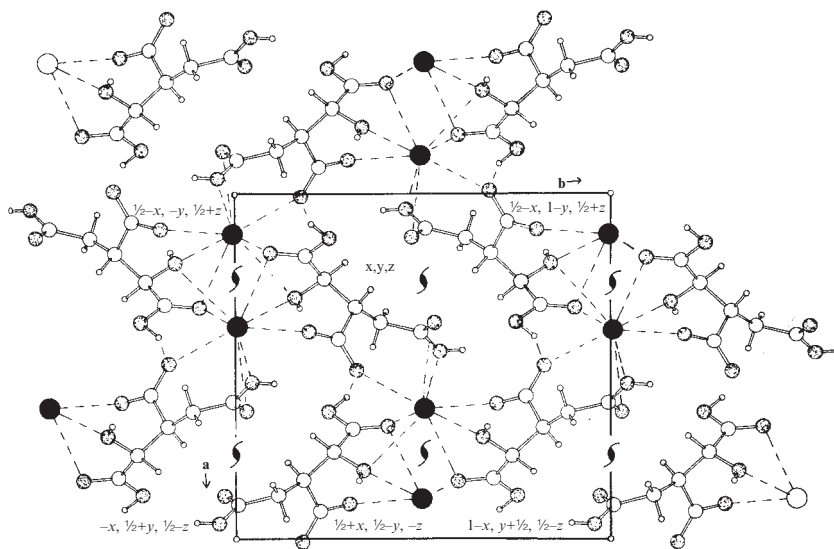


Fig. 7.7 A structure that crystallizes in the space group $P2_12_12_1$.

Contents of the unit cell of potassium dihydrogen isocitrate (van der Helm et al., 1968). The space group (see Figure 7.6) requires that, for each atom at x, y, z , there should be equivalent atoms at $1/2 - x, -y, 1/2 + z$; $1/2 + x, 1/2 - y, -z$; and $-x, 1/2 + y, 1/2 - z$. These are indicated on the diagram (oxygen stippled, potassium dark, hydrogen small). Interactions via hydrogen bonding and metal coordination are indicated by broken lines. This figure illustrates how anions cluster around a cation (dark spheres, K^+) and how this clustering, together with hydrogen bonding, is a major determinant of the structure.

combined with the symmetry elements of the 32 crystallographic point groups (involving reflection, rotation, and rotation-inversion symmetry), plus, in addition, the translational symmetry elements of glide planes and screw axes, the result is just 230 arrangements. These 230 space groups are compatible with the geometrical requirements of three-dimensional crystal lattices, that is, that the space-group symmetry should generate exactly the same arrangement of objects from unit cell to unit cell. There are thus 230 three-dimensional space groups, ranging from that with no symmetry other than the identity operation (symbolized by $P1$, the P implying primitive) to those with the highest symmetry, such as $Fm\bar{3}m$, a face-centered cubic space group. These 230 space groups represent the 230 distinct ways in which objects (such as molecules) can be packed in three dimensions so that the contents of one unit cell are arranged in the same way as the contents of every other unit cell.

It is interesting to note that these 230 unique three-dimensional combinations of the possible crystallographic symmetry elements were derived independently in the last two decades of the nineteenth century by Evgraf Stepanovich Fedorov in Russia, Artur Moritz Schönflies in Germany, and William Barlow in England (Schönflies, 1891; Fedorov, 1891; Barlow, 1894). It was not until several decades later that anything was known of the actual atomic structure of even the simplest crystalline solid. Since the introduction of diffraction methods for studying the structure of crystals, the space groups of many thousands of crystals

have been determined. It has been found that about 60% of the organic compounds studied crystallize in one of six space groups.**

All 230 space groups, and the systematically absent Bragg reflections found for them in the diffraction pattern, are listed in *International Tables*, Volume 1 or A, which is in constant use by X-ray crystallographers (Wyckoff, 1922; Astbury and Yardley, 1924; Hahn, 2005). Part of a specimen page from Volume 1 is shown in Figure 7.6. The symmetry operations in a space group must ensure that the next unit cell has the same contents as the original, and that it packs against the original unit cell with no gaps or spaces. Once the space group is determined from the systematically absent Bragg reflections in the X-ray diffraction pattern and by other means, if needed, *only the structure of the contents of the asymmetric unit*, not the entire unit cell, *need be determined*. The contents of the rest of the cell (and of the entire structure) are then known by application of the symmetry operations of the space group. An example is shown in Figure 7.7. An excellent way to obtain an introduction to space groups is to work one's way through the 17 plane groups listed just before the space groups in *International Tables for Crystallography*, Volume A, *Space-group Symmetry* (Hahn, 2005).

**The centrosymmetric space groups $P2_1/c$, $P\bar{1}$, $C2/c$, and $Pbca$ and non-centrosymmetric space groups $P2_12_12_1$ and $P2_1$.

Space group ambiguities

The principal method used to determine the space group of a crystal is that of determining which Bragg reflections are systematically absent in the space group. These are listed in *International Tables*, Volume A. As shown in an example at the beginning of this chapter, these systematic absences depend on the translational symmetry of the space group (screw axes, glide planes, face- or body-centering); that is, a two-fold screw axis resulted in systematic absences for $h00$ when h is odd. Therefore, space groups with the same translational symmetry elements (for example, $P2_1$ and $P2_1/m$)[†] will have the same systematic absences in their diffraction patterns, giving rise to an ambiguity in the determination of the space group.

However, there are ways of overcoming this problem. If the crystal contains only one enantiomorph of an asymmetric molecule, then the space group cannot contain a mirror or glide plane or a center of symmetry, since these symmetry elements convert one enantiomorph into the other. As a result, if the ambiguity involves a pair of space groups, one centrosymmetric and the other noncentrosymmetric (such as $P1$ and $P\bar{1}$ or $P2_1$ and $P2_1/m$), then a distinction can be made if the crystal contains molecules of only one chirality, since the crystal cannot then be centrosymmetric. In other cases the distinction can usually be made, as described in more detail in Chapter 8, by a consideration of the distribution of intensities in the diffraction pattern, since centrosymmetric structures have a higher proportion of Bragg reflections of very low intensity than do noncentrosymmetric structures. Other diagnostic methods involve tests of physical properties, including the

[†] Equivalent positions for $P2_1$ are x, y, z and $-x, 1/2 + y, -z$. Equivalent positions for $P2_1/m$ are $x, y, z; -x, -y, -z; -x, 1/2 + y, -z; \text{ and } x, 1/2 - y, z$.

piezoelectric and pyroelectric effects (see Chapter 2). These effects are found only for noncentrosymmetric crystals. Still another method of distinguishing between space groups is to analyze the vectors in the Patterson map, described in Chapter 9. Finally, a consideration of the chemical identity of the contents of the unit cell may help resolve any space group ambiguity.

The following example of such an ambiguity may be of interest. The protein xylose isomerase, consisting of four identical subunits bound in a tetramer, crystallizes in the space group $I222$ or $I2_12_12_1$ with two molecules (eight subunits) in the unit cell. The systematic absences in Bragg reflections are, unfortunately, the same for both space groups, so here is an example of a space group ambiguity. This follows because the space-group absences for a body-centered unit cell are such that $h + k + l$ must be even, while the three screw axes require $h00$ with h even, $k00$ with k even, and $l00$ with l even; these last three requirements are included in the first condition, so that it does not make any difference to the systematic absences whether or not the screw axes are there. However, each unit cell for either space group contains eight asymmetric units, and therefore one subunit (one quarter of the molecule) must be the asymmetric unit (together with solvent, not considered here). If the space group were $I2_12_12_1$ the protein would be an infinite polymer, because of the requirements of the two-fold screw axes, contrary to physical evidence. Therefore the space group is $I222$, so that the subunits are related to each other by two-fold rotation axes rather than two-fold screw axes.

Chirality

Chirality is the handedness of a structure (Greek: *cheir* = hand); that is, if a structure cannot be superimposed on its mirror image it is said to be chiral or enantiomorphous. We are most familiar with this in the example of the asymmetric carbon atom—that is, a carbon atom connected to four different chemical groups so that two types of molecules, related to each other by a mirror plane, are found. This chirality, however, can also extend to the crystal structure itself. For example, silica crystallizes in a helical arrangement that has a handedness shown in the external shape of the crystal—small hemihedral[‡] faces appear in such a way as to give crystals that are mirror images of each other. The observation of such hemihedry was used by Louis Pasteur in 1848 to separate sodium ammonium tartrate into its left- and right-handed enantiomers (Pasteur, 1848; Patterson and Buchanan, 1945). Solutions of these pure enantiomers rotate the plane of polarization of light in opposite directions. When such resolution[§] occurs the space group must contain no mirror planes, glide planes, or centers of inversion (i.e., any symmetry operation that would convert a left-handed structure into a right-handed structure). Such crystals also exhibit pyroelectric and piezoelectric properties as a result of their asymmetry. Pasteur's

[‡] Called “hemihedral” because only half the number of faces expected for a centrosymmetric structure is observed.

[§] The term “resolution” is used in a different sense from that in the caption to Figure 6.6. Here it is used to mean the separation of enantiomers. The term is also used to describe the process of distinguishing individual parts of an object, as when viewing them through a microscope.

resolution of sodium ammonium tartrate was possible because the space group was one for a noncentrosymmetric structure, so the two crystal forms looked different. If an asymmetric molecule crystallizes in a centrosymmetric space group, then there are equal numbers of left- and right-handed molecules in the crystal structure. This will be discussed further in Chapter 10.

Space groups of chiral objects

Chiral molecules, such as proteins and nucleic acids, cannot crystallize in space groups with centers of symmetry, mirror planes, or glide planes, because otherwise molecules with the opposite chirality would also be required. There are 65 space groups that are suitable for such chiral molecules (see Appendix 7). In all, there are three types of space groups. 90 space groups are centrosymmetric and contain equal numbers of both enantiomers (left-handed and right-handed species) in the crystal. There are, however, 75 other space groups that are neither centrosymmetric nor chiral; that is, while the space group is noncentrosymmetric, the unit cell still contains equal numbers of both enantiomers (see Appendix 7). Some space groups among those for chiral molecules are designated as “polar space groups.” They do not have a defined origin, for example, because, as in the space group $P2_1$, there is only one screw axis and it moves an atom at x, y, z to $-x, 1/2 + y, -z$ (by convention along the b axis). So y can have any value for the first atom in a list of atomic coordinates; its value then defines the origin that has been selected (but this is not defined by the space group), so that all other atoms are correctly related in space to the first atom. The polar space groups are indicated in Appendix 7. This polar property of the crystal must be remembered when atomic coordinates are being refined, as described later in Chapter 11. It also implies that opposite crystal faces perpendicular to the b axis may have different physical characteristics, as will be described in Chapter 10.

Summary

Symmetry in the contents of the unit cell is revealed to some extent by the symmetry of the diffraction pattern and by the systematically absent Bragg reflections (see Appendix 2). The probable space group of the crystal can be deduced from this information about the diffraction pattern. Knowledge of the space group may also give information on molecular packing, even before the structure has been determined.

- (1) There are 14 distinct three-dimensional lattices (the Bravais lattices), corresponding to seven different crystal systems.
- (2) Point-symmetry operations leave at least one point within an object fixed in space. Those characteristic of crystals consist of:

- (a) n -fold rotation axes (1, 2, 3, 4, 6) and
 - (b) n -fold rotatory-inversion axes ($\bar{1}$, $\bar{2}$ or m , $\bar{3}$, $\bar{4}$, or $\bar{6}$).
- (3) These point-symmetry operations can be combined in 32 and only 32 distinct ways to give the three-dimensional crystallographic point groups.
- (4) Combination of point-symmetry operations with translations gives space-symmetry operations by way of:
- (a) n -fold screw axes, n_r , and
 - (b) glide planes.
- (5) All these operations may act on a given motif in the asymmetric portion of the structure. They can be combined in just 230 distinct ways, giving the space groups which can be used to describe crystal structures composed of multiple unit cells, each with identical structural components within them.

The derivation of trial structures. I. Analytical methods for direct phase determination

8

As indicated at the start of Chapter 4, after the diffraction pattern has been recorded and measured, the next stage in a crystal structure determination is solving the structure—that is, finding a suitable “trial structure” that contains approximate positions for most of the atoms in the unit cell of known dimensions and space group. The term “trial structure” implies that the structure that has been found is only an approximation to the correct or “true” structure, while “suitable” implies that the trial structure is close enough to the true structure that it can be smoothly refined to give a good fit to the experimental data. Methods for finding suitable trial structures form the subject of this chapter and the next. In the early days of structure determination, trial and error methods were, of necessity, almost the only available way of solving structures. Structure factors for the suggested “trial structure” were calculated and compared with those that had been observed. When more productive methods for obtaining trial structures—the “Patterson function” and “direct methods”—were introduced, the manner of solving a crystal structure changed dramatically for the better.

We begin with a discussion of so-called “direct methods.” These are analytical techniques for deriving an approximate set of phases from which a first approximation to the electron-density map can be calculated. Interpretation of this map may then give a suitable trial structure. Previous to direct methods, all phases were calculated (as described in Chapter 5) from a proposed trial structure. The search for other methods that did not require a trial structure led to these phase-probability methods, that is, direct methods. A direct solution to the phase problem by algebraic methods began in the 1920s (Ott, 1927; Banerjee, 1933; Avrami, 1938) and progressed with work on inequalities by David Harker and John Kasper (Harker and Kasper, 1948). The latter

authors used inequality relationships put forward by Augustin Louis Cauchy and Karl Hermann Amandus Schwarz that led to relations between the magnitudes of some structure factors (see Glossary). These proved very useful, enabling them to derive relationships between the relative phases of different structure factors, and therefore to determine the crystal structure of decaborane (Kasper et al., 1950). This provided a previously unthought-of chemical structure for this molecule and greatly augmented our understanding of the structure and chemistry of the boron hydrides. Many scientists and mathematicians worked on the derivation of phase relationships in direct methods from this time on.* David Sayre provided an important equation that led to his demonstration of the structure of hydroxyproline (Sayre, 1952), while Herbert Hauptman and Jerome Karle worked on the probabilistic basis of direct methods (Karle and Hauptman, 1950; Hauptman and Karle, 1953). These, and the studies of many others, led to the equations of direct methods that are used today, and to the production of computer programs to do the analysis (Germain et al., 1971, for example) together with initially much-needed teaching on how to interpret the results of their use correctly.

*There have been many involved in the development of direct methods, in the programming of methods to use them, and in teaching people how to do it. These include (in alphabetical order), in the earlier stages, William Cochran, Joseph Gillis, David Harker, Herbert Hauptman, Isabella Karle, Jerome Karle, John S. Kasper, Peter Main, David Sayre, George Sheldrick, Michael Woolfson, and William H. Zachariasen. Many others also merit our appreciation of the ease with which crystal structures can generally be determined.

“Direct methods” make use of two important facts: (1) that the intensities of Bragg reflections contain the structural information that peaks (representing atoms) are well resolved from each other (the principle of *atomicity*), and (2) that the background is fairly flat, and that this background should not be negative, because this would imply a negative electron density (the principle of *positivity*). These two conditions are true for X-ray diffraction, where atoms generally scatter by an amount that depends on their atomic number. The basic assumption that atoms are resolved from each other results in a requirement of high resolution, usually 1.1 Å or better, for direct methods. In the case of neutron diffraction, the electron-density map may have negative peaks because atoms, such as hydrogen, with a negative scattering factor for neutrons, are present. In spite of this, direct methods appear to work for neutron structures as well (Verbist et al., 1972). Centrosymmetric structures (with the positional coordinates of each atom at x, y, z , matched by those of an equivalent atom at $-x, -y, -z$) are considered first here, because the problems presented by noncentrosymmetric structures are more formidable. Techniques other than “direct methods” for deriving trial structures and the principles upon which they are based are discussed in Chapter 9.

It is possible to derive relations among the phases of different Bragg reflections. The basic assumption of direct methods is that the intensities in the X-ray diffraction pattern contain phase information (because the phases are constrained to give atomic peaks and positive electron density and this limits their values). It means that direct methods can be viewed as a mathematical problem—the control of the phase angles of density waves because of the principles of atomicity and positivity. How can the many density waves be aligned (as required by their

individual phases) so that the resultant electron-density map shows peaks or a flat background with no negative areas? What must their phases be to satisfy these conditions?

In crystal structures with a center of symmetry at the origin and no appreciable anomalous-dispersion effects, each structure factor has a phase angle of 0° or 180° , so that $\cos a$ is just $+1$ or -1 and $\sin a = 0$. Therefore, in a centrosymmetric structure, $F = |F| \cos a = +|F|$ or $-|F|$, and one often speaks of the *sign of a structure factor*; when the phase angle a is 0° we write “+” and when it is 180° we write “-”. If N Bragg reflections have been observed for the structure, 2^N electron-density maps would need to be calculated, representing all possible combinations of signs for all N independent structure factors. One of these 2^N maps must represent the true electron density, but how could one tell which one it is? For even as few as twenty Bragg reflections, more than one million different maps would need to be calculated ($2^{20} = 1,048,576$), and most structures of interest have of the order of 10^3 – 10^6 unique Bragg reflections. Since the contributions from Bragg reflections with high values for the structure factor amplitude will tend to dominate any electron-density map calculated, only the most intense Bragg reflections need be considered initially when one is trying to obtain an approximation to the correct map. However, even with as few as ten terms, the number of possible maps is 1024, much too high a number to make any simple trial-and-error method practicable. With a noncentrosymmetric crystal structure, a phase angle may be anywhere between 0° and 360° and one would have to calculate an impossibly large number of maps to ensure having at least approximately correct phase angles for even ten Bragg reflections.

Relationships can be found among the signs of the structure factors, and these relationships involve the magnitudes of the larger structure factors normalized (that is, modified) in a certain way, as will be described in this chapter. If you want to know what a given structure factor of known relative phase contributes to the overall electron density in a unit cell (its density wave), it is easy to plot this. Suppose that $F(1\ 0\ 0)$ for a centrosymmetric structure is large (see Figure 8.1). If this Bragg reflection has a positive sign (phase angle of 0°), then the computed electron-density map has a peak near the origin at $x = 0$ and a hole at $x = 1/2$. By contrast, if this Bragg reflection has a negative sign, there is a peak at $x = 1/2$ and a hole at $x = 0$. Therefore the fact that this Bragg reflection is intense in a centrosymmetric structure implies that there must be a peak in the electron-density map near either $x = 0$ or $x = 1/2$, whatever the sign (phase) to be associated with $F(1\ 0\ 0)$. If $F(2\ 0\ 0)$ is considered, it can be seen in Figure 8.1 that a peak at either 0 or $1/2$ implies a positive sign for $F(2\ 0\ 0)$. Consequently, *if $F(1\ 0\ 0)$ and $F(2\ 0\ 0)$ are intense, $F(2\ 0\ 0)$ is probably positive* no matter whether the sign of $F(1\ 0\ 0)$ is positive or negative. Figure 8.1 shows also that when only these terms are summed, a positive sign for $F(2\ 0\ 0)$ results in an “electron density” that has a shallower negative trough than does

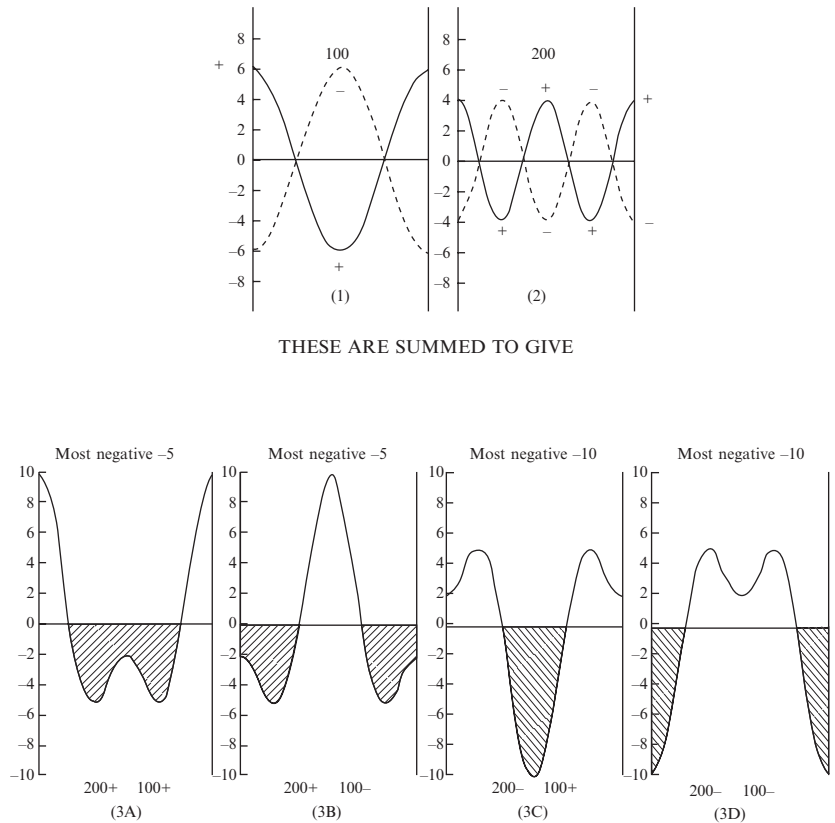


Fig. 8.1 Summing density waves.

In centrosymmetric structures, the phase angle of any structure factor $F(hkl)$ is either 0° or 180° . “Electron-density maps” based on one structure factor (“density wave”) are shown for $F(1\ 0\ 0)$ and $F(2\ 0\ 0)$. In general, for centrosymmetric structures, if $F(hkl)$ is large, whatever its sign, and $F(2h2k2l)$ is also large, then the latter is probably positive (a phase of 0°). (1) Possible situations for $F(1\ 0\ 0)$: solid line— F positive, phase 0° ; dotted line— F negative, phase 180° . (2) Possible situations for $F(2\ 0\ 0)$; solid line— F positive, phase 0° ; dotted line— F negative, phase 180° . (3) Summations for the four combinations of possible situations in (1) and (2), showing the deep negative areas obtained when $F(2\ 0\ 0)$ is given a phase of 180° (C, D). The $F(0\ 0\ 0)$ term, which has been omitted, is always positive and therefore when it is included the sum is always more positive at each given point (see Figure 6.2).

Areas of negative electron density are shaded. The inferences on the position of an atom (at x) from these electron-density maps are: 3A, $x = 0$; 3B, $x = 1/2$; 3C, 3D, $x = 1/4, 3/4$. The last two have more negative troughs and so are excluded. Therefore we conclude 200 is + (phase angle 0°) and x is 0 and/or $1/2$.

the electron density that results when a negative sign is assigned to $F(2\ 0\ 0)$ (regardless of the sign of $F(1\ 0\ 0)$). Thus the phase of $F(2\ 0\ 0)$ is probably +.

The principle of positivity of electron density may be extended to three dimensions. For example, David Sayre noted that the functions $\rho(r)$ and $\rho^2(r)$ in a crystal composed of identical atoms are similar in appearance. From analyses of the relationship between these two

functions and of their Fourier transforms, he showed that

$$\sum_K \sum H \sum F(K)F(H-K) = VsF(H) \quad (8.1)$$

This is the equation that bears his name (Sayre, 1952; see also Viterbo, 1992; Shmueli, 2007). In this equation $H = h, k, l$ and $K = h', k', l'$; V is the unit cell volume; s is the sign of the hkl Bragg reflection; and the summations are over all values of K .

If one considers probabilities (denoted \approx), rather than certainties (denoted $=$), it can be shown that, for a centrosymmetric structure, one obtains a *triple product*

$$sF(H) sF(K) \approx sF(H+K) \quad (8.2)$$

where sF means the “sign of F ” and $F(H)$, $F(K)$, and $F(H+K)$ are all intense Bragg reflections. The symbol \approx means “is probably equal to.” It should be noted that a special case of Eqn. (8.2) is

$$s(2h\ 0\ 0) \approx [s(h\ 0\ 0)]^2 \approx + \quad (8.3)$$

because whatever the sign of $F(h00)$, its square is positive. This is in agreement with our qualitative argument for $F(2\ 0\ 0)$ and $F(1\ 0\ 0)$ above and in Figure 8.1. In Figure 8.2 it is shown that if $F(3\ 0\ 0)$ is known to be positive and $F(2\ 0\ 0)$ is known to be negative, then, if all three are strong Bragg reflections, $F(5\ 0\ 0)$ is probably (but not definitely) negative. Again, this is shown to be consistent with the principle of positivity of electron density. Two types of sets of triple products of phases (see Eqn. 8.2) merit attention at this point. A “structure invariant” is a linear combination of the phases that is totally independent of the choice of origin; even if the origin is changed, the invariant remains unchanged. The same is true for “structure seminvariants” except that the origin change must be one that is allowed by space-group symmetry constraints. The identification of structure invariants and seminvariants helps to fix an origin and enantiomorph for the structure under study.

In practice, these analytical methods of phase determination are carried out on “normalized structure factors”—that is, values of the structure factor $|F(hkl)|$ modified to remove the fall-off in the individual scattering factors f with increasing scattering angle 2θ (see Figures 5.4 and 8.3). A normalized structure factor, $E(hkl)$, represents the ratio of a structure factor $F(hkl)$ to $(\sum f_j)^{1/2}$, where the sum is taken over all atoms in the unit cell at the value of $\sin \theta/\lambda$ appropriate to the values of h , k , and l for the Bragg reflection and includes an overall vibration factor. This sum, $(\sum f_j)^{1/2}$, represents the root-mean-square value that all $|F(hkl)|^2$ measurements would have (at that value of $\sin \theta/\lambda$) if the structure were a random one, composed of equal atoms (see the discussion of the Wilson plot at the end of Chapter 4):

$$|E(hkl)| = \frac{|F(hkl)|}{(\varepsilon \sum f_j)^{1/2}} \quad (8.4)$$

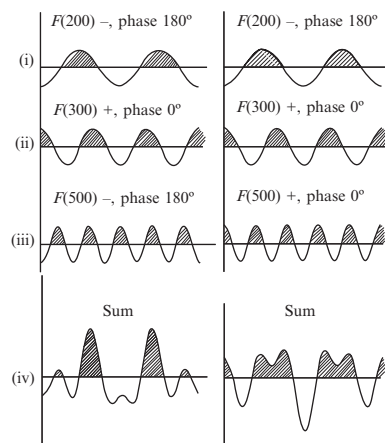


Fig. 8.2 Aiming for nonnegative electron density.

If $|F(2\ 0\ 0)|$, $|F(3\ 0\ 0)|$, and $|F(5\ 0\ 0)|$ are all large they must contribute significantly to the final electron-density map (via “density waves”). Suppose that it is found that $F(2\ 0\ 0)$ has a negative sign and $F(3\ 0\ 0)$ has a positive sign; the areas in which each then contributes in a positive manner to the electron-density map are shaded in (i) and (ii) on the left. The regions in which these areas overlap, near $x = \pm 0.3$, correspond to regions to which $F(5\ 0\ 0)$ contributes positively only if the sign of the term $F(5\ 0\ 0)$ is negative, that is, a phase of 180° , as indicated in (iii). On summation of these terms with the indicated signs the background is reduced, as in (iv); if $F(5\ 0\ 0)$ has a positive sign, that is, a phase of 0° , the map is far less satisfactory. The relation among these signs may then be written (where s means “the sign of”)

$$s(5\ 0\ 0) \approx s(2\ 0\ 0)s(3\ 0\ 0)$$

which is a special case of Eqn. (8.2). This follows from the discussion in the text since deep negative troughs (areas of negative electron density) are not satisfactory or physically meaningful. With proper phasing, the background is reduced to a value closer to zero. Thus in (iv) on the left the most negative value of the electron density is $-4\ \text{e}/\text{\AA}$, while for (iv) on the right, which has a less satisfactory set of phases, the most negative value of the electron density is $-9\ \text{e}/\text{\AA}$. The addition of data for $F(000)$ will probably result in an almost nonnegative map if $F(500)$ has a phase of 180° .

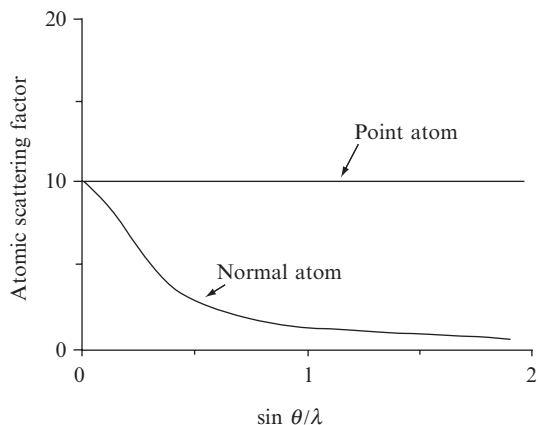


Fig. 8.3 X-ray scattering by point atoms and normal atoms.

Theoretical point atoms have no width and no vibrational amplitude. As a result there is no fall-off in value as $\sin \theta / \lambda$ increases. By contrast, real normal atoms have width and vibrational amplitude and their atomic scattering factors fall off at high $\sin \theta / \lambda$.

** Contained in the expression for $E(hkl)$ is a factor, ε , that corrects for the fact that Bragg reflections in certain reciprocal lattice zones or rows (for example, $0k0, hk0$, etc.) have higher average intensities in certain space groups than do general Bragg reflections (hkl). It is an integer, 1, 2, or 4, depending on the crystallographic point group and the type of Bragg reflection (h , k , and/or $l = 0$).

where ε is a constant (an epsilon factor)**, 1, 2, or 4, depending on the crystal class, and the summation is from $j = 1$ to N . This use of $E(hkl)$ values is approximately equivalent to considering each atom to be a point atom (an extremely sharp peak occupying a very small volume in the electron-density map). As a result, high-order Bragg reflections (high $\sin \theta / \lambda$), which normally are weaker because of the intensity fall-off of atomic scattering factors f with $\sin \theta$ values, may have large $|E|$ values that would play an appropriate role in the structure determination (rather than being ignored because of their low values when $|F|$ is used).

Information on significant features of the structure is contained in the very intense and very weak Bragg reflections; these have different distributions when the structure is centrosymmetric and when it is non-centrosymmetric (Wilson, 1949). The centrosymmetric distribution has a higher proportion of Bragg reflections with very low intensities. An analysis of the $E(hkl)$ values in the diffraction pattern (the "distribution of $E(hkl)$ values") shows that they contain (as, of course, do the $F(hkl)$ values as well) information on whether the structure is centrosymmetric or noncentrosymmetric. For example, the mean value of $E(hkl)$ is 0.798 for a centrosymmetric structure and 0.886 for a noncentrosymmetric structure. The value that the crystallographer more commonly uses for this test is $|E^2 - 1|$, which is theoretically 0.968 for a centrosymmetric structure and 0.736 for a noncentrosymmetric structure. These values are calculated from the diffraction data that have just been measured, and they probably will indicate which symmetry the crystal has.

Once a table of $|E(hkl)|$ values has been prepared, it is usual to rank these $E(hkl)$ values in decreasing order of magnitude. Usually one works with the strongest 10 percent of them. Then one looks for groups of three Bragg reflections that satisfy the condition that their indices

are numerically related in the manner described in Eqn. (8.2); this selection of “triple products” [$E(hkl)$, $E(h', k', l')$, $E(h + h', k + k', l + l')$] is generally made by computer. If each of the three Bragg reflections in a triple product has a high $E(hkl)$ value, the product of their three signs is probably positive. This listing is called the “ Σ_2 ” or “sigma 2” listing (see Eqn. (8.2) and Figure 8.2). The summation symbol Σ is used in this naming because, in the probability formula, summations are involved. The “ Σ_1 ” relations (see Eqn. (8.3) and Figure 8.1) are simpler because they involve only pairs of intense Bragg reflections related by $E(hkl)$ and $E(2h, 2k, 2l)$ and contain the implication that the sign of $E(2h, 2k, 2l)$ is probably positive in a centrosymmetric structure (see Figure 8.1 and Eqn. (8.3)). The general equation used is

$$s[E(hkl)] \approx \left[\sum_{h', k', l'} E(h', k', l') E(h - h', k - k', l - l') \right] \quad (8.5)$$

The probability aspects of these sign relationships are very important. If we replace h, k, l by H and h', k', l' by K , the probability that a triple product is positive in a centrosymmetric structure (that is, $s_H \approx s_K s_{H-K}$) is[†]

$$P_+ = \frac{1}{2} + \frac{1}{2} \tanh \left(\frac{E_H E_K E_{H-K}}{N^{1/2}} \right) \quad (8.6)$$

(where N is the number of equal atoms in the unit cell[‡]). Furthermore, the probability that $E(hkl) \equiv E_H$ is positive is

$$P_+ = \frac{1}{2} + \frac{1}{2} \tanh \left(|E_H| \sum_K \frac{E_K E_{H-K}}{N^{1/2}} \right) \quad (8.7)$$

where the summation Σ is over all values of $K = (h', k', l')$, and $P_+ = 1$ indicates a sign of +1, while $P_+ = 0$ indicates that it is 0.[§] These probability aspects of direct methods result in a requirement for a large amount of diffraction data.

Solving the structure of a centrosymmetric structure

We will now describe the steps in the determination of a centrosymmetric structure by direct methods. When the list of “triple products” [$E(hkl)$, $E(h'k'l')$, and $E(h + h', k + k', l + l')$] has been prepared, the derivations of their signs requires some initial choices of signs. Initially, in three dimensions, one has a choice of the signs of three Bragg reflections for many centrosymmetric space groups; these choices determine which of the possible positions is used for the origin of the unit cell. The choice does not alter the structure, it just defines where the unit-cell origin is. In selecting three origin-fixing Bragg reflections,

[†] \tanh , the hyperbolic tangent of x , is $\{(e^x - e^{-x})/(e^x + e^{-x})\}$.

[‡] We advance from Eqn. (8.5) to Eqn. (8.6) by incorporating a commonly used abbreviation that has developed in the literature of direct methods: $H \equiv (h, k, l)$, $K \equiv (h', k', l')$, and hence $H + K \equiv (h + h', k + k', l + l')$. Note that, since $-K$ and K have the same E 's (in sign and magnitude) in a centrosymmetric structure, then a relation between H and K and a relation between H and $-K$ are equivalent.

[§] For unequal atoms, $(1/N^{1/2})$ in Eqns. (8.6) and (8.7) is replaced by $\sigma_3 \sigma_2^{-3/2}$, where $\sigma_n = \Sigma Z_j^n$, the summation being from 1 to N , and N is the number of atoms with atomic number Z_j for the j th atom.

An illustration of the successive application of Eqn. (8.2) to derive the signs of some of the strongest Bragg reflections for a structure. Values of $|E|$ are derived from those for $|F|$, chiefly to eliminate the effects of thermal vibration and to treat each atom as if all its electrons were concentrated at a point. Values of $|E|$ are used in deriving sign relationships because their magnitudes depend only on the arrangement and relative atomic numbers of the atoms.

Monoclinic example:

$$|F(hkl)| \neq |F(\bar{h}kl)|$$

$$k+l \text{ even} \quad s(hkl) = s(h\bar{k}l) = s(\bar{h}k\bar{l}) = s(\bar{h}\bar{k}\bar{l})$$

$$s(\bar{h}kl) = s(\bar{h}\bar{k}l) = s(hk\bar{l}) = s(h\bar{k}\bar{l})$$

$$k+l \text{ odd} \quad s(hkl) = s(\bar{h}\bar{k}\bar{l}) = -s(h\bar{k}l) = -s(\bar{h}k\bar{l})$$

$$s(\bar{h}kl) = s(h\bar{k}\bar{l}) = -s(hk\bar{l}) = -s(\bar{h}\bar{k}\bar{l})$$

The compound studied is 2-keto-3-ethoxybutyraldehyde-bis (thiosemicarbazone), space group $P2_1/c$. The above sign relationships for this space group are to be found in *International Tables*, Volume A.

Relation to be used [Eqn. (8.2)]:

$$s(h+h', k+k', l+l') \approx s(h, k, l) s(h', k', l')$$

| | | | | |
|--------------|------|---|---|--|
| hkl | E | + | } | Signs chosen arbitrarily fixing the origin. (If one or all of these signs had been negative another allowable origin would have resulted.) |
| 331 | 3.74 | + | | |
| $\bar{9}67$ | 3.25 | + | | |
| $\bar{13}14$ | 2.92 | + | | |

| hkl | E | Relationships used | Sign found | (Notes) |
|--------------|------|---|------------|---|
| 1200 | 4.35 | (600)(600) | + | (+)(+) = (-)(-) = + |
| 600 | 2.80 | | ? | |
| $\bar{25}14$ | 3.49 | ($\bar{12}00$)($\bar{13}14$) | + | ++ = + |
| $\bar{22}45$ | 2.22 | (331)(2514) | + | ++ = + |
| 642 | 2.86 | | a | An additional undetermined sign is chosen and is temporarily designated a |
| 1842 | 2.92 | (1200)(642) | a | +a = a |
| 973 | 2.07 | (331)(642) | a | +a = a |
| $\bar{22}61$ | 2.30 | ($\bar{13}\bar{1}4$)($\bar{9}7\bar{3}$) | -a | -(+a) = -a |
| $\bar{19}32$ | 2.84 | ($3\bar{3}1$)($\bar{22}61$) | -a | +(-a) = -a |
| | | ($\bar{13}\bar{1}4$)($\bar{6}4\bar{2}$) | | -(+a) = -a |
| $\bar{7}32$ | 2.14 | (1200)($\bar{19}32$) | -a | +(-a) = -a |
| 2510 | 2.03 | (1842)($7\bar{3}\bar{2}$) | - | $\left\{ \begin{array}{l} a(-a) = - \\ a(-a) = - \end{array} \right.$ |
| | | (642)($19\bar{3}\bar{2}$) | | |

Eventually the sign of some Bragg reflection could be found both in terms of a and independently of it; this established the fact that the sign of a was probably +. If this had not happened it would have been necessary to calculate two maps, one with the sign of a positive and one with the sign of a negative.

Fig. 8.4 Numerical use of Eqn. (8.2) to derive phases of a crystal structure.

it is essential for them to be different with respect to the evenness or oddness of their individual indices, and h , k , and l must not all be even. In the numerical example in Figure 8.4, arbitrary signs were chosen for $F(3\ 3\ 1)$ (odd, odd, odd), $F(\bar{9}\ 6\ 7)$ (odd, even, odd), and $F(\bar{13}\ 1\ 4)$ (odd, odd, even) at the start.

The reader may ask where negative signs for phases come from. The relationships of signs of Bragg reflections with negative values of h , k , and/or l to that of a Bragg reflection with all indices positive are listed for each space group in *International Tables*, Volume A. For example, in the space group $P2_1/c$, if $k + l$ is odd, then $F(hkl) = -F(h\bar{k}l) = -F(\bar{h}k\bar{l})$. Negative signs are introduced into the sign relationships in this way. It is essential to have some negative terms in the calculation of the E -map, because an E -map with all signs positive will give a high peak at the origin, a rarely observed feature in complex structures; in fact this E -map with all signs positive resembles a Patterson function (to be described in the next chapter), but cannot be interpreted as an electron-density map.

From the list of "triple products" it should be possible to derive, for the set of $E(hkl)$ values, a set of signs that have been determined with acceptable probabilities (see the example in Figures 8.4 and 8.5). If difficulties occur, it may be necessary to choose another set of origin-fixing Bragg reflections. It may also be necessary to assign symbolic signs ("a", "b", etc.) to certain Bragg reflections and generate the signs of other Bragg reflections in terms of these symbols with the hope that eventually the actual signs of these symbols may become clear. This process is referred to as "symbolic addition" (Zachariasen, 1952; Karle and Karle, 1966). For example, in Figure 8.4 it is deduced that the sign of symbol "a" is positive. If n symbols have been used but their signs cannot be determined in this way, it will be necessary to compute 2^n E -maps.

The derivation of signs for a monoclinic centrosymmetric structure is shown in Figure 8.4. Some sign relationships could be immediately deduced from a knowledge of the monoclinic space group relationships among $F(hkl)$ appropriate for this structure. Others were then deduced from these new signs and some arbitrarily chosen signs. This process was continued until the signs of 836 out of the 872 strongest terms were found with no sign ambiguity (although it is usually not necessary to work with this many terms). Part of the resulting Fourier synthesis computed using $E(hkl)$ values (an E -map) is shown in Figure 8.5.

The crystal structure of hexamethylbenzene was reported by Kathleen Lonsdale in 1928 and showed that the benzene ring is planar and has six-fold symmetry (Lonsdale, 1928). The arrangement of atoms in

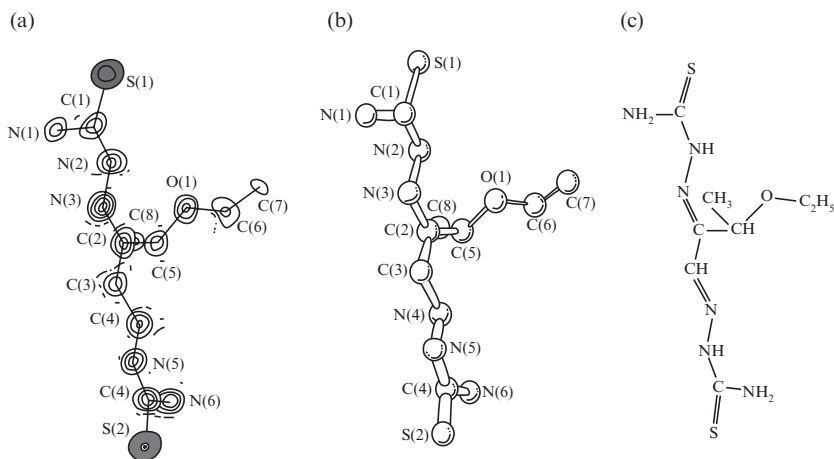


Fig. 8.5 An excerpt from an E -map.

(a) A three-dimensional map calculated with phases derived as in Figure 8.4 and $|E|$ values rather than values of $|F|$ as amplitudes (see Gabe et al., 1969). This is a composite map; each peak has been drawn as it appears in the section in which it has the highest value. It is a simple matter to pick out the entire molecule, 2-keto-3-ethoxybutyaldehyde-bis(thiosemicarbazone), from this map. The molecular skeleton and the presumed identity of each atom have been added to the peaks. (b) A ball-and-stick drawing of the molecule. (c) The chemical formula of the molecule.

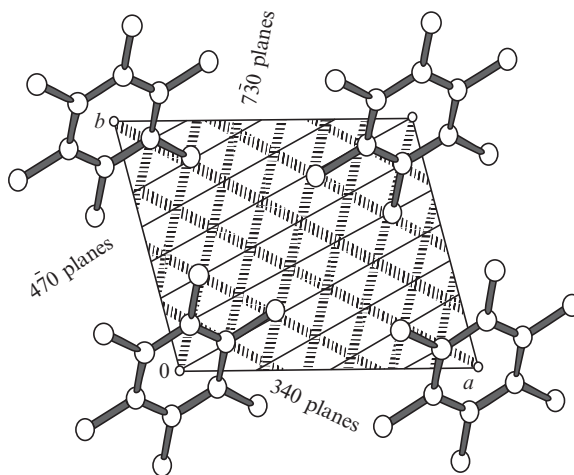


Fig. 8.6 A triple product in diffraction by hexamethylbenzene.

Shown is the crystal structure of hexamethylbenzene (Phase II) (Lonsdale, 1928). Maxima of the density waves of three intense Bragg reflections, 340 , $7\bar{3}0$, and $4\bar{7}0$, are diagrammed with the molecular structure superimposed. Note that all of the carbon atoms lie at the intersection of maxima of the density waves of these three Bragg reflections.

the unit cell is shown in Figure 8.6. Three strong Bragg reflections, 340 , $7\bar{3}0$ and $4\bar{7}0$, form a triple product (inspect the indices) and, although direct methods were not used in 1928, they illustrate the principle. The maxima of the density waves of these three Bragg reflections are shown in this figure. Note how the carbon atoms each lie on the intersections of three density-wave maxima.

The final stage is the calculation of an E -map. This is an electron-density map calculated with $E(hkl)$ values rather than $F(hkl)$ values (so that atoms are sharper, corresponding to point atoms) (see Figure 8.5a). If all has gone well, the structure will be clear in this map. Sometimes only part of the structure is revealed in an interpretable way and the rest may be found from successive electron-density maps or different electron-density maps. Sometimes the general orientation and connectivity of the molecule are found, but the positioning in the unit cell is wrong because some subsets of signs are in error. This problem is usually recognizable when distances between atoms are calculated and some nonbonded atoms are too close to others. In this case, the development of signs must be done again, this time following some new path, such as selecting origin-fixing Bragg reflections or assigning symbols to a different set of Bragg reflections.

Solving the structure of a noncentrosymmetric crystal

The derivation of phases for noncentrosymmetric structures is more complicated because the values for the phases are not simply 0° or 180° . For noncentrosymmetric crystal structures, an additional formula may be used to derive approximate values for the phase angle ϕ_H :

$$\phi_H \approx \sum_K (\phi_{H-K} + \phi_K) \quad (8.8)$$

where, as before, $H \equiv h, k, l$; $K \equiv h', k', l'$; ϕ is the phase angle of the structure factor; and the brackets refer to an average over all values of K , where $H = (K) + (H - K)$. The so-called “tangent formula,”

$$\tan \phi_H = \frac{\sum_K (|E_K| |E_{H-K}| \sin(\phi_K + \phi_{H-K}))}{\sum_K (|E_K| |E_{H-K}| \cos(\phi_K + \phi_{H-K}))} = \text{tangent formula} \quad (8.9)$$

is used extensively to calculate and also to refine phases for noncentrosymmetric structures. The probability function for

noncentrosymmetric structures is more complicated than that given in Eqns. (8.6) and (8.7). It is:

$$P(\phi_H) = \frac{\exp[-4x \cos(\phi_H - \phi_K - \phi_{H-K})]}{\int_0^{2\pi} \exp(4x \cos \gamma) d\gamma} \quad (8.10)$$

where $x = |E_H E_K E_{H-K}|/N^{1/2}$ and γ is a dummy variable. Higher-order structure invariants and seminvariants (quartets, quintets, for example) are also used in structure determination by direct methods. These are sets of more than three Bragg reflections with indices that have a zero sum. A so-called “negative quartet,”

$$\phi_H + \phi_K + \phi_L + \phi_{-H-K-L} = \pi \quad (8.11)$$

has a phase sum that is probably near 180° rather than 0° (Hauptman, 1974). It is useful not only in phase determination, but also for finding the correct solution if there are several possibilities. Some important computer programs currently in use for determining crystal structures include SHELXS and SHELXD (Sheldrick, 2008), Shake-and-Bake (Miller et al., 1993; Miller et al., 1994), SIR (Burla et al., 2005), and SUPERFLIP (Palatinus and Chapuis, 2007), but there are many more. The reader is advised to consult the World Wide Web for the most suitable program for use for a current problem. In addition, much useful information is provided in the various volumes of *International Tables* (see the reference list).

Dual-space algorithms, which involve iterative cycles of Fourier transforms between real and reciprocal space with changes at each step, have proved very useful in the determination of the structures of macromolecules. Some important methods of phase improvement for proteins involve “density modification.” If the boundaries between solvent and protein have been determined in the electron-density map, the relative phases can be improved by “flattening” the solvent area (“solvent flattening”). Improved phases are then obtained by a Fourier transform (Hoppe and Gassmann, 1968; Wang, 1985; Leslie, 1987). Another example is provided by “real-space averaging” or “non-crystallographic symmetry averaging,” in which electron densities (in real space) of two units are averaged. “Histogram matching” can also be applied to protein structures; in this, the initial electron densities are modified to conform to an expected distribution. The Shake-and-Bake (SnB) program is a phase-determining procedure for solving crystal structures by direct methods, and it has been incorporated into SHELXD (Schneider and Sheldrick, 2002). It alternates phase refinement in reciprocal space by use of the minimal principle (the shake) with real-space constraints through some form of electron-density modification (the bake) (Miller et al., 1993; Miller et al., 1994). The minimal

principle involves a residual described as a “minimum-variance, phase invariant.” All phases are initially determined by computation from a random atomic arrangement and are refined by minimizing this residual. They are then Fourier transformed, and peaks are selected from the resulting electron-density map and used for a new trial structure for the next cycle of the method. While used successfully for small structures, the SnB program has also provided *ab initio* solutions (meaning no preliminary experimentally determined phase information but good resolution of 1.1 Å or higher) for protein structures involving as many as 1000 independent nonhydrogen atoms. Another dual-space structure determination method is the charge-flipping algorithm, which is an iterative process that requires a complete set of diffraction intensities to atomic resolution, but does not require any information on the symmetry or chemical composition of the crystal structure (Oszlányi and Sütö, 2005; Palatinus and Chapuis, 2007). A random set of phases is assigned to the measured structure factors and their Fourier transform is calculated. All electron densities that fall below a selected positive value (to be selected by the user) are inverted (the charge-flipping step). The modified electron-density map is then Fourier transformed and the new phases from the charge-flipped map are combined with the original observed data, the structure amplitudes $|F(hkl)|$. Then follows a new iteration cycle. The process is repeated until a satisfactory structure is obtained. Results can be checked, for example, by “random omit maps,” in which a selected proportion, say one third, of the highest peaks in an electron-density map are deleted, and the remaining atoms are used to calculate new phases and start a new cycle (Bhat and Cohen, 1984; Bhat, 1988). Then one can check if the deleted atoms appear in the new electron-density map.

In an attempt to improve the resolution of a measured data set, the “free lunch algorithm” (also called “nonmeasured reflection extrapolation”) was introduced by Eleanor Dodson, developed by Carmelo Giacovazzo, and named by George Sheldrick “since one is apparently getting something for nothing” (Caliandro et al., 2005; Yao et al., 2005). It extends the resolution of the measured data significantly by simply inventing the missing data. This is done by Fourier transformation of the existing experimental F_o map using the Wilson plot to obtain the overall scale factor for the made-up data. Unexpectedly, it was found that the introduction of unmeasured structure amplitudes produced phases that improved the resulting electron-density map and led, in many cases, to a structure solution (Usón et al., 2007). For some reason random structure amplitudes are better than zero structure amplitudes for those high-resolution data that cannot be measured experimentally (Caliandro et al., 2007; Dodson and Woolfson, 2009).

Overview

Direct methods for both centrosymmetric and noncentrosymmetric structures have been programmed for many high-speed computers. Since the equations involve probabilistic rather than exact relations, uses of direct methods are most successful when care is taken initially in the choice of the origin-fixing and symbolically assigned phases. These are used to determine the phases of a good number of intense Bragg reflections. In many structure analyses a reasonable approximate (“trial”) structure has been recognizable from an E -map calculated with only 5 or 10 percent of the observed Bragg reflections, although often larger fractions are used, as in the example illustrated in Figures 8.4 and 8.5. Generally these “direct methods” result in a structure that can be refined (Chapter 11), and so the structure may be considered to be determined. A variety of excellent computer programs generally ensure a correct structure. For several reasons, however, such success may be elusive with some structures. There are many possible problems that can arise in using these methods, such as a poor choice of origin-fixing Bragg reflections, the derivation of too few triple products so that some signs are generated with lower probabilities than one would like, and a preponderance of positive signs for the derived signs so that the resulting E -map has a huge peak at the origin even though there is no heavy atom in the structure. However, with care and experience these problems can usually, although not always, be overcome.

Summary

There are limits to the possible phase angles for individual Bragg reflections in both centrosymmetric and noncentrosymmetric structures. This follows from the constraints on the electron density; it must be nonnegative throughout the unit cell and it must contain discrete, approximately spherical peaks (atoms). For three intense related Bragg reflections in a centrosymmetric structure, the signs are related by

$$sF(H) \approx sF(K)sF(H + K)$$

where s means “sign of”; $H \equiv h, k, l$; $K \equiv h', k', l'$; $H + K \equiv h + h', k + k', l + l'$; and F is a structure factor or E value. From such relationships it is often possible to derive phases for almost all strong Bragg reflections and so to determine an approximation to the structure (a “trial” structure) from the resulting electron-density map. Similar methods are available for noncentrosymmetric structures.

The steps in the determination of a structure by “direct methods” consist of:

- (1) Making a list of E values in decreasing order of magnitude and working with the highest 10 percent or so.
- (2) Analysis of the statistical distribution of E values to determine if the structure is centrosymmetric or noncentrosymmetric. This is important if there is an ambiguity in the space group determined from systematically absent Bragg reflections.
- (3) Derivation of triple products among the high E values.
- (4) Selection of origin-fixing Bragg reflections.
- (5) Development of signs or phases for as many E values as possible using triple products and probability formulae.
- (6) Calculation of E -maps and the selection of the structure from the peaks in the map.

All of these steps are now incorporated into computer programs in wide use.

9

The derivation of trial structures. II. Patterson, heavy-atom, and isomorphous replacement methods

* In the three decades from the mid 1930s to the mid 1960s, the most powerful method of analysis of the diffraction pattern of a crystal was the Patterson method. It revolutionized structure determination because no longer was it necessary to propose a correct trial structure before analysis. For the first time it provided a means for solving most structures if good diffraction data were available.

The two methods to be described here, the Patterson method* and the isomorphous replacement method, have made it possible to determine the three-dimensional structures of large biological molecules such as proteins and nucleic acids. In addition, the Patterson function is still useful for small-molecule studies if problems are encountered during the structure analysis. If a crystal structure determination proves to be difficult, the Patterson map should be determined to see if it is consistent with the proposed trial structure.

The Patterson method involves a Fourier series in which only the indices (h, k, l) and the $|F(hkl)|^2$ value of each diffracted beam are required (Patterson, 1934, 1935). These quantities can be obtained directly by experimental measurements of the directions and intensities of the Bragg reflections. The Patterson function, $P(uvw)$, is defined in Eqn. (9.1). It is evaluated at each point u, v, w in a three-dimensional grid with axes u, v , and w that are coincident with the unit-cell axes x, y, z ; the grid fills a space that is the size and shape of the unit cell:

$$P(uvw) = \frac{1}{V_c} \sum_{\text{all } h,k,l} |F(hkl)|^2 \cos 2\pi(hu + kv + lw) \quad (9.1)$$

No phase information is required for this map, because $|F(hkl)|^2$, unlike $F(hkl)$, is independent of phase. *There is only one Patterson function for a given crystal structure.* For reasons that we explain shortly, a plot of this function is often called a vector map. Appendix 8 gives some useful background information and further details.

The Patterson function at a point u, v, w may be thought of as the convolution** of the electron density with itself in the following manner:

** See the Glossary.

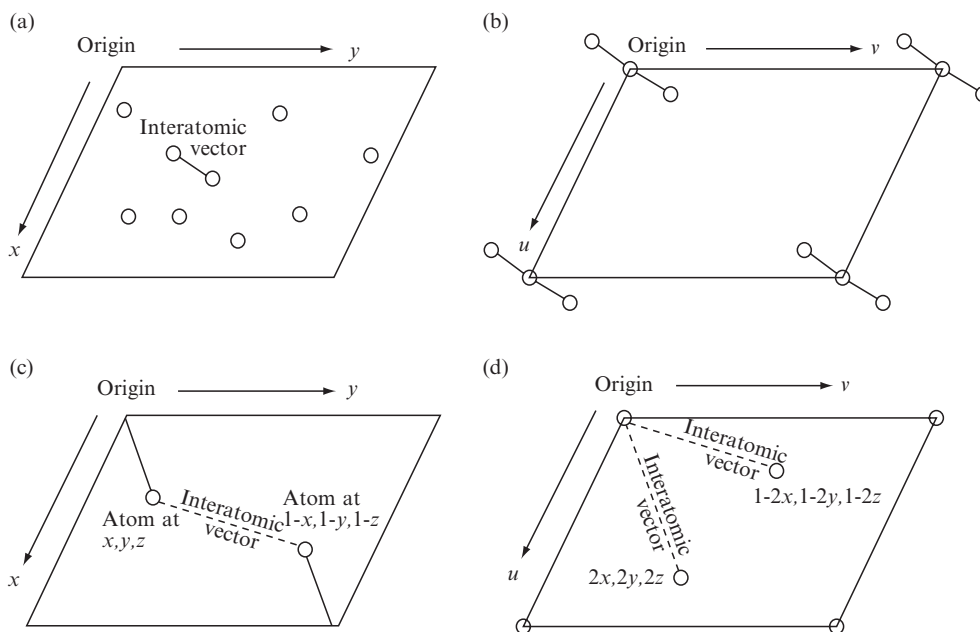


Fig. 9.1 Peaks in a Patterson (vector) map.

A Patterson map represents all interatomic vectors in a crystal structure, positioned with one end of the vector at the origin of the Patterson map. (a) Atoms in a crystal structure showing one interatomic vector, which will appear as shown in (b) in the Patterson map. (c) Two atoms related by a center of symmetry in a crystal structure. (d) The corresponding Patterson map showing vector coordinates.

$$P(uvw) = V_c \iiint_{\text{whole cell}} \rho(x, y, z) \rho(x+u, y+v, z+w) dx dy dz \quad (9.2)$$

Equation 9.2 is obtained by multiplying the electron density at all points x, y, z in the unit cell (that is, $\rho(x, y, z)$) with the electron density at points $x+u, y+v$, and $z+w$ (that is, $\rho(x+u, y+v, z+w)$). This Patterson function, $P(u, v, w)$, can be thought of as the sum of the appearances of the structure when one views it from each atom in turn, a procedure illustrated in Figure 9.1. It is as if an atomic-scale elf sat on an atom, took a snapshot of his surroundings, then moved to the next atom and superimposed his second snapshot on the first, and so forth.[†] Essentially the Patterson map samples the crystal structure at all sites separated by a vector u_0, v_0, w_0 and notes if there is electron density at both ends of this vector; if this is so an interatomic vector has been localized. Therefore, if any two atoms in the unit cell are separated by a vector u_0, v_0, w_0 in the three-dimensional structure (or electron-density map), there will be peak in the Patterson map at the site u_0, v_0, w_0 .

The Patterson map [Eqns. (9.1) and (9.2)] is flat, near zero, except for peaks that represent the orientation and length of every interatomic vector in the structure. The vector between any two atoms is the distance between them and the direction in space that a line connecting them would take. The heights of the peaks in the Patterson map are

[†] H. F. Judson, in *The Eighth Day of Creation* (Judson, 1996), uses the analogy of a cocktail party in describing the Patterson function. If there are one hundred guests at a party, there must have been one hundred invitations. The host would have to make almost five thousand introductions if he wanted to be sure everyone met each other, and this would involve ten thousand attempts to remember a new name. If the shoes of the guests are nailed to the floor, their handshakes must involve different lengths and directions of arms and different strengths of grip. This analogy may help some readers understand the meaning of the vectors in a Patterson map; they are interatomic vectors of different lengths and directions, with heights proportional to the product of the atomic numbers of the atoms at each end of the vector. If each partygoer could then recount every handshake and the direction, distance, and strength of it, then the location of every guest in the room would be known. Of course one would only use this very complicated method (five thousand vectors to locate one hundred people) if it were absolutely necessary.

proportional to the values of $Z_i Z_j$, where Z_i is the atomic number of the atom, i , at one end of the vector and Z_j is that of the atom, j , at the other end. The high peak that occurs at the origin of the Patterson function represents the sum of all the vectors between an individual atom and itself. It is important to note that a Patterson map is centrosymmetric whether or not the structure itself is centrosymmetric.[‡] This is because a vector from atom B to atom A has the opposite direction but the same magnitude as a vector from atom A to atom B, so that these two vectors, $A \rightarrow B$ and $B \rightarrow A$, are related by a center of symmetry. The symmetry of a Patterson map is generally not the same as that of the electron-density map for the same crystal structure, but is like the Laue symmetry. Symmetry elements containing translations (glide planes and screw axes) are replaced by mirror planes or simple rotation axes, respectively, and there is always the center of symmetry just described.

[‡]This center of symmetry is evident in Figure 9.1c.

If there is a peak in the Patterson map at a position related to the origin of the map by a certain vector (with components u, v, w , corresponding to a certain distance and direction from the origin), then *at least one position of that particular vector in the corresponding crystal structure has both ends on atomic positions.* (Remember that a vector is characterized by a certain length and direction, but its origin may be anywhere). If there are many pairs of atomic positions related by a particular vector, or if there are only a few but the atoms involved have high atomic numbers, then the Patterson function will have a high peak at that particular position u, v, w . If the value of the Patterson function at a given position is very low, there is no interatomic vector in the structure that has that particular length and direction.

The Patterson map for a one-dimensional structure with identical atoms at $x = \pm 1/3$ is shown in Figure 9.2. The values of the function given by Eqn. (9.1) are designated $P(u)$, and positions in the one-dimensional map by u . An interesting feature of this map is that the same result would be obtained from a structure in which the atoms were at $x = \pm 1/6$. As shown in Figure 9.2, these two structures differ only in that the location of the origin of the unit cell has been changed; the *relative* positions of the atoms are the same in both solutions of the map.

Thermal motion and disorder of atoms will cause a broadening of the vector peaks and a lowering of their heights in the Patterson map. This broadening can be reduced by “sharpening” the peaks. One method of doing this is an artificial conversion of the atoms to point scatterers by dividing each $|F(hkl)|$ by the average scattering factor for the value of $\sin \theta/\lambda$ at which it was measured. Normalized structure factors $|E(hkl)|$ fit this criterion and are commonly used with unity subtracted from their square so that the origin Patterson peak will be removed. This means that the coefficients used to compute the map are modified from $|F(hkl)|^2$ to $|E(hkl)|^2 - 1$. The resulting origin-removed, sharpened

Patterson map is

$$P(uvw) = \frac{1}{V_c} \sum_{\text{all } h,k,l} |E(hkl)^2 - 1| \cos 2\pi(hu + kv + lw) \quad (9.3)$$

There are areas in a Patterson map, called "Harker sections" or "Harker lines," where symmetry operators involving translational components (such as screw axes or glide planes) lead to useful information, especially if a heavy atom is present (Harker, 1936). Therefore if the space group lists atoms at x, y, z and $1/2 - x, -y, 1/2 + z$, there will be peaks at $w = 1/2$ in the Patterson map and they represent vectors

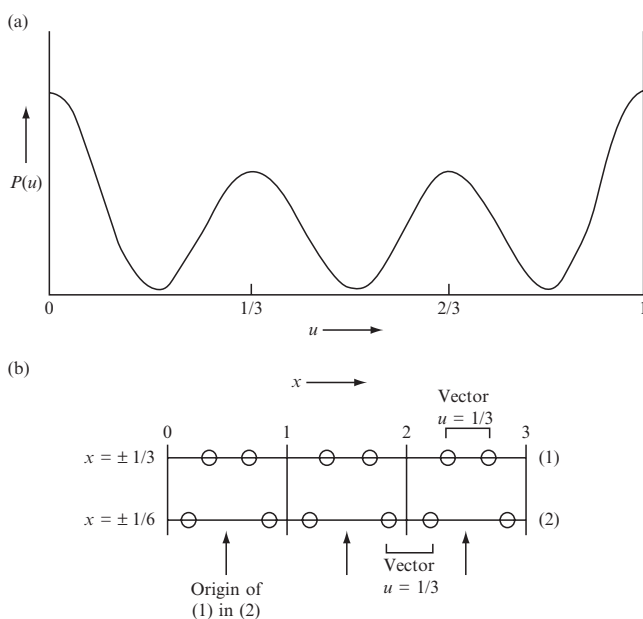


Fig. 9.2 The calculation of a Patterson map for a one-dimensional structure.

(a) The equation of the Patterson function in one dimension is

$$P(u) = \frac{1}{a} \sum_{\text{all } h} |F|^2 \cos 2\pi(hu)$$

The function plotted is $P(u)$ computed for a one-dimensional structure from the following hypothetical "experimental" data:

| | | | | | | | |
|---------|----|----|----|---|---|---|---|
| h | -3 | -2 | -1 | 0 | 1 | 2 | 3 |
| $ F ^2$ | 4 | 1 | 1 | 4 | 1 | 1 | 4 |

(b) There are two structures consistent with this map, one with atoms at $x = \pm 1/3$ and one with atoms at $x = \pm 1/6$. As shown, these two structures are related simply by a change of origin.

between symmetry-related atoms at z and at $z + 1/2$. Therefore a perusal of the Patterson map at $w = 1/2$ for a structure with this particular space group may help solve the structure, especially if a heavy atom is present.

A problem with Patterson maps is that there are N^2 interatomic-vector peaks within a unit cell that contains N independent atoms. N of these peaks lie at the origin and, since the Patterson map has a center of symmetry, there are $(N^2 - N)/2$ independent vectors in the map. When N becomes at all large (even as small as 20), the $(N^2 - N)/2$ vector peaks in the Patterson map necessarily overlap one another, since they have about the same width as atomic peaks and occupy a volume equal to that occupied by the N atoms of the structure. For example, when $N = 20$ there are $20 \times 19/2 = 190$ Patterson peaks in the same volume that the 20 atomic peaks occupy in the electron-density map. With crystals of very large molecules, such as proteins, the overlap may become hopeless to resolve, except for the peaks arising from the interactions between atoms of very high atomic number, since a Patterson peak has a height proportional to the product of the atomic numbers of the two atoms involved in the vector it represents.

The structure shown in Figure 6.6, for which the Patterson map is shown in Figure 9.3, contains only 12 nonhydrogen (O, N, or C) atoms in the asymmetric unit. The great complexity of the Patterson map compared with the electron-density map is obvious. In this example, similar orientations of the six-membered rings in space-group-related molecules give rise to very similar sets of six interatomic vectors, the vectors in each set having nearly the same magnitude and direction, thereby giving a high peak in the Patterson map (see peaks B, C, and D in Figures 9.3a and b). Similarly oriented five-membered rings also lead to high peaks (peaks A and E). The slope of the ring system is clear in Figures 9.3c and d. This figure demonstrates the large amount of structural information available in a Patterson map. However, since all nonhydrogen atoms in the structure are similar in atomic number, and the chemical formula was unknown until the structure was determined, the Patterson map was too complicated to analyze when first obtained. Some Patterson maps that were much easier to interpret will be described later in this chapter.

Until the advent of computer-assisted direct methods in the late 1960s, analysis of Patterson maps was the most important method for getting at least a partial trial structure, especially for crystals containing one or a few atoms of atomic number much higher than those of the other atoms present. In principle, for all but the largest structures, a correct trial structure can always be found from the Patterson distribution, but it is often very difficult to unravel the map, especially when the chemical formula of the compound being studied is not known. Some people, however, find it a fascinating mental exercise to try to deduce at least part of a crystal structure from a Patterson map.

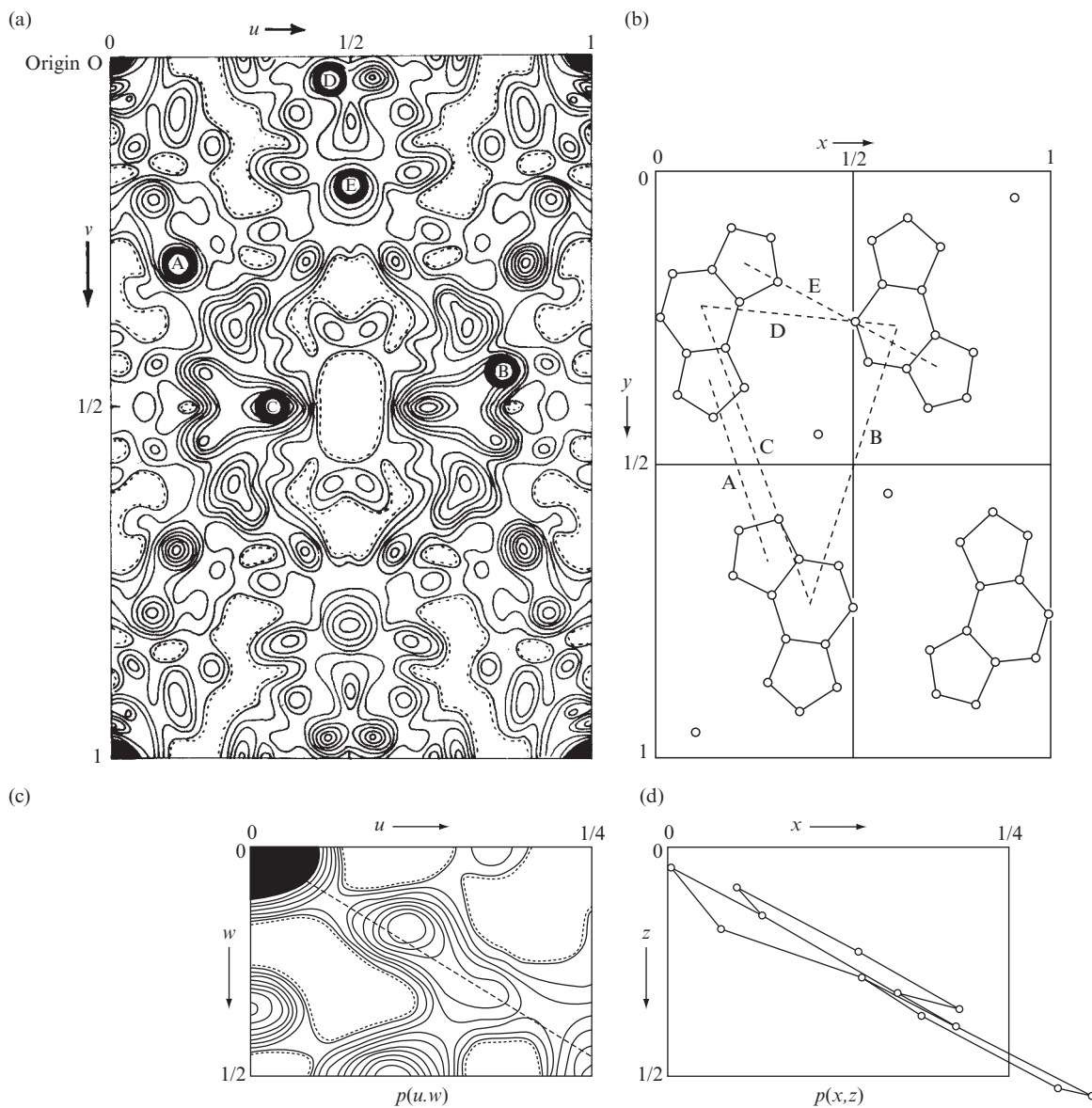


Fig. 9.3 The analysis of a Patterson map.

- (a) A two-dimensional Patterson map, $P(u, v)$, a projection down the w axis, of an azidopurine is shown. The peaks in the $P(u, v)$ map that correspond to the multiple superposition of vectors from ring to ring are lettered A to E and are shown in both (a) and (b).
- (b) The interpretation of the map shown in (a).
- (c) The $P(u, w)$ map, a projection down the v axis, for the same structure, indicating the slope of the ring. The contour interval is arbitrary.
- (d) One molecule shown for comparison with the Patterson map in (c).

Data from Glusker et al. (1968).

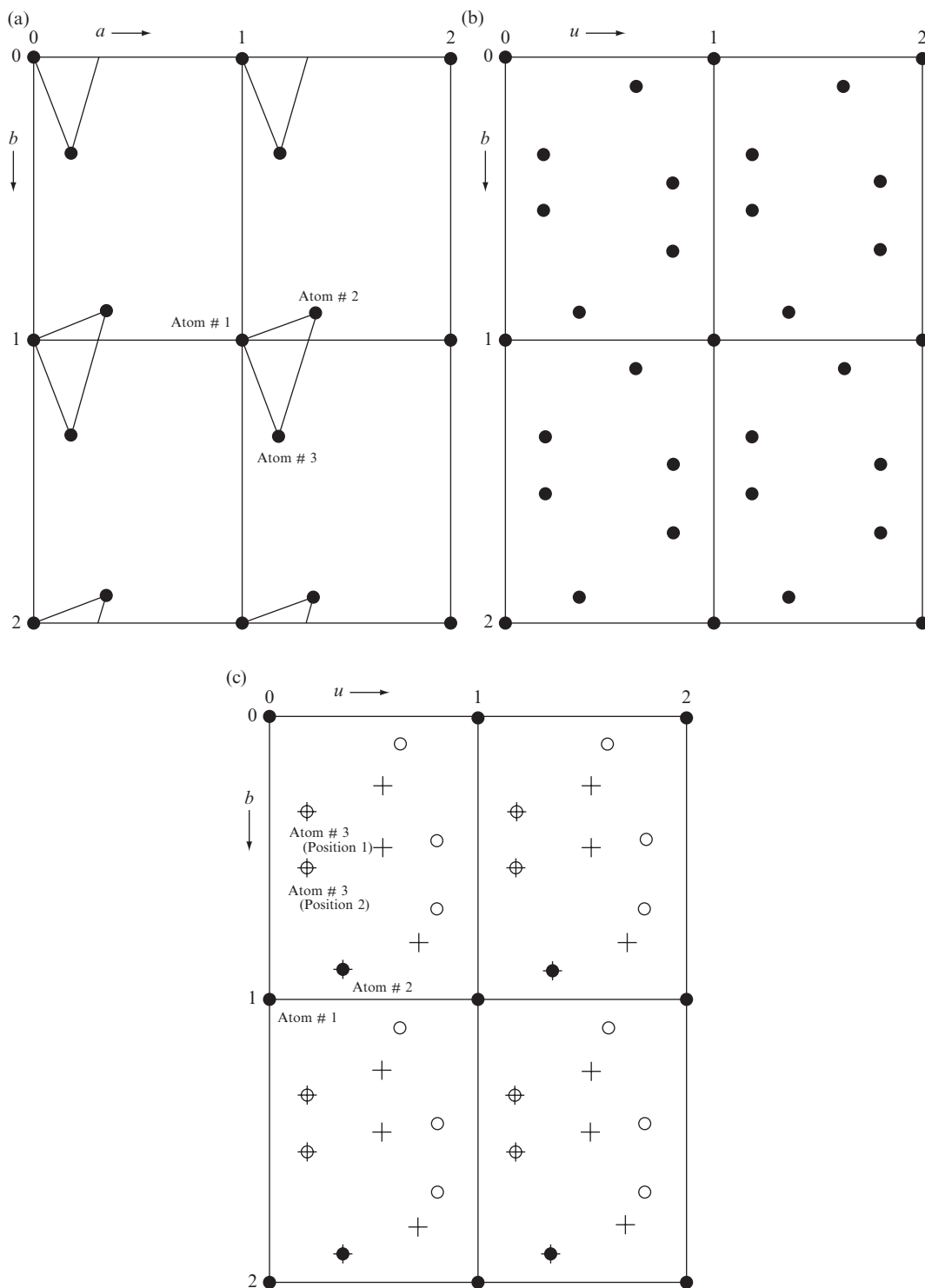


Fig. 9.4 The vector superposition method.

Patterson superposition methods

There are several methods, and many are quite powerful, for finding the structure corresponding to a Patterson map by transcribing $P(uvw)$ upon itself with different relative origins. One of the simplest methods for analyzing the Patterson map of a compound that contains an atom in a known position (such as a heavy atom that has been located in the Patterson map) is to calculate, graphically or by computer, a “vector superposition map.” The origin of the Patterson map is put, in turn, always in the same orientation, at each of the symmetry-related positions of the known heavy atom, and the values of $P(uvw)$ are noted at all points in the unit cell. The lowest value of $P(uvw)$ in the different superposed Patterson maps is recorded for each point; the resulting vector superposition map is therefore also known as a *minimum function*. The principle underlying this approach is that it isolates the vectors arising from the interaction of the known heavy atom with all other atoms in the structure. A schematic example is illustrated in Figure 9.4. In some of the maps there will be other peaks at this same position, corresponding to other vectors in the structure, but the possible ambiguity that such peaks might introduce is minimized by recording the lowest value of $P(uvw)$ in any of the superposed maps. This method can be used even if no atomic positions are known, simply by moving each Patterson peak in turn onto the origin, as in the schematic example illustrated in Figure 9.4.

Rotation and translation functions

Sometimes a structure contains a complex molecule, with (necessarily) a multitude of vectors, but may include a group for which all the vectors are known (relative to one another) rather precisely—for example, a benzene ring in a phenyl derivative. The vector map of this grouping can then be calculated and the resulting vector arrangement can be compared with the arrangement of peaks around the origin of the Patterson map. There will be many more peaks in this region of the Patterson map than those arising from the known structural features alone, but, in at least one relative orientation of the two maps, all peaks in the vector map of the phenyl group will fall in positive areas

-
- (a) Crystal structure.
 - (b) Patterson map of the structure shown in (a).
 - (c) Vector superposition. A search for the position of a third atom when the positions of the first two (#1 and #2, filled circles) are known. The Patterson map illustrated in (b) has been placed (i) with the origin on the position of atom #1 (to give open circles) and then, by superposition of peaks, (ii) with the origin on the position of atom #2 (to give crosses). Four unit cells are shown. It can be seen that there are four positions within each unit cell where overlap of Patterson peaks occurs (a circle and cross superposed). Two of these are, necessarily, at the positions of atom #1 (the origin) and atom #2; the other two are possible positions for atom #3; that is, there are two solutions to the vector map at this stage. In practice, this ambiguity is not found when many atoms are present, and the method will often show the structure clearly. Note that the two solutions to the structure problem are mirror images of each other.

of the Patterson map (although they will not necessarily all lie at maxima if the Patterson peaks are composite, as they usually are). This method, which involves rotation of the Patterson map, is illustrated in Figure 9.5. The fit of the calculated and observed Patterson maps can be optimized with a computer by making a “rotational search” to examine all possible orientations of one map with respect to the other and to assess the degree of overlap of vectors as a function of the angles through which the Patterson map has been rotated. The maximum overlap normally occurs (except for experimental errors) at or near the correct values of these rotation angles, thus giving the approximate orientation of the group. Then the Patterson map can be searched for vectors between groups in symmetry-related positions, and the exact position of the group in the unit cell can be found and used as part of a trial structure.

This method has been adapted to aid in the search for information on the relationship between molecules if there are more than one in the asymmetric unit. Sometimes, in crystalline proteins or other macromolecules, there is what is referred to as “noncrystallographic symmetry”; for example, a dimer of two identical subunits may be contained in one asymmetric unit. Thus, there are two identical structures with different positions and orientations within the asymmetric unit. If, however, one copy of the Patterson map of this dimer is rotated on another copy of the map, there will be an orientation of the first relative to the second that gives a high degree of peak overlap (McRee, 1993; Drenth, 2007; Sawaya, 2007). This is called a “self-rotation function.” The results can be plotted in three dimensions in a map that describes the rotation angles that achieved superposition of the two maps. A large peak is expected at the rotation angles at which one subunit (or molecule) becomes aligned upon another. For example, the relative orientations of two subunits in the same asymmetric unit may be determined because the rotations required for superposition are directly related to the orientation of the noncrystallographic (local) symmetry element of the dimer, usually a two-fold axis (Rossmann and Blow, 1962). Thus a rotation function, plotted as a contour map, provides information on the results (as peaks) of the overlap of one Patterson function with the rotated version of another Patterson function. In a similar way, it may be possible to find the translational components of the noncrystallographic symmetry elements, but this is often considerably more difficult (Crowther and Blow, 1967).

This concept of a probe and the finding of its location in the unit cell by examination of the Patterson map is known as “molecular replacement,” (Rossmann, 1972). For protein studies the probe may be structural data from a similar protein such as a mutant of the same protein. The method involves positioning the probe within the unit cell of the target crystal so that the calculated diffraction pattern matches that observed experimentally. The search is broken into two parts, as described above—rotation then translation, each providing three parameters. This method is very useful if atomic coordinates for

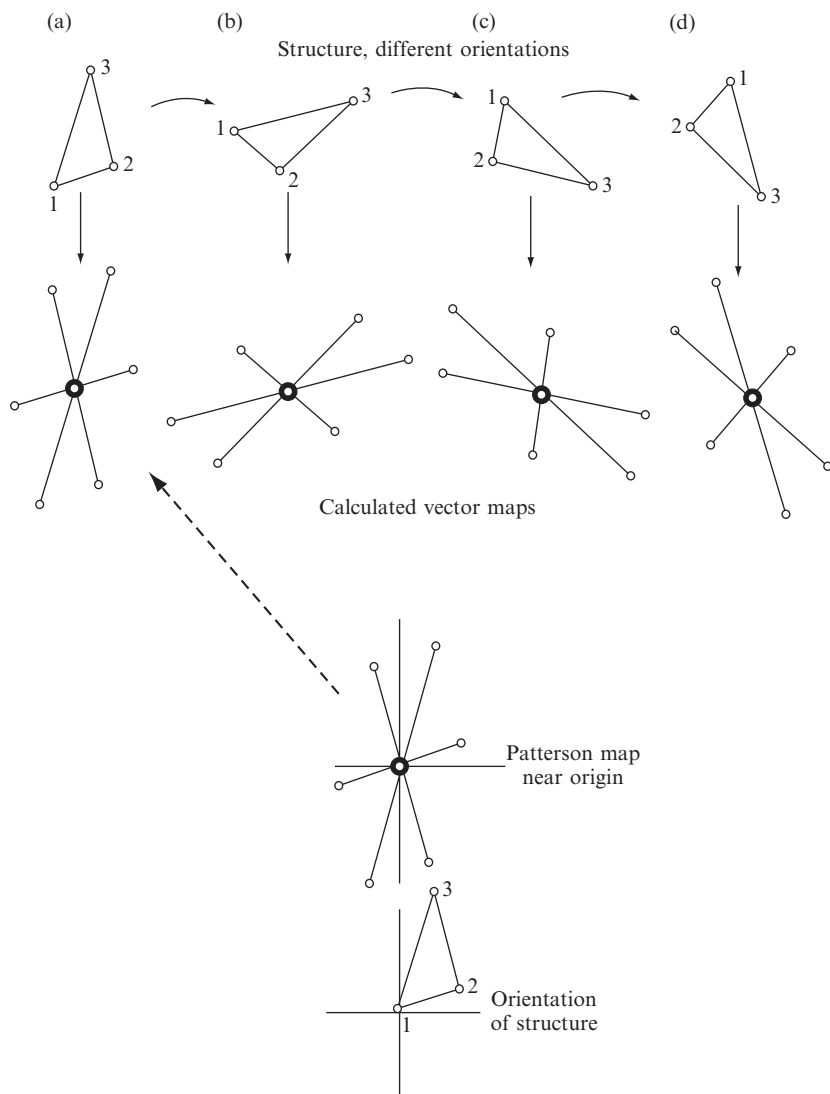


Fig. 9.5 A Patterson search by rotation.

This is a schematic example. If the dimensions of a molecule or part of a molecule in a crystal structure are known, but its orientation (and position) in the unit cell is unknown, the *orientation* may often be found by a comparison of calculated and observed vector maps around the origin. The *position* of the molecule will have to be found in some other way. A comparison of vector maps calculated from trial structures in various orientations with the Patterson map calculated from experimental data indicates that model (a) (above, left) has the trial structure in its correct orientation. The orientations in (b) to (d) are incorrect.

a similar structure, such as a similar protein from a different biological source, have already been reported.

The heavy-atom method

In the *heavy-atom method*, one or a few atoms in the structure have an atomic number Z_i considerably greater than those of the other atoms present. Figure 5.2c showed that if one atom has a much larger atomic scattering factor than the others, then the phase angle for the whole structure will seldom be far from that of the single heavy atom alone, unless, of course, many of the other atoms happen to be in phase with one another, a most improbable circumstance. Heavy atoms thus dominate the scattering of a structure, as illustrated in Figure 5.2c. If the molecule of interest does not contain such an atom, then a derivative, containing, for example, bromide or iodide, can often be prepared, with the hope that the molecular structural features of interest will not be modified in the process (Dauter et al., 2000). Heavy atoms can usually be located by analysis of a Patterson map, although this depends on how many are present and how heavy they are relative to the other atoms present. In Appendix 9 some data relevant to the Patterson function are given for an organic compound containing cobalt, a derivative of vitamin B₁₂ with formula $C_{45}H_{57}O_{14}N_5CoCl \cdot C_3H_6O \cdot 3H_2O$; cobalt has an atomic number of 27 versus 6 for carbon, 7 for nitrogen, and 8 for oxygen. Therefore the scattering of cobalt, that is, $|F(hkl)|^2$, is 12–20 times greater than that of any of the three lighter atoms. The appearances of two Patterson projections for this substance are shown in Figure 9.6. In spite of the presence of many other peaks, the cobalt–cobalt peaks are heavier than most of those due to the other vectors and dominate the map. The position of the cobalt atom in the unit cell was thus found from these two Patterson projections ($P(uv)$ and $P(uw)$). In a similar way, the location of a heavy atom in a protein structure can be found. In Figure 9.7, the heavy-atom position in a protein crystal structure is found from the three Harker sections.

Once the heavy atom has been located, the assumption is then made that it dominates the diffraction pattern, and the relative phase angle for each diffracted beam for the whole structure is approximated by that for a structure containing just the heavy atom. Figure 9.8 illustrates the application of the heavy-atom method to the structure of the vitamin B₁₂ derivative just mentioned, which contained one cobalt atom, one chlorine atom, and about seventy carbon, nitrogen, and oxygen atoms (the structure used for the Patterson map illustrated in Figure 9.6). The first approximation to the electron density was phased with the cobalt atom alone. Peaks in it near the metal atom that were most compatible with known features of molecular geometry were used, together with the metal atom, in a calculation of phase angles for a second approximate electron-density map. This process was continued until the entire structure had been found. The combined use of

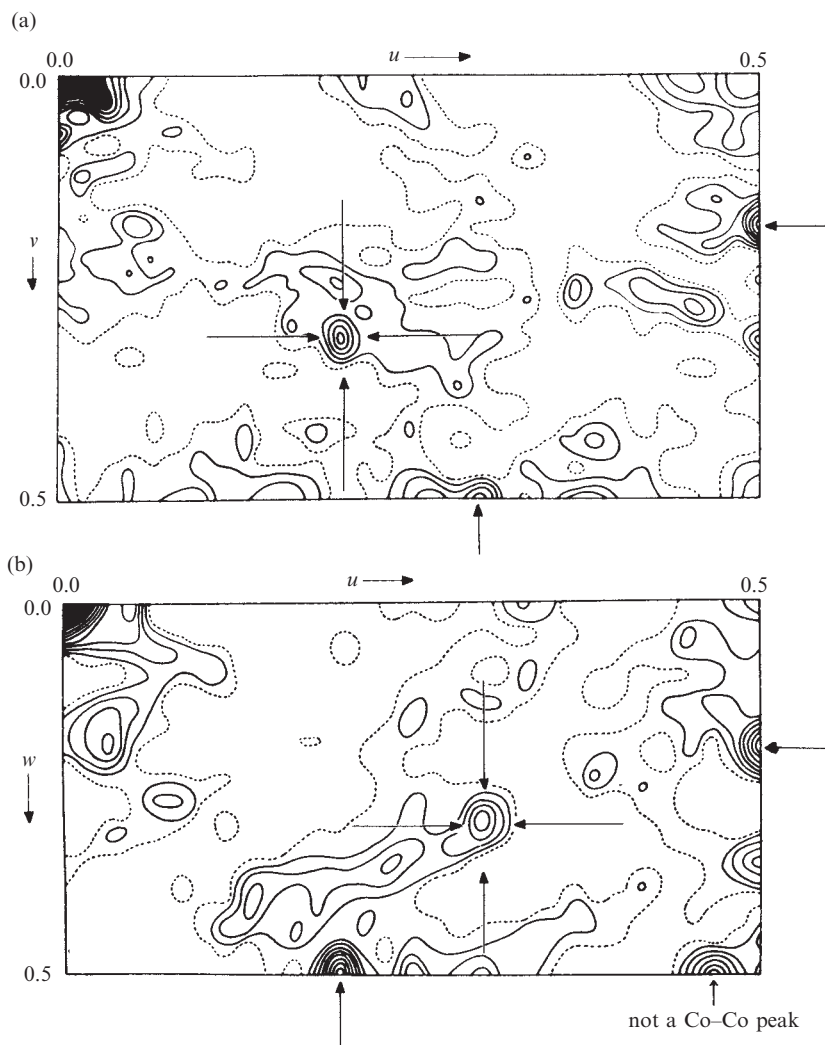


Fig. 9.6 Patterson projections for a cobalt compound in the space group $P2_12_12_1$.

Peaks identified as arising from cobalt–cobalt interactions are indicated by arrows. See Appendix 9 for an analysis of these maps.

(a) $P(u, v)$ Patterson projection down the c -axis. Co–Co peaks appear at 0.00, 0.00; 0.20, 0.32; 0.50, 0.18; 0.30, 0.50.

(b) $P(u, w)$ Patterson projection down the b -axis. Co–Co peaks appear at 0.00, 0.00; 0.30, 0.30; 0.50, 0.20; 0.20, 0.50.

Note that these particular Patterson maps are projections, not Harker sections, but that Harker peaks at half each unit-cell direction (u and $v = 0.50$ in (a) and u and $w = 0.50$ in (b)) helped solve the location of the cobalt atom.

From *Proceedings of the Royal Society* (Hodgkin et al. (1959), p. 312, Figure 3). Published with permission.

Patterson maps and heavy-atom methods made it possible for structures of moderate complexity to be solved in the 1950s and 1960s and, for a while, was the most powerful tool in the analysis of structures of moderate complexity (molecules with, say, 30 to 100 atoms). Direct methods are now more commonly used to solve such structures (small and moderate-sized), because these methods have become much more

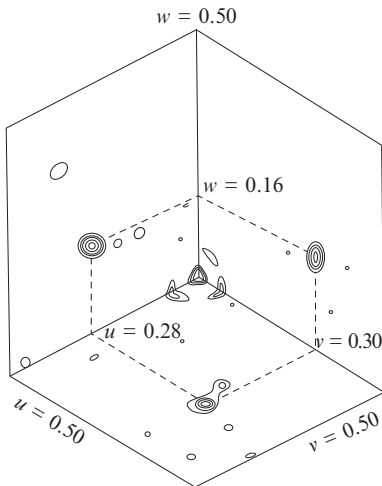


Fig. 9.7 The heavy-atom method. A difference Patterson map.

The macromolecule crystallizes in the space group $I222$. Atomic positions are $(0, 0, 0$ or $1/2, 1/2, 1/2) + (x, y, z; -x, -y, z; x, -y, -z; -x, y, -z)$. Three Harker sections have peaks at $u = 2x, v = 2y, w = 0$, at $u = 2x, v = 0, w = 2z$, and at $u = 0, v = 2y, w = 2z$. The heavy atom is therefore found to lie at $x = 0.14, y = 0.35$, and $z = 0.42$.

powerful with the greatly increased availability of high-speed, high-capacity computers. One minor drawback of the heavy-atom method is that when the heavy atom has an atomic number sufficiently high to dominate the vector distribution, it will necessarily also contribute strongly to the X-ray scattering. If it is desirable to know the structure very precisely, it may be better to work on the structure of a compound that does not contain a heavy atom as a derivative. However, now, with precise low-temperature measurements and high-resolution data, it is generally possible to locate hydrogen atoms in small structures, even if a very heavy atom, such as tungsten or mercury, is present. In addition, Patterson maps can permit a search for vectors of a specific length, such as the S-S distance of a disulfide bridge or the vector between two metal ions that share a particular functional group.

The isomorphous replacement method

Isomorphous crystals are similar in shape, unit-cell dimensions, and structure. They have similar (but not identical) chemical compositions (for example, when one atom has a different atomic number in the two structures) (Mitscherlich, 1822). Ideally, the substances are so closely similar that they can generally form a continuous series of solid solutions, so that, for example, a colorless crystal of potash alum will continue crystal growth on a crystal of chrome alum. When the term “isomorphous” is used for a crystal of a biological macromolecule, it implies that the crystal, with and without a heavy-atom compound soaked into the water channels of the protein or else genetically engineered into the structure, has the same unit-cell dimensions and space group. As a result it is assumed that the macromolecules are in the same positions and orientations in the two crystals.

The high scattering power of heavy atoms has been used to help solve the structures of biological macromolecules. The isomorphous replacement method that will be discussed next has been used in large number of protein structure determinations. The Patterson map of a protein is too complex, with too many overlaps of peaks, for direct interpretation, but the location of a heavy atom, if it can be introduced into a protein crystal, can be found. Data for both the protein and its “heavy-atom derivative” are used to determine perturbations to intensities caused by the addition of heavy atoms. With multiple isomorphous replacement, the aim is to make some alteration in the crystal and examine how this change perturbs the structure factors. From the measured intensities, plus the changes on the introduction of different heavy atoms, it may be possible to obtain phases for each Bragg reflection (Bokhoven et al., 1949; Harker, 1956). For example, if a protein has a molecular weight of 24,000, it contains approximately 2000 carbon, nitrogen, and oxygen atoms. Then, at $\sin \theta = 0^\circ$, the mean value of

$$\langle |F_P|^2 \rangle = \sum_{j=1}^{2000} f_c^2$$

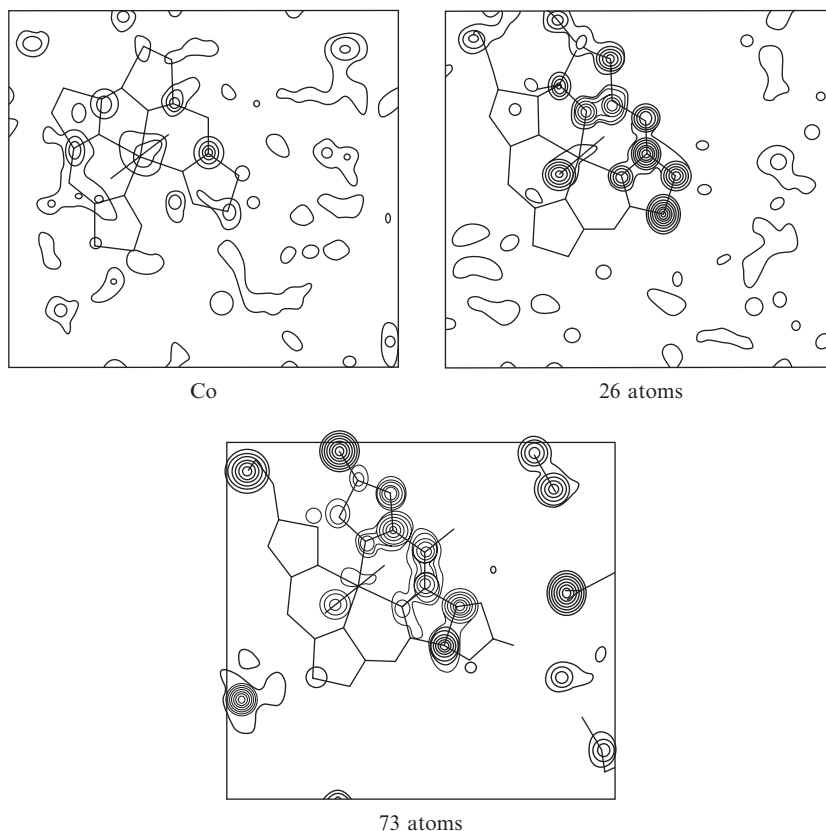


Fig. 9.8 The heavy-atom method.

One section through a three-dimensional electron-density map for a structure with 73 atoms (including various solvent molecules, but not hydrogen atoms) in the asymmetric unit is shown at three different stages of the structure analysis. In the calculation of the first map, only a cobalt atom was used to determine phases. For the second map, 26 atoms were used (one Co, 25 C and N), chosen from peaks in the first map. The third map was phased with the positions of all 73 atoms. Most of the features of the map phased with 73 atoms can be found, at least weakly, in the map phased with the heavy atom alone, although in the latter map there are many extra peaks that do not correspond to any real atoms. Note the general reduction in the background density as the correct relative phase angles are approached. Since these are sections of a three-dimensional map, some atoms that lie near but not in the plane of the section are indicated by lower peaks than would represent them if the section passed through their centers. Other atoms implied by the skeletal formula lie so far from this section that no peaks corresponding to them occur here.

From *Proceedings of the Royal Society* (Hodgkin et al. (1959), p. 328, Figure 14). Published with permission.

is about 98,000. If one uranium atom, atomic number 92, is added, this value of $\langle |F_P|^2 \rangle$ is increased to approximately 106,000, an 8 percent change in average intensity. Differences in intensities of the native protein and the heavy-atom derivative can be measured, many of which will significantly exceed the average. Therefore the position of the uranium atom should be obtainable from the intensity differences.

If a protein crystal is soaked in a solution of a heavy-atom compound (such as a uranyl salt), the heavy-atom compound will be distributed throughout the solvent channels in the crystal by diffusion. In some cases the heavy atom will bind to a specific group on the macromole-

cule, and this binding may occur in an ordered arrangement within the macromolecular crystal. The difference between the diffracted intensities of the “heavy-atom derivative” of the protein crystal (structure factors F_{PH}) and the diffracted intensities of the “native protein” without any added heavy atom (structure factors F_P) can be used to reveal the position of the heavy atom by a “difference Patterson map.” This is done with a Patterson map that uses $||F_{PH}|^2 - |F_P|^2|$ as coefficients. In other cases, however, with this method of soaking heavy atoms into the native protein, nonspecific binding of the heavy atom may occur, since there are many binding groups on the surface of a protein. If this does happen, that particular heavy-atom derivative can probably not be used for structure determination because of the disorder of its position. To prevent random binding it is necessary to stop the soaking after an appropriate time, determined experimentally, in the hope that only specific binding will occur; the concentration of the heavy-atom salt is often critical for this. An alternative method, which involves attempting to crystallize proteins from solutions containing heavy-atom salts, has not proved very satisfactory, because the crystals so obtained are often not isomorphous with the native crystal. Crystals must be isomorphous for the use of the isomorphous replacement method that will now be described. When a pair or series of isomorphous crystals can be found, isomorphous replacement is a powerful method for the determination of *phase angles*, especially for complex structures for which purely analytical methods (see Chapter 8) are inadequate. It has provided the basis for the solution of many of the macromolecular crystal structures determined to date.

Isomorphous crystals are crystals with essentially identical cell dimensions and atomic arrangements but with a variation in the nature of one or more of the atoms present. The alums constitute probably the best-known example of a series of isomorphous crystals. “Potash alum,” $KAl(SO_4)_2 \cdot 12H_2O$, grows as colorless octahedra, while “chrome alum,” $KCr(SO_4)_2 \cdot 12H_2O$, forms dark lavender crystals of the same shape and structure. The Cr(III) atom in chrome alum is in the same position in the unit cell as the Al(III) atom in potash alum. A common experiment in isomorphism is to grow a crystal of chrome alum suspended from a thread and then to continue to grow it in a solution of potash alum. The result is an octahedral crystal with a dark center surrounded by colorless material (Holden and Singer, 1960). In general, however, isomorphous pairs (involving isomorphous replacement of one atom by another) are difficult to find for crystals with small unit cells, because variations of atomic size usually cause significant structural changes when substitution is tried. Even with large unit cells, patience and ingenuity are usually needed to find an isomorphous pair for a compound being studied. The rewards from this method are enormous—the entire three-dimensional molecular architecture of a protein molecule, found with minimal chemical assumptions.[§] Max Perutz searched for years for ways to solve the structure of hemoglobin, and succeeded when he devised this isomorphous replacement method

[§] Usually information about the sequence of the amino acids in the protein chain is needed to interpret the electron-density maps, especially in poorly resolved regions of the structure.

(Green et al., 1954). The existence of isomorphism between a protein and a heavy-atom derivative may be demonstrated by the determination that their unit-cell dimensions do not differ by more than about 0.5 percent, and that there are differences in the diffraction intensity patterns. It is hoped that there is only a change in the site of isomorphous replacement and that most of the crystal structure of the native and the heavy-atom-substituted protein is the same.

After a Patterson map has been calculated and the position of the heavy atom has been found for each derivative, it is possible to calculate the relative phases of the Bragg reflections directly by a proper consideration of the changes in intensity from one crystal to another.

The method for calculating phase angles by the isomorphous replacement method is illustrated in Appendix 8 in a numerical example involving a centrosymmetric crystal. The atoms or groups of atoms (M and M') that are interchanged during preparation of the isomorphous pair must be located, usually from a Patterson map, as described earlier. This allows calculation of their contributions, F_M and $F_{M'}$. If F_M and $F_{M'}$ are positive (they necessarily have the same sign, since their only difference is in the amount of scattering power in the atom or group of atoms), then the overall F values (F_T) must differ in the same way that F_M and $F_{M'}$ differ. Since the absolute magnitudes of these measured values of F are known and the difference equivalent to the change in M can be computed, it is possible to find signs for F_T and $F_{T'}$. The solutions to the equations are in practice inexact, because of experimental errors and also because the remainder of the structure, R , may move slightly during the replacement of one ion group by another. In an interesting variation to the isomorphous replacement method, it has been found that the relationship between structures in a crystal before and after radiation damage can be used to determine phases. For the "radiation-damage-induced phasing" (RIP) method, two data sets of the same crystal are measured. Between the two data collections the crystal is exposed to a very, very large dose of X-rays. The structural changes as a result of radiation damage (by analogy with heavy-atom insertion) are enough to make it possible to determine the phasing, especially if a few somewhat heavier atoms, such as sulfur, are present in the structure (Ravelli et al., 2003).

With noncentrosymmetric structures, the situation is greatly complicated by the fact that the phase angle may have any value from 0 to 360°. This is the case for biological macromolecules. If the heavy-atom position can be found from the Patterson map, then F_H and the relative phase angle α_H can be computed for a given diffracted beam for each derivative. The construction for graphical determination of the phase angle for the protein (P) is shown in Figure 9.9. For each heavy-atom derivative (PH_1 and PH_2), two possible values[¶] for the phase angle for the protein are found; in the example in Figure 9.9, these are near 53° and 322° for PH_1 (Figure 9.9a) and near 56° and 155° for PH_2 (Figure 9.9b). The phase angle for the free protein for this particular diffracted beam must therefore be near 54°. This process of estimating the

¶ With reference to Figure 9.9a, the law of cosines also illustrates the two-fold ambiguity in the phase angle determined from just one heavy-atom derivative:

$$\begin{aligned} a_P &= a_H \\ &+ \cos^{-1} \{ (F_{PH}^2 - F_P^2 - F_H^2) / 2F_P F_H \} \\ &= a_H \pm a' \end{aligned}$$

Thus two values of a_P , that is, $a_H + a'$ and $a_H - a'$, are possible and it is necessary to study several heavy-atom derivatives with substituted heavy atoms in different positions in the unit cell; the value of a_P that is common to these different studies is determined in this way.

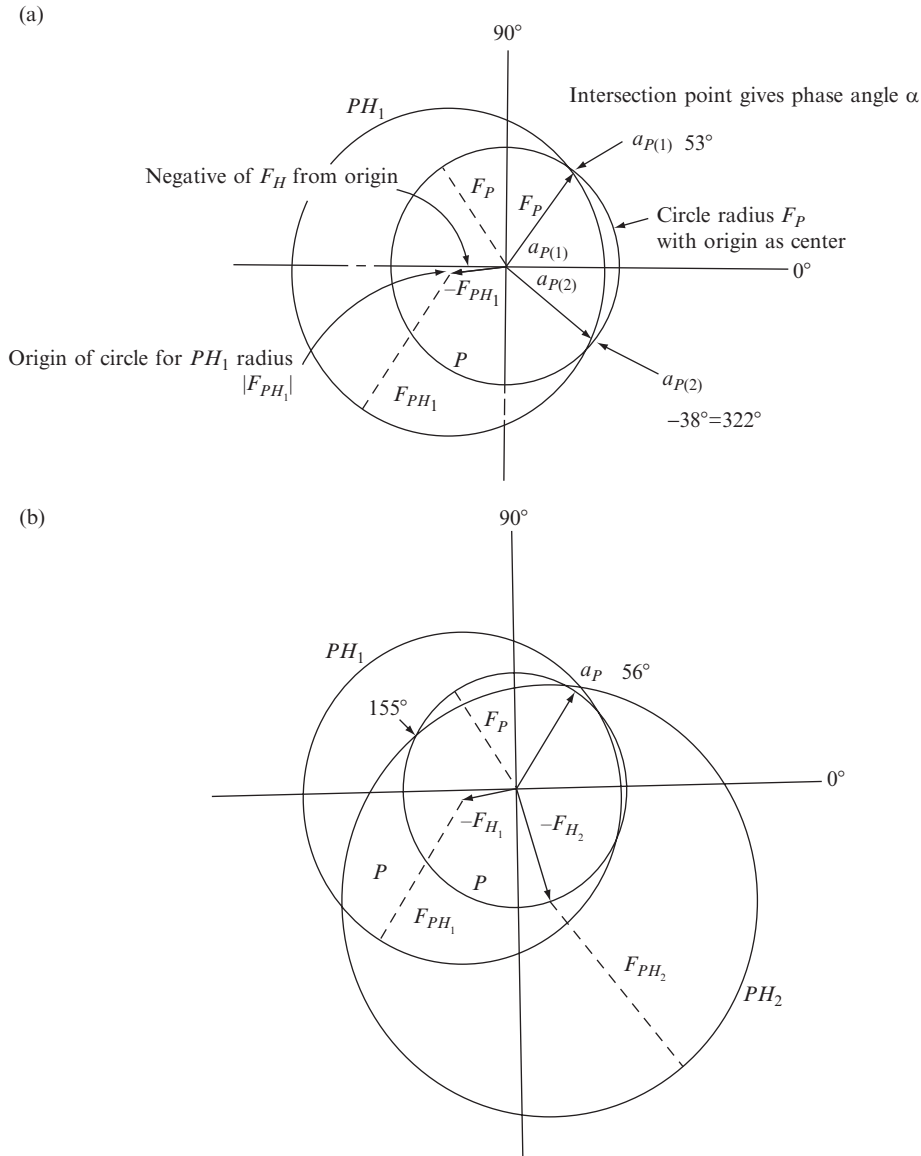


Fig. 9.9 Isomorphous replacement for a noncentrosymmetric structure.

Graphical evaluation of the relative phase, α_P , of a Bragg reflection, indices hkl , diffracted with a structure factor $|F_P|$ from a protein crystal. The diagrams illustrate the following equation: $F_P = F_{PH} - F_H$, where P = "native protein," H = heavy atom, PH = protein heavy-atom derivative.

- (a) One heavy-atom derivative is available, with a structure factor $|F_{PH1}|$ for the Bragg reflection hkl . A circle with radius $|F_P|$ is drawn about the origin. From the position of the heavy atom, determined from a difference Patterson map, it is possible to calculate both the structure amplitude and the phase of the heavy-atom contribution ($|F_{H1}|$, phase angle α_{H1}). A line of length $|F_{H1}|$ and phase angle $-\alpha_{H1}$ (i.e., $\alpha_{H1} + 180^\circ$ to give $-F_{H1}$) is drawn. With the end of this vector as center, a circle with radius $|F_{PH1}|$ is drawn. It intersects the circle with radius $|F_P|$ at two points, corresponding to two possible phase angles, $\alpha_{P(1)}$ and $\alpha_{P(2)}$, for the native protein.
- (b) When two or more heavy-atom derivatives are available, then the process described in (a) is repeated and, in favorable circumstances, only one value of phase angle for the native protein is obtained. Thus, a second derivative is needed to remove the two-fold ambiguity of case (a). This method, of course, depends on accurate measurements of $|F_P|$, $|F_{PH1}|$, and $|F_{PH2}|$ and involves the assumption that no other perturbation than the addition of a heavy atom to the native protein has occurred. Additional derivatives are sometimes needed to improve the accuracy of the phase angles.

phase angle must be repeated for each diffracted beam in the diffraction pattern; usually more than two heavy-atom derivatives (in addition to the free protein) are studied, so that the phases can be more accurately determined. A measure of the error in phasing is provided by a figure of merit, m . This is the mean cosine of the error in the phase angle; it is near unity if the circles used in deriving phases (Figure 9.9) intersect in approximately the same positions. For example, if the figure of merit is 0.8, the phases are in error, on the average, by $\pm 40^\circ$, if it is 0.9, the mean error is $\pm 26^\circ$.

Thus the stages in the determination of the structure of a protein involve the crystallization of the protein, the preparation of heavy-atom derivatives, the measurement of the diffraction patterns of the native protein and its heavy-atom derivatives, the determination of the heavy-atom positions, the computation of phase angles (Figure 9.9), and the computation of an electron-density map using native-protein data and the phase angles so derived from isomorphous replacement. The map is then interpreted in terms of the known geometry of polypeptide chains so that initially this backbone of the protein is traced through the electron-density map. This was formerly done by model building (using a half-silvered mirror in a "Richards box" so that a ball-and-stick model and the electron-density map were superimposed and therefore could be visually compared). Nowadays it is more common for this interpretation of the electron-density map to be done with the help of computer graphics (as shown in Figure 9.10).

The isomorphous replacement method was one of the most used methods for determining macromolecular structure, is now being replaced by experimental methods that involve anomalous dispersion ("MAD" and "SAD" phasing). They will be described in Chapter 10, where their advantages will be described.

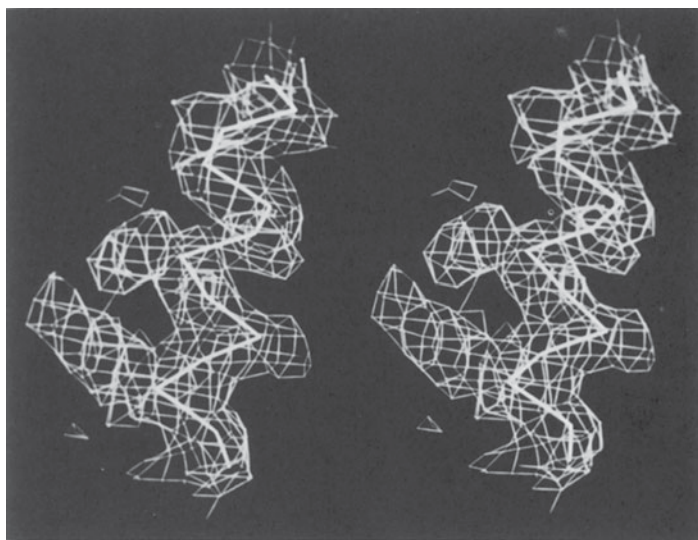


Fig. 9.10 Protein backbone fitting by computer-based interactive graphics.*

*Areas of high electron density are stored in the computer as three-dimensional information and are represented by cage-like structures on a video screen. Any desired view can be generated. The backbone of the molecule is represented as a series of vectors, each 3.8 Å in length (the distance between α -carbon atoms in a polypeptide chain). Each vector is positioned with one end on an α -carbon atom; the other end of the vector is rotated until it lies in an appropriate area of high electron density. Then coordinates of both ends of the vector are stored in the computer, the process is repeated, and the most likely location of the next α -carbon atom is sought. Such vectors are represented in this figure, a stereopair** photographed from a video screen, as heavy solid lines. In this way the "backbone," that is, the positions of the carbon atoms of the polypeptide backbone of the protein (excluding side chains), may be found.

(Photograph courtesy Dr. H. L. Carrell.)

** Such stereodiagrams can be viewed with stereoglasses, or readers can focus on the two images until an image between them begins to form, and then allow their eyes to relax until the central image becomes three-dimensional. This process requires practice and usually takes 10 seconds or more.

Multiple Bragg reflection

A very different but important approach to phase measurement involves “double reflection.” This is a physical effect that occurs when the crystal is oriented so that two reciprocal lattice points, h_1, k_1, l_1 and h_2, k_2, l_2 , lie simultaneously in the diffracting position; that is, both lie on the surface of the sphere of reflection (the Ewald sphere) at the same instant. The result is two beams that are diffracted in the direction normally expected for h_1, k_1, l_1 , and which interfere with each other. One is the normally expected $h_1 k_1 l_1$ Bragg reflection (the primary beam), and the other, also in the $h_1 k_1 l_1$ direction, results from the $h_2 k_2 l_2$ Bragg reflection (the secondary beam) acting as the incident beam for the $h_1 - h_2, k_1 - k_2, l_1 - l_2$ Bragg reflection (the coupling beam). The amplitude of the resultant Bragg reflection gives information on the phase difference of these two waves. This effect is variously described as the Renninger effect (Renninger, 1937), the *Umweganregung* effect (if $I(h_1 k_1 l_1)$ is increased at the expense of $I(h_2 k_2 l_2)$), or the *Aufhellung* effect (if $I(h_1 k_1 l_1)$ is decreased). When a ψ -scan of the peak (through a very small angle) is done it is found that there is an asymmetry, shown in Figure 9.11, that depends on the value of the phase invariant. Therefore a direct reading of α_{sum} is obtained:

$$\alpha_{\text{sum}} = \underbrace{a(-h_1, -k_1, -l_1)}_{\text{primary beam}} + \underbrace{a(h_2, k_2, l_2)}_{\text{secondary beam}} + \underbrace{a(h_1 - h_2, k_1 - k_2, l_1 - l_2)}_{\text{coupling beam}} \quad (9.4)$$

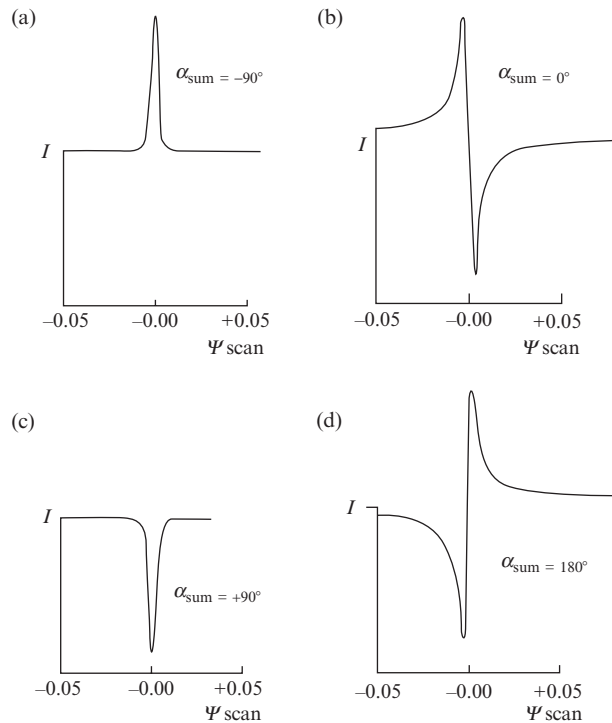


Fig. 9.11 Multiple Bragg reflections.

Some idealized ψ -scans and values of $\alpha_{\text{sum}}(hkl)$ derived from peak profiles. If the crystal is noncentrosymmetric, intermediate phase sum values will be found.

This is like a triplet phase relationship but is an equality rather than a probability. A highly precise (six-circle) diffractometer is needed for this experiment but, when available, such an instrument has provided experimental data that have been used with good success (Hümmer and Billy, 1986; Shen, 1998). Thus an experimental way of measuring origin-independent structure invariants is provided.

Summary

The Patterson map

The map computed with amplitudes $|F(hkl)|^2$, but no phase information, will give a vectorial representation of the atomic contents of the unit cell. The Patterson function, $P(uvw)$, is expressed in the coordinate system u, v, w in a cell of the same size and shape as that of the crystal. It is calculated by

$$P(uvw) = \frac{1}{V} \sum_{\text{all } h,k,l} \sum_{\text{all } h,k,l} |F(hkl)|^2 \cos 2\pi(hu + kv + lw)$$

The peaks in this map occur at points whose distances from the origin correspond in magnitude and direction with distances between atoms in the crystal, because

$$P(uvw) = V \iiint \rho(x, y, z) \rho(x + u, y + v, z + w) dx dy dz$$

Ideally this map can be interpreted in terms of an atomic arrangement. In practice, however, this is only possible if there are comparatively few atoms in the structure or if some are very heavy. The map may also be “sharpened” and the high origin peak removed if values of $\{|E(hkl)|^2 - 1\}$ rather than $|F(hkl)|^2$ are used. A rotation of a Patterson map can be used to identify the angle between two identical molecules when noncrystallographic symmetry is present.

The heavy-atom method

If one or a few atoms of high atomic number are present, they will dominate the scattering. These atoms can generally be located from a Patterson map and the phases of the entire structure approximated by the phases of the heavy atom(s). In the resulting electron-density map, portions or all of the remainder of the structure will usually be revealed, leading to improved phases and successively better approximations to the structure.

Isomorphous replacement method

For very large structures, such as those of proteins, the isomorphous replacement method is a good method for the experimental determination of phase angles. Two crystals are isomorphous if their space

groups are the same and their unit cells and atomic arrangements are essentially identical. Since protein crystals contain solvent channels, if heavy atoms (in solution) are soaked into them and the resulting crystals are isomorphous with the unsubstituted (“native”) crystal, a comparison of the two diffraction patterns will give relative-phase information. If the positions of these added or replaced atoms can be found from Patterson maps, their contributions to the phase angle of each Bragg reflection can be calculated, and if the atoms are sufficiently heavy, differences in intensities for the two isomorphs can be used to determine the approximate phase angle for each Bragg reflection. At least two heavy-atom derivatives are necessary for noncentrosymmetric structures.

Multiple Bragg reflection

If the crystal is oriented so that two reciprocal lattice points lie simultaneously in the diffracting position, that is, both lie on the surface of the sphere of reflection at the same instant, the resulting diffracted beam contains information on a structure invariant involving three Bragg reflections—the primary beam, the secondary beam, and the coupling beam. This method requires specialized equipment.

Anomalous scattering and absolute configuration

10

The concept of the carbon atom with four bonds extending in a tetrahedral fashion was put forward by van't Hoff and Le Bel in 1874. It coincided with the realization that such an arrangement could be asymmetric if the four substituents were different, as shown in Figure 10.1a (van't Hoff, 1874; Le Bel, 1874). Thus, for any compound containing one such asymmetric carbon atom, there are two isomers of opposite chirality (individually called enantiomers), for which three-dimensional representations of their structural formulas are related by a mirror plane. Aqueous solutions of these enantiomers rotate the plane of polarized light in opposite directions. As discussed in Chapter 7, Pasteur showed that crystals of sodium ammonium tartrate had small asymmetrically located faces and that crystals with these so-called "hemihedral faces" rotated the plane of polarization of light clockwise, while crystals with similar faces in mirror-image positions rotated this plane of polarization counterclockwise. Thus the external form (that is, the morphology) of the crystals illustrated in Figure 10.1b was used to separate enantiomers (see Patterson and Buchanan, 1945). Pure enantiomers can only crystallize in noncentrosymmetric space groups unless both isomers are present.

But even if the chemical formula and the three-dimensional structure of a molecule such as tartaric acid have been determined by standard X-ray diffraction methods, there is an ambiguity about the absolute configuration. Information about the absolute configuration is not contained in the diffraction pattern of the crystal as it is normally measured. Thus, although the substituents on the asymmetric carbon atoms have been identified, and even the detailed three-dimensional geometry of the molecule has been determined, it is not known which of the two enantiomers (mirror-image forms, analogous to those shown in Figure 10.1a) represents the three-dimensional structure of a particular individual molecule that has some distinguishing chiral property, such as the ability to rotate the plane of polarized light to the right. In other words, what is the absolute structure of the dextrorotatory form of the compound under study?

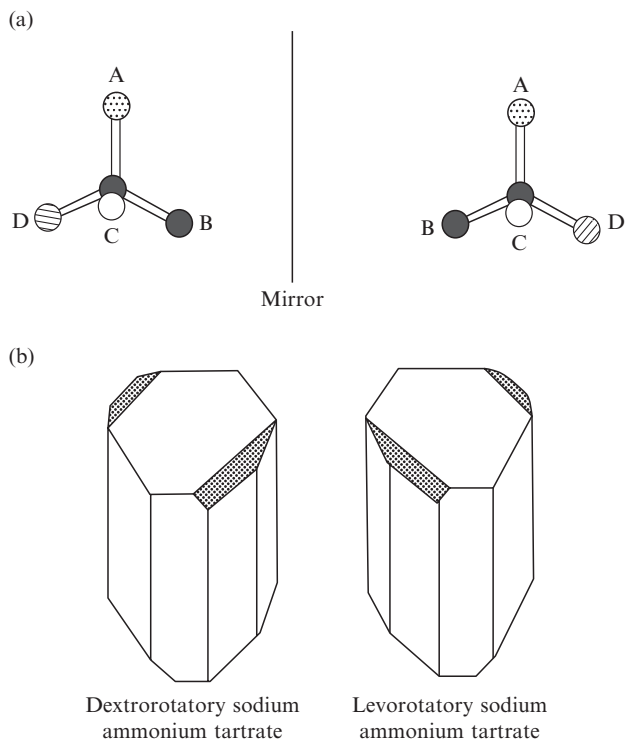


Fig. 10.1 Absolute configurations.

- (a) The asymmetric carbon atom. If A, B, C, and D attached to the tetrahedral carbon atom are all different, there are two chiral isomers related to each other by a mirror plane. In a similar way, the entire structure of a crystal may be chiral.
- (b) Hemihedral faces (shaded) on sodium ammonium tartrate crystals (used by Pasteur to differentiate dextrorotatory from levorotatory forms).

A means of determining the absolute configurations of molecules was, however, provided by X-ray crystallographic studies. It was made possible by the observation that the absorption coefficient of an atom for X-rays shows discontinuities when plotted as a function of the wavelength of the incident X-radiation. These discontinuities, shown in Figure 10.2, are graphically described as “absorption edges.” At wavelengths at the absorption edge of an atom, the energy (inversely proportional to wavelength) of the incident X rays is sufficient either to excite an electron in the strongly absorbing atom to a higher quantum state or to eject the electron completely from the atom. This has an effect on the phase change of the X rays on scattering. The scattering factor for the atom becomes “complex,” and the factor f is replaced by

$$f = f_i + f'_i + if''_i \quad (10.1)$$

where f' and f'' vary with the wavelength of the incident radiation. While f' causes no change in phase (it remains at 180°), f'' causes a phase change of 90° , which is the reason that the Friedel-pair symmetry breaks down. The value of f'' is largest when the wavelength is near

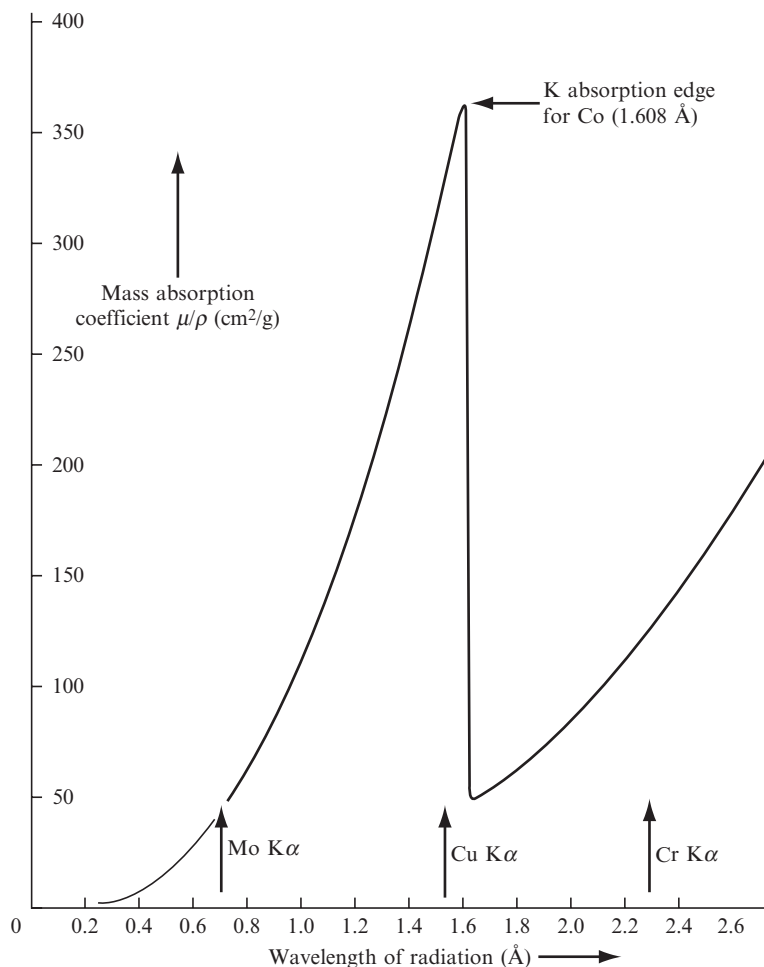


Fig. 10.2 Absorption of X rays of various wavelengths by a cobalt atom.

The mass absorption coefficient for cobalt as a function of wavelength. Note the discontinuity near the absorption edge (1.608 Å); beyond it, there is a gradual increase in the coefficient as the wavelength of the radiation increases.

the absorption edge (as for cobalt in a structure studied with copper K α radiation; see Figure 10.2).

When visible light passes through transparent matter, such as a glass prism or a colorless crystal, its speed is decreased from the value it had in a vacuum. This decreased speed depends on the wavelength of the light. The refractive index of a material is the ratio of the velocity of light *in vacuo* to its velocity when it passes through this medium. Since white light consists of rays with a variety of wavelengths (from red to violet), rays with different wavelengths will be refracted at slightly different angles when they enter a material at an angle. This separation of light so that the individual colors of the component waves become visible is called "dispersion." The violet and blue rays (of shorter wavelengths) are slowed more and therefore are bent to a greater extent

than are the red and orange rays, with longer wavelengths; rays with shorter wavelengths have a larger refractive index. The result of such dispersion is a beautiful rainbow-like display of colors, such as that seen when sunlight passes through and exits a glass prism. This dispersion becomes “anomalous” when an energy absorption band is encountered and a discontinuity occurs; the dispersion is normal on either side of the absorption band, but at the absorption edge the refractive index is larger for longer wavelengths, rather than shorter as is normal. In this area near an absorption edge this plot of wavelength versus refractive index shows an increase of refractive index with wavelength (so that blue light is less refracted than red), the opposite of normal expectation. This is called “anomalous dispersion” or “anomalous scattering,” meaning that one is studying the area of a spectrum near an absorption edge.

All atoms scatter anomalously to some extent, but at wavelengths near the absorption edge of a scattering atom, anomalous scattering will be especially noticeable. If an atom in the structure absorbs, at least moderately, the X rays being used, then this absorption will result in a *phase change for the X rays scattered by that atom, relative to the phase of the X rays scattered by the other atoms of the structure, the equivalent of advancing or delaying the radiation for a short time as shown in Figure 10.3* [that is, equivalent to a hesitation (“gulp”) at the time of scattering].

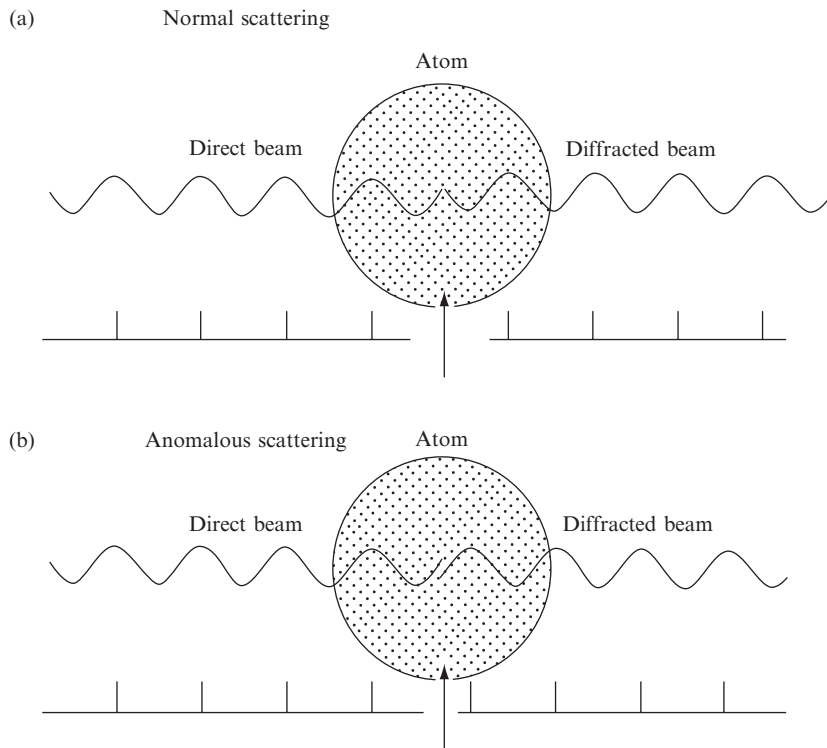


Fig. 10.3 Phase change on anomalous scattering.

(a) Normal scattering with a phase change of 180° . (b) Anomalous scattering with a different phase change.

This implies that in order to demonstrate anomalous scattering, the crystal must contain at least two different types of atoms. The phase change caused by f'' changes the path length of the scattered radiation, as illustrated schematically in Figure 10.3, and the result is an effect on the intensities of the diffracted beams. When there is none of this so-called “anomalous scattering,” the intensities of the Bragg reflections with indices h, k, l and $\bar{h}, \bar{k}, \bar{l}$ are the same (Friedel’s Law). When there is anomalous scattering, the intensities of these two Bragg reflections may be different because of changes in effective path differences between scattered waves arising from the phase change on absorption by the anomalously scattering atom.

The difference in intensities may alternatively be thought of as a result of the complex nature of the scattering factor, f_i [see Eqn. (10.1)], so that the absolute value of $F(hkl)$ is different from that of $F(-h, -k, -l)$, as illustrated in Figure 10.4. We showed in Eqn. (10.1) that if there is an anomalous scatterer in the crystal, f is replaced by $f + f' + if''$. Let $A' = G(f + f') + A$ and $B' = H(f + f') + B$, where A and B refer to the rest of the structure and G and H to the anomalous scatterer. Remember that f and f' scatter with a phase change of 180° , while f'' scatters with a phase change of 90° . As a result, since

$$F(hkl) = (A' + iGf'') + i(B' + iHf'') = (A' - Hf'') + i(B' + Gf'') \quad (10.2)$$

$$|F(hkl)|^2 = (A' - Hf'')^2 + (B' + Gf'')^2 \quad (10.3)$$

and similarly

$$F(\bar{h}\bar{k}\bar{l}) = (A' + iGf'') - i(B' + iHf'') = (A' + Hf'') - i(B' - Gf'') \quad (10.4)$$

$$|F(\bar{h}\bar{k}\bar{l})|^2 = (A' + Hf'')^2 + (B' - Gf'')^2 \quad (10.5)$$

it then follows that

$$|F(hkl)|^2 - |F(\bar{h}\bar{k}\bar{l})|^2 = 4f''(B'G - A'H) \quad (10.6)$$

Thus, when the incident X-radiation is of a wavelength near that of the absorption edge of an atom in a noncentrosymmetric structure, $|F(hkl)|$ does not equal $|F(\bar{h}\bar{k}\bar{l})|$. Under normal conditions the wavelength of the X-radiation used for a diffraction experiment is far from any absorption edge and these two quantities, $|F(hkl)|$ and $|F(\bar{h}\bar{k}\bar{l})|$, are equal. If anomalous scattering occurs, the magnitude of the difference between $|F(hkl)|^2$ and $|F(\bar{h}\bar{k}\bar{l})|^2$ for the two Bragg reflections (called “Friedel pairs” or “Bijvoet pairs”) is a function of f'' (which depends on how near the incident radiation is to the absorption edge) and the positional parameters of both the anomalous scatterer and the rest of the structure.

It is possible from Eqn. (10.6) to calculate the expected differences between $|F(hkl)|^2$ and $|F(\bar{h}\bar{k}\bar{l})|^2$ for a given enantiomorph (with a specific absolute configuration). In practice, the indices of the Bragg reflections are assigned so that h, k , and l are in a right-handed system. Therefore the axes of x, y, z (that is, \mathbf{a}, \mathbf{b} , and \mathbf{c}) must also be in a right-handed system. Values of $|F|^2$ for pairs of Bragg reflections hkl and $\bar{h}\bar{k}\bar{l}$ are measured and the magnitude and sign of their difference are

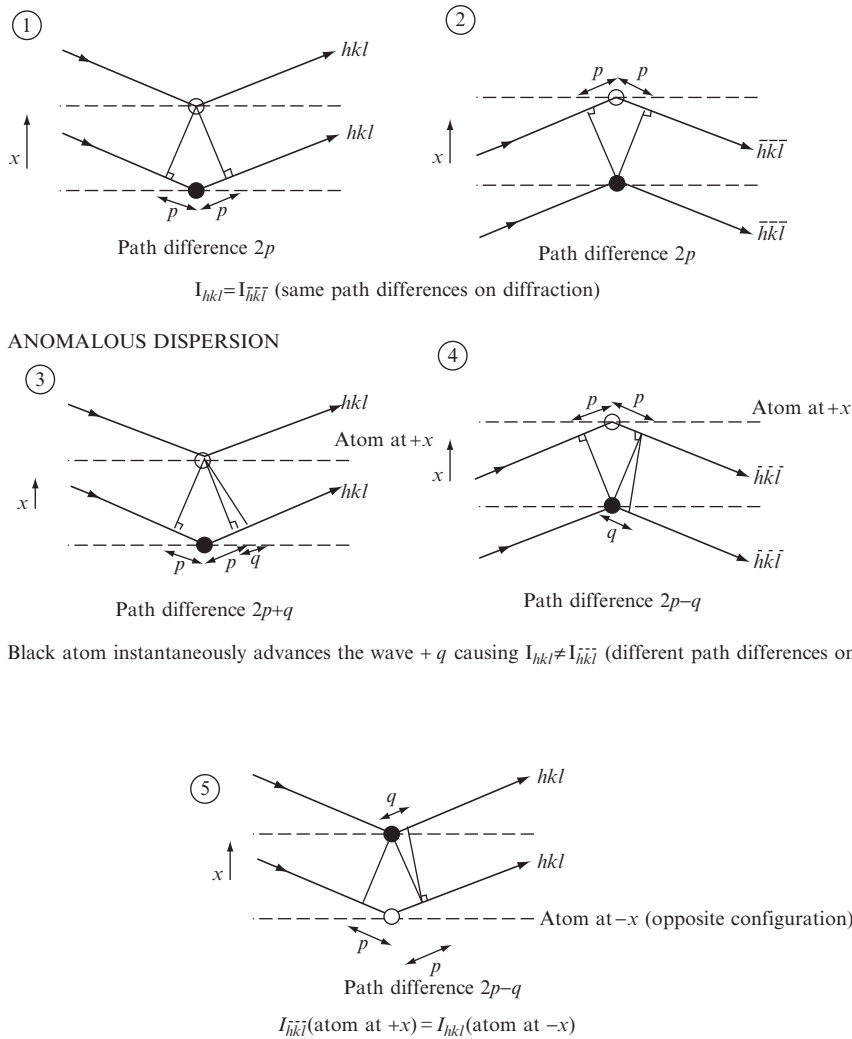


Fig. 10.4 Path differences on anomalous scattering in a noncentrosymmetric structure.

Effect of anomalous scattering on the path lengths of diffracted X-ray beams. Suppose that for a particular reflection the anomalous scatterer (black circles) causes in effect a path difference, q , in addition to the usual difference of $2p$ between the radiation scattered by a normal scatterer at this position and by a normal scatterer at some other position (open circles). As shown, the path difference for the hkl reflection with anomalous scattering is $2p + q$ and that for the $\bar{h}\bar{k}\bar{l}$ reflection is $2p - q$. If no anomalous scattering had occurred, these would be the same—namely, $2p$. Since the intensity of a diffracted beam depends on the path differences between waves scattered by the various atoms in the unit cell, the result of anomalous scattering is an intensity difference between hkl and $\bar{h}\bar{k}\bar{l}$. It is possible to compute values of $|F(hkl)|$ and $|F(\bar{h}\bar{k}\bar{l})|$ and see which should be the larger. If for many reflections the relations of the calculated values to the experimentally measured values are the same as those calculated for the model, then the model has the correct handedness (configuration); if not, the configuration of the model must be changed. That is, if $|F_o(hkl)| > |F_o(\bar{h}\bar{k}\bar{l})|$, then we must necessarily have $|F_c(hkl)| > |F_c(\bar{h}\bar{k}\bar{l})|$. See Appendix 11.

compared with the calculated value of $4f''(B'G - A'H)$ [see Eqn. (10.6)]. G and A' are cosine terms and do not change sign if the "handedness" of the system in which the model is calculated is changed. However, B' and H are sine terms, and if the signs of x , y , and z for all the atoms in the model are reversed, then B' and H change sign. Therefore, if $(|F(hkl)|^2 - |F(\bar{h}\bar{k}\bar{l})|^2)$ and $(B'G - A'H)$ have opposite signs, the values of x , y , and z in the model must be replaced by $-x$, $-y$, $-z$ to give the correct model. An example is given in Appendix 11. The result of *maintaining the same handedness for the axes in real and reciprocal space* is a three-dimensional representation of the molecule from which the absolute configuration can be seen directly.

In order to establish the absolute configuration of a crystal structure it is necessary (if anomalous scattering has taken place) to compare $I(hkl)$ and $I(\bar{h}\bar{k}\bar{l})$, note which is larger, and compare this information with the result of a structure factor calculation done with a model of the structure. If there is not agreement between the signs of these observed and calculated intensity differences, the handedness of the model should be reversed. The signs of the differences should be correct in all cases where they are large (keeping in mind the standard uncertainties of their measurements). Alternatively, a Flack parameter, x , can be calculated. This is obtained by the equation

$$I(hkl) = (1 - x)|F(hkl)|^2 + x|F(\bar{h}\bar{k}\bar{l})|^2 \quad (10.7)$$

and is often part of the least-squares refinement (Flack, 1983). The value found for x for all data generally lies between 0 and 1. If x is near 0 with a small standard uncertainty, the absolute structure that has been obtained is probably correct. If x is near 1, then the signs of all x , y , and z in the structure must be reversed. If x is near 0.5, the crystal may be racemic or twinned, and further investigation is necessary.

In 1930 Coster, Knol, and Prins were able to determine the absolute configuration of a zinc blende (ZnS) crystal (Coster et al., 1930).^{*} This contains, in one direction (a polar axis) through the crystal (the one perpendicular to the 111 face), pairs of layers of zinc and sulfur atoms separated by a quarter of the spacing in that direction and then another pair one cell translation away, and so on (Figure 10.5). The sense or polarity of that arrangement was determined by the use of radiation (gold, $\text{AuL}\alpha_1$, $\lambda = 1.276 \text{ \AA}$, $\text{AuL}\alpha_2$, $\lambda = 1.288 \text{ \AA}$) near the K-absorption edge of zinc (1.283 \AA). The $\text{AuL}\alpha_1$ radiation caused anomalous scattering by the zinc atoms, but the $\text{AuL}\alpha_2$ radiation did not. As a result it was shown that the shiny ($\bar{1}\bar{1}\bar{1}$) faces have layers of sulfur atoms on their surfaces and the dull (111) faces have layers of zinc atoms on their surfaces (see Figure 10.5).

This method was extended, as described above and in Appendix 11, by Bijvoet, Peerdeman, and van Bommel in 1951 to establish the absolute configuration of (+)-tartaric acid in crystals of its sodium rubidium double salt using zirconium radiation, which is scattered anomalously by rubidium atoms and ions (Bijvoet et al., 1951). The result is shown in Figure 10.6a. The absolute configuration was unknown until that time;

^{*} Zinc blende, ZnS, crystallizes in a cubic unit cell, $a = 5.42 \text{ \AA}$, space group $F\bar{4}3m$. The structure contains Zn at $(0,0,0)$, $(0, 1/2, 1/2)$, $(1/2, 0, 1/2)$, and $(1/2, 1/2, 0)$ and sulfur at $(1/4, 1/4, 1/4)$, $(1/4, 3/4, 3/4)$, $(3/4, 1/4, 3/4)$, and $(3/4, 3/4, 1/4)$. The shiny, well-developed faces have sulfur atoms on their surfaces, while the rougher, matte faces have zinc on their surfaces. When pressure is applied perpendicular to the 111 face, the shiny faces become, by the piezoelectric effect, positively charged and the matte faces become negatively charged.

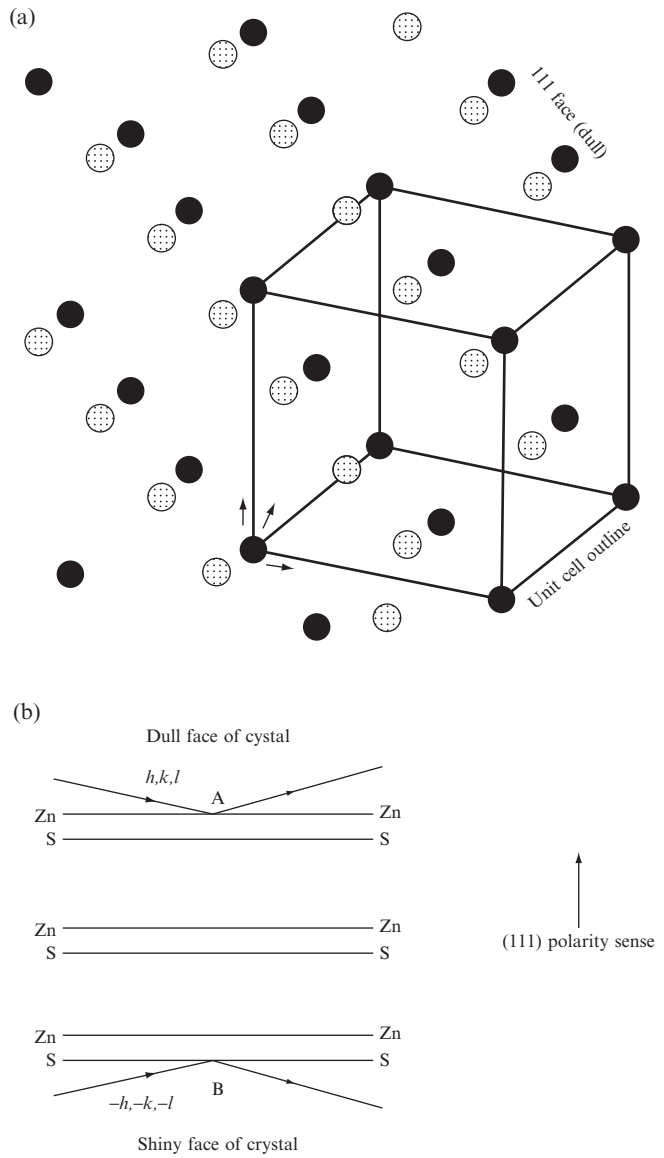


Fig. 10.5 Polarity sense of zinc blende.

- (a) The structure of zinc blende, showing the arrangement of zinc and sulfur atoms. Two views are shown, one down an axis and the other to show the planes of atoms in the [111] direction. Zinc blende is often called sphalerite. Zn black, S stippled.
- (b) Reflections from the two faces of zinc blende (dull and shiny) will have different relative path differences for the zinc and the sulfur atoms (compare with Figure 10.4). If the radiation is near the absorption edge of zinc, the two types of reflections will have different intensities, allowing one to determine (as did Coster, Knol, and Prins in 1930) that the dull face has zinc atoms on the surface and the shiny face has sulfur atoms on the surface.

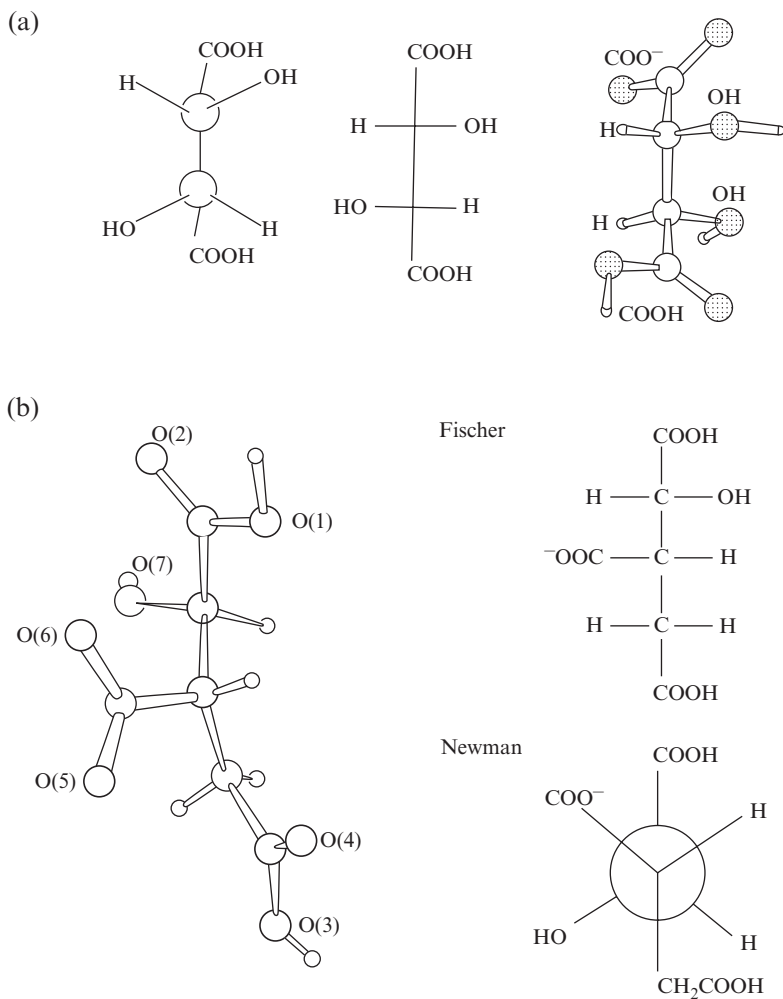


Fig. 10.6 Absolute configurations of biological molecules.

- (a) Absolute configuration of (+)-tartaric acid (dextrorotatory tartaric acid). Note that in the actual structure (right) the chain of four carbon atoms has effectively a planar zigzag arrangement. In the formula on the left, and by convention in all "Fischer formulas," vertical carbon chains are represented as planar but with successive bonds always directed into the page. Thus, in the formulas in the center and left here, the lower half of the molecule has been rotated 180° relative to the upper half as compared with the actual structure. This affects the conformation but not the absolute configuration of the molecule. The conformation of tartaric acid illustrated on the left is a possible one for this molecule, but it is of higher energy (because bonds are eclipsed) than that shown on the right, the conformation observed in the crystals studied by Bijvoet et al. (1951). Still other conformers may exist in solution or in other crystals.
- (b) Absolute configuration of the potassium salt of (+)-isocitric acid (isolated from the plant *Bryophyllum calycinum*). Fischer and Newman formulas are shown. The correct designation of this enantiomer is 1*R*:2*S*-1-hydroxy-1,2,3-propanetricarboxylate. The torsion angles are shown in Figure 12.5.

From *Acta Crystallographica* **B24** (1968), p. 585, Figure 4.

fortunately that which was found was the one arbitrarily chosen from the two possibilities half a century earlier by Fischer (Fischer, 1890, 1894), so the current organic chemistry textbooks did not have to be changed. The absolute configurations of many other molecules have been determined either by X-ray crystallographic methods or by chemical correlation with those compounds for which the absolute configuration had already been established (see Figure 10.6b). Values of anomalous scattering factors, especially those near the absorption edge, have been measured in detail with synchrotron radiation (see, for example, Templeton et al., 1980).

But how can absolute configuration be represented? The *R/S* system of doing this involved assigning a priority number to the atoms around an asymmetric (carbon) atom so that atoms with greater atomic number have the higher priority (Cahn et al., 1966). If two atoms have the same priority, *their* substituents are considered until differentiation of priorities can be established (otherwise, of course, the central atom is not asymmetric). Then the structure is viewed with the atom of lowest priority directly behind the central (carbon) atom and the other substituents are examined. Then if the order of the substituents going from highest to lowest priority is clockwise, the central atom is designated *R* (Latin *rectus*, right). If it is anticlockwise, the central atom is designated *S* (Latin *sinister*, left). As a result, once the absolute configuration is established and each asymmetric tetrahedral atom has an *R* or *S* designation, sufficient information is provided from these designations to make it possible to build a model with this correct absolute configuration.

The effect of anomalous scattering was used to solve the structure of a small protein, crambin, containing 45 amino acid residues (and which crystallized with 72 water and 4 ethanol molecules per protein molecule) (Hendrickson and Teeter, 1981). The nearest absorption edge of sulfur is at 5.02 Å, but for CuK α radiation, wavelength 1.5418 Å, the values of f' and f'' are 0.3 and 0.557, respectively, for sulfur. Pairs of reflections [$|F(hkl)|$ and $|F(\bar{h}\bar{k}\bar{l})|$] were measured to 1.5 Å resolution (the crystals scatter to 0.88 Å resolution); sulfur atom positions were calculated from Patterson maps with $|\Delta F|^2$. While it was necessary to take into account possible errors in such measurements of the differences of two large numbers, it was, in fact, possible to determine the positions of the three disulfide links (six sulfur atoms). The structure was then determined from an analysis of the Fourier map calculated on the heavy-atom parameters of the sulfur atoms together with a partial knowledge of the amino acid sequence.

SAD and MAD phasing

The use of anomalous scattering in structural work has increased recently since the advent of “tunable” synchrotron radiation—that is, X rays whose wavelength may, within certain limits, be selected at

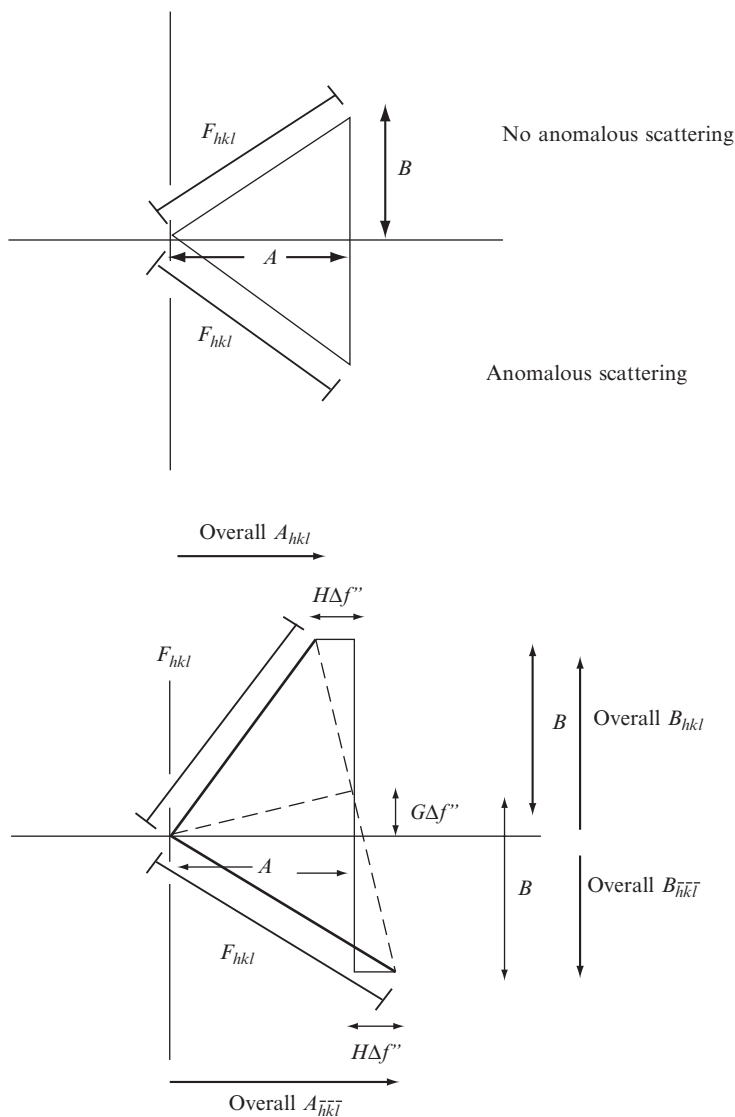


Fig. 10.7 Effects of anomalous scattering on F values.

The top diagram shows the structure factor vectors for $F(hkl)$ and $F(-h, -k, -l)$ in the absence of anomalous scattering and the lower diagram shows the effect of anomalous scattering on such a diagram. When there is anomalous scattering, $A(hkl) \neq A(-h, -k, -l)$. The same occurs for B values, as shown (see Chapter 5 and especially Figure 5.1 for the fundamentals of such diagrams).

will. As a result it is possible to measure the diffraction pattern of a macromolecular crystal with X-radiation of wavelengths near and also far from the absorption edges of any anomalous scatterers present. Two data sets can be measured, one near and one far from any absorption edge of atoms in the crystal. The integrity of the crystal during so much radiation exposure is maintained by flash freezing. For example, the

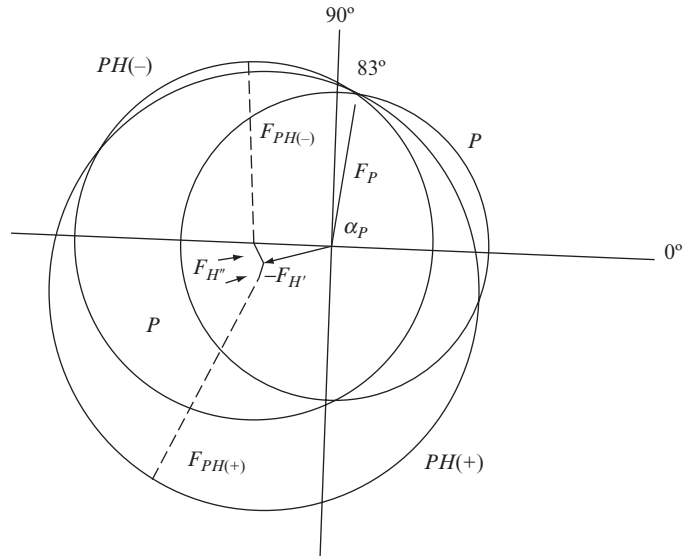


Fig. 10.8 Isomorphous replacement plus anomalous scattering (noncentrosymmetric).

The effect of anomalous scattering by an atom M , introduced to replace another atom, may be used to resolve the ambiguity in phase-angle determination by the isomorphous replacement method. The effect of anomalous scattering (Appendix 11) is to introduce a phase shift, which means in effect, to change the atomic scattering factor of atom M from a "real" quantity, f , to a "complex" one, $(f + f') + if''$. Suppose A and B refer to that part of the structure that does not scatter anomalously, and A' and B' to the total structure without any f'' component; then $A' = G(f + f') + A$ and $B' = H(f + f') + B$, where G and H refer to geometric components for the anomalous scatterer, M . A'' and B'' are components of the structure when anomalous scattering is present, and A''_M and B''_M are components for the anomalous scatterer M alone. Then

$$A''_M = G(f + f' + if'') = A_M + Gf' + iGf''$$

$$B''_M = H(f + f' + if'') = B_M + Hf' + iHf''$$

Then, for the entire structure, including anomalous-scattering effects, we have

$$A'' = A + Gf + Gf' + iGf'' = A' + iGf''$$

$$B'' = B + Hf + Hf' + iHf'' = B' + iHf''$$

As shown in Appendix 11, we have for the entire structure with anomalous scattering (by separating and squaring the "real" and "imaginary" components)

$$|F(hkl)| = \sqrt{(A' - Hf'')^2 + (B' + Gf'')^2}$$

$$|F(\bar{h}\bar{k}\bar{l})| = \sqrt{(A' + Hf'')^2 + (B' - Gf'')^2}$$

(see Figure 10.4). Therefore, $|F(hkl)|$ and $|F(\bar{h}\bar{k}\bar{l})|$ are different; the intensity of each reflection is measured to see which is the greater, as shown in Appendix 11.

A diagram to illustrate the determination of a phase angle for a macromolecule (that is, α_P) by the combination of isomorphous replacement and anomalous scattering is shown. This diagram is constructed in a similar way to Figure 9.9. Circles of radii $|F_{PH(+)}|$ and $|F_{PH(-)}|$ (for reflections of the heavy-atom derivative with indices h, k, l and $-h, -k, -l$, respectively) are drawn with centers at $-(\mathbf{F}_{H'} + \mathbf{F}_{H''})$ and $-(\mathbf{F}_{H'} - \mathbf{F}_{H''})$, respectively. There are now three circles, radii $|F_P|$, $|F_{PH(+)}|$, and $|F_{PH(-)}|$, and these intersect at a phase angle of α_P (83°). This is probably the phase angle of this reflection, h, k, l , for the native protein.

method of anomalous scattering may be combined with isomorphous replacement in protein structure determination. Three data sets are needed for this. One involves the protein crystal, and one a heavy-atom derivative of this protein. A third data set is measured with X rays of a wavelength that will cause maximal anomalous scattering by the heavy atom. The heavy-atom position is located from the first two data sets, and phase information is aided by the nonequivalent Friedel pairs of Bragg reflections; these remove ambiguities in phase determination (see Figures 10.7 and 10.8). This makes it possible to obtain approximate phases from just one heavy-atom derivative.

The multiwavelength anomalous dispersion (MAD) method, suggested by Wayne Hendrickson, is now a method of choice for phase determination (Hendrickson, 1991). Generally proteins that are used have been biologically expressed in a medium that contains only selenomethionine. As a result the protein contains selenomethionine in its sequence where methionine would normally be expected. Therefore the strong anomalous signal of selenium can be used to derive phases. X-ray diffraction data are measured near the absorption edge (where f'' has a maximum value, 1.15 electrons), and also at one or two wavelengths remote from any absorption edge. Only one crystal is needed, and the data are generally measured at a synchrotron source.

In the single-wavelength anomalous dispersion (SAD) method, diffraction data for one wavelength of radiation are measured on a heavy-atom-containing protein, not necessarily near an absorption edge. Since when heavy atoms are soaked into a crystal they may attach to various side chains in a disordered manner, the strategy has been to generate a protein with a heavy atom, such as that in iodophenylalanine, chemically incorporated into one amino acid (Dauter, 2004). The value of f'' for iodine is 6.91 electrons for $\text{CuK}\alpha$ radiation. Alternatively, chromium $\text{K}\alpha$ radiation ($\lambda = 2.2909 \text{ \AA}$) may be used to locate sulfur, which has an anomalous signal (f'') of 1.14 electrons for $\text{CrK}\alpha$ radiation, twice that for $\text{CuK}\alpha$ radiation (Yang et al., 2003). This means that naturally occurring protein side chains such as those of methionine or cysteine are sufficient to provide phasing with $\text{CrK}\alpha$ radiation. Also, the data collection can be done in a laboratory and no tuning of radiation wavelength is needed; a simple X-ray tube can be used. The phase ambiguity that comes from measuring just one data set can be aided by direct methods or by density modification. Obviously crystallographers are now experimenting with different wavelengths of radiation and different possible anomalous scatterers, and the trend is to study a crystal that contains only the molecule under study (and not variations such as heavy-atom derivatives).

Sine-Patterson map

A modified Patterson map can be used to determine the absolute configuration of a structure provided Bijvoet pairs of reflections have been

measured and correctly indexed. The map is calculated with a function with $\{|F(hkl)|^2 + |F(\bar{h}\bar{k}\bar{l})|^2\}$ as coefficients and a cosine term; this gives peaks corresponding to Eqn. (9.1), that is, vectors between atoms. Another function, with $\{|F(hkl)|^2 - |F(\bar{h}\bar{k}\bar{l})|^2\}$ as coefficients and a sine term, known as the sine-Patterson map,

$$P_s(u, v, w) = \frac{1}{V_c} \sum_{\text{all } hkl} \sum_{\text{all } hkl} \left\{ |F(hkl)|^2 - |F(\bar{h}\bar{k}\bar{l})|^2 \right\} \sin 2\pi(hu + kv + lw) \quad (10.8)$$

will have only vectors between anomalously and nonanomalously scattering atoms, and these peaks are positive if the vector is from an anomalously scattering atom to a normal atom, and negative if the vector is in the other direction. This map is asymmetric. Thus the absolute configuration of the structure may be determined from such a map (Okaya et al., 1955).

What effect does anomalous scattering have on the calculated electron density, since a term in the scattering factor now has an “imaginary” component? The answer is that the calculated electron density must be real, and, to obtain this, any effect of anomalous scattering (which involves a complex scattering factor) must be removed (as described in Appendix 11) (Patterson, 1963). This, of course, also removes any means of distinguishing one enantiomorph from the other; such information is contained only in the anomalous-scattering data.

Summary

If an atom in the crystal appreciably absorbs the X rays used, there will be a phase change for the X rays scattered by that atom relative to the phase of the X rays scattered by a nonabsorbing atom at the same site. This phase change on absorption leads to anomalous scattering and, for a noncentrosymmetric structure, results in differences in values of $|F(hkl)|^2$ and $|F(\bar{h}\bar{k}\bar{l})|^2$ that are not found in the absence of anomalous scattering. If the structure contains only one enantiomorph of a molecule, its absolute configuration may be determined by a comparison of the signs of the observed and calculated values of $(|F(hkl)|^2 - |F(\bar{h}\bar{k}\bar{l})|^2)$.

**STRUCTURE
REFINEMENT
AND STRUCTURAL
INFORMATION**

**Part
III**

This page intentionally left blank

Refinement of the trial structure

11

When approximate positions have been determined for most, if not all, of the atoms, it is time to begin the refinement of the structure. In this process the atomic parameters are varied systematically so as to give the best possible agreement of the observed structure factor amplitudes (the experimental data) with those calculated for the proposed trial structure. Common refinement techniques involve Fourier syntheses and processes involving least-squares or maximum likelihood methods. Although they have been shown formally to be nearly equivalent—differing chiefly in the weighting attached to the experimental observations—they differ considerably in manipulative details; we shall discuss them separately here.

Many successive refinement cycles are usually needed before a structure converges to the stage at which the shifts from cycle to cycle in the parameters being refined are negligible with respect to their estimated errors. When least-squares refinement is used, the equations are, as pointed out below, nonlinear in the parameters being refined, which means that the shifts calculated for these parameters are only approximate, as long as the structure is significantly different from the “correct” one. With Fourier refinement methods, the adjustments in the parameters are at best only approximate anyway; final parameter adjustments are now almost always made by least squares, at least for structures not involving macromolecules.

Fourier methods

As indicated earlier (Chapters 8 and 9, especially Figure 9.8 and the accompanying discussion), Fourier methods are commonly used to locate a portion of the structure after some of the atoms have been found—that is, after at least a partial trial structure has been identified. Initially, only one or a few atoms may have been found, or maybe an appreciable fraction of the structure is now known. Once approximate positions for at least some of the atoms in the structure are known, the phase angles can be calculated. Then an approximate electron-density

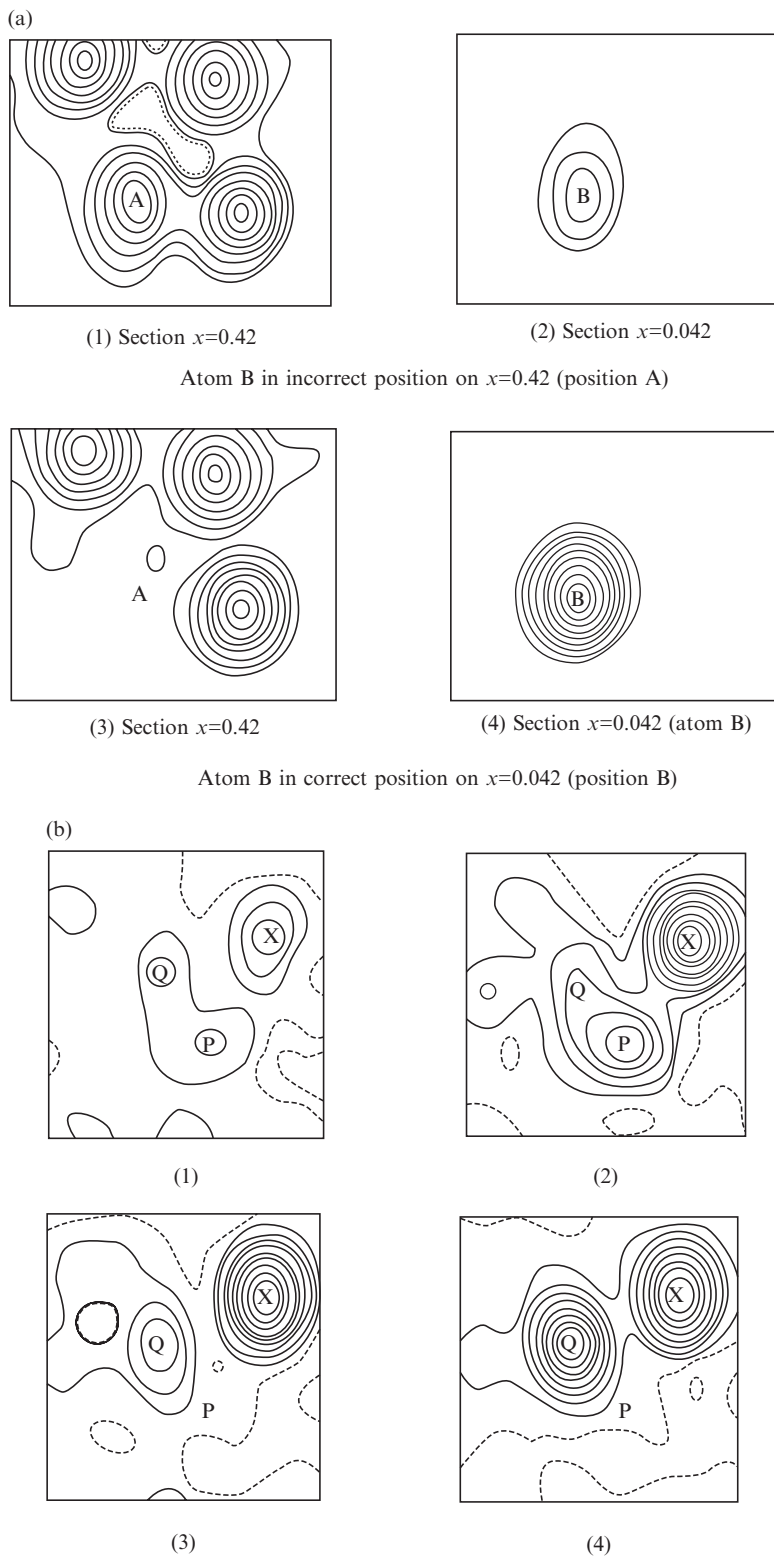


Fig. 11.1 Fourier maps phased with partially incorrect trial structures.

map calculated with *observed* structure amplitudes and *computed* phase angles will contain a blend of the true structure (from the structure amplitudes) with the trial structure (from the calculated phases). If the trial structure contains most of the atoms of the true structure, at or near their correct positions, the resulting electron-density map will contain peaks representing the trial structure, but, additionally, at other sites, peaks representing atoms that were omitted from the trial structure but that are really present. Conversely, if an atom in the trial structure has been incorrectly chosen, the corresponding peak in the electron-density map will usually be significantly lower than normal, so that its location will be questionable. Finally, if an atom was put into the calculation near, but not at, its correct position, the resulting peak in the electron-density map will usually have moved a slight amount from the input position towards (but not usually as far as) the correct position. Examples of these effects for a noncentrosymmetric structure are shown in Figure 11.1. In centrosymmetric structures, the phase angles are either 0° or 180° and a slight error in the structure may not have a large effect on most phase angles. Therefore, a map computed with observed $|F(hkl)|$ values and computed phase angles may be almost correct even if the model used was slightly in error. However, with noncentrosymmetric structures, for which the phase angles may have any value from 0° to 360° , there will be at least small errors in most of the phases, and consequently the calculated electron-density map will be weighted more in the direction of the trial structure used to calculate the phases than it would be if the structure were centrosymmetric.

It is usual, when most or all of the trial structure is known, to compute *difference maps* rather than normal electron-density maps. For difference maps, the coefficients for the calculation are $(|F_o| - |F_c|)$ and the phase

-
- (a) *The effect of an atom in the wrong position.* This example is from a noncentrosymmetric structure. In (1), one atom, B, was inadvertently included (an input typographical error) at the wrong position (marked by an A) in the structure factor calculation. The electron-density map phased with this incorrect structure contains a peak at the wrong position, but this peak is lower in electron density than the others near it. A small peak occurs in the correct position, B, shown in (2), although none was introduced there in the phasing. Corresponding sections of a correctly phased map are shown in (3) and (4); the spurious "atom" at A above has disappeared and the correct peak, B, is now a pronounced one.
- (b) *The effect of an atom near but not at the correct position.* The appearance of a particular section in successive electron-density maps is shown as the structure used for phasing becomes more nearly correct. The map (1) was computed from the positions of two heavy atoms (positions not shown) and from this the location of atom X was correctly (as it turned out) deduced. But in (2) an atom was incorrectly placed at P; it can be seen that the peak for this atom is elongated in the direction of the correct position, Q. In (3) only atom X (of P, Q, and X) was included in the phasing and peak Q now is more clearly revealed. In (4) the peak at Q is now established as correct. A total of 2, 62, 54, and 68 atoms out of 73 were used in the phasing of maps (1), (2), (3), and (4), respectively.
From Hodgkin et al., 1959, p. 320, Figures 8 and 9.

angles are those computed for the trial structure. The difference map is thus the difference of an “observed” and a “calculated” map (both with “calculated” phases). In this map a positive region implies that not enough electrons were put in that area in the trial structure, while a negative region suggests that too many electrons were included in that region in the trial structure. For example, if an atom is included in the trial structure with too high an atomic number, a trough appears at the corresponding position; if it is included (at the correct position) with too low an atomic number or omitted entirely, a peak appears. Hydrogen atoms can be located from difference maps calculated from a trial structure that includes all the heavier atoms present (see Figure 11.2), although often hydrogen atoms are put at geometrically calculated positions and then refined. Another use of difference maps is in macromolecular structure determination, to locate the binding sites of inhibitors, substrates, or products.

Figure 11.3 shows some examples of further uses of difference maps for refinement of parameters. If an atom has been included near but not at the correct position, the location at which it was input will lie in a negative region, with a positive region in the direction of the correct position. The amount of the shift needed to move the atom to the correct position is indicated by the slope of the contours between the negative and positive regions. If an atom is left out of the trial structure (as in “omit maps”) it will appear in the correct position as a peak, provided, of course, that the phase angles used in computing the electron-density map are approximately correct. If an atomic displacement factor is too small in the calculated trial structure, a trough will appear at the atomic position because the electrons in that atom have been assumed in the trial structure to be confined to a smaller volume than in fact they are, and hence to have too high a total electron density. Similarly, if the atomic displacement factor is too large in the trial structure, a peak will appear in the difference map. If the atom vibrates anisotropically, that is, different amounts in different directions, but has been assumed to be isotropic, peaks will occur in directions of greater motion and troughs in directions of lesser motion. In summary, if there is a positive area in a difference map, consider adding more electron density at that position; a negative area indicates too much electron density at that location in the trial structure.

The process of Fourier refinement can be adapted for automatic operation with a high-speed computer. Instead of evaluating the electron density at the points of a fixed lattice, we calculate it, together with its first and second derivatives, at the positions assumed for the atomic centers at this stage. The shifts in the atomic positions* and temperature-factor parameters can then be derived from the slopes and the curvatures in different directions. When this *differential-synthesis* method is used, it is normally applied to the difference density. In fact, however, the method is used much less extensively than least-squares refinement, for the latter is somewhat more convenient for computer application and has the advantage

* The shift required in x is

$$\begin{aligned}\Delta x &= \frac{-\partial \Delta \rho}{\partial x} / \frac{\partial^2 \rho}{\partial x^2} \\ &= \frac{-(\text{gradient of difference Fourier at } x_0)}{(\text{curvature of electron density at } x_0)}\end{aligned}$$

where x_0 is the input position.

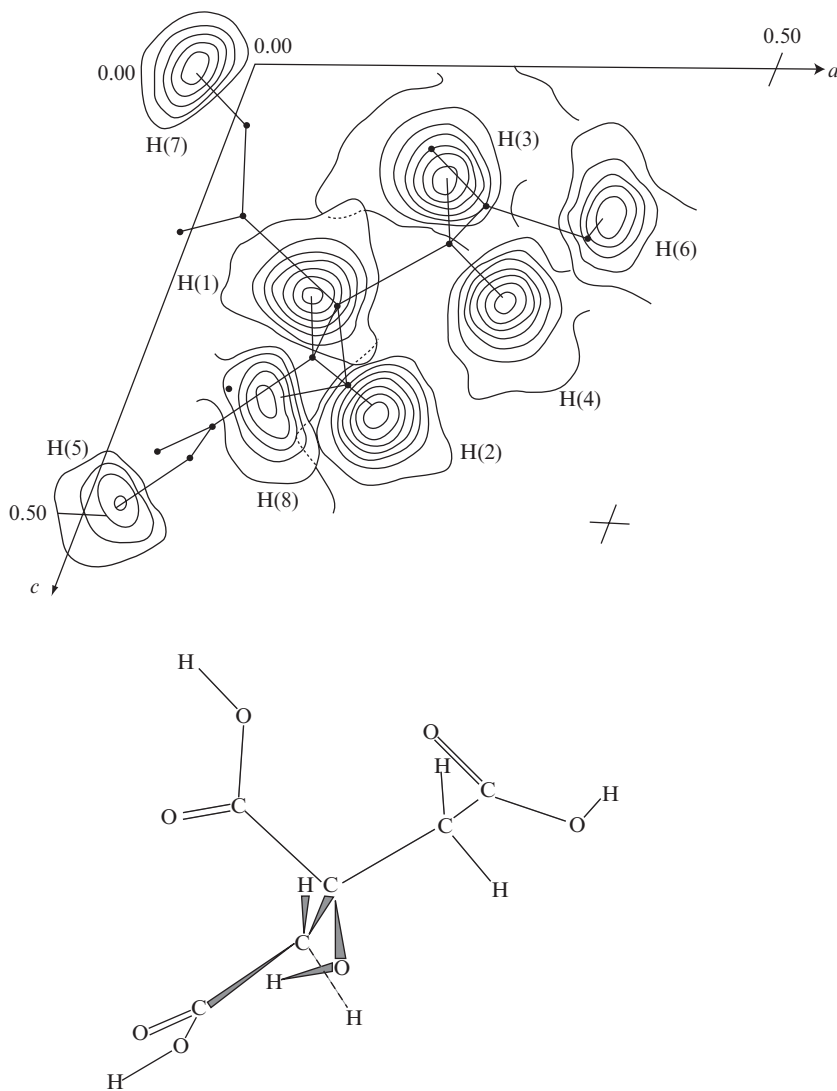


Fig. 11.2 Hydrogen atoms found from a difference map.

This is a composite map of sections of a difference map for a monoclinic structure, anhydrous citric acid, viewed down b . Eight sections containing hydrogen atoms are shown here. The contour interval is 0.1 electrons per cubic Å; the zero contour is omitted. Solid circles show the final positions of the heavier atoms that were used in the phase-angle calculation. Peaks occur in the map at positions in which not enough electron density has been included in the structure factor calculation, and thus at the positions of hydrogen atoms omitted from the phase-angle calculation. The molecular formula is shown below the map, on the same scale and in the same orientation.

From Glusker et al., 1969, *Acta Crystallographica* **B25**, p. 1066, Figure 1.

of a statistically sounder weighting scheme for the experimental observations.

One of the best criteria of a good structure determination is a flat difference map at the end of the refinement (because now the values of the observed and calculated structure amplitudes are approximately

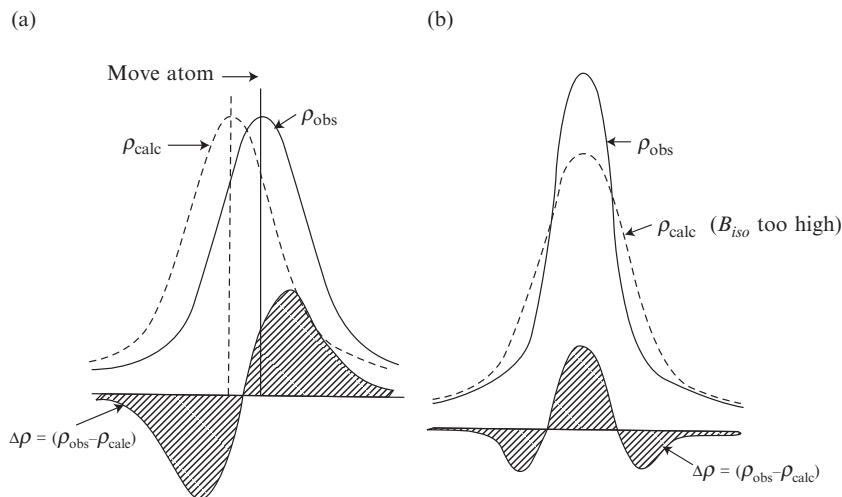


Fig. 11.3 Refinement by difference maps.

A difference map (the difference between the observed and calculated electron density, $\rho_{\text{obs}} - \rho_{\text{calc}}$) may be used to refine atomic positions and temperature factors. In a difference map a peak (a region of positive electron density) implies that not enough electron density was included in the model at that position, and a trough (a region of negative electron density) implies the opposite.

- (a) *An error in the position of an atom.* The peak in ρ_{calc} shows the approximate position used in the calculation of structure factors. The peak in ρ_{obs} is nearer to the correct position. Therefore, the assumed atomic position should be moved (to the right) in the direction of the positive peak in the difference map.
- (b) *Incorrect atomic displacement parameter.* If the displacement parameter exponent is too high in the model used to phase the map, the atom is vibrating through too large a volume. A peak surrounded by a region of negative density occurs at the atomic position, indicating that the exponent should be decreased to give a higher and narrower peak (and thus B should be decreased).

equal). It is possible to have a good average agreement of $|F_{\text{o}}|$ and $|F_{\text{c}}|$, and thus a low discrepancy index, R , and yet to have many ($|F_{\text{o}}| - |F_{\text{c}}|$) values contributing to a peak or trough in a given area of the map, indicating some error in the structure. Therefore, at the end of every structure determination, a difference map should be calculated and scanned for any peaks.

One question that always arises in discussions of Fourier refinement is: How good must the trial structure be, or how nearly correct must the phases be, for the process to converge? This question cannot be answered precisely. For an ordinary small-molecule structure analysis, if most of the atoms included are within about 0.3 \AA (approximately half their radius) of their correct sites, then a few that are farther away and even one or two that may be wholly spurious can be tolerated. When the initial phases are poor, the first approximations to the electron density will contain much false detail (as illustrated in Figures 9.8 and 11.1b), together with peaks at or near the correct atomic positions. The sorting of the real from the spurious is difficult, especially with noncentrosymmetric structures; experience, chemical information, and a sound knowledge of the principles of structural chemistry are all desirable, and a good deal of caution is essential. A very astute or fortunate crystallographer may be able to recognize portions of a molecule of known

structure in a map produced from an extremely poor trial structure, but such perspicacity is uncommon.

Most investigators currently view electron-density and difference maps on a computer screen. There are several mouse-driven three-dimensional interactive programs such as O (Jones et al., 1991) and COOT (Emsley and Cowtan, 2004) that show electron densities as three-dimensional wire-frame entities. These can be rotated by the user to better view them, and a diagram of a three-dimensional trial structure can be overlaid on them. Some refinement can even take place at the computer screen as the trial structure diagram is moved to best fit the map. When the user is satisfied with the fit, the program will then generate the atomic coordinates of the new and better position of the model and these coordinates can be further refined.

The method of least squares

The method of least squares, first used by Legendre (1805), is a common technique for finding the best fit of a *particular assumed model* to a set of experimental data when there are more experimental observations than parameters to be determined. Parameters for the assumed model are improved by this method by minimizing the sum of the squares of the deviations between the experimental quantities and the values of the same quantities calculated with the derived parameters of the model. The method of least squares is often used to calculate the best straight line through a series of points, when it is known that there is an experimental error (assumed random) in the measurement of each point. The equation for a line may be calculated such that the sum of the squares of the deviations from the line is a minimum. Of course, if the points, which were assumed to lie on a straight line, actually lie on a curve (described very well by a nonlinear equation), the method will not tell what this curve is, but will approximate it by a straight line as best it may. It is possible to “weight” the points; that is, if one measurement is believed to be more precise than the others, then this measurement may, and indeed should, be given higher weight than the others. The weight $w(hkl)$ assigned to each measurement is inversely proportional to its precision, that is, the square of the standard uncertainty (formerly known as the estimated standard deviation).

The least-squares method has been extended to the problem of fitting the observed diffraction intensities to calculated ones (Hughes, 1946), and has been for more than six decades by far the most commonly used method of structure refinement, although this practice has not been without serious criticism.** Just as in a least-squares fit of data to a straight line (a two-parameter problem), the observed data are fitted to those calculated for a particular assumed model. If we let $\Delta|F(hkl)|$ be the difference in the amplitudes of the observed and calculated structure factors, $|F_o| - |F_c|$, and let the standard uncertainty of the experimental value of $F_o(hkl)^2$ be $[1/w(hkl)]$, then, according to the theory of

** These criticisms are based in part on the fact that the theory of the least-squares method is founded on the assumption that the experimental errors in the data are normally distributed (that is, follow a Gaussian error curve), or at least that the data are from a population with finite second moments. This assumption is largely untested with most data sets. Weighting of the observations may help to alleviate the problem, but it depends on a knowledge of their variance, which is usually assumed rather than experimentally measured. For a discussion of some of these points, see Dunitz's discussion of least-squares methods (Dunitz, 1996).

† The equations can be formulated with $|F^2|$ rather than $|F|$, so that the equation parallel to Eqn. (11.1) then becomes

$$Q = \sum w(hkl)[\Delta|F^2(hkl)|]^2$$

Most crystallographers prefer refinement that involves F^2 for a variety of reasons, including ease of refining twinned structures, calculating weights for the least-squares refinement, and dealing with weak Bragg reflections (which may have negative values of F^2 from the nature of the measurement process).

‡ These six vibration parameters, different for each atom j , are symbolized in various ways (see Chapter 12). Here we represent them as b^{11} , b^{22} , b^{33} , b^{12} , b^{23} , and b^{31} , with sometimes an additional subscript to denote the atom j . As mentioned later, more parameters may be needed to describe the atomic motion in extreme circumstances.

errors, the best parameters of the model assumed for the structure are those corresponding to the minimum value of the quantity[†]

$$Q = \sum w(hkl)[\Delta|F(hkl)|]^2 \quad (11.1)$$

in which the sum is taken over all unique diffraction maxima. In an analysis of the equations that define F_c , the effects of small changes in the atomic parameters are considered, and changes are found that will difference between F_o and F_c [and thus the sum in Eqn. (11.1)]. Since even the problem of fitting data to a two-parameter straight line involves much calculation, this method requires a high-speed, large-memory computer.

The variable parameters that are used in the minimization of Q in Eqn. (11.1) normally include an overall scale factor for the experimental observations; the atomic position parameters x , y , and z for each atom, j ; and the atomic displacement parameters for each atom, *which may number as many as six*.[‡] Occasionally, when disorder is present, occupancy factors (varying from 0 to 1, and perhaps correlated with those of other atoms) may be refined for selected atoms. Thus *in a general case* there may be as many as $(9N + 1)$ or even a few more parameters to be refined for a structure with N independent atoms.

If the total number of parameters to be refined is p , then the minimization of Eqn. (11.1) involves setting the derivatives of Q with respect to *each* of these parameters equal to zero. This gives p independent simultaneous equations. The derivatives of Q are readily evaluated. Clearly, at least p experimental observations are needed to define the p parameters, but, in fact, since the observations usually have significant experimental uncertainty, it is desirable that the number of observations, m , exceeds the number of variables by an appreciable factor. In most practical cases with three-dimensional X-ray data, m/p is of the order of 5 to 10, so that the equations derived from Eqn. (11.1) are greatly overdetermined.

Unfortunately, the equations derived from Eqn. (11.1) are by no means linear in the parameters, since they involve trigonometric and exponential functions, whereas the straightforward application of the method of least squares requires a set of linear equations. *If* a reasonable trial structure is available, then it is possible to derive a set of linear equations in which the variables are the *shifts* from the trial parameters, rather than the parameters themselves. This is done by expanding in a Taylor series about the trial parameters, retaining only the first-derivative terms on the assumption that *the shifts needed are sufficiently small that the terms involving second- and higher-order derivatives are negligible*:

$$\Delta|F_c| = \frac{\partial|F_c|}{\partial x_1} \Delta x_1 + \frac{\partial|F_c|}{\partial y_1} \Delta y_1 + \dots + \frac{\partial|F_c|}{\partial b_{33,n}} \Delta b_{33,n} \quad (11.2)$$

The validity of this assumption depends on the closeness of the trial structure to the correct structure. If conditions are unfavorable, and Eqn. (11.2) is too imprecise, the process may sometimes converge to

a false minimum rather than to the minimum corresponding to the correct solution or may not converge at all. Thus this method of refinement also depends for its success on the availability at the start of a reasonably good set of phases—that is, a good trial structure. Since the linearization of the least-squares equations makes them only approximate, several cycles of refinement are needed before convergence is achieved. However, the linear approximation becomes better as the solution is approached because the neglected higher-derivative terms, which involve high powers of the discrepancies between the approximate and true structures, become negligible as these discrepancies become small.

It is often desirable in a least-squares refinement to introduce various constraints or restraints on the atomic parameters to make them satisfy some specific criteria, usually geometrical. Constraints are limits on the values that parameters in a least-squares refinement may take. For example, they may relate two or more parameters, or may assign fixed values to certain parameters. As a result they reduce the number of independent parameters to be refined and are mathematically rigid with no standard uncertainty. For example, suppose that the structure is disordered in some way, or that the available diffraction data are of limited resolution. The individual atomic positions obtained by the usual least-squares process for some of the atoms will then have relatively high standard uncertainties and the geometrical parameters derived from these positions may not be of high significance. If geometrical constraints are introduced—for example, constraining a phenyl ring to be a regular hexagon of certain dimensions, or merely fixing certain bond lengths or bond angles or torsion angles within a particular range of values—the number of parameters to be refined will be significantly reduced and the refinement process accelerated. By contrast, restraints are assumptions that are treated like additional data that need to be refined against. For example, a phenyl group would be described as an “approximately regular hexagon” with a standard uncertainty within which it is supposed to be refined. Constraints remove parameters and restraints add data.

If the trial model used in a least-squares refinement is incorrect or partially incorrect, there are almost always indications that this is so. The discrepancy index R may not drop to an acceptable value, and the parameters may show certain anomalies. For example, if a false atom has inadvertently been included in the initial trial structure, it may move to a chemically unreasonable position, perhaps too close to another atom, and its temperature factor will increase strikingly to a value far higher than that normally encountered for any real atom. This corresponds physically to a very high vibration amplitude—that is, a smearing of the atom throughout the unit cell, an almost infallible sign that there is no atom in the actual structure at the position assumed in the trial structure.

At the conclusion of any least-squares refinement process, it is always wise to calculate a difference Fourier synthesis. If it is zero everywhere,

within experimental error, then the least-squares procedure is a reasonable one. If it is not, and the peaks in it are not attributable to light atoms that have been left out of the structure factor calculations or to some other understandable defect of the model, then it is distinctly possible that the least-squares procedure may have converged to a false minimum because the initial approximation (the trial structure) was not sufficiently good. Another plausible trial structure must be sought and refinement tried again.

The maximum likelihood method

Maximum likelihood estimation is an increasingly commonly employed statistical method that is used to refine a statistical model to experimental data, and thereby provide improved estimates of the parameters of this model (Murshudov et al., 1997; Terwilliger, 2000). It deals in conditional probability distributions, that is, probabilities that are conditional upon additional variables, and aims to maximize their likelihoods. For example, if we know that the probability of data A is dependent upon model B, we can find the likelihood of model B given the data A. Stephen Stigler compares maximum likelihood to the choice that prehistoric men made of “where and how to hunt and gather,” that is, experience and acute observation which indicates how best to do something (Stigler, 2007). The likelihood function for macromolecular structures is proportional to the conditional distribution of experimental data when the parameters are known. The conditional probability distributions for each Bragg reflection are multiplied together and the result is the joint conditional probability distribution. This includes the experimental data plus any phase information and any experimental standard uncertainties that may be available. The aim of the method is to find those values of the parameters that make the observed data most likely. The necessary equations are contained in the program REFMAC (Vagin et al., 2004), which will minimize atomic parameters to satisfy either a maximum likelihood or a least-squares residual. The method has been used with great success, and, if the data have been measured to very high resolution, approaches least squares as a good refinement method.

The correctness of a structure

What assurance is there that the changes suggested by difference maps, least-squares methods, or maximum likelihood estimations are correct? Are the suggested changes really improvements that will make the trial structure more nearly resemble the actual distribution of scattering matter in the crystal? In fact, if the experimenter is injudicious or unfortunate, some changes may actually make the model worse, since an image formed with incorrect phases will always contain false

detail—for example, peaks that may seem to suggest atoms but that really arise from errors in the phases. If the model is altered in a grossly incorrect way (or if it was inadequate in the first place), the “refinement” process may converge to a quite incorrect solution. What then are the criteria for assessing the likely correctness of a structure that has been determined by the refinement of approximate phases? There are no certain tests, but the most helpful general criteria are the following. (A number of erroneous structures have been reported because of inadequate attention to these criteria.)

- (1) The agreement of the individual observed structure factor amplitudes $|F_o|$ with those calculated for the refined model should be comparable to the estimated precision of the experimental measurements of the $|F_o|$. As stressed in Chapter 6, the discrepancy index, R [Eqn. (6.9)], is a useful but by no means definitive index of the reliability of a structure analysis.
- (2) A difference map phased with the final parameters of the refined structure should reveal no fluctuations in electron density greater than those expected on the basis of the estimated precision of the electron density.
- (3) Any anomalies in the molecular geometry and packing, or other derived quantities—for example, abnormal bond distances and angles, unusually short nonbonded intramolecular or intermolecular distances, and the like—should be scrutinized with the greatest care and regarded with some skepticism. They may be quite genuine, but if so they should be interpretable in terms of some unusual properties of the crystal or the molecules and ions in it.

If writers of crystallographic papers have done their work properly, the information needed for a reader to assess the precision and accuracy of the reported results will be given. The precision of an experimental result, usually expressed in terms of its standard uncertainty, is a measure of the reproducibility of the observed value if the experiment were to be repeated. Accuracy, on the other hand, gives the deviation of a measurement from the value accepted as true (if that is known). The standard uncertainties of the various observed results—distances, angles, and so on—can be *estimated* by statistical methods, using as a basis the estimated errors of the prime experimental quantities, the intensities and directions of the diffracted radiation and the instrumental parameters of the equipment used. The basic assumption involved in the estimation of standard uncertainties is that fluctuations in observed quantities are due solely to *random* errors, which implies that the fluctuations are about an average value that agrees with the “true value.” However, it is very important to recognize that there may be *systematic* errors, too, arising from failure to correct for various effects, which may be either known—for example, the effect of absorption on the intensities—or unknown—for example, inadequacies of the model because of lack of knowledge of the way in which molecular motion occurs in the crystal. Uncorrected systematic errors can cause

the reported values to differ from the “true” values by considerably more than would be estimated on the basis of the precision; that is, the accuracy may be low even if the precision is high. As in any experiment, it is far harder to assess the accuracy than the precision, because many systematic errors are unsuspected; the best way to detect systematic errors is to compare many distinct measurements of the quantity of interest, under different experimental conditions and by different methods if possible.[§]

[§] A classic example of this approach led to the discovery of the noble gases by Rayleigh and Ramsey through a comparison of highly precise measurements of the density of nitrogen prepared from various pure nitrogen-containing compounds with that of a sample obtained by fractionation of liquid air.

If the distribution of errors is normal, statistical tables can be used to assess the probability that one observation or derived quantity is “significantly” different from another—that is, that the difference arises not merely from random errors but rather is one that further sufficiently precise measurements could verify. If two measurements differ from one another by twice the standard uncertainty (s.u.) of either, the probability is about 5 percent that the difference between them represents a random fluctuation; if they differ by 2.7 times the s.u., the probability is only about 1 percent that the difference represents a random fluctuation—in other words, there is about 99 percent probability that they represent two distinct values, which further precise measurements would verify as being different. It is a matter of taste what one accepts as being “significantly different”; some people accept the 2 s.u. (or “95 percent confidence”) level, while those who are more conservative may choose the 2.7 s.u. (or “99 percent confidence”) level, or an even higher one. Because systematic errors are so difficult to eliminate, the standard uncertainties calculated on the assumption that only random errors are present are usually quite optimistic as estimates of the *accuracy* of the results, however valuable they may be as measures of *precision*. Hence, in comparing results from different studies—for example, in comparing two bond lengths, or in trying to decide whether a bond angle is significantly different from that expected on the basis of some theoretical model—it is usually sound not to regard the difference as significant unless it is at least three or more times the s.u. For example, if a bond length is measured to be 1.560 Å with an s.u. of 0.007 Å, it is probably not significantly different from one measured to be 1.542 Å.

There are several known sources of systematic errors in even the more precise crystal structure analyses published to date. Most of these effects are under study in various laboratories and some of the most careful recent studies take them into account. They include:

- (1) Scattering factor curves (uncorrected for thermal motion) are normally assumed to be spherically symmetrical, which is clearly not correct for bonded atoms. Extensive studies (both theoretical and experimental) of this asymmetry, which is detectable only in the most precise work, are now under way.
- (2) The motions of some molecules in crystals are very complicated, and the usual ellipsoidal approximation for the motion of each atom may be a considerable oversimplification, especially if the motion is appreciable. Furthermore, in some crystals the corre-

lated motions of molecules in different unit cells—so-called “lattice vibrations”—may give rise to appreciable “thermal diffuse scattering” (e.g., streaks extending out from the usual Bragg diffraction peaks). Correction must be made for such effects in the most precise work.

- (3) Many errors that can in principle be eliminated—for example, those arising from absorption or instrumental effects—may not have been properly taken into account.
- (4) Sometimes the diffracted beam is rediffracted in the crystal when two planes are in a position to “reflect” simultaneously. This can give rise to significant errors in measurements of intensities.

Failure to correct for systematic errors may occur because the errors are regarded as minor and the corrections too complicated to be worthwhile, because an appropriate method of correction is not known, or because the source of error is overlooked. A critical reader will seek to discover what the author has done about known sources of systematic errors. Of course, it takes experience to assess the likely effects of having ignored some of them. Because of the ever-present possibility of systematic errors in even the most careful work, it is usually unwise to regard measured interatomic distances in crystals as more accurate than to the nearest 0.01 \AA , although the stated precision may be as low as 0.001 \AA . An exception is the now relatively unusual circumstance that the distance involves no parameters at all other than the unit-cell dimensions, for example, the Na^+ to Cl^- distance in NaCl or the C-C distance in diamond, each of which can be measured accurately to better than 0.001 \AA at any given temperature. However, even when an interatomic distance is known with high precision and apparent accuracy, it must always be remembered that it represents only the distance between the average positions of the atoms as they vibrate in the crystal. For substances such as rock salt, the root-mean-square amplitude of vibration of the atoms at room temperature is 0.08 \AA , and for organic molecules it is larger by a factor of two or three.

Summary

Since there are so many measured reflections (50 to 100 or more per atom in precise structure determinations), the “trial structure” parameters, representing atomic positions and extents of vibration, may be refined to obtain the best possible fit of observed and calculated structure factors.

Difference Fourier methods

Either electron-density or difference electron-density maps may be calculated, the latter being especially useful in the later stages of refinement. A peak in a difference map indicates too little scattering matter in the trial structure, a trough too much. For example, if a hydrogen

atom is left out of a trial structure, a peak will show where the atom must lie in the corrected trial structure. In general a model is adjusted appropriately to give as flat a final difference map as possible; this map should ideally be zero everywhere, but fluctuations will occur as a result of experimental uncertainties or inadequacies of the model used.

Least-squares/maximum likelihood methods

In any crystal structure analysis there are many more observations than parameters to be determined. The best parameters corresponding to some assumed model of the structure are found by minimizing the sum of the squares of the discrepancies between the observed values of $|F|$ (or $|F|^2$) and those calculated for an appropriate trial structure (or a partially refined version of it). Maximum likelihood methods are now increasingly used for structure refinement. These two methods of refinement have only been practicable for three-dimensional data since the advent of high-speed computers.

The correctness of a structure

All the following criteria should be applied:

- (1) The agreement of individual structure factor amplitudes with those calculated for the refined model should be consistent with the estimated precision of the experimental measurements of the observations.
- (2) A difference map, phased with final parameters for the refined structure, should reveal no fluctuations in electron density greater than those expected on the basis of the estimated precision of the electron density.
- (3) Any anomalies in molecular geometry or packing should be scrutinized with great care and regarded with some skepticism.

Structural parameters: Analysis of results

12

The results of an X-ray structure analysis are coordinates of the individual, chemically identified atoms in each unit cell, the space group (which gives equivalent positions), and displacement parameters that may be interpreted as indicative of molecular motion and/or disorder. Such data obtained from crystal structure analyses may be incorporated into a CIF or mmCIF (Crystallographic Information File or Macromolecular Crystallographic Information File). These ensure that the results of crystal structure analyses are usefully archived. There are many checks that the crystallographer can make to ensure that the CIF or mmCIF file is correctly informative. For example, the automated validation program PLATON (Spek, 2003) checks that all data reported are up to the standards required for publication by the International Union of Crystallography. It does geometrical calculations on the structure, illustrates the results, finds if any symmetry has been missed, investigates any twinning, and checks if the structure has already been reported. We now review the ways in which these atomic parameters can be used to obtain a three-dimensional vision of the entire crystal structure.

Calculation of molecular geometry

When molecules crystallize in an orthorhombic, tetragonal, or cubic unit cell it is reasonably easy to build a model using the unit-cell dimensions and fractional coordinates, because all the interaxial angles are 90° . However, the situation is more complicated if the unit cell contains oblique axes and it is often simpler to convert the fractional crystal coordinates to orthogonal coordinates before calculating molecular geometry. The equations for doing this for bond lengths, interbond angles, and torsion angles are presented in Appendix 12. If the reader wishes to compute interatomic distances directly, this is also possible if one knows the cell dimensions ($a, b, c, \alpha, \beta, \gamma$), the fractional atomic coordinates (x, y, z for each atom), and the space group. For example, the

square of the distance between two points (x_1, y_1, z_1) and (x_2, y_2, z_2) is

$$\begin{aligned}
 l^2 &= [(x_1 - x_2)a]^2 + [(y_1 - y_2)b]^2 + [(z_1 - z_2)c]^2 \\
 &\quad - [2ab \cos \gamma (x_1 - x_2)(y_1 - y_2)] - [2ac \cos \beta (x_1 - x_2)(z_1 - z_2)] \\
 &\quad - [2bc \cos \alpha (y_1 - y_2)(z_1 - z_2)] \\
 &= [\Delta x a]^2 + [\Delta y b]^2 + [\Delta z c]^2 - [2ab \cos \gamma \Delta x \Delta y] \\
 &\quad - [2ac \cos \beta \Delta x \Delta z] - [2bc \cos \alpha \Delta y \Delta z]
 \end{aligned} \tag{12.1}$$

where $\Delta x = x_1 - x_2$, and so forth. This provides an equation for calculating a bond length or other type of interatomic interaction. If the three distances between atoms A, B, and C, where $AB = l_1$, $AC = l_2$, $BC = l_3$, are known, then the angle $B-A-C = \delta$ may be calculated with the law of cosines,

$$\cos \delta = \frac{l_1^2 + l_2^2 - l_3^2}{2l_1 l_2} \tag{12.2}$$

These two equations [Eqns. (12.1) and (12.2)] are used for most of the preliminary information necessary for analyzing a crystal structure.

Some illustrations of results from some very simple crystal structure studies are shown in Figures 12.1–12.3. For example, sodium chloride, NaCl (Figure 12.1), crystallizes at room temperature in the space group $Fm\bar{3}m$, a face-centered cubic space group, and the unit-cell dimension is $a = 5.6402(2) \text{ \AA}$; the 2 in parentheses is a measure of the standard uncertainty in the last place quoted, so that it could be read as $a = 5.6402 \pm 0.0002 \text{ \AA}$. Since this crystal structure involves a sodium ion at the origin ($x = y = z = 0.0$) and a chloride ion at $1/2, 0, 0$, each ion is surrounded by six of the opposite type so that there is no significant buildup of charge (positive or negative) in the crystal. It can be readily calculated that the nearest distance between cations and anions is 2.82 \AA . Integration of the experimental electron densities of Na and Cl, assuming that the minimum of electron density between them defines the edge of each atom or ion, shows that they are ions rather than atoms (see Dunitz, 1996). Potassium chloride has a similar structure in a unit cell with $a = 6.2931(2) \text{ \AA}$ and therefore a $K^+ \dots Cl^-$ distance of 3.15 \AA . On the other hand, cesium chloride has a cubic unit cell with a cesium ion at the origin and a chloride ion in the center of the cell at $x = y = z = 1/2$ to give a primitive unit cell (*not a body-centered unit cell, because the atoms at the origin and the center of the unit cell are different*), so that the space group is primitive, $Pm\bar{3}m$. Since the unit-cell edge is $a = 4.120(2) \text{ \AA}$, the $Cs^+ \dots Cl^-$ distance is $4.120 \times (\sqrt{3})/2 = 3.57 \text{ \AA}$. Iron pyrite, FeS_2 (Figure 12.2), also crystallizes in a cubic unit cell, space group $Pa\bar{3}$, $a = 5.4175(5) \text{ \AA}$, with an iron atom at the origin and a sulfur atom at x, x, x , where $x = 0.39$. Iron atoms are shown in black in this figure, with Fe–S distances of 3.05 \AA . Sulfur atoms are speckled, and S–S bonds that are about 2.06 \AA in length are illustrated in this figure

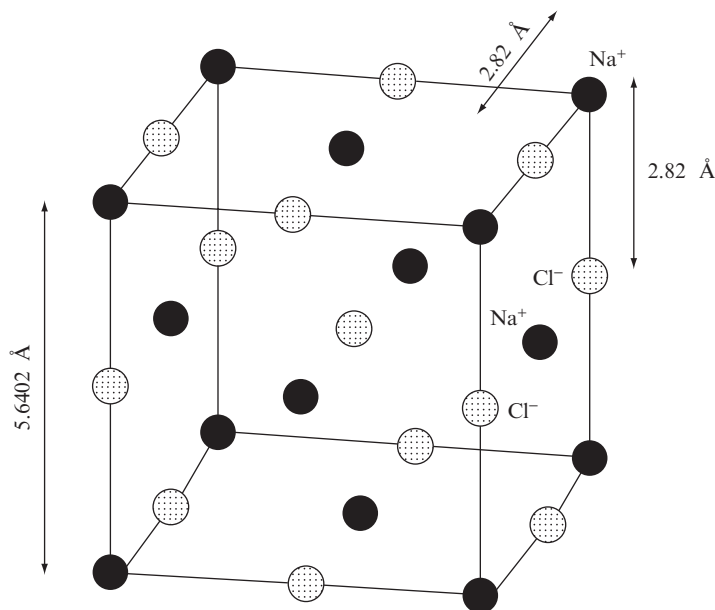


Fig. 12.1 Crystal structure of sodium chloride.

Sodium chloride (Na^+ black, Cl^- stippled circles) (Bragg, 1913).

4Na^+ at $0, 0, 0; 0, 1/2, 1/2; 1/2, 0, 1/2; 1/2, 1/2, 0$ and 4Cl^- at $1/2, 0, 0; 0, 1/2, 0; 0, 0, 1/2; 1/2, 1/2, 1/2$.

with black bonds. Diamond, shown in Figure 12.3, crystallizes in a cubic unit cell, $a = 3.5597 \text{ \AA}$, space group $Fd\bar{3}m$, with eight carbon atoms per unit cell (Bragg and Bragg, 1913). The crystal structure clearly show the tetrahedral surroundings of each carbon atom and the result is the hardest mineral known. The nearest neighbor to an atom at the origin is the atom at $x = y = z = 1/4$, so that the C–C distance is $3.5597 \times (\sqrt{3})/4 = 1.541 \text{ \AA}$, the C–C–C bond angle is 109.5° , and the C–C–C–C torsion angles are 60° or 180° depending on which carbon atom is chosen as the fourth (see equations in Appendix 12). Approximate atomic and ionic radii for many common ions in crystals have been derived from data such as these. There is always an element of arbitrariness in assigning radii, and no set is completely consistent, because ions are not “hard spheres,” their effective radii varying somewhat with environment. Some typical values, however, are: Na^+ , $0.95\text{--}1.17 \text{ \AA}$; K^+ , $1.33\text{--}1.49 \text{ \AA}$; Cl^- , $1.64\text{--}1.81 \text{ \AA}$; F^- , $1.16\text{--}1.36 \text{ \AA}$ (Frausto da Silva and Williams, 2001; Brown, 2006). A general analysis of ionic crystals was written by Linus Pauling in 1929, in which he showed how charged groups congregate in a crystal and aim to stay distant from hydrophobic groups (Pauling, 1929).

Of course, much more complicated structures than those illustrated in Figures 12.1–12.3 are now being studied, and the amount of information on bond lengths and the environments of various chemical groupings is escalating. Examples of historical interest include the phthalocyanines (Robertson, 1936), the boron hydrides (Lipscomb,

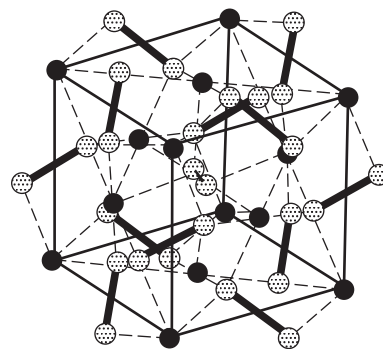


Fig. 12.2 Crystal structure of iron pyrite.

Iron pyrite (fool’s gold), FeS_2 (Fe black, S stippled). Space group $Pa\bar{3}$, unit-cell dimensions $a = 5.417 \text{ \AA}$ (Bragg, 1913).

4Fe at $0, 0, 0; 0, 1/2, 1/2; 1/2, 0, 1/2; 1/2, 1/2, 0$ (as Na^+ in NaCl); 8S at $\pm(x, x, x; 1/2 + x, 1/2 - x, -x; -x, 1/2 + x, 1/2 - x; 1/2 - x, -x, 1/2 + x; \text{where } x = 0.39)$.

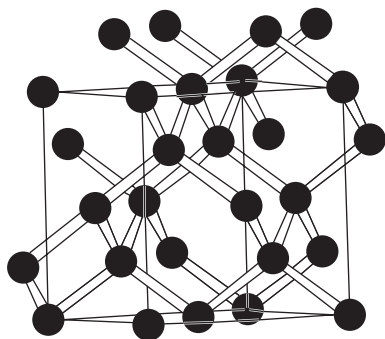


Fig. 12.3 Crystal structure of diamond.

The crystal structure of diamond, showing three-dimensional bonding throughout the crystal (Bragg and Bragg, 1913). This three-dimensional structure accounts for its hardness.

C at $0, 0, 0; 0, \frac{1}{2}, \frac{1}{2}; \frac{1}{2}, 0, \frac{1}{2}; \frac{1}{2}, \frac{1}{2}, 0; \frac{1}{4}, \frac{1}{4}, \frac{1}{4}; \frac{1}{4}, \frac{3}{4}, \frac{3}{4}; \frac{3}{4}, \frac{1}{4}, \frac{3}{4}; \frac{3}{4}, \frac{3}{4}, \frac{1}{4}$.

1954), vitamin B₁₂ (Hodgkin et al., 1957), myoglobin (Kendrew et al., 1960), hemoglobin (Perutz et al., 1968; Perutz, 1976), lysozyme (Phillips, 1966), and tobacco mosaic virus (Stubbs et al., 1977). Data on the results of X-ray and neutron diffraction studies on crystal structures of small and medium-sized molecules containing at least one carbon atom are available on the Cambridge Structural Database (CSD). This database is maintained by the Cambridge Crystallographic Data Centre in Cambridge, England, founded by Olga Kennard (Allen, 2002). Data files are also available on other types of crystal structures, including inorganic structures (the Inorganic Crystal Structure Database, ICSD) (Bergerhoff and Brown, 1987) and proteins (the RCSB Protein Data Bank) (Bernstein et al., 1977; Berman et al., 2003). A search of the World Wide Web will show the reader that there are many other crystallographic databases available and many computer-based methods of extracting structural information from them.

Molecular conformations

The torsion angles in a molecular structure are frequently of interest (see Appendix 12). These are a measure of the amount of twist about a bond and are defined, for a bonded series of four atoms (A–B–C–D), as the angle of rotation about a bond B–C needed to make the projection of the line B–A coincide with the projection of the line C–D, when viewed along the B–C direction. The positive sense is clockwise for this rotation. Thus the torsion angle is a representation of the structure viewed so that the atom C is completely obscured by atom B, as shown in Figure 12.4. A chain of methylene (–CH₂–) groups will generally have a staggered conformation so that torsion angles are 180° for C–C–C–C and 60° for C–C–C–H or H–C–C–H. The torsion angle is actually independent of the direction of view; that is, the A–B–C–D torsion angle equals the D–C–B–A torsion angle. However, for a pair of enantiomers (mirror images) the torsion angles of equivalent sets of

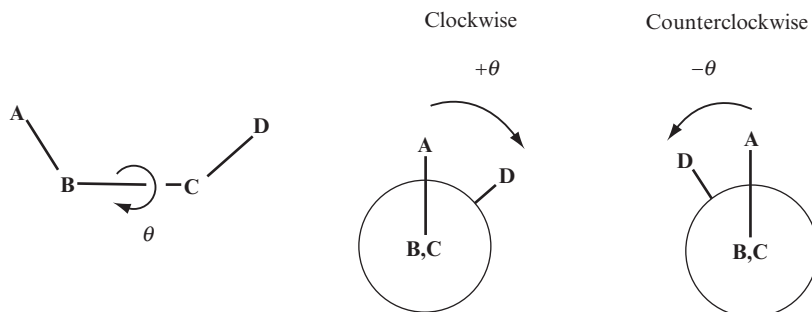


Fig. 12.4 Torsion angles.

Torsion angles measure the amount of twist about a chemical bond. For four bonded atoms A–B–C–D, the torsion angle about the central B–C bond is the extent to which the A–B bond has to be rotated clockwise so that it will eclipse the C–D bond.

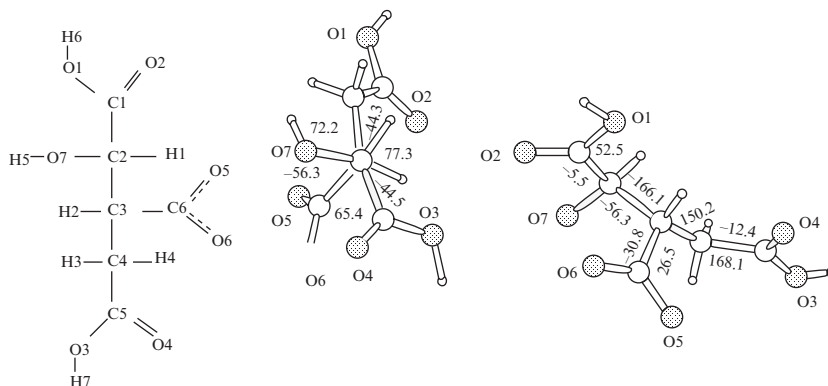


Fig. 12.5 Torsion angles in the isocitrate ion.

The isocitrate ion (see Figure 10.6b), showing some relevant torsion angles.

atoms have opposite signs (Figure 12.4, compare the two diagrams on the right of this Figure). An example of torsion angles in a structure is shown in Figure 12.5. Many studies of molecular structures involve lists of torsion angles because these angles can indicate similarities (or significant variations) in conformation (for example in sugars and in steroids). Another very useful calculation is that of the *least-squares plane* through a group of atoms in a molecule. Such planes can be used points of reference in describing the rest of the molecule, particularly when the shapes of molecules are being compared.

Intermolecular interactions

If one wishes to determine intermolecular distances (that is, distances between atoms in different molecules), then space-group symmetry information aids the calculations. The results are particularly useful for investigating the presence of hydrogen bonds and also for checking whether two molecules are unusually close to each other (an indication either of an unexpected intermolecular interaction or of an incorrect structure). For example, if the compound crystallizes in the space group $P2_12_12_1$, then, by use of Eqn. (12.1) and the information in Figure 7.6, the distance may be calculated, for example, between one atom at x_1, y_1, z_1 and another at $\frac{1}{2} - x_2, 1 - y_2, \frac{1}{2} + z_2$ (where x_1, y_1, z_1 and x_2, y_2, z_2 are the coordinates of two atoms in one molecule). Systematic calculations of distances and angles are now done almost entirely by computer programs, which search for all distances (intramolecular and intermolecular) within a selected range (in Å) around each atom in a chosen molecule. Analysis of intermolecular packing has, in several instances, led to an improved understanding of molecular interactions (see, for example, Bürgi et al., 1973; Kitaigorodsky, 1973; Rosenfield, 1977; Brown, 1988).

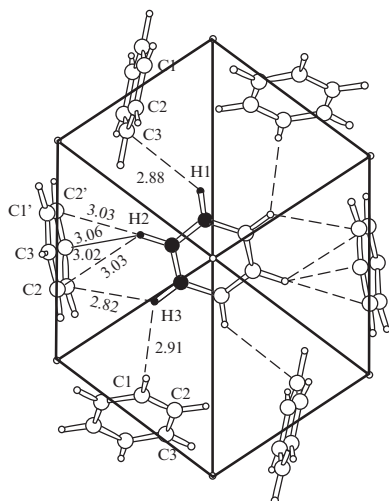


Fig. 12.6 Crystal structure of benzene.

Benzene, space group $Pbca$, $a = 7.44$, $b = 9.55$, $c = 6.92$ Å. Atoms at $\pm\{x, y, z; 1/2 + x, 1/2 - y, -z; -x, 1/2 + y, 1/2 - z; 1/2 - x, -y, 1/2 + z\}$

| Atom | x | y | z |
|------|---------|---------|---------|
| C(1) | -0.0569 | 0.1387 | -0.0054 |
| C(2) | -0.1335 | 0.0460 | 0.1264 |
| C(3) | -0.0774 | -0.0925 | 0.1295 |
| H(1) | -0.0976 | 0.2447 | -0.0177 |
| H(2) | -0.2409 | 0.0794 | 0.2218 |
| H(3) | -0.1371 | -0.1631 | 0.2312 |

The asymmetric unit is indicated by black atoms (Cox and Smith, 1954; Bacon et al., 1964).

* Dunitz (1996) has an extensive discussion of calculations of standard uncertainties of derived quantities, including the need for taking correlations between different parameters into account.

** The name "temperature factor" has persisted to denote the constants in the exponential factors in Eqns. (12.3) and (12.4), despite the fact that it has long been recognized that vibrations persist at low temperatures, and that a static disorder may simulate a dynamic one if studies are made only at a single temperature. We use "displacement factor" here in recognition of this problem, that is, that the factor may represent thermal motion and/or disorder of the atom involved (Trueblood et al., 1996).

Benzene, for example, has been studied in the crystalline state at -3°C and by neutron diffraction at -55°C , -135°C , -150°C , and -258°C (because it is a liquid at room temperature) (Cox and Smith, 1954; Bacon et al., 1964; Jeffrey et al., 1987). The last two neutron studies were done on deuterobenzene, C_6D_6 . The structure is illustrated in Figure 12.6. The crystals are orthorhombic, space group $Pbca$, with cell dimensions $a = 7.44$, $b = 9.55$, and $c = 6.92$ Å, and with half of a molecule (in black) in the asymmetric unit. Atomic coordinates are listed in the caption to this figure, which shows the molecular packing. The average C-C bond is 1.390 Å and the average C-H bonds are 1.07 Å in length. As shown in the figure, one hydrogen atom of one molecule points toward the π -electron system of the aromatic ring of a neighboring molecule. This kind of C-H... π -electron interaction occurs in many crystal structures of aromatic compounds.

Precision

All the quantities listed in a structure analysis (bond lengths, inter-bond angles, torsion angles, and least-squares planes) have errors that result from experimental errors in the diffraction measurements (see Chapter 4). Furthermore, the atomic scattering model used is not an exact representation of the electron density, merely the sum of ellipsoidal electron densities around each atomic nucleus. Estimates of errors, including those of unit-cell dimensions, may be made from least-squares refinements of the appropriate data, and their values can be used to assess the standard uncertainties in bond lengths, bond angles, and torsion angles. Unsuspected systematic errors may also be present.

As pointed out in Chapter 11, it is always necessary to quote a standard uncertainty with any computed geometrical quantity.* The standard uncertainty of a bond length is a function both of the precision in measurement of $|F(hkl)|$ values (expressed in the R value) and of the relative atomic numbers of the various atoms in the structure. For example, the standard uncertainty of a C-C bond in a structure containing only carbon and hydrogen atoms may be 0.002 Å for an R value of 0.05 , but can increase to 0.02 Å or more for a structure with $R = 0.05$ that contains a heavy atom.

Atomic and molecular motion and disorder

The extent of atomic motion from vibration and/or disorder of each atom in a structure can also be measured.** However, before deriving their values it is important that absorption and other factors that affect the intensity distribution be taken into account; otherwise the parameters will not be a true representation of atomic motion or disorder.

The effect of the vibration of atoms in crystals on the scattering of X rays by these atoms has been discussed in Figure 5.4 and the

accompanying text. The simplest assumption that can be made is that the motion of each atom is the same in all directions; that is, that the motion is isotropic. The decrease of scattering intensity that results from this motion then depends only on the scattering angle and not on the particular orientation of the crystal with respect to the incident X-ray beam. As indicated in Figure 5.4c, such isotropic motion causes an exponential decrease of the effective atomic scattering factors as the scattering angle, 2θ , increases. The scattering factor for an atom at rest, f , is replaced by

$$f e^{-B_{\text{iso}}(\sin^2 \theta)/\lambda^2} \quad (12.3)$$

B_{iso} is related to the average of the square of the amplitude of vibration, $\langle u^2 \rangle$, by $B_{\text{iso}} = 8\pi^2 \langle u^2 \rangle \cong 79 \langle u^2 \rangle$. For a typical B value of around 4 \AA^2 (for an atom in an organic molecule at room temperature), this means that $\langle u^2 \rangle$ is about 0.05 \AA^2 , and the root-mean-square vibration amplitude, $\langle u^2 \rangle^{1/2}$, is then around 0.22 \AA . At liquid nitrogen temperatures (near 100 K), B values are typically reduced by a factor of 2 or 3 from those at room temperature, and the root-mean-square amplitude will then be of the order of 0.15 \AA . Atomic displacement parameters can be used to establish atomic type if the chemical formula of the compound under study is not known. This was true for the azidopurine that was used to demonstrate resolution in Figure 6.6 (Glusker et al., 1968). When the structure was refined with all atoms as carbon atoms it was found that the atomic displacement factors were lower for the nitrogen atoms, so that the chemical formula was thereby established.

However, it is clear that the approximation of isotropic motion is a poor one for atoms in most crystals, because the environments of these atoms are far from isotropic. The increasing availability of high-speed computers during the last three decades has made it worthwhile to attempt to collect precise intensity data and to analyze these data for relatively subtle effects, such as more complicated patterns of atomic and molecular motion. The next simplest approximation after isotropic motion is to assume that the motion is ellipsoidal—that is, that it can be described by the six parameters of a general ellipsoid rather than the single parameter characteristic of a sphere. These six parameters define the lengths of three mutually perpendicular axes describing the amount of motion in these directions, and the orientation of these ellipsoidal axes relative to the crystal axes. Figure 12.7 illustrates this representation of atomic motion in a portion of the structure of sodium dihydrogen citrate. This diagram was drawn with the computer program ORTEP (Johnson, 1965), which automatically generates stereoscopic images of molecules and represents the molecular motion by ellipsoids. These “thermal ellipsoids,” calculated from the atomic displacement factors, show the amount that an atom is displaced in a given direction (indicated by the shape of the ellipsoid, a cigar shape indicating much motion or displacement). The ellipsoid also indicates the direction of maximum motion. The plot of ellipsoids is made at a

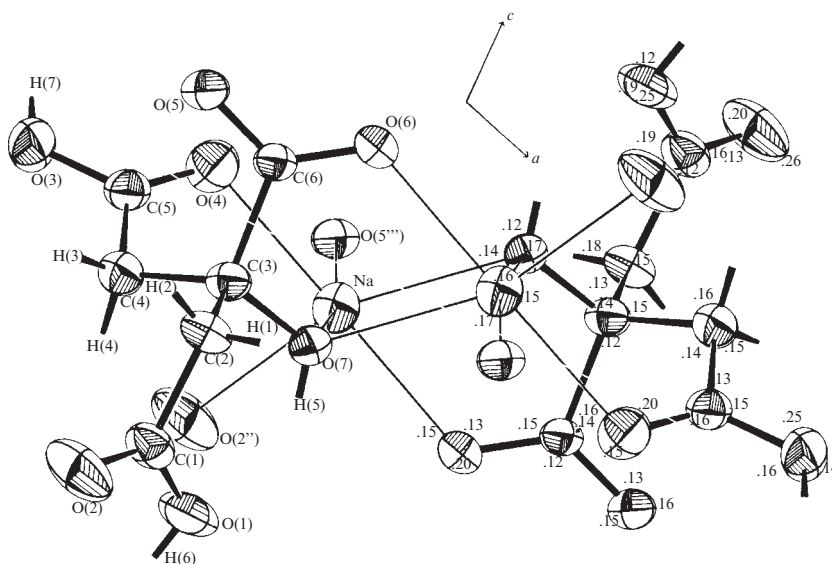


Fig. 12.7 Anisotropic molecular motion.

The anisotropic motion of atoms is usually described by “thermal ellipsoids,” as in this example, taken from a study of the structure of sodium dihydrogen citrate and drawn with the program ORTEP (Johnson, 1965). Two complete dihydrogen citrate ions and two sodium ions are shown, grouped around a center of symmetry in the middle of the figure. Two atoms [O(5) and O(2)] of each of two other dihydrogen citrate ions are also shown. In order to simplify the figure, hydrogen atoms are not drawn, but their positions are labeled and the bonds to them are displayed. The thick lines represent covalent bonds; the thin ones denote coordination interactions of oxygen atoms with the sodium ion. The “thermal motion ellipsoids,” calculated from the displacement factors, are drawn at 67% of the probability density function for each atom. The three numbers near each of the ellipsoids in the right half of the drawing indicate the root-mean-square displacements (Å) along the three principal axes of that ellipsoid. The anisotropy of the motion is very evident for some of the atoms, especially for those at the ends of the ion; for these peripheral atoms, the motion is always greatest in directions perpendicular to the bonding direction. This result is just what one would expect, and thus is evidence for the reality of this interpretation of the diffraction data. (From Glusker et al. (1965), p. 564, Figure 2.)

selected percentage of the probability density function for the electron density of each atom, that is, the probability of finding an electron in a defined volume of the crystal. It is noteworthy that both the degree of anisotropy and the extent of atomic motion itself vary in different parts of the citrate ion, being greatest for some of the peripheral atoms, such as O(2).

The usual way of taking this kind of ellipsoidal motion into account in the structure factor equations is by means of an anisotropic exponential factor analogous to that in Eqn. (12.3), with six anisotropic vibration parameters, b^{ij} (with superscripts in their labels), as multipliers of the indices for each reflection hkl in the exponent, thus:

$$e^{-(b^{11}h^2+b^{22}k^2+b^{33}l^2+b^{12}hk+b^{23}kl+b^{31}hl)} \quad (12.4)$$

Increasingly, anisotropic vibration parameters are reported as components of a symmetric tensor, U , rather than as b values, because the latter are dimensionless and their magnitudes cannot be related to vibration amplitudes without taking the cell dimensions into account.

The relation between the U^{ij} and b^{ij} values is simple:

$$U^{ii} = b^{ii}/2\pi^2 a_i^{*2}, \quad U^{ij} = b^{ij}/4\pi^2 a_i^* a_j^* \quad (i \neq j) \quad (12.5)$$

The mean square vibration amplitude in any direction, specified by the cosines l of the angles this direction makes with reciprocal axes, is given by

$$\langle u^2 \rangle = U^{11}l_1^2 + U^{22}l_2^2 + U^{33}l_3^2 + 2U^{12}l_1l_2 + 2U^{23}l_2l_3 + 2U^{31}l_3l_1 \quad (12.6)$$

The anisotropic vibration parameters b^{ij} or U^{ij} differ from atom to atom in a structure. The effect of temperature is illustrated in the ellipsoids in Figure 12.8. At the lower temperature, the atoms fill less space.

This ellipsoidal description of atomic motion is a convenient one for computation, unlike more complex models that may be more realistic physically, and it has proved adequate for most structure analyses to date. It is, however, clear that the motions of atoms in crystals may frequently be more complicated; for example, the atoms may move along arcs rather than straight lines, or under the influence of an anharmonic potential function that is steeper on one side of the equilibrium position than on the other. Analysis of such motion requires the best possible data and more complete equations describing the motion (Johnson, 1969). One needs to beware of possible problems; for example, appreciable uncorrected absorption errors in a crystal of irregular shape may be compensated for by spurious anisotropy of motion of some atoms in the structure. However, by suitable choice of radiation and crystal size and shape, such absorption errors can be minimized or corrected for, and the reality of derived anisotropies of atomic motion in many structures has been firmly established.

Rigid-body motion

Some molecules may be regarded as nearly rigid bodies, which implies that when they move the relative positions of all atoms (and consequently all interatomic distances) remain constant. The motion may thus be considered to be motion of the molecule as a whole. This is clearly only an approximation, because there are always "internal" vibrations—motion of an atom in the molecule relative to its neighbors—but in many crystals the overall motion of the molecules (or ions) is far greater than the internal vibrations. Analysis of the individual anisotropic thermal parameters of molecules in crystals sometimes reveals striking patterns of molecular motion, which can frequently be correlated with the shape of the molecule and the nature of its surroundings in the crystal. The molecular motion may, in general, be described in terms of three components: a translational motion (vibration along a straight-line path), a librational motion (vibration along an arc), and a combination of translation and libration that may be regarded as vibration along a helical path (Schomaker and Trueblood, 1968; Dunitz et al., 1988). Libration is shown in Figure 12.9.

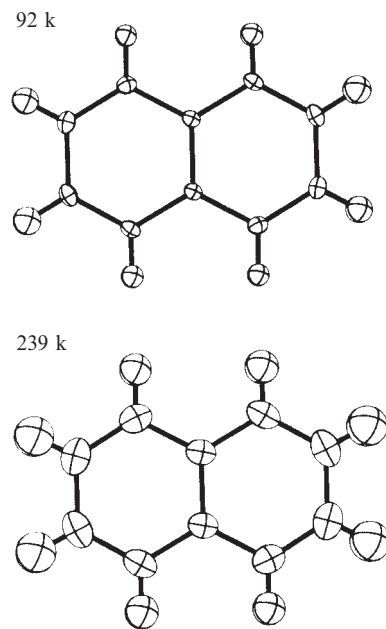


Fig. 12.8 Root-mean-square displacements at two different temperatures.

Two views of naphthalene, measured with X rays at 92 K (upper diagram) and 239 K (lower diagram). Note the smaller root-mean-square displacements of the atoms at the lower temperature.

(From Brock and Dunitz (1982). Photograph courtesy C. P. Brock and J. D. Dunitz).

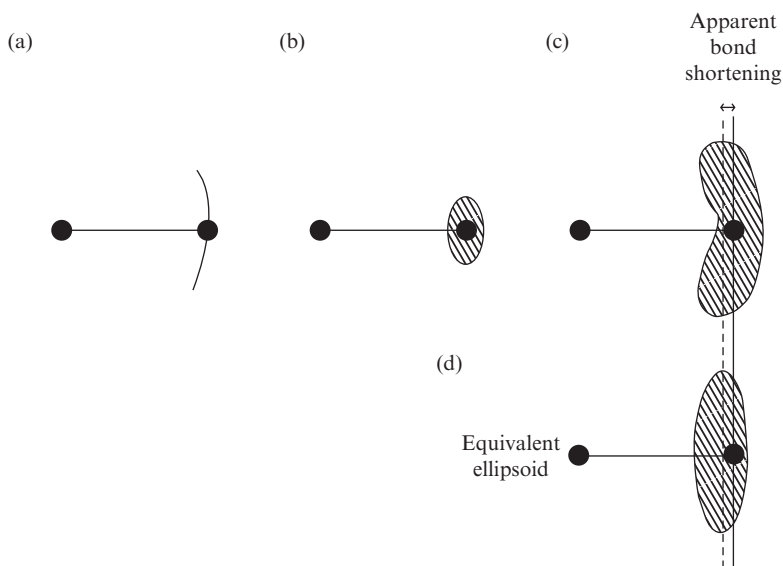


Fig. 12.9 Libration.

Libration causes apparent but not real bond shortening. The movement of the librating atom takes the form of an arc. This is, however, introduced into the structure as an ellipsoid with the result that the bond appears to be shorter, as shown.

Some molecules that are not completely rigid may be composed of segments that are themselves rigid, coupled together in a nonrigid way—for example, molecules such as biphenyl and its derivatives, with appreciable torsional oscillation about the inter-ring bond, or torsional oscillation of the methyl groups in durene (1,2,4,5-tetramethylbenzene). Methods have been developed for analysis of internal torsional motion and similar motions in many molecules, and it has been possible to obtain, from diffraction data, rough estimates of force constants for and barriers to such motions. Since bond-stretching vibrations are small, it was noted by Fred Hirshfeld that a bond length should not change much even if the two atoms composing it are vibrating. This means that the two atoms should move in synchrony along the direction of the bond, but not necessarily in other directions (Hirshfeld, 1976); the anisotropic displacement factors should reflect this condition. This is shown (especially at the higher temperature) in Figure 12.8.

One important consequence of librational motion is that *intra* molecular distances appear to be somewhat foreshortened, especially for distances that are perpendicular to axes about which there is appreciable librational motion. This is shown in Figure 12.9. Approximate corrections to intramolecular distances are not hard to make if the pattern of motion is known, but with molecules that are not rigid, the corrections are not themselves precise, and consequently the corrected distances cannot be. This is an example of a systematic error that can make the accuracy of a derived result considerably poorer than

would be implied by a statistical analysis based on the assumption that only random errors were present. Only wide limits can usually be put on *intermolecular* distances if there is appreciable molecular motion, because the correlation (if any) of the motion of one molecule with that of its neighbors is unknown.

Neutron diffraction

In many ways neutron and X-ray diffraction complement each other, since they involve different phenomena. Neutrons are scattered by nuclei (or any unpaired electrons present, the magnetic moment of the electron interacting with that of the neutron). Although there have been a few studies of the distribution of unpaired electrons (e.g., in certain orbitals of selected transition metal ions), such applications have been rare, and in most crystal diffraction studies with neutrons, all electrons are paired and the scattering of the neutrons is essentially by the nuclei present. X rays, on the other hand, are scattered almost entirely by the electrons in atoms. Hence, if the center of gravity of the electron distribution in an atom does not coincide with the position of the nucleus, atomic positions determined by the two methods will differ. Such differences are particularly noticeable for the positions of hydrogen atoms, unless X-ray data have been collected to an usually high angle corresponding to a $\sin \theta/\lambda$ of near 1.2, nearly twice as great as usual (and thus corresponding to nearly eight times as many data, if all reflections are collected). One disadvantage of neutron diffraction is that larger crystals are needed than for X-ray structure analysis in order to get sufficient diffraction intensity with the neutron flux available from the present reactors. In order to collect data on myoglobin, a crystal with minimum dimensions of 2 mm was needed. One advantage of neutrons is that they do not cause as much radiation damage as do X rays.

The amount of scattering by nuclei does not vary much (or in any regular way) with atomic number. This fact may be used to clear up some ambiguities in an X-ray study. Typical scattering-factor data for X rays and neutrons are listed in Appendix 5. Hydrogen has a negative[†] scattering factor for neutrons (as shown in Figure 12.10 and Appendix 5) while deuterium has a positive one, both quite high, so that these two isotopes may readily be distinguished; as far as X rays are concerned, they are identical (Peterson and Levy, 1952). Neutron diffraction can thus be useful in studying the structures of reaction products that have been labeled with deuterium. It is also possible with neutrons to distinguish atoms with nearly the same atomic number that cannot readily be distinguished with X rays (for example, Fe, Co, and Ni), because their scattering power for neutrons may be very different. Atomic positions for hydrogen or deuterium may be determined as accurately as those for uranium and many other heavy atoms. This is a particularly important advantage of neutron diffraction

[†] If a nucleus has a negative scattering factor, the radiation scattered by that nucleus differs in phase by 180° ($\cos 180^\circ = -1$) from the radiation that would be scattered from a nucleus that has a positive scattering factor and is situated at the same position.

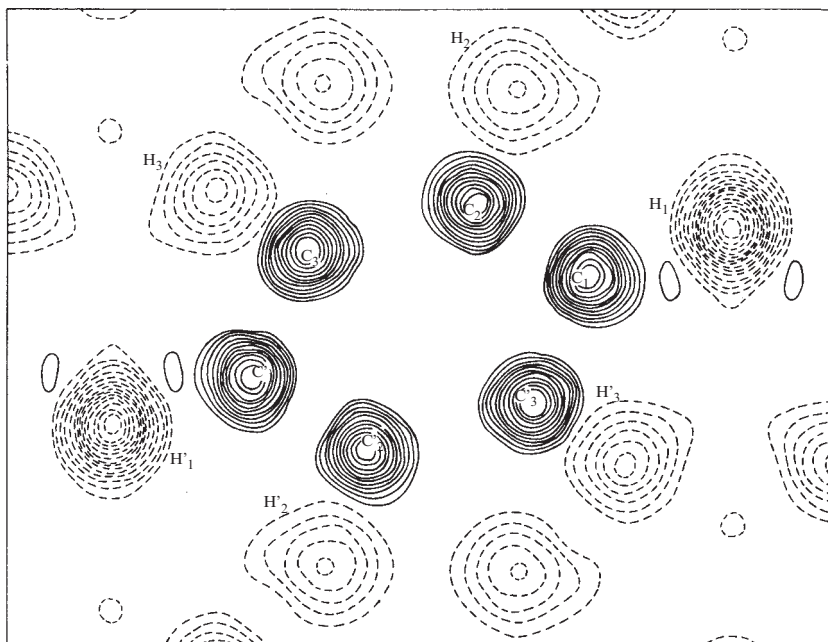


Fig. 12.10 Projection of the neutron scattering density for crystalline benzene.

Positive density (mainly at carbon atom positions) is indicated by full lines; negative density (mainly at hydrogen atom positions) by broken lines. The unlabeled hydrogen atoms are parts of other benzene molecules. The ring plane is not perpendicular to the direction of the projection; thus the ring does not appear as a regular hexagon. The deeper trough at H_1 and H_1' results from the fact that there are two hydrogen atoms superimposed on each other at these positions in this projection.

(Figure courtesy of Dr. G. E. Bacon.)

studies. There may also be anomalous scattering with neutrons, as with X rays. Since nuclei are extremely small relative to the usual neutron wavelengths, which are about 1 \AA , the intensity of neutrons scattered from a stationary nucleus would not decrease markedly at high angles, as it would for X rays. Atomic vibrations, even at low temperature, will, however, cause a decrease of intensity at high angles, as with X rays (Figure 5.4).

The combined use of neutron and X-ray diffraction to solve a biochemical problem is illustrated by the analysis of the structure of lithium glycolate (Johnson et al., 1965). Deuterated glycolic acid, HO-CHD-COOH , was prepared biochemically and the structure of the lithium salt determined by X-ray diffraction methods. Since hydrogen and deuterium have the same atomic number they were each located but could not be distinguished by this X-ray method. Crystals of the lithium salt were prepared using lithium hydroxide enriched with the isotope of atomic weight 6. It was then possible to determine the absolute configuration of the lithium salt by neutron diffraction because the scattering amplitude of ${}^6\text{Li}$ is anomalous to neutrons ($0.18 + 0.025i \times 10^{-12} \text{ cm}$) and the scattering amplitudes of hydrogen and deuterium (-0.378 and $+0.65 \times 10^{-12} \text{ cm}$, respectively) are so

different. This then identified which hydrogen in the molecule was H and which was D and also established the absolute configuration of this glycolate stereoisomer that is acted on by the enzyme lactate dehydrogenase.

Studies of proteins can yield a wealth of structural information because deuterium and hydrogen can be distinguished, and therefore the ionization state of the functional groups in a protein can be found. If the conditions, such as the pH of the crystallization medium, are changed, then the effect of the change on these ionization states will be helpful in understanding how an enzyme accommodates to substrate or inhibitor binding and how hydrogen atoms move throughout the active site. For example, a lysine group may have two or three hydrogen atoms attached to its terminal nitrogen atom; both situations have been seen in neutron studies of the enzyme xylose isomerase (Katz et al., 2006).

Deformation density and difference density studies

The disposition of the electron density in a molecule is of particular interest to chemists since it provides information on what keeps the atoms together in a molecule. The valence-electron scattering of X rays is mainly concentrated in Bragg reflections with low $\sin \theta/\lambda$ values. In order to view the valence-electron density by means of difference electron-density maps, it is necessary to obtain precise and unbiased positional and temperature parameters; this requires high-order data, for which the spherical-atom approximation is more closely valid. When diffraction data are measured to the maximum scattering angles for shorter-wavelength X rays, such as MoK α radiation ($\lambda = 0.7107 \text{ \AA}$) or, even better, AgK α radiation ($\lambda = 0.5609 \text{ \AA}$), and especially when measurements are made at low temperatures, a large number of experimental data result and the structure perceived in the X-ray experiment—that is, the electron density—is seen at much higher resolution; atoms are therefore located with very high precision.

Some information on the detailed electron distribution in molecules may be obtained by high-resolution X-ray diffraction studies, particularly if the results are combined with neutron diffraction studies. It is possible to look at bonding effects that occur when atoms combine to form molecules. For example, a “deformation density” map may be obtained by calculating the difference electron density between the experimental map and that calculated from the “promolecule” electron density obtained from a model consisting of spherical atoms. This and the other maps described here are affected by the precision of the data used to obtain them and the correctness of the proposed structures. Superpositions that involve computing either an “X – X” map (a difference map using atomic positions from an analysis of only the

high-order X-ray diffraction data) or an “X – N” map (a difference map using atomic positions from a neutron diffraction analysis, and hence atomic nuclear positions) are used to examine the differences between the map from experimental data and that from the promolecule. There are some differences in results from X-ray and neutron studies, and therefore the same displacement parameters (generally from the neutron structure) are used with both the X-ray and neutron atomic coordinates. It has already been pointed out that X-ray diffraction studies give information on the electron density throughout the crystal while neutron diffraction studies give information on atomic nuclei. Therefore the difference between the two maps obtained will contain peaks in positions expected for bonding electrons and for lone pairs of electrons. For several molecules that have been studied (e.g., oxalic acid), quite good agreement exists between the experimental deformation density and a theoretical one, provided the latter model is sufficiently sophisticated [i.e., an extended basis set is used in the theoretical calculation (Pople, 1999)]. For example, the centroid of the electron density of a hydrogen atom is displaced from the nucleus (defined by neutron data) toward the atom it is linked to, as expected for chemical bonding. The future of this area of analysis is bright (Coppens, 1997; Dittrich et al., 2007).

Summary

Molecular geometry

This may be computed from the unit-cell dimensions and symmetry and the values of x , y , and z for each atom that have been derived from electron-density maps or by least-squares methods. Bond lengths, interbond angles, torsion angles, least-squares planes through groups of atoms, and the angles between such planes give much useful chemical information. It is common for crystal structures to be displayed in publications as stereopairs.†

† Such stereodiagrams can be viewed with stereoglasses or the reader can focus on the two images until an image between them begins to form. The reader should allow his/her eyes to relax until the central image becomes three-dimensional. This process requires patience and may take 10 seconds or more.

Atomic and molecular motion and disorder

The fall-off in intensity with increasing scattering angle becomes more pronounced with increasing vibrations of atoms. Atomic vibration itself becomes greater as the temperature of the specimen rises. For spherically symmetrical motion, the reduction in intensity is simply represented by an exponential, $e^{-2B_{\text{iso}}[(\sin^2 \theta)/\lambda^2]}$. Thermal motion is frequently represented by more sophisticated models, such as an ellipsoid. Atomic disorder can also provide intensity fall-off. With both atomic vibration and disorder the effective size of the atom, which is an average of all such atoms in the crystal, appears to be increased in volume while keeping the same number of electrons within that volume.

Neutron diffraction

Neutrons are scattered by atomic nuclei or by unpaired electrons; X rays are scattered significantly only by the electrons in atoms. Scattering factors for neutrons do not vary systematically with atomic number or atomic weight. Neutron diffraction studies can often clear up ambiguities in X-ray work, and, when the two methods are compared, may give information on the electron distribution that is due to chemical bonding in the molecule. Neutron diffraction is used in protein structural studies, often after an enzyme has been soaked in D_2O in order to insert deuterium in the place of labile hydrogen atoms. The deuterium atoms can be located in the protein electron-density map and therefore it is possible to determine how many (and the percentage of each) H or D atoms are on the oxygen, nitrogen, or sulfur atoms of side chains; this means that neutron crystallography provides a probe of the location of an H or D atom in a hydrogen bond and hence the local pH in a protein (for example, distinguishing $-NH_2$ from $-NH_3^+$).

13

Micro- and noncrystalline materials

The crystalline state is characterized by a high degree of internal order. There are two types of order that we will discuss here. One is *chemical order*, which consists of the connectivity (bond lengths and bond angles) and stoichiometry in organic and many inorganic molecules, or just stoichiometry in minerals, metals, and other such materials. Some degree of chemical ordering exists for any molecule consisting of more than one atom, and the molecular structure of chemically simple gas molecules can be determined by gaseous electron diffraction or by high-resolution infrared spectroscopy. The second type of order to be discussed is *geometrical order*, which is the regular arrangement of entities in space such as in cubes, cylinders, coiled coils, and many other arrangements. For a compound to be crystalline it is necessary for the geometrical order of the individual entities (which must each have the same overall conformation) to extend *indefinitely* (that is, apparently infinitely) in three dimensions such that a three-dimensional repeat unit can be defined from diffraction data. Single crystals of quartz, diamond, silicon, or potassium dihydrogen phosphate can be grown to be as large as six or more inches across. Imagine how many atoms or ions must be identically arranged to create such macroscopic perfection!

Sometimes, however, this geometrical order does not extend very far, and microarrays of molecules or ions, while themselves ordered, are disordered with respect to each other on a macroscopic scale. In such a case the three-dimensional order does not extend far enough to give a sharp diffraction pattern. The crystal quality is then described as “poor” or the crystal is considered to be *microcrystalline*, as in the naturally occurring clay minerals.

On the other hand, in certain solid materials the spatial extent of geometrical order may be less than three-dimensional, and this reduced order gives rise to interesting properties. For example, the geometrical order may exist only in two dimensions; this is the case for mica and graphite, which consist of planar structures with much weaker forces between the layers so that cleavage and slippage are readily observed. In a similar way, certain biological structures such as membranes and

micelles have less than three-dimensional order. Sometimes, however, geometrical order can be increased by external forces. For example, “liquid crystals” can be *temporarily* aligned in three dimensions by externally applied electric or magnetic fields (hence their use in liquid crystal displays in watches, computers, and other instruments). Even less geometrical order is shown by fibers such as silk, hair, and some long-chain polymers that have essentially only one-dimensional order.

Many times there is no evident geometric order beyond the immediate near-neighbor environment of the fundamental building unit. This is characteristic of liquids, glasses, and rubbers, whose spherically symmetrical diffraction patterns indicate that in no direction in space is there geometric order extensive enough to define a period. Such materials are described as *amorphous* and the only regularities seen in the diffraction pattern are those due to recurring bond distances. Thus diffraction patterns from amorphous materials provide information about interatomic distances only when a particular distance stands out from the average of all—usually because it is heavily weighted either by frequent occurrence or by involvement of atoms with scattering factors that are large relative to those of the other atoms present, but occasionally simply because it is unique, with no other distances of comparable magnitude occurring in the sample.

Liquid diffraction

Careful diffraction studies of liquids have provided much valuable structural information on time-averaged interatomic distances; these are spherically symmetrical in space and therefore are generally represented by radial distribution functions, that is, radially averaged electron-density maps. Examples, calculated from the diffraction patterns of water at various temperatures, are shown in Figure 13.1. These show the expected interatomic distances (O–H, O...O, and H...O) and the effects of neighboring molecules, which change as the temperature is raised.

Glass diffraction

Traditional glass, used throughout history to construct containers, windows, and ornaments, is made by fusion of a mixture of lime, silica, and soda and subsequent blowing or pressing of the product into the desired shape. Such glass is, of course, solid at ordinary temperatures. Glass stemware made from it is often referred to as “crystal” in spite of the fact that it is not crystalline. Its diffraction pattern has a halo-like appearance, resembling the diffraction pattern of a liquid; this demonstrates clearly that it is not crystalline and that there is

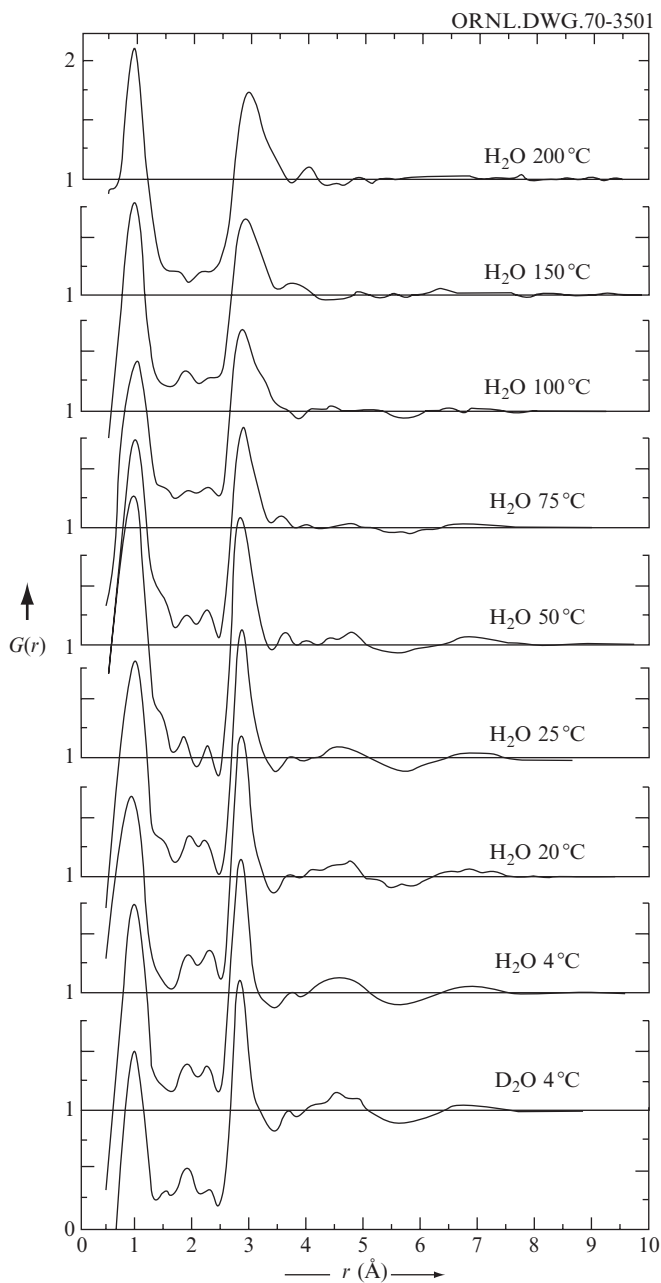


Fig. 13.1 Radial distribution functions.

Radial distribution curves obtained by X-ray diffraction studies on liquid water at temperatures from 4° C to 200° C are shown. Sample pressures were atmospheric up to 100° C; above 100° C, the pressure was equal to the vapor pressure. The vertical coordinate, $G(r)$, for the curves represents a normalized radial distribution function; that is, it gives information on the number of neighbor atoms or molecules at a distance r from an average atom or molecule in the system compared with that expected for a liquid without distinct structure.

no well-defined geometrical order within it. The best model to date of such glass consists of random chains, nets, and three-dimensional arrays of SiO_4 tetrahedra, linked together through oxygen atoms, with appropriately situated cations. Many attempts have been made to fit models with different kinds of short-range order to the observed diffraction patterns and to other quantitative physical and chemical data available on various glasses. This is done in an effort to define more precisely what might be meant by “the structure of glass” (Warren, 1940; Tanaka et al., 1985).

In contrast to the traditional glasses that are the products of fusion and can be “thawed” and reworked without crystallizing, there are now known to be many other glass-forming composition systems and, as a result, there are several ways of generating glasses and other amorphous materials. Each of these gives rise to properties that are useful. For example, amorphous metal films can be made by “splat cooling”—that is, a jet of liquid metal is directed onto a cold surface and therefore is cooled to a solid so rapidly from the melt that it has been deprived of the time required for crystal organization. Another industrial example is provided by the use of a chemical reaction in the gas phase to generate an extremely fluffy amorphous “soot” that may be sintered and compressed to three-dimensional solidity without crystallizing. Optical-waveguide–laser communication technology depends in large measure on the purity, composition control, and perfection of such processes, achievable by starting with pure gases, such as silicon tetrafluoride and oxygen, and reacting them to form a condensed phase of pure silica “soot” where, presumably, the surface is both highly energetic and unique such that particles “join” under pressure without melting (sintering) to form a continuum; such sintering without melting precludes the possibility of any crystallization. A third example is provided by glass-ceramics, which, although noncrystalline as formed, cannot be heated to the softening point because they undergo crystallization from the solid state; this crystallization must be controlled carefully in order to obtain a glass-ceramic with the desired physical properties.

The peak near 1 \AA represents the intramolecular O–H interaction and that at 2.9 \AA represents hydrogen-bonding interactions between oxygen atoms of neighboring water molecules. A sequence of broad peaks follows, notably those near 4.5 \AA and 7 \AA , and they may be attributed to preferred distances of separation for second and higher coordination shells. At distances large compared with atomic dimensions, and also with increasing temperature, the values of $G(r)$ merge to unity—that is, to the value for a structureless liquid.

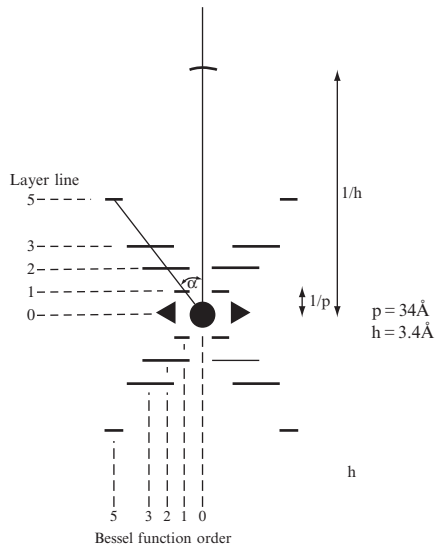
In liquid water the average coordination in the first shell represents about 4.4 molecules (independent of temperature), compared with exactly 4 molecules in ice, in support of the idea that the increase in density when ice melts is due to a small increase in the average coordination number in the first coordination shell. Other details in the distribution curves are compatible with an approximately tetrahedral coordination of molecules, as found in ice.

The curves were kindly provided by Dr. A. H. Narten from Oak Ridge National Laboratory Report 4378, June 1970.

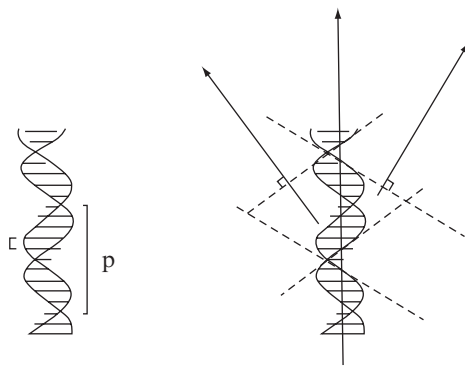
(a)



(b)



(c)



(d)

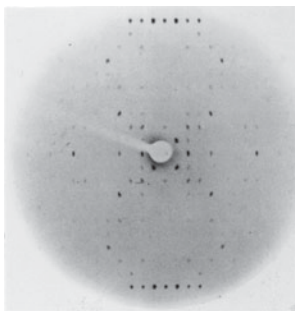


Fig. 13.2 Some diffraction patterns of DNA and polynucleotides.

Diffraction patterns of DNA and of a synthetic polynucleotide. Each diffraction photograph has been taken with the fiber axis vertical.

Fiber diffraction

Fibers have disordered strands aligned within them along the fiber axis (the meridian). If the fiber is rotated about this axis the diffraction pattern does not change much. The diffraction patterns in Figure 3.9 show the effect on the diffraction pattern of partial but incomplete internal order. Figure 3.9d displays quite effectively the result of one-dimensional internal order (characteristic of certain fibers), with elongated streaks instead of spots on the photograph. Many fibers are composed of units with helical structures, with some order along the axis of the helix, but often little order in the packing of adjacent helical units. DNA, certain fibrous proteins, and many other natural and synthetic materials have such structures. An X-ray photograph of DNA is shown in Figure 13.2a; note that the fiber axis is vertical in Figure 13.2, but horizontal in Figure 3.9d.

The coordinates of the atoms in a helical structure are best described by cylindrical polar coordinates, and the scattering factor of a cylindrical system is most appropriately represented in terms of Bessel functions. A zeroth-order Bessel function is high near the origin and then dies away like a ripple in a pond, while higher-order Bessel functions are zero at the origin and then rise to a peak at a distance proportional to their order and then die away, again like a ripple. These Bessel functions are used in calculating the Fourier transform of a helix, which describes the scattering pattern of the helix. The “cross” that is so striking in Figure 13.2a is characteristic of helical diffraction patterns. The diffraction pattern is analyzed in Figure 13.2b and its relationship to DNA structure is shown in Figure 13.2c. Because the helix is periodic along the axial direction, layer lines are formed. Two chief pieces of information may be derived from such a photograph as that in Figure 13.2a. These are the distance between “equivalent” units of the helical structure

-
- (a) B-DNA, the diffraction of which is illustrated, is a form of DNA in which the individual molecules are packed together less regularly. This fibrous noncrystalline form is that for which Watson and Crick first proposed their famous DNA helical structure. The fibers are randomly oriented around the fiber axes, and a helical diffraction pattern with a characteristic cross is obtained. Remember that short spacings in reciprocal space (the diffraction photograph) represent large spacings in real space. The peaks at the top and bottom of the photograph represent the stacked DNA bases, 3.5 Å apart. The “cross” represents spacings between the turns of the helix. (Photograph courtesy of Dr. R. Langridge.) (Langridge et al., 1957.)
- (b) Analysis of the diffraction pattern of DNA shown in Figure 13.2a.
- (c) DNA structure showing the stacked bases and the phosphodiester backbone. Periodicities in the structures of both of these are seen in the diffraction photograph.
- (d) Precession photograph of a crystalline decameric polynucleotide CGAQTTCGATCGn (Grzeskowiak et al., 1991). This photograph is a sampling of the fiber diffraction pattern in (a). Therefore it is clear which is the direction of stacked bases (vertical). (Photograph courtesy of Dr. Richard E. Dickerson.)

(for example, the base pairs in DNA) and the distance along the helix needed for one complete turn. From these two data the pitch of the helix can be deduced (see Watson and Crick, 1953; Franklin and Gosling, 1953; Wilson, 1966; Holmes and Blow, 1965; Squire, 2000).

The diffraction pattern of a crystalline dodecameric fragment of DNA is shown in Figure 13.2d (Dickerson et al., 1985; Grzeskowiak et al., 1991). Note that Figure 13.2d represents a sampling of the diffraction pattern in Figure 13.2a, so that one immediately knows the orientation of the molecules in the crystal (for example, the fiber direction). High-resolution studies of polynucleotides have provided much information on nucleic acid structure and function.

Small-angle scattering

Structural features that are large compared with the wavelength of the radiation being used cause significant scattering only at small angles (Figures 3.1 and 5.4). “Small-angle scattering” at angles 2θ no larger than a few degrees is thus used to measure long-range structure. For example, for a biological macromolecule it may be used to measure the radius of gyration and to study the hydration of the macromolecule. It has been widely applied to the study of liquids, polymers, liquid crystals, and biological membranes. The radiation used may be X rays (small-angle X-ray scattering, SAXS) or neutrons (small-angle neutron scattering, SANS). The method is very useful because it can provide information on partially or totally disordered systems. Therefore particles can be studied under physiological conditions (Guinier and Fournet, 1955; Brumberger, 1994; Koch et al., 2003; Kasai and Kakudo, 2005).

Powder diffraction

The diffraction pattern of a powder (packed in a capillary tube) may be considered that of a single crystal but with the pattern of the crystal in all possible orientations (as are the crystallites in the capillary tube). Powder diffraction is an extremely powerful tool for the identification of crystalline phases and for the qualitative and quantitative analyses of mixtures (Cullity, 1978). It is used for analysis of unit-cell parameters as a function of temperature and pressure and to determine phase diagrams (diagrams showing the stable phases present as a function of temperature, pressure, and composition). A very useful compilation

of common powder diffraction patterns, the Powder Diffraction File (PDF), is maintained by the International Centre for Diffraction Data (ICDD). This file contains d -spacings (related to angle of diffraction) and relative intensities of observable diffraction peaks. A comparison of a powder diffraction pattern obtained experimentally with the highest diffracted intensities of some powder diffraction patterns in the file, a search that can be done by computer, will often reveal the chemical composition of a powder. Thus, the method is of great importance industrially and forensically. For example, the composition of particles in an industrial smokestack may be determined by analysis of the diffraction pattern. Other useful information can also come from powder diffraction studies. For example, an analysis of profile broadening (Figure 13.3) can lead to an estimate of average crystallite sizes in the specimen.

Powder methods may even be used for simple structural studies. There are now sophisticated methods, originally introduced by Hugo Rietveld in 1967, for the adjustment of parameters to give the best fit with an experimental powder diffraction pattern (Rietveld, 1969; Young, 1993; Jenkins and Snyder, 1996). The technique is now used for the structure determination of simple structures and can provide precise unit-cell dimensions, atomic coordinates, and temperature factors in the same way that crystal diffraction studies do. The Rietveld method is, of course, of great value when suitably large crystals cannot be grown. It uses a least-squares approach to obtain agreement between a theoretical line profile and the measured diffraction profile. The introduction of this technique was a significant step forward in the diffraction analysis of powder samples as, unlike other techniques at that time, it was able to deal reliably with strongly overlapping reflections. Larger and larger structures are now being tackled.

Summary

Studies of structures that are not fully crystalline

The diffraction patterns of liquids and glasses are spherically symmetrical and only radial information can be obtained. However, from substances exhibiting partial order, more information may be derived. For example, for a helical structure, the pitch of the helix and the repeat distance along it can be deduced.

Powder diffraction

The diffraction pattern of a powder also gives only radial information, since the powder contains crystallites in all possible orientations.

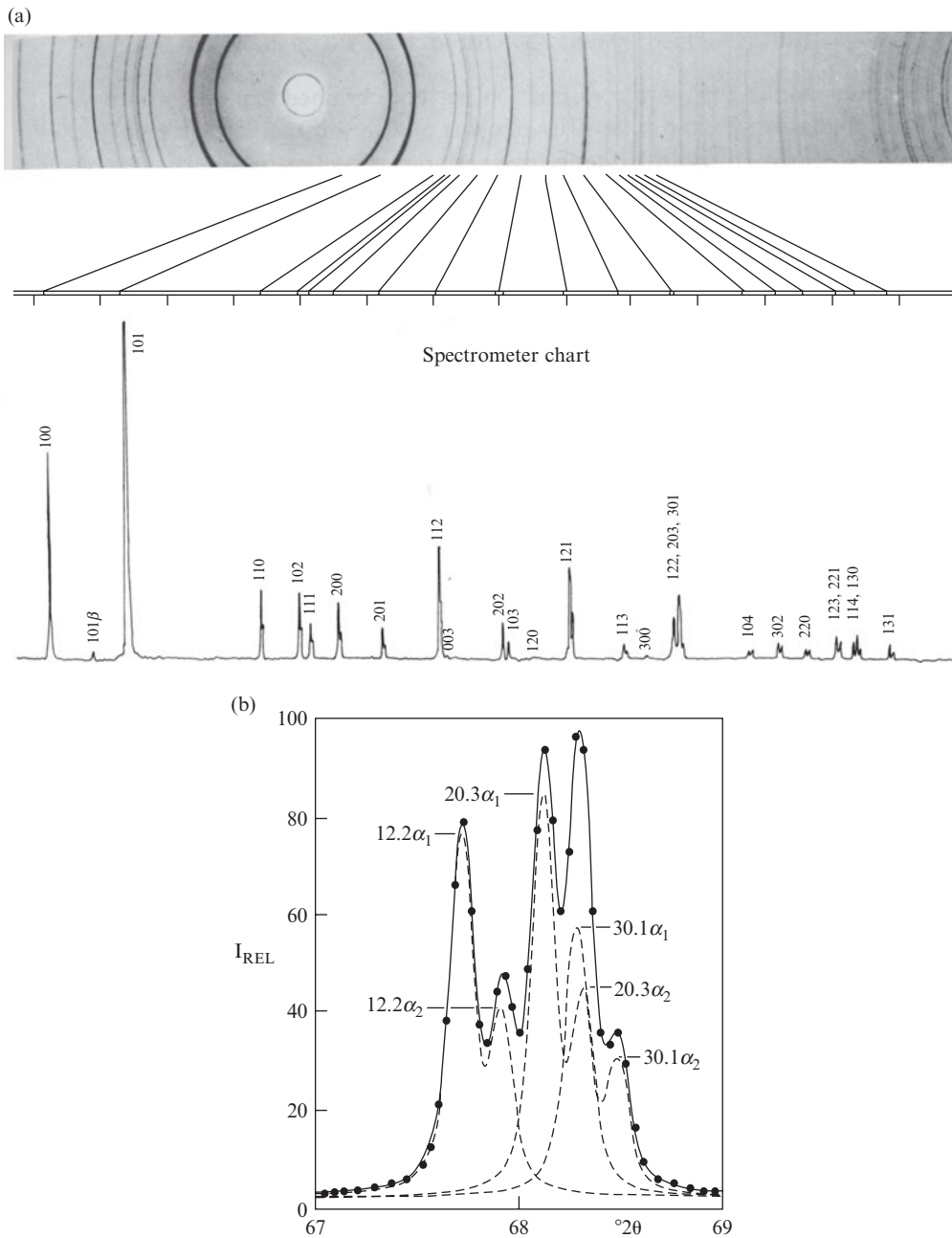


Fig. 13.3 Powder diffraction.

- (a) Comparison of an 11.46 cm diameter powder camera film (upper photograph) with a scanned diffractometer pattern of quartz (with copper $K\alpha$ radiation).
- (b) Profile fitting of a portion of the diffraction pattern of quartz. The dots are experimental points from step-scanning and the dashed lines are the individual results for each reflection. The sum is represented by a solid line. In this figure the peak identifications "12.2," "20.3," and "30.1" represent, respectively, the 122, 203, and 301 Bragg reflections for this crystal. Note the separation of the α_1 and α_2 wavelengths of the radiation (wavelengths 1.5405 Å and 1.5443 Å, respectively).

(Photographs and diagram courtesy of Dr. William Parrish.)

Powder diffraction is used for the identification of crystalline phases and for the qualitative and quantitative analysis of mixtures. When suitable crystals are not available, the Rietveld method has made evident the power of powder diffraction to determine three-dimensional crystal structures that otherwise could not have been studied.

14

Outline of a crystal structure determination

Small-molecule crystals

The stages in a crystal structure analysis by diffraction methods are summarized in Figure 14.1 for a substance with fewer than about 1000 atoms. The principal steps are:

- (1) First it is necessary to obtain or grow suitable single crystals; this is sometimes a tedious and difficult process. The ideal crystal for X-ray diffraction studies is 0.2–0.3 mm in diameter. Somewhat larger specimens are generally needed for neutron diffraction work. Various solvents, and perhaps several different derivatives of the compound under study, may have to be tried before suitable specimens are obtained.
- (2) Next it is necessary to check the crystal quality. This is usually done by finding out if the crystal diffracts X rays (or neutrons) and how well it does this.
- (3) If the crystal is considered suitable for investigation, its unit-cell dimensions are determined. This can usually be done in 20 minutes, barring complications. The unit-cell dimensions are obtained by measurements of the locations of the diffracted beams (the reciprocal lattice) on the detecting device, these spacings being reciprocally related to the dimensions of the crystal lattice. The space group is deduced from the symmetry of, and the systematic absences in, the diffraction pattern.
- (4) The density of the crystal may be measured if the crystals are not sensitive to air, moisture, or temperature and can survive the process. Otherwise an estimated value (about 1.3 g cm^{-3} if no heavy atoms are present) can be used. This will give the formula weight of the contents of the unit cell. From this it can be determined if the crystal contains the compound chosen for study, and how much solvent of crystallization is present.
- (5) At this point it is necessary to decide whether or not to proceed with a complete structure determination. The main question is, of course, whether the unit-cell contents are those expected. One must try to weigh properly the relevant factors, among which are:

- (i) Quite obviously, the intrinsic interest of the structure.
- (ii) Whether the diffraction pattern gives evidence of twinning, disorder, or other difficulties that will make the analysis, even if possible, at best of limited value. This will depend in part on the type of information sought.

If the answer to (ii) is unfavorable, another crystal specimen or polymorph (with a different crystalline form) may be sought. However, under happy circumstances, one can proceed.

- (6) Once a decision has been made to proceed, the next stage is to record, usually with a diffractometer equipped with an area detector (e.g., CCD or imaging plate), the locations and intensities of the accessible diffraction maxima. The intensities must then be appropriately correlated, averaged, and multiplied by various geometrical factors to convert them to relative values of $|F|$. For a typical molecular structure, there may be between 10^3 and 10^4 unique diffraction maxima to be measured, or even more with a very large molecule. The normal time involved in the collection and estimation of these intensity data is from a few hours to several days, the exact amount depending on the equipment available and the experience and other concurrent obligations of the experimenter. The data processing is done with a computer as are all subsequent steps, appreciably reducing the necessary time involved in the analysis.
- (7) Next it is necessary to attempt to get a "trial structure" or approximate relative phases. Generally, direct methods and Patterson methods are carried out with a computer-based "black box," indicated by shading in the flow chart. The excellent software now available will make most of the necessary structure solution decisions that the user requires. However, if problems arise, an understanding of the entire process will be necessary (hence this book). If all goes well, the normal procedure is to try some of the direct-methods programs, or to calculate a three-dimensional Patterson map with the aim of finding any heavy atom(s), or some recognizable portion of the molecule that may be present. Meanwhile, measurement of diffraction data on other related compounds whose crystal structures may prove easier to solve (if this one is unusually stubborn) should be considered; every laboratory has its collection of unsolved structures, some of which yield to new and improved methods or brighter minds that come along, and a few of which persist indomitably against all challengers.
- (8) Hydrogen atoms, which are weak diffractors of X rays, are often visible in a difference electron-density map. Alternatively, their positions can often be calculated. Refinement (usually by a least-squares method) may then be carried out. One way to ensure that hydrogen atoms are correctly placed is to do a neutron diffraction study on a deuterated specimen.

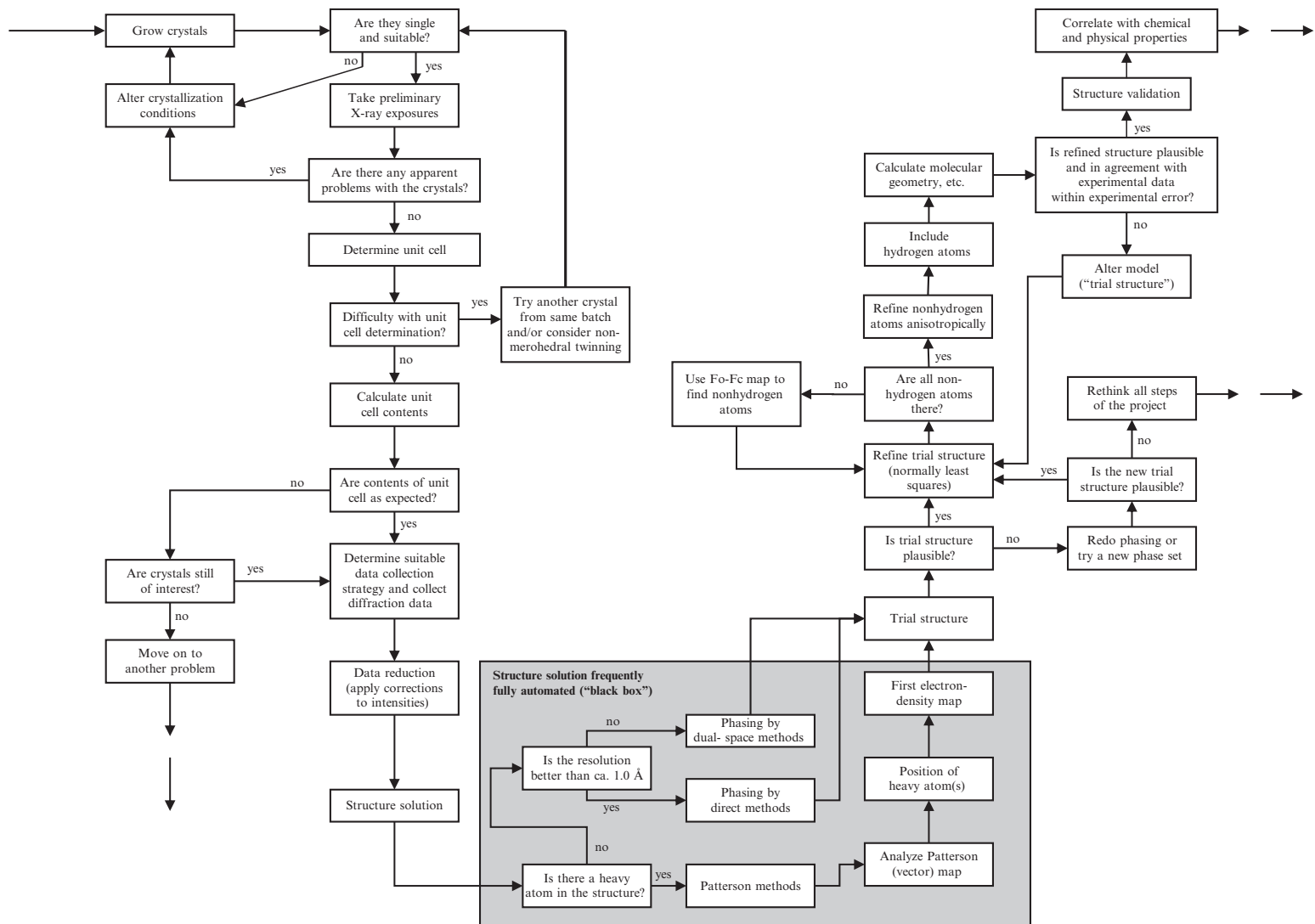


Fig. 14.1 The course of a structure determination by single-crystal X-ray diffraction. Flow diagram for determination of small structures (10^2 or fewer atoms per asymmetric unit). (We are grateful to Dr. Peter Müller for help in the preparation of this diagram.)

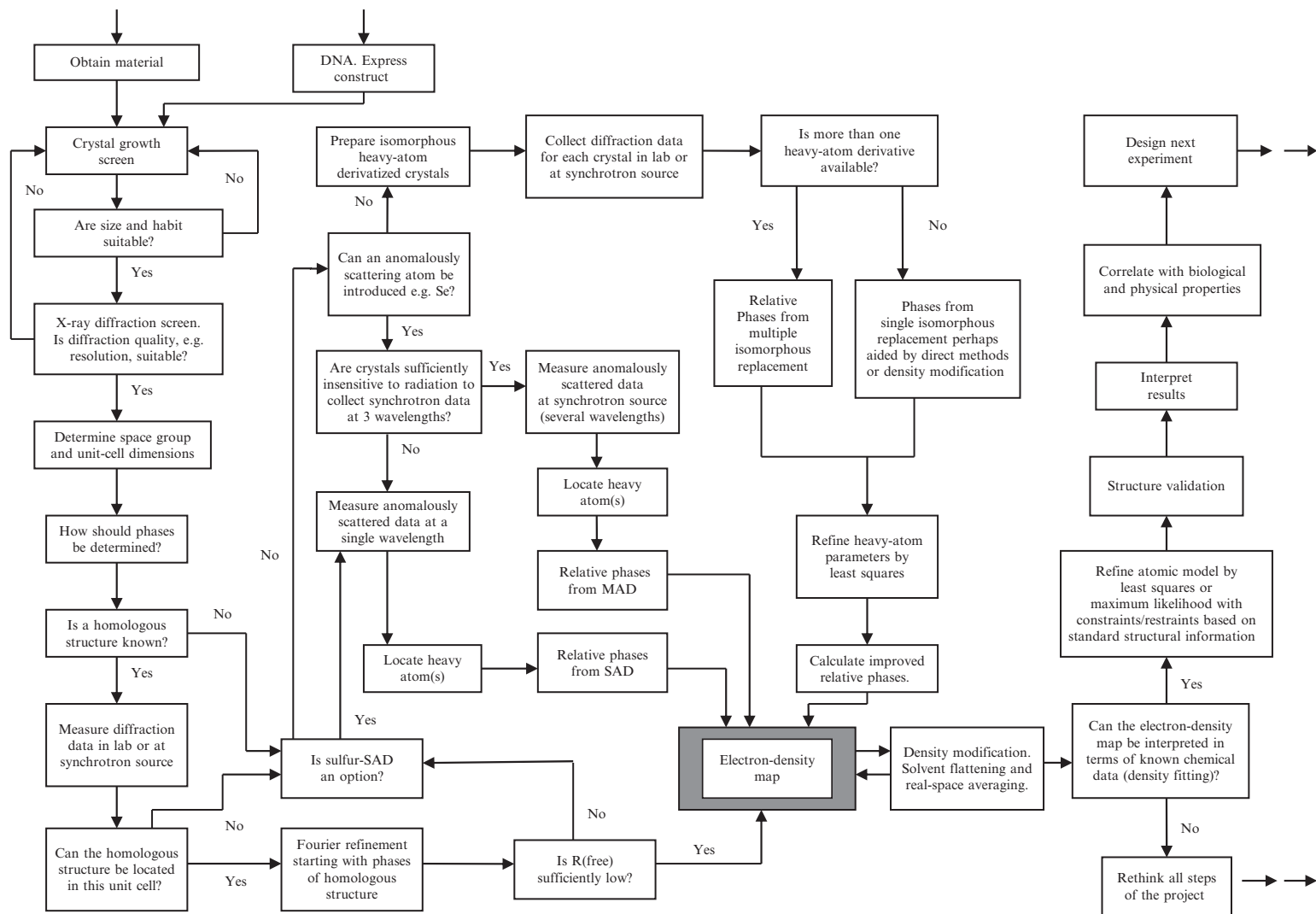


Fig. 14.2 The course of a structure determination by single-crystal X-ray diffraction.

Flow diagram for determination of macromolecular structures (10^3 or more atoms per asymmetric unit).

(We are grateful to Drs. David Eisenberg and Peter Müller for help in the preparation of this diagram.)

- (9) A satisfactory trial structure is one that is chemically plausible and for which there is good agreement between observed and calculated structure factors. It must then be refined, as discussed earlier. The resulting structure should have an R index [Eqn. (6.9)] consistent with the precision of the data that were collected, and should meet the criteria discussed earlier under the heading “The correctness of a structure” in Chapter 11 (see Müller, 2009).
- (10) When the refinement is complete, the molecular geometry can be calculated and analyzed.
- (11) One by-product of a complete and successful structure analysis of an optically active material can be a determination of its absolute configuration, provided that it contains an atom that absorbs sufficiently the X rays being used. This technique has been applied to many organic natural products and was discussed and illustrated in Chapter 10.

Macromolecular crystals

When a macromolecule is crystallized, somewhat different techniques are used to determine its structure (Figure 14.2). The principal steps are:

- (1) The material is obtained either by extraction from a biological or chemical specimen, or, if it is a protein, by cloning its gene into a high-expression system. The material so produced needs to have been carefully purified; mass spectrometry and electrophoretic techniques help here. Suitable single crystals are then (hopefully) grown by vapor diffusion of solvent or related methods (Chapter 2 and Figure 2.1). If a suitable crystal is obtained, it is mounted, ready for diffraction studies.
- (2) The unit-cell dimensions, space group, and density are determined. These will indicate if the analysis is feasible or not. Sometimes a subunit of an enzyme or other large macromolecule is the asymmetric unit. This should make the structure analysis feasible. On the other hand, it sometimes happens that several molecules comprise the asymmetric unit. This is not always unfortunate, because the resulting additional symmetry in the Patterson function may provide valuable help in solving the structure.
- (3) Then it is necessary to assess the degree of order in the crystal under study. This is determined by the measurable Bragg reflections at the highest $\sin \theta/\lambda$ values (which indicate the expected resolution of the measured structure). It must then be decided whether the ultimate resolution will be sufficient to provide information about the detailed structure. If the resolution is

poor, one must try to grow better crystals or look for another source of the biological macromolecule (e.g., a different animal or bacterium).

- (4) The next question is whether there is a homologous structure already reported in the crystallographic literature. The structure being sought (the homologous structure) probably has approximately the same amino acid sequence and similar enzymatic activity to the protein investigated (the protein under study). To find out if there is such a homologous structure in the crystallographic literature, it is necessary to search the Protein Data Bank; this is available on the World Wide Web. If such a homologous protein can be found, it is assumed that the foldings of both proteins (the homologous protein and the protein under study) are similar. Therefore diffraction data for the protein under study are measured. An attempt is then made, usually by Patterson methods, to determine the location of the homologous protein molecule in the unit cell of the protein crystal under study. If this works out, the phases for the crystal under study can be calculated and refined and an electron-density map produced.
- (5) If no homologous structure is available, there might be an opportunity for sulfur-SAD phasing if sulfur is present in the molecule. This method is currently used frequently and it does not require any heavy metals or homologous structures, only good data to 2.5 Å resolution. Single-wavelength anomalously scattered X-ray data plus direct methods (to locate the sulfur atoms) will give phases for an electron-density map.
- (6) In the absence of sulfur or a strong anomalous scatterer, it will be necessary to make conventional heavy-atom derivatives, measure the diffraction data for the native crystal and each of its heavy-atom derivatives that have been successfully crystallized, and then determine the phases by isomorphous replacement. For some proteins, side chains containing heavy atoms, such as selenium, iodine, or bromine, may be genetically engineered into them. The best heavy atoms are those that scatter anomalously with X rays from either a laboratory X-ray tube or a synchrotron source (with the possibility of X-ray wavelength tuning to required values). The heavy-atom parameters are then refined by least-squares methods. Improved phases are then derived, and an electron-density map is computed.
- (7) If an atom with a strong anomalous signal can be introduced into the crystal, the measurement of anomalous data is probably the best way to go (that is, by MAD or SAD phasing). If anomalous data [i.e., $I(hkl)$ and $I(\bar{h}\bar{k}\bar{l})$] are an option it is necessary to determine if the crystal will survive many data collections, since X rays damage protein crystals. The single-wavelength anomalous

dispersion (SAD) method (mentioned above for sulfur-containing proteins) is used if the crystals are fragile or if it is more convenient to study them in the investigator's laboratory with standard X-ray tubes. Sturdier crystals can be studied by the multiwavelength anomalous dispersion (MAD) method, in which several data sets at different wavelengths near and far from the absorption edge of the anomalously scattering atom are measured. Selenomethione is often introduced in place of methionine in proteins and acts as the anomalous scatterer. The advantage of MAD phasing is that only one crystal is needed, but it is generally necessary to go to a synchrotron source to obtain the required X-ray wavelengths.

- (8) In each of these methods, the result is an electron-density map. This is probably a good place to stress that this map does not constitute "data," and to remind the reader that the primary experimental data are the Bragg reflections. The map is totally dependent on the phases that have been input into the calculation. These phases may be improved by density modification, which includes solvent flattening for crystal structures with large areas occupied by solvent and real-space averaging for structures with noncrystallographic symmetry.
- (9) If a protein crystal structure is under study, it is usual first to "trace the chain" of the polypeptide backbone. The determination of side-chain coordinates for the protein follows from a knowledge of the amino acid sequence of the protein and the fitting of a model of each amino acid to the electron density on a computer screen. Without sequence information, the analysis of the electron-density map is difficult unless phasing is good to atomic resolution (as is the case with increasingly many investigations). If the macromolecule under study is a nucleic acid, the phosphate groups and the bases are sought from the electron-density map as a preliminary to phasing the electron-density map.
- (10) For an enzyme, the question of the location of the active site of the catalytic process then arises. This may often be found by soaking into native crystals either inhibitors, poor substrates (if the substrate is too good, reaction may readily occur), or cofactors. Then diffraction data are measured and a difference electron-density map is calculated using phases from both the native protein and the liganded complex. In this way the site of attachment of a substrate may be evident, suggesting that this is the active site of the enzyme. At this stage, neutron diffraction studies on deuterated proteins and/or their ligands can yield powerful information on the protonation state of each functional group under the particular experimental conditions at which the crystals formed. Therefore a combination of X-ray and neutron diffraction investigations is encouraged.

Concluding remarks

We have attempted to present enough about the details of structure determination so that an attentive reader can appreciate how the method works. As mentioned earlier, a glossary and list of references (including a short bibliography) have been included so that those interested may delve further into the subject. Do not forget to use search engines in the World Wide Web, as there are many useful articles and reprints available for study. We will now summarize by answering our initial questions.

Why use crystals and not liquids or gases?

A crystal has a precise internal order and gives a diffraction pattern that can be analyzed in terms of the shape and contents of one repeating unit, the unit cell. This internal order is lacking in liquids and gases and for these only radial information may be derived. Such information may be of use in distinguishing between possible structures, but, for detailed results in terms of molecular structure and intermolecular interactions, the analysis of crystals (or powders) is necessary.

Why use X rays or neutrons and not other radiation?

These radiations are scattered by the components of atoms and have wavelengths that are of the same order of magnitude as the distances between atoms in a crystal (approximately 10^{-10} m). Hence they lead to diffraction effects on a scale convenient for observation and measurement.

What experimental measurements are needed?

The unit-cell dimensions and the density of the crystal, and the indices and intensities of all observable Bragg reflections.

What are the stages in a typical structure determination?

These stages have been described above in detail for both small molecules and macromolecules, and further information may be obtained from the World Wide Web. The stages involve the preparation of a

crystal, the indexing and measurement of intensities in the diffraction pattern, the determination of a “trial structure,” and the refinement of this structure.

Why is the process of structure analysis often lengthy and complex?

Because 50 to 100 distinct intensity measurements are needed per atom in the asymmetric unit for a resolution of 0.75 \AA , because the determination of a trial structure may be difficult, because the refinement requires much computation, and because in the end so much structural information is obtained that analysis of it takes time. Many structures are readily or even automatically solved, while others, tackled by the same competent crystallographer, may take months or years to solve. It is hard for the noncrystallographer, who may have been led to believe that the determination of structure is now almost automatic, to comprehend this “never-never land” in which crystallographers occasionally find themselves while trying to arrive at a trial structure for certain crystals.

Why is it necessary to “refine” the approximate structure that is first obtained?

Because the initially estimated phases may give a poor image of the scattering matter. Since the least-squares equations are not linear, many cycles of refinement are usually necessary. By refinement, one can tell whether the approximate structure is correct and obtain the best possible atomic positions consistent with the experimental data and the assumed structural model.

How can one assess the reliability of a structure analysis?

By checking the standard uncertainties of the derived results, by considering measures of the agreement of the values of the observed $|F_o|$ with the values of the calculated $|F_c|$, by the absence of any unexplained peaks in a final difference map, and by the chemical reasonableness of the resulting structure.

We hope we have made it possible for you to read accounts of X-ray structure analyses with some appreciation of the scope and the limitations of the work described. Perhaps you are even interested enough to want to try the techniques yourself. If so, trust that this introduction serves as a useful background and reference. But also

we hope that you realize that there is more to the crystallographer's discipline than just diffraction methods. When the crystal structure is known, it is a first step in the interpretation of physical properties, chemical reactivity, or biological function in terms of the three-dimensional structures and conformations of the component molecules or ions.

Appendices

Appendix 1: The determination of unit-cell constants and their use in ascertaining the contents of the unit cell

Unit-cell dimensions

Unit-cell dimensions may be determined, with X rays of a known wavelength, from values of 2θ for Bragg reflections of known indices; 2θ is the deviation of the diffracted beam from the direct beam. The Bragg equation is then used, i.e., $n\lambda = 2d \sin \theta$; d_{hkl} = spacing between crystal planes (hkl).

Example

Monoclinic cell, $a = 23.033 \text{ \AA}$, $b = 7.670 \text{ \AA}$, $c = 9.928 \text{ \AA}$, $\alpha = \gamma = 90^\circ$, $\beta = 100.12^\circ$, $\sin \beta = 0.98445$, $\lambda = 1.5418 \text{ \AA}$ [$a \sin \beta = 22.675 = d_{100}$, $c \sin \beta = 9.774 = d_{001}$].

Experimental measurements

| h | k | l | $2\theta(^\circ)$ | $\theta(^\circ)$ | $\sin \theta$ | $n\lambda/2 \sin \theta(\text{\AA})$ | | |
|-----|-----|-----|-------------------|------------------|---------------|--------------------------------------|-------------|------------------|
| 20 | 0 | 0 | 85.68 | 42.84 | 0.67995 | 22.675 | } d_{100} | } $a \sin \beta$ |
| 22 | 0 | 0 | 96.82 | 48.41 | 0.74791 | 22.676 | | |
| 0 | 4 | 0 | 47.41 | 23.705 | 0.40203 | 7.670 | d_{010} | b |
| 0 | 0 | 10 | 104.14 | 52.07 | 0.78876 | 9.774 | d_{001} | $c \sin \beta$ |

Conclusion: $a = 23.033 \text{ \AA}$, $b = 7.670 \text{ \AA}$, $c = 9.928 \text{ \AA}$, $\beta = 100.12^\circ$.

Unit-cell contents

Let W = weight in grams of one gram-formula weight of the contents of the unit cell.

V = the unit-cell volume in cm^3 of this weight of the crystal.

$N_{\text{Avog.}}$ = Avogadro's number = number of molecules in a gram molecule = 6.02×10^{23} .

Unit-cell volume = $1726 \text{ \AA}^3 = 1726 \times 10^{-24} \text{ cm}^3$.

Observed density (by flotation) = 1.34 g/cm^3 .

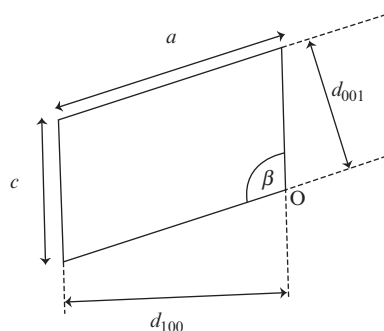


Fig. A1.1 Unit cell with b perpendicular to the plane of the paper.

If the density of a crystal is known (or guessed), it is possible to determine what is in the crystal. N_{Avog} unit cells occupy $1726 \times 10^{-24} \times 6.02 \times 10^{23} \text{ cm}^3 = V = 1039 \text{ cm}^3$.

Crystal density = $W/V = W/1039 \text{ g/cm}^3 = 1.34 \text{ g/cm}^3$.

Therefore $W = 1392$.

But W also equals $(ZM + zm)$,

where Z is the number of molecules of the compound (molecular weight M) per unit cell, and z is the number of molecules of solvent of crystallization (molecular weight m) per unit cell. In this example, M is known to be 340 and $m = 18$ (for water).

$$(Z \times 340) + (z \times 18) = 1392.$$

The monoclinic symmetry of the unit cell suggests that Z is 4, or a multiple of 4, leading to the conclusion that $Z = 4$ and $z = 2$ ($W = 1396$) is the correct solution, and that the solution $Z = 3$ and $z = 20$ ($W = 1380$), which is equally probable from the calculated weight alone, is much less likely, because of the monoclinic symmetry.

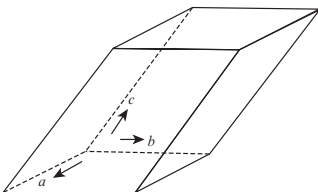
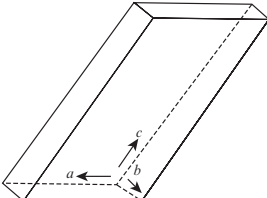
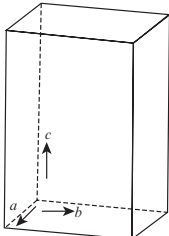
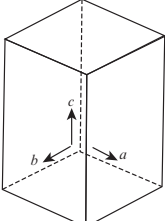
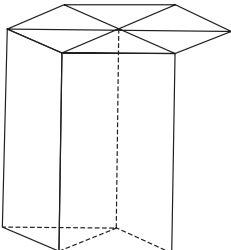
Appendix 2: Some information about crystal systems and crystal lattices

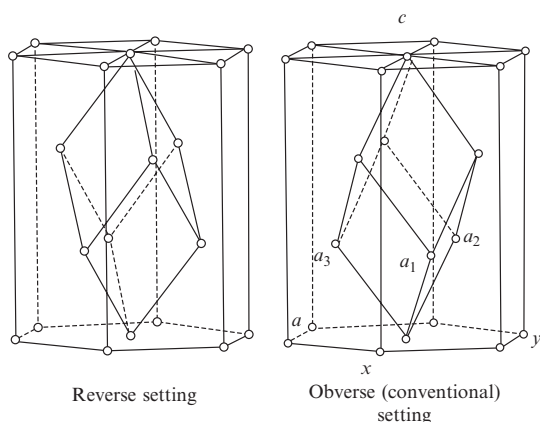
There are seven crystal systems defined by the minimum symmetry of the unit cell. It is conventional to label the edges of the unit cell a , b , c and the angles between them α , β , γ , with α the angle between b and c , β that between a and c , and γ that between a and b . If the crystal lattice has six-fold symmetry, sometimes four axes of reference are used. These are x , y , u , z , where x , y , and u lie in one plane inclined at 120° to each other and with z perpendicular to them. The indices of Bragg reflections are then $hkil$ with the necessary condition that $i = -(h + k)$. We use the simpler cell here. For the seven crystal systems, the minimum symmetry and the diffraction symmetry are:

| | Minimum point group symmetry of a crystal in this system | Diffraction symmetry (Laue symmetry) |
|--------------------------|--|--------------------------------------|
| 1. Triclinic | None (one-fold rotation axis). | $\bar{1}$ |
| 2. Monoclinic | Two-fold rotation axis parallel to b . | $2/m$ |
| 3. Orthorhombic | Three independent mutually perpendicular two-fold rotation axes. | mmm |
| 4. Trigonal/rhombohedral | Three-fold rotation axis parallel to $(a + b + c)$ | $\bar{3}$ or $\bar{3}m$ |
| 5. Tetragonal | Four-fold rotation axis parallel to c . | $4/m$ or $4/mmm$ |
| 6. Hexagonal | Six-fold rotation axis parallel to c . | $6/m$ or $6/mmm$ |
| 7. Cubic | Four intersecting three-fold rotation axes along the cube diagonals. | $m\bar{3}$ or $m\bar{3}m$ |

Here a number, 1, 2, 3, 4, or 6, implies a rotation axis. If there is a line over it, such as $\bar{3}$, then it is an inversion axis. A mirror plane perpendicular to the rotation axis is n/m , but if the mirror plane is parallel to the rotation axis it is nm ; see *International Tables*, Volume A (Hahn, 2005).

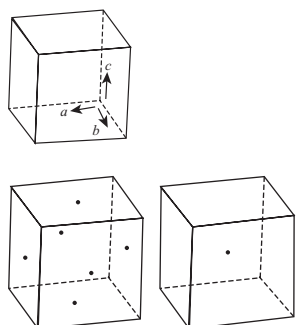
Diagrams of the unit cells are shown below, together with symmetry-imposed restrictions on the unit-cell dimensions.

| Diagrams of unit cells | Crystal system | Rotational symmetry elements and cell-dimension restrictions |
|--|------------------------|--|
|  | Triclinic | No rotational symmetry. No restrictions on axial ratios or angles. |
|  | Monoclinic | b chosen along the two-fold rotation axis. ^a Angles made by b with a and by b with c must be 90° . |
|  | Orthorhombic | Three mutually perpendicular two-fold rotation axes chosen as a , b , c coordinate axes. No restrictions on axial ratios. All three angles must be 90° . |
|  | Tetragonal | Four-fold rotation axis chosen as c . Two-fold rotation axes perpendicular to c . Lengths of a and b identical. All angles must be 90° . |
|  | Hexagonal ^b | c is chosen along the six-fold axis. Two-fold rotation axes perpendicular to c . Angle between a and b must be 120° ; other two angles must be 90° . |



Rhombohedral

Three-fold rotation axis along one body diagonal of unit cell. This makes all three axial lengths necessarily the same and all three interaxial angles also necessarily equal. There is no restriction on the value of the interaxial angle, α .



Cubic

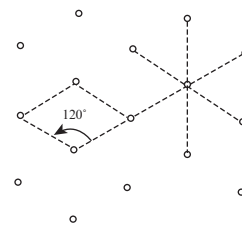
Three-fold rotation axes along all four body-diagonals of unit cell. Four-fold axes parallel to each crystal axis. Two-fold axes are also present. All axial lengths are identical by symmetry. All angles must be 90° .

Face-centered (*F*)
and
body-centered (*I*)

Symmetry at each crystal lattice point is the same as for simple cubic. *F* has four crystal lattice points per cubic unit cell, the extra three being at face centers. *I* has two points per unit cell, the extra one being at the center of the cell.

^a This means that if the cell is rotated $360^\circ/2 = 180^\circ$ about an axis parallel to \mathbf{b} , the cell so obtained is indistinguishable from the original.

^b The six-fold axis present in hexagonal crystal lattices is perhaps not evident from the shape of the unit cell, because the inclusion of the cell edges as solid lines in the diagram obscures the symmetry. If only the crystal lattice points are shown in a layer normal to the unique c -axis (one cell is outlined here on the right in dashed lines), the six-fold symmetry is apparent (ignoring the dotted lines). There is a six-fold rotation axis perpendicular to the plane of the paper at every crystal lattice point; it is indicated by the dashed lines drawn from one crystal lattice point.



There are five additional Bravais lattices that are obtained by adding face-centering and body-centering to certain of the seven space lattices just listed. Face-centering involves a crystal lattice point at the center of opposite pairs of faces, and is designated *F* if all faces are centered and *A*, *B*, or *C* if only one pair of faces is centered. In body-centered unit cells, there is a crystal lattice point at the center of the unit cell; a body-centered cell is designated *I*. These centerings cause additional systematic absences in the measured Bragg reflections (h, k, l) as follows:

- A* $(k + l)$, odd, absent.
- B* $(l + h)$, odd, absent.
- C* $(h + k)$, odd, absent.
- F* $(h + k), (k + l), (l + h)$, all odd, absent.
- I* $(h + k + l)$, odd, absent.

The 14 Bravais lattices are:

| | | | | |
|--------------|----------|----------|----------|----------|
| Triclinic | <i>P</i> | | | |
| Monoclinic | <i>P</i> | <i>C</i> | | |
| Orthorhombic | <i>P</i> | <i>C</i> | <i>F</i> | <i>I</i> |
| Tetragonal | <i>P</i> | <i>I</i> | | |
| Hexagonal | <i>P</i> | | | |
| Rhombohedral | <i>P</i> | | | |
| Cubic | <i>P</i> | <i>F</i> | <i>I</i> | |

(*C* in monoclinic can alternatively be *A* or *I*; *C* in orthorhombic can alternatively be *A* or *B*. *P* in rhombohedral is often called *R*.)

Addition of symmetry elements to these Bravais lattices give the 230 space groups. Some of these symmetry elements also cause systematic absences in the diffraction pattern. For example, for a two-fold screw axis parallel to **a**, *h* in the *h* 0 0 Bragg reflections is only even, and for a four-fold screw axis parallel to **a**, *h* in the *h* 0 0 reflections is only a multiple of 4. For a glide plane perpendicular to **a** with translation *b*/2 (which is a *b* glide), *k* in the 0*kl* reflections is only even. For more details, see *International Tables*, Volume A (Hahn, 2005), or *X-ray Crystallography* by M. J. Buerger, Chapter 4, pp. 82–90 (Buerger, 1942).

Appendix 3: The reciprocal lattice

The relation between the crystal lattice (real space) and the reciprocal lattice (reciprocal space) may be expressed most simply in terms of vectors. Some of the relationships between these two lattices are illustrated in Figure 3.7d. The point *hkl* in the reciprocal lattice is drawn at a distance $1/d_{hkl}$ from the origin and in the direction of the perpendicular between (*hkl*) lattice planes. If we denote the fundamental translation vectors of the crystal lattice by **a**, **b**, and **c**, and the volume of the unit cell by V_c , and then use the same symbols, starred, for the corresponding quantities of the reciprocal lattice, the relation between the two lattices is

$$\mathbf{a}^* = \frac{\mathbf{b}^* \times \mathbf{c}^*}{V_c}, \quad \mathbf{b}^* = \frac{\mathbf{c}^* \times \mathbf{a}^*}{V_c}, \quad \mathbf{c}^* = \frac{\mathbf{a}^* \times \mathbf{b}^*}{V_c} \quad (\text{A3.1})$$

with $V_c = \mathbf{a} \cdot \mathbf{b} \times \mathbf{c} = 1/V_c^*$.

The vectors of the crystal lattice and the reciprocal lattice are thus oriented as follows: any fundamental translation of one lattice is perpendicular to the other two fundamental translations of the second lattice. Thus **a**^{*} is perpendicular to both **b** and **c**, **b** is perpendicular to both **a**^{*} and **c**^{*}, and so on. The vectors of the crystal lattice and the reciprocal lattice are therefore said to form an “adjoint set” in the sense that this term is used in tensor calculus; they satisfy the condition that the scalar product of any two corresponding fundamental translation vectors, one from each of the two lattices, is unity, and the scalar product of any two noncorresponding vectors of the two lattices is zero, because, as mentioned above, they are mutually perpendicular. This is expressed by

$$\mathbf{a}_i^* \cdot \mathbf{a}_j = \delta_{ij} \begin{cases} = 1, & \text{if } i = j \\ = 0, & \text{if } i \neq j \end{cases} \quad (\text{A3.2})$$

That is,

$$\mathbf{a} \cdot \mathbf{a}^* = \mathbf{b} \cdot \mathbf{b}^* = \mathbf{c} \cdot \mathbf{c}^* = 1$$

and

$$\mathbf{b} \cdot \mathbf{a}^* = \mathbf{c} \cdot \mathbf{a}^* = \mathbf{c} \cdot \mathbf{b}^* = \mathbf{a} \cdot \mathbf{b}^* = \mathbf{a} \cdot \mathbf{c}^* = \mathbf{b} \cdot \mathbf{c}^* = 0$$

As stressed in Chapter 3, if a structure is arranged on a given lattice, its diffraction pattern is necessarily arranged on a lattice reciprocal to the first. The fact that any fundamental translation of the crystal lattice is perpendicular to the other two fundamental translations of the reciprocal lattice, and the converse, is an example of a quite general relation: *every reciprocal lattice vector is perpendicular to some plane in the crystal lattice and, conversely, every crystal lattice vector is perpendicular to some plane in the reciprocal lattice*. Furthermore, if the indices of a crystal lattice plane are (hkl) (in the sense defined in the caption of Figure 2.4), the reciprocal lattice vector \mathbf{H} perpendicular to this plane is the vector from the origin of the reciprocal lattice to the reciprocal lattice point with indices hkl . It is expressed as

$$\mathbf{H} = h\mathbf{a}^* + k\mathbf{b}^* + l\mathbf{c}^* \quad (\text{A3.3})$$

In a monoclinic unit cell,

$$d_{100} = a \sin \beta = \frac{1}{a^*}$$

We have the relation, for this Bragg reflection 100, where $h = 1$,

$$|\mathbf{H}| = |h\mathbf{a}^*| = h/d_{100} \quad (\text{A3.4})$$

or

$$|\mathbf{H}_{100}| = |\mathbf{a}^*| = 1/d_{100}$$

A comparison with the Bragg equation for 100 with the appropriate values of d and θ ,

$$h\lambda = 2d \sin \theta \quad \text{or} \quad h/d = \frac{2 \sin \theta}{\lambda} \quad (\text{A3.5})$$

$$\lambda = 2d_{100} \sin \theta_{100} \quad \text{or} \quad 1/d_{100} = 2 \sin \theta_{100}/\lambda$$

indicates that in this case

$$|\mathbf{H}| = \frac{2 \sin \theta}{\lambda} \quad (\text{A3.6})$$

This relation holds quite generally.

$$|\mathbf{H}_{100}| = 2 \sin \theta_{100}/\lambda \quad (\text{A3.7})$$

$$|\mathbf{H}_{hkl}| = 2 \sin \theta_{hkl}/\lambda$$

The equations relating the real and reciprocal unit-cell dimensions are given in Buerger (1942) (Chapter 18, p. 360) and Stout and Jensen (1989) (p. 31). Some

of these are listed below:

$$a^* = bc \sin \alpha / V, b^* = ac \sin \beta / V, c^* = ab \sin \gamma / V$$

where

$$V = abc \sqrt{1 - \cos^2 \alpha - \cos^2 \beta - \cos^2 \gamma + 2 \cos \alpha \cos \beta \cos \gamma}$$

$$V^* = 1/V$$

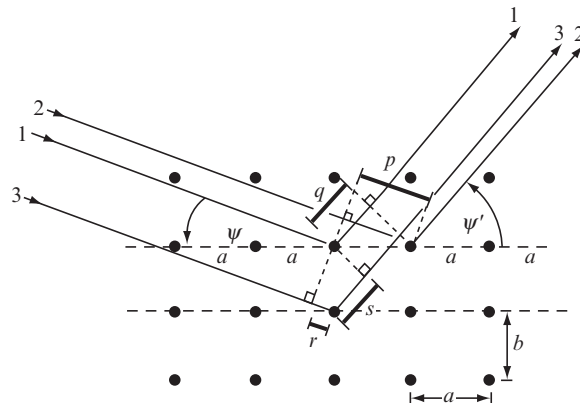
$$\cos \alpha^* = (\cos \beta \cos \gamma - \cos \alpha) / \sin \beta \sin \gamma$$

$$\cos \beta^* = (\cos \alpha \cos \gamma - \cos \beta) / \sin \alpha \sin \gamma$$

$$\cos \gamma^* = (\cos \alpha \cos \beta - \cos \gamma) / \sin \alpha \sin \beta$$

Appendix 4: The equivalence of diffraction by a crystal lattice and the Bragg equation

For simplicity we will consider diffraction by a two-dimensional orthogonal crystal lattice (a rectangular net), but the treatment can be generalized to three dimensions and to the nonorthogonal case. Suppose the crystal lattice has sides a and b for each unit cell and that X rays are incident upon the crystal lattice from a direction such that the incident beams make an angle ψ with the crystal lattice rows in the a direction. Consider the scattering (the diffracted beam) in the direction ψ' with respect to the a direction. Because a and b are crystal lattice translations, any atom in the structure will be repeated periodically with



DIFFRACTION BY A CRYSTAL

Fig. A4.1

spacings a and b . Thus atoms may be imagined to be present at the crystal lattice points in Figure A4.1 (they will normally also be present at other points, lying between these crystal lattice points, but spaced identically in each unit cell). If scattering is to occur in the direction specified by ψ' , then the radiation scattered in that direction from every crystal lattice point must be exactly in phase with that from every other crystal lattice point. (If scattering from any two crystal lattice points is somewhat out of phase, that from some other pair of crystal lattice points will be out of phase by a different amount, and the net sum over all crystal lattice points, considering the crystal to be essentially infinite, will consist of equal positive and negative contributions and thus will be zero.)

Consider waves 1 and 2, scattered by atoms separated by a (Figure A4.1). For these waves to be just in phase after scattering, the path difference (PD_1) must be an integral number (h) of wavelengths (ray 1 travels a distance q , while ray 2 travels a distance p):

$$PD_1 = p - q = a \cos \psi - a \cos \psi' = h\lambda \quad (\text{A4.1})$$

Similarly, the path difference for waves 1 and 3, scattered by atoms separated by b , must also be an integral number of wavelengths (ray 3 travels a distance $r + s$ more than ray 1):

$$PD_2 = r + s = b \sin \psi + b \sin \psi' = k\lambda \quad (\text{A4.2})$$

where k is some integer.

Both of these conditions must hold simultaneously. They are sufficient conditions to ensure that the scattering from all atoms in this two-dimensional net will be in phase in the direction ψ' . In three dimensions, another similar equation, corresponding to the spacing in the third (noncoplanar) direction, must be added. Each of these equations describes a cone. In three dimensions, the three cones intersect in a line corresponding to the direction of the diffracted beam, such that the conditions $h\lambda = PD_1$, $k\lambda = PD_2$, and $l\lambda = PD_3$ all are satisfied simultaneously. This is why, when a three-dimensional crystal diffracts, there are very few diffracted beams for any given orientation of the incident beam with respect to the (stationary) crystal. The chance that all three conditions will be satisfied at once is small.

Now let us see how this set of conditions can be related to the Bragg equation. Consider several parallel planes, I, II, and III, each passing through a set of crystal lattice points and making equal angles, θ , with the incident and scattered beams (Figure A4.2). The planes make an angle α with the a axis. The angles ψ and ψ' are defined as in Figure A4.1, and so

$$\theta = \psi + \alpha = \psi' - \alpha \quad (\text{A4.3})$$

Substituting for ψ and ψ' from Eqn. (A4.3) into Eqns. (A4.1) and (A4.2), we find

$$h\lambda = 2a \sin \alpha \sin \theta \quad (\text{A4.4})$$

$$k\lambda = 2b \cos \alpha \sin \theta \quad (\text{A4.5})$$

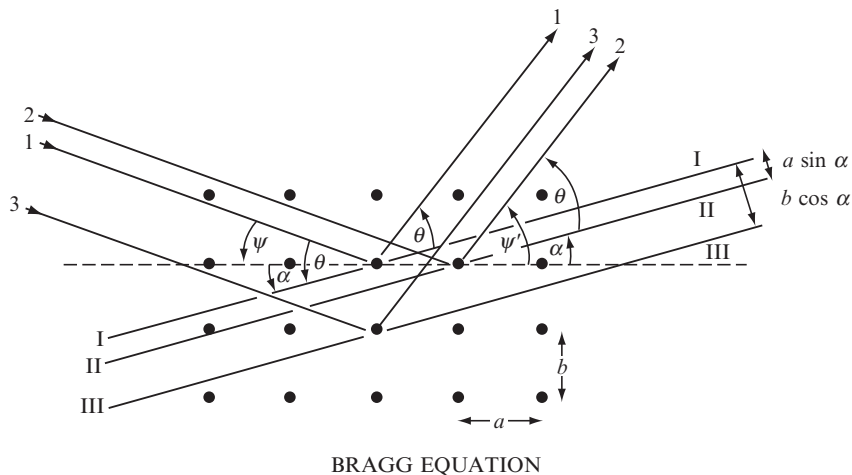


Fig. A4.2

or

$$\frac{2 \sin \theta}{\lambda} = \frac{h}{a \sin \alpha} = \frac{k}{b \cos \alpha} \quad (\text{A4.6})$$

Now $a \sin \alpha$ is just the spacing between planes I and II, while $b \cos \alpha$ is just the spacing between planes I and III. If we let d_{hkl} represent the spacing between any two planes in a set of equidistant planes parallel to I, and let n be some integer, we can write Eqn. (A4.6) generally as

$$\frac{2 \sin \theta}{\lambda} = \frac{n}{d_{hkl}} \quad (\text{A4.7})$$

which is the Bragg equation, $n\lambda = 2d \sin \theta$, Eqn. (3.1).

The indices ($H K$) of the "reflecting planes," I, II and III, are determined, as described in the caption to Figure 2.4, by measuring the intercepts on the axes as fractions of the cell edges. From Figure A4.2 it can be seen that the intercepts along \mathbf{b} and \mathbf{a} are in the ratio $\tan \alpha$, whence

$$(b/K)/(a/H) = \tan \alpha \quad (\text{A4.8})$$

or

$$H/K = (a \tan \alpha)/b \quad (\text{A4.9})$$

Equation (A4.6) then shows the relation of H and K to the indices of the Bragg reflection ($h k$),

$$\frac{H}{K} = \frac{a \sin \alpha}{b \cos \alpha} = \frac{h}{k} \quad (\text{A4.10})$$

That is, in conclusion, h and k , the indices of the Bragg reflection, are proportional to H and K , the indices of the reflecting plane.

Appendix 5: Some scattering data for X rays and neutrons

| Element | Nuclide | X rays | | Neutrons ^a $b/10^{-12}$ cm | Neutrons normalized to ¹ H as -1.00 |
|--|--------------------|---------------------------|--|--|--|
| | | $\sin \theta/\lambda = 0$ | $\sin \theta/\lambda = 0.5/\text{\AA}$ | | |
| (relative to scattering by one electron) | | | | | |
| H | ¹ H | 1.0 | 0.07 | -0.38 | -1.00 |
| | ² H = D | 1.0 | 0.07 | 0.65 | 1.71 |
| Li | ⁶ Li | 3.0 | 1.0 | 0.18 + 0.025i | 0.71 + 0.066i |
| | ⁷ Li | 3.0 | 1.0 | -0.25 | -0.66 |
| C | ¹² C | 6.0 | 1.7 | 0.66 | 1.74 |
| | ¹³ C | 6.0 | 1.7 | 0.60 | 1.58 |
| O | ¹⁶ O | 8.0 | 2.3 | 0.58 | 1.53 |
| Na | ²³ Na | 11.0 | 4.3 | 0.35 | 0.92 |
| Fe | ⁵⁴ Fe | 26.0 | 11.5 | 0.42 | 1.11 |
| | ⁵⁶ Fe | 26.0 | 11.5 | 1.01 | 2.66 |
| | ⁵⁷ Fe | 26.0 | 11.5 | 0.23 | 0.61 |
| Co | ⁵⁹ Co | 27.0 | 12.2 | 0.25 | 0.66 |
| Ni | ⁵⁸ Ni | 28.0 | 12.9 | 1.44 | 3.79 |
| | ⁶⁰ Ni | 28.0 | 12.9 | 0.30 | 0.79 |
| | ⁶² Ni | 28.0 | 12.9 | -0.87 | -2.29 |
| U | ²³⁸ U | 92.0 | 53.0 | 0.85 | 2.24 |

^a The quantity b is the neutron coherent scattering amplitude.

In the final column on the right of the table we have listed neutron scattering amplitudes arbitrarily normalized to a value of -1.0 (for ¹H) in order to illustrate more clearly the small range of amplitudes observed as compared with that observed for X-ray scattering. For the nuclides considered here, the range of scattering amplitudes for X rays is about 10^2 at $\theta = 0^\circ$ and nearly 10^3 at $\sin \theta/\lambda = 0.05 \text{\AA}^{-1}$, whereas for neutrons it is near 6, independent of scattering angle.

Appendix 6: Proof that the phase difference on diffraction is $2\pi(hx + ky + lz)$

The phase difference for the $h00$ Bragg reflection for diffraction by two atoms one unit cell apart is $(360h^\circ = 2\pi h)$ radians. However, if the atoms are only the fraction x of the cell length apart then the phase difference will be $2\pi hx$ radians. This may be extended to three dimensions to give $2\pi(hx + ky + lz)$ as the phase

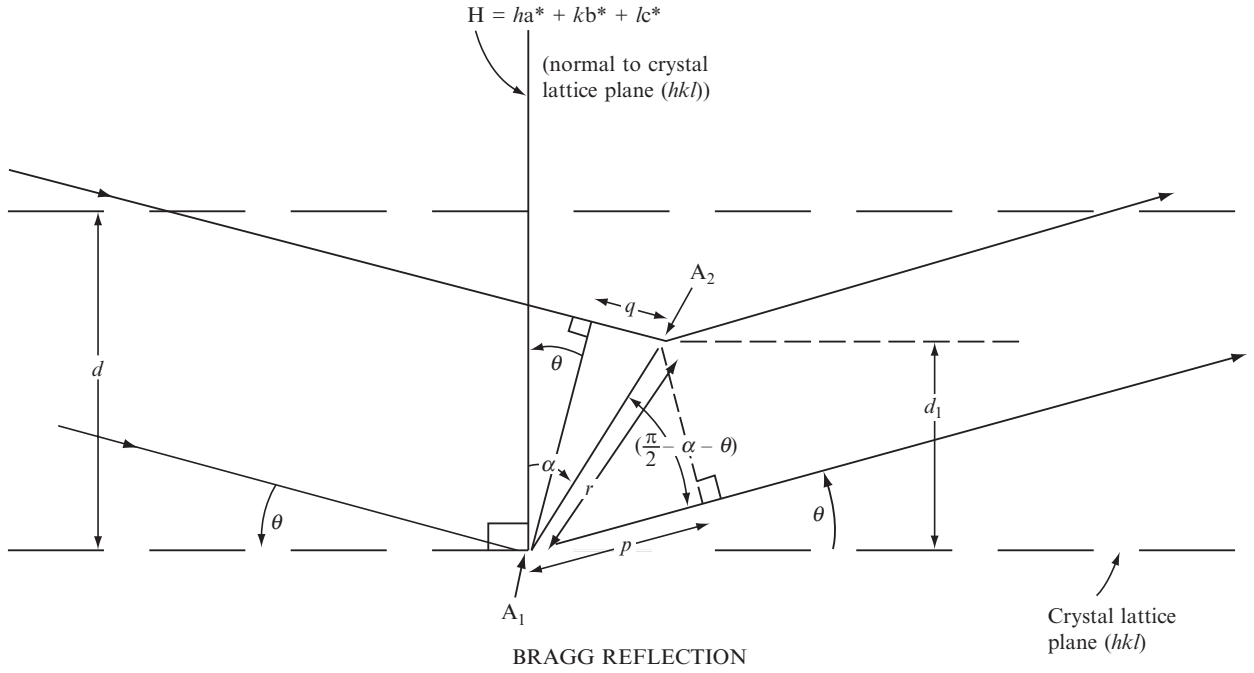


Fig. A6.1

difference for the hkl Bragg reflection for two atoms, one at $0, 0, 0$ and the other at x, y, z .

A proof is given below:

Let A_1 and A_2 be two scattering points (atoms) separated by a vector \mathbf{r} (Figure A6.1). An inspection of the angles in the region of A_1 and A_2 shows that the phase difference for the beams scattered from these atoms at the angle θ is

$$2\pi \frac{p - q}{\lambda} \text{ radians}$$

where

$$p = |\mathbf{r}| \cos \left(\frac{\pi}{2} - \alpha - \theta \right) = |\mathbf{r}| \sin(\alpha + \theta)$$

$$= |\mathbf{r}| \sin \alpha \cos \theta + |\mathbf{r}| \cos \alpha \sin \theta \tag{A6.1}$$

$$q = |\mathbf{r}| \sin(\alpha - \theta) = |\mathbf{r}| \sin \alpha \cos \theta - |\mathbf{r}| \cos \alpha \sin \theta \tag{A6.2}$$

This leads to

$$p - q = 2|\mathbf{r}| \cos \alpha \sin \theta \tag{A6.3}$$

Therefore, from Eqn. (A6.3),

$$\frac{2\pi(p - q)}{\lambda} = 2\pi \frac{2 \sin \theta}{\lambda} |\mathbf{r}| \cos \alpha \tag{A6.4}$$

But the reciprocal lattice vector (see Eqn. A3.7) is

$$\mathbf{H} = h\mathbf{a}^* + k\mathbf{b}^* + l\mathbf{c}^* \quad (\text{A6.5})$$

and is normal to the crystal lattice plane (hkl) .

$$|\mathbf{H}| = \frac{2 \sin \theta}{\lambda} \quad (\text{A6.6})$$

Since α is the angle between \mathbf{H} and \mathbf{r} , where $\mathbf{r} = a\mathbf{x} + b\mathbf{y} + c\mathbf{z}$, then, by Eqns. (A6.4) and (A6.6),

$$\frac{2\pi(p - q)}{\lambda} = 2\pi |\mathbf{H}| |\mathbf{r}| \cos(\text{angle between } \mathbf{H} \text{ and } \mathbf{r})$$

Therefore, the phase difference on diffraction is

$$\frac{2\pi(p - q)}{\lambda} = 2\pi \mathbf{H} \cdot \mathbf{r} = 2\pi(hx + ky + lz)$$

since

$$\mathbf{a}^*_i \cdot \mathbf{a}_j = \delta_{ij} \begin{cases} = 1, & i = j \\ = 0, & i \neq j \end{cases}$$

Appendix 7: The 230 space groups

Noncentrosymmetric space groups, chiral molecules (one hand only) in them. These are the 65 space groups that proteins and nucleic acids, which are chiral, crystallize in.

| | |
|--------------------|---|
| Triclinic (polar) | $P1$ |
| Monoclinic (polar) | $P2, P2_1, C2$ |
| Orthorhombic | $P222, P222_1, P2_12_12, P2_12_12_1, C222_1, C222, F222,$ $I222, I2_12_12_1$ |
| Tetragonal (polar) | $P4, P4_1, P4_2, P4_3, I4, I4_1$ |
| Tetragonal | $P422, P42_12, P4_122, P4_12_12, P4_222, P4_22_12, P4_322,$ $P4_32_12, I422, I4_122$ |
| Trigonal (polar) | $P3, P3_1, P3_2, R3$ |
| Trigonal | $P312, P321, P3_112, P3_121, P3_212, P3_221, R32$ |
| Hexagonal (polar) | $P6, P6_1, P6_5, P6_2, P6_4, P6_3$ |
| Hexagonal | $P622, P6_122, P6_522, P6_222, P6_422, P6_322$ |
| Cubic | $P23, F23, I23, P2_13, I2_13$ |
| Cubic | $P432, P4_232, F432, F4_132, I432, P4_332, P4_132,$ $I4_132$ |

Noncentrosymmetric space groups, both enantiomers in them.

| | |
|--------------|--|
| Monoclinic | Pm, Pc, Cm, Cc |
| Orthorhombic | $Pmm2, Pmc2_1, Pcc2, Pma2, Pca2_1, Pnc2, Pmn2_1, Pba2, Pna2_1, Pnn2, Cmm2, Cmc2_1, Ccc2, Anm2, Abm2, Ana2, Aba2, Fmm2, Fdd2, Imn2, Iba2, Ima2$ |
| Tetragonal | $P\bar{4}, I\bar{4}$ $P4mm, P4bm, P4_2cm, P4_2nm, P4cc, P4nc, P4_2mc, P4_2bc, I4mm, I4cm, I4_1md, I4_1cd$ $P\bar{4}2m, P\bar{4}2c, P\bar{4}2_1m, P\bar{4}2_1c, P\bar{4}m2, P\bar{4}c2, P\bar{4}b2, P\bar{4}n2, I\bar{4}m2, I\bar{4}c2, I\bar{4}2m, I\bar{4}2d$ |
| Trigonal | $P\bar{3}, R\bar{3}$ $P3m1, P31m, P3c1, P31c, R3m, R3c$ |
| Hexagonal | $P\bar{6}$ $P6mm, P6cc, P6_3cm, P6_3mc$ $P\bar{6}m2, P\bar{6}c2, P\bar{6}2m, P\bar{6}2c$ |
| Cubic | $P\bar{4}3m, F\bar{4}3m, I\bar{4}3m, P\bar{4}3n, F\bar{4}3c, I\bar{4}3d$ |

Centrosymmetric space groups, both enantiomers in them.

| | |
|--------------|--|
| Triclinic | $P\bar{1}$ |
| Monoclinic | $P2/m, P2_1/m, C2/m, P2/c, P2_1/c, C2/c$ |
| Orthorhombic | $Pmmm, Pnnn, Pccm, Pban, Pmma, Pnna, Pmna, Pcca, Pbam, Pccn, Pbcm, Pnnm, Pnmn, Pbcn, Pbca, Pnma, Cmcm, Cmca, Cmmm, Cccm, Cmma, Ccca, Fmmm, Fddd, Immm, Ibam, Ibca, Imma$ |
| Tetragonal | $P4/m, P4_2/m, P4/n, P4_2/n, I4/m, I4_1/a$ $P4/nmn, P4/mcc, P4/nbm, P4/nnc, P4/mbm, P4/mnc, P4/nmm$ $P4/ncc, P4_2/mmc, P4_2/mcm, P4_2/nbc, P4_2/nnm, P4_2/mbc, P4_2/mnm, P4_2/nmc, P4_2/ncm, I4/mmm, I4/mcm, I4_1/amd, I4_1/acd$ |
| Trigonal | $P\bar{3}1m, P\bar{3}1c, P\bar{3}m1, P\bar{3}c1, R\bar{3}m, R\bar{3}c$ |
| Hexagonal | $P6/m, P6_3/m$ $P6/nmm, P6/mcc, P6_3/mcm, P6_3/mmc$ |
| Cubic | $Pm\bar{3}, Pn\bar{3}, Fm\bar{3}, Fd\bar{3}, Im\bar{3}, Pa\bar{3}, Ia\bar{3}$ $Pm\bar{3}m, Pn\bar{3}n, Pm\bar{3}n, Pn\bar{3}m, Fm\bar{3}m, Fm\bar{3}c, Fd\bar{3}m, Fd\bar{3}c, Im\bar{3}m, Ia\bar{3}d$ |

The first letter shows the Bravais lattice type (P, A, B, C, R, I, F). Then follow the symmetry operation symbols. Monoclinic unit cells have \mathbf{b} unique. The obverse setting is used for rhombohedral R space groups (listed in trigonal).

Appendix 8: The Patterson function

The Patterson function, deduced by A. L. Patterson in 1934, is a Fourier series, analogous to Eqn. (6.1), in which the coefficients of $|F|$ are replaced

by $|F|^2$:

$$P(uvw) = \frac{1}{V} \sum_{\text{all } h,k,l} \sum |F|^2 \exp[-2\pi i(hu + kv + lw)] \quad (\text{A8.1})$$

This function was an extension from the suggestion of Zernike and Prins in 1927 that, because there may be local order in a liquid, there should be diffraction effects. For example, in a monatomic liquid such as mercury, the nearest neighbors of a given atom should never be at a distance less than two atomic radii, and seldom much more. There is more disorder for second nearest neighbors and, as the distance from the atom under consideration increases, the arrangement becomes random. Zernike and Prins showed that measurements of the diffraction pattern could be used to calculate the *average radial distribution* of matter in a liquid or powdered crystal (Zernike and Prins, 1927). The term “radial” is used because the distribution is averaged over all directions and depends only on the distance from its origin. The term “average” implies that the distribution function found represents the average of the distributions of neighbors around each of the atoms in the sample whose diffraction pattern has been used.

These ideas were extended to crystals by Patterson, who recognized the key fact that, because of the high degree of order in the crystal, the averaging over all directions could be eliminated and detailed information about both the *magnitudes* and the *directions* of the interatomic vectors (that is, both radial and angular information) could be obtained (Patterson, 1934, 1935).

It is easiest to consider first a one-dimensional case and then extend it to three dimensions. A one-dimensional electron density distribution map, $\rho(x)$, for a regularly repeating cell, length a , can be expressed by Eqn. (A8.2) and is illustrated in Figure A8.1:

$$\rho(x) = \frac{1}{a} \sum_{\text{all } h} F(h) \exp(-2\pi i h x) \quad (\text{A8.2})$$

Consider the distribution of electron density about an arbitrary point, x , in the unit cell. The electron density at a point $+u$ from x is $\rho(x+u)$. Patterson defined the weighted distribution, WD, about the point x by allotting to the distribution about x a weight that was equal to $\rho(x) dx$, the total amount of scattering material in the interval between x and $x+dx$:

$$\text{WD} = \rho(x+u)\rho(x) dx \quad (\text{A8.3})$$

It can be seen that, for a given value of dx , the weighted distribution is large *only* if both $\rho(x)$ and $\rho(x+u)$ are large, and is thus small if either or both are small.

Values of weighted distributions are summed by integrating over all values of x in the cell, keeping u constant, so that the average weighted distribution of density, $P(u)$, is

$$P(U) = a \int_0^1 \rho(x)\rho(x+u) dx \quad (\text{A8.4})$$

$$= \frac{1}{a} \int_0^1 \left[\sum_{\text{all } h} F(h) \exp(-2\pi i h x) \right] \left[\sum_{\text{all } h'} F(h') \exp[-2\pi i h'(x+u)] \right] dx \quad (\text{A8.5})$$

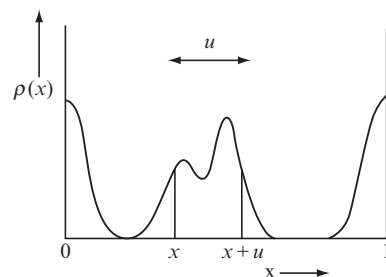


Fig. A8.1

The properties of the complex exponential are such that the integral in Eqn. (A8.5) vanishes unless $h = -h'$; consequently, Eqn. (A8.5) leads to

$$\begin{aligned} P(u) &= \frac{1}{a} \sum_{\text{all } h} F(h)F(-h) \exp(2\pi i h u) \\ &= \frac{1}{a} \sum_{\text{all } h} |F(h)|^2 \exp(2\pi i h u) \end{aligned} \quad (\text{A8.6})$$

since $a(\bar{h}) = -a(h)$ and, by Eqn. (5.18), $F(h)F(-h) = |F|^2 e^{i a} e^{-i a} = |F|^2$.

This function, $P(u)$, may be visualized by imagining a pair of calipers set to measure a distance u . One point of the calipers is set on each point in the cell in turn; since the unit cell is repeated periodically, the situation at x is repeated at $x - 1, x + 1, x + 2, \dots$. The sum of all the products of values of $\rho(x)$ at the two ends of the calipers then gives $P(u)$. As the electron density is nearly zero between atoms and is high near atomic centers, the positions of peaks in $P(u)$ correspond to vectors between atoms; in other words, large values of $\rho(x)\rho(x + u)$ give large contributions to $P(u)$.

These equations may be extended to three dimensions, letting V_c = the volume of the unit cell, so that from the definition

$$P(u, v, w) = V_c \int_0^1 \int_0^1 \int_0^1 \rho(x, y, z) \rho(x + u, y + v, z + w) dx dy dz \quad (\text{A8.7})$$

after substitution of values for ρ and integration, most terms are zero, leaving

$$P(u, v, w) = \frac{1}{V_c} \sum_{\text{all } h,k,l} |F(hkl)|^2 \exp[2\pi i(hu + kv + lw)] \quad (\text{A8.8})$$

This equation can easily be reduced to Eqn. (A8.9),

$$P(u, v, w) = \frac{F^2(000)}{V_c} + \frac{2}{V_c} \sum_{h \geq 0} \sum_{\text{all } k,l} |F|^2 \cos 2\pi(hu + kv + lw) \quad (\text{A8.9})$$

excluding $F^2(000)$

by noting that $|F|^2(hkl) = |F|^2(\bar{h}\bar{k}\bar{l})$ and

$$e^{i\phi} = \cos \phi + i \sin \phi \quad (\text{A8.10})$$

and then grouping Bragg reflections in pairs, hkl and $\bar{h}\bar{k}\bar{l}$. For every such pair, the value of ϕ for hkl is equal in magnitude and opposite in sign to that for $\bar{h}\bar{k}\bar{l}$ for each point u, v, w and thus, since $\cos \phi = \cos(-\phi)$ while $\sin \phi = -\sin(-\phi)$, the sine terms in the expansion of Eqn. (A8.8) cancel when summed over each of these pairs of Bragg reflections.

To summarize, the importance of the Patterson function is that peaks in it occur at points to which vectors from the origin correspond very closely in direction and magnitude with vectors between atoms in the crystal and that no preliminary assumptions are needed because $|F|^2$ values are independent of phase and can be derived directly from the measured intensities.

Appendix 9: Vectors in a Patterson map

A certain derivative of vitamin B₁₂ crystallizes in the space group $P2_12_12_1$ and contains Co, Cl, O, N, C, and H, with atomic numbers 27, 17, 8, 7, 6, and 1, respectively.

- (a) The expected approximate relative heights of typical peaks in the Patterson map are

| | | |
|-------|----------------|-----|
| Co-Co | 27×27 | 729 |
| Co-Cl | 27×17 | 459 |
| Cl-Cl | 17×17 | 289 |
| Co-O | 27×8 | 216 |
| Co-C | 27×6 | 162 |
| O-O | 8×8 | 64 |
| H-H | 1×1 | 1 |

(This map will then be dominated by Co-Co and Co-Cl vectors unless there are accidental overlaps of other peaks.)

- (b) Derivation of the coordinates of vectors between symmetry-related positions of any atom (for example, Co) in terms of its atomic position parameters:

- (i) Atomic positions:
 (1) x, y, z
 (2) $1/2 - x, -y, 1/2 + z$
 (3) $1/2 + x, 1/2 - y, -z$
 (4) $-x, 1/2 + y, 1/2 - z$

- (ii) Interatomic vectors between symmetry-related atoms are expected at the following positions, corresponding to the differences in coordinates of the various atomic positions:

| | | | |
|----------------|----------------|----------------|----------------------------|
| $u = 0$ | $v = 0$ | $w = 0$ | (position 1 to position 1) |
| $u = 1/2 - 2x$ | $v = -2y$ | $w = 1/2$ | (position 2 to position 1) |
| $u = 1/2$ | $v = 1/2 - 2y$ | $w = -2z$ | (position 3 to position 1) |
| $u = -2x$ | $v = 1/2$ | $w = 1/2 - 2z$ | (position 4 to position 1) |

(The vector between any other positions—for example, 2 to 4 or 4 to 3—either is identical to one of these, or is related by a two-fold axis or by a center of symmetry at the origin. Every Patterson map is centrosymmetric.)

- (c) The actual Patterson map for this crystal shows peaks at, among other positions:

| | | |
|------------|------------|------------|
| u | v | w |
| 0.00 | 0.00 | 0.00 |
| ± 0.20 | ± 0.32 | 0.50 |
| 0.50 | ± 0.18 | ± 0.20 |
| ± 0.30 | 0.50 | ± 0.30 |

- (d) A comparison of these observed peak positions with the general expectations in (b) above shows that a consistent set of coordinates for the Co

atom is $x = 0.15$, $y = 0.16$, $z = 0.10$. (See Hodgkin et al. (1957), p. 228 and Hodgkin et al. (1959), p. 306.)

Appendix 10: Isomorphous replacement (centrosymmetric structure)

$$F_T = F_M + F_R$$

M = replaceable atom or group of atoms

R = the rest of the structure

If the position of M is known, then F_M is known. If two isomorphous crystals are studied, it is assumed that the position of the remainder of the structure is the same in each. Then, for one crystal,

$$F_T = F_M + F_R$$

while for the second one,

$$F_{T'} = F_{M'} + F_R$$

* See Glusker et al.(1963).

The experimentally obtained data* consist of $|F_T|$ and $|F_{T'}|$ derived from the measured intensities. F_M and $F_{M'}$ are computed from the positions of M and M' , found by an analysis of the Patterson map. The signs of F_T and $F_{T'}$ may then be obtained, as illustrated in the following table.

| h | k | l | $ F_T $ | $ F_{T'} $ | $F_{Rb} - F_K$ (calculated from known metal position) | Sign of F for Rb computed | Sign of F for K computed |
|-----|-----|-----|---------|------------|--|-----------------------------------|----------------------------------|
| | | | Rb salt | K salt | | | |
| 0 | 1 | 1 | 16 | 20 | +33 | + | - |
| 0 | 1 | 3 | 132 | 78 | -59 | - | - |
| 0 | 2 | 1 | 63 | 70 | -11 | + | + |
| 0 | 2 | 2 | 56 | 31 | +29 | + | + |
| 0 | 4 | 0 | 102 | 50 | +61 | + | + |
| 0 | 4 | 1 | 6 | 12 | +17 | + | - |
| 0 | 5 | 2 | 9 | 16 | +21 | + | - |
| 0 | 5 | 3 | 38 | 9 | -50 | - | + |

For example, for the 0 1 1 Bragg reflection it is known, from computed values of F_{Rb} and F_K , that the difference is approximately +33 between F_T for the rubidium salt (for which the experimental value is ± 16) and F_T for the potassium salt (for which the experimental value is ± 20). This is only possible if F_{Rb} is +16 and F_K is -20, an experimental difference ($F_{Rb} - F_K$) of +36. For the 0 1 3

Bragg reflection, the calculated value of $(F_{\text{Rb}} - F_{\text{K}})$ is -59 and the experimental values are ± 132 for F_{Rb} and ± 78 for F_{K} . This difference of -59 indicates that F_{Rb} is -132 and F_{K} is -78 , an experimental difference of -54 . Some phases may be ambiguous, in which case they must then be omitted.

Appendix 11: Diffraction data showing anomalous scattering

The following values of $|F|$ for five pairs of reflections hkl and $\bar{h}\bar{k}\bar{l}$ from a crystal of potassium dihydrogen isocitrate** (Figure 10.6b), measured with chromium radiation, show the effect of anomalous scattering as a result of the presence of potassium ions in the structure. With these data the effect was sufficiently large that the absolute configuration of the sample could easily be determined. The $|F_c|$ values given here were calculated for the absolute configuration of the dihydrogen isocitrate ion given in Figure 10.6b; for the enantiomorphous form, the corresponding values for hkl and $\bar{h}\bar{k}\bar{l}$ would be reversed.

The effect of anomalous scattering on the electron density calculation was discussed by A. L. Patterson (Patterson, 1963). He showed how to correct the value of F so that the effect is removed, and in so doing, demonstrated that to use $F(\bar{h}\bar{k}\bar{l})$ or $F(hkl)$ to compute electron density is not correct when anomalous scattering is appreciable:

$$|F_{\pm}|^2 = A^2 + B^2 + (\delta_1^2 + \delta_2^2)(A_d^2 + B_d^2) + 2\delta_1(AA_d + BB_d) - 2\sigma\delta_2(AB_d - BA_d) \quad (\text{A11.1})$$

where A and B are the components of the structure factors for the normally scattering atoms and A_d and B_d are those for the anomalously scattering atoms. σ has a value of $+1$ for $F(hkl)$ and -1 for $F(\bar{h}\bar{k}\bar{l})$. $\delta_1 = f'_d/f_d$ and $\delta_2 = f''_d/f_d$. As a result two quantities were defined:

$$S = 1/2\{|F_+|^2 + |F_-|^2\} = A^2 + B^2 + 2\delta_1(AA_d + BB_d) + (\delta_1^2 + \delta_2^2)(A_d^2 + B_d^2) \quad (\text{A11.2})$$

$$D = 1/2\{|F_+|^2 - |F_-|^2\} = -2\delta_1(AB_d - BA_d) \quad (\text{A11.3})$$

Thus the average of the intensities of Bijvoet-related pairs of reflections (hkl and $\bar{h}\bar{k}\bar{l}$) may be computed by Eqn. (A11.2) and the differences may be computed by Eqn. (A11.3), provided the structure is known. If the sign of D is wrong, then the structure model has the wrong absolute configuration.

The term that should be used in computing an electron density map is

$$|F|_0 = \{S - 2\delta_1(AA_d + BB_d) - (\delta_1^2 + \delta_2^2)(A_d^2 + B_d^2)\} \quad (\text{A11.4})$$

Thus it is best, if accurate electron density maps are required, to measure diffraction data far from the absorption edge of any atom in the structure. Data measured near an absorption edge can be used to establish the absolute configuration.

** See van der Helm et al. (1968), p. 578.

| h | k | l | $ F_o $ | $ F_c $ |
|-----|-----|-----|---------|---------|
| 1 | 3 | 1 | 19.0 | 19.2 |
| -1 | -3 | -1 | 22.9 | 23.7 |
| 1 | 3 | 2 | 6.4 | 6.6 |
| -1 | -3 | -2 | 11.7 | 11.7 |
| 1 | 3 | 3 | 26.3 | 25.7 |
| -1 | -3 | -3 | 20.7 | 20.0 |
| 4 | 5 | 2 | 7.2 | 7.0 |
| -4 | -5 | -2 | 2.5 | 2.7 |
| 7 | 1 | 2 | 9.2 | 9.0 |
| -7 | -1 | -2 | 13.1 | 12.9 |

Appendix 12: Molecular geometry

Transformation from fractional coordinates to Cartesian coordinates

The fractional coordinates of atomic positions, x, y, z in a unit cell of dimensions a, b, c , α, β, γ , may be expressed in Cartesian coordinates, X, Y, Z (in units of Å), as follows:

$$\begin{aligned} X &= xa + yb \cos \gamma + zc \cos \beta \\ Y &= yb \sin \gamma + z\{c(\cos \alpha - \cos \beta \cos \gamma)/\sin \gamma\} \\ Z &= zcW/\sin \gamma \end{aligned}$$

where

$$W = \sqrt{1 - \cos^2 \alpha - \cos^2 \beta - \cos^2 \gamma + 2 \cos \alpha \cos \beta \cos \gamma}$$

The orientation of the Cartesian axes relative to the crystallographic axes is:

- A parallel to \mathbf{a} ;
- B in the \mathbf{a}, \mathbf{b} plane perpendicular to \mathbf{a} ;
- C perpendicular to A and B .

Interatomic distances

Distance A-B:

$$\begin{aligned} d_{A-B} &= \sqrt{(X_A - X_B)^2 + (Y_A - Y_B)^2 + (Z_A - Z_B)^2} \\ &= \sqrt{\Delta X_{A-B}^2 + \Delta Y_{A-B}^2 + \Delta Z_{A-B}^2} \end{aligned}$$

Interbond angles

$$\text{Angle A-B-C} = \arctan(\sqrt{1 - c_A^2}/c_A)$$

where

$$c_A = -(\Delta X_{A-B}\Delta X_{B-C} + \Delta Y_{A-B}\Delta Y_{B-C} + \Delta Z_{A-B}\Delta Z_{B-C})/d_{B-C}d_{A-B}$$

Torsion angles

$$\text{Torsion angle A-B-C-D} = \arctan(s_T/c_T)$$

where

$$s_T = (\Delta X_{AB}v_1 + \Delta Y_{AB}v_2 + \Delta Z_{AB}v_3)/d_{AB}$$

and

$$c_T = u_1v_1 + u_2v_2 + u_3v_3$$

where

$$u_1 = (\Delta Y_{AB}\Delta Z_{BC} - \Delta Z_{AB}\Delta Y_{BC})/(d_{AB}d_{BC})$$

$$u_2 = (\Delta Z_{AB}\Delta X_{BC} - \Delta X_{AB}\Delta Z_{BC})/(d_{AB}d_{BC})$$

$$u_3 = (\Delta X_{AB}\Delta Y_{BC} - \Delta Y_{AB}\Delta X_{BC})/(d_{AB}d_{BC})$$

$$v_1 = (\Delta Y_{BC}\Delta Z_{CD} - \Delta Z_{BC}\Delta Y_{CD})/(d_{BC}d_{CD})$$

$$v_2 = (\Delta Z_{BC}\Delta X_{CD} - \Delta X_{BC}\Delta Z_{CD})/(d_{BC}d_{CD})$$

$$v_3 = (\Delta X_{BC}\Delta Y_{CD} - \Delta Y_{BC}\Delta X_{CD})/(d_{BC}d_{CD})$$

Glossary

Absent Bragg reflections. (See Unobserved Bragg reflections.)

Absolute configuration. The structure of a crystal or molecule expressed in an absolute frame of reference. The configuration of a molecule or crystal is the relationship in space of the atoms within it. It is generally defined by atomic coordinates (see Atomic parameters) with respect to three independent axes, each of which has directionality; these axes provide an absolute frame of reference. Absolute configuration describes a real-space relationship and gives the actual three-dimensional structure as one would see it if it were lifted out of the viewing screen; we can immediately see it is “left handed” or “right handed.” Bijvoet and co-workers, in 1951, used the difference between $I(hkl)$ and $I(\bar{h}\bar{k}\bar{l})$ for zirconium radiation in crystals showing anomalous scattering by rubidium ions to determine the absolute configuration of sodium rubidium (+)-tartrate.

Absolute scale, scale factor. Structure amplitudes are on an absolute scale when they are expressed relative to the amplitude of scattering by a single classical point electron under the same conditions. A scale factor is required to convert measured structure amplitudes (from experiment) to absolute values. This scale factor is generally found from a Wilson plot (q.v.) or by comparison with calculated values for a model structure.

Absorption correction. (See Linear absorption coefficient.)

Absorption edge. At absorption edges the plot of absorption versus X-ray wavelength shows an abrupt drop and then rises again. These sharp discontinuities, called absorption edges, occur at energies at which the incident X rays can excite a bound electron in a particular atom to a higher vacant orbital or can eject it altogether. The inner-shell vacancy left by this electron is then filled by another electron falling from an outer shell. The energy (and hence wavelength) of this process depends on the difference in energy of the levels that this second electron has moved between.

Accuracy. Deviation of a measurement from the value accepted as true (cf. Precision).

Amorphous solid. A material without a real or apparent crystalline nature; it contains no long-range ordering of atoms. Many substances that appear superficially to be amorphous may, in fact, be composed of many tiny crystals.

Amplitude. The height of a wave measured from its mean value. For a vertically symmetric wave (such as a sinusoidal wave), it is half the peak-to-valley (maximum to minimum) displacement. The square of the amplitude gives a measure of the intensity of the wave.

Angle of incidence. The angle that a ray of light that is impacting on a surface makes with a line perpendicular to (i.e., normal to) the surface at the point of incidence. The Bragg angle, θ , which is half the angle between the direct beam and a diffracted beam, is the complement of this, and the angle of incidence is $(90^\circ - \theta)$.

Angle of reflection. The angle between a ray that is reflected by a surface and the normal to the surface at the point of reflection. (See Angle of incidence.)

Ångström unit. The unit of length used in crystal structure analyses, named after Anders J. Ångström, a Swedish spectroscopist. $1 \text{ \AA} = 10^{-10} \text{ m} = 10^{-8} \text{ cm} = 10^{-7} \text{ mm} = 10^{-4} \text{ \mu m} = 0.1 \text{ nm} = 100 \text{ pm}$.

Anisotropic. Exhibiting physical properties that are non-spherical, that is, have different values when measured along axes with different directions.

Anomalous dispersion. “Dispersion” is the passage of light through a medium, such as glass in a prism or a crystal, so that the light is separated into its component parts, that is, beams of different (rainbow) colors. The refractive index of a material is the ratio of the velocity of light *in vacuo* to its velocity when it passes through this medium. Blue light (which is shorter in wavelength than red light and which has a larger refractive index than does red light) is bent more than red light when it enters a medium. This is “normal dispersion.” If, however, the

wavelength of the light (or X rays) is near an absorption edge (q.v.) of one type of atom in the structure, there will be a large discontinuity in the curve of refractive index against wavelength. In a plot of wavelength versus refractive index the refractive index increases with wavelength and blue light is less refracted than red, the opposite of normal expectation. This is called “anomalous dispersion.” All atoms scatter anomalously to some extent, but when the wavelength is near the absorption edge of a scattering atom, anomalous dispersion will be especially strong. It will cause a phase change on scattering other than the normal value of 180° , and diffraction data will not obey Friedel’s Law (q.v.). In noncentrosymmetric crystals intensities of pairs of Bragg reflections $I(hkl)$ and $I(\bar{h}\bar{k}\bar{l})$, normally the same, will be different if a strong anomalous scatterer is present. These intensity differences can be used to determine the absolute configuration (q.v.) of the crystal and its constituent molecules.

Anomalous scattering. An effect caused by high absorption at wavelengths near an absorption edge (q.v.). In noncentrosymmetric crystals, Bragg reflections hkl and $\bar{h}\bar{k}\bar{l}$ from opposite faces (that is, in directions at 180° to one another) are caused to have different intensities, contrary to the requirement of Friedel’s Law (q.v.). These differences in intensity ($I(hkl)$ versus $I(\bar{h}\bar{k}\bar{l})$) may be used to determine the absolute configuration (q.v.) of chiral crystals (see Anomalous dispersion).

Area detector. An electronic device, such as a charge-coupled device (q.v.), for measuring the intensities of a large number of Bragg reflections at one time. It gives information on the intensity and direction of each Bragg reflection and is equivalent to electronic film.

Asymmetric unit. The smallest portion of a crystal structure from which the entire structure can be generated from the space-group symmetry operations (including translations). The asymmetric unit may consist of part of a molecule, a whole molecule, or all or part of several molecules not related by crystallographic symmetry.

Atomic displacement parameters, displacement parameters. Displacements of atoms in the unit cell from their equilibrium positions as a result of atomic vibration or disorder. Because static displacements from one unit cell to another will simulate vibrations of an atom, the term “displacement parameters” is used unless it is clear that the displacements are caused by temperature effects only, and not by static disorder.

Atomic parameters or atomic coordinates. A set of numbers that specifies the position of an atom in a crystal structure with respect to a selected coordinate system,

usually the crystal axes, and the extent of its vibration and disorder from unit cell to unit cell. Atomic coordinates are generally expressed as dimensionless quantities x , y , z (fractions of unit-cell edges, measured in directions parallel to these edges), but sometimes as lengths (with dimensions), with respect to either the axial directions of the crystal or an orthogonal Cartesian coordinate system (q.v.). Additional parameters include thermal or displacement parameters (one parameter if isotropic, six if anisotropic), and, for disordered structures, parameters that define the atomic occupancy factors.

Atomic scattering factor, scattering factor, form factor. The scattering power of an atom for X rays, f_i , is defined relative to the scattering of X rays by a single electron under the same conditions. It depends on the number of electrons in the atom (approximately the atomic number) and the angle of scattering 2θ . This scattering power, which is for an atom at rest, not vibrating, falls off as the scattering angle increases. By contrast, for neutron scattering this reduction in scattering power at higher scattering angles does not occur, because the scattering object, the atomic nucleus, is so small. Atomic scattering factors can be computed, usually as a function of the scattering angle, from theoretical wave functions for free atoms (neutral or charged). They are modified by anomalous scattering (q.v.), which occurs to some extent at all wavelengths. The value f_i is replaced by $f_i + f'_i + if''_i$ (see Chapter 10). The effect is largest if the incident-beam wavelength is near an absorption edge of the scattering atom; at most other wavelengths it is often ignored.

Automated diffractometer. A computer-controlled instrument that automatically measures and records the intensities of the Bragg reflections. It may measure Bragg reflections sequentially or may have a detector that can measure large numbers of reflections at the same time. For sequential measurement, the mutual orientations of the crystal and of the detector with respect to the source of radiation are assessed by computer from some initial diffraction data on some 20–30 selected Bragg reflections. The computer then provides an orientation matrix that specifies the orientation of the crystal and detector with respect to the X-ray beam. Electromechanical devices under computer control then drive the gears that move the crystal orienter and detector to the desired angular settings for each Bragg reflection in turn, and scan and measure the intensity and scattering angle for each $I(hkl)$; they also open and close the X-ray shutter. The newer technology now involves the use of area detectors to record large numbers of Bragg reflections simultaneously through a continuum of angular rotations, while

the data are evaluated during the collection of the data or processed at a later time.

Avogadro's number. Named after Amedeo Avogadro, who, in 1811, proposed that equal volumes of all gases at the same pressure and temperature contain the same number of molecules. Avogadro's number is the number of molecules in a gram molecule of material (its molecular weight in grams), 6.022×10^{23} per mol.

Axial lengths and angles. These are the unit-cell lengths and angles, $a, b, c, \alpha, \beta, \gamma$. They are generally reported in Å and degrees.

Axial ratios. The ratios of the axial lengths, customarily expressed with the value of b equal to unity. These ratios may be deduced from measurements of the angles between faces on a crystal, and are useful in identifying the composition of crystals.

Axis of rotation or axis of symmetry, rotation axis. When an object can be rotated by $(360/n)^\circ$ about an axis passing through it, and, as a result, give an object indistinguishable from the first, then the original object is said to possess an n -fold axis of rotation.

Azimuthal scan. The azimuth of a line is the angle between the vertical plane containing the line and the plane of the meridian. If you stood at the center of the earth, the north pole would be at an azimuthal angle of 0° , and, measuring angles clockwise from the meridian (longitude through Greenwich), east at 90° , south at 180° , and west at 270° . An azimuthal scan (also called a psi-scan or ψ -scan) of diffraction data is measured as the crystal rotates about the diffraction vector (q.v.). This scan is used to make an empirical absorption correction (q.v.) and to avoid possible errors due to double reflections (q.v.).

Bessel function. Bessel's differential equation arises in numerous problems, especially in polar and cylindrical coordinates. The solutions of this equation are called Bessel functions, named for Friedrich Bessel, a German mathematician and astronomer. These functions, which give graphs that look like damped cosine or sine waves, are available in computer mathematics libraries. They are used for structures that are best defined by polar or cylindrical coordinates, such as nucleic acids. They also appear in the probability theory that underlies direct methods.

Best plane. The plane through a group of atoms that satisfies the least-squares (see Method of least squares) criterion of planarity.

Bijvoet differences. In 1951 Johannes Martin Bijvoet and fellow crystallographers in the Netherlands demonstrated

that it is experimentally possible to determine the absolute configuration of an optically active molecule in the crystalline state from the effects of anomalous dispersion. They showed that this information is available in the differences in intensity between Bragg reflections $I(hkl)$ and $I(\bar{h}\bar{k}\bar{l})$ when the incident X rays have a wavelength near the absorption edge (q.v.) of at least one (but not all) of the atoms in the asymmetric unit of the crystal.

Birefringence. Double refraction, that is, the separation of a ray of light on passing through a crystal into two unequally refracted, plane-polarized rays of orthogonal polarizations; these are called the "ordinary ray," which obeys the normal laws of refraction, and the "extraordinary ray," which does not. This effect occurs in crystals in which the velocity of light is not the same in all directions; that is, the refractive index is anisotropic. Uniaxial crystals, such as calcite or quartz, have one direction (the anisotropy axis or optic axis) along which double refraction does not occur, and are characterized by two refractive indices; biaxial crystals have two such axes of anisotropy and three refractive indices.

Body-centered unit cell. A unit cell having a lattice point at its center ($x = y = z = 1/2$) as well as at each corner ($x = y = z = 0$ or 1).

Bragg. Father, William Henry Bragg, pioneered instrumental methods for measuring X-ray diffraction patterns. Son, William Lawrence Bragg, developed methods for analyzing the experimental data in terms of the atomic structure of the crystal. They shared the Nobel Prize in Physics in 1915 (W. L. Bragg then being only 25 years old).

Bragg reflection, reflection. Since diffraction by a crystal may be considered as reflection from a set of lattice planes (a view suggested by William Lawrence Bragg), the term "Bragg reflection" has come to be used to denote a diffracted beam. While this is correct, the term "reflection" (without the "Bragg") is also used. The more definitive term "Bragg reflection" is used in this book.

Bragg's Law or Bragg equation. Each diffracted beam is considered as a "Bragg reflection" from a family of parallel lattice planes, hkl . If the angle between the n th order of diffraction of X rays, wavelength λ , and the normal (perpendicular) to a set of crystal lattice planes is $(90^\circ - \theta_{hkl})$, and the perpendicular spacing between successive lattice planes is d_{hkl} , then

$$n\lambda = 2d_{hkl} \sin \theta_{hkl} \quad \text{Bragg's Law}$$

When X rays strike a crystal they will be diffracted when, and only when, this equation is satisfied. With this equation, W. L. Bragg first identified the integers h, k , and l of the

Laue equations with the Miller indices of the lattice planes that cause that Bragg reflection.

Bravais lattice. One of the 14 possible arrays of points repeated periodically in three-dimensional space such that the arrangement of points surrounding any one of the points is identical in every respect to that surrounding any other point in the array. They are obtained by combining the seven crystal systems (q.v.) with one of the lattice centerings, that is, P = primitive, I = body-centered, F = face-centered, and A , B , or C = single-face-centered, and eliminating equivalent results (giving 14 rather than 42 Bravais lattices). They were studied by Auguste Bravais.

Bremsstrahlung. X rays (specifically “braking radiation”) that are produced when accelerated electrons are suddenly decelerated by a collision with the electrical field of an atom in the metal target of an X-ray tube. This radiation has a continuous spectrum with respect to wavelength, and is generally considered background to characteristic X rays (q.v.).

Calculated phase angle or calculated phase. The phase angle, $\alpha(hkl)$, relative to a chosen origin, computed from the atomic positions (x , y , z) of a model structure. The equations that lead to its value are as follows:

$$\begin{aligned} A(hkl) &= \sum f \cos 2\pi(hx + ky + lz) \text{ and} \\ B(hkl) &= \sum f \sin 2\pi(hx + ky + lz) \\ F(hkl) &= A(hkl) + iB(hkl) \text{ and} \\ |F(hkl)|^2 &= [A(hkl)]^2 + [B(hkl)]^2 \\ \alpha(hkl) &= \tan^{-1}[B(hkl)/A(hkl)] \end{aligned}$$

where f includes the scattering factor and displacement factor of the atom and each summation is over all atoms in the unit cell.

Cartesian coordinate system. The three-dimensional position of a point (x , y , and z) can be located by reference to three orthogonal (mutually perpendicular) axes with units of equal length (e.g., Å or cm) along these axes. The location is defined by distances from an origin, measured parallel to these axes. (Named after René Descartes, the mathematician and philosopher.)

Cauchy–Schwarz inequality. The square of the sum of the products of two variables (a and b here) for a particular range of values is less than or equal to the product of the sums of the squares of these two variables for the same range of values:

$$|\sum ab|^2 \leq \{\sum a^2\} \{\sum b^2\}$$

In this equation each sum Σ is over the same range, e.g., from 1 to N . This equation, the result of studies by Augustin Louis Cauchy, Viktor Yakovlevich Bunyakovsky, and Karl Hermann Amandus Schwarz, is used in direct methods of phase determination (see Chapter 8).

Center of symmetry or center of inversion. A point through which an inversion operation is performed, converting an object at x , y , z into its enantiomorph at $-x$, $-y$, $-z$ if the center of inversion is at 0, 0, 0 (see Inversion).

Centrosymmetric crystal structure. A crystal structure for which the space group, and therefore the arrangement of atoms, contains a center of symmetry. When the unit-cell origin is chosen at the center of symmetry, the phase angle for each Bragg reflection is either 0° or 180° .

Characteristic X rays. X rays of definite wavelength, characteristic of the target (generally a metal) and produced when that target is bombarded by fast electrons. Characteristic X rays are emitted when an electron that has been displaced from an inner shell of the atom being excited (an atom in the target material) is replaced by another electron that falls in from an outer shell. This gives radiation of a wavelength corresponding to the difference in the energies of the two shells in the target atom.

Charge-coupled device area detector, position-sensitive detector. A position-sensitive electronic device for measuring the intensities of a large number of diffracted intensities at one time. It gives information on the direction (exact point of impact on the detector) and intensity of each diffracted beam and behaves like electronic film. It is a photoelectric radiation sensor that acts, when hit by a photon, by generating electron–hole pairs. The electric charges so formed, which are proportional to the radiation intensity at that point in space, are collected in pixels (picture elements) formed by an array of gates, and transferred by application of a differential voltage across the gates.

Chiral. A chiral object or structure cannot be superimposed (with complete equivalence) upon its mirror image (Greek: *cheir* = hand). Left and right hands provide excellent examples of chiral objects.

Chi-square. The sum of the quotients obtained from the square of the difference between the observed (x_i) and mean or averaged ($\langle x \rangle$) values of a quantity when divided by the square of its standard uncertainty (s.u.), $\sigma(x_i)$. The relationship is $\chi^2 = \{\sum (x_i - \langle x \rangle)^2\} / \sigma(x_i)^2$.

Chi-square test. A test for the mathematical fit of the distribution of chi-square to a standard frequency

distribution. This gives the likelihood that an observed distribution arose from fluctuations of random sampling rather than from systematic error. Tables of probability values (likelihoods) are available.

Cleavage. The property of many crystals of splitting readily (usually upon impact) in one or more definite directions to give smooth surfaces, always parallel to actual or possible crystal faces.

Coherent scattering. Scattering in which the incoming radiation interacts with all the scatterers in a coordinated manner so that the scattered waves have definite relative phases and can interfere with each other. The energy of the scattered photon is the same as that of the incident photon. (See also Incoherent scattering.)

Collimator. A device for producing a parallel beam of radiation.

Complex number. An expression of the form $a + ib$, where a and b are real numbers and $i = \sqrt{-1}$. The word "complex" here implies that the number is composed of two or more separable parts, that is, a and ib .

Configuration. The configuration of a molecule consists of the relationships in space of the atoms within it.

Conformation. One of the likely shapes of a molecule. Generally applied to molecules for which there is a possibility for rotation about bonds. Different rotational positions about bonds are represented by torsion angles (q.v.).

Constraints. Constraints are limits on the values that parameters in a least-squares refinement may take. They reduce the number of parameters and are mathematically rigid with no standard uncertainty. A common constraint is a reduction in the number of parameters defining a group of atoms that is being refined. This simplifies the refinement. For example, a benzene ring may be constrained to six parameters, three defining position and three defining orientation in the unit cell. Atoms in special positions may also need to be constrained so that they do not move during refinement. Constraints remove parameters and restraints add data. (Think of a dog constrained in a cage in which he fits tightly and is not able to move.) (See Restraints.)

Contact goniometer. A device for measuring angles between faces of a crystal by making direct contact with the crystal faces with two straight edges and then measuring the angle between these straight edges.

Contour map. In crystal structure analysis, this is a map showing electron or nuclear density by means of contour lines drawn at regular intervals. It resembles a

topographic map, with peaks representing areas of high electron or nuclear density. The map is drawn with contour lines at regular intervals of electron or nuclear density. (See Electron-density map.)

Convolution. One mathematical function folded with another. To calculate the convolution of the plots of two mathematical functions, we set the origin of the plot of the first function in turn on every point of the plot of the second function, multiply the value of the first function in each position by the value of the second at that point, and then the results are added together for all such possible operations. For two functions $A(x, y, z)$ and $B(x, y, z)$, the convolution of A and B at the point (u_0, v_0, w_0) is

$$c(u_0, v_0, w_0) = \int_{-\infty}^{+\infty} \int_{-\infty}^{+\infty} \int_{-\infty}^{+\infty} A(x, y, z) B(x + u_0, y + v_0, z + w_0) dx dy dz$$

Note that a crystal structure is the convolution of a crystal lattice and the contents of one unit cell.

Correlation of parameters. The extent to which two mathematical variables, such as atomic parameters, are dependent on each other. For example, position parameters of an atom that has been refined by least squares in an oblique coordinate system are correlated to an extent that is dependent upon the cosine of the interaxial angle. Parameters related by crystallographic symmetry are completely correlated. Displacement occupancy factors are often highly correlated, and this may be evident in the output of a least-squares refinement.

Crystal. A solid that contains a very high degree of long-range three-dimensional internal order of the component atoms, molecules, or ions.

Crystal class. (See Crystallographic point group.)

Crystal lattice. Crystals are solids composed of groups of atoms repeated at regular intervals in three dimensions with the same orientation. If each such group of atoms is replaced by a representative point, the collection of points so formed provides the space lattice, or crystal lattice. The meaning is specific for this arrangement of points, and the term "lattice" should not be used to denote the entire atomic arrangement.

Crystal morphology. (See Morphology.)

Crystal structure. The mutual arrangement of the atoms, molecules, or ions that are packed together in a regular way (on a crystal lattice) to form a crystal.

Crystal system. There are seven crystal systems, best classified in terms of their symmetry. They are: triclinic, monoclinic, orthorhombic, tetragonal, cubic, trigonal, and hexagonal. As a result of their symmetries they lead to the seven fundamental shapes for unit cells consistent with the 14 Bravais lattices (q.v.).

Crystallographic point group, crystal class. A point group is a group of symmetry operations that leave at least one point unmoved within an object when the symmetry operation is carried out. There are 32 crystallographic point groups (crystal classes) that contain rotation and rotatory-inversion axes ($n = 1, 2, 3, 4, 6$). The crystallographic point groups characterize the external symmetry of well-formed crystals.

Cubic unit cell. A unit cell in which there are three-fold rotation axes along all four body diagonals. All axial lengths are therefore identical by symmetry, and all interaxial angles must be 90° ($a = b = c$, $\alpha = \beta = \gamma = 90^\circ$).

Data reduction. Conversion of measured intensities, $I(hkl)$, to structure amplitudes $|F(hkl)|$ or to $|F^2(hkl)|$, by application of various factors including Lorentz, polarization, and absorption corrections (q.v.).

Database. A collection of data on a particular subject, such as atomic coordinates from crystal structure determinations. These data are readily retrievable by computer.

Defect. A crystal lattice imperfection. This may be due to impurities. A point defect is a vacancy or an interstitial atom. A line defect is a dislocation in the crystal lattice.

Deformation density. The difference between the experimental electron density in a molecule (with all its distortions as a result of chemical bonding) and the promolecule density (q.v.) (a model of the molecule with a spherical electron density around each isolated free atom). The deformation-density map contains information on chemical bonding, although this information is modified by errors in the phases and the measured intensities of the Bragg reflections and inadequacies in the calculated scattering factors of free atoms.

Deliquescence. The property that some crystals have of attracting and absorbing moisture from the surrounding atmosphere and dissolving gradually, eventually becoming a solution.

Density modification, solvent flattening. A computational method for improving phases, particularly when a unit cell contains a high proportion of solvent as do macromolecular crystals. When an electron-density map is calculated with $|F(hkl)|$ and an initial set of possible

relative phases, the map will probably be noisy if the relative phases are not very good. However, the outline of an "envelope," the protein-solvent boundary, may be evident. The overall density of atoms in aqueous areas of the crystal (involving oxygen-oxygen distances near 2.7 \AA) is lower than in the interior of the molecule (involving C-C, C-O, and C-N distances near 1.4 \AA). An "envelope" defining the approximate boundary of the molecule is determined from the electron-density map. All of the electron density outside this envelope, that is, the electron density in the solvent area, is then set to a single low value (the average for disordered water) and a new set of phases is then determined by Fourier inversion of this "solvent-flattened" map. The process is used to improve the phases and may be repeated, if necessary.

Difference synthesis or difference map. A Fourier map for which the input Fourier coefficients are the differences between measured structure factors and those calculated from a proposed structural model. Such a map will have peaks at positions in which there is not enough electron density in the trial structure, and troughs where too much is included. It is an exceedingly valuable tool both for locating missing atoms and for correcting the positions of those already present in the trial structure.

Differential synthesis. A method of refining parameters of an atom from a mathematical consideration of the slope and curvature of the difference synthesis (q.v.) in the region of each atom.

Diffraction. When radiation passes by the edges of an opaque object or through a narrow slit, the waves appear to be deflected and they produce fringes of parallel light and dark bands. This effect may best be explained as the interference of secondary waves generated in the area of the slit or the opaque object. These secondary waves, so generated, interfere with one another, and the intensity of the beam in a given direction is determined by a superposition of all the wavelets in that direction. When light passes through a narrow slit all the waves will be in phase in the forward direction. In any other direction, each secondary wave traveling in a given direction will be slightly out of phase with its neighbors by an amount that depends on the wavelength of the light and the angle of deviation from the direct beam. The shorter the wavelength, the more a wave is out of phase with its neighbor. In X-ray crystallography, the radiation is X rays and the slit is replaced by the electron clouds of atoms in a crystal which scatter the X rays. Because the crystal contains a regularly repeating atomic arrangement, the beams diffracted from one unit cell may be in phase with those from other unit cells and can reinforce each other to

produce a strong diffracted beam. The scattering from the arrangement of atoms within the unit cell will modify the intensities of these beams.

Diffraction grating. A series of close, equidistant parallel lines, usually ruled on a polished surface. Because of the regularity of the ruled lines, this grating can be used to produce diffraction spectra.

Diffraction pattern. The intensity pattern obtained when radiation is diffracted by an object that has a regular spacing with similar dimensions to that of the wavelength of the radiation.

Diffraction plane. The plane containing the incident beam, the location point of diffraction by the crystal, and the diffracted beam.

Diffraction symmetry. Symmetry in the intensities of Bragg reflections with indices (hkl) related by a change of sign (e.g., $-h, -k, -l$) or permutation (k, l, h). The diffraction symmetry must adhere exactly to one of the Laue groups; a small difference from Laue group symmetry is allowed when anomalous-dispersion effects are present.

Diffraction vector. A vector perpendicular to the lattice planes hkl causing a Bragg reflection. This vector bisects the directions of the incident and diffracted beams and lies in their plane. (See Diffraction plane.)

Diffraction pattern. An instrument for measuring the directions and intensities of Bragg reflections in the diffraction pattern of a crystal (see Automated diffractometer). For serial measurements, the required orientations of the crystal and detector with respect to the X-ray source are computed from initial data on some Bragg reflections. The orientations necessary for the measurement of all of the diffraction data are achieved by computer-directed commands to electromechanical devices that position the components of the instrument at the required settings. Alternatively, an area detector may be used that can measure many Bragg reflections at one time.

Diffuse scattering. Halos or streaks that appear around or between intense Bragg reflections and indicate the presence of disorder in the structure (static disorder), or high thermal motion of atoms (dynamic disorder).

Dihedral angle. The dihedral angle between two planes is the angle between the planes, often defined (with the same result) as the angle between the normals (perpendiculars) to these planes. If the planes, with an angle θ between them, have equations

$$a_1x + b_1y + c_1z + d_1 = 0 \text{ and } a_2x + b_2y + c_2z + d_2 = 0$$

then

$$\cos \theta = \frac{a_1a_2 + b_1b_2 + c_1c_2}{\sqrt{(a_1^2 + b_1^2 + c_1^2)(a_2^2 + b_2^2 + c_2^2)}}$$

Direct methods or direct phase determination. A method of deriving phases of Bragg reflections by consideration of probability relationships among the phases of the more prominent Bragg reflections. These relationships come from the conditions that the structure is composed of atoms (giving independent, isolated peaks in the electron-density map) and that the electron density must be positive or zero everywhere (not negative). Only specific values for the relative phases of Bragg reflections are consistent with these conditions.

Direct space. There are two types of lattices important in crystallography: the crystal lattice, commonly called the direct lattice, and the reciprocal lattice. Each of these two lattices can be thought of as existing in a space defined by its coordinate system. Direct space is the space where the atoms of the crystal structure reside. Reciprocal space is the space where the diffraction intensities reside.

Discrepancy index. (See R value.)

Dislocation. A discontinuity in the otherwise regularly periodic three-dimensional structure of a crystal resulting in a defect, often an imperfect alignment between lattice rows. There are two common varieties of dislocations: edge and screw dislocations. Edge dislocations form where only part of one plane of atoms or molecules exists in the crystal and, because atoms or molecules are missing, causes stress as a result of distortions of nearby planes. These dislocations can move through the crystal as a result of shear stress applied perpendicular to the dislocation line. On the other hand, screw dislocations also have a dislocation line, but a helical path is formed around it. This dislocation involves a displacement of rows of atoms or molecules along a plane.

Disordered crystal structure. Lack of regularity in the internal arrangement within a crystalline material. For example, there may not be an exact register of the contents of one unit cell with those of all others. Such disorder may be revealed by large displacement parameters in the least-squares refinement or by the presence of diffuse scattering, either as halos or streaks, around intense Bragg reflections.

Dispersion. Variation, as a function of wavelength, in the velocity of light in a material (such as a crystal) and hence variation in the refractive index (q.v.) of the medium. For example, the spreading of white radiation by a prism or

grating into a colored (rainbow-type) beam is due to dispersion of light. The variation of velocity with wavelength is usually smooth, but at strongly absorbed wavelengths of the incident radiation the curve may be discontinuous, leading to anomalous dispersion (q.v.).

Displacement parameters. (See Atomic displacement parameters.)

Distribution of intensities, intensity distribution. The number of intensities in selected ranges of the diffraction pattern and their overall variation. Intensities from a noncentrosymmetric crystal tend to be clustered more tightly around their mean value than do those from a centrosymmetric one. This forms the basis for one test for the presence or absence of a center of symmetry in the crystal.

Domain. A small region of a crystal containing a completely oriented structure.

Double reflection. X rays that are diffracted by one set of lattice planes may then be diffracted by another set of planes that, by chance, are in exactly the right orientation for this. The twice-reflected resultant beam emerges in a direction that corresponds to a single Bragg reflection from a third set of planes, whose Miller indices are the sums of the indices of the two sets of planes producing the Bragg reflection. This double reflection that is, by chance, traveling in the same direction as an original singly diffracted beam will enhance or weaken the intensity of the latter. The effect may even cause an ambiguity in the space group determination if a systematically absent Bragg reflection gains intensity by it. It can generally be eliminated by reorienting the crystal or by changing the wavelength of the incident X rays. The effect is also called the “Renninger effect” after its discoverer, Moritz Renninger.

Dynamical diffraction. Diffraction theory in which the modification of the primary beam on passage through the crystal is important. The mutual interactions of the incident and scattered beams are taken into account. This is important for perfect crystals and for electron diffraction by crystals.

E-map. A Fourier map (equivalent to an electron-density map) with phases derived by “direct methods” and normalized structure factors (q.v.) $|E(hkl)|$, replacing $|F(hkl)|$ in the Fourier summation. Since the $|E(hkl)|$ values correspond to sharpened atoms (with no fall-off as a function of $\sin \theta/\lambda$), the peaks on the resulting map are more easy to identify than those in an electron-density map computed with $|F(hkl)|$ values.

E-values. (See Normalized structure factors.)

Efflorescence. A change in the surface of a crystal that results in a powder as a result of loss of water (or some other solvent) of crystallization on exposure to air.

Elastic scattering. When radiation is scattered elastically, there is no exchange of energy or momentum between the incoming radiation and the scatterer, so that there is no change in wavelength between the incident (incoming) and scattered (outgoing) radiation. This is the type of scattering described in this book.

Electron density. The number of electrons per unit volume (usually per cubic Å).

Electron-density map. A representation of the electron density at various points in a crystal structure. Electron density is expressed as the concentration of electrons per unit volume (in electrons per cubic Å) and is highest near atomic centers. The map is calculated using a Fourier synthesis—that is, a summation of waves of known amplitude, frequency, and relative phase. The input consists of $|F(hkl)|$ and $a(hkl)$. The three-dimensional map can be viewed and manipulated on a computer screen. Summation of the electron-density values (in electrons per cubic Å) over the volume expected to be occupied by one atom will give the atomic number (the total number of electrons in that volume) of the peak; this calculation, however, depends on good scaling and a near-perfect model.

Enantiomorph. A molecule or crystal that is not identical to its mirror image when superimposed on it.

Epitaxy. The oriented overgrowth of one crystalline material on the surface of another. Generally there is some match of periodicity between the two.

Epsilon factor, ϵ . This is a factor used in computing normalized structure factors (E-values, q.v.) that takes into account the fact that, depending on which of the 230 space groups the crystal belongs to, there may be certain groups of Bragg reflections in areas of the reciprocal lattice that will have an average intensity greater than that for the general Bragg reflections. The ϵ factor is used to correct for these differences.

Equivalent positions. The complete set of atomic positions produced by the operation of the symmetry elements of the space group upon any general position, x, y, z , in the unit cell.

Equivalent reflections. There are eight measurements for each h, k, l , of each Bragg reflection corresponding to combinations of positive or negative values of each h, k, l . Those that are equivalent by the symmetry of the crystal have (within experimental error) identical intensities. For high-symmetry crystals, other Bragg reflections

may also be equivalent, e.g., hkl , klh , and lkh for cubic crystals. In the absence of anomalous dispersion (q.v.), $|F(hkl)| = |F(\bar{h}\bar{k}\bar{l})|$.

Estimated standard deviation. (See Standard uncertainty.)

Euler's formula. $e^{i\theta} = \cos \theta + i \sin \theta$.

Eulerian angles. The three successive angles of rotation needed to transform one set of Cartesian coordinates into another or describe the orientation of a rigid body in terms of a defined set of axes. They are named after the Swiss mathematician Leonhard Euler.

Ewald sphere, sphere of reflection. A geometric construction for considering conditions for diffraction by a crystal in terms of its reciprocal lattice rather than its direct (real) crystal lattice. It is a sphere, of radius $1/\lambda$ (for a reciprocal lattice with dimensions $d^* = \lambda/d$), drawn with its diameter along the incident beam. The origin of the reciprocal lattice is positioned at the point at which the incident beam emerges from the Ewald sphere. The crystal (and its reciprocal lattice) can then be rotated. Whenever a reciprocal lattice point P touches the surface of the Ewald sphere, the conditions for a diffracted beam are satisfied. A Bragg reflection with the indices of that reciprocal lattice point P will result. Thus, for any orientation of the crystal relative to the incident beam, it is possible to predict which reciprocal lattice points, and thus which planes in the crystal, will be in a "reflecting position" (in the sense used by Bragg).

Extinction. An effect that reduces the intensity of a Bragg reflection to less than the expected value. This means that the X-ray beam has been weakened as it passes through the crystal. Extinction is evidenced by a tendency for $|F_o|$ to be systematically smaller than $|F_c|$ for very intense Bragg reflections. Primary extinction occurs when the incident beam passes through a single block of a perfect crystal. Part of the beam may be reflected twice so that it returns to its original direction but is out of phase with the main beam, thus reducing the intensity of the latter. However, when a crystal has a mosaic structure (q.v.), part of the incident beam will be diffracted by one mosaic block and therefore may not be available for diffraction by a following block. As a result the second block contributes less than expected to the diffracted beam. This is called secondary extinction. Extinction of this kind can sometimes be reduced by dipping the crystal in liquid nitrogen, thereby increasing its mosaicity.

Face-centered unit cell. A unit cell with a lattice point at the origin and at the center of a face. If all faces are cen-

tered, the designation is F ; if only faces perpendicular to the a axis are centered, the description is A (in which case the face-centered atom lies in the bc plane). Analogous conditions pertain to B and C .

Faces of a crystal. The flat, smooth surfaces of a crystal that intersect with other faces giving sharp edges. They show symmetrical relationships that may reveal the point-group symmetry (see Point group) of the internal structure of the crystal.

Figure of merit. A numerical quantity used for indicating comparative effectiveness. In crystallographic studies it is used to indicate an estimate of the average precision in the selection of phase angles. It is particularly used in protein crystallography where phase angles are derived by isomorphous replacement methods.

Film scanner. A device for measuring the intensities of spots on an X-ray diffraction photograph. This is done by a light beam that is caused to scan the photograph systematically. The intensity of the beam transmitted through the film is recorded for each point on the film.

Filter. A semitransparent material that absorbs some or all of the radiation passing through it. It is possible to choose appropriate filters with different wavelength absorptivities to select a narrow wavelength range.

Focusing mirror system. Two bent metal mirrors that deflect the X-ray beam and produce a small, intense beam with a narrow angular divergence, a uniform beam profile, and a low background intensity. They are useful for experiments involving crystals with large unit cells.

Form factor. (See Atomic scattering factor.)

Fourier analysis. The breaking down of a periodic mathematical function into its component cosine and sine waves (harmonics), which have specific amplitudes and frequencies. The procedure was initiated by Jean Baptiste Joseph Fourier, a French mathematician and physicist.

Fourier map. A map computed for a periodic function by addition of waves of known amplitude, frequency, and relative phase. The term is generally used for an electron-density or difference electron-density map.

Fourier synthesis or Fourier series. A method of summing waves (such as scattered X rays) to obtain a periodic function (such as the representation of the electron density in a crystal). It is a mathematical function $f(t)$ that is periodic with a period T (so that $f(t + T) = f(t)$), and is represented by a sum of sine and cosine terms (an infinite

series) of the form

$$f(t) = a_0/2 + a_1 \cos 2\pi(t/T) + a_2 \cos 2\pi(2t/T) \\ + \dots + b_1 \sin 2\pi(t/T) + b_2 \sin 2\pi(2t/T) + \dots$$

The Fourier theorem states that any periodic function may be resolved into cosine and sine terms involving known constants. Since a crystal has a periodically repeating internal structure, this can be represented, in a mathematically useful way, by a three-dimensional Fourier series, to give a three-dimensional electron-density map. In X-ray diffraction studies the magnitudes of the coefficients are derived from the intensities of the Bragg reflections; the periodicities of the terms are derived from the Miller indices h , k , l of the Bragg reflections, but the relative phases of the terms are rarely determined experimentally.

Fourier transform. A mathematical procedure used in crystallography to interrelate the electron density and the structure factors. In X-ray diffraction the structure factor, F , is related to the electron density, ρ , by

$$F = \int_{-\infty}^{\infty} \rho e^{i\phi} dV_c \text{ and, conversely, } \rho = (1/V_c) \sum F e^{-i\phi}$$

summing for all Bragg reflections. In these equations, $\phi = 2\pi(hx + ky + lz)$, and V_c is the volume of the unit cell. Summation replaces integration in the latter equation because the diffraction pattern of a crystal is observed only at discrete points. F is the Fourier transform of ρ , and ρ is the inverse Fourier transform (because of the negative sign) of F . (Note that $e^{ix} = \cos x + i \sin x$). See Glusker et al. (1994), p. 204, for a detailed worked-out example of a Fourier transform. Most such calculations are now done by computer.

Fractional coordinates. Coordinates of atoms expressed as fractions of the unit-cell lengths a , b , and c (see Atomic parameters).

Fraunhofer diffraction. Diffraction observed with parallel incident radiation, as in the diffraction by slits described in Chapter 3. Named after Joseph von Fraunhofer.

Friedel's Law. This law, named after Georges Friedel, states that $|F(hkl)|^2$ values of centrosymmetrically related Bragg reflections are equal (even for an acentric crystal structure): $|F(hkl)|^2 = |F(\bar{h}\bar{k}\bar{l})|^2$. This law holds only under conditions where anomalous scattering (q.v.) can be ignored.

Gaussian distribution. In many kinds of experiments repeated measurements follow a Gaussian or normal error distribution, which is a probability density function,

named for Carl Friedrich Gauss, a German mathematician and scientist. It is a symmetrical bell-shaped curve of the form $y = A \exp(-x^2/B)$, where x is the deviation of a variable from its mean value and $\sigma^2 = B/2$ is its variance (the square of its standard uncertainty, s.u.). 68% of values lie within 1 s.u. of the mean, 95% lie within 2 s.u., and 99.7% within 3 s.u.

Geiger counter. A discharge tube filled with inert gas that can briefly conduct electricity if ions have been produced in the gas by ionizing radiation. The conduction is amplified by the gas tube and the amplified effect can then be detected electronically. This device, invented by Johannes (Hans) Wilhelm Geiger and improved with assistance from Walther Müller, can count radiation events but cannot provide the identities of the types of radiation being counted.

Glide plane. A glide plane involves reflection across the plane combined with translation in a direction parallel to the plane. It is designated by a , b , or c if the translation is, respectively, $a/2$, $b/2$, or $c/2$, by n if the translation is $(a+b)/2$, $(a+c)/2$, or $(b+c)/2$, i.e., halfway along one of the face diagonals, and by d if the translation is $(a+b)/4$, $(b+c)/4$, $(c+a)/4$, or $(a+b+c)/4$.

Goniometer. An instrument for measuring angles, such as those between the faces of a crystal. (See Contact goniometer and Reflecting goniometer.)

Goniometer head. A device for orienting (by movable arcs) and aligning (by translational motion) a crystal ready for diffraction studies. The crystal, mounted on the goniometer head, is adjusted so that it is always in the center of the collimated X-ray or neutron beam.

Group (mathematical). A collection or set of symmetry elements that obeys the following conditions. One element must be the identity element. The product of any two elements must also be an element. For every symmetry element in the group there must be another that is its inverse, so that when the two are multiplied together the identity element is obtained.

Habit of a crystal. The appearance of a crystal, as seen in the relative development of different faces.

Harker-Kasper inequalities, inequality relationships. Space-group-dependent inequalities among unitary structure factors (q.v.) that allow for the determination of the phases of certain intense Bragg reflections in a centrosymmetric crystal. These provided, in 1947, one of the earliest successful methods for solving the phase problem by direct methods. Named for David Harker and John Kasper.

Harker sections. Certain areas or projections of the Patterson map that contain many vectors between space-group-equivalent atoms. For example, if there are atoms at both x and $x + 1/2$ then the Patterson map will contain information on them in the Harker section at $u = 1/2$.

Heavy-atom derivative of a protein. The product of soaking a solution of a salt of a metal of high atomic number into a crystal of a protein. Many protein crystals contain aqueous channels that permit the interaction of a heavy-atom compound with functional groups of the protein. The heavy atom must be substituted in only one (or a few) ordered position(s) per molecule of protein, and the unmodified crystal and its heavy-atom derivative must be isomorphous. Then the isomorphous replacement method (q.v.) can be used to determine the phases of the Bragg reflections.

Heavy-atom method. A method of deriving phase angles in which the phases calculated from the position of a heavy atom are used to compute the first approximate electron-density map, from which further portions of the structure are recognizable as additional peaks in this map.

Hexagonal unit cell. A unit cell containing a six-fold rotation axis parallel to one axis (arbitrarily chosen as c) and also two-fold rotation axes perpendicular to c . These symmetry relations dictate that the lengths of a and b should be identical, that the angle between a and b is 120° , and that the other two angles are 90° ($a = b$, $\alpha = \beta = 90^\circ$, $\gamma = 120^\circ$).

Homometric structure. A crystal structure with a uniquely different arrangement of atoms from another crystal structure, but having the same sets of interatomic vectors, and hence the same Patterson map (see Patterson function).

Identity operation. A symmetry operation that leaves apparently totally unchanged anything upon which it operates.

Image plate. A detector surface that behaves like photographic film and can be used to store X-ray intensities as latent images in the form of color centers. The stored image is scanned by laser light to extract data. The image plate is erasable and can be used many times. It is more sensitive than photographic film and useful because intensities can be retrieved electronically.

Imperfect crystal. An ideally imperfect crystal is composed of small mosaic blocks that are small but are not precisely aligned with each other. An imperfect crystal ideally shows no primary and usually very little secondary extinction (see Extinction).

Improper symmetry operation, symmetry operation of the second kind. Any symmetry operation (q.v.) that converts a chiral object into its enantiomorph (that is, a right-handed object into a left-handed object). Such operations include mirror planes, glide planes, centers of symmetry, and rotation-inversion axes.

Incoherent scattering. Scattering in which the incoming radiation interacts independently with each scatterer. The scattered waves have random, unrelated phases.

Indices. Indices are used to describe the faces of a crystal and the orders of diffraction—that is, to refer to a specific crystal face or Bragg reflection (using indices h, k, l) (see Miller indices).

Inelastic scattering. With inelastic scattering of X rays by electrons or of neutrons by nuclei, there is an exchange of energy and momentum on impact, resulting in a small wavelength (energy) change for the X rays or neutrons.

Inequality. A mathematical statement that the value of one expression is not equal to the value of another expression. The expression that is greater is usually specified.

Inequality relationships. (See Harker–Kasper inequalities.)

Integrated intensity. The total intensity measured at the detector as a Bragg reflection is scanned. The intensity may be scanned over one, two, or three dimensions.

Intensity distribution. (See Distribution of intensities.)

Interference. The mutual effect of two waves traveling in the same direction on each other. If one wave is in phase with another, the second wave enhances the intensity of the first. The interference is then said to be “constructive.” If they are partially or totally out of phase with each other, the intensity will be decreased and the interference will be described as “destructive.”

Inversion. Conversion of an object into its enantiomorph by projecting it along a line through a center of symmetry (also called a center of inversion) and extending it an equal distance beyond this center. If the center of symmetry is at the origin $(0, 0, 0)$, every point x, y, z , after passing through this center, becomes $-x, -y, -z$.

Isomorphism. Similarity of crystal shape, unit-cell dimensions, and structure between two substances of similar (but not identical) chemical composition (for example, when one atom has a different atomic number in the two structures). Ideally, the substances are so closely similar that they can generally form a continuous series of solid solutions.

Isomorphous replacement method. A method for deriving phases by comparing the intensities of corresponding Bragg reflections from two or more isomorphous crystals (such as heavy-atom derivatives). If the locations in the unit cell of those atoms that vary between each isomorph have been found, for instance from a Patterson map, then the phase of each Bragg reflection can be assessed if a sufficient number of isomorphs is studied (at least two if the structure is noncentrosymmetric).

Isotropic. Exhibiting properties that are the same in all directions throughout a material of interest.

Isotropic displacement factor. An atomic displacement parameter (q.v.) that represents an equal amplitude of vibration or displacement in all directions through the crystal. At the beginning of a least-squares refinement of a structure, all atoms are considered to have isotropic displacement parameters but in the later stages, anisotropic displacement parameters are usually assigned to appropriate atoms.

Kinematical diffraction. Diffraction theory in which it is assumed that the incident beam only undergoes simple diffraction on its passage through the crystal. No further diffraction occurs that would change the beam direction after the first diffraction. This type of diffraction is considered in this book. (See Dynamical diffraction.)

Lagrange multiplier. An artificial variable used in least-squares calculations that is introduced in order to find the maximum or minimum of a function that is subject to constraints. Named after Joseph Louis Lagrange.

Lattice planes. Planes through at least three non-colinear crystal lattice points.

Laue class or Laue symmetry. Symmetry in the intensities of the diffraction pattern beyond that expected by Friedel's Law (q.v.), named for Max Theodor Felix von Laue, a German physicist. The Laue symmetry of the diffraction pattern of a crystal is the point-group symmetry of the crystal plus a center of symmetry. There are the 11 Laue groups, obtained by adding a center of symmetry (if absent) to the 32 crystallographic point groups (q.v.).

Laue equations. Equations that, like the Bragg equation, express the conditions for diffraction in terms of the path differences of the scattered waves. The path differences must be an integral number of wavelengths for diffraction (that is, reinforcement) to occur. This condition must be true simultaneously in three dimensions.

Laue photograph. Diffraction photograph produced by sending a beam of X rays that has a wide range of

wavelengths ("white" X rays) along a principal axis of a stationary crystal. It demonstrates well the diffraction symmetry.

Law of Constancy of Interfacial Angles. In all crystals of a given type from a given compound, the angles between corresponding faces have a constant value. This law, of course, applies to only one particular form of a polymorphous crystalline material. Interfacial angles are measured with a goniometer (contact or reflecting) (q.v.).

Law of Rational Indices. A rational number is an integer or the quotient of two integers. The Law of Rational Indices, first proposed by Haüy in 1784, states that all of the faces of a crystal may be described, with references to three non-colinear axes, by three small whole numbers. (See Miller indices.)

Layer line. When a crystal is rotated or oscillated about a principal axis of a crystal, the diffraction spots on a cylindrical film surrounding the crystal are arranged in a series of straight lines called layer lines. They are perpendicular to the axis of rotation.

Least-squares method. (See Method of least squares.)

Libration. A form of rigid-body vibrational motion that may be described as a vibration along an arc rather than along a straight line.

Linear absorption coefficient, absorption correction. A factor to correct for the reduction in intensity of X rays as a result of absorption when the beam passes through a crystal. It is the ratio of the intensities of X rays entering and leaving a crystal of thickness t . This ratio is $\exp(\mu t)$, where μ is the linear absorption coefficient of the crystal (with units of cm^{-1}); it is a function of the atomic composition of the crystal and the wavelength of the X rays.

Linear equation. An equation that uses only constants or the product of a constant with the first power of a single variable, for example $y = ax + b$ or $d = ax + by + cz$.

Liquid crystal. A substance, such as *para*-azoxyanisole, that has observable optical anisotropy, as does a crystal, but behaves in other ways as a liquid. Thus the term refers to a state of matter with structural order intermediate between that of normal liquids and of crystalline solids.

Lorentz factor. A correction factor used in the reduction of intensity diffraction data to $|F(hkl)|^2$ values that takes into account the time that it takes for a given Bragg reflection (represented as a reciprocal lattice point with finite size) to pass through the surface of the Ewald sphere (q.v.). The value of this Lorentz factor depends on the scattering angle and on the geometry of the measurement of the

Bragg reflection. For a standard four-circle diffractometer the Lorentz factor is $(1/\sin 2\theta)$.

MAD phases. MAD = multiwavelength anomalous dispersion. A crystal containing highly anomalous scatterers, such as heavy atoms in a protein, is used to collect diffraction data at several carefully chosen X-ray wavelengths. The scattering factor for the heavy atom varies for data measured near and far from its absorption edge. As a result, sufficient information may be obtained from these data sets to determine phases and solve the crystal structure. The heavy atom may be a metal or metal complex. This method works well when, for example, sulfur is replaced by selenium in a protein structure.

Method of least squares, least-squares method. A statistical method for obtaining the best fit of a large number of observations to a given equation. This is done by minimizing the sum of the squares of the deviations of the experimentally observed values from those values calculated with the equation to be fitted. The individual terms in the sum are usually weighted to take into account their relative precision. In crystal structure analyses, atomic coordinates and other parameters are used to calculate values of $|F(hkl)|$, and these calculated values may be fitted by the least-squares method to the appropriate experimentally measured structure factors (so that the sum of the squares of their deviations is minimized). Ideally, there should be at least ten experimental measurements for each parameter to be determined. In a similar way, the least-squares criterion can be applied to the computation of a plane through a group of atoms and to many other geometrical problems.

Miller–Bravais indices. In the hexagonal lattice (c unique), there are three axes perpendicular to c inclined at 120° to each other. Therefore four indices, $hkil$, rather than the usual three Miller indices, hkl , are used in this hexagonal case, where $i = -(h + k)$.

Miller indices. A set of three integers (h , k , and l) that identifies a face of a crystal, a set of lattice planes, or a particular order of Bragg reflection from these planes. They are named for William Hallows Miller, a British mineralogist. For sets of lattice planes with Miller indices h , k , and l , the plane nearest the origin makes intercepts a/h , b/k , and c/l with the unit-cell axes a , b , and c . The “Law of Rational Indices” (q.v.) states that the indices of the faces of a crystal are usually small integers, seldom greater than three. The importance of the Bragg equation is that it identifies the integers h , k , l that specify the “order” of diffraction in the Laue equations with the Miller indices of the lattice planes causing the “Bragg reflection.”

Minimum function. A method of analyzing a Patterson map that involves setting the origin of the Patterson map in turn on the known positions of certain atoms, and then recording the minimum value throughout the map for all of these superpositions. The resulting three-dimensional map, a minimum-function map, should contain an indication of additional atoms in the crystal structure.

Mirror plane. A mirror plane converts an object into its mirror image. This image lies as far behind the mirror plane as the original object lies in front of it. If the mirror plane is perpendicular to b , it converts a chiral object at x, y, z into its enantiomorph (q.v.) at $x, -y, z$.

Modulated structure. A regular structure that is modified by a periodic or partially periodic perturbation. This is revealed by additional halos or spots around Bragg reflections in the diffraction pattern.

Molecular replacement method. The use of rotation and translation functions (q.v.), of noncrystallographic symmetry (q.v.), or of structural information from related structures to determine a protein crystal structure. The method is primarily used for macromolecules. It is used when a new investigation involves a protein or other large molecule that is similar to one for which the atomic coordinates are already available. The Patterson function is used to compare the relative orientations and positions of the two molecules, giving a rotation matrix and a translation vector between them. From these, a model of the new structure is available for refinement.

Monochromatic. Consisting of radiation of a single wavelength.

Monochromator. An instrument used to select radiation of a single wavelength. Some monochromators are crystals, such as graphite crystals, and an intense Bragg reflection from the crystal is selected as the new incident beam for diffraction studies. Gratings may also be used. Often monochromator crystals are bent or even doubly bent (for example, silicon crystals at a synchrotron source). The beam exiting the monochromator is the incident beam for diffraction studies.

Monoclinic unit cell. A unit cell in which there is a two-fold rotation axis parallel to one unit-cell axis (usually chosen as \mathbf{b}); as a result there are no restrictions on the axial ratios, but $\alpha = \gamma = 90^\circ$.

Morphology, crystal morphology. The shape or form of a material. With crystals, a description of the crystal faces and the angles between them can often be used for identification.

Mosaic structure or mosaic spread. A measure of the degree of orientational inhomogeneity in a particular crystal. Bragg's Law (q.v.) implies that X-ray diffraction occurs only when the orientation of the crystal with respect to the incident beam exactly satisfies the Bragg equation, $n\lambda = 2d \sin \theta$. In practice, however, diffraction is appreciable over several tenths of a degree around the Bragg angle because the crystal is composed of a mosaic of tiny blocks of unit cells differing slightly in orientation. The misalignment of these blocks of unit cells is small, of the order of 0.2° to 0.5° for most crystals. (See Extinction.)

Mother liquor. The solution in which the crystals under study were grown. If the crystal is not stable in air, as for a protein, it is maintained in a capillary in contact with its mother liquor during data collection. An alternative to capillary mounting is freezing. Most protein data sets are now measured at 100 K. This reduces radiation damage (q.v.) and keeps the mother liquor in place.

Multiple Bragg diffraction. Further diffraction of a Bragg reflection by a second set of lattice planes. This occurs when *two reciprocal lattice planes lie simultaneously on the surface of the Ewald sphere*. It affects the intensity of the Bragg reflection, and a detailed analysis of the effect can lead to some phase information. (See Double reflection.)

Multiple isomorphous replacement. When heavy-metal compounds are bound to a protein in a crystal they perturb the diffraction pattern. This gives information on possible values for the phase angle if at least two heavy-atom derivatives have been studied.

Neutron diffraction. Neutrons of wavelengths near 1 \AA can be used for diffraction by crystals. Neutrons are scattered by atomic nuclei, but their scattering factors are not a regular function of the atomic number of the scattering atom. Therefore their diffraction data give information that complements that from X-ray diffraction. The location of deuterium atoms (replacing some of the hydrogen atoms in a structure) by neutron diffraction is much more precise than for X-ray diffraction. This is because the neutron scattering of deuterium is similar to that of carbon, while, by contrast, the X-ray scattering of both hydrogen and deuterium is very small. Larger crystals are required currently for neutron diffraction than for X-ray diffraction studies.

Noncentrosymmetric structure. A crystal structure with no center of symmetry in its atomic arrangement. The phase angle of most Bragg reflections may have any value between 0° and 360° (0 and 2π radians). An electron-density map calculated with relative phases of a trial structure will generally show the features of the trial structure even if this structure is partially wrong. However,

some features of the correct structure may also appear in the electron-density map.

Noncrystallographic symmetry. Local symmetry within the asymmetric unit of a crystal structure that is not accounted for by the space-group symmetry. For example, the asymmetric unit of a crystalline protein may contain a dimer whose two subunits may have identical molecular structures but, since they are not related by crystallographic symmetry, may have different environments. This noncrystallographic symmetry in macromolecules can be used as an aid in structure determination.

Nonlinear optics. In linear optics light, as it passes through a material, may be deflected or delayed but its wavelength remains unchanged. In nonlinear optics the dielectric polarization does not correspond linearly to the electric field of the light. Now that intense sources of light, such as lasers, are available, these effects are of technological use. An interesting effect is second-harmonic generation, or frequency doubling, in which light with half the wavelength is generated on passage through a non-centrosymmetric crystal. It can be used to test for a center of symmetry in the structure, in which case no frequency doubling is observed.

Normal equations. Any set of simultaneous equations involving experimental unknowns and derived from a larger number of observational equations in the course of a least-squares adjustment of observations. The number of normal equations is equal to the number of parameters to be determined.

Normalized structure factors, E-values. The ratio of the value of the structure amplitude, $|F(hkl)|$, to its root-mean-square expectation value. It is denoted by $|E(hkl)| = |F(hkl)|/(\epsilon \Sigma f_j)^{1/2}$, where $(\Sigma f_j)^{1/2}$ is the root mean square scattering factor, corrected for thermal motion and disorder (see Epsilon factor for a definition of ϵ).

Nucleation of crystals. The action of a tiny seed crystal, dust particle, or other "nucleus" in starting a crystallization process. An example is provided in the seeding of a cloud with crystalline material (silver iodide, which has almost the same unit-cell dimensions as ice) so that ice crystals will be formed that may act as rainmakers.

Observational equation. An equation expressing a measured value as some function of one or more unknown quantities. Observational equations are reduced to normal equations during the course of a least-squares refinement.

Occupancy factor. A parameter that defines the partial occupancy of a given site by a particular atom. It is most frequently used to describe disorder in a portion of a

molecule, or for describing nonstoichiometric situations—for example, when a solvent molecule is being lost to the atmosphere.

Omit map. A difference map in which part of the structure in a specific area of the unit cell is omitted from the phasing calculation. The resulting electron-density map is then examined to check if the proposed structure can still be recognized in that area. This technique is generally used for large macromolecules such as proteins.

Optic axis. The direction in a birefringent crystal along which the ordinary and extraordinary rays travel at the same speed. Uniaxial crystals have one such axis; biaxial crystals have two.

Optical activity. The ability of a substance to rotate the plane of polarization of plane-polarized light.

Order of diffraction. An integer associated with a given interference fringe of a diffraction pattern. The diffraction is first order if it arises as a result of a radiation path difference of one wavelength. The n th order corresponds to a path difference of n wavelengths.

Orientation matrix. A matrix that provides a connection between the orientation of the diffractometer circles and the production of a Bragg reflection so that the indices hkl of the Bragg reflection can be related to the orientation of the chosen unit cell of the crystal, and the intensity of the Bragg reflection can then be measured.

Origin of a unit cell. The point in a unit cell (usually one corner), chosen by the investigator, from which x , y , and z axes originate. It is designated “0, 0, 0” for its values of x , y , and z .

Orthogonal system. Reference axes that are mutually perpendicular.

Orthorhombic unit cell. A unit cell in a lattice in which there are three mutually perpendicular two-fold rotation axes (parallel to the three reference axes a , b , and c); as a result, while there are no restrictions on axial ratios, all interaxial angles are necessarily equal to 90° ($\alpha = \beta = \gamma = 90^\circ$).

Oscillation photograph. A photograph of the diffraction pattern obtained by oscillating the crystal through a small angular range.

Parallelepiped. A six-sided figure, each side of which is a parallelogram, and opposite sides of which are parallel to each other.

Parity group. A set of structure factors whose three Miller indices (h , k , and l) are odd (o) or even (e) in an identical

way. There are eight parity groups for three indices (eee, eeo, eoe, eoo, oee, oeo, ooe, and ooo).

Path difference. This term is used in diffraction to describe the difference in distance that two beams travel when “scattered” from different points. As a result of such path differences, the two beams may or may not be in phase with each other.

Patterson function. A Fourier summation that has the squares of the structure factor amplitudes as coefficients and all phases zero. Because these values of $|F(hkl)|^2$ can be obtained (after some geometric corrections) directly from the diffraction intensities, the map can be computed directly with no phase information required.

$$P(uvw) = \frac{1}{V_c} \sum_{\text{all } h,k,l} \sum |F(hkl)|^2 \cos 2\pi(hu + kv + lw)$$

Ideally, the positions of the maxima in the map represent the end points of vectors between atoms, all referred to a common origin. There is only one Patterson map for a given crystal structure, but the input may be enhanced to make the interpretation easier. If values of $|F(hkl)|^2$ are modified by an exponential or similar function that enhances those Bragg reflections with high values of $\sin \theta/\lambda$, the resulting interatomic vectors appear as sharper peaks. The map is named for Arthur Lindo Patterson, a physicist.

Perfect crystal. A crystal in which the unit cells and their contents are in perfect register.

Phase. The phase is the point to which the crest of a given wave has advanced in relation to a standard position, for example the origin of the unit cell. It is usually expressed as a fraction of the wavelength in angular measure, with one cycle or period being 2π radians or 360° ; that is, if the crests differ by Δx for a wavelength λ , the phase difference is $\Delta x/\lambda$ or $2\pi \Delta x/\lambda$ radians or $360 \Delta x/\lambda$ degrees (see also Calculated phase). If two waves of the same wavelength travel in the same direction, their phase difference is the difference between the positions of crests (peaks) between the two. The relative phase of a structure factor is expressed relative to the phase of a wave scattered at the chosen origin of the unit cell (or some other defined position) in the same direction: $\alpha(hkl) = \tan^{-1}(B(hkl)/A(hkl))$, where $A(hkl)$ and $B(hkl)$ are components of the structure factor $F(hkl)$. If the crystal structure is centrosymmetric and the origin is set at a center of symmetry, the phase is 0° or 180° (0 or π radians) according to a positive or negative sign of $A(hkl)$; $B(hkl) = 0$. When we use “relative phase” we remind the reader that its value depends on the chosen location of the origin of the unit cell; that is,

a structure factor does not usually have a fixed phase; its relative phase depends on where the unit-cell origin has been chosen to be.

Phase problem. The problem of determining the phase angle (relative to a chosen origin) for each Bragg reflection, so that an electron-density map may be calculated from a Fourier series with structure factors (including both amplitude and relative phase) as coefficients. "Solving a structure" requires determining phases.

Photometry. Measurement of the ratio of the intensity of a constant source of light to that of an equivalent beam of light after it has passed through a selected position on a piece of photographic film. In this way the intensity of a Bragg reflection that has been recorded on film can be measured.

Piezoelectric effect. The generation of a small potential difference across certain crystals when they are subjected to stress such as pressure (the direct effect), or the change in the shape of a crystal that accompanies the application of a potential difference across a crystal (the inverse effect). The effect is found only for noncentrosymmetric crystals; examples are provided by quartz and Rochelle salt.

Planck constant. The Planck constant (h), named after Max Planck, defines the size of a quantum of electromagnetic radiation. It is the proportionality constant between the energy of a photon (in joules) and the frequency (in oscillations per second) of the wave that it represents. $h = 6.626 \times 10^{-34} \text{ J s}$ or $\text{kg m}^2 \text{ s}^{-1}$.

Plane groups. The groups of symmetry elements that lead to those symmetry operations that produce regularly repeating patterns in two dimensions. There are 17 plane groups (listed in *International Tables*), meaning that there are 17 symmetry variations of wallpaper (if it has a two-dimensional repeating pattern).

Plane polarization. Electromagnetic radiation, such as visible light and X rays, contains electric vectors of its waves and if the radiation is plane-polarized, all of these are confined to a single plane.

Pleochroism. The property of certain crystals of appearing to have different colors when viewed from different directions under transmitted white light (dichroism if only two colors).

Point group. A group of symmetry operations that leave unmoved at least one point within the object to which they apply. Symmetry elements include simple rotation and rotatory-inversion axes; the latter include the center of

symmetry and the mirror plane. Since one point remains invariant, all rotation axes must pass through this point and all mirror planes must contain it. A point group is used to describe isolated objects, such as single molecules or real crystals. (See Group (mathematical).)

Poisson distribution. A distribution of measurements applied to rare events in which the number of such events occurring in a fixed period of time depends only on the length of this time interval and is independent of previous events. The mean and variance of the distribution are equal so that the standard uncertainty is proportional to the square root of the measured value. The distribution is named after the French mathematician Siméon Denis Poisson.

Polar axis. An axis in a crystal that has different properties at its two ends (meaning that it has directionality, like an arrow). Such properties include crystal face development and charge accumulation.

Polarization factor. A correction factor for intensity data that takes into account the reduction in intensity of X-ray scattering due to the state of polarization of the incident beam. If the incident X rays are not polarized, the factor is $(1 + \cos^2 2\theta)/2$. It will be further modified if a monochromator was used to provide the incident radiation.

Polymorphism. Property of crystallizing in two or more forms with distinct structures (dimorphism if only two forms), generally depending on the conditions of crystallization. Polymorphs have different unit cells and different atomic arrangements within them.

Position-sensitive detector. (See Charge-coupled device area detector.)

Powder diffraction. Diffraction by a powder consists of lines or rings rather than separate diffraction spots. The diffraction pattern obtained is like that expected for a set of randomly oriented crystals. For diffraction studies the powder is either glued to a glass fiber, placed on a flat surface (e.g., a microscope slide), or, if it is unstable in air, put in a sealed capillary tube.

Precession photograph. A photograph of the diffraction pattern that is an undistorted magnified image of a given layer of the reciprocal lattice. The necessary camera and crystal motions involve the precession of one crystal axis about the direction of the direct beam. The film is continuously maintained in the plane perpendicular to this precessing axis. The photograph resulting from this complicated set of motions is simple to interpret, and the indices (h, k, l) of the diffraction spots may readily be found by inspection.

Precipitant. A chemical used to promote crystallization but not denaturation of a protein. Examples are highly soluble inorganic salts (ammonium sulfate or sodium chloride) and organic polyethers (polyethyleneglycols of a selected molecular weight range.)

Precipitation. The act of separation of a solid mass from solution. A precipitant (q.v.) will assist this.

Precision. A measure of the experimental uncertainty in a measured quantity, an indication of its reproducibility (cf. Accuracy).

Primitive unit cell. The unit cell of the smallest possible volume for a given space lattice. The term is used to differentiate this unit cell from a centered cell or other nonprimitive cells. When a primitive cell is chosen, the symbol *P* is included in the space-group designation.

Principal axes of thermal ellipsoids. Three mutually perpendicular directions, along two of which the amplitudes of vibration of an atom, represented by an ellipsoid, are at a maximum and at a minimum. Each axis is characterized by an amplitude and a direction.

Probability density function. The probability that a random variable will take on a particular value in an infinitesimal time interval, divided by the length of the interval.

Probability relationships. In crystallographic use, this term refers to equations that express the probability that a phase angle will have a certain value. Such equations are the basis of phase determination by direct methods.

Promolecule density. The electron density of spherically symmetrical free atoms without effects from chemical bonding or other factors that distort the electron density.

Proper symmetry operation. A symmetry operation that maintains the handedness of an object. Such operations include translations, rotation axes, and screw axes.

Proportional counter. A radiation detector that produces a measurable amplified voltage pulse of height proportional to the energy of photons hitting it; it gives a linear response at high counting rate.

Pyroelectric effect. The development of a small potential difference across certain crystals as the result of a temperature change.

R value or R factor, discrepancy index, residual. An index that gives a measure of the disagreement between observed and calculated structure amplitudes and therefore a crude (and sometimes misleading) measure of the correctness of a derived model for a crystal structure and the quality of the experimental data. It is defined as

$$R = \Sigma(|F_o| - |F_c|) / \Sigma|F_o|$$

and values of 0.02 to 0.06 are considered good for present-day small-molecule structure determinations. However, some partially incorrect structures have had *R* values below 0.10, and many basically correct but imprecise structures have higher *R* values.

Racemic mixture. A mixture composed of equal amounts of dextrorotatory and levorotatory forms (enantiomorphs) of the same compound. It displays no optical rotatory power.

Radiation damage. Damage caused by radiation. Since a crystal is constantly irradiated by X rays during a diffraction experiment, such damage can be an important source of error. As a result of such damage, molecules in the crystal may move, be ionized, form free radicals, or interact with other species in the crystal. Sometimes sets of three or more Bragg reflections are measured at regular intervals during intensity data measurement by a diffractometer in order to monitor any radiation damage. However, with area detector data, radiation (and other) damage is checked by average counts per image and any drop thereof. Radiation damage by X rays is dramatically reduced by low-temperature data collection. By contrast, neutrons do not generally damage a crystal.

Raw data. Diffraction data when they are first measured, before correction and other factors are applied to them.

Real space. (See Direct space.)

Real-space averaging. A computational method for improvement of phases, when there are two or more identical chemical units in the crystallographic asymmetric unit. In a trial electron-density map, the electron densities of the two identical units are averaged. Then a new set of phases is computed by Fourier transformation of the averaged structure, and, with these, a new electron-density map is synthesized with the observed $|F(hkl)|$ values. By iteration of this procedure, the electron-density map can be improved. This method is commonly used in refining large crystal structures.

Reciprocal lattice. The lattice defined by axes \mathbf{a}^* , \mathbf{b}^* , \mathbf{c}^* , related to the crystal lattice or direct lattice (with axes \mathbf{a} , \mathbf{b} , \mathbf{c}) in a reciprocal manner such that \mathbf{a}^* is perpendicular to \mathbf{b} and \mathbf{c} ; \mathbf{b}^* is similarly perpendicular to \mathbf{a} and \mathbf{c} ; and \mathbf{c}^* is perpendicular to \mathbf{a} and \mathbf{b} . The repeat distance, d^* , between points in a particular row of the reciprocal lattice is inversely proportional to the interplanar spacing, d , between the nets of the crystal lattice that are normal to this row of points ($d^* = \lambda/d$).

Refinement of a crystal structure. A process of improving the parameters of an approximate (trial) structure until the

best fit of calculated structure factor amplitudes to those observed is obtained. This is usually done by the method of least squares (q.v.). Since the dependence of the structure amplitudes on atomic parameters is not linear, the process involves a series of iterations until convergence is reached. To avoid falling into physically meaningless minima, it is important to start with a good set of initial parameters.

Reflecting goniometer. A device for measuring the angles between crystal faces by measuring the angle through which a crystal has to be rotated from a position at which one face reflects a narrow beam of light into a stationary detector to a position at which a second face reflects.

Reflection. (See Bragg reflection.)

Refraction. The change in direction that occurs when a beam of radiant energy passes from one medium into another in which its velocity is different. (See Refractive index.)

Refractive index. The ratio of the velocity of light *in vacuo* to its velocity as it passes through the material under study. It is evident when a stick is placed in a tumbler full of water. The stick appears bent at the surface of the water. When a colorless, clear object (such as a crystal) is immersed in a colorless medium of the same refractive index, the object becomes invisible.

Residual. (See *R* value.)

Resolution. The ability to distinguish adjacent parts of an object when examining it with radiation, that is, the process of distinguishing two adjacent objects (high resolution) as separate entities rather than as a single, blurred object (low resolution). Most X-ray structures of small molecules are determined to a "resolution" of 0.75–0.9 Å or better. At this resolution each atom is fairly distinct. The resolution improves with an increase in the maximum value of $\sin \theta / \lambda$ at which Bragg reflections are measured. Sometimes the quality of the crystal or the wavelength of the radiation limits the resolution that may be obtained experimentally.

A second use of this term is for the separation of enantiomorphs.

Restraints. Limits on the possible values that parameters may have. For example, additional observations, such as known bond distances and angles, can be added to the least-squares equations, and these must hold true for the results of the least-squares refinement. Restraints are used like data and one refines against them. They come with a standard uncertainty or elasticity that should be obeyed. Constraints remove parameters and restraints

add data. Constraints rigidly relate certain parameters or assign specific values to them, while restraints give ranges to target values for certain parameters. (Think of a dog restrained by a flexible leash of a selected length.) (See Constraints.)

Rhombohedral unit cell. A unit cell in which there is a three-fold rotation axis along one body diagonal of the unit cell. This symmetry requirement makes all three axial lengths necessarily the same and all three interaxial angles necessarily equal, although their values are not restricted ($a = b = c$, $\alpha = \beta = \gamma$). This is an alternative description of unit cells in trigonal space groups that are centered if they are drawn in the hexagonal representation. The difference between the trigonal and hexagonal systems is the symmetry; a hexagonal unit cell has a six-fold rotation axis, while a trigonal unit cell has only a three-fold axis. The rhombohedral unit cell, denoted *R*, is a third of the volume of the hexagonal representation. The hexagonal setting ($a = b \neq c$, $\alpha = \beta = 90^\circ$, $\gamma = 120^\circ$), which has obverse and reverse settings (see Appendix 2), is, however, usually preferred.

Right-handed coordinate system. A system of three axes, *x*, *y*, and *z*, in which a rotation from *x* to *y*, coupled with a translation along *z*, corresponds to the action of a right-handed screw moving clockwise into a piece of wood (with *x* to *y* as the clockwise motion and *z* the direction into the wood). If the thumb, index finger, and middle finger of the right hand are extended in mutually perpendicular directions, then these digits point to the positive directions of *x*, *y*, and *z*, respectively.

Rigid-body model. A model of vibration that assumes a molecule (or a specific part of it) to be rigid, so that, during vibration, all its interatomic distances are constant and all atoms move in synchrony.

Rotating-anode generator. An X-ray tube in which an electron beam hits a wheel of target material rotating at high speed. The anode moves while the X-ray beam remains fixed, so that the heat generated during X-ray production is spread over a larger area than in a conventional sealed X-ray tube. This provides a higher intensity of X rays than obtained with a conventional sealed X-ray tube.

Rotation axis. (See Axis of rotation.)

Rotation function. A function that describes a measure of the degree of correspondence between (1) a set of interatomic vectors that has been calculated for a known structure and (2) the Patterson function of that crystal. It is expressed by a map of the rotation about the origin of one of these functions with respect to the other. Peaks in

this map define a likely orientation of the known fragment of the structure. The orientation of a known part of a structure may often be found through such comparison. In a self-rotation function, the Patterson map is compared with itself. Peaks in this function will indicate the relationship between molecules if there is more than one in the asymmetric unit.

Rotation photograph. A photograph of the diffraction pattern obtained by rotating a crystal continuously about a fixed axis, sometimes normal to some set of reciprocal lattice planes.

Rotatory-inversion axis. Rotation by $360^\circ/n$ combined with inversion through a center of symmetry (on that axis) to give an enantiomorph of the original object.

SAD phases. SAD = single-wavelength anomalous dispersion. A single set of anomalous-dispersion data is measured with $\text{CuK}\alpha$ radiation for a crystal containing a heavy atom such as iodine or bromine. Alternatively, a sulfur-containing structure may be measured with $\text{CrK}\alpha$ radiation. In both cases the data can be collected in a laboratory (rather than at a synchrotron source), but the phase ambiguity persists (because only one data set was measured). This ambiguity is generally resolved by direct methods, such as by locating all the anomalously scattering atoms in the structure.

Salting out. Precipitating, coagulating, or separating a substance from a solution by the addition of a salt.

Saturated solution. A solution is saturated when the solute and solution are at equilibrium. This occurs when the maximum amount of solute has been dissolved in the solvent, and is usually dependent on the temperature and pressure.

Scale factor. (See Absolute scale.)

Scattering angle. The angle at which the scattered wave deviates from the direct beam. Conventionally, in X-ray diffraction, the direct X-ray beam is deviated by an angle $2\theta_{hkl}$.

Scattering factor. (See Atomic scattering factor.)

Scattering vector. The reciprocal lattice vector associated with (and perpendicular to) a set of reflecting crystal-lattice planes hkl ,

$$H = ha^* + kb^* + lc^*$$

Its magnitude is given by $H = 1/d_{hkl} = 2 \sin \theta_{hkl} / \lambda$, where d_{hkl} is the interplanar spacing. The order of diffraction, n , is contained in the Miller indices hkl as a multiplying factor.

Scintillation counter. A device for measuring the intensity of an X-ray beam. It makes use of the fact that X rays cause certain substances to emit visible light by fluorescence. The intensity of this visible light is proportional to the intensity of the incident X-ray beam and is amplified by a photomultiplier and then counted. The substance generally used as the X-ray detector is a sodium iodide crystal, activated by a small amount of thallos ion.

Screw axis. A screw axis, designated n_r , is a symmetry operation that involves rotation about the axis by $360^\circ/n = 2\pi/n$ coupled with a translation parallel to the axis by r/n of the unit-cell length in that direction. A two-fold screw axis through the origin of the unit cell and parallel to \mathbf{b} converts an object at x, y, z to one at $-x, \frac{1}{2} + y, -z$. The translation component leads to the generation of an infinitely repeating periodic pattern in the direction of translation. The enantiomorphic identity remains the same if a screw axis is used.

Series-termination error. An effect in a periodic function that results from a truncation of the number of terms in a Fourier series. Ideally, an infinite amount of data is necessary for the calculation of a Fourier series. In practice, only a finite number of data are measured in a diffraction pattern. This leads to a truncation of the Fourier series so that peaks in the resulting Fourier syntheses may be surrounded by series of ripples, which are especially noticeable around a heavy atom. The use of difference syntheses (q.v.) obviates most of the effects of series-termination errors.

Sigma Two formula (Σ_2). A formula used in direct methods. It relates the phases of three intense Bragg reflections to each other.

Simulated annealing. Annealing is a method used to make steel or glass more soft and less brittle, and involves heating and then cooling. This process is simulated in crystallographic refinements by adjusting the parameters of a macromolecule to simulate "heating" of the molecule (by increasing the displacements or vibrations), and then "cooling" it so as to minimize the energy. In this way a global minimum may be more readily obtained than with other methods of refinement, such as least-squares methods, where a local minimum, but not the deepest minimum, may be the end point of a refinement.

Sinusoidal wave. A wave described by a function $y(t) = A \sin(\omega t + \theta)$, where A = amplitude, ω = angular frequency, and θ = phase. Sine and cosine functions are both sinusoidal waves, with different phases [$\cos x = \sin(x + \pi/2)$]. A sinusoidal wave retains its wave shape when added to another sinusoidal wave (see Fourier synthesis).

Small-angle scattering. The study of matter by analysis of the diffraction of X rays with diffraction angles smaller than a few degrees—that is, θ less than 1° , for copper radiation. This scattering occurs when the sample is composed of particles with dimensions of the order of several hundred to several thousand Å. Measurement of the intensity distribution gives information on the low-resolution structure of the diffracting material; for example, it will give the radius of gyration of the particles, which is a measure of the size of the particle.

Solvent flattening. (See Density modification.)

Space group. A group of symmetry operations consistent with an infinitely extended, regularly repeating three-dimensional pattern. There are 230 such groups, which can be identified (although sometimes with some ambiguity) from the systematic absences in the diffraction pattern combined with the intensity data (see Distribution of intensities) and the Laue symmetry (see Laue class). A space group may be considered as the group of operations that converts one molecule or asymmetric unit into an infinitely extending pattern of such units. The 230 space groups are listed in detail in *International Tables for Crystallography*, Vol. A (Hahn, 2005).

Space group ambiguity. Sometimes more than one space group fits a set of systematic absences in the intensities of Bragg reflections for a given crystal. Other methods, such as information on the crystal contents and their possible symmetry or employing characteristics of the intensity distribution, may have to be used to determine the correct space group.

Spallation. Spallation is the ejection of material on impact. It can involve high-energy incident particles that bombard an atomic nucleus, ejecting particles such as neutrons. Neutrons are obtained when short bursts of high-energy pulsed protons are used to bombard a target of heavy nuclei (such as mercury, lead, or uranium) several times a second. Each proton produces several high-energy neutrons, which are slowed down by moderators to useful energies for diffraction studies.

Sphere of reflection. (See Ewald sphere.)

Standard uncertainty (s.u.). A measure of the precision of a quantity. If the distribution of errors is normal, then there is a 99% chance that a given measurement will differ by less than 2.7 s.u. from the mean. A bond length 1.542(7) Å (1.542 Å with an s.u. of 0.007 Å) is, by the usual criteria, not considered significantly different from one measured as 1.528(7) Å (2 s.u. away). This term is sometimes called an “estimated standard deviation” (e.s.d.).

Stoichiometry. The quantitative relationship of constituents implied by a chemical formula or equation.

Structure factor. The structure factor $F(hkl)$ is the value, at a reciprocal lattice point, of the Fourier transform of the electron density in the unit cell. The wave scattered by the contents of the unit cell in the direction of the hkl Bragg reflection is described in amplitude and phase by the structure factor $F(hkl)$. The structure factor has both a magnitude (amplitude) and a phase (relative to the origin of the unit cell). The magnitude of the structure factor, $|F(hkl)|$, is the ratio of the amplitude of the radiation scattered in a particular direction by the contents of one unit cell to that scattered by a classical point electron at the origin of the unit cell under the same conditions. The structure factor depends on the chemical identities and arrangement in the unit cell of the constituent atoms, and on the direction of scattering with respect to the incident X-ray beam. For the relationship between structure factors and electron density, see Fourier transform.

Structure invariant. A linear combination of the phases of a particular set of Bragg reflections that does not change when the position of the origin of the unit cell is changed; that is, this linear combination of phases is totally independent of the choice of origin.

Structure seminvariant. Bragg reflections whose phases remains unchanged (except by an integral multiple of 2π radians) when the location of the origin is changed (provided this origin change is allowed by space-group symmetry constraints).

Superposition methods. Analysis of a Patterson map by setting the origin of the Patterson map in turn on the positions of certain atoms whose positions may already be known, and then recording those areas of the superposed maps in which peaks appear that are derived from both maps. The resulting map is called a vector superposition map and may contain information that allows one to derive the atomic arrangement.

Symbolic addition method. A direct-method procedure, in which phases for a few Bragg reflections are represented by algebraic symbols (such as a, b, or c) when needed during phase assignment. The meaning of the symbolic phases, such as + and – for 0° and 180° for a centrosymmetric structure, may then become evident during the subsequent analysis (for example, if the phase becomes a^2 which must be positive). Otherwise, electron-density maps with all possible values for the undetermined symbols must be computed, and hopefully one of these will be obvious as the correct structure.

Symmetry element. A point, a line, or a plane on or about which a particular symmetry operation is performed. The actual operation is a “symmetry operation” (q.v.).

Symmetry operation. In crystal structures (assumed infinite in extent), the possible symmetry operations include axes of rotation and rotatory inversion, screw axes, and glide planes, as well as lattice translations. Symmetry operations convert an object into a replica of itself. Translation and rotation are proper symmetry operations, while reflection and inversion are improper symmetry operations, which convert an object into the mirror image of itself.

Symmetry operation of second kind. (See Improper symmetry operation.)

Synchrotron radiation. Radiation emitted by very high-energy electrons, such as those in an electron storage ring, when their path is bent by a magnetic field. This radiation is characterized by a continuous spectral distribution (which can, however, be “tuned” by appropriate selection), a very high intensity, a pulsed time structure, and a high degree of polarization. Its high intensity makes it useful for rapid data collection on macromolecular crystals and its tunability makes it convenient for collecting anomalous scattering data.

Systematically absent reflections. Bragg reflections that are too weak to be observed by the method of measurement used and for which h , k , and l values are systematic in terms of evenness or oddness (for example, an absence of all Bragg reflections for which $h + k$ is odd, indicative of C-face centering in the unit cell). Systematic absences depend only upon symmetry in the atomic arrangement. There are two types of systematic absences: (1) those arising from translational symmetry elements, i.e., screw axes and glide planes, and (2) those that arise from a decision to use a nonprimitive unit cell, and are an artifact of the way we index Bragg reflections. Systematic absences are of great use in deriving the space group of a crystal.

Tangent formula. A formula used in direct methods of phase determination that allows the development of additional phases.

Taylor series. A power series that expresses a function as an infinite sum of terms that can be calculated from values of its derivatives at a single point. In this power series, the coefficients are the corresponding derivatives divided by the factorial of the order of the derivative. The higher the power in a term, the smaller its value. The series is named after Brook Taylor, an English mathematician, who followed the earlier work of James Gregory.

Temperature factor. An exponential expression by which the scattering of an atom is reduced as a consequence of vibration (or a simulated vibration resulting from static disorder). For isotropic motion the exponential factor is $\exp(-B_{\text{iso}} \sin^2 \theta / \lambda^2)$, with B_{iso} called, loosely but commonly, the “isotropic temperature factor.” B_{iso} equals $8\pi^2 \langle u^2 \rangle$, where $\langle u^2 \rangle$ is the mean square displacement of the atom from its equilibrium position. For anisotropic motion the exponential expression contains six parameters, the anisotropic vibration or displacement parameters, which describe ellipsoidal rather than isotropic (spherically symmetrical) motion or average static displacements. (See Atomic displacement parameters.)

Tetragonal unit cell. A unit cell in which there is a four-fold rotation axis parallel to one axis (arbitrarily chosen as c); as a result, the lengths of a and b are identical and all interaxial angles are 90° ($a = b$, $\alpha = \beta = \gamma = 90^\circ$).

Thermal diffuse scattering. Diffuse scattering results from a departure from the regular periodic character of a crystal lattice. It is evident as diffuse spots or blurs around normal diffraction spots. If it is a temperature-dependent effect, it is called thermal diffuse scattering. This can be analyzed to give information on the elastic properties of crystals and the force constants between their constituent atoms.

Thermal-motion corrections. Adjustments to intramolecular dimensions from a crystal structure determination for distortions arising from atomic vibrations, especially libration (q.v.). The appropriate corrections depend on a model for specifying the correlations between the motions of the several atoms.

Time-of-flight neutrons. Neutrons from a reactor arrive at a detector array at times determined by their energies. They come in pulses (as a result of the action of mechanical choppers) and their energies (and wavelengths) are determined from the time it takes for them to travel to and hit the detector. Their velocities v are related to the wavelength by $\lambda = h/mv = (h/m)(t/L)$, where h is Planck’s constant, m is the mass of a neutron, and t is the time of flight for a path length L . This equation gives essential information for analysis of a Laue-type diffraction pattern. Time-of-flight detectors can record the different wavelengths one after the other.

Torsion angle (sometimes called “conformational angle”). The torsion angle (or angle of twist) about the bond B–C in a series of bonded atoms A–B–C–D is defined as the angle of rotation needed to make the projection of the line B–A coincide with the projection of the line C–D, when viewed along the B–C direction. The positive sense is clockwise.

If the torsion angle is 0° or 180° , the four atoms lie in the same plane. Enantiomers have torsion angles of equal absolute value but opposite sign.

Translation. The word “translation” has two different meanings in crystallography. Generally it indicates the symmetry element (of one unit cell length) that is typical of lattices, or some fraction of that. It is also used when all atoms of a molecule move the same distance in the same direction along the same or parallel lines.

Translation function. A function that can be calculated in order to determine (with respect to the unit-cell axes) how a molecule, for which the orientation has been found (see Rotation function), is positioned with respect to the origin of the unit cell. This function is important in structure analysis in macromolecular crystallography.

Trial-and-error method. A method that involves postulating a structure (that is, assuming locations of the atoms in the unique part of the unit cell), calculating structure factors F_c , and comparing their magnitudes with the scaled observed values $|F_o|$. Since the number of trial structures that must be tested increases with the number of parameters, such methods have generally been applied in solving only the simplest structures.

Trial structure. A possible structure for a crystal (found by one of several methods), which is tested by a comparison of calculated and observed structure factors and by the results of an attempted refinement of the structure.

Triclinic unit cell. A unit cell in which there are no rotation axes or mirror planes. As a result there are no restrictions on axial ratios or interaxial angles.

Trigonal unit cell. (See Rhombohedral unit cell.)

Triple-product sign relationship. The sign relationship $s(h, k, l) s(h', k', l') s(-h - h', -k - k', -l - l') \approx +1$, where \approx means “is probably equal to” and s means “the sign of.”

Twin. A composite crystal built from two or more crystal specimens that have grown together in a specific relative orientation.

Unit cell. The basic building block of a crystal, repeated infinitely in three dimensions. It is characterized by three vectors, \mathbf{a} , \mathbf{b} , and \mathbf{c} , that form the edges of a parallelepiped. The angles between these vectors are α (between \mathbf{b} and \mathbf{c}), β (between \mathbf{a} and \mathbf{c}), and γ (between \mathbf{a} and \mathbf{b}).

Unit-cell dimensions. The unit-cell dimensions a , b , c , α , β , γ , of a crystal structure.

Unitary structure factor. The ratio of the structure amplitude, $|F(hkl)|$, to its maximum possible value—that is,

the value it would have if all atoms scattered exactly in phase. It is denoted by U . $U(hkl) = |F(hkl)| / |\sum f_j|$, where f_j is the scattering factor of atom j at the $\sin \theta / \lambda$ value of $F(hkl)$.

Unobserved Bragg reflections, absent Bragg reflections. Bragg reflections that are too weak to be measured by the apparatus in use. The term is also used for Bragg reflections for which the intensity $I(hkl)$ is less than $n\sigma(I)$, where n is chosen (usually 2–3), and σ is the s.u. of $I(hkl)$.

Variance. The mean square deviation of a frequency distribution from its arithmetic mean. The variance is the square of the standard uncertainty σ . For a random variable x , the variance is $\Sigma[(x_i - x_m)^2/n]$, where x_m is the mean value of x , and n is the number of measurements.

Vector. A quantity that requires for its complete description a magnitude, direction, and sense. It is often represented by a line, the length of which specifies the magnitude of the vector, and the orientation of which specifies the direction of the vector. The sense of the vector is then indicated by an arrowhead at one end of the line. Two vectors may be added together by placing the second vector with its origin on the end (arrowhead) of the first. The resultant vector is the directed line from the origin of the first vector to the end of the second. This process of addition can be continued infinitely. The scalar product, $\mathbf{a} \cdot \mathbf{b}$, is $|a||b| \cos \gamma$, where γ is the angle from \mathbf{a} to \mathbf{b} . The vector product, $\mathbf{a} \times \mathbf{b}$, is a vector with direction normal to both \mathbf{a} and \mathbf{b} , and magnitude $|a||b| \sin \gamma$.

Wavefront. All points reached at a given instant in time by a series of waves as they move through any material.

Wavelength. The distance between two similar points on a wave system, for example, the crests of a cosine wave.

Weight of a measurement. A number assigned to express the relative precision of each measurement. In least-squares refinement the weight should be proportional to the reciprocal of the square of the standard uncertainty of the measurement. Other weighting schemes frequently are used.

Weissenberg camera. This is an oscillation camera in which the camera is translated (moved) as the crystal rotates so that Bragg reflections can be indexed more readily than for a simple oscillation photograph that lacks this simultaneous motion of camera and crystal. It is named after Karl Weissenberg, an Austrian physicist.

White radiation. Any radiation, such as X rays or sunlight, with a continuum of wavelengths.

Wilson plot. A plot of the logarithm of the average ratio of the observed Bragg intensities to the theoretical values expected for a random arrangement of the same (stationary) atoms in the unit cell, in successive ranges (shells) of $\sin^2 \theta / \lambda^2$. Such a plot typically approaches a straight line, whose intercept yields the factor needed to place the observed intensities on an absolute scale (q.v.) and whose slope yields an average isotropic displacement parameter for the entire structure. The plot was designed by Arthur James Cochran Wilson, a crystallographer.

X-ray camera. A device for holding film in an appropriate manner to intercept and record an X-ray diffraction pattern.

X-ray tube. The basic parts of an X-ray tube are a source of electrons and a metal anode that emits the X-rays, enclosed

in a glass envelope under vacuum. Tubes may be classified according to the nature of these parts.

X rays. Electromagnetic radiation of wavelength 0.1–100 Å, produced by bombarding a target (generally a metal such as copper or molybdenum) with fast electrons. It is found that X rays of definite wavelengths, characteristic of the target element (characteristic X rays, q.v.), plus a continuous background of X rays (bremsstrahlung, q.v.), are produced. Characteristic X rays are produced when electrons from the innermost shells (K or L) are ejected from atoms in the target material. When an electron from an outer shell falls back into the vacant shell, energy is emitted in the form of X rays with a specific wavelength. The spectrum of the emitted X rays has a maximum intensity at a few wavelengths characteristic of the target material.

References and further reading

- Abbé, E. Beiträge zur Theorie des Mikroskops und der mikroskopischen Wahrnehmung. [Contributions to the theory of the microscope and microscopic observations.] *Archiv für Mikroskopische Anatomie (Archiv für Entwicklungsmechanik der Organismen)* **9**, 413–468 (1873).
- Allen, F. H. The Cambridge Structural Database: A quarter of a million crystal structures and rising. *Acta Crystallographica* **B58**, 380–388 (2002).
- Astbury, W. T. and Yardley, K. [Lonsdale] Tabulated data for the examination of the 230 space-groups by homogeneous X rays. *Philosophical Transactions of the Royal Society (London)* **A244**, 221–257 (1924).
- Avrami, M. Direct determination of crystal structure from X-ray data. *Physical Review* **54**, 300–303 (1938).
- Bacon, G. E. *Neutron Diffraction*. 1st edition (1955). 2nd edition (1962). 3rd edition, Oxford University Press: Oxford (1975).
- Bacon, G. E., Curry, N. A., and Wilson, S. A. A crystallographic study of solid benzene by neutron diffraction. *Proceedings of the Royal Society (London)* **A279**, 98–110 (1964).
- Banerjee, K. Determinations of the signs of the Fourier terms in complete crystal structure analysis. *Proceedings of the Royal Society (London)* **A141**, 188–193 (1933).
- Barlow, W. Über die Geometrischen Eigenschaften homogener starrer Strukturen und ihre Anwendung auf Krystalle. [On the geometrical properties of homogeneous rigid structures and their application to crystals.] *Zeitschrift für Kristallographie und Mineralogie* **23**, 1–63 (1894).
- Barlow, W. and Pope, W. J. The relation between the crystalline form and chemical constitution of simple inorganic substances. *Transactions of the Chemical Society (London)* **91**, 1150–1214 (1907).
- Bentley, W. A. *Snow Crystals*. McGraw-Hill: New York (1931).
- Bergerhoff, G. and Brown, I. D. Inorganic Crystal Structure Database. In: *Crystallographic Databases. Information Content, Software Applications, Scientific Applications*, Section 2.2, pp. 77–95. International Union of Crystallography: Bonn, Cambridge, Chester (1987).
- Bergfors, T. M. (ed.). *Protein Crystallization: Techniques, Strategies, and Tips: A Laboratory Manual*. 1st edition (1999). 2nd edition, International University Line: La Jolla, CA (2009).
- Bergman, T. Variarum Crystallorum Formae a Spatho Orthae. [Various crystal shapes explained by the position of heavenly bodies.] *Nova Acta Regiae Societatis Scientiarum Upsaliensis* **1**, 150–155 (1773). English translation: Cullen, E. *Physical and Chemical Essays*. 3 volumes. J. Murray: London (1784).
- Berman, H. M., Henrick, K., and Nakamura, H. Announcing the worldwide Protein Data Bank. *Nature Structural Biology* **10**, 980 (2003).
- Bernal, J. D. Carbon skeleton of the sterols. *Chemistry and Industry* **51**, 466 (1932).
- Bernal, J. D. and Crowfoot, D. X-ray photographs of crystalline pepsin. *Nature* **133**, 794–795 (1934).
- Bernstein, F. C., Koetzle, T. F., Williams, G. J. B., Meyer, E. F. Jr, Brice, M. D., Rodgers, J. R., Kennard, O., Shimanouchi, T., and Tasumi M. The Protein Data Bank: A calculator-based archival file for macromolecular structures. *Journal of Molecular Biology* **112**, 535–542 (1977).
- Bhat, T. N. Calculation of an OMIT map. *Journal of Applied Crystallography* **21**, 279–281 (1988).
- Bhat, T. N. and Cohen, G. H. OMITMAP: An electron density map suitable for the examination of errors in a macromolecular model. *Journal of Applied Crystallography* **17**, 244–248 (1984).
- Bijvoet, J. M., Kolkmeijer, N. H., and McGillavry, C. H. *X-ray Analysis of Crystals*. Interscience: New York; Butterworths: London (1951). Originally *Röntgenanalyse van Kristallen*. [X-ray Analysis of Crystals.] 2nd edition, revised. D. B. Centen: Amsterdam (1948).
- Bijvoet, J. M., Peerdeman, A. F., and van Bommel, A. J. Determination of the absolute configuration of optically active compounds by means of X rays. *Nature* **168**, 271–272 (1951).

- Blundell, T. L. and Johnson, L. N. *Protein Crystallography*. Academic Press: New York, 1976.
- Bokhoven, C., Schoone, J. C., and Bijvoet, J. M. On the crystal structure of strychnine sulfate and selenate. III. [001] projection. *Proceedings of the Koninklijke Nederlandse Akademie van Wetenschappen* **52**, 120–121 (1949).
- Bragg, W. L. The structure of some crystals as indicated by their diffraction of X rays. *Proceedings of the Royal Society (London)* **A89**, 248–277 (1913).
- Bragg, W. H. IX Bakerian lecture. X-rays and crystal structures. *Transactions of the Royal Society (London)* **A215**, 253–274 (1915).
- Bragg, W. H. and Bragg, W. L. The structure of the diamond. *Nature* **91**, 557 (1913).
- Bravais, A. Mémoire sur les systèmes formés par des points distribués régulièrement sur un plan ou dans l'espace. *Journal de l'École Polytechnique (Paris)*. **19** (cahier 33), 1–128 (1850). English translation: Shaler, A. J. On the system formed by points regularly distributed on a plane or in space. *Crystallographic Society of America Memoir # 1* (Monograph # 4), New York (1949).
- Brock, C. P. and Dunitz, J. D. Temperature dependence of thermal motion in crystalline naphthalene. *Acta Crystallographica* **B38**, 2218–2228 (1982).
- Brown, I. D. What factors determine cation coordination numbers? *Acta Crystallographica* **B44**, 545–553 (1988).
- Brown, I. D. *The Chemical Bond in Inorganic Chemistry: The Bond Valence Model*, IUCr Monographs on Crystallography 12. Oxford University Press: Oxford (2006).
- Brumberger, H. (ed.). *Modern Aspects of Small-Angle Scattering*, NATO Science Series C. Kluwer/Springer: New York (1994).
- Buerger, M. J. *X-ray Crystallography*. Wiley: New York (1942).
- Buerger, M. J. *The Precession Method in X-ray Crystallography*. Wiley: New York (1964).
- Bunn, C. W. *Chemical Crystallography. An Introduction to Optical and X-ray Methods*. 1st edition (1946). 2nd edition, Oxford at the Clarendon Press: Oxford (1961).
- Bürgi, H. B., Dunitz, J. D., and Shefter, E. Geometrical reaction coordinates. Nucleophilic addition to a carbonyl group. *Journal of the American Chemical Society* **95**, 5065–5067 (1973).
- Burke, J. G. *Origins of the Science of Crystals*. University of California Press: Berkeley, Los Angeles (1966).
- Burla, M. C., Caliendo, R., Camalli, M., Carrozzini, B., Cascarano, G. L., De Caro, L., Giacovazzo, C., Polidori, G., and Spagna, R. SIR2004: An improved tool for crystal structure determination and refinement. *Journal of Applied Crystallography* **38**, 381–388 (2005).
- Cahn, R. S., Ingold, C. K., and Prelog, V. Specification of molecular chirality. *Angewandte Chemie International Edition* **5**, 385–415 (1966).
- Caliandro, R., Carrozzini, B., Cascarano, G. L., De Caro, L., Giacovazzo, C., and Siliqi, D. Phasing at resolution higher than the experimental resolution. *Acta Crystallographica* **D61**, 556–565 (2005).
- Caliandro, R., Carrozzini, B., Cascarano, G. L., De Caro, L., Giacovazzo, C., and Siliqi, D. Advances in the free lunch method. *Journal of Applied Crystallography* **40**, 931–937 (2007).
- Carslaw, H. S. *Introduction to the Theory of Fourier's Series and Integrals*. 3rd edition. Macmillan and Company: London (1930).
- Chadwick, J. The existence of a neutron. *Proceedings of the Royal Society (London)* **A136**, 692–708 (1932).
- Chayen, N. E. Methods for separating nucleation and growth in protein crystallization. *Progress in Biophysics and Molecular Biology* **88**, 329–337 (2005).
- Coppens, P. *X-ray Charge Densities and Chemical Bonding*, IUCr Texts on Crystallography 4. Oxford University Press: Oxford (1997).
- Coster, D., Knol, K. S., and Prins, J. A. Unterschiede in der Intensität der Röntgenstrahlenreflexion an den beiden 111 Flächen der Zinkblende. [Difference in the intensities of X-ray reflection from the two sides of the 111 plane of zinc blende.] *Zeitschrift für Physik* **63**, 345–369 (1930).
- Cotton, F. A. *Chemical Applications of Group Theory*. 2nd edition. Wiley-Interscience: New York, London, Sydney (1971).
- Cox, E. G. and Smith, J. A. S. Crystal structure of benzene at -3° . *Nature* **173**, 75 (1954).
- Crowther, R. A. and Blow, D. M. A method of positioning a known molecule in an unknown crystal structure. *Acta Crystallographica* **23**, 544–548 (1967).
- Cullity, B. D. *Elements of X-Ray Diffraction*. 1st edition (1956). 2nd edition (1978). 3rd edition, with S. R. Stock, Addison-Wesley: Reading, MA (2001).
- Curie, J. and Curie, P. Développement, par pression, de l'électricité polaire dans les cristaux hémihédres à faces inclinées. *Comptes Rendus de l'Académie des Sciences (Paris)* **91**, 294–295 (1880).
- Dauter, Z. Phasing in iodine for structure determination. *Nature Biotechnology* **22**, 1239–1240 (2004).
- Dauter, Z., Dauter, M., and Rajashankar, K. R. Novel approach to phasing proteins: Derivatization by short

- cryo-soaking with halides. *Acta Crystallographica* **D56**, 232–237 (2000).
- Davissou, C. and Germer, L. H. The scattering of electrons by a single crystal of nickel. *Nature* **119**, 558–560 (1927).
- de Broglie, M. L. Radiations.—Ondes et quanta. [Radiation—waves or quanta.] *Comptes Rendus de l'Académie des Sciences (Paris)* **1177**, 507–510 (1923).
- de Sénarmont, H., Verdet, E., and Fresnel, L. F. (eds.). *Œuvres Complètes d'Augustin Fresnel*. Volume 1, pp. 129–170. Imprimerie Impériale: Paris (1866).
- de Wolff, P. M. and Gruber, B. Niggli lattice characters: Definition and graphical representation. *Acta Crystallographica* **A47**, 29–36 (1991).
- Debye, P. Interferenz von Röntgenstrahlen und Wärmebewegung. [X-ray interference and thermal motion.] *Annalen der Physik* **43**, 49–95 (1914). English translation in: *Collected Papers of Peter J. W. Debye*, pp. 3–39. Interscience: New York (1954).
- DeLucas, L. J., Moore, K. M., and Long, M. M. Protein crystal growth and the International Space Station. *Gravitational and Space Biology Bulletin* **12**, 39–45 (1999).
- Dianoux, A. J. and Lander, G. H. *Neutron Data Booklet*. 2nd edition. Institut Laue-Langevin, Old City Publishing: Philadelphia, London, Paris (2003).
- Dickerson, R. E., Kopka, M. L., and Pjura, P. Base sequence, helix geometry, hydration, and helix stability in B-DNA. In: *Biological Macromolecules and Assemblies*, Volume 2, *Nucleic Acid and Interactive Proteins* (eds. F. Jurnak and A. McPherson). Chapter 2, pp. 38–126. Wiley: New York (1985).
- Dittrich, B., Koritsanszky, T., Volkov, A., Mebs, S., and Luger, P. Novel approaches to the experimental charge density of vitamin B₁₂. *Angewandte Chemie, International Edition* **46**, 2935–2938 (2007).
- Dodson, E. J. and Woolfson, M. M. ACORN2: New developments of the ACORN concept. *Acta Crystallographica* **D65**, 881–891 (2009).
- Dougherty, J. P. and Kurz, S. K. A second harmonic analyzer for the detection of non-centrosymmetry. *Journal of Applied Crystallography* **9**, 145–158 (1976).
- Drenth, J. *Principles of Protein X-ray Crystallography*. 1st edition (1994). 2nd edition (1999). 3rd edition, Springer-Verlag: New York (2007).
- Duane, W. The calculation of the X-ray diffracting power at points in a crystal. *Proceedings of the National Academy of Sciences of the United States of America* **11**, 489–493 (1925).
- Ducruix, A. and Giegé, R. (eds.). *Crystallization of Nucleic Acids and Proteins. A Practical Approach*. 1st edition (1992). 2nd edition, Oxford University Press: Oxford (1999).
- Dunitz, J. D. *X-Ray Analysis and the Structure of Organic Molecules*. Cornell University Press: Ithaca, NY (1979). Revised edition, Wiley-VCH: New York (1996).
- Dunitz, J. D., Schomaker, V., and Trueblood, K. N. Interpretation of atomic displacement parameters from diffraction studies of crystals. *Journal of Physical Chemistry* **92**, 856–867 (1988).
- Emsley, P. and Cowtan, K. Coot: Model-building tools for molecular graphics. *Acta Crystallographica* **D60**, 2126–2132 (2004).
- Ewald P. P. Zur Theorie der Interferenzen der Röntgenstrahlen in Kristallen. *Physikalische Zeitschrift*, **14**, 465–472 (1913). English translation: Cruickshank, D. W. J., Juretschke, H. J., and Kato, N. P. P. *Ewald and His Dynamical Theory of X-ray Diffraction*. International Union of Crystallography Monographs on Crystallography 2, pp. 114–123. Oxford University Press/International Union of Crystallography: Oxford (1992).
- Ewald, P. P. Das “Reziproke Gitter” in der Strukturtheorie. Teil I: Das Reziproke eines einfachen Gitter. [The “reciprocal lattice” in the theory of structure. Part 1. The reciprocal of a primitive lattice.] *Zeitschrift für Kristallographie* **56**, 129–156 (1921).
- Ewald, P. P. Introduction to the dynamical theory of X-ray diffraction. *Acta Crystallographica* **A25**, 103–108 (1969).
- Fedorov, E. S. Simmetriia pravil'nykh sistem figur. [The symmetry of real systems of configurations.] *Zapiski Imperatorskogo S. Petersburgskogo Mineralogicheskogo Obshchestva* [Transactions of the Mineralogical Society of St. Petersburg] **28**, 1–146 (1891). English translation: Harker, D. and Harker, K. *Symmetry of Crystals*, American Crystallographic Association Monograph No. 7, pp. 50–131. American Crystallographic Association: Buffalo, NY (1971).
- Feynman, R. P., Leighton, R. B., and Sands, M. *The Feynman Lectures on Physics: Mainly Mechanics, Radiation and Heat*. Addison-Wesley: Reading, MA; Palo Alto, CA; London (1963).
- Fischer, E. Synthesen in der Zuckergruppe. I. [Syntheses of sugars. I.] *Berichte der Deutschen Chemischen Gesellschaft* **23**, 2114–2141 (1890).
- Fischer, E. Synthesen in der Zuckergruppe. II. [Syntheses of sugars. II.] *Berichte der Deutschen Chemischen Gesellschaft* **27**, 3189–3232 (1894).
- Flack, H. D. On enantiomorph-polarity estimation. *Acta Crystallographica* **A39**, 876–881 (1983).
- Fourier, J. B. J. *Théorie Analytique de la Chaleur*. Firmin Didot: Paris (1822). [English translation with notes: Freeman, A. *Analytical Theory of Heat*. Cambridge University

- Press: London (1878); republication by Dover Phoenix Editions: New York (1955); digital version (2009).]
- Franklin, R. E. and Gosling, R. G. Molecular configuration in sodium thymonucleate. *Nature* **171**, 740–741 (1953).
- Frausto da Silva, J. J. R. and Williams, R. J. P. *The Biological Chemistry of the Elements: The Inorganic Chemistry of Life*. 2nd edition. Oxford University Press: New York (2001).
- Friedel G. Sur les symétries cristallines que peut révéler la diffraction des rayons Röntgen. [Concerning crystal symmetry revealed by X-ray diffraction.] *Comptes Rendus de l'Académie des Sciences (Paris)* **157**, 1533–1536 (1913).
- Friedrich, W., Knipping, P., and Laue, M. Interferenz-Erscheinungen bei Röntgenstrahlen [Interference phenomena with X rays.] *Sitzungsberichte der mathematisch-physikalischen Klasse der Königlichen Bayerischen Akademie der Wissenschaften zu München*, pp. 303–322 (1912). English translation: Stezowski, J. J. In: *Structural Crystallography in Chemistry and Biology* (ed. Glusker, J. P.), pp. 23–39. Hutchinson & Ross: Stroudsburg, PA (1981). [Max Laue became Max von Laue after his article was published].
- Gabe, E. J., Taylor, M. R., Glusker, J. P., Minkin, J. A., and Patterson, A. L. The crystal structure of 2-keto-3-ethoxybutyaldehyde-bis(thiosemicarbazone). *Acta Crystallographica* **B25**, 1620–1631 (1969).
- Germain, G., Main, P., and Woolfson, M. M. The application of phase relationships to complex structures. *Acta Crystallographica* **A27**, 368–376 (1971).
- Gibbs, J. W. *Vector Analysis. A Text-book for the Use of Students of Mathematics and Physics. Founded upon the Lectures of J. Willard Gibbs, Ph.D., LL.D. Formerly Professor of Mathematical Physics in Yale University.* (By Wilson, E. B.) Yale University Press: New Haven, CT (1901).
- Glasser, L. Fourier transforms for chemists. Part I. Introduction to the Fourier transform. *Journal of Chemical Education* **64**, A228–A233 (1987a).
- Glasser, L. Fourier transforms for chemists. Part 2. Fourier transforms in chemistry and spectroscopy. *Journal of Chemical Education* **64**, A260–A268 (1987b).
- Glusker, J. P., Patterson, A. L., Love, W. E., and Dornberg, M. L. X-ray crystal analysis of the substrates of aconitase. IV. The configuration of the naturally occurring isocitric acid as determined from potassium and rubidium salts of its lactone. *Acta Crystallographica* **16**, 1102–1107 (1963).
- Glusker, J. P., van der Helm, D., Love, W. E., Dornberg, M. L., Minkin, J. A., Johnson, C. K., and Patterson, A. L. X-ray crystal analysis of the substrates of aconitase. VI. The structures of sodium and lithium dihydrogen citrates. *Acta Crystallographica* **19**, 561–572 (1965).
- Glusker, J. P., van der Helm, D., Love, W. E., Minkin, J. A., and Patterson, A. L. The molecular structure of an azidopurine. *Acta Crystallographica* **B24**, 359–366 (1968).
- Glusker, J. P., Minkin, J. A., and Patterson, A. L. X-ray crystal analysis of the substrates of aconitase. IX. A refinement of the structure of anhydrous citric acid. *Acta Crystallographica* **B25**, 1066–1072 (1969).
- Glusker, J. P., Lewis, M., and Rossi, M. *Crystal Structure Analysis for Chemists and Biologists*. VCH: New York (1994).
- Green, D. W., Ingram, V. M., and Perutz, M. F. The structure of haemoglobin. IV. Sign determination by the isomorphous replacement method. *Proceedings of the Royal Society(London)* **A225**, 287–307 (1954).
- Grimaldi, F. M. *Physicomathesis de Lumine, Coloribus, et Iride, aliisque annexis*. [Physical insights into light, colors, and the spectrum (rainbow).] Vittorio Bonati: Bologna, Italy (1665).
- Groth, P. H. R. von. *Chemische Kristallographie*. 5 volumes. Leipzig: Engelmann (1906–1919).
- Guinier, A. and Fournet, G. *Small Angle Scattering of X-rays*. John Wiley: New York (1955).
- Grzeskowiak, K., Yanagi, K., Privé, G. G., and Dickerson, R. E. The structure of B-helical C-G-A-T-C-G-A-T-C-G and comparison with C-C-A-A-C-G-T-T-G-C. The effect of base pair reversals. *The Journal of Biological Chemistry* **266**, 8861–8883 (1991).
- Hahn, T. (ed.). *International Tables for Crystallography, Volume A, Space-group Symmetry*. Kluwer Academic (2005).
- Hajdu, J., Machin, P. A., Campbell, J. W., Greenhough, T. J., Clifton, I. J., Zurek, S., Gover, S., Johnson, L. N., and Elder, M. Millisecond X-ray diffraction and the first electron density map from Laue photographs of a protein crystal. *Nature* **329**, 178–181 (1987).
- Harburn, G., Taylor, C. A., and Welberry, T. R. *Atlas of Optical Transforms*. Bell and Sons: London (1975).
- Harker, D. The application of the three-dimensional Patterson method and the crystal structures of proustite, Ag_3AsS_3 , and pyrargyrite, Ag_3SbS_3 . *Journal of Chemical Physics* **4**, 381–390 (1936).
- Harker, D. The determination of the phases of the structure factors of non-centrosymmetric crystals by the method of double isomorphous replacement. *Acta Crystallographica* **9**, 1–9 (1956).
- Harker, D. and Kasper, J. S. Phases of Fourier coefficients directly from crystal diffraction data. *Acta Crystallographica* **1**, 70–75 (1948).
- Harp, J. M., Timm, D. E., and Bunick, G. J. Macromolecular crystal annealing: Overcoming increased mosaicity associ-

- ated with cryocrystallography. *Acta Crystallographica* **D54**, 622–628 (1998).
- Hartree, D. R. The wave mechanics of an atom with a non-Coulomb central field. Part I—Theory and methods. Part II—Some results and discussion. *Proceedings of the Cambridge Philosophical Society* **24**, 89–110, 111–132 (1928).
- Hartshorne, N. H. and Stuart, A. *Crystals and the Polarising Microscope*. 2nd edition. Edward Arnold: London (1950).
- Hauptman, H. On the identity and estimation of those cosine invariants, $\cos(\psi_1 + \psi_2 + \psi_3 + \psi_4)$, which are probably negative. *Acta Crystallographica* **A31**, 472–476 (1974).
- Hauptman, H. A. and Karle, J. *Solution of the Phase Problem I. The Centrosymmetric Crystal*. American Crystallographic Association Monograph No. 3. The Letter Shop: Washington, DC (1953).
- Häuy, R.-J. *Essai d'une théorie sur la structure des cristaux appliquée à plusieurs genres de substances cristallisées*. [Essay on a theory on the structure of crystals applied to various types of crystalline materials.] Gougué and Née de la Rochelle: Paris (1784).
- Häuy, R. J. *Traité de Minéralogie*. [Treatise on Mineralogy.] 5 volumes. Chez Louis: Paris (1801).
- Havighurst, R. J. The distribution of diffracting power in sodium chloride. *Proceedings of the National Academy of Sciences of the United States of America* **11**, 498–502 (1925).
- Helliwell, J. R. *Macromolecular Crystallography with Synchrotron Radiation*. Cambridge University Press: Cambridge (1992).
- Hendrickson, W. A. Determination of macromolecular structures from anomalous diffraction of synchrotron radiation. *Science* **254**, 51–58 (1991).
- Hendrickson, W. A. and Teeter, M. M. Structure of the hydrophobic protein crambin determined directly from the anomalous scattering of sulfur. *Nature* **290**, 107–113 (1981).
- Hirshfeld, F. Can X-ray data distinguish bonding effects from vibrational smearing? *Acta Crystallographica* **A32**, 239–244 (1976).
- Hodgkin, D. C., Kamper, J., Lindsey, J., Mackay, M., Pickworth, J., Robertson, J. H., Shoemaker, C. B., White, J. G., Prosen, R. J., and Trueblood, K. N. The structure of vitamin B₁₂. I. An outline of the crystallographic investigations of vitamin B₁₂. *Proceedings of the Royal Society (London)* **A242**, 228–263 (1957).
- Hodgkin, D. C., Pickworth, J., Robertson, J. H., Prosen, R. J., Sparks, R. A., and Trueblood, K. N. The structure of vitamin B₁₂. II. The crystal structure of a hexacarboxylic acid obtained by the degradation of vitamin B₁₂. *Proceedings of the Royal Society (London)* **A251**, 306–352 (1959).
- Holden, A. and Singer, P. *Crystals and Crystal Growing*. New York: Doubleday (1960).
- Holmes, K. C. and Blow, D. M. The use of X-ray diffraction in the study of protein and nucleic acid structure. In *Methods in Biochemical Analysis* (ed. Glick, D.), Vol. 13, pp. 113–239. Wiley: New York (1965). Reprinted by Interscience: New York (1966).
- Hooke, R. *Micrographia. Some Physiological Descriptions of Minute Bodies Made by Magnifying Glasses with Observations and Inquiries Thereupon*. J. Martyn and J. Allestry (for the Royal Society): London (1665).
- Hoppe, W. and Gassmann, J. Phase correction, a new method to solve partially known structures. *Acta Crystallographica* **B24**, 97–107 (1968).
- Hughes, E. W. The crystal structure of melamine. *Journal of the American Chemical Society* **68**, 1970–1975 (1946).
- Hümmer, K. and Billy, H. Experimental determination of triplet phases and enantiomorphs of non-centrosymmetric structures. I. Theoretical considerations. *Acta Crystallographica* **A42**, 127–133 (1986).
- Huygens, C. *Traité de la lumière*. [Treatise on light.] Pierre van der Aa: Leyden (1690). English translation: Thompson, S. P. *Treatise on Light*. Macmillan: London (1912).
- James, R. W. *The Optical Principles of the Diffraction of X-Rays*. G. Bell and Sons: London (1948, 1950, 1954, 1962); Cornell University Press: Ithaca, NY (1965).
- Jeffrey, G. A., Ruble, J. R., McMullan, R. K., and Pople, J. A. The crystal structure of deuterated benzene. *Proceedings of the Royal Society (London)* **A414**, 47–57 (1987).
- Jenkins, R. and Snyder, R. *Introduction to X-ray Powder Diffractometry*. Wiley-Interscience: New York (1996).
- Jenkins, F. A. and White, H. E. *Fundamentals of Optics*. 3rd edition. McGraw-Hill: New York (1957).
- Johnson, C. K. *ORTEP: A FORTRAN Thermal-Ellipsoid Plot Program for Crystal Structure Illustrations*. ORNL Report #3794. Oak Ridge National Laboratory: Oak Ridge, TN (1965).
- Johnson, C. K. Addition of higher cumulants to the crystallographic structure-factor equation: A generalized treatment for thermal-motion effects. *Acta Crystallographica* **A25**, 187–194 (1969).
- Johnson, C. K., Gabe, E. J., Taylor, M. R., and Rose, I. A. Determination by neutron and X-ray diffraction of the absolute configuration of an enzymatically formed α -monodeuteroglycolate. *Journal of the American Chemical Society*, **87**, 1802–1804 (1965).

- Jones, T. A., Zou, J. Y., Cowan, S. W., and Kjeldgaard, M. Improved methods for building protein models in electron density maps and the location of errors in these models. *Acta Crystallographica* **A47**, 110–119 (1991).
- Judson, H. F. *The Eighth Day of Creation: Makers of the Revolution in Biology*. 1st edition, Simon and Schuster: New York (1979). 2nd edition, Cold Spring Harbor Laboratory Press: Cold Spring Harbor, NY (1996).
- Kantardjiev, K. A. and Rupp, B. Matthews coefficient probabilities: Improved estimates for unit cell contents of proteins, DNA, and protein–nucleic acid complex crystals. *Protein Science* **12**, 1865–1871 (2003).
- Karle, J. and Hauptman, H. The phases and magnitudes of the structure factors. *Acta Crystallographica* **3**, 181–187 (1950).
- Karle, J. and Karle, I. L. The symbolic addition procedure for phase determination for centrosymmetric and noncentrosymmetric crystals. *Acta Crystallographica* **21**, 849–859 (1966).
- Kasai, N. and Kakudo, M. *X-ray Diffraction by Macromolecules*. Kodansha: Tokyo, and Springer: Berlin, Heidelberg, New York (2005).
- Kasper, J. S., Lucht, C. M., and Harker, D. The crystal structure of decaborane, B₁₀H₁₄. *Acta Crystallographica* **3**, 436–455 (1950).
- Katz, A. K., Li, X., Carrell, H. L., Hanson, B. L., Langan, P., Coates, L., Schoenborn, B. P., Glusker, J. P., and Bunick, G. J. Locating active-site hydrogen atoms in D-xylose isomerase: Time-of-flight neutron diffraction. *Proceedings of the National Academy of Sciences* **103**, 8342–8347 (2006).
- Kendrew, J. C., Dickerson, R. E., Strandberg, B. E., Hart, R. G., Davies, D. R., Phillips, D. C., and Shore, V. C. Structure of myoglobin. A three-dimensional Fourier synthesis at 2 Å resolution. *Nature* **185**, 422–427 (1960).
- Kepler, J. *Strena seu de nive sexangula*. [The six-cornered snowflake]. Godefridum Tambach: Francofurti ad Moenum (1611). English translation: Hardie, C. *The Six-cornered Snowflake*. Clarendon Press: Oxford (1966).
- Kitaigorodsky, A. I. *Molecular Crystals and Molecules*. Physical Chemistry Monographs Volume 29. Academic Press: London (1973).
- Koch, M. H., Vachette, P., and Svergun, D. I. Small-angle scattering: A view on the properties, structures and structural changes of biological macromolecules in solution. *Quarterly Review of Biophysics* **36**, 147–227 (2003).
- Ladd, M. F. C. and Palmer, R. A. *Structure Determination by X-ray Crystallography*. 4th Edition. Kluwer Academic/Plenum: New York (2003).
- Lamzin, V. S., Perrakis, A., and Wilson, K. S. The ARP/wARP suite for automated construction and refinement of protein models. In: *International Tables for Crystallography*, Volume F: *Crystallography of biological macromolecules*. Rossmann, M. G. and Arnold, E. (eds.). Kluwer Academic: Dordrecht, pp. 720–722 (2001).
- Langridge, R., Seeds, W. E., Wilson, H. R., Hooper, C. W., Wilkins, M. H. F., and Hamilton, L. D. Molecular structure of deoxyribonucleic acid (DNA). *Journal of Biophysical and Biochemical Cytology* **3**, 767–778 (1957).
- Le Bel, J. A. Sur les relations qui existent entre les formules atomiques des corps organiques, et le pouvoir rotatoire de leurs dissolutions. [On the relations which exist between the atomic formulas of organic compounds and the rotatory power of their solutions.] *Bulletin de la Société Chimique de France* **22**, 337–347 (1874). English translation: Benfy, O. T. In: *Classics in the Theory of Chemical Combinations*, pp. 151–171. Dover: New York (1963).
- Legendre, A. M. Appendix. Sur la méthode des moindres carrés. In: *Nouvelles Méthodes pour la Détermination des Orbites des Comètes*, pp. 72–75. Courcier: Paris (1805). English translation: Harvey, G. On the method of minimum squares, employed in the reduction of experiments, being a translation of the appendix to an essay of Legendre's entitled "Nouvelles Méthodes pour la Détermination des Orbites des Comètes," with remarks. *Edinburgh Philosophical Journal* **7**, 292–301 (1822).
- Leslie, A. G. W. A reciprocal-space method for calculating a molecular envelope using the algorithm of B. C. Wang. *Acta Crystallographica* **A43**, 134–136 (1987).
- Lima-de-Faria, J. (ed.). *Historical Atlas of Crystallography*. Kluwer Academic: Dordrecht, Boston, London (1990).
- Lipscomb, W. N. Structures of the boron hydrides. *Journal of Chemical Physics* **22**, 985–988 (1954).
- Lipson, H. and Cochran, W. *The Crystalline State*, Volume III, *The Determination of Crystal Structures*. Cornell University Press: Ithaca, NY; G. Bell and Sons: London (1966).
- Lonsdale, K. The structure of the benzene ring. *Nature* **122**, 810 (1928).
- Matthews, B. W. Solvent content of protein crystals. *Journal of Molecular Biology* **33**, 491–497 (1968).
- McPherson, A. *Preparation and Analysis of Protein Crystals*. Wiley: New York (1982).
- McRee, D. E. *Practical Protein Crystallography*. 1st edition (1993). 2nd edition, Academic Press: San Diego (1999).
- Miller, R., DeTitta, G. T., Jones, R., Langs, D. A., Weeks, C. M., and Hauptman, H. A. On the application of the

- minimal principle to solve unknown structures. *Science* **259**, 1430–1433 (1993).
- Miller, R., Gallo, S. M., Khalak, H. G., and Weeks, C. M. SnB: Crystal structure determination via shake-and-bake. *Journal of Applied Crystallography* **27**, 613–621 (1994).
- Miller, W. H. *A Treatise on Crystallography*. Pitt Press (Deighton): Cambridge, and Parker: London (1839).
- Mitchell, D. P. and Powers, P. N. Bragg reflection of slow neutrons. *Physical Review* **50**, 486–487 (1936).
- Mitscherlich, E. Sur la relation qui existe entre la forme cristalline et les proportions chimiques. I. Mémoire sur les arseniates et les phosphates. [On the relationship that exists between crystal form and chemical proportions. I. Note on arsenates and phosphates.] *Annales des Chimie et des Physique* **19**, 350–419 (1822).
- Moffat, K., Szebenyi, D., and Bilderback, D. X-ray Laue diffraction from protein crystals. *Science* **223**, 1423–1425 (1984).
- Müller, P. Practical suggestions for better crystal structures. *Crystallography Reviews* **15**, 57–83 (2009).
- Murshudov, G. N., Vagin, A. A., and Dodson, E. J. Refinement of macromolecular structures by the maximum-likelihood method. *Acta Crystallographica* **D53**, 240–253 (1997).
- Niggli, P. *Krystallographische und Strukturtheoretische Grundbegriffe*, Volume 7, Part 1, pp. 108–176. Handbuch der Experimentalphysik. Akademische Verlagsgesellschaft: Leipzig, Germany (1928).
- Nyburg, S. C. *X-ray Analysis of Organic Structures*. Academic Press: New York (1961).
- Okaya, Y., Saito, Y., and Pepinsky, R. New method in X-ray crystal structure determination involving the use of anomalous dispersion. *Physical Review* **98**, 1857–1858 (1955).
- Oldfield, T. J. Automated tracing of electron-density maps of proteins. *Acta Crystallographica* **D59**, 483–491 (2003).
- Oszlányi, G. and Süto, A. Ab initio structure solution by charge flipping. II. Use of weak reflections. *Acta Crystallographica* **A61**, 147–152 (2005).
- Ott, H. Zur Methodik der Strukturanalyses. [On a method of structure analysis.] *Zeitschrift für Kristallographie* **66**, 136–153 (1927).
- Palatinus, L. and Chapuis, G. SUPERFLIP—a computer program for the solution of crystal structures by charge flipping in arbitrary dimensions. *Journal of Applied Crystallography* **40**, 786–790 (2007).
- Pasteur, L. Mémoire sur la relation qui peut exister entre la forme cristalline et la composition chimique et sur la cause de la polarisation rotatoire. [Note on the relationship of crystalline form to chemical composition, and on the cause of rotatory polarization.] *Comptes Rendus de l'Académie des Sciences (Paris)* **26**, 535–538 (1848).
- Patterson, A. L. A Fourier series method for the determination of the components of interatomic distances in crystals. *Physical Review* **46**, 372–376 (1934).
- Patterson, A. L. A direct method for the determination of the components of interatomic distances in crystals. *Zeitschrift für Kristallographie* **90**, 517–542 (1935).
- Patterson, A. L. Treatment of anomalous dispersion in X-ray diffraction data. *Acta Crystallographica* **16**, 1255–1256 (1963).
- Patterson, T. S. and Buchanan, C. Historical and other considerations regarding the crystal form of sodium-ammonium *d*- and *l*-tartrate, potassium *d*- and *l*-tartrate, potassium-ammonium *d*- and *l*-tartrate, and potassium racemate. *Annals of Science* **5**, 288–295, 317–324 (1945).
- Pauling, L. The principles determining the structure of complex ionic crystals. *Journal of the American Chemical Society* **51**, 1010–1026 (1929).
- Perutz, M. F. Stereochemistry of cooperative effects in haemoglobin. *Nature* **228**, 726–734 (1976).
- Perutz, M. F., Muirhead, H., Cox, J. M., Goaman, L. C. G., Mathews, F. S., McGandy, E. L., and Webb, L. E. Three-dimensional Fourier synthesis of horse oxyhaemoglobin at 2.8 Å resolution: (I) X-ray analysis. *Nature* **219**, 29–32 (1968).
- Peterson, S. W. and Levy, H. A. A single crystal neutron diffraction determination of the hydrogen position in potassium bifluoride. *Journal of Chemical Physics* **20**, 704–707 (1952).
- Phillips, D. C. The three-dimensional structure of an enzyme molecule. *Scientific American* **215**, 78–90 (1966).
- Phillips, F. C. *An Introduction to Crystallography*. 3rd edition, Longmans, Green: London (1963). 4th edition, Oliver and Boyd: Edinburgh (1971).
- Planck, M. Über das Gesetz der Energieverteilung im Normalspektrum. [On the law of distribution of energy in the normal spectrum.] *Annalen der Physik* **4**, 553–563 (1901).
- Pople, J. A. Nobel Lecture: Quantum chemical models. *Reviews of Modern Physics* **71**, 1267–1274 (1999).
- Porter, A. B. On the diffraction theory of microscopic vision. *Philosophical Magazine* **11**, 154–166 (1906).
- Ravelli, R. G. B., Leiros, H. K. S., Pan, B., Caffrey, M. and McSweeney S. Specific radiation damage can be used to solve macromolecular structures. *Structure* **11**, 217–224 (2003).

- Renninger, M. "Umweganregung," eine bisher unbeachtete Wechselwirkungserscheinung bei Raumgitterinterferenzen. ["Detour-excitation," a hitherto unobserved interaction in space-lattice interference.] *Zeitschrift für Physik* **106**, 141–176 (1937).
- Rietveld, H. M. A profile refinement method for nuclear and magnetic structures. *Journal of Applied Crystallography* **2**, 65–71 (1969).
- Robertson, J. M. An X-ray study of phthalocyanines. Part II. Quantitative structure determination of the metal-free compound. *Journal of the Chemical Society* 1195–1209 (1936).
- Romé de Lisle, J. B. L. *Essai de Cristallographie, ou Description des Figures Géométriques propres à Différens Corps du Règne Minéral, connus vulgairement sous le Nom de Cristaux*. [Essay on crystallography, or a description of geometric figures, characteristic of different materials in the mineral kingdom, known commonly under the name of crystals.] 1st edition. Didot, Knappen & Delaguette: Paris (1772).
- Röntgen, W. C. Über eine neue Art von Strahlen. *Sitzungsberichte der Würzburger Physikalischen-Medizinischen Gesellschaft*, pp. 132–141 (1895). English translation: Stanton, A. On a new kind of ray. *Science* **3**, 227–231 (1896); *Nature (London)* **53**, 274–276 (1896).
- Rosenfield, R. E. Jr., Parthasarathy, R., and Dunitz, J. D. Directional preferences of nonbonded atomic contacts with divalent sulfur. 1. Electrophiles and nucleophiles. *Journal of the American Chemical Society* **99**, 4860–4862 (1977).
- Rossmann, M. G. (ed.). *The Molecular Replacement Method*. Gordon and Breach: New York (1972).
- Rossmann, M. G. and Blow, D. M. The detection of subunits within the crystallographic asymmetric unit. *Acta Crystallographica* **15**, 24–31 (1962). See also Tollin, P. and Rossmann, M. G. A description of various rotation function programs. *Acta Crystallographica* **21**, 53–57 (1966).
- Rubin, B. H., Stallings, W. C., Glusker, J. P., Bayer, M. E., Janin, J., and Srere, P. A. Crystallographic studies of *Escherichia coli* citrate synthase. *Journal of Biological Chemistry* **258**, 1297–1298 (1983).
- Sawaya, M. R. Characterizing a crystal from an initial native dataset. In: *Macromolecular Crystallography Protocols*, Volume 2, *Structure Determination*. Doublé, S. (ed.). Methods in Molecular Biology 364. Humana Press: Totowa, NJ (2007).
- Sayre, D. The squaring method: A new method for phase determination. *Acta Crystallographica* **5**, 60–65 (1952).
- Sayre, D. Report on a project on three-dimensional imaging of the biological cell by single-particle X-ray diffraction. *Acta Crystallographica* **A64**, 33–35 (2008).
- Schneer, C.J. (ed.) *Crystal Form and Structure*. Dowden, Hutchinson and Ross. Stroudsburg, Pennsylvania (1977).
- Schneider, T. R. and Sheldrick, G. M. Substructure solution with SHELXD. *Acta Crystallographica* **D58**, 1772–1779 (2002).
- Schoenflies, A. *Krystallsysteme und Krystallstruktur*. [Crystal systems and crystal structures.] B. G. Teubner: Leipzig (1891). 2nd edition (1923). Reprinted, Springer: Berlin (1984).
- Schomaker, V. and Trueblood, K. N. On the rigid-body motion of molecules in crystals. *Acta Crystallographica* **B24**, 63–76 (1968).
- Shapiro, D., Thibault, P., Beetz, T., Elser, V., Howells, M., Jacobsen, C., Kirz, J., Lima, E., Miao, H., Neiman, A. M., and Sayre, D. Biological imaging by soft X-ray diffraction microscopy. *Proceedings of the National Academy of the United States of America* **102**, 15343–15346 (2005).
- Sheldrick, G. M. A short history of SHELX. *Acta Crystallographica* **A64**, 112–122 (2008).
- Shen, Q. Solving the phase problem using reference-beam X-ray diffraction. *Physical Review Letters* **80**, 3268–3271 (1998).
- Shmueli, U. *Theories and Techniques of Crystal Structure Determination*, IUCr Texts on Crystallography 9, International Union of Crystallography, Oxford Science Publications. Oxford University Press: New York (2007).
- Snook, C. F., Purdy, M. D., and Wiener, M. C. Use of a crystallization robot to set up sitting-drop vapor-diffusion crystallization and in situ crystallization screens. *Journal of Applied Crystallography* **33**, 344–349 (2000).
- Sommerfeld, A. Remarks in: *La Structure de la Matière*. [The structure of matter.] *Rapports et Discussions du Conseil de Physique tenu à Bruxelles du 27 au 31 Octobre 1913 sous les auspices de l'Institut International de Physique Solvay*, p. 131. [Publication delayed because of the Great War.] Gauthier-Villars: Paris (1921).
- Spek, A. L. Single-crystal structure validation with the program PLATON. *Journal of Applied Crystallography* **36**, 7–13 (2003).
- Squire, J. M. Fibre and muscle diffraction. In: *Structure and Dynamics of Biomolecules. Neutron and Synchrotron Radiation for Condensed Matter Studies*. Fanchon, E., Geissler, E., Hodeau, J.-L., Regnard, J.-R., and Timmins, P. A. (eds.), Chapter 14, pp. 272–301. Oxford University Press: New York (2000).
- Steno [Stensen], N. *De Solido intra Solidum Naturaliter Contento. Dissertationis Prodromus*. [The prodromus to a

- dissertation concerning solids naturally contained within solids.] *Ad Serenissimum Ferdinandum II. Magnum Erturiae Ducem. Stellæ Florentiæ* (1669). English translation: Oldenburgh, H. Published by J. G. Winter: London (1671).
- Stewart, R. F., Davidson, E. R., and Simpson, W. T. Coherent X-ray scattering for the hydrogen atom in the hydrogen molecule. *Journal of Chemical Physics* **42**, 3175–3187 (1965).
- Stigler, S. M. The epic story of maximum likelihood. *Statistical Science* **22**, 598–620 (2007).
- Stoicheff, B. P. High resolution Raman spectroscopy of gases. II. Rotational spectra of C₆H₆ and C₆D₆ and internuclear distances in the benzene molecule. *Canadian Journal of Physics* **32**, 339–346 (1954).
- Stout, G. H. and Jensen, L. H. *X-ray Structure Determination: A Practical Guide*. Macmillan: New York (1968). 2nd edition, Wiley-Interscience: New York (1989).
- Stubbs, G., Warren, S., and Holmes, K. Structure of RNA and RNA binding site in tobacco mosaic virus from 4-Å map calculated from X-ray fibre diagrams. *Nature* **267**, 216–221 (1977).
- Tanaka, Y., Ohtomo, N., and Katayama, M. A diffraction study of SiO₂ glass—an analysis of neutron and X-ray data by a liquid model. *Journal of the Physical Society of Japan* **54**, 967–976 (1985).
- Taylor, C. A. and Lipson, H. *Optical Transforms: Their Preparation and Application to X-ray Diffraction Problems*. G. Bell and Sons: London (1964).
- Templeton, D. H., Templeton, L. K., Phillips, J. C., and Hodgson, K. O. Anomalous scattering of X-rays by cesium and cobalt measured with synchrotron radiation. *Acta Crystallographica* **A36**, 436–442 (1980).
- Terwilliger, T. C. Maximum-likelihood density modification. *Acta Crystallographica* **D56**, 965–972 (2000).
- Thomson, J. J. *Conduction of Electricity through Gases*, p. 268 (1903). 2nd edition, p. 321 (1906). 3rd edition, with Thomson, G. P., in two volumes, Volume II, p. 256 (1928 and 1933). Merchant Books, Cambridge University Press: Cambridge.
- Trueblood, K. N., Bürgi, H.-B., Burzlaff, H., Dunitz, J. D., Gramaccioni, C. M., Schulz, H. H., Shmueli, U., and Abrahams, S. C. Atomic displacement parameter nomenclature. Report of a subcommittee on atomic displacement parameter nomenclature. *Acta Crystallographica* **A52**, 770–781 (1996).
- Usón, I., Stevenson, C. E., Lawson, D. N., and Sheldrick, G. M. Structure determination of the O-methyltransferase NovP using the “free lunch algorithm” as implemented in SHELXE. *Acta Crystallographica* **D63**, 1069–1074 (2007).
- Vagin, A. A., Steiner, R. S., Lebedev, A. A., Potterton, L., McNicholas, S., Long, F., and Murshudov, G. N. REF-MAC5 dictionary: Organisation of prior chemical knowledge and guidelines for its use. *Acta Crystallographica* **D60**, 2284–2295 (2004).
- van der Helm, D., Glusker, J. P., Johnson, C. K., Minkin, J. A., Burow, N. E., and Patterson, A. L. X-ray crystal analysis of the substrates of aconitase. VIII. The structure and absolute configuration of potassium dihydrogen isocitrate isolated from *Bryophyllum calycinum*. *Acta Crystallographica* **B24**, 578–592 (1968).
- van't Hoff, J. H. *Voorstel tot Uitbreiding der Tegenwoordige in de Scheikunde gebruikte Structuurformules in de Ruimte, benevens een daarmee samenhangende Opmerking omtrent het Verband tusschen Optisch Actief Vermogen en chemische Constitutie van Organische Verbindingen*. [Proposal for the extension of the structural formulae now in use in chemistry into space, together with a related note on the relation between the optical active power and the chemical constitution of organic compounds.] J. Greven: Utrecht (1874), and *Archives Néerlandaises des Sciences Exactes et Naturelles* **9**, 445–454 (1874). English translation: *Arrangement of Atoms in Space*. Longmans, Green: London (1898).
- Verbist, J. J., Lehmann, M. S., Koetzle, T. F., and Hamilton, W. C. Direct methods in neutron crystallography: Structure of L-proline monohydrate by symbolic addition and tangent refinement. *Nature* **235**, 328–329 (1972).
- Viterbo, D. Solution and refinement of crystal structures. In: *Fundamentals of Crystallography*. Giacovazzo, C. (ed.), Chapter 5, pp. 320–401. International Union of Crystallography, Oxford University Press (1992).
- von Halban, H. and Preiswerk, P. Preuve expérimentale de la diffraction des neutrons. (Experimental proof of the diffraction of neutrons.) *Comptes Rendus de l'Académie des Sciences (Paris)* **203**, 73–75 (1936).
- Wahlstrom, E. E. *Optical Crystallography*. 5th edition. Wiley: New York, Chichester, Brisbane, Toronto (1979).
- Waller, I. Zur Frage der Einwirkung der Wärmebewegung auf die Interferenz von Röntgenstrahlen. [On the question of the influence of heat motion on the scattering of Röntgen rays.] *Zeitschrift für Physik* **17**, 398–408 (1923).
- Wang, B.-C. Resolution of phase ambiguity in macromolecular crystallography. *Methods in Enzymology* **115**, 90–112 (1985).
- Warren, B. E. X-ray diffraction study of the structure of glass. *Chemical Reviews* **26**, 237–255 (1940).
- Waser, J. Pictorial representation of the Fourier method of X-ray crystallography. *Journal of Chemical Education* **45**, 446–451 (1968).

Watson, J. D. and Crick, F. H. C. A structure for deoxyribose nucleic acid. *Nature* **171**, 737–738 (1953).

Weissenberg, K. Ein neues Röntgengoniometer. [A new X-ray camera.] *Zeitschrift für Physik* **23**, 229–238 (1924).

Willis, B. T. M. and Carlile, C. J. *Experimental Neutron Scattering*. Oxford University Press: Oxford (2009).

Willis, B. T. M. and Pryor, A. W. *Thermal Vibrations in Crystallography*. Cambridge University Press: Cambridge (1975).

Wilson, A. J. C. Determination of absolute from relative X-ray intensity data. *Nature* **150**, 151–152 (1942).

Wilson, A. J. C. The probability distribution of X-ray intensities. *Acta Crystallographica* **2**, 318–321 (1949).

Wilson, A. J. C. Largest likely values for the reliability index. *Acta Crystallographica* **3**, 397–398 (1950).

Wilson, C. *Single Crystal Neutron Diffraction from Molecular Materials*, Series on Neutron Techniques and Applications Volume 2. World Scientific: Singapore (2000).

Wilson, H. R. *Diffraction of X-rays by Proteins, Nucleic Acids and Viruses*. Arnold: London (1966).

Wood, E. A. *Crystals and Light: An Introduction to Optical Crystallography*. Van Nostrand: New York (1977).

Wyckoff, R. W. G. *The Analytical Expression of the Results of the Theory of Space Groups*. Publication 38. Carnegie Institution of Washington (1922). 2nd edition (1930).

Yang, C., Pflugrath, J. W., Courville, D. A., Stence, C. N., and Ferrara, J. D. Away from the edge: SAD phasing from the sulfur anomalous signal measured in-house with chromium radiation. *Acta Crystallographica* **D59**, 1943–1957 (2003).

Yao, J.-X., Woolfson, M. M., Wilson, K. S., and Dodson, E. J. A modified ACORN to solve protein structures at resolutions of 1.7 Å or better. *Acta Crystallographica* **D61**, 1465–1475 (2005).

Young, R. A. (ed.). *The Rietveld Method*. Oxford University Press: Oxford (1993).

Young, T. Lecture XXXIX. On the nature of light and colours. In: *A Course of Lectures on Natural Philosophy and the Mechanical Arts*, pp. 457–471 (1807).

Zachariasen, W. H. A new analytical method for solving complex crystal structures. *Acta Crystallographica* **5**, 68–73 (1952).

Zernike, F. and Prins, J. A. Die Beugung von Röntgenstrahlen in Flüssigkeiten als Effekt der Molekülanordnung. [The diffraction of X rays in liquids as an effect of the molecular arrangement.] *Zeitschrift für Physik* **41**, 184–194 (1927).

Acta Crystallographica and other IUCr journals

The international organization to which most crystallographers belong, through various national associations, is the International Union of Crystallography (IUCr), which holds congresses and symposia every three years and sponsors publications and compilations. The tables of data published by the IUCr provide not only useful information, but also an explanation of each area of crystallography that is referred to. The reader is urged to browse through *International Tables* (see below), particularly the plane groups in Volume A, and some of the details of the experimental methods that are clearly described in Volume C.

Some journals for crystallographers that are published by the International Union of Crystallography are: *Acta Crystallographica*, *Journal of Applied Crystallography*, and *Journal of Synchrotron Radiation*. Structure determinations are also reported in *Structure Reports*, *Zeitschrift für Kristallographie*, *Inorganic Chemistry*, *Journal of the American Chemical Society*, *Journal of the Chemical Society*, *Acta Chemica Scandinavica*, and *Helvetica Chimica Acta*, among others. *Acta Crystallographica* Sections E and F are online only; all other IUCr journals are available in print and online.

IUCr journals

Acta Crystallographica. ISSN 0365-110X, 1948–1967, <http://journals.iucr.org/q/>

Acta Crystallographica Section A: Crystal Physics, Diffraction, Theoretical and General Crystallography. ISSN 0567-7394, 1968–1982, <http://journals.iucr.org/a/>

Acta Crystallographica Section A: Foundations of Crystallography. Schwarzenbach, D. (ed.), ISSN 0108-7673, 1983–, <http://journals.iucr.org/a/>

Acta Crystallographica Section B: Structural Crystallography and Crystal Chemistry. ISSN 0567-7408, 1968–1982, <http://journals.iucr.org/b/>

Acta Crystallographica Section B: Structural Science. Brock, C. P. (ed.), ISSN 0108-7681, 1983–, <http://journals.iucr.org/b/>

Acta Crystallographica Section C: Crystal Structure Communications. Linden, A. (ed.), ISSN 0108-2701, 1983–, <http://journals.iucr.org/c/>

Acta Crystallographica Section D: Biological Crystallography. Baker, E. N. and Dauter, Z. (eds.), ISSN 0907-4449, 1993–, <http://journals.iucr.org/d/>

Acta Crystallographica Section E: Structure Reports Online. Harrison, W. T. A., Simpson, J., and Weil, M. (eds.), ISSN 1600-5368, 2001–, <http://journals.iucr.org/e/>

Acta Crystallographica Section F: Structural Biology and Crystallization Communications. Einspahr, H. M. and Weiss, M. S. (eds.), ISSN 1744-3091, 2005–, <http://journals.iucr.org/f/>

Journal of Applied Crystallography. Pyzalla, A. R. (ed.), ISSN 0021-8898, 1968–, <http://journals.iucr.org/j/>

Journal of Synchrotron Radiation. Ice, G. E., Kwick, Å., and Ohta, T. (eds.), ISSN 0909-0495, 1994–, <http://journals.iucr.org/s/>

International Tables for Crystallography (available as books or online)

International Tables for X-ray Crystallography, Volume 1, Symmetry Groups. Henry, N. F. M. and Lonsdale, K. (eds.). International Union of Crystallography, Kynoch Press: Birmingham, UK (1969).

(*International Tables for Crystallography* is available from Wiley.)

Volume A, *Space-group Symmetry*. Hahn, T. (ed.), ISBN 978-0-7923-6590-7 (2005), <http://it.iucr.org/A/>, IUCr/Springer.

Volume A1, *Symmetry Relations Between Space Groups*. Wondratschek, H. and Müller, U. (eds.), ISBN 978-1-4020-2355-2 (2004), <http://it.iucr.org/A1/>, IUCr/Springer.

Volume B, *Reciprocal Space*. Shmueli, U. (ed.), ISBN 978-1-4020-8205-4 (2008), <http://it.iucr.org/B/>, IUCr/Springer.

Volume C, *Mathematical, Physical and Chemical Tables*. Prince, E. (ed.), ISBN 978-1-4020-1900-5 (2004), <http://it.iucr.org/C/>, IUCr/Kluwer Academic.

Volume D, *Physical Properties of Crystals*. Authier, A. (ed.), ISBN 978-1-4020-0714-9 (2003), <http://it.iucr.org/D/>, IUCr/Kluwer Academic.

Volume E, *Subperiodic Groups*. Kopsk'y, V. and Litvin, D. B. (eds.), ISBN 978-1-4020-0715-6 (2002), <http://it.iucr.org/E/>, IUCr/Kluwer Academic.

Volume F, *Crystallography of Biological Macromolecules*. Rossmann, M. G. and Arnold, E. (eds.), ISBN 978-0-7923-6857-1 (2001), <http://it.iucr.org/F/>, IUCr/Kluwer Academic.

Volume G, *Definition and Exchange of Crystallographic Data*. Hall, S. R. and McMahon, B. (eds.), ISBN 978-1-4020-3138-0 (2005), <http://it.iucr.org/G/>, IUCr/Springer.

Useful books

All teachers of X-ray crystallography, including the present authors, have their favorite sources of information. We have chosen those that we consider to have a simple or clarifying approach. Those readers who wish to delve further into the subject should follow the bibliogra-

phies given in some of the books listed. We have tried to keep to a minimum the number of different books referred to, thus necessarily omitting some worthy ones. A few books are mentioned for the browser because they seem delightful, but they are not essential for those with limited time or budget. At the beginning of this book we stated that this is a book that tries to explain “why it is possible to do it,” not “how to do it.” There are many excellent texts listed here that address both, some concentrating on “how to do it.”

The World Wide Web, Google, for example, contains almost everything you would want to know about X-ray and neutron diffraction and their use in structure determination. Many articles are available in full, even some of the historical articles listed in the text. However, the URLs of many informative teaching sites seem to change with time and therefore we have not included them.

Bentley, W. A. *Snow Crystals*. McGraw-Hill: New York (1931). See also Martin, J. B. *Snowflake Bentley*. Houghton-Mifflin: New York (1998).

Bijvoet, J. M., Burgers, W. G., and Hägg, G. (eds.). *Early Papers on Diffraction of X-rays by Crystals* (Volume I, Volume II). Published for the International Union of Crystallography by A. Oosthoek's Uitgeversmaatschappij N.V.: Utrecht (1969, 1972).

Blow, D. *Outline of Crystallography for Biologists*. Oxford University Press: Oxford (2002).

Bragg, W. L., Phillips, D. C., and Lipson, H. *The Development of X-ray Analysis*. New York: Dover (1992).

Clegg, W., Blake, A.J., Gould, R.O., and Main, P. *Crystal Structure Analysis Principles and Practice*. Oxford University Press: Oxford (2001).

Ewald, P. P. (ed.). *Fifty Years of X-ray Diffraction*. Published for the International Union of Crystallography by A. Oosthoek's Uitgeversmaatschappij N.V.: Utrecht (1962).

Giacovazzo, C., Monaco, H. L., Viterbo, D., Scordari, F., Gilli, G., Zanotti, G., and Catti, M. *Fundamentals of Crystallography*. 1st edition (1992). 2nd edition, IUCr and Oxford Science Publications: Oxford (2002).

Glusker, J. P. (ed.). *Structural Crystallography in Chemistry and Biology*. Benchmark Papers in Physical Chemistry and Chemical Physics. Hutchinson Ross: Stroudsburg, PA and Woods Hole, MA (1981).

Hammond, C. *The Basics of Crystallography and Diffraction*. International Union of Crystallography Texts on Crystallography 5. 1st edition (1997). 2nd edition (2001). 3rd edition, Oxford University Press: Oxford, New York (2009).

Jenkins, R. and Snyder, R. *Introduction to X-ray Powder Diffractometry*. Wiley-Interscience: New York (1996).

Lonsdale, K. *Crystals and X-rays*. D. van Nostrand: New York (1949).

Luger, P. *Modern X-ray Analysis on Single Crystals*. W. de Gruyter: Berlin, New York (1980).

Massa, W. *Crystal Structure Determination*. 2nd edition, Springer-Verlag: Berlin, Heidelberg, New York. (2004). Translated by Gould, R. O. Originally published in German as *Kristallstrukturbestimmung*, B. G. Teubner GbmH: Stuttgart, Leipzig, Wiesbaden (2002).

McPherson, A. *Introduction to Macromolecular Crystallography*. 2nd edition. Wiley: Hoboken, NJ (2009).

Müller, P., Herbst-Irmer, R., Spek, A. L., Schneider, T. R., and Sawaya, M. R. *Crystal Structure Refinement: A Crystallographer's Guide to SHELXL*. Oxford University Press: Oxford (2006).

Pecharsky, V. and Zavalij, P. *Fundamentals of Powder Diffraction and Structural Characterization of Materials*. Springer/Kluwer Academic: New York (2003).

Rhodes, G. *Crystallography Made Crystal Clear*. Academic Press: San Diego (2000).

Sands, D. E. *Introduction to Crystallography*. W. A. Benjamin (1969, 1975). Dover Publications: Mineola, NY (1975).

Schwarzenbach, D. *Kristallographie*. Springer: Berlin (2001).

Steadman, R. *Crystallography*. Van Nostrand Reinhold: Wokingham (1982).

Woolfson, M. M. *An Introduction to X-ray Crystallography*, Cambridge University Press: Cambridge (1997).

International Union of Crystallography Commission on Crystallographic Teaching teaching pamphlets

1. A non-mathematical introduction to X-ray diffraction. C. A. Taylor.
2. An introduction to the scope, potential and applications of X-ray analysis. M. Laing.
3. Introduction to the calculation of structure factors. S. C. Wallwork.
4. The reciprocal lattice. A. Authier.

5. Close-packed structures. P. Krishna and D. Pandey.

6. Pourquoi les groupes de symétrie en cristallographie. D. Weigel.

7. Solving the phase problem when heavy atoms are in special positions. L. Hohne and L. Kutchabsky.

8. Anomalous dispersion of X-rays in crystallography. S. Caticha-Ellis.

9. Rotation matrices and translation vectors in crystallography. S. Hovmöller.

10. Metric tensor and symmetry operations in crystallography. O. Rigault.

11. The stereographic projection. E. J. W. Whittaker.

12. Projections of cubic crystals. I. O. Angell and M. Moore.

13. Symmetry. L. S. Dent Glasser.

14. Space group patterns. W. M. Meier.

15. Elementary X-ray diffraction for biologists. J. P. Glusker.

16. The study of metals and alloys by X-ray powder diffraction methods. H. Lipson.

17. An introduction to direct methods. The most important phase relationships and their application in solving the phase problem. H. Schenk.

18. An introduction to crystal physics. E. Hartmann.

19. Introduction to neutron powder diffractometry. E. Arzi.

20. Crystals—a handbook for school teachers. E. A. Wood.

21. Crystal packing. A. Gavezzotti and H. Flack.

22. Matrices, mappings, and crystallographic symmetry. H. Wondratshek.

23. Teaching crystallographic and magnetic point group symmetry using three-dimensional rendered visualizations. M. de Graef.

These pamphlets are available on the Web and can be copied (full text or pdf). The copyright in these materials resides with the International Union of Crystallography. The electronic editions available from the Web site may be freely copied and redistributed for educational or research purposes only.

Index of scientists referred to in the text

Note: no dates listed for living persons.

- Ångström, Anders Jonas (1814–1874) 236
- Avogadro, Lorenzo Romano Amedeo Carlo (1776–1856) 238
- Avrami, Melvin (Melvin, Mael A.) 115
- Banerjee, Kedaeswar (1900–1975) 115
- Barlow, William (1845–1934) 3, 110
- Bergman, Torbern Olof (1735–1784) 10
- Bessel, Friedrich (1784–1846) 238
- Bijvoet, Johannes Martin (1892–1980) 157, 236, 238
- Bragg, William Henry (1862–1942) 43, 238
- Bragg, William Lawrence (1890–1971) 3, 43, 45, 238
- Bravais, Auguste (1811–1863) 20, 239
- Bunyakovsky, Viktor Yakovlevich (1804–1889) 239
- Cauchy, Augustin-Louis (1789–1857) 116, 239
- Chadwick, James (1891–1974) 56
- Cochran, William (1922–2003) 37, 116
- Coster, Dirk (1889–1950) 157, 158
- Curie, Pierre and Jacques (1859–1906) and (1856–1941) 22
- Davison, Clinton Joseph (1881–1958) 3
- de Broglie, Louis-Victor-Pierre-Raymond (1892–1987) 56
- Debye, Peter (Petrus) Josephus Wilhelms (1884–1966) 83
- Descartes, René (1506–1650) 239
- Dodson, Eleanor 127
- Dunitz, Jack David 173, 186
- Euler, Leonhard Paul (1707–1783) 244
- Ewald, Paul Peter (1888–1985) 52, 53
- Fedorov (Fyodorov) Evgraf Stepanovich (1853–1919) 110
- Feynman, Richard Phillips (1918–1988) 35
- Fischer, Hermann Emil (1852–1919) 159, 160
- Flack, Howard D. 157
- Fourier, Jean Baptiste Joseph (1768–1830) 86, 244
- Frankenheim, Moritz Ludwig (1801–1869) 20
- Fresnel, Augustin-Jean (1788–1827) 26
- Friedel, Georges (1865–1933) 245
- Friedrich, Walther (1883–1968) 3, 9, 41, 44, 48
- Gauss, Johann Carl Friedrich (1777–1855) 245
- Geiger, Hans Wilhelm (1882–1945) 245
- Germer, Lester Halbert (1896–1971) 3
- Giacovazzo, Carmelo 127
- Gibbs, Josiah Willard (1839–1903) 33
- Gillis, Joseph (1911–1993) 116
- Gregory, James (1638–1675) 256
- Grimaldi, Francesco Maria (1618–1663) 26
- Harker, David (1906–1991) 115, 116, 245
- Hauptmann, Herbert 116
- Haüy, René Just (1743–1822) 10, 247
- Hendrickson, Wayne Arthur 163
- Hirshfeld, Fred L. (1927–1991) 190
- Hooke, Robert (1635–1703) 10
- Hughes, Edward Wesley (1904–1987) 173
- Huygens, Christiaan (1629–1695) 26
- James, Reginald William (1891–1964) 27
- Judson, Horace Freeland 131
- Karle, Isabella Helen (Lugoski) 116
- Karle, Jerome 116
- Kasper, John Simon (1915–2005) 115, 116, 245
- Kennard, Olga (Weisz) 184
- Kepler, Johannes (1571–1630) 10
- Knipping, Paul (1883–1935) 3, 9, 41, 44, 48
- Knol, Kornelis Swier 157, 158
- Lagrange, Joseph-Louis (Lagrangia, Giuseppe Lodovico) (1736–1813) 247
- le Bel, Joseph Achille (1847–1930) 151
- Legendre, Adrien-Marie (1752–1833) 173
- Lipson, Henry Solomon (1910–1991) 37
- Lonsdale, Kathleen (Yardley) (1903–1971) 3, 123
- Main, Peter 116
- Matthews, Brian 51
- Miller, William Hallows (1801–1880) 15, 245, 247, 248
- Mitchell, Dana Paul (1899–1966) 3, 56
- Müller, Walther (1905–1979) 245
- Newman, Melvin Spencer (1908–1993) 159
- Nicol, William (1770–1851) 48
- Niggli, Paul (1888–1953) 17
- Ott, Heinrich (1894–1962) 115
- Parrish, William (1915–1991) 204
- Pasteur, Louis (1822–1895) 112, 151, 152
- Patterson, Arthur Lindo (1902–1966) 130, 228, 229, 233, 250
- Pauling, Linus Carl (1901–1994) 183
- Peerdeman, Antonius Franciscus 157
- Perutz, Max Ferdinand (1914–2002) 144
- Planck, Max (1858–1947) 57, 251, 256
- Poisson, Siméon Denis (1781–1840) 251
- Pope, William Jackson (1870–1939) 3
- Powers, Philip Nathan (1912–1988) 3, 56
- Preiswerk, Peter (1907–1972) 3
- Prins, Jan Albert (1899–1986) 157, 158, 229
- Ramsey, William (1852–1916) 178
- Rayleigh, Lord (John William Strutt) (1842–1919) 178
- Renninger, Moritz (Mauritius) (1905–2009) 243
- Richards, Frederic Middlebrook (1925–2009) 147

- Rietveld, Hugo M. 203
 Romé de Lisle (L'Isle) Jean Baptiste Louis
 (1736–1790) 10
 Röntgen, Wilhelm Conrad (1845–1923) 3
- Sayre, David 116, 118
 Schönflies, Artur Moritz (1853–1928) 110
 Schwarz, Karl Hermann Amandus
 (1843–1928) 116, 239
 Sheldrick, George Michael 116, 127
 Steno, Nicolaus (Stensen, Niels)
 (16389–1686) 10
 Stoicheff, Boris Peter (1924–2010) 3
- Taylor, Brook (1685–1731) 174, 256
 Taylor, Charles Alfred (1922–2002)
 38
 Thomson, John Joseph (1856–1940) 27
- van Bommel, Adrianus Johannes 157
 van't Hoff, Jacobus Henricus
 (1852–1911) 151
 von Halban, Hans (1908–1964) 3
 von Fraunhofer, Joseph (1787–1826) 245
 von Laue, Max Theodor Felix
 (1879–1960) 3, 9, 41, 44, 45, 48, 52,
 56, 247
- Waller, Ivar (1898–1991) 83
 Weissenberg, Karl (1893–1976)
 257
 Whewell, William (1794–1866) 15
 Wilson, Arthur James Cochran
 (1914–1995) 66, 258
 Woolfson, Michael Mark 116
- Young, Thomas (1773–1829) 26
- Zachariasen, Fredrik William Houlder
 (1906–1979) 116
 Zernike, Fritz (1888–1966) 229

Index

An italic entry is a Glossary definition of that specific entry.

- absolute configuration 151–164, 210, 236
absolute scale of $|F(hkl)|$ 65–67, 236
absolute zero temperature 83
absorption correction 65–67
absorption edge 152–155, 160, 233, 236
accuracy 177–180, 236
algebraic representation of waves 72–74, 85
alum (potash and chrome) 142, 144
ammonium sulfate 12, 252
amorphous materials 196, 197, 236
amplitude 6, 27–29, 72–82, 236
angle, interbond 182, 234
angle, torsion 184, 185, 234, 235, 240, 256, 257
angles of incidence and reflection 42, 236
Ångström unit 236
anisotropic displacement parameters (atomic motion) 79, 82–84, 174, 186–192, 194, 236, 237, 256
annealing 50
anomalous dispersion and scattering 56, 151–164, 192, 211, 233, 236, 237
area detector, proportional counter 62, 237, 252
asymmetric carbon atom 151, 152
asymmetric unit 20–21, 101–102, 111, 237
atomic displacement parameters 79, 82–84, 170–172, 187–191, 237, 247, 256
atomic number 132, 191
atomic parameters or atomic coordinates 71, 80–82, 100, 168–173, 181–184, 225–227, 237
atomic scattering factor, scattering factor 77–85, 152, 178, 187, 237, 249
atomic size (radius) 78, 79, 183
atomicity (direct methods) 116
automated diffractometer 237, 238, 242
Avogadro's number 9, 216, 238
axial lengths and angles 51, 52, 59, 71, 94, 202, 206, 210, 213, 216, 221, 238, 248, 257
axis of rotation or axis of symmetry, rotation axis 238
azimuthal scan (absorption correction) 238

base stacking (DNA) 200, 201, 202
beam stop, beam catch 48, 50, 54, 59
benzene 3, 125, 186, 192
beryl 106
beryllium window (X-ray tube) 48, 54
Bessel function 201–202, 238
best plane (least squares) 238
biaxial crystals 250
Bijvoet differences 155, 238
biological macromolecules 50, 51, 130, 142, 162, 163, 170, 202, 210–212
birefringence 21, 22, 48, 238, 250
body-centered unit cell 24, 111, 112, 182, 219, 238, 239
bond lengths 181–183, 190
bonding electrons (deformation density) 193–194, 241
Bragg's Law (Bragg equation) 25, 41–45, 52, 221–224, 238
Bragg reflection 25, 37, 41–48, 52, 55, 57–67, 80–82, 86–90, 93, 99–102, 120–129, 145–150, 156–158, 161–164, 225–227, 232, 233, 238, 239, 242–244, 247–252, 255
Bravais lattice 20, 21, 24, 101, 109, 113, 219, 220, 228, 239, 241
Bremsstrahlung 54, 55, 239

calculated phase angle or calculated phase 85, 96, 239, 250–251
calcite (Iceland spar) 22, 238
Cambridge Structural Database 184
capillary tubes (crystal mounting) 49, 249, 251
Cartesian coordinate system 234, 237, 239, 244
Cauchy–Schwarz inequality 239
center of symmetry (center of inversion) 19, 21, 24, 104, 113, 117, 132, 239
centrosymmetric structure 111, 113, 117, 118, 120, 121, 123, 128, 145, 169, 228, 232, 233, 239, 250
cesium chloride 182
characteristic X rays 54, 55, 258, 239
charge-coupled device area detector (CCD) 47, 60, 63, 64, 207, 237, 239
charge-flipping algorithm 127
chirality 109, 112, 113, 237, 239
chosen origin of unit cell 82, 89, 97, 109
citric acid, citrates, and isocitrates 12, 110, 159, 171, 185, 188, 233
cleavage (crystal) 240
coherent scattering 240
collimator 48, 55, 56, 59, 240
complex representation of waves 75–77, 85, 240
computer graphics program ORTEP 83, 187, 188
computers and computer graphics 95, 96, 126, 127, 129, 134, 142, 147, 170, 173, 176, 180, 181, 212, 237
conditional probability distributions 176
configuration 159, 240
conformation (torsion angles) 184, 185, 234, 235, 240, 256, 257
constraints 175, 240, 253
constructive interference 28–33, 43, 44, 67
convolution 17, 240
coordinates 71, 80–82, 100, 168–173, 181–184, 225–227, 237
copper radiation 54–56, 98
correctness of trial structure 96, 97, 176–179
correlation of parameters 240
crambin 160
cryocrystallography 50
crystal 9, 14–24, 240
crystal density 17, 51, 52, 216, 217
crystal disorder and imperfection (defect) 11, 66, 79, 83, 241, 242, 246
crystal growth (crystallization) 10–13
crystal lattice 17–21, 23, 25, 35, 36, 39, 42–45, 59, 109, 179, 217–220, 222–227, 240, 242
crystal morphology 9, 15–17, 151, 152, 248, 251
crystal mounting 48–52, 58–62, 191
crystal structure 71, 98, 181–195, 222, 240
crystal system 19, 20, 101, 109, 217–220, 241
Crystallographic Information File (CIF) 181
crystallographic point group, crystal class 105, 241
cubic unit cell 19, 20, 23, 37, 48, 110, 181, 217, 219, 220, 227, 228, 241
cylindrical polar coordinates 201, 238

data collection 46–67
data reduction 65–67, 241
defect (crystal) 9, 11, 241, 242
deformation density 193–194, 241
deliquescence 13, 241

- density and density determination (crystal) 51, 52, 213
 density modification, solvent flattening 126, 163, 241
 density wave 88–96, 116–119
 destructive interference 28–33, 43, 44, 67
 detection device 63–64, 239, 245–246, 252, 254, 258
 deuterated proteins 207, 212
 deuterium atoms 191, 192, 195, 207, 249
 dextrorotatory 151, 152, 159
 diamond 15, 179, 183, 184, 196
 dichroism 251
 difference electron-density map 96, 167–173, 176–180, 241, 244
 difference Patterson map 142, 144
 differential synthesis 170, 241
 diffraction 27–45, 52, 53, 71, 101, 113, 200, 241, 242, 250, 251
 diffraction photograph 9, 23, 25–35, 67, 94, 222–224
 diffraction vector 58, 242
 diffractometer 47, 59–64, 237, 242
 diffuse scattering 242, 256
 dihedral angle 242
 dimorphism 251
 direct methods or direct phase determination 115–129, 163, 207, 211, 242, 243, 255, 256
 discrepancy index, *R* value 97, 100, 172, 175, 177, 186, 210, 252
 disordered crystal structure 9, 11, 66, 132, 186, 242
 dispersion 153, 154, 236, 242, 243
 disulfide bridge 142, 160
 DNA 8, 200, 201, 202
 domain 243
 double reflection (Renninger effect) 88, 99, 147–150, 243, 249
 double refraction 21, 22, 250
 dual-space algorithms 126
 dynamical diffraction 52, 243

 efflorescence 13, 243
Eighth Day of Creation 131
 elastic scattering 26, 243
 electron density 86, 91, 243
 electron diffraction 3, 9, 26, 196
 electron microscopy 14, 15, 25
 electron-density map 7, 62, 71, 72, 77, 84–100, 116–129, 140, 143, 167, 179, 212, 240, 241, 243–245, 250
 electrons (X-ray scatterers in atoms) 35, 45, 78
E-map 123–125, 128, 129, 243
 enantiomorph, enantiomer 106, 111, 112, 151, 164, 185, 239, 243, 252, 253, 257
 envelope (diffraction pattern) 29–35, 45, 83
 epitaxy 243
 epsilon factor 120, 243, 249
 equipment for diffraction 57–68
 equivalent positions 111, 243
 equivalent reflections 243, 244
 Euler's formula 244
 Eulerian angles 244
E-values, normalized structure factors 122, 132, 243, 249
 Ewald sphere, sphere of reflection 52, 53, 148, 244, 247, 249
 exponential representation of waves 75–77, 87
 extinction (primary and secondary) 244, 246, 249

 face-centered cubic unit cell 23, 110, 111, 182, 219, 239, 244
 faces of a crystal 15–17, 244
 fiber diffraction 200–202
 figure of merit 147, 244
 film, X-ray 60, 244
 Fischer formula 159, 160
 Flack parameter 157
 flash freezing 50, 163
 focusing mirror system 56, 244
 four-circle diffractometer 61, 62
 Fourier series 86, 130, 167, 170, 229, 244, 245, 254
 Fourier synthesis 7, 86–91, 96, 175, 243, 244, 245, 250
 Fourier transform 87, 91–93, 126, 245, 255
 fractional coordinates 181, 245
 Fraunhofer diffraction 245
 free lunch algorithm 127
 freezing 249
 frequency doubling 22, 249
 frequency of X rays 82
 Friedel's law 87, 152, 155, 163, 237, 245

 Gaussian distribution (error curve) 173, 245
 Geiger counter 245
 glass 10, 199
 glide plane 21, 24, 106–114, 132, 133, 245, 256
 glycogen phosphorylase *b* 62
 goniometer and goniometer head 16, 49, 50, 57, 60, 62, 240, 245, 253
 graphical representation of waves 72, 73, 84
 graphite 196
 grating, diffraction 31–35
 green laser 22
 group (mathematical) 103, 245

 habit of a crystal 245
 Harker sections and projections 133, 141, 246
 Harker–Kasper inequalities, inequality relationships 245
 heavy-atom derivative of a protein 142–144, 146, 147, 163, 211, 246
 heavy-atom method 75, 140–144, 149, 246
 helical diffraction 201, 202
 hemihedry 112, 151, 152

 hemoglobin 144, 184
 hexagonal unit cell 19, 20, 23, 217, 218, 220, 227, 228, 241, 246, 253
 hexamethylbenzene 3, 123–125
 histogram matching 126
 homometric structure 246,
 hydrogen atoms 170, 171, 191, 192, 207
 hydrogen bond 185, 199

 Iceland spar (calcite) 22, 238
 identity operation 103, 246
 image plate 47, 63, 64, 207, 246
 improper symmetry operation, symmetry operation of second kind 246
 incoherent scattering 246
 indexing of crystal faces 15–17
 indices, Miller (*h, k, l*) 15–17, 71, 246
 inelastic scattering 26, 246
 Inorganic Structure Database 184
 intensity 27, 28, 67, 80, 243
 interatomic distances 99, 181–185, 197, 234
 interatomic vectors 131–136, 253
 interbond angles 182, 234
 interfacial angles 10, 16
 interference 28, 246
 intermolecular packing 185
 International Centre for Diffraction Data (ICDD) 203
International Tables 21, 102, 109, 111, 122, 123, 126, 218, 220, 251, 255, 268, 269
 interpreting diffraction data 71–85
 inversion operation (through a point) 103, 239, 246
 iron pyrite 182, 183
 isomorphous replacement method 99, 130, 142–147, 149, 150, 162, 211, 232, 246, 247
 isotropic displacement factor 79, 187, 247, 256

 kappa geometry (diffractometer) 61, 62
 kinematical diffraction 52, 247

 Lagrange multiplier 247
 lattice, (crystal) 17–21, 23, 25, 35, 36, 39, 42–45, 109, 179, 217–220, 222–227, 240, 242, 247
 Laue method 44, 57, 62, 64, 247, 256
 Laue symmetry 132, 242, 247, 255
 Law of Constancy of Interfacial Angles 10, 247
 Law of Rational Indices 15, 247, 248
 layer line (diffraction) 59, 247
 least-squares method of refinement 167, 173–176, 180, 203, 207, 211, 214, 248
 least-squares plane (in a molecule) 185
 lens 5, 6, 26
 libration 189–191, 247
 linear absorption coefficient, absorption correction 247
 liquid crystals 197, 247

- liquid diffraction 198, 203
lithium glycolate (absolute configuration) 192–193
loop (crystal mounting) 49, 50
Lorentz and polarization factors 65, 247, 248, 251
- macromolecules 49–51, 126, 142, 162, 163, 181, 202, 210–212, 249
MAD (multiple wavelength anomalous dispersion) phasing 147, 160, 163, 211, 212, 248
Matthews coefficient 51
maximum likelihood methods 176, 180
mean-square amplitude of displacement 85, 189
method of least squares, least-squares method 238, 248
mica 196
microcrystalline materials 196
microscope 4, 5, 25, 48, 49
Miller indices (*hkl*) 15–17, 62, 243, 246, 247, 248, 254
Miller–Bravais indices (*hkil*) 248
minimum function 137, 248
minimum-variance phase invariant 127
mirror plane 21, 24, 103, 105, 106, 113, 132, 151, 248
Macromolecular Crystallographic Information File (mmCIF) 181
modulated structure 248
molecular geometry and packing 181–195, 234, 235
molecular motion 8, 178, 179, 186–191
molecular replacement method 138–140, 248
molecular transform 35
monochromators and monochromatic radiation 50, 54–56, 248
monoclinic unit cell 19, 20, 23, 37, 122, 123, 171, 216, 217, 218, 220, 221, 227, 228, 241, 248
morphology (crystal) 9, 10, 15–17, 151, 152, 248
mosaic structure or mosaic spread 11, 246, 249
mother liquor 10–13, 49, 50, 249
multiple Bragg diffraction 148–150, 249
multiple isomorphous replacement 142, 249
myoglobin 37, 38, 184
- naphthalene 189
negative quartet 126
negative scattering factor 116, 191
neutron scattering amplitudes 225
neutrons and neutron diffraction 3, 4, 7, 9, 13, 25, 26, 47, 51, 56, 57, 63, 64, 99, 191–193, 195, 202, 207, 212, 225, 249
Newman formula 159
Nicol prism 48
Niggli reduced cell 17, 18
- noncentrosymmetric crystal structure 22, 95, 112, 125, 128, 145, 146, 156, 164, 169, 172, 228, 243, 249, 251
noncrystallographic symmetry 138, 249
noncrystallographic symmetry averaging (real-space averaging) 126, 252
nonlinear optics 249
nonmeasured reflection extrapolation method 127
normal equations (least squares) 249
normalized structure factors, *E*-values 119, 132, 243, 249
nucleation of crystals 11–13, 249
nucleic acids and nucleotides 113, 200–202
- observational equations (least squares) 249
occupancy factor 174, 249
omega block (kappa diffractometer) 61
omit map 127, 170, 250
optic axis 250
optical activity 250
optical diffraction pattern 38–41
optical properties of crystals 21, 22
order of diffraction 30, 31, 94, 248, 250
orientation matrix 250
origin of a unit cell 81, 250
origin-fixing reflections 128, 129
ORTEP (Oak Ridge Thermal Ellipsoid Plot) 83, 187, 188
orthogonal system 74, 76, 77, 237, 250
orthorhombic unit cell 19, 20, 23, 109, 181, 217, 218, 220, 227, 228, 241, 250
oscillation camera 250, 257
oscillation of crystal 52
- parallelepiped 14, 250, 257
parity group (direct methods) 250
particle size 255
path difference (PD) 78, 88, 89, 156, 222–224, 250
Patterson map, Patterson function 115, 123, 130–147, 145, 149, 160, 207, 210, 211, 228–232, 246–248, 250, 253–255
Patterson superposition methods 137
peak heights in Patterson map 131
pentagonal tiles 104
pharmacognosy 10
phase 6, 28, 32, 72, 81, 84, 96, 250, 251, 254, 255
phase angle 72–74, 81, 86, 88, 91, 118, 126, 130, 144, 147, 244
phase angle ambiguity 145–147, 163
phase change 154
phase difference 29, 225–227, 250
phase problem 86–100, 251
phase sum 126
phenyl group geometry 137, 175
phi-scans 148
photographic film 63, 251
phthalocyanine molecule 40, 41, 184
piezoelectric effect 22, 112, 157, 251
- Planck constant 57, 251, 256
plane groups 21, 111, 251
plane-polarized light 22, 151, 238, 250, 251
pleochroism 251
point groups and point symmetry 19, 20, 103, 114, 217–220, 251
Poisson distribution 251
polar space group 113
polarity sense 157, 158, 251
polarization factor 65, 251
polarized light 22, 48
polarized X rays 25, 56
polymorphism 207, 251
positivity (direct methods) 116, 117
potassium chloride 37, 38, 182
powder diffraction 202–205, 251
Powder Diffraction File (PDF) 203
precession camera and method 35, 37, 58–60, 201, 251
precipitant and precipitation (salting out) 12, 13, 252, 254
precision 177, 178, 186, 252
primitive unit cell 20, 23, 24, 109, 182, 239, 252
principal axes of thermal ellipsoid 188, 252
probabilities 119, 121
probability density function 245, 252
probability distributions 176, 252
promolecule density 252
proper symmetry operations 252
protein crystals 8, 12, 14, 60, 83, 99, 113, 126, 138, 142–147, 150, 193, 195, 210–212, 246, 248, 250, 252
Protein Databank 184, 211
protein relative phases 145–147
pycnometer (density) 51
pyroelectric effect 22, 112, 252
- quartets and quintets (direct methods) 126
quartz 196, 204, 251
- R* value, *R* factor, *R* index, discrepancy index 97, 100, 172, 175, 177, 186, 210, 252
R/S (*rectus/sinister*) system (absolute configuration) 160
racemic mixture 252
radial distribution function 197, 198, 229
radiation damage 50, 51, 211, 249, 252
radiation-damage-induced phasing (RIP) 145
radius of gyration 255
real-space averaging 126, 252
reciprocal lattice point (*hkl*) 80, 91, 206, 252
reciprocal space 29, 33–41, 52, 53, 59, 92, 120, 220–222, 225–227, 244, 249, 251, 252
refinement of a crystal structure 46, 167–180, 252, 253
reflection (symmetry operation) 110

- refraction and refractive index 21, 153, 154, 242, 253
- relative phase angle 4, 6, 27, 28, 72, 80, 81, 86, 88, 91, 100, 207
- reliability of a structure analysis 176–179
- Renninger effect 88, 99, 147–150, 243, 249
- residual (*R* value) 97, 100, 172, 175, 177, 186, 210, 252
- resolution (electron density) 94, 97, 98, 99, 253
- resolution (separation of enantiomers) 112, 253
- restraints 175, 253
- rhombohedral unit cell 19, 20, 23, 217, 219, 220, 228, 253
- Richards box 147
- Rietveld method 203, 205
- right-handed coordinate system 253
- rigid-body motion 189–191, 253
- robot setup for crystallization 13
- Rochelle salt 251
- root-mean-square amplitude of vibration 187
- rotating-anode X-ray generator 56, 59, 253
- rotation axis (symmetry operation) 19, 21, 24, 103–105, 110, 250, 256
- rotation function or search 137, 138, 149, 253, 254
- rotation photograph 254
- rotational symmetry 217–220
- rotatory-inversion axis 104, 105, 110, 241, 254, 256
- SAD (single wavelength anomalous dispersion) phasing 147, 160, 163, 211, 212, 254
- sampling regions (diffraction pattern) 31–41, 45
- saturated solution 254
- scattering angle 2θ 71, 254
- scattering factor, form factor 77–85, 152, 155, 178, 187, 237, 24,
- scattering vector 254
- scintillation counter 63, 254
- screw axis 21, 24, 106–112, 132, 133, 254, 256
- second-harmonic generation (SHG) 22, 249
- selenomethionine 163, 212, 248
- self-rotation function 138
- series-termination error 254
- sharpened Patterson function 132
- shift in atomic parameter 170
- sigma 2 formula (Σ_2) 121, 254
- sign of a structure factor 117
- silica and silicates 197, 199
- simulated annealing 254
- sine-Patterson map 163
- sinusoidal wave 6, 72, 73, 254
- slit diffraction 26–35, 45, 83
- small-angle scattering 202, 255
- snowflake 10
- sodium chloride 3, 179, 182, 183, 252
- solvent flattening 126, 163, 241
- space group 21, 24, 101, 109, 110, 113, 114, 122, 181, 206, 210, 227, 228, 239, 243, 255
- space group ambiguities 111, 112, 255
- space shuttle 13
- space-group symmetry 20, 101, 103, 106, 109, 112, 237, 249
- spallation (of neutrons) 57, 255
- sphere of reflection, Ewald sphere 52, 53, 148, 244, 247, 249
- standard uncertainty (s.u.) 177, 178, 255
- stereopairs 147
- stoichiometry 196, 255
- structure factor amplitude 86, 87, 88, 96, 161, 167, 236
- structure factor 65, 80, 82, 86, 87–93, 118, 144, 157, 210, 251, 126, 255
- structure invariant and structure seminvariant 119, 126, 255
- summing density waves 117–119
- superposition method Patterson 255
- superposition of waves 72–77, 93
- symbolic addition procedure 123, 255
- symmetry 101–114
- symmetry element 101, 103, 251, 256
- symmetry of crystal 19–21
- symmetry operation 101, 133, 251, 255, 256
- synchrotron radiation 25, 47, 56, 160–163, 212, 256
- systematic errors 177, 179, 186
- systematically absent reflections 102, 109, 111, 256
- tangent formula 125, 256
- tartaric acid, tartrate 112, 152, 157, 159, 236
- Taylor series 174, 256
- temperature effects 189, 198
- tetragonal unit cell 19, 20, 23, 181, 217–220, 227, 228, 241, 256
- theoretical calculations 194
- thermal diffuse scattering 179, 256
- thermal motion 132, 186–194, 256
- time-of-flight neutrons 256
- tobacco mosaic virus 184
- torsion angle 184, 185, 190, 234, 235, 240, 256, 257
- translation (lattice) 35, 254
- translation (motion) 189
- translation function 138, 257
- translational symmetry 14, 103, 257
- trial structure 46, 88, 96, 97, 100, 115, 167–180, 207, 210, 257
- trial-and-error method 117, 257
- triclinic unit cell 19, 20, 23, 217–220, 227, 228, 241, 257
- trigonal unit cell 19, 20, 23, 217, 227, 228, 241, 253
- triple-product sign (triplet phase) relationship 119, 121, 123–125, 129, 149, 257
- twinning 13, 174, 257
- uniaxial crystals 250
- unit cell 10, 14–19, 23, 35, 51, 181, 216, 217, 250, 251, 257
- unit cell dimensions 51, 52, 59, 71, 94, 202, 210, 213, 216, 221, 238, 248, 257
- unitary structure factor 257
- unobserved Bragg reflections, absent Bragg reflections 257
- uranyl (heavy-atom) derivative 143
- vapor diffusion method (crystal growth) 12
- vector 75, 132, 220, 242, 257
- vector map 131, 139
- vector superposition method 136, 137
- vectorial representation of waves 74–77, 85
- viewing stereodiagrams 147, 194
- virus structures 8, 184
- vitamin B₁₂ 140, 141, 143, 184, 231
- water 198, 199
- wavelengths 72, 99, 153, 160, 249
- weight of a measurement 173–176, 257
- Weissenberg camera 58, 257
- white (polychromatic) radiation 56, 64, 257
- Wilson plot 66, 127, 236, 258
- World Wide Web 126, 184, 211, 269
- X rays 3, 25, 26, 37, 47, 52–57, 216, 237, 258
- X-ray diffraction 3–8, 37, 59, 99, 191, 206, 225–227, 244, 245, 249
- X-ray tube 48, 52–56, 253, 258
- X – X and X – N maps 193–194
- xylose isomerase 112, 193
- zinc blende (sphalerite) 157, 158